FEASIBILITY STUDY OF CONTINUOUS FOR LIVE LOAD STEEL BRIDGES

By

DANIEL ENRIQUE MORALES

Bachelor of Science

Oklahoma State University

Stillwater, Oklahoma

2004

Submitted to the Faculty of the
Graduate College of
Oklahoma State University
in partial fulfillment of
the requirements for
the Degree of
MASTER OF SCIENCE
December, 2006

FEASIBILITY STUDY OF CONTINUOUS FOR LIVE

LOAD STEEL BRIDGES

Thesis Approved:

_____Dr. Charles M. Bowen_____
Thesis Adviser

_____Dr. Robert Emerson_____

_____Dr. Steven Gipson_____

_____Dr. A. Gordon Emslie_____
Dean of the Graduate College

Acknowledgments

I would like to thank the Oklahoma Transportation Center for funding the research project.

Dr. Bowen has been a great adviser throughout the project. Thank you for helping me to look at things like a good engineer would. I'd also like to thank the entire faculty and staff of the Civil and Environmental Engineering Department at Oklahoma State. You all have made my academic years a very rewarding experience.

All of the friends I have met or worked with at Oklahoma State have also helped to enrich my college years. If it was either studying for a mid-term together or just talking about life issues; I had a friend. There are too many of you to count, but I am still grateful to all of you.

I am grateful for my family. Thanks Dad for encouraging me to stick with the structural side of Civil Engineering. Thanks Mom and Jon for listening to me talk about the many trials and tribulations of being a student and telling me to keep going. Thank you to my entire family for all of your love and support throughout the years.

Thanks Kat. You know that I wouldn't have been able to do this without you. You are my true love always and forever.

TABLE OF CONTENTS

CHAPTER **PAGE**

CHAPTER **PAGE**

LIST OF TABLES

TABLE **PAGE**

LIST OF FIGURES

FIGURE **PAGE**

FIGURE **PAGE**

NOMENCLATURE

CLL	Continuous for Live Load
DOT	Department of Transportation
BDI	Bridge Diagnostics Inc.
STS	Structural Testing System
LRFD	Load Resistance Factor Design
AASHTO	American Association of State Highway and Transportation Officials

CHAPTER 1

INTRODUCTION

1.1 BACKGROUND

Currently in the U.S. the precast-concrete market dominates in the short to medium span range bridges (span length < 150 feet). The material and labor savings associated with the use of precast-concrete is the biggest incentive for practicing engineers in choosing this material. Due to the rising material cost of steel and greater erection cost, fewer short and medium span steel bridges are being constructed (Azizinamini, Lampe, Yakel 2003).

In 1995 the American Iron and Steel Institute developed design aids for short span bridges with the objective of improving simplicity, cost effectiveness, and fatigue resistance. The design aids included a set of plans for pre-designed bridges with varying types of girders and computer software that allows the user to customize the design for different projects (Rubiez 1996). The design aids employed many of the cost effective refinements in steel bridge design.

Some of the refinements in steel bridge design include the use of unpainted weathering steel, which has long-term maintenance cost savings. Using simplified diaphragm and cross frame details also helps to lower fabrication costs. Wider girder

spacing can be utilized through the use of stay-in-place metal deck forms ultimately decreasing the total steel weight. Another advance is the use of jointless and integral abutments providing a jointless bridge. Jointless bridges eliminate leaky joints and offer long-term maintenance cost savings. According to Weaver (1996) the development of the Load Resistance Factor Design (LRFD) yields a more cost effective design compared with the previous design method, Allowable Stress Design (ASD) due to material savings. Elastomeric bearing pads are being used at supports because of the low initial cost and low maintenance costs (Weaver 1996, Mistry 1994, Rubiez 1996). A summary of these refinements can be found in Table 1.1 below. Even with all of these new practices, the precast concrete bridges are still heavily favored in the short to medium span range bridges.

Table 1.1: Advances in Steel Bridge Design

Old Practice	New Practice
Lead-Based Paint	Weathering Steel
Close Girder Spacing	Wide Girder Spacing
Removable Deck Forms	Permanent Metal Deck Forms
Expansion Joints	Integral & Jointless Abutments
Pin, Roller, Rocker	Elastomeric Bearing Pad
Complex Framing Details	Simple Framing Details
Non-Composite Design	Composite Design
Allowable Stress Design	Load Factor Design

Another approach to the problem was developed by Dr. Atorod Azizinamini at the University of Lincoln Nebraska utilizing sponsorship of the Nebraska Department of

Roads. The solution is called the continuous for live load method (CLL). The method employs a simple span configuration that handles the non-composite dead loads and a continuous span configuration for composite dead and live loads. A concrete diaphragm at the pier connects the two simply supported spans thus making them structurally continuous. The CLL method is very similar to the method in which many prestressed concrete bridges are constructed.

1.2 BASIC CONCEPTS BEHIND CLL

The purpose of the CLL method is to provide a more cost effective design method for short to medium span steel bridges. This is accomplished through the simplification of the details used in steel bridges, which in turn yields a decrease in the erection and fabrication costs of a bridge. A continuous span steel bridge utilizes bolted field splices located approximately at the dead load inflection points (away from the piers) to connect two steel girders. Refer to Figure 1.1 below.

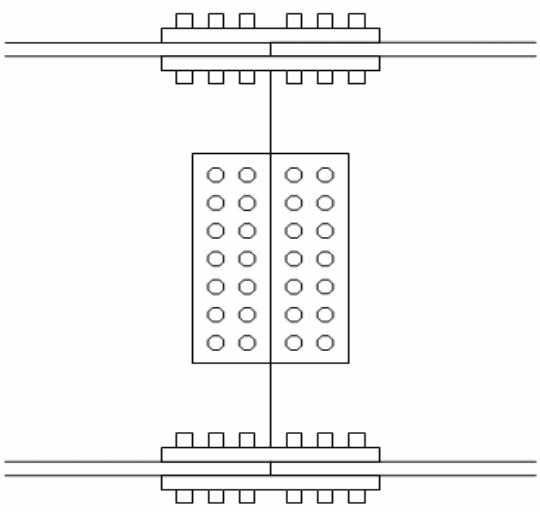

Figure 1.1: Bolted Steel Splice

Normally this procedure requires two cranes to hold up each girder to properly align each girder to be connected with the field splice as illustrated in Figure 1.2.

Figure 1.2: Traditional Bolted Steel Splicing

Employing the continuity detail eliminates the need for two cranes in that the steel girders rest on the pier to be connected later at that location by the concrete diaphragm. Refer to Figure 1.3 for a traditional continuous steel bridge and Figure 1.4 for a simply supported steel bridge.

Figure 1.3: Traditional Continuous Steel Bridge

Figure 1.4: Simply Supported Steel Bridge

Please refer to figure 1.5 for the CLL detail.

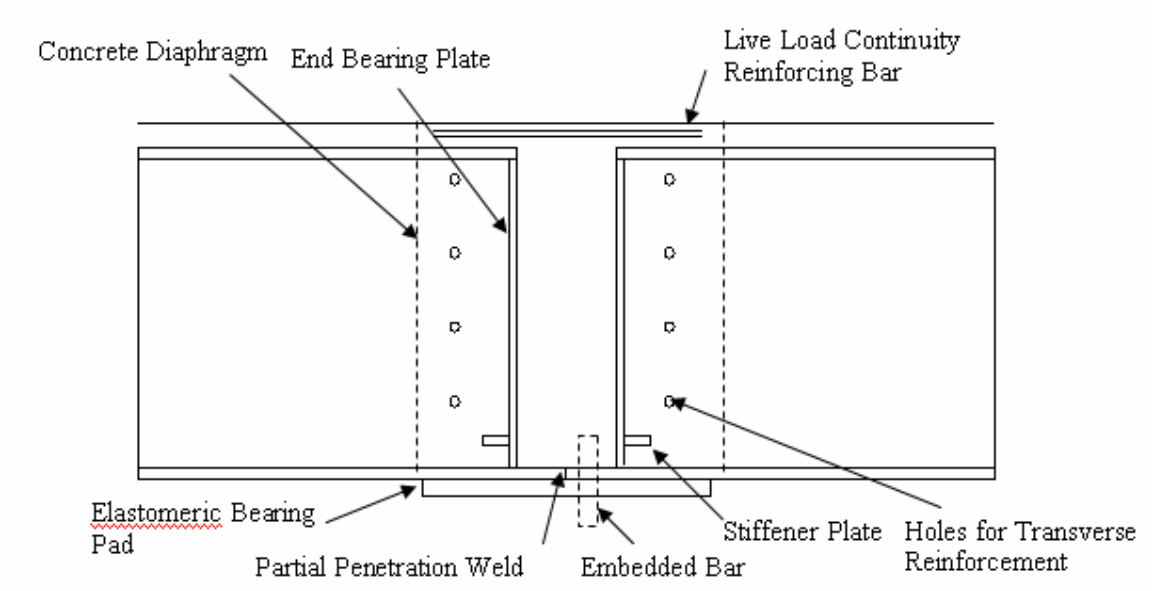

Figure 1.5: CLL Detail @ Pier

Traffic disruption is reduced due to quicker erection time. The elimination of a splice away from the pier cuts fabrication costs and the use of one less crane cuts erection costs.

One big advantage to the CLL method is what is referred to as the equalization of the moment requirements in the girder. For a distributed load in a continuous system, the maximum negative moment at the pier is twice the maximum positive moment located between supports. In a CLL configuration, the dead load is supported by a simply supported system, and then the system is converted to a continuous one by connecting the two members at the pier. With the live load superimposed on a continuous system, the maximum positive and negative moments are closer in magnitude than using a fully continuous system from the beginning. This equalization may allow for one type of girder cross section along an entire span length. Combining the moment diagram of a simply supported span with that of a continuous span configuration equalizes the moment. The dead load of the structure is placed in a simply supported fashion, and the live load is placed in a continuous fashion. Looking at the moment diagram of a continuous span one notes that the negative moment is largest at the interior supports while the positive moment at midspan locations is significantly lower. For simply supported spans only positive moments occur with the maximum moment located at midspan. The combination of these two configurations yields a lower negative moment requirement at the interior supports while increasing the positive moment requirement the midspan. Figure 1.6 illustrates this concept.

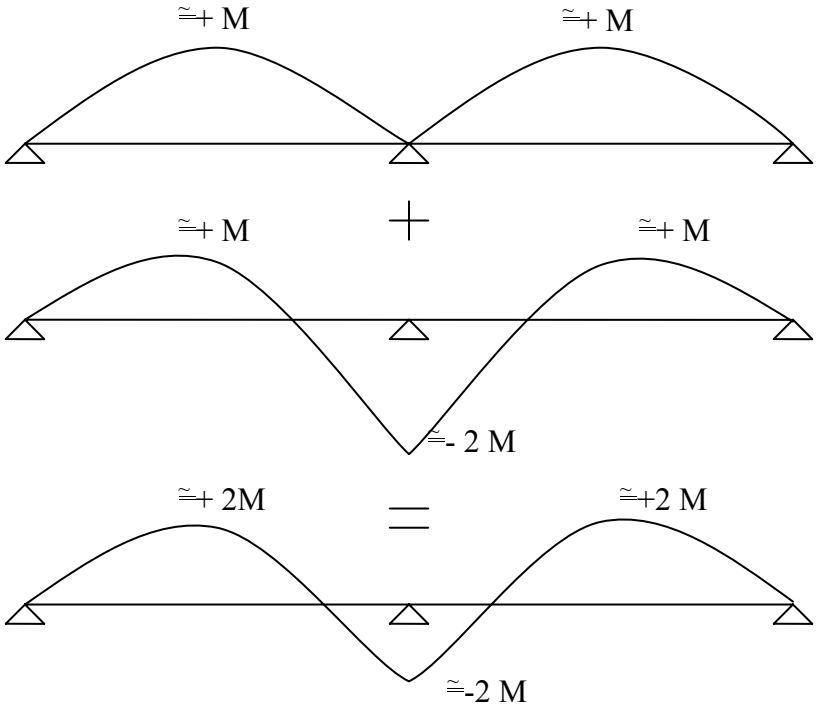

Figure 1.6: CLL Basic Concepts

Structurally speaking, the CLL method can allow for one type of steel girder for the entire length of a span in a bridge. Many times in steel bridge construction the cross section of the steel girders fluctuates along the length of the bridge. Field splices connect two different girders in order to satisfy the positive and negative flexure requirements imposed by the loadings. The CLL method reduces the maximum negative moment located at the interior supports that is associated with a continuous span configuration, and helps make the positive and negative moments more equal.

There are many other advantages to using the CLL method. For example, the girders acting in a simply supported fashion for the non-composite loads only require single curvature camber. (Non-composite loads implies any loading that occurs before the concrete slab has hardened, while composite loading implies any loading that occurs

after the concrete slab has hardened.) Continuous girders would require a double curvature camber. A greater portion of the deck will be in compression due to the equalization of moment. This helps to reduce tension cracking in the slab.

1.3 PROJECT OBJECTIVES AND SCOPE

This thesis involves the investigation into the feasibility of the continuous for live load (CLL) concept of steel bridge construction from an engineering and economical standpoint. One of the main objectives in this study will also be to determine if the CLL concept devised actually performed as designed in-situ, as opposed to laboratory and computer simulation only. The tasks below were used to accomplish these objectives.

1) Literature review
2) Solicite opinions and recommendations from the State Departments of Transportation (DOT) concerning current practices and experiences with construction of a CLL bridge
3) Examination of the economic feasibility of CLL
4) Perform a computer analysis of a CLL bridge using linear finite element analysis
5) Perform load test on CLL bridge
6) Analyze results of the load test and computer model to determine the degree of continuity achieved by the CLL concept

The literature survey constitutes reviews of journal articles and theses pertaining to the CLL concept. The articles and theses all describe either the structural concept of CLL or give an account of the experiences with construction of a CLL bridge. A questionnaire sent to all of the DOTs was utilized to gauge the current practices of steel bridge construction and inquire about any CLL bridges previously constructed.

A CLL bridge located in Las Cruces, New Mexico was chosen for one of the load tests. It is a twin three-span composite concrete slab on steel girder bridge. Another bridge located in Hatch, New Mexico was also chosen to load test. STAAD Pro 2004 was used to conduct a linear Finite Element Analysis of both bridges under live loading. The bridge will be modeled in both a continuous and simple span configuration in STAAD. Finally, the load test results and the finite element analysis results will be compared to show which configuration the bridge models the closest.

CHAPTER 2

LITERATURE REVIEW & SURVEY

2.1 INTRODUCTION

This chapter will outline the supplementary information gathered concerning the CLL method. Due to the fact that the continuous for live load concept is still a relatively new concept, not a lot of research has been conducted. However, conducting a nationwide survey of DOT's helped to uncover articles about the CLL concept written by engineers. The other main source of information used is the original thesis written concerning CLL titled, *Toward Development of a Steel Bridge System – Simple for Dead Load and Continuous for Live Load*, written by N. Lampe, et al.

2.2 LITERATURE REVIEW

Henkle (2001) reviewed a CLL bridge in Las Cruces, New Mexico that was constructed in 2001 on U.S. Highway 70. According to Henkle, the bridge was designed with the objective in mind to reduce fabrication costs. Henkle notes many design advantages associated with the CLL concept. Full penetration welds and field splices are eliminated except for the continuity plate (which will be discussed in Chapter 3).

Another advantage discussed is that more of the deck is put in compression, which helps to complement concrete's compressive strength capabilities and reduce tension cracking. The more equal positive and negative moment also helps to keep constant the thickness of the web plate in a steel girder.

Engel, Miller, and Swanson helped to design and construct a CLL bridge (PIC-22) in Ohio. The authors note that the bridge was built specifically to ensure quick and fast construction to reduce traffic to the public. The bridge was part of a research project involving the Ohio Department of Transportation, University of Cincinnati, and several engineering firms with the purpose to identify quick and easy construction methods. To reduce construction time ODOT engineers employed the CLL concept for this bridge.

The new bridge consists of a six span continuous composite slab on steel girder bridge. Five steel girders support a concrete deck that is 44'-2" wide. Engineers designed the steel girders as simply supported, which were later made continuous through the use of concrete integral diaphragms at the piers. This particular bridge became Ohio's longest jointless bridge due to the use of integral abutments.

Figure 2.1: View of Integral Abutment

Despite some unexpected delays the bridge was still completed 10 days earlier than expected. The project was deemed a success in terms of quick construction speed.

As part of a research project, Lin (2004) load tested the PIC-22 bridge in Ohio to analyze the level of continuity that the concrete diaphragm provides. Strain data collected in the test was converted to moments at specific locations, and this was plotted vs. the location of the load vehicle. The measured converted moments were compared with two computer models. One computer model was a one-dimension, six span, simply supported beam with fixed ends representing the abutments. Another model was a one-dimension, six span, fully continuous beam with fixed ends representing the abutments.

By plotting the test data with the two computer models, Lin (2004) concluded that the bridge behaved much more like a continuous structure than a simply supported structure. These were only qualitative observations and no quantitative conclusions were made. However, Lin (2004) concluded that the pier diaphragms provided an adequate level of continuity.

Two other bridges located in Tennessee also utilize the CLL concept. Wasserman (2004) aided in the design of these two bridges. According to Wasserman, two distinct methods of construction were used. The first method employs a simple span for the dead loads (which include the weight of the steel girders and wet concrete slab) and a continuous span for the live loads. The other method employs a simple span for only the dead load of beams and continuous span for the dead load of the concrete slab and all of the live loads.

Wasserman notes that the first method involves designing the steel girders to carry their self-weight and the weight of the slab in a non-composite condition with

simply supported end restraints. Once the concrete deck is poured and hardens, the bridge is now considered composite and behaves in a continuous manner for all of the dead and live loads. The only dead loads that would be considered once the bridge becomes composite are concrete bridge barriers. A bridge on State Route 35 over Brown Creek and Harper Avenue in Maryville, Tennessee utilized this method of construction.

Wasserman indicates that the second method involves designing a beam with the same cross sectional properties the full length of the bridge, which meets the maximum positive moment requirements. The girders are placed in a simply supported fashion and then connected by bolting a cover plate to the top flanges of adjoining stringers. The gap between the bottom flanges is filled with two trapezoidal plates, which are welded to the flanges. Once the girders are locked into place the slab and diaphragm is poured. A bridge on the DuPont Access Road over State Route 1 in New Johnsonville, Tennessee utilized this method. Figure 2.2 below illustrates the connection.

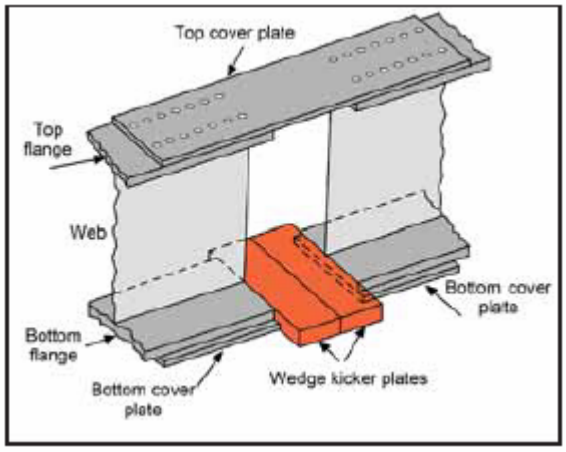

Figure 2.2: Detail of CLL Connection @ DuPont Access Road New Johnsonville, Tennessee (Talbot 2005)

According to Wasserman, the simple span for dead load of the beams and continuous for all other loads proved to be more favorable in terms of economy and

structural efficiency. Overall both methods save on material and shipping costs. Girder erection is also less expensive because of the smaller cranes that are required. The economic feasibility of this method compared with utilizing prestressed concrete girders for both bridges is discussed in Chapter 3.

Research was conducted by Azizinamini, Lampe, and Yakel (2003) at the University of Lincoln Nebraska in association with the Nebraska Department of Roads to develop an economical steel bridge system for short to medium span bridges. Data from the National Bridge Inventory (NBI) that was compiled by the Federal Highway Administration (FHWA) was utilized to perform a market analysis. The analysis showed that the amount of short to medium span steel bridges has declined. The authors note that several reasons were attributed to the decline:

- Intricate and expensive details
- High costs of bolts used for bolted connections
- Over design of steel bridges
- Complexity of steel bridge design compared to that of prestressed concrete bridge design

The CLL concept was theorized in order to develop a more economical steel bridge system for short span lengths. Several different configurations for continuity transfer of loads were analyzed with varying span lengths to determine the most efficient load carrying system in terms of moment capacity. Span lengths of 100ft, 120ft, and 150ft were used with four different configurations of load distribution. Case 1 utilized

two girders acting as simple spans for dead loads and continuous for live loads with non-integral piers. Case 2 utilized girders acting continuous for all loads with non-integral piers. Case 3 utilized girders acting as simple spans for dead loads and continuous for live loads with integral piers. Case 4 utilized girders acting continuous for all loads with integral piers. For an integral pier the concrete diaphragm is cast directly on top of the pier allowing for interaction between the diaphragm and pier. A thin layer of foam is placed on top of the pier before the concrete diaphragm is cast to form a non-integral pier.

Using finite element analysis software, it was determined that integral piers gave negligible effects in terms of moment capacity for the shorter spans of 100ft and 120ft. Of the two configurations utilizing non-integral piers, Case 1 had several benefits such as increasing the maximum positive moment while decreasing the maximum negative moment. This configuration thus allows for the same cross section of the steel girder for the entire span length. The simple for non-composite loads and continuous for composite load design was used for further investigation (Azizinamini, Lampe, Yakel 2003).

The Military Road Bridge in Omaha, Nebraska was reconstructed utilizing the CLL concept. The designs of this bridge were in accordance with American Association of State Highway and Transportation Officials (AASHTO) and Load and Resistance Factor Design (LRFD). A cost comparison between the original construction and new construction showed savings of 4% to 8% in material and fabrication costs (Azizinamini, Lampe, Yakel 2003).

The authors also constructed a full-scale model of the connection of a two span CLL bridge. The model was subjected to a fatigue test of 2,000,000 cycles of loads

simulating 75 years of truck traffic loading. The model suffered no deterioration of stiffness or strength. It was also determined that for a two span bridge with 100 foot spans, the negative moment could be reduced by 35% with an increase of 17% in positive moment. An increase of 5% in girder weight was required for this adjustment. It was concluded by the authors that the intensive lab testing and the cost comparison indicated the CLL method was a successful alternative to fully continuous construction.

2.3 DOT SURVEY

A survey written by Daniel Morales (found in Appendix C) was sent to the fifty DOT's across the nation in order to gain their thoughts and opinions concerning the economics of steel bridge design and those economics as compared to pre-stressed concrete bridges. The survey also helped to determine where any CLL bridges may have been constructed. Out of the 50 states, almost half (24) states returned the survey.

Of the many statements made by the DOT bridge engineers, several comments emerged many times. Some conclusions that were made from the surveys are:

1.) Pre-stressed concrete bridges are generally more economical than steel bridges in the short span range (spans < 110 ft)

2.) Simplifying the steel design details saves costs in fabrication and erection

3.) Erection time of steel bridges is considerably longer than most pre-stressed concrete bridges

4.) Optimizing the amount of bolts and splices helps to significantly lower costs

The CLL method in theory would help to improve these negative qualities associated with steel bridges. The CLL method would help to simplify the fabrication and reduce the erection time of steel bridge construction. The next chapter will explore whether there truly are any economic savings.

CHAPTER 3

CONTINUITY DETAIL

3.1 INTRODUCTION

This chapter will outline the development of the CLL detail and investigate the economic feasibility of the method. The continuity detail is the mechanism in which the two simply supported spans are connected to, in theory, create a continuous span. Any cost or time savings will be investigated and quantified for several bridges where CLL has been used. Since the development of the first continuity detail at the University of Nebraska-Lincoln, the CLL method has been used on steel bridges in several states. The details have changed slightly from bridge to bridge but the overall concepts have stayed in tact. This chapter will also highlight and explore the differences between connections.

3.2 CONTINUITY DETAIL

The continuity detail is the connection of steel girders at the interior supports, which helps to enable a continuous moment transfer for the live load. The continuity detail was first proposed by Dr. Atorod Azizinamini at the University of Lincoln – Nebraska. From this first continuity detail many other DOT's around the country have

used the same concepts of CLL to create their own detail of the continuity connection. Although the details have not changed much from state to state, it is important to note differences or similarities in order to determine what is needed for the detail to function properly.

The first detail designed by Dr. Azizinamini was very basic in nature in order to provide the simplest connection detail to cut fabrication costs. The detail is shown below in Figure 3.1.

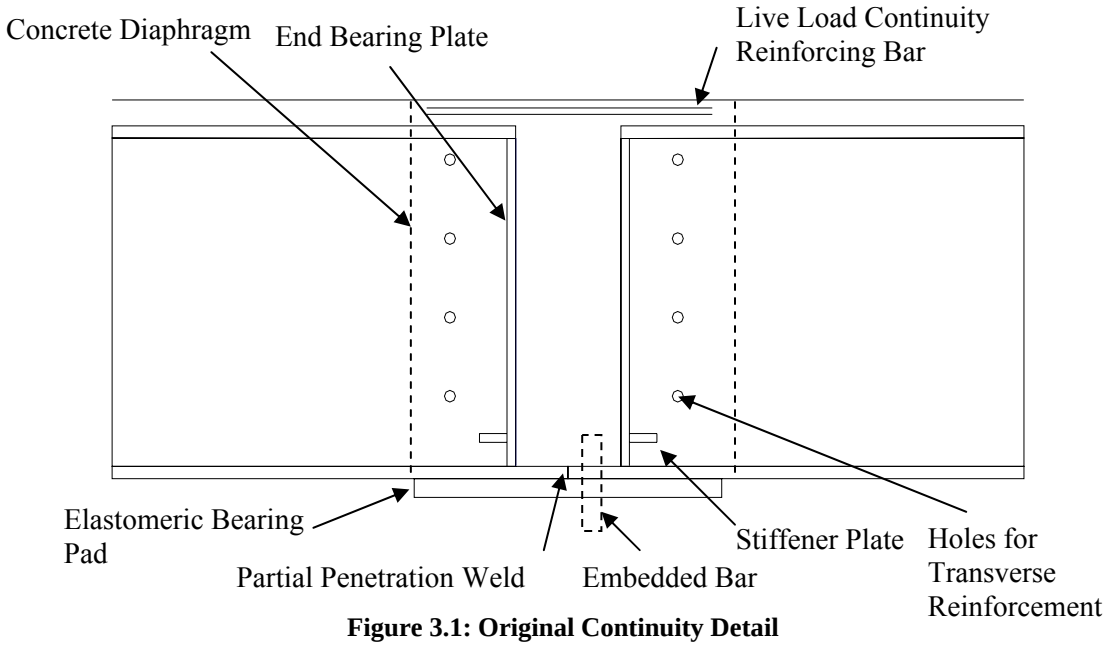

Figure 3.1: Original Continuity Detail

The two girders rest on top of an elastomeric bearing pad, which extends the entire width of the concrete diaphragm. The diaphragm is a concrete block that is formed at the intersection of the two steel girders. The bottom flanges are extended further than the top flanges to close the gap between girder ends. The bottom flanges are then connected by partial penetration welds. The reasoning behind this extension is to avoid the crushing of

concrete between girder ends bottoms as the continuity detail induces negative moment (and hence compression in the bottom flange).

A bearing stiffener plate is welded to both girder ends to ensure that the concrete poured between the girders does not fail due to the large compressive stresses. The bearing plates were stiffened through the use of stiffener plates attached near to the compression zone. Several holes are drilled into the girder web cross section to allow for transverse reinforcement in the concrete diaphragm. This transverse reinforcement runs the entire length of the concrete diaphragm to resist the tensile bending stresses in the concrete. Instead of using anchor bolts, several reinforcement bars extend up from the pier into the concrete diaphragm to connect the two. The reinforcement in the concrete deck above the top flanges extends into the concrete diaphragm to help ensure live load continuity. The concrete diaphragm was first poured to about two-thirds full to make the girders partially continuous. Next the concrete deck along with the rest of the diaphragm is poured allowing the girders to handle the rest of the non-composite system dead loads. Once the concrete cures, the system handles any superimposed dead loads or live loads in a continuous and composite fashion.

A variation to the original connection proposed by Dr. Azizinamini was implemented on a bridge in Omaha Nebraska. It carries Sprague Street over I-680. The variation includes a 2 in. thick plate that is welded to the bottom of each end plate. The bottom flanges are no longer extended beyond the top flanges as with the first detail. The detail is shown below in Figure 3.2 below.

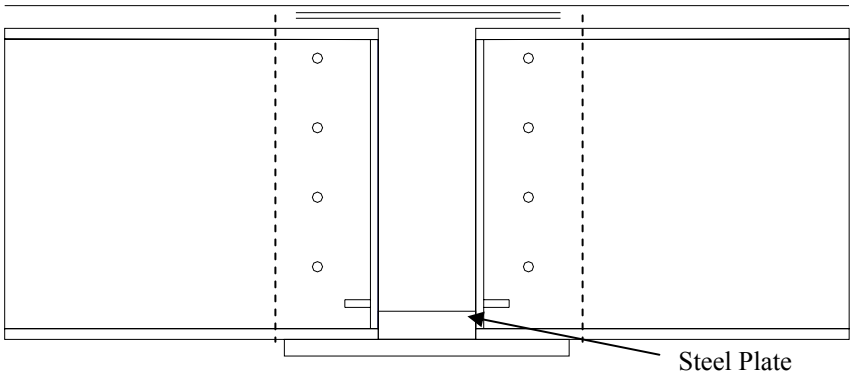

Figure 3.2: Alternative to Original Continuity Detail

The logic behind the thick plate at the bottom is to avoid any concrete crushing between the bottom flanges by preventing the longitudinal movement that the bottom flanges experience under loading. Finite element analysis research conducted by Dr. Azizinamini indicated a possibility for concrete crushing due to the large compressive stresses. It was thought this method would reduce the risk of concrete crushing as compared to the previous design. Dr. Azizinamini performed extensive lab testing on several prototypes to develop this final detail.

The state of Ohio utilized the CLL concept in the reconstruction of a bridge on state route 22 in Circleville, OH. The continuity detail used for this bridge is very similar to the detail developed by Dr. Azizinamini. The continuity detail used on the bridge in Circleville Ohio is shown in Figure 3.3 below.

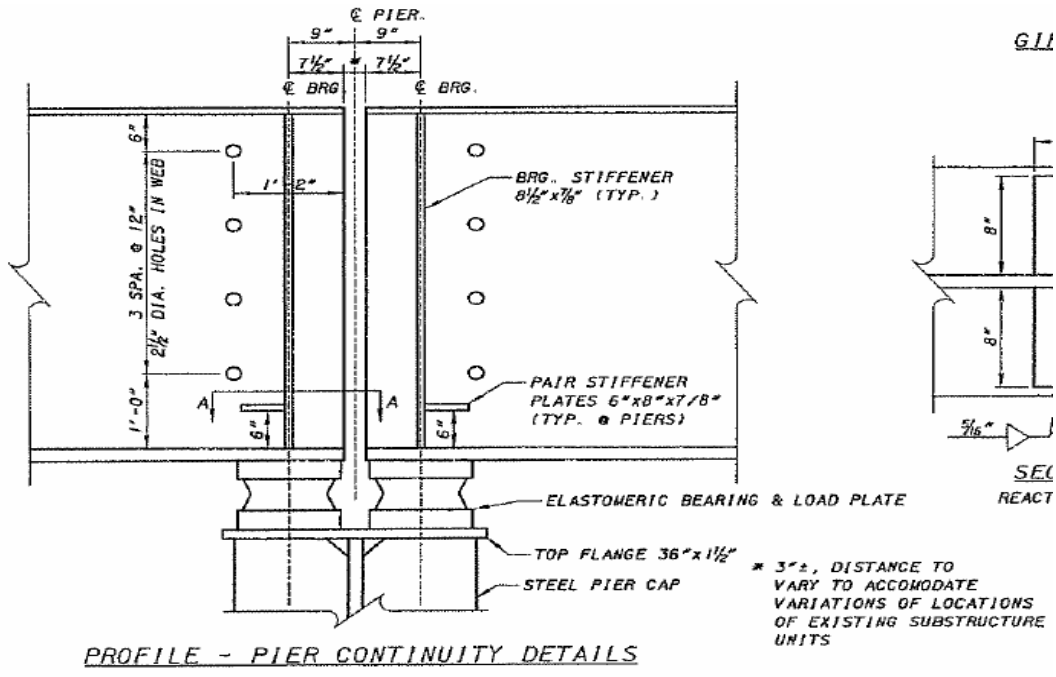

Figure 3.3: Continuity Detail of PIC-22 Bridge

Both girders rest on elastomeric bearing pads and both girder ends have bearing stiffeners, which also act as transverse shear stiffeners. There are also horizontal stiffener plates located near at the bottom of the flanges to stiffen the bearing stiffeners against the compressive concrete forces associated with negative flexure.

The major difference between this connection and the University of Lincoln Nebraska's connection is that the Circleville bridge leaves a gap between the bottom flanges. This small difference makes this type of connection a little simpler due to the fact that any type of welding is eliminated. It was thought by the designers that the bearing stiffeners would be enough to prevent the concrete between the girders from crushing. The slab was poured concurrently with the concrete diaphragms, which can be different depending on different state's own DOT regulations. It is required by some DOT regulations that the deck in the positive moment regions be poured before the deck

in the negative moment regions. The reasoning behind this procedure is to avoid cracking over the piers in continuous bridges (Engel 2004).

The Tennessee DOT utilized two different types of continuity details on two different bridges. The first detail is much like the ones used in Ohio and Nebraska. A bridge in Maryville, Tennessee on state route 35 was constructed using the first detail. The girders rest on neoprene bearing pads however, and anchor bolts are utilized in this connection to lock the girders into the piers. Two steel plates were welded to both girder ends to act as bearing stiffeners. The girder ends were locked into place first by means of an initial pour in the concrete diaphragm. Then the rest of the diaphragm was poured concurrently with the slab. Figure 3.4 illustrates the detail at the bridge in Maryville Tennessee.

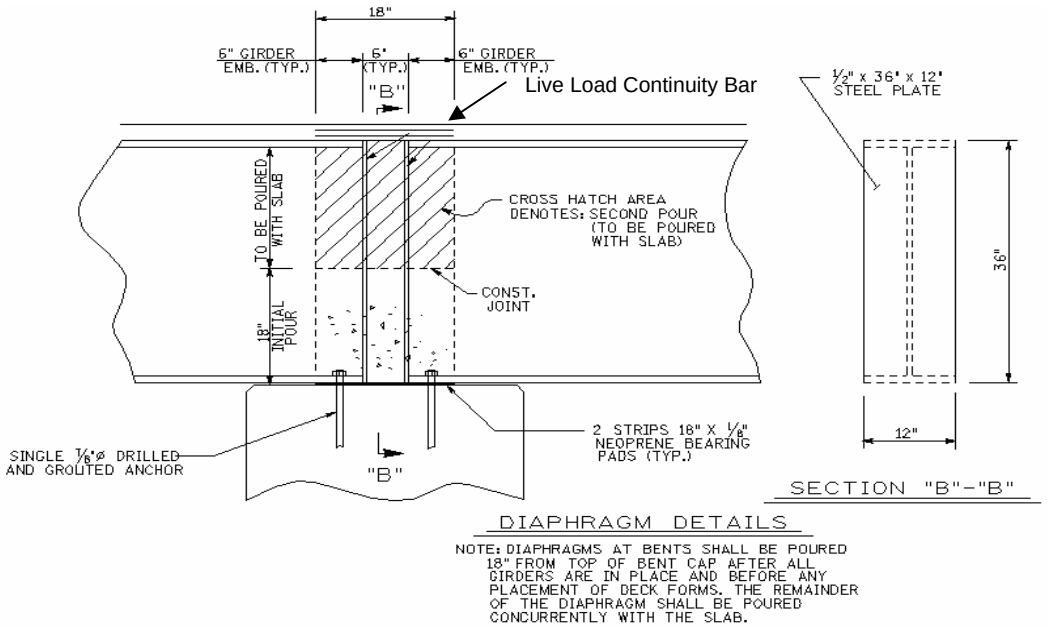

Figure 3.4: Continuity Detail of State Route 35 Bridge in Maryville Tennessee (Wesserman 2004)

A bridge in New Johnsonville, Tennessee over state route 1 used another type of continuity detail that was different from the one previously described. The major

difference between details is the inclusion of a bolted connection plate, which joins the top tension flanges of each girder. The connection was bolted before pouring the concrete in the diaphragm or the slab. This action results in only the dead load of the steel girders to be put in a simply supported configuration while all other loads are handled in a continuous fashion. The compression flanges were joined by two trapezoidal plates that were wedged in between the girders and later welded. Figure 3.5 contains the continuity detail of this bridge in New Johnsonville Tennessee highlighting the wedge kicker plates and cover plate. (Note: The figure which was taken directly from Wasserman's article mistakenly does not show bolts connecting the top cover plate)

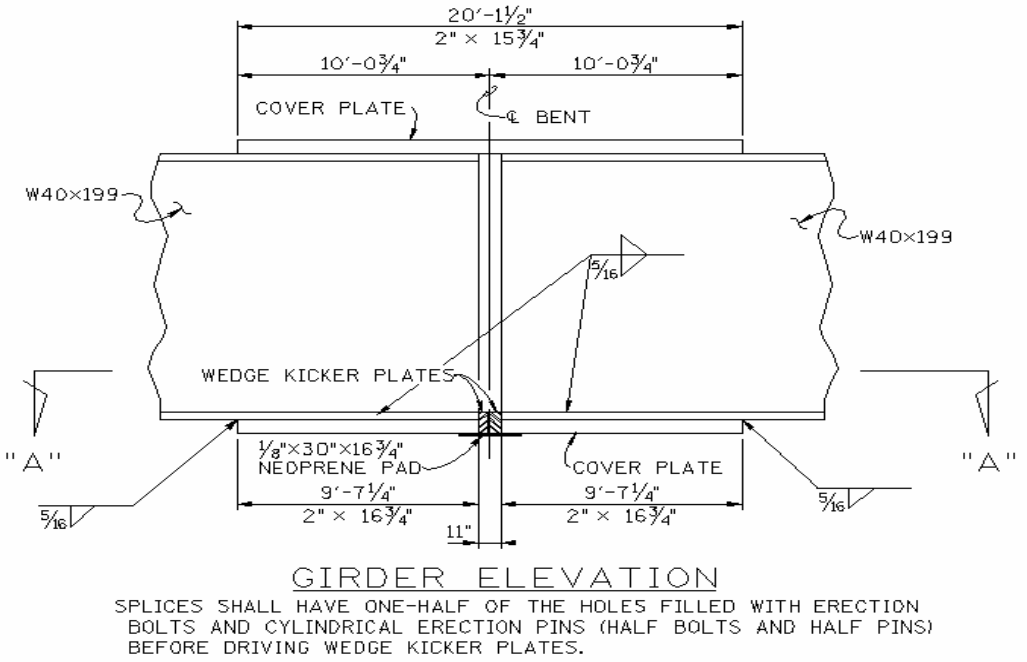

Figure 3.5: DuPont Access Road Bridge in New Johnsonville Tennessee (Wesserman 2004)

The two bridges used for case studies in this report have a similar continuity detail to that of the bridge in New Johnsonville, TN. The Las Cruces and Hatch bridges both have what is called a continuity plate that joins the tension flanges at the diaphragms.

The major difference with the continuity plate is that unlike the Tennessee bridge, the bolts on the plate are not tightened until after the concrete is poured in the positive moment region of the deck. The positive moment region of the deck constitutes a majority of the deck, which puts the dead load of the girders and concrete slab in a simply supported fashion. After this portion of the slab is poured, the bolts on the plate are tightened and the negative moment region and concrete diaphragm is poured. The reasoning behind this is to reduce any potential cracking of the slab at the negative moment regions and to allow for the use of the bolted connection. The continuity plate provides a level of redundancy in case of failure of the longitudinal steel in the slab in the negative moment region. Figures 3.6 & 3.7 illustrate the continuity detail and plate.

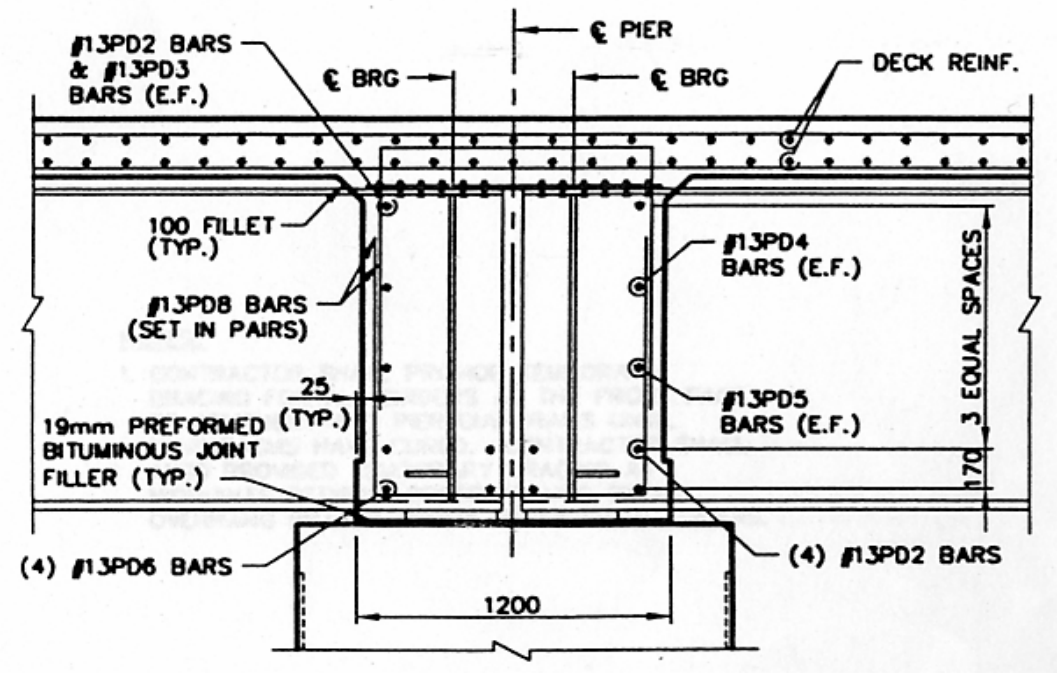

Figure 3.6: Las Cruces Bridge Continuity Detail (Wade 2000)

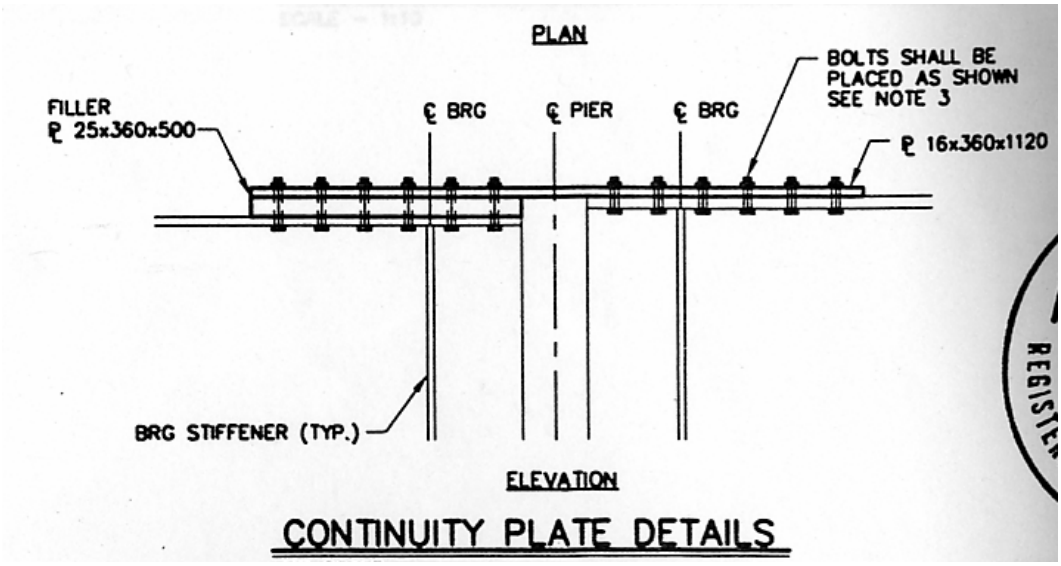

Figure 3.7: Las Cruces Bridge Continuity Plate Detail (Wade 2000)

Figure 3.8 shows the continuity detail for the bridge in Hatch New Mexico.

As before, the bearing stiffeners help to reduce concrete crushing between girder ends. The braced bearing stiffener is used in order to avoid using a much thicker stiffener plate. The holes for transverse reinforcement also carry the tensile bending stresses that the concrete diaphragm experiences in flexure.

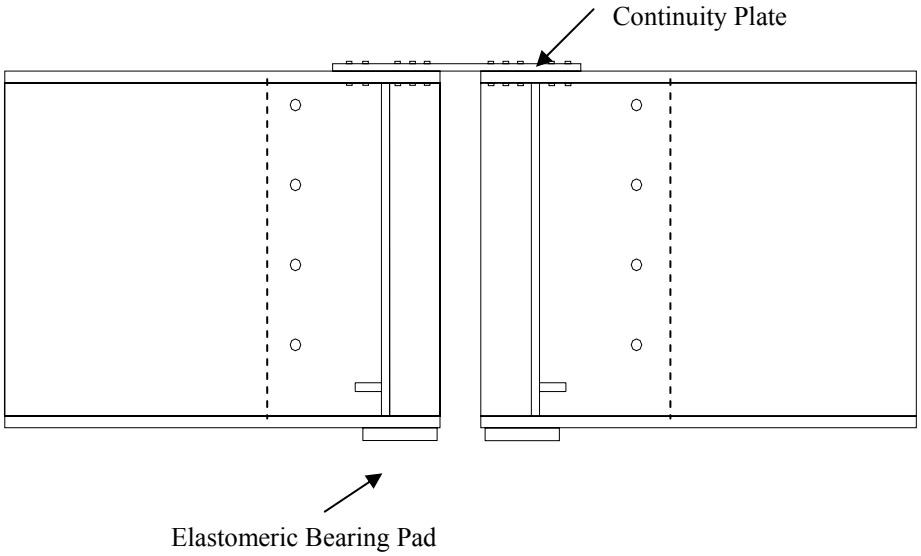

Figure 3.8: Hatch Bridge Continuity Detail

3.3 ECONOMIC FEASIBILITY

One of the main factors in determining the success or failure of the CLL method is economic feasibility. As mentioned previously, concrete bridges have increased in numbers in the short span bridge range due to economy. The CLL method theoretically has cost and time savings, which make steel bridges more competitive in the short span bridge range. The best way to determine the validity of this comment is to examine the bridges that have been constructed for any cost or time savings.

3.3.1 Cost savings

A critical component determining the success or failure of the continuous for live load concept is whether it can save money or not. Some of the bridges mentioned earlier were examined to identify cost savings earned or lost using the CLL method. The cost savings were identified by examining the bids of a project or through testimonials provided by the engineers and contractors who helped build the bridges. The CLL method was predicted to have cost savings in terms of material, fabrication, and labor.

The material savings come in the form of a single steel cross section that is needed for the entire length of the bridge. The shift of the moment between the positive and negative regions in a CLL design allows for one type of cross section, which can help with decreasing the total material costs. The fabrication costs are reduced by eliminating or simplifying the splice detail (ex. Las Cruces Bridge & Hatch Bridge). Some labor savings are also predicted for the ease of construction as compared with standard steel

continuous bridges. This is because with the CLL method, the girders rest on piers which are later connected by concrete diaphragms. A steel splice between piers requires the use of two cranes perfectly aligning the girders in mid-air while a steel worker bolts the splice on.

The bridge in Las Cruces New Mexico had reported cost savings in all of the aforementioned areas. Interviews with the engineer, contractor, and fabricator conducted by John Stouffer at New Mexico State University proved useful in determining the cost savings. Fabrication costs were reduced by $0.20/lb compared with traditional steel design. This correlates to an 18% to 28% savings in fabrication compared with traditional continuous steel bridges. The reduction of intermediate stiffeners and the simplicity of the continuity detail helped to drastically lower fabrication costs. The fabricator noted that the simplicity of the steel components helped to reduce labor costs.

The Las Cruces Bridge was double bid with the CLL option and a prestressed concrete girder option. This allowed the designers to determine which method would be the most cost effective. Table 3.1 on the next page contains the bids of two contractors alongside the engineer's estimate. It matches the bids of two contractors with the engineer's estimate. The CLL Bridge is more competitive with the prestressed concrete bridge as compared with a traditional continuous steel bridge.

Table 3.1: Las Cruces Bridge Bid Information

CLL Bridge		
Engineer's Estimate	Contractor A	Contractor B
$2,802,912.15	$2,991,280.74	$2,573,201.60
Concrete Girders		
Engineer's Estimate	Contractor A	Contractor B
$2,981,890.30	$2,865,279.23	$2,595,285.50

The CLL bridge is more economical than the concrete girder bridge for the Engineer's Estimate and Contractor B's bid. Only Contractor A's bid for the CLL bridge was more expensive than the concrete girder bridge. However, the CLL bridge is within 5% difference of the concrete girder option for Contractor A's bid. The differences are small, but show CLL is competitive with pre-cast concrete.

Other bridges utilizing CLL have also seen cost savings. The Military Road Bridge in Nebraska was constructed after the CLL method was proposed by Dr. Atorod Azizinamini. The bridge was part of a rehabilitation project replacing an older structurally deficient bridge. The bridge proved to yield a 4 to 8% savings in material and girder fabrication costs as compared to conventional continuous steel girder bridges (Azizinamini 2003). Another CLL bridge was constructed in Omaha, Nebraska over I-680 having span lengths of 97ft. each. Conventional continuous steel bridges in that area at the time were estimated at $0.75/lb. The I-680 bridge was constructed at $0.52/lb (Azizinamini 2004). This correlates with a 31% reduction in material costs.

Several CLL bridges constructed in Tennessee were also investigated to note any cost savings. As mentioned previously two types of CLL bridges were constructed in Tennessee: simple span for dead loads and continuous for live loads and simple span for dead load of beam only and continuous for the dead load of the slab and all live loads. The first type of CLL bridge was constructed in Maryville carrying State Route 55 over Brown Creek. The second type of CLL bridge was constructed in New Johnsonville carrying the DuPont Access Road over State Route 1. The TDOT experienced improved

cost savings utilizing the second type of CLL method. A cost comparison between the CLL bridges and precast concrete girder option can be seen in the Table 3.2 on the following page. State averages of concrete girder prices were used in the comparison.

Table 3.2: Cost Comparisons of Tennessee CLL Bridges

State Route 55 Bridge	
Steel Girders (CLL Method)	Prestressed I-Beam Concrete Girders (Type III)
$290,475.46	$257,880.11
% Difference	**12.6%**
DuPont Access Road	
Steel Girders (CLL Method)	Prestressed I-Beam Concrete Girders (Type III)
$137,650.24	$124,411.38
% Difference	**10.6%**

The first bridge was bid at $0.72/lb while the second bridge had a lowest bidder of $0.56/lb. The cost savings show that steel bridges are not as competitive with concrete bridges as the bridge in Las Cruces. This can be due many factors. Of the many factors the most notable difference might be due to the fact that the pre-cast concrete girder market is more developed in Tennessee. However, the purpose of developing the continuous for live load steel bridge systems in Tennessee was to make steel bridge systems more competitive. In terms of this objective Tennessee DOT engineers feel as though they have accomplished this.

Another possible reason for the noticeable difference between prices can be attributed to the fact that the average for that year did not reflect many constructed bridges. It was noted through communication with Tennessee DOT engineers that the

average price did not reflect many bridges utilizing the Type III prestressed concrete beams. Therefore the concrete girder estimate is only an estimate and does not constitute an exact cost as the steel girder cost does.

3.3.2 Time Savings

Time savings on a project can relate to money saved, especially in the users' costs. Just like the cost savings portion, the information gathered for the time savings was provided by testimonials of engineers and contractors working on the various jobs. The predicted time savings of using the CLL method come from the simplicity of the continuity detail itself. Only one crane is needed instead of two, and it is much easier to connect two steel stringers when they are resting on a pier beforehand. Using one crane decreases the erection time and cost and also reduces traffic disruption. User cost (cost of having the bridge out for the bridge users) is increasingly a strong consideration for state DOT's when considering a project.

The bridge in Las Cruces experienced some of the benefits of a CLL system. As previously noted, only one crane was needed to erect the steel girders. Time was saved resting the girders on the piers and later connecting them by a concrete diaphragm in lieu of field splicing. For this particular bridge traffic was detoured completely away from the bridge therefore the contractor did not experience the time savings from using only one crane. Overall, the contractor saved eight days on the duration of the project, as compared to traditional continuous bridge construction. However, some difficulty was experienced in placing the continuity plate that was bolted onto the top of the girder flanges. The contractor felt as though the plate was "excessive", and that the rebar in the

deck was sufficient to provide live load continuity. The contractor noted however that the plate was still easier to install compared with a regular splice because the worker can actually have safe ground to stand on instead of being suspended by a lift in the air. There were still time savings even with the relatively minor issues concerning the installation of the continuity plate.

The Fast Track PIC-22 bridge in Circleville Ohio had a considerable amount of time savings when using the CLL method. The bridge carried Route 22 over the Scioto River and was a major route for the farming business in Circleville. The road is a high traffic area and is vital to the economy of the town. The bridge reconstruction needed to be accomplished very quickly in order to keep traffic disruption down. The engineers and contractors felt as though making the steel girders simple for dead and continuous for live load would greatly decrease construction time. The bridge was constructed in just 48 days as opposed to the predicted 60 days. Hence, a total of eleven days were saved using this method. The contractor noted that setting the girders on top of the pier caps allowed to the girders to be placed quickly and effectively.

Several bridges in Tennessee experienced improved construction speed with using the CLL method. Smaller less capacity cranes were used in placing the steel beams compared with precast/prestressed concrete beams of similar span length. There was reduced traffic disruption in both of the bridges constructed continuous for live load. The use of only one crane helps to allow more traffic flow. Although no actual days were cut off from the total construction time, time was saved in the erection of the beams. Both projects were finished on schedule however with no delays.

3.4 SUMMARY

This chapter focused the logic behind constructing bridges using the CLL method. The continuity detail that facilitates the method was also outlined. The economic feasibility of the method is also investigated by studying several bridges constructed across the U.S. Any cost and time savings were noted where they appeared. The predicted savings came in the form of reduced material and fabrication costs and reduced erection times.

Bridges in Nebraska, Ohio, Tennessee, and New Mexico were heavily researched. A summary of the economic feasibility study results from each bridge is listed below.

Nebraska

Military Road Bridge

- 4% to 8% savings in material and fabrication costs compared w/ conventional continuous steel bridges

Sprague Street & I-680 Bridge

- Steel cost $0.52/lb compared w/ conventional continuous steel bridges costing $0.75/lb

Ohio

PIC-22 Bridge

- CLL was used to help reduce total construction time by 11 days

Tennessee

State Route 55 Bridge

- CLL steel girders were within 13% of the cost of concrete precast/prestressed girders

DuPont Access Road Bridge

- CLL steel girders were within 11% of the cost of concrete precast/prestressed girders

New Mexico

Las Cruces Bridge

- Fabrication costs were reduced by $0.20/lb compared with traditional steel design
- Correlates to an 18% to 28% savings in fabrication compared with traditional continuous steel bridges
- Bridge was double-bid w/ concrete girder option and CLL steel option was competitive within 5%
- Saved 8 days with using CLL compared w/ traditional continuous steel bridges

CHAPTER 4

LAS CRUCES CASE STUDY

4.1 INTRODUCTION

The previous chapter identified the continuity detail and how it works to resist the live load in a continuous fashion. This chapter will focus on if indeed the continuity detail functions as designed. Specifically, this chapter investigates if the continuity detail actually allows for the transfer of moment across the joint to essentially make the system continuous. To address this question, in-situ load testing was performed on two CLL bridges in New Mexico. These load tests provide the experimental data necessary to help determine if the detail works in an in-situ application. This chapter will focus on the first of the bridge tests, a structure located in Las Cruces, New Mexico.

4.2 BRIDGE DESCRIPTION

The first case study conducted was on the Las Cruces Bridge. The bridge is located along U.S. Highway 70 at the Sonoma Ranch Boulevard intersection. The Las Cruces Bridge consists of twin bridges, one bridge is eastbound and the other is westbound. Figure 4.1 gives an elevation view of the bridge.

Figure 4.1: Las Cruces Bridge

For this particular study, the westbound bridge was load tested. The Las Cruces Bridge is a three span composite slab on girder bridge. Four plate girders spaced at approximately 10'2" support a 38'4" road width. A cross-sectional view of the girders, concrete deck, and concrete diaphragm can be found in Figure 4.2. The three span lengths are 78'10", 119'10", and 78'10". The plate girders for the shorter spans are slightly smaller than those of the longer span. The steel cross sections can be found in Figure 4.3.

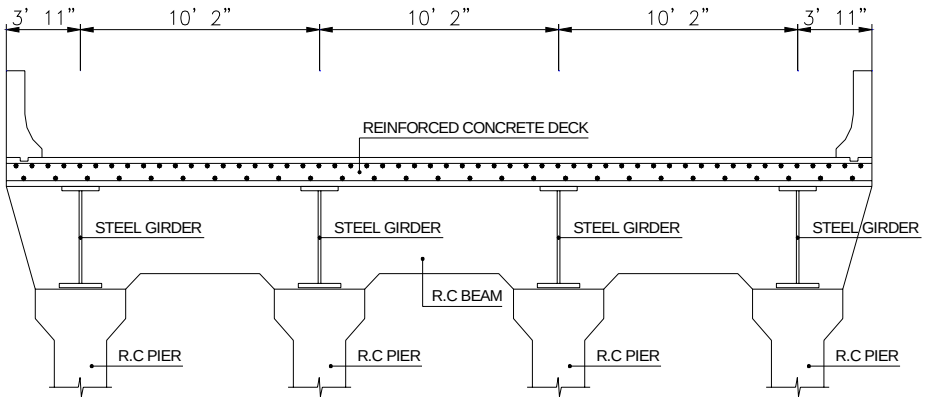

Figure 4.2: Cross Sectional View of Girders

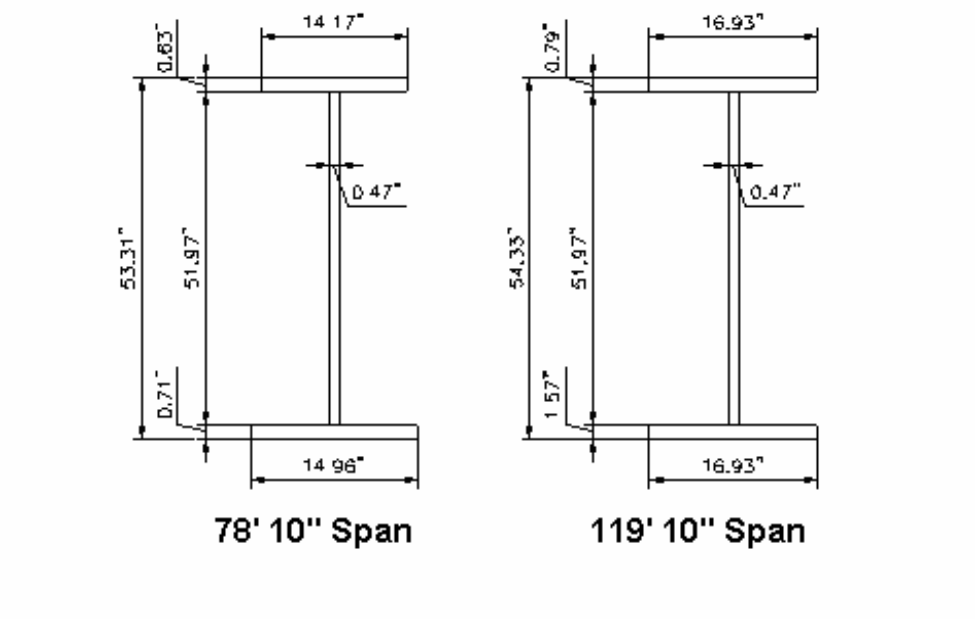

Figure 4.3: Steel Cross Section

The 8.5” concrete slab is made composite with the plate girders through the use of shear studs. Three shear 1” diameter studs, 6” long are spaced evenly transversely across the top of the plate girders. The stud spacing varies longitudinally along each plate girder depending on the amount of composite action required.

The bottom girder flanges are welded to a sole plate at all of the abutments and piers. Elastomeric bearing pads rest beneath the sole plates, which are attached to anchor bolts coming up from the concrete pier. Figure 4.4 gives a view of the bearing detail.

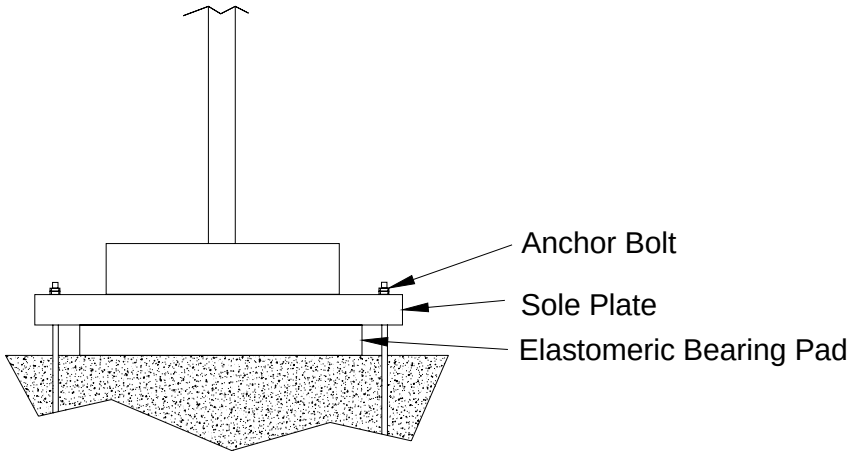

Figure 4.4: Bearing Detail @ Pier

After the concrete diaphragms are poured on top of these bearings, bituminous joint filler is applied between the concrete diaphragm and the concrete pier below.

The top flanges of each girder end are connected by using a bolted steel plate. Because the bridge has different girder heights a filler was placed between the top of the short girder and the continuity plate. For this particular bridge the bolts were not tightened until after the positive moment region of the deck had been poured. Then the concrete diaphragm and negative moment region were poured. As mentioned previously the purpose is to avoid cracking of the deck in the negative moment region.

4.3 LAS CRUCES LOAD TEST

The research team utilized a load test to help determine the amount of continuity that the concrete diaphragms actually provide. In this test, strain gages were placed at strategic locations on the bridge. The strains obtained can be converted to stress (all linear-elastic behavior) and either the moments or stresses at a particular location of the

bridge can be plotted against the location of the truck on the bridge. The plots show the type of flexure that a member is exhibiting, which can be used as a preliminary check as to whether the girders are behaving continuously. Therefore if there is any indication of negative flexure near the piers, some degree of continuity is present. If no negative flexure is exhibited near the supports then this would indicate simply supported spans.

The Las Cruces Bridge was load tested on December 18, 2005. The bridge was instrumented the day before due to the large number of strain gages applied. The test consisted of pseudo-static and dynamic loading conditions. Pseudo-static is defined as the truck slowly crossing the bridge at a relatively slow speed, approximately 4-5 mph. Several loading paths were utilized in order to examine the behavior of the structure under various loading conditions, and to ensure that the continuity (if present) was repeatable for various loads.

4.3.1 Truck and Strain Gages

A dump truck was provided by the New Mexico Department of Transportation for the load test. The truck (filled with gravel) had a gross weight of 55,600 lbs and axle spacings of 15’5” and 4’3”. The dump truck is pictured in Figure 4.5.

Figure 4.5: Dump Truck

The same truck was utilized for the Hatch Bridge Test as well. The truck traveled in a westbound direction for the test. The axle weights and spacings are illustrated in the Figure 4.6.

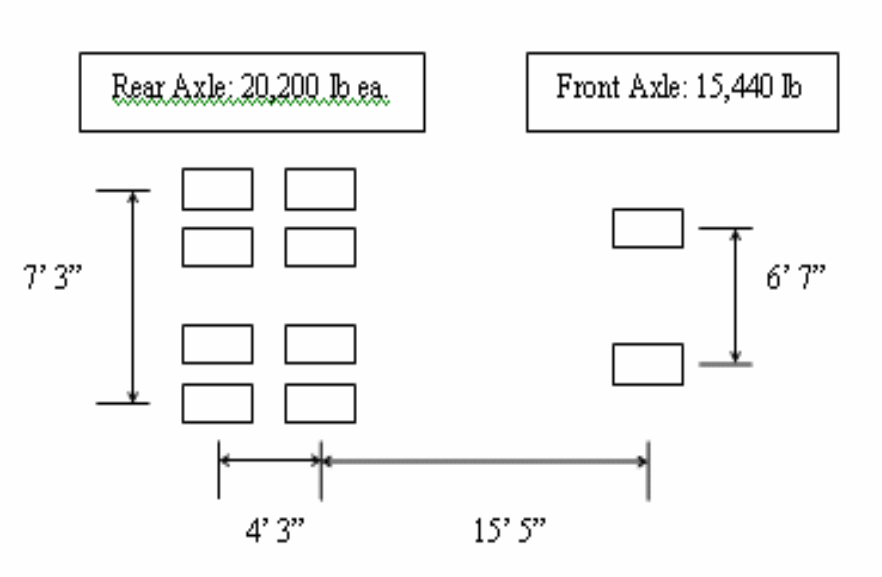

Figure 4.6: Axle Weights

Testing equipment (Structural Testing System II) developed by BDI (Bridge Diagnostics Inc.) was used for the load test. The system transmitted the strain data recorded from the strain gages to a laptop the computer where it was stored. Sampling rates vary from 1 Hz to 100 Hz. The BDI-STS-II system is pictured in Figure 4.7 on the following page. The system can be run on standard 110-220VAC power coming from a generator or 12VDC coming from a car battery that is run through a power inverter.

Figure 4.7: BDI STS-II Data Retrieval System

A laptop was used to store the gage data, and the program WinSTS was installed on the computer to control the testing system and gages. WinSTS runs with the operating system Windows 2000 & XP.

Aluminum strain gages were used for the load testing. The strain gage consists of a full wheatstone bridge with 4 active 350Ω foil gages with a 4-wire hookup and is approximately three inches in length. The gage has a strain range of $\pm$ 4000 $\mu\varepsilon$, a sensitivity of 500 $\mu\varepsilon$/mV/V, and an accuracy of $\pm$ 2%. The strain gage can be attached to steel, prestressed concrete, reinforced concrete, or timber. Two methods of attaching the gages to the steel members were employed. One method consists of using C-clamps to lock the gages onto the steel. This method was used for the bottom flange locations. The

second method consisted of using quick drying adhesive to glue the gages to the steel. A view of gages attached utilizing both methods can be found in Figure 4.8.

Figure 4.8: Installed Strain Gages

The gage location was first grinded to obtain a smooth surface and a thin layer of the adhesive (brand name, Loctite 410) was applied to the tabs on the bottom of the gage. Then an adhesive accelerator (brand name, Loctite Tak Pak 7452) was applied to the adhesive. This method was utilized for gages at the top flange and mid-web locations.

4.3.2 Instrumentation Plan

The main purpose of the load test was to determine whether the concrete diaphragms provide continuity or not. With this objective in mind, the gage locations were chosen based on the type of flexure that the beam should exhibit when fully continuous. A continuous beam with multiple supports exhibits negative flexure close to the interior supports. Hence, if the bridge girders are truly behaving in a continuous manner, then the girders should experience negative flexure around the interior pier

supports. Therefore gages were placed on both sides of one of the interior piers to examine the flexure present at that location. Gages were also placed at mid span locations to view the maximum positive bending stresses in the beam. Lastly, gages were placed near the abutment to determine if the supports supplied rotational constraint.

As a joint venture, New Mexico State University helped to conduct the load tests. The NMSU Team also used BDI testing equipment for the load test. During the test, two BDI-STS systems recorded the data onto two separate laptops. The NMSU Team had a capacity of 20 gages while the OSU Team had a capacity of 40 gages. The total of 60 gages allowed more gages to be placed at each test location.

At each gage location it was decided that at least two gages would be placed. At least two gages are needed to draw the stress and strain profile (the research team assumed plane sections remain plane, and hence a linear stress/strain over the depth of the cross section). Because the bridge was composite, having two gage locations can also help determine the amount of composite action in the bridge. Three gages were placed at most locations in order to provide a more accurate strain profile. A gage was placed at the top of the bottom flange, mid-web, and the bottom of the top flange. Due to the limited number of strain gages the locations close to the abutment received only two gages. Gages at that location were placed at the top of the bottom flange and mid-web. Gage locations started at the abutment and ended at the midspan of the second span. Refer to Figure 4.9 for the instrumentation plan.

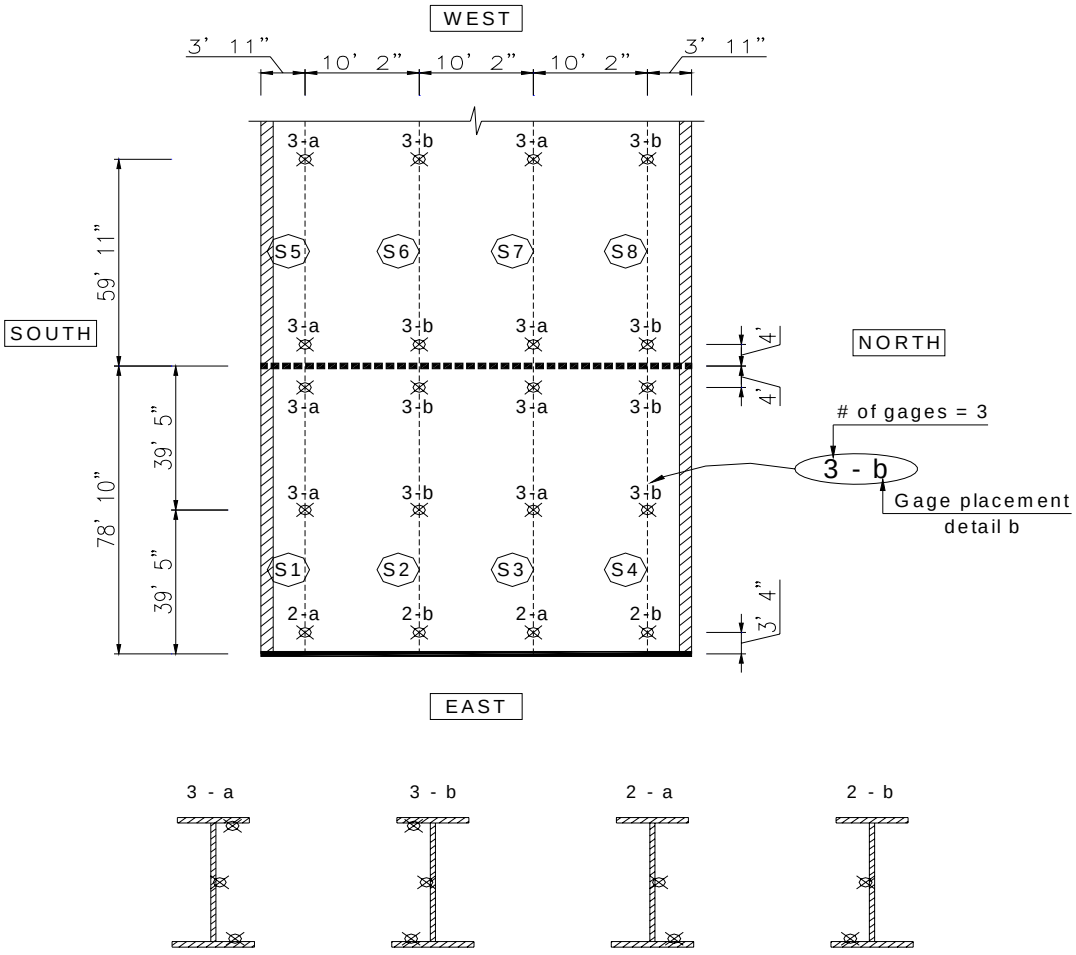

Figure 4.9: Instrumentation Plan

4.3.3 Load Test

Two types of load tests were performed on the Las Cruces Bridge: pseudo-static and dynamic testing. Although only the pseudo-static load test results were used directly for this research project, dynamic testing can give help to determine the effects of impact loading. A sampling rate of 40Hz was chosen for the pseudo-static load tests which provided enough data for the slow speed of the truck. A greater sampling rate of 66Hz

was chosen for the dynamic load tests. The increased sampling rate is necessary in order to obtain more data corresponding to the relatively short interval of loading.

Eight loading paths were used in the test, spanning the entire width (transversely) of the road. The load paths are shown in Figure 4.10.

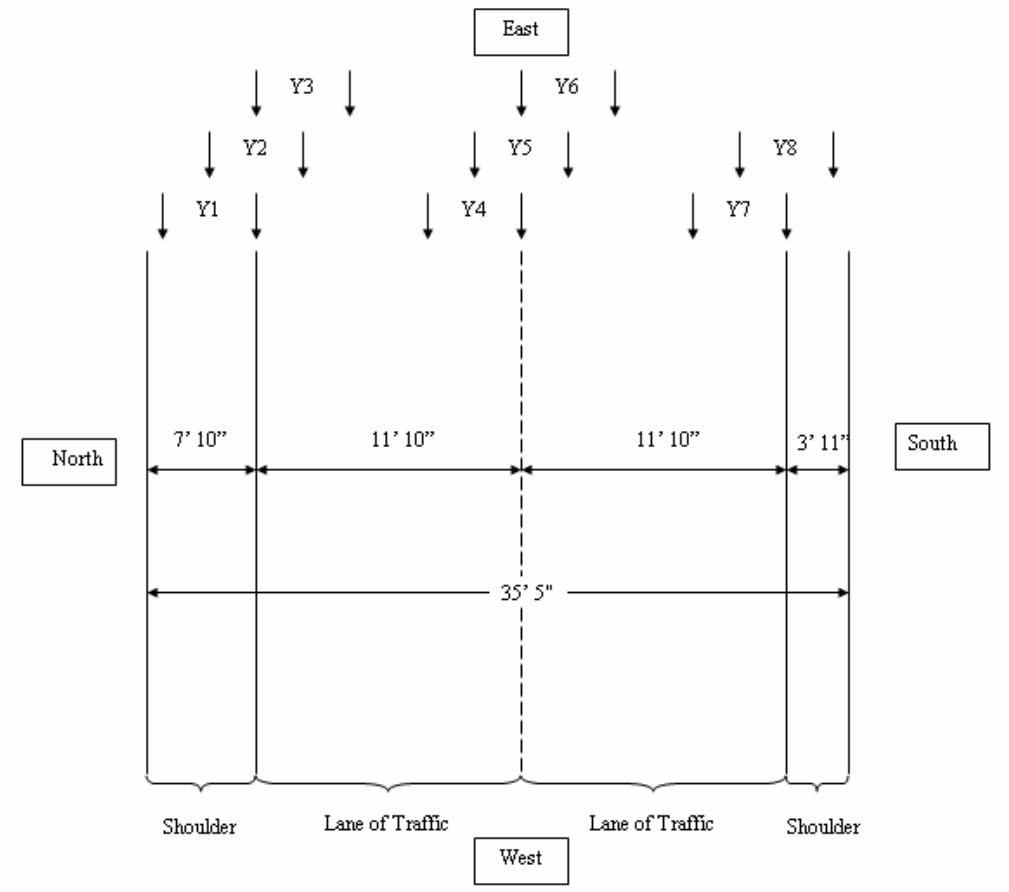

Figure 4.10: Loading Paths

Truck Positions

Y1: Driver side wheel on northern solid line
Y2: Centered about northern solid line located 8' away from northern barrier
Y3: Passenger side wheel on northern solid line
Y4: Driver side wheel on the striped center line
Y5: Centered about the striped center line
Y6: Passenger side wheel on striped center line
Y7: Driver side wheel on southern solid line
Y8: Centered about southern line located 4' away from southern barrier

The load test started at 10 feet before the first abutment and ended at the abutment on the other side of the bridge. The northern span of the twin bridge was used for the load test with the truck traveling in a westerly direction. Two runs were completed on each load path to determine repeatability of the testing data obtained.

An auto-clicker was used to track the location of the truck throughout the testing. The auto-clicker, shown in the figure below, consists of camera that is connected to a box housing a radio.

Figure 4.11: BDI Auto Clicker

The device rests on top the wheel well through adjustable straps that are hooked onto hooks. A reflective wheel clamp is attached to the wheel which returns the light emitted from the camera marking each tire revolution. The device then triggers the radio which equates to a "click" or full wheel revolution on the program. A radio that is attached to the STS system receives the click, and the system records the revolution. The revolution was determined through averaging five revolutions. Alternately the circumference of the wheel can be found to determine one full wheel revolution.

4.3.4 Test Results

The results of the test were expressed in terms of stress at a particular point versus truck location (longitudinally on the bridge) plots. Essentially, it is a plot of a stress influence line. Influence lines are a plot of a specific structural quantity as a function of position of load. Influence lines can help illustrate the type of flexure a specific location will experience under a moving load. Please refer to Figure 4.12 for a sample plot.

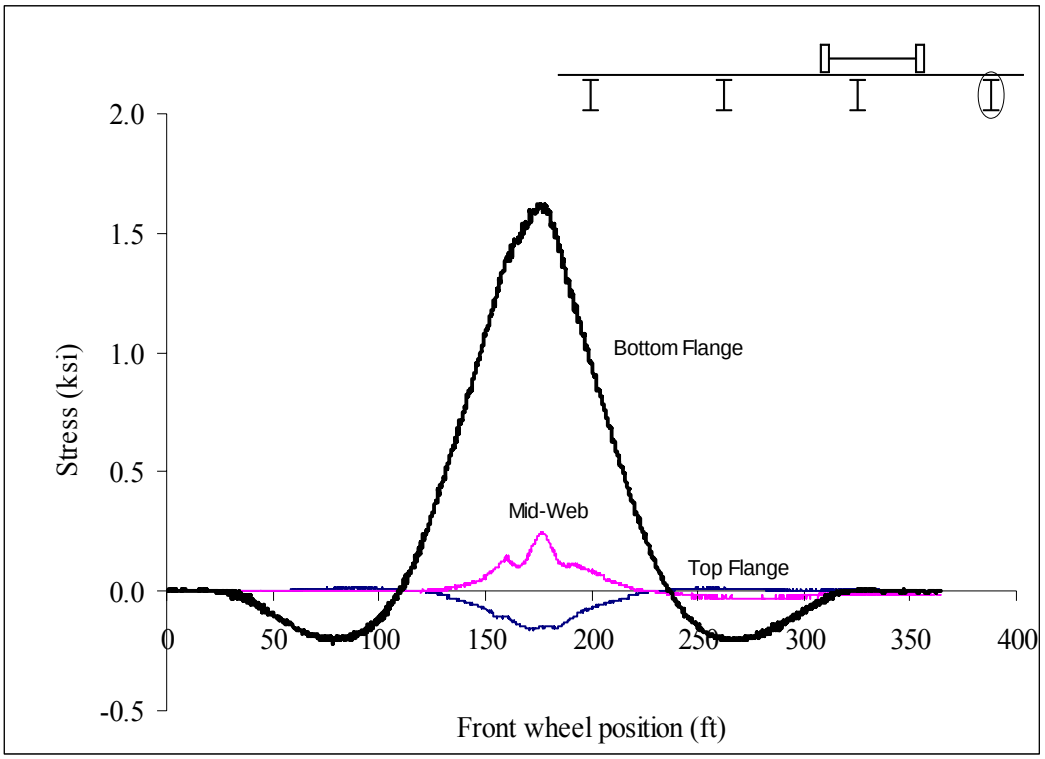

Figure 4.12: Sample Plot Run 3 S8 @ Midspan

The recorded microstrains were converted into units of stress by multiplying by the modulus of elasticity of steel (29 E3 ksi). Please refer to Appendix A for all of the stress plots created from the test. Each plotted line has text next to it to denote the gage location on the particular cross section. Stress plots for both runs of each loading path

were created and examined for repeatability. Examining these multiple plots revealed that each run was very similar indicating repeatability of the data. Figures 4.13 & 4.14 illustrate the repeatability of the data.

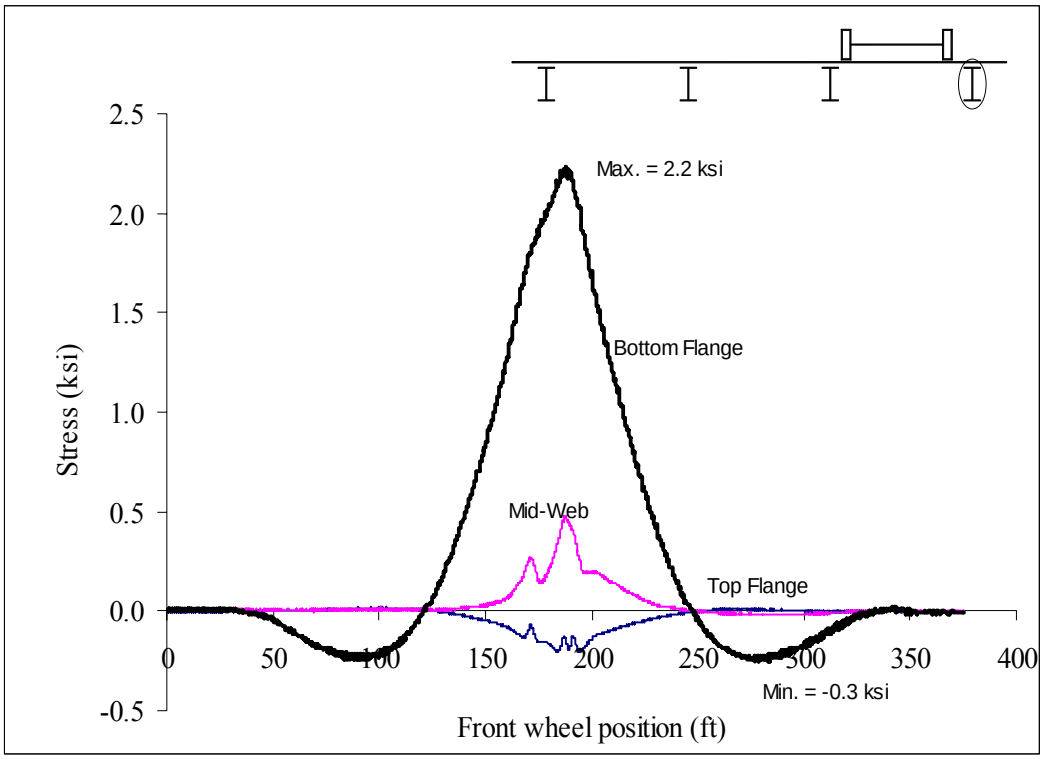

Figure 4.13: First Trial Run 2 S8 @ Midspan

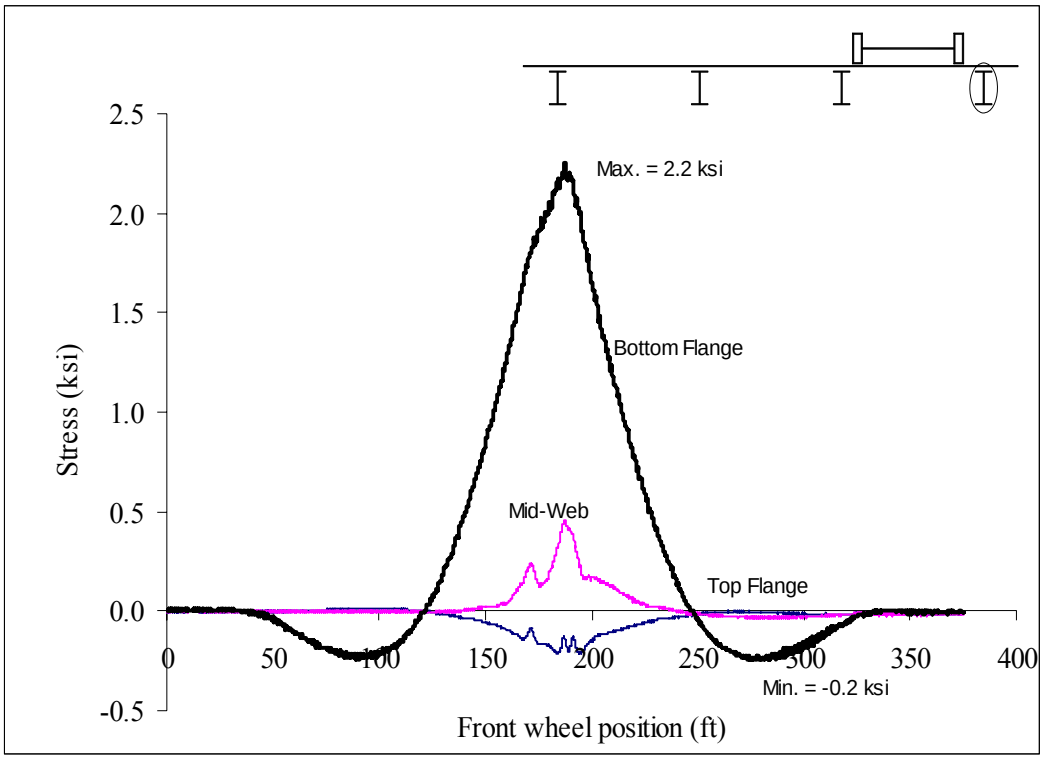

Figure 4.14: Second Trial Run 2 S8 @ Midspan

The stress plots revealed several unusual results. The unusual behavior particularly pertained to the mid-web stresses. The three unusual cases were:

1. Stresses at mid-web were EQUAL or LARGER than the bottom flange stress
2. Stresses at mid-web were SMALLER than the bottom flange stress but with the opposite sign
3. Stresses at mid-web were very small

Figure 4.15 displays how many unexpected results were found and at what locations. One possible explanation for the first two cases is the occurrence of biaxial bending. The

Figure 4.15: Unusual Test Results Diagram Las Cruces Bridge Test

strain gages are only able to read pure axial stresses of tension or compression. Biaxial bending would cause the gage to record unusual stresses. To determine if biaxial bending was occurring gages would need to be attached on both sides of the cross section. When talking with BDI technical specialists it was determined that the third case could be due to gage slipping. If the gage slipped then the brittle bond created between the tabs and steel surface through the use of glue would be broken. Once the bond is broken the gage records little to no stress at all.

Because of the anomalies and possible biaxial influence, only the flange gages were used for the analysis. Only one gage is needed per location to show if the member is exhibiting positive or negative flexure. Due to this the mid-web stresses were ignored and the bottom flange stresses were used.

The main objective of the testing is to verify continuity transfer. The two main locations of concern to verify continuity as mentioned previously are at the midspan and near the interior supports. The influence lines for a midspan and support location can be found in Figure 4.16.

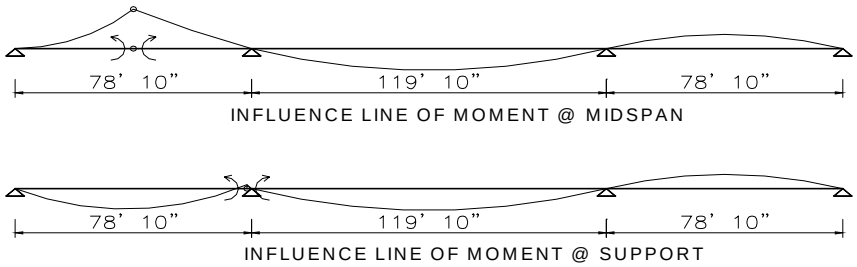

Figure 4.16: Influence Lines of Moment

Influence lines of moment indicate the type of flexure at a fixed particular point whether it be positive or negative as the position of loading is variant. If the influence

line indicates a positive value (above the original undeflected shape) then this corresponds with positive flexure. If the influence line indicates a negative value (below the undeflected shape) then this corresponds with negative flexure.

Once the influence lines are drawn, they can be compared to the load test results. In essence, the theoretical moment influence lines are being compared with the experimental stress influence lines. When examining a midspan location it can be seen that the beam exhibits positive flexure when the truck is located near midspan. When the truck is on an adjoining span the beam exhibits negative flexure at the previous midspan. A connection providing no continuity would correlate with little stresses at the gage location when the truck is loaded on another span. Refer to Figure 4.17 for a midspan stress plot.

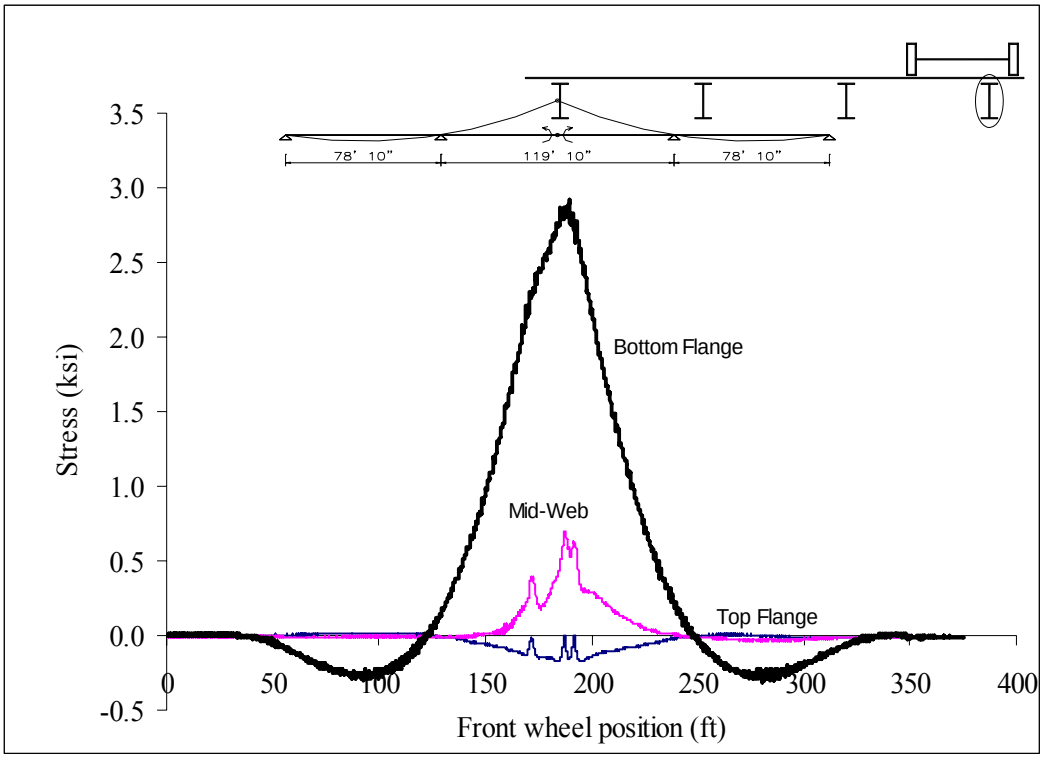

Figure 4.17: Stress Plot @ Midspan Location w/ Influence Line

The interior support gage locations exhibit negative flexure when the truck is loaded on either span that is joined at that interior support. The beam exhibits positive flexure at an interior pier location when the truck is on a span not joined by that interior support. Figure 4.18 shows a stress plot at an interior support location.

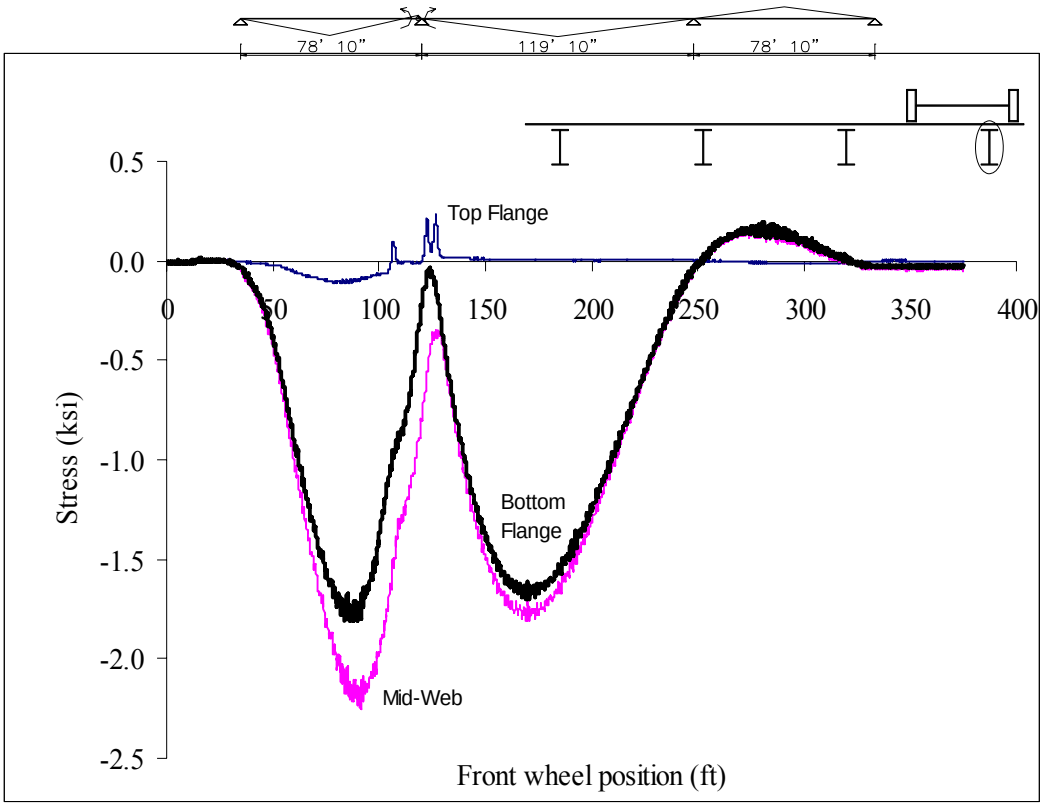

Figure 4.18: Stress Plot @ Support Location w/ Influence Line

The influence lines can indicate how continuity affects the moment or flexure from one span to the next. This is a qualitative evaluation of whether continuity is transferred. A computer analysis of the bridge also helps to verify the continuity transfer. However, by inspection the data would indicate that moment is transferred across the interior supports, as would be expected in a continuous structure. If the continuity detail

was not functioning, the structure would respond closer to simple supports at interior pier locations

4.4 FINITE ELEMENT ANALYSIS

A finite element analysis was performed on the Las Cruces Bridge to qualitatively verify the field test results and continuity detail enabling a moment transfer across the pier. STAAD Pro 2004 was chosen for the analysis due to the simplicity and flexibility of the program. The program has non-linear capabilities, however, a linear analysis was used for the purposes of this research.

4.4.1 Model Description

In modeling this structure, it was necessary to capture the composite nature of the structure in a reliable, yet simple manner. Previous research has shown that the use of rigid links to represent shear connectors is effective in modeling a composite beam model in computer finite element analysis (Tedesco et al 1995, Liang et al 2005, Mabsout et al 1997, Chung et al 2005). The composite beam model used for the Las Cruces Bridge consisted of beam and shell elements. The entire steel cross section consists of shell elements, while the shear connectors or rigid links are represented as beam elements. The beam elements are then rigidly connected to the concrete deck which consists of a series of shell elements. Figure 4.19 shows the typical composite cross section.

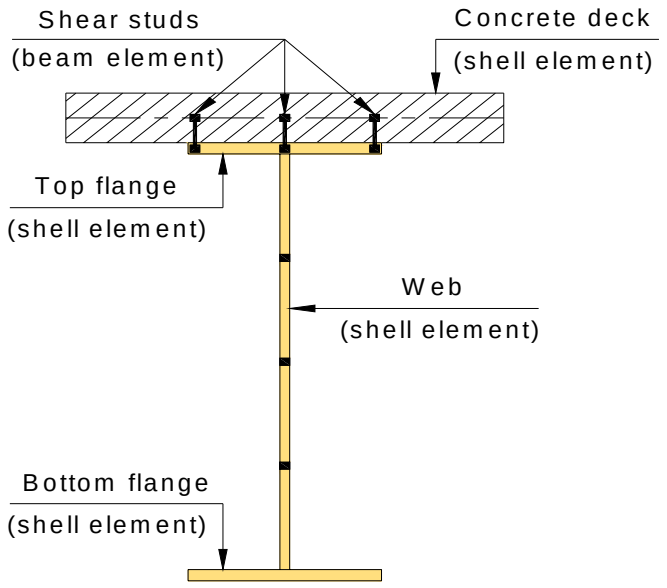

Figure 4.19: Composite Beam Model (Dang 2006)

The shell thicknesses were assigned to the model according to cross sectional dimensions found in the plan drawings. The material properties were also assigned such as the concrete compressive strength and modulus of elasticity. The modulus of elasticity used for the steel was 29,000 ksi while the modulus of elasticity used for the concrete was 3,600 ksi. The modulus of concrete was calculated according to ACI (American Concrete Institute) 318-02 specifications utilizing the compressive strength that was given on the as-built drawings. The shear stud spacing was set at 9.5" to ensure a fully composite model.

In considering the boundary conditions it was decided to utilize pinned connections at the abutment and interior pier locations. In actuality the abutment behaves somewhere in between a fixed and pinned connection. This was determined by observing negative flexure in the beams near the abutments. Simple spans would have no moments

at the beam ends. Please refer to Figure 4.20 for plot illustrating the negative flexure experienced at the abutment.

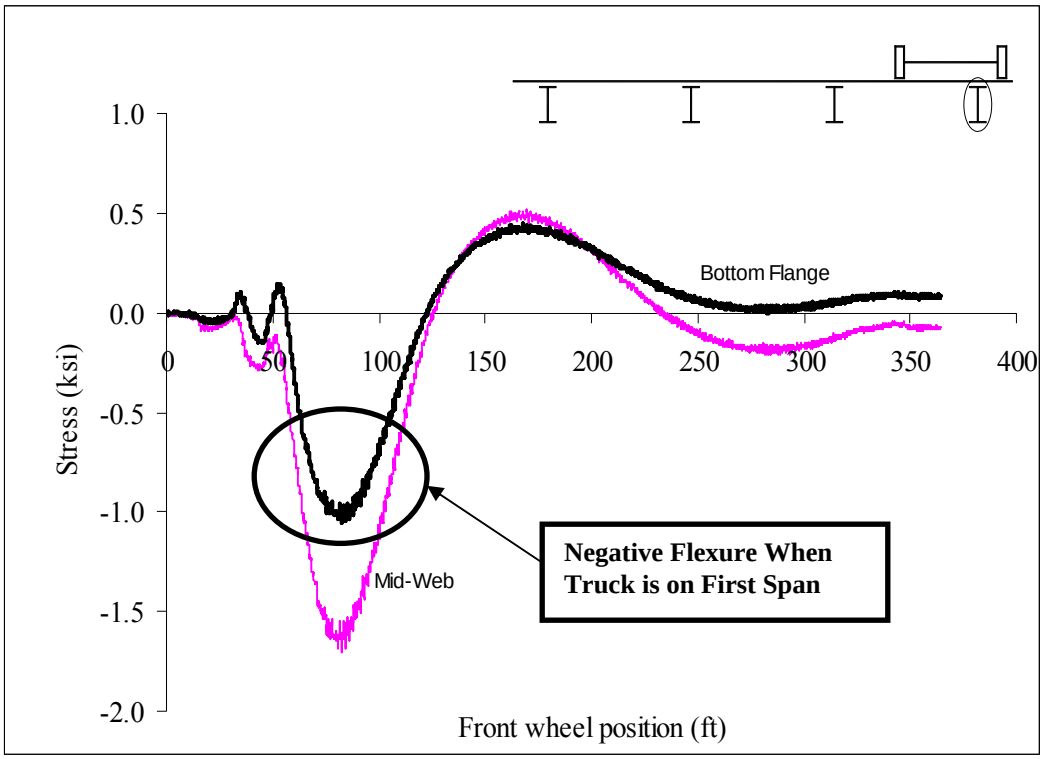

Figure 4.20: Appearance of Negative Flexure for S4 @ 2 ft from abutment

The beam end is encased in concrete which provides some rotational constraint. Figure 4.21 illustrates the abutment detail.

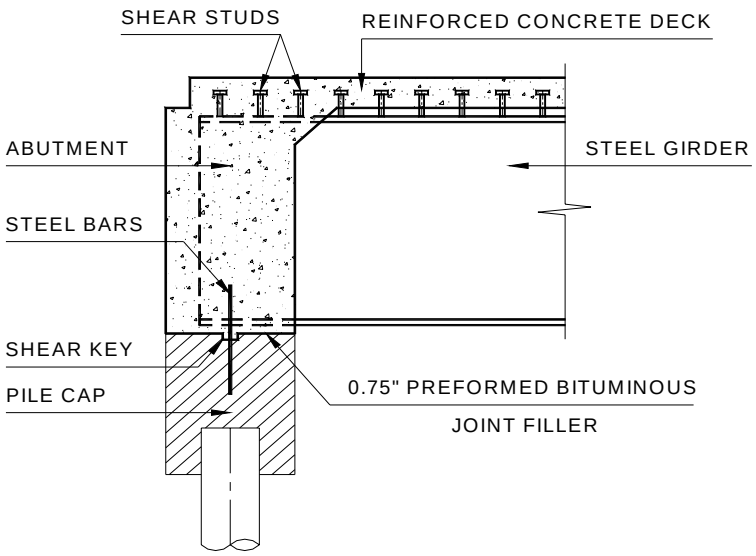

Figure 4.21: Abutment Detail (Dang 2006)

A more detailed report covering the finite element portion of this research was written by Chi Dang (Oklahoma State University, unpublished). The report compares several different models with different types of boundary conditions. Rotational springs are utilized to more closely match the true behavior of the bridge. Only models with pinned supports were studied for this thesis. The logic behind using pinned supports only was to keep the boundary conditions basic and uniform throughout the model. The two models utilized were: a fully continuous model and a simply supported span model. These two models represent the extremes in terms of continuity transfer from one span to the next.

4.4.2 Loading

The dump truck used in the field test was modeled as six point loads. The axle weights were used to determine the weight that each tire carries. For simplicity two longitudinal truck locations were utilized for each load path. The stress plots were examined to determine the truck positions that produced the maximum response. The

maximum response correlates with a peak on the stress plot. For this field test, placing the front wheel of the truck at roughly 56' and 140' from the abutment produced the maximum response. Please refer to Figure 4.22 below for the loading locations.

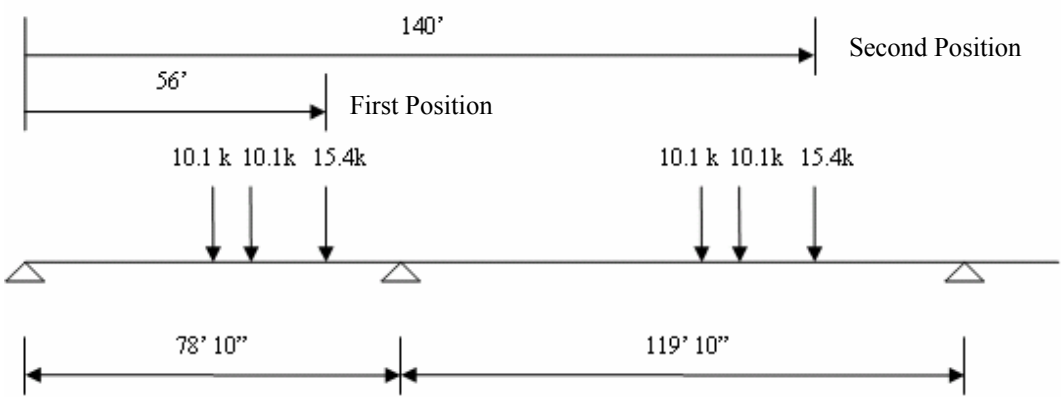

Figure 4.22: Las Cruces Load Locations

Hence, for the computer modeling to compare maximum stresses, the loads were placed at these two locations.

4.4.3 Finite Element Analysis Results

Two models were analyzed using STAAD Pro 2004. The first model (Model 1) represents a fully continuous pinned end connection bridge, while the second model (Model 2) represents a simply supported pinned end connection bridge. In order to compare the stresses from the field results to the stresses from the computer model the calculated moments obtained were converted into stress at the locations of the applied gages. With this conversion, the bottom flange stresses were examined in comparing the field results with the analysis results. Only the load paths which directly loaded each

stringer were considered in the comparison in order to compare substantial amounts of stresses. Table 4.1 contains the bottom flange stresses of the field results compared with the bottom flange stresses from the finite element analysis.

Table 4.1: STAAD & Field Results (Las Cruces Bridge)

Run	Member	Gage Location	Bottom Flange Stresses (ksi)				
			Field	Model 1	% Difference	Model 2	% Difference
8	S1	Abutment	-1.8	0.18	-110%	0.24	-113%
		Midspan	3.7	5.01	35%	5.96	61%
		Support	-2.9	-2.93	1%	0.09	-103%
	S5	Support	-2	-1.6	-20%	0.04	-102%
		Midspan	3	3.3	10%	4.22	41%
6	S2	Abutment	-0.8	0.08	-110%	0.11	-114%
		Midspan	2.3	2.28	-1%	2.7	17%
		Support	-2.2	-1.47	-33%	0.05	-102%
	S6	Support	-1.3	-0.77	-41%	0.01	-101%
		Midspan	2.25	1.79	-20%	2.25	0%
4	S3	Abutment	-1	0.07	-107%	0.1	-110%
		Midspan	3.1	2.14	-31%	2.54	-18%
		Support	-1.8	-1.35	-25%	0.04	-102%
	S7	Support	-1.15	-0.7	-39%	0.01	-101%
		Midspan	2	1.63	-19%	2.05	2%
1	S4	Abutment	-1	0.19	-119%	0.25	-125%
		Midspan	3.4	5.13	51%	6.1	79%
		Support	-1.8	-3.05	69%	0.09	-105%
	S8	Support	-1.9	-1.66	-13%	0.04	-102%
		Midspan	2.85	3.43	20%	4.38	54%

Please refer to Figure 4.23 and 4.24 for graphical representations of these results. Each of these figures represent a plot of maximum stresses from the field test results and one finite element analysis model along a single longitudinal line of girders. Therefore, if one desires to visually examine the accuracy of the computer model against the field results at a particular testing location along the beam (ex. abutment, midspan, or near a pier) then it can be done easily.

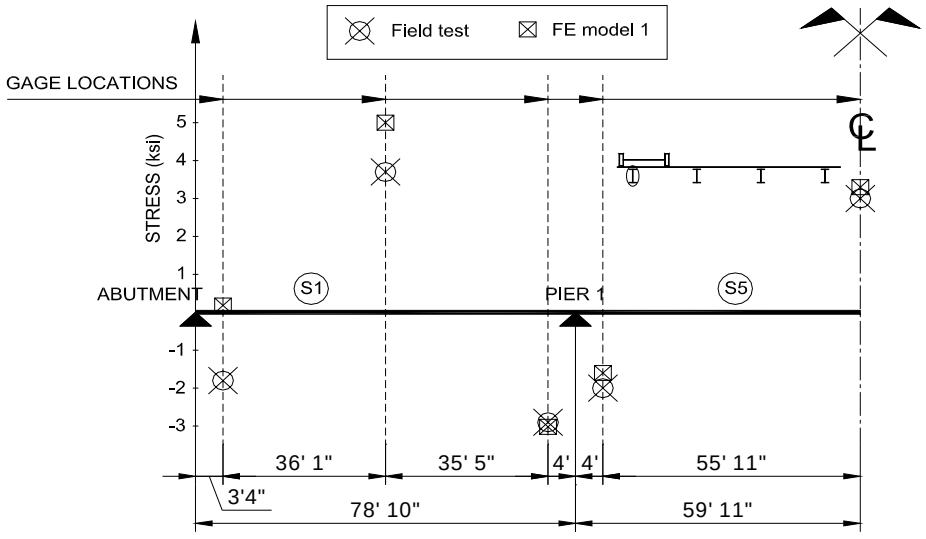

Figure 4.23: Las Cruces Load Test Results vs. FEA Results of Bottom Flange Stresses of S1 & S5 (Model 1)

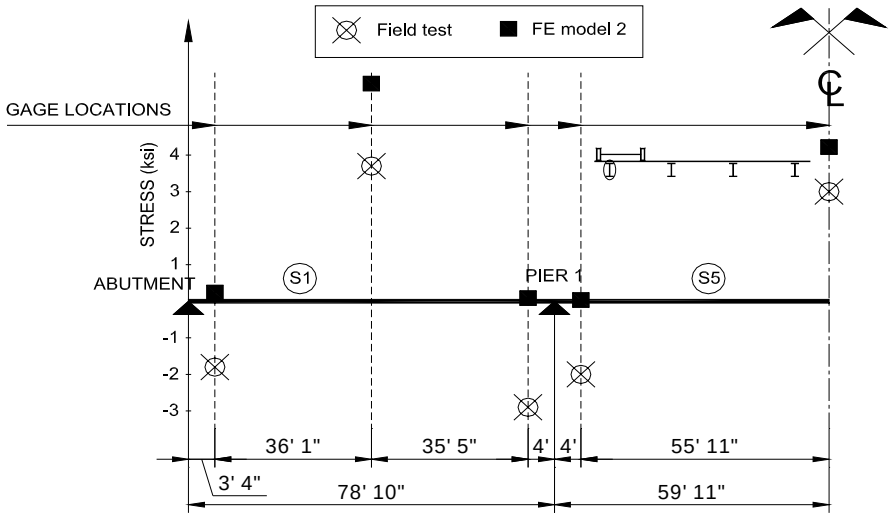

Figure 4.24: Las Cruces Load Test Results vs. FEA Results of Bottom Flange Stresses of S1 & S5 (Model 2)

Refer to Appendix A for a complete set of the finite element results compared to the field load tests. In most cases the first model is more representative of the actual field test results. To determine which model more accurately captures the in-situ response, first, the midspan stresses were compared. The midspan stresses of model 2 are in most cases

significantly greater (From -18% to 79% higher) than the midspan field test results. This increase in stress is to be expected because there is greater moment at the midspan of a simply supported case compared with a continuous case. Because pinned connections were used at the abutments, the stresses at midspan were much greater for model 1 than the field results.

Another location to compare is near the interior supports. The bottom flange stresses near the interior supports should be negative due to negative flexure. The bottom flange stresses in model 1 more closely match the field test results in most locations. As expected, model 2 exhibits little to no stress near the interior supports. This is another indication that the field results show (at least qualitatively) a moment transfer across the piers.

4.5 SUMMARY

This chapter focused on a case study of a bridge located in Las Cruces New Mexico. A field load test was conducted on the bridge to verify the continuity transfer supplied by the concrete diaphragm.

Several abnormalities were discovered in examining the test data. Mid-web stresses at several locations on the bridge were found to have either too great of a value or the opposite sign. It was theorized that the abnormal mid-web stresses could be due to biaxial bending. However, due to the nature of the research the exact cause was not determined to have an effect on the determining the continuity. When examining

influence lines, it was determined that the bridge is maintaining a certain degree of continuity.

Comparing the field results with the finite element analysis results showed that the bridge exhibited some degree of continuity. Model 1 (continuous model) was on average 6% greater than the field results at all midspan locations, while model 2 (simply supported model) was on average 30% greater than the field results at all midspan locations. Model 1 (continuous model) was on average 13% less than the field results at all pier locations, while model 2 (simply supported model) was on average 102% less than the field results at all pier locations.

The continuous behavior of the bridge can be quantified by calculating ratios. If the midspan stresses of the continuous case are divided by the midspan stresses of the simply supported case then this ratio can be compared with the ratio of the actual field results divided by the simply supported case. Comparing ratios shows that the average midspan stress ratio for the continuous case is 0.82 while the field results also had an average ratio of 0.82. Therefore, the bridge showed that it maintained a degree of continuity that agrees with the computer model analysis.

CHAPTER 5

HATCH CASE STUDY

5.1 INTRODUCTION

The previous chapter concentrated on the results of a load test conducted on a bridge in Las Cruces New Mexico. This chapter focuses on another CLL bridge which is located in Hatch, New Mexico. Essentially, the Hatch field load test will seek to verify the results of the Las Cruces test, and provide repeatability of the data and conclusions reached. Most prominently, to investigate if the continuity detail performed as designed.

5.2 BRIDGE DESCRIPTION

The second case study was conducted on the Hatch Bridge. The bridge is on NM 187 crossing east-west over the Rio Grande River. The bridge is a five span composite slab on steel girder bridge. The spans are 104’2”, 105’, 105’, 105’, and 104’2” in length. A picture of the Hatch Bridge is shown in Figure 5.1.

Figure 5.1: Hatch Bridge

Four plate girders spaced at 8’7” support a 31’6” road width. The same cross section is utilized for all of the plate girders.

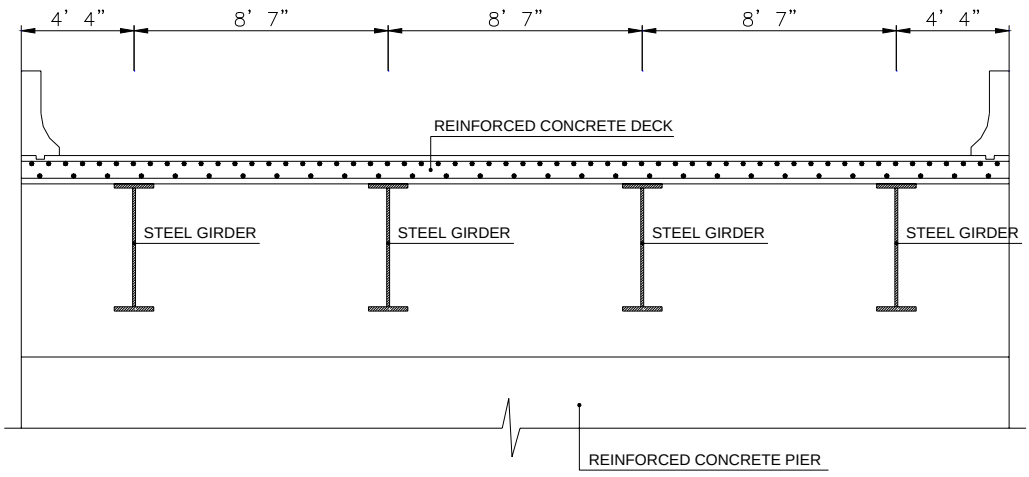

Figure 5.2: Cross Section View of Bridge

The cross sectional dimensions are shown in the figure below.

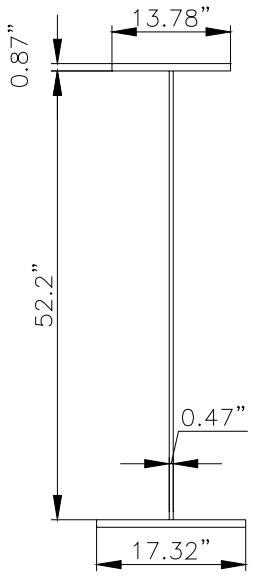

Figure 5.3: Steel Cross Section

The Hatch Bridge has a 9” concrete slab that is made composite through the use of shear studs that are 1.25” in diameter. Each row of shear studs consists of three evenly spaced studs which are machine welded to the top flange. Each shear stud is approximately 6” in height.

All of the girder ends rest on a sole plate atop an elastomeric bearing pad. The plate and pad are attached to the concrete below via anchor bolts. The top flanges of the girder ends are joined at the interior supports through the use of a continuity plate detail. Please refer to Figure 5.4 for the continuity detail of Hatch Bridge.

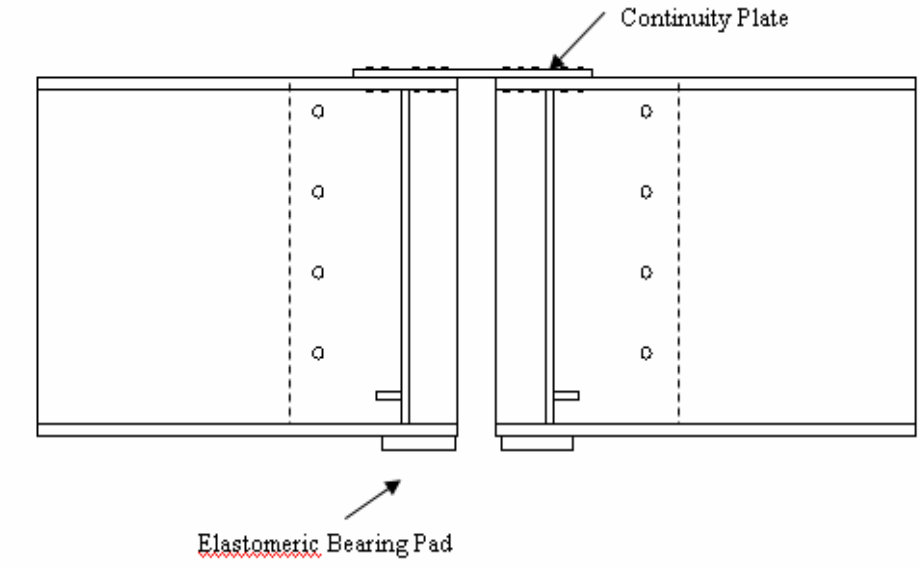

Figure 5.4: Hatch Bridge Continuity Detail

The plate is connected to the top flanges by bolts which are tightened after the deck is poured. The bolts are staggered along the length of the plate in between the shear studs. Please refer to Figure 5.5.

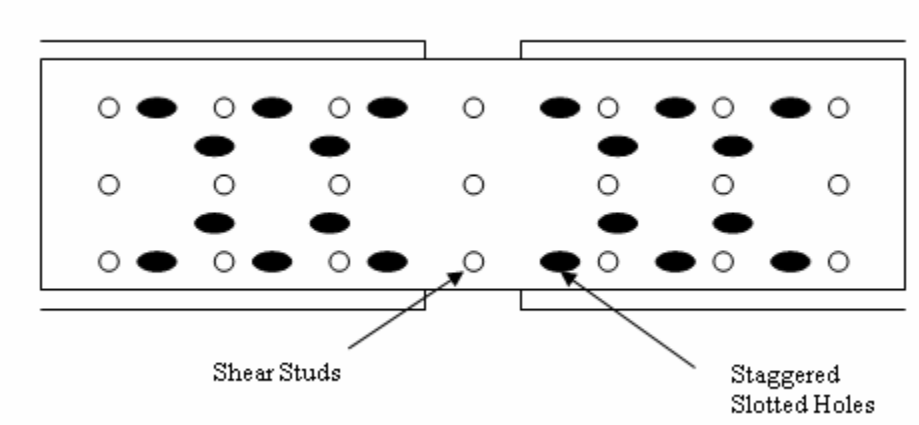

Figure 5.5: Top View of Slotted Bolt Holes

Unlike the Las Cruces bridge, the entire bridge deck was poured before tightening the bolts.

5.3 HATCH LOAD TEST

The Hatch Bridge was load tested on December 19, 2005. The Hatch Bridge was load tested in a similar fashion and purpose as the Las Cruces Bridge; to determine if the concrete diaphragm is providing continuity across the piers. Pseudo-static and dynamic load tests were performed on the bridge, however only the pseudo-static results are presented here.

5.3.1 Instrumentation Plan

To examine the continuity provided by the concrete diaphragm, gage locations were chosen to measure either negative or positive strain to be compared to the strain expected in a fully continuous configuration. Gages were placed 3 feet from each side of the interior supports to determine if the continuity detail provided enough rotational restraint to cause negative flexure. Gages were also placed at midspan to measure the strain as compared to what would be expected with a fully continuous structure.

A single gage at each location was sufficient to study the continuous behavior of the bridge. However, at least two gages are needed at each location to draw the strain profile (over the depth of the cross section) so gages were placed at the bottom flange and mid-web. Two gages were placed at every location except for one location close to an interior support. At each location gages were placed at the bottom flange and mid-web. The location near the interior support had three gages which were placed at the bottom of the top flange, at mid-web, and at the top of the bottom flange. Due to the increased number of spans in comparison with the Las Cruces Bridge, gages were placed on only

three of the five spans. Gage locations started at the midspan of the first span to the midspan of the third span. The gaging plan can be found in Figure 5.6.

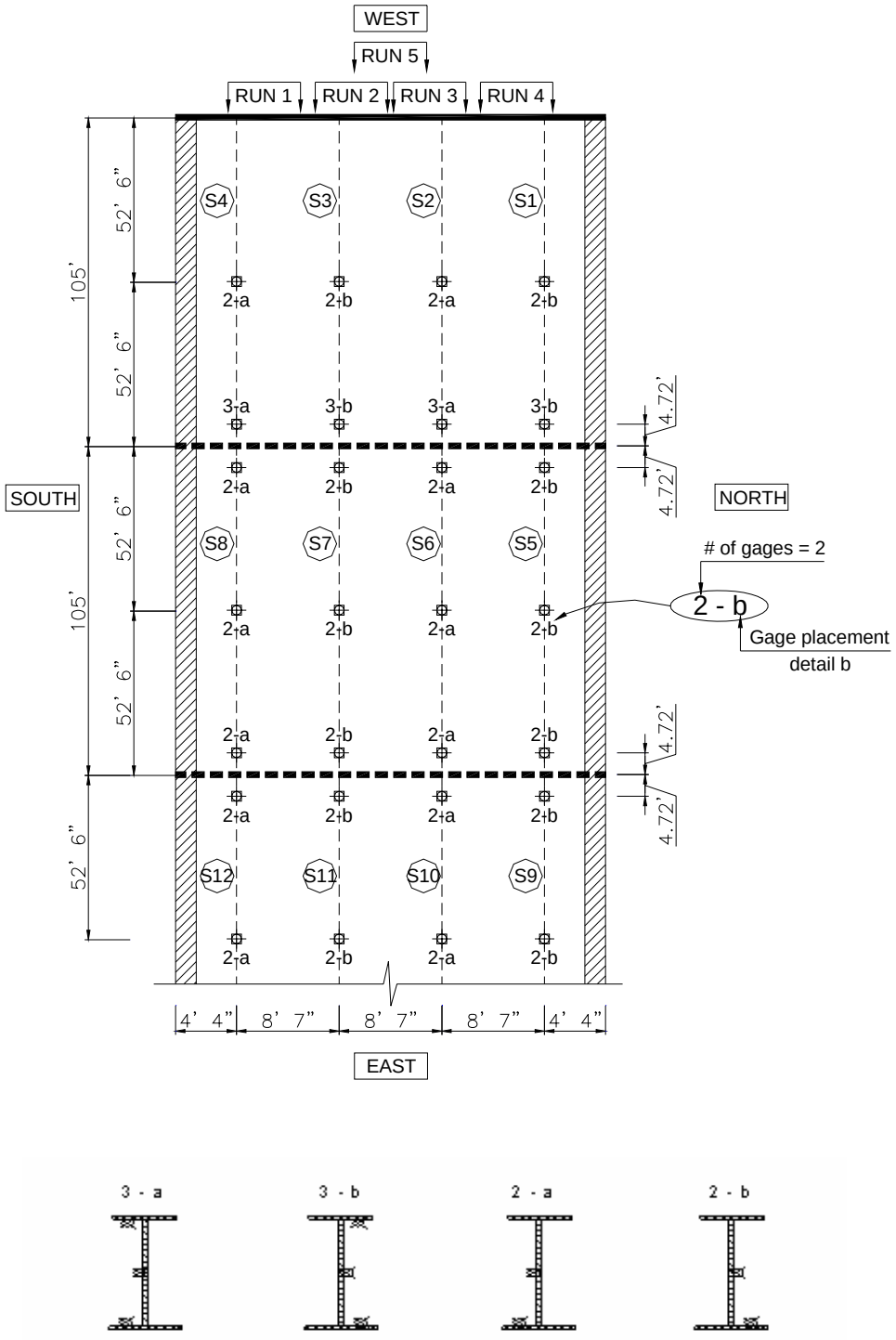

Figure 5.6: Instrumentation Plan of Hatch Bridge

5.3.2 Load Test

Two types of tests were conducted as on the Las Cruces Bridge. The sampling rate employed for the pseudo static test was 40 Hz. A sampling rate of 66 Hz was used for the dynamic testing to capture enough data due to the increased speed of the truck.

The truck traveled east on the bridge in five different loading positions. Five loading paths covered the width of the road starting at 2 feet from the barrier. Each loading path was run two times. The loading paths are outlined in Figure 5.7. As previously discussed, the system starts recording data at the first click sent by the auto clicker. This occurs at half of a wheel revolution behind the starting line. The starting line for the Hatch Bridge was 10 feet before the first abutment while the ending was at the second abutment. The auto-clicker measuring each wheel revolution contained a radio which was set to the same channel as the radios utilized by the Oklahoma State University system and the New Mexico State University system.

5.3.3 Test Results

Strain was recorded and then converted to stress assuming elastic behavior. Plots were created showing the stress recorded at each location versus the location of the truck. Essentially an influence stress plot was created for each gage location. Since the gages were mounted on the inside of the flanges (web side) the strain was adjusted linearly out to the extreme fibers. The two runs for each path were checked against each other for repeatability. Figures 5.8 & 5.9 illustrate the repeatability of the data.

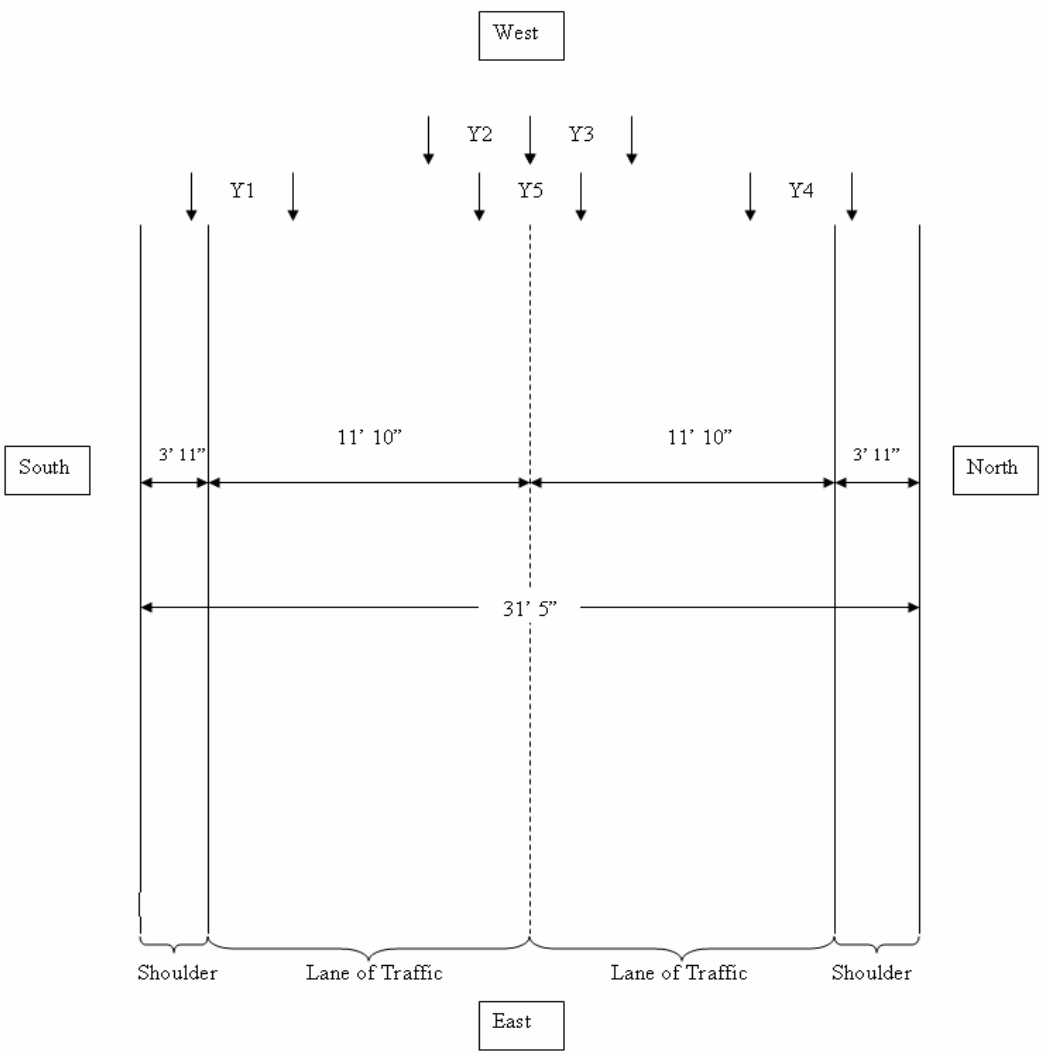

Figure 5.7: Loading Paths

Truck Positions

Y1: Passenger side wheel is 2' away from southern barrier
Y2: Driver side wheel on striped center line
Y3: Passenger side wheel on striped center line
Y4: Driver side wheel is 2' away from northern barrier
Y5: Centered about striped center line

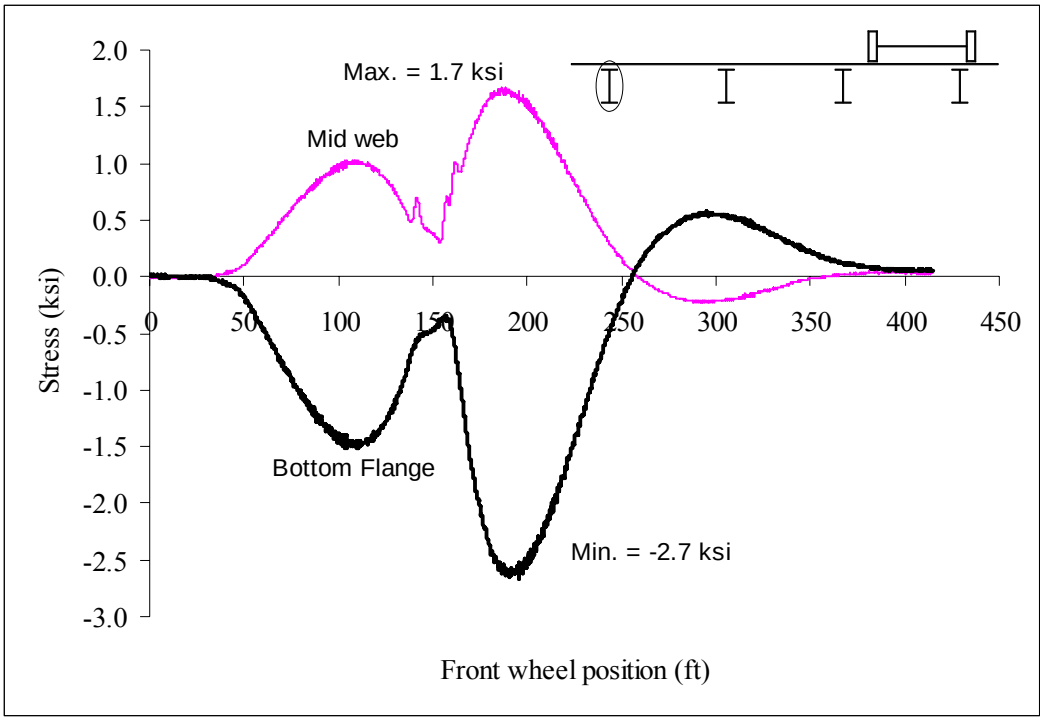

Figure 5.8: First Trial Run 1 S8 @ Support

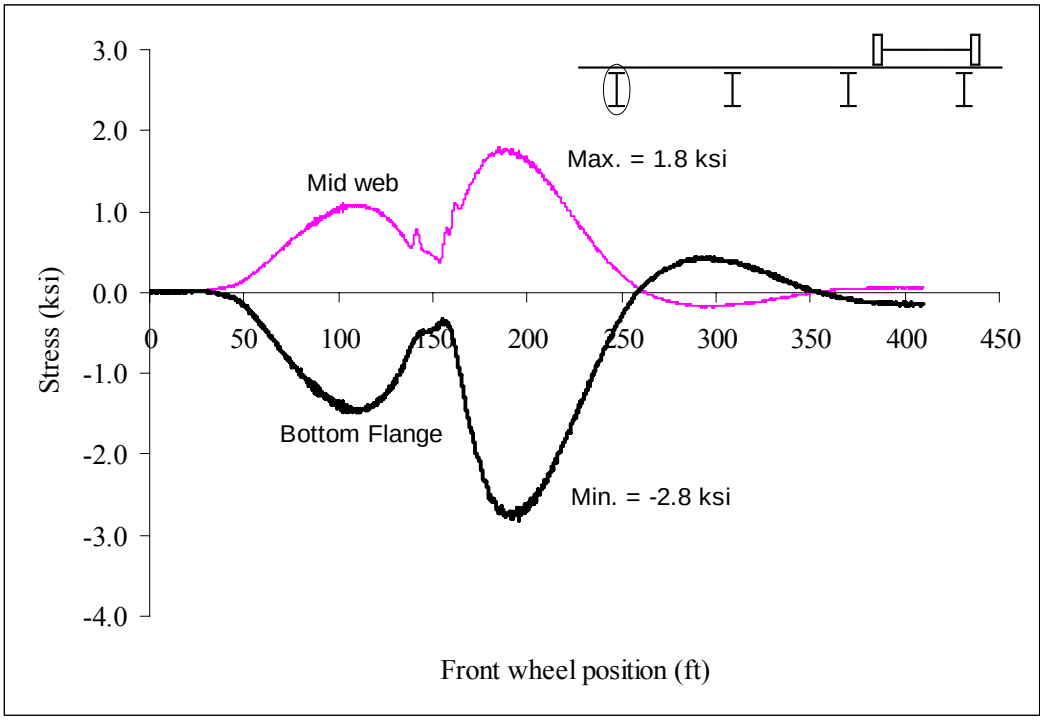

Figure 5.9: Second Trial Run 1 S8 @ Support

The unusual results obtained from the Las Cruces Test also occurred in the Hatch Load Test. The three anomalies are:

1. stresses at mid-web were EQUAL or LARGER than the bottom flange stress
2. stresses at mid-web were SMALLER than the bottom flange stress but with the opposite sign
3. stresses at mid-web were very small

The most likely cause for the unusual midweb stresses is bi-axial bending. However, it was felt only one gage was needed per location to determine if the bridge exhibited continuity. For this particular bridge, most gage locations recorded strains at the midweb and bottom flange. Figure 5.10 displays the number of unusual results that were found and at what locations. The three unusual results are marked each time they occur and at what locations on the bridge. Any results that do not display the unusual qualities are marked as "Usual" and are identified at different locations on the bridge.

Figure 5.10: Unusual Test Results Diagram Hatch Bridge Test

Influence lines were drawn for each testing location. Refer to Figure 5.11 below.

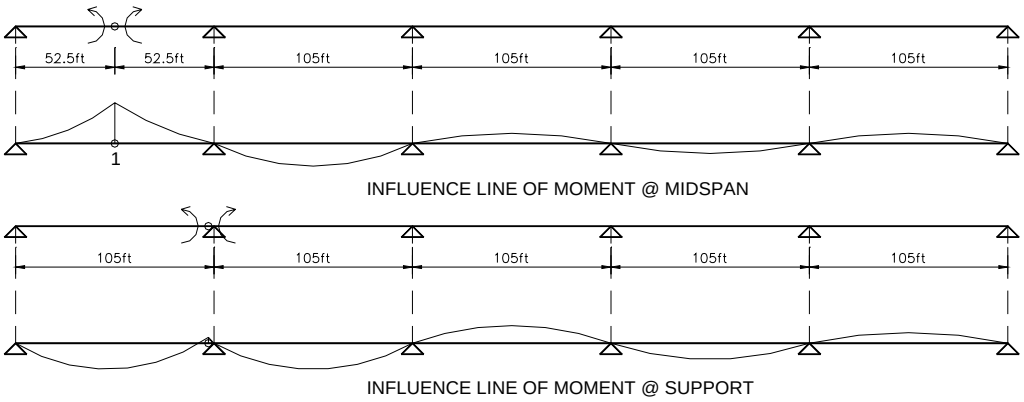

Figure 5.11: Influence Lines of Moment

Each influence line represents a single location longitudinally. Negative values on the influence line indicate a negative moment at the selected point, and positive values indicate a positive moment at the selected point as the load crosses the span. Influence lines were created for midspan and near support locations.

The influence lines were examined along with the stress versus truck location plots for analysis purposes. A midspan examination revealed that when the truck is loaded directly on the gage location the beam exhibits positive bending. This correlates with a tensile axial strain reading from the gage at the bottom flange and a compressive axial strain reading from the gage at the top flange. When the truck is loaded on spans that are next to the original span the location exhibits negative flexure. This correlates with a compressive axial strain reading from the gage at the bottom flange. Figure 5.12 is a stress plot of a midspan location with the corresponding influence line.

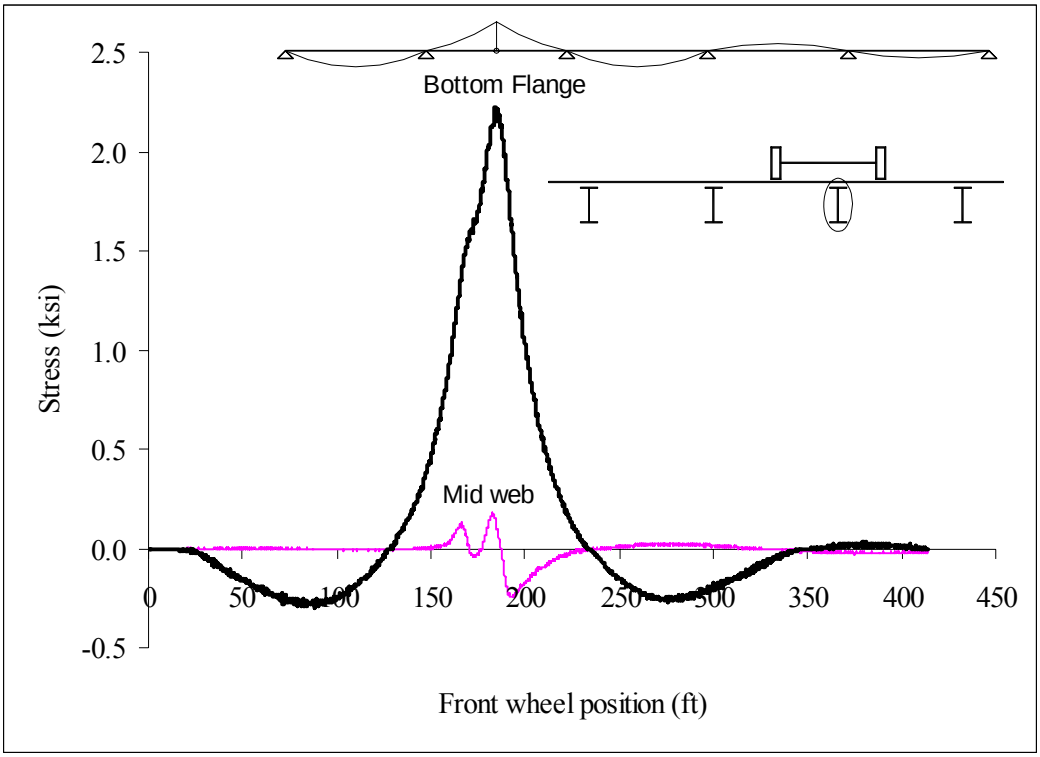

Figure 5.12: Stress Plot @ Midspan Location w/ Influence Line

The bottom flange gages near the interior supports exhibited negative strain when the truck is loaded on the two closest spans (thus correlating with negative flexure). The bottom flange gage reads positive strain when the truck is on a span on either side of the two closest spans (thus correlating with positive flexure). As with the midspan location, influence lines and tests results were compared. Figure 5.13 is a stress plot near a support location with the corresponding influence line.

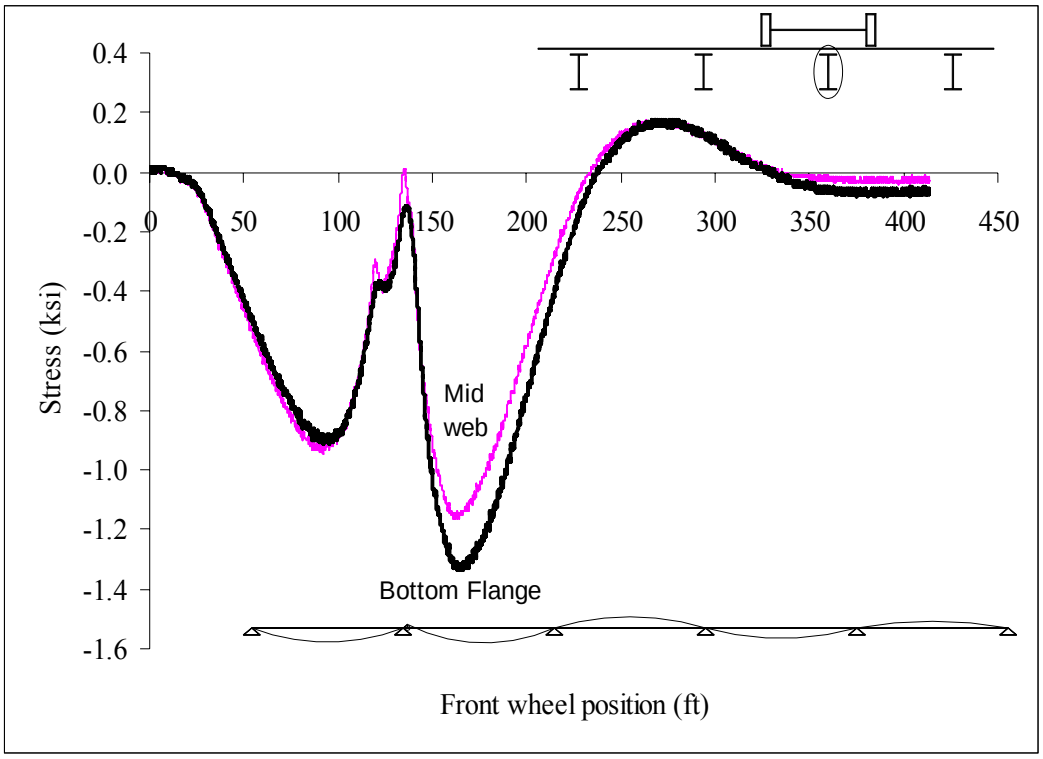

Figure 5.13: Stress Plot @ Support Location w/ Influence Line

Since the influence lines and the data compared favorably in a qualitative fashion, the conclusion was that the concrete diaphragm does provide continuity in the Hatch Bridge. Utilizing computer models will help to demonstrate to what degree the girders behave continuously.

5.4 FINITE ELEMENT ANALYSIS

STAAD Pro 2004 was again used to perform a finite element analysis on Hatch Bridge. Due to the fact that the Hatch Bridge was designed in a similar fashion to the Las Cruces Bridge many of the same modeling techniques were used. The Hatch Bridge was also a slab-on-girder composite bridge, therefore a composite cross section was needed for the analysis. As before the rigid link system was utilized to simulate composite action

between the concrete slab and steel girder. Pinned connections were also used for the boundary conditions.

5.4.1 Model Description

The same type of composite cross section model from the Las Cruces Bridge was used for the Hatch Bridge. The steel stringer and concrete deck consisted of a series of shell elements. Beam elements were used to represent the shear connectors. These beam elements served as rigid links connecting the steel stringer to the concrete deck. The shell element thicknesses and material properties were assigned according to the design drawings. Again the modulus of elasticity of steel used was 29,000 ksi while the modulus of elasticity of concrete used was 3,600 ksi. These material properties were taken from the as-built drawings. The rigid links were spaced at 10" in order to ensure full composite action.

Pinned connections were used to represent the boundary conditions. The abutment and interior support details are very similar in design to the Las Cruces Bridge, therefore the same boundary conditions were utilized. A continuous pinned end model and a simply supported pinned end model were created to determine which model more closely represents the bridge behavior as compared to the field tests.

5.4.2 Loading

Six concentrated point loads represented the six wheels of the test truck. Three longitudinal truck positions were used for each load path. The stress plots were examined to determine the truck location that produced the maximum response. The

stress plots peaked when the front wheel of the truck was roughly at 79’ 4”, 179’ 4”, and 279’ 4” from the abutment. Please refer to Figure 5.14 for relative loading positions.

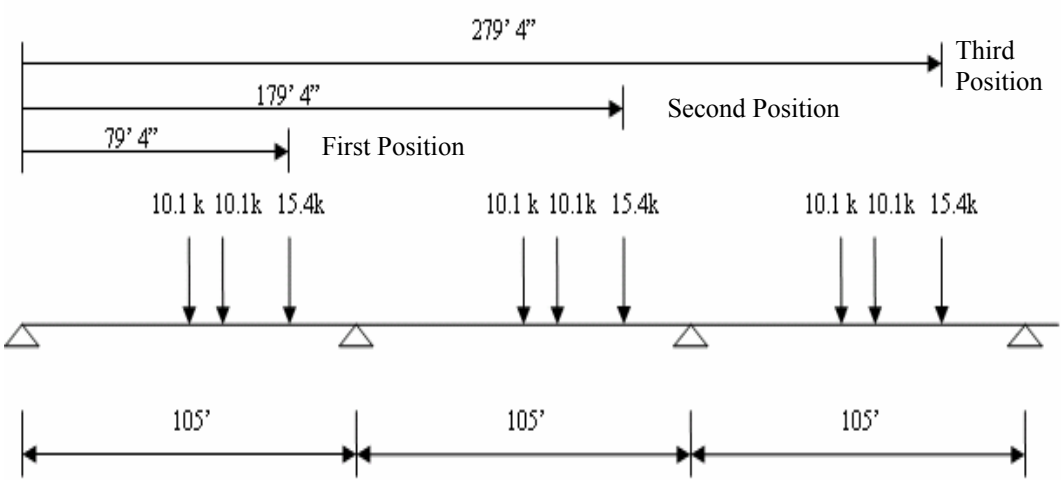

Figure 5.14: Hatch Loading Locations

5.4.3 Finite Element Analysis Results

The two aforementioned models were analyzed in STAAD Pro 2004. One load path was considered for each stringer that almost directly loaded it. Table 5.1 gives a side by side comparison of the bottom flange stresses recorded from the field test and the bottom flange stresses from the analysis. Model 1 is representative of the continuous case while model 2 is the simply supported case.

Table 5.1: STAAD & Field Results (Hatch Bridge)

Run	Member	Gage Location	Bottom Flange Stresses (ksi)				
			Field	Model 1	% Difference	Model 2	% Difference
4	S1	Midspan	**3.8**	5.04	33%	5.96	57%
		Support 1	**-2.7**	-2.41	-11%	0	-100%
	S5	Support 1	**-2.2**	-1.79	-19%	0	-100%
		Midspan	**3.6**	4.27	19%	5.59	55%
		Support 2	**-2.6**	-1.94	-25%	0	-100%
	S9	Support 2	**-2**	-1.97	-2%	0	-100%
		Midspan	**3.4**	3.89	14%	5.23	54%
3	S2	Midspan	**2.6**	3.27	26%	3.79	46%
		Support 1	**-1.5**	-1.48	-1%	0	-100%
	S6	Support 1	**-1.3**	-1.11	-15%	0	-100%
		Midspan	**2.2**	2.79	27%	3.51	60%
		Support 2	**-1.6**	-1.2	-25%	0	-100%
	S10	Support 2	**-1.3**	-1.24	-5%	0	-100%
		Midspan	**2.5**	2.44	-2%	3.17	27%
2	S3	Midspan	**2.7**	3.28	21%	3.79	40%
		Support 1	**-1.8**	-1.48	-18%	0	-100%
	S7	Support 1	**-1.1**	-1.11	1%	0	-100%
		Midspan	**2.7**	2.79	3%	3.51	30%
		Support 2	**-1.1**	-1.2	9%	0	-100%
	S11	Support 2	**-0.9**	-1.24	38%	0	-100%
		Midspan	**2.5**	2.44	-2%	3.17	27%
1	S4	Midspan	**3.8**	5.04	33%	5.96	57%
		Support 1	**-2.8**	-2.41	-14%	0	-100%
	S8	Support 1	**-2.6**	-1.79	-31%	0	-100%
		Midspan	**4.2**	4.27	2%	5.59	33%
		Support 2	**-2.2**	-1.94	-12%	0	-100%
	S12	Support 2	**-2.4**	-1.97	-18%	0	-100%
		Midspan	**3.9**	3.89	0%	5.23	34%

Refer to Figures 5.15 and 5.16 for graphical representations of these results. As before these plots display the maximum stresses from the field results compared with the finite element analysis results for a single longitudinal line of girders. Recall from the instrumentation plan that the maximum stress can be visually examined for the midspan or close to pier locations on up to three spans.

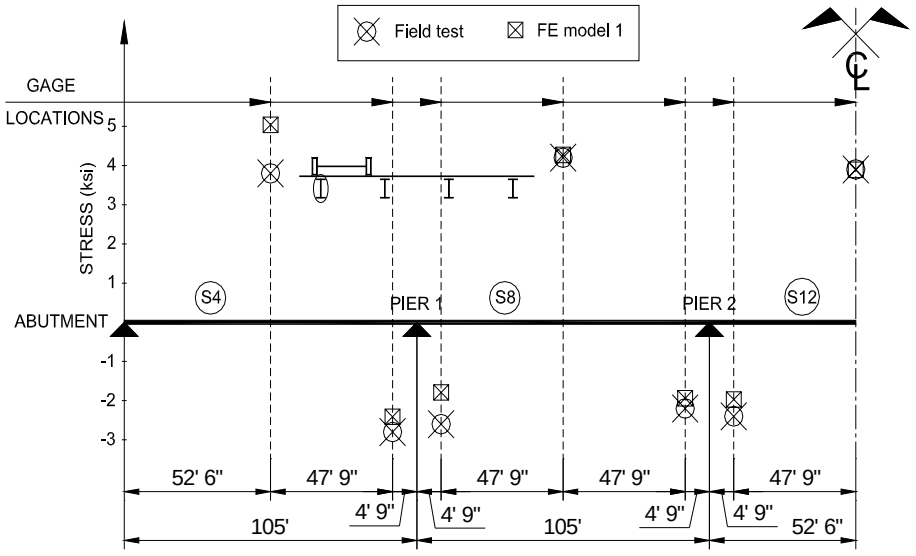

Figure 5.15: Hatch Load Test Results vs. FEA Results of Bottom Flange Stresses of S4, S8, & S12 (Model 1)

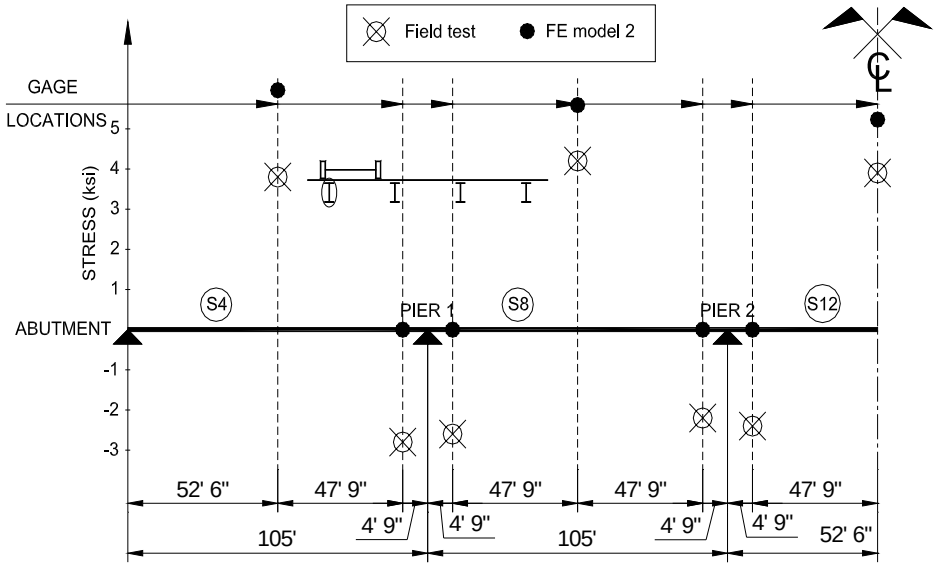

Figure 5.16: Hatch Load Test Results vs. FEA Results of Bottom Flange Stresses of S4, S8, & S12 (Model 2)

When examining the table it can be seen that the first model is closer to the actual field test results in most cases. Examining both the midspan and near pier stresses can

help to determine whether the bridge behaves more like model 1 or model 2. The midspan stresses of model 2 are significantly greater than the midspan field test results. This increase in stress is to be expected because there is greater moment at the midspan of a simply supported case compared with a continuous case therefore resulting in an increased stress. Because pinned connections were used at the abutments, the stresses at midspan were much greater for model 1 than the field results. Observing the interior supports can also help to determine the continuous behavior of the bridge. If the bridge behaves in a continuous fashion then the bottom flange stresses near the interior supports should be negative due to negative flexure that would be expected. If the structure acted in a simply supported fashion (as modeled by model 2), it would be expected the field test results would have little or no stress. As expected, the bottom flanges near the interior supports in model 2 exhibits little to no stress, while the stresses in model 1 show a considerable amount of stress. This would indicate that the continuity detail does indeed function to transfer moment from span to span.

5.5 SUMMARY

This chapter focused on a case study of a bridge located near Hatch New Mexico. A field load test was conducted on the bridge to verify the continuity transfer supplied by the concrete diaphragm. The same unusual results discovered in the Las Cruces Bridge were also found in the Hatch Bridge. Mid-web stresses at several locations on the bridge were found to have either an unusually high value or the opposite sign. It was again theorized that the abnormal mid-web stresses could be due to biaxial bending. However,

it was concluded that this abnormality did not have an effect on determining if the concrete diaphragm supplied continuity across the support. The comparisons of the influence lines for moment with the stress plots show qualitatively that continuity is being transferred across the concrete diaphragm.

A comparison between the field results and the finite element analysis showed that the bridge behaves much more like model 1 (continuous model) than model 2 (simply supported model). Model 1 was on average 15% greater than the field results at all midspan locations, while model 2 was on average 43% greater than the field results at all midspan locations. Model 1 was on average 9% less than the field results at all pier locations, while model 2 was on average 100% less than the field results at all pier locations. The individual percent differences between the field results and model 1 are rather close with the greatest difference being 38%.

The continuous behavior of the bridge can be quantified by calculating ratios. Dividing the results of the finite element analysis midspan stresses of the continuous case by the midspan stresses of the simply supported case can be compared with the ratio of actual field results divided by the midspan stresses of the simply supported case. Comparing ratios shows that the average midspan stress ratio for the finite element continuous case was 0.80 while the field results had an average ratio of 0.70. Therefore, it was concluded that this indicated the bridge demonstrated a degree of continuity that reasonably agrees with the computer model analysis.

CHAPTER 6

SUMMARY AND CONCLUSIONS

6.1 OVERVIEW OF PROJECT SCOPE

In an attempt to make steel bridges more economical in the short to medium span range the Continuous for Live Load (CLL) method was developed by Dr. Atorod Azizinamini at the University of Nebraska Lincoln. The method consists of placing the steel girders of a bridge in a simply supported configuration for the dead load and a continuous configuration for the live loads. The bridge is then retrofitted into a continuous structure by use of a concrete diaphragm at the interior supports. Pre-cast concrete girder bridges utilize this same technology in making the bridge CLL. However, due to this method being relatively new for steel bridges little research has been conducted into the use of CLL.

The objective of this research was to examine the economic feasibility of using CLL as a viable alternative/economically competitive to pre-stressed concrete bridges in the short to medium span lengths. Also the CLL method was tested to verify if it did indeed provide continuity as designed. Two in-situ bridge field load tests were conducted to examine this portion of the project. A literature review was conducted to gather any

current information, while a DOT survey was written in order to gather information on economical steel bridge design.

Two bridges in New Mexico were chosen to load test as a joint venture between Oklahoma State University and New Mexico State University. The first bridge is located near Las Cruces and the second bridge is located near Hatch. Each steel bridge was constructed continuous for live load with the addition of a steel continuity plate joining the top flanges of the girders.

6.2 PROJECT RESULTS

There are two other methods that the CLL method for steel bridges was compared against in terms of cost and time savings: traditional steel bridge design and pre-cast pre-stressed concrete girder bridges. In all cases the CLL method was cost and time effective compared with traditional continuous steel bridges. The CLL steel bridges proved to be competitive in terms of cost and time savings as compared with pre-cast pre-stressed concrete girder bridges. However, the difficulty in comparing these two types of bridges lies in the fact that the material costs of steel and concrete are always in constant flux. Whenever cost drives the project, a DOT will choose that type of material simply because it is more cost effective to do so at the time. Another difficulty in comparing these two types of bridges is that the fabrication market for one material in a particular state can be much more developed than the other material. Therefore any cost and time savings coming from the CLL method do not necessarily prove to make steel as or more competitive with concrete in the short to medium span range of bridges.

The other major area of interest addressed in this project was whether or not CLL performs as designed in field applications. Two CLL bridges were load tested and the results were compared with finite element computer analysis model results. The results showed that both bridges behaved much more like a fully continuous bridge than a simply supported span bridge.

The level of continuity transfer was quantified for both bridges. The continuity transfer was quantified through a ratio of the finite element analysis midspan stresses of the continuous case divided by the finite element analysis midspan stresses of the simply supported case. This ratio theoretically represents the greatest amount of continuity transfer. That ratio was compared with the midspan stresses of the field results divided by the finite element analysis midspan stresses of the simply supported case. This ratio represents the amount of continuity transfer that the bridge is exhibiting. The Las Cruces Bridge had a ratio of 0.82 for the continuous case and 0.82 for the field results. The Hatch Bridge had a ratio of 0.80 for the continuous case and 0.70 for the field results. Both bridges exhibited a significant amount of continuity transfer.

Although the bridges proved to be continuous it might be necessary to check these bridges again in the future. The bridge in Las Cruces was built in 2001 while the bridge in Hatch was built in 2004. These bridges are fairly new and there is some concern how the concrete diaphragm will fair with time. Future load testing would help to prove that continuity is or is not maintained. Specifically, the continuity connection with the steel reinforcement providing the live load continuity is of concern. As mentioned previously, the concrete deck on bridges has been known to fail due to the corrosion of the steel.

6.3 CONCLUSIONS

Using the CLL method on steel bridges proved to be economical in comparison to traditional continuous steel bridges. CLL bridges proved to be relatively economical compared with pre-cast pre-stressed concrete girders. One case in New Mexico proved that a CLL bridge can be real competitive with pre-cast concrete girder bridges. However, another case in Tennessee proved that a CLL bridge was only slightly competitive to a pre-cast concrete girder bridge. The constant fluctuation of the steel and concrete material costs based on the economy and local markets make it difficult to give any long term conclusions. However, it was proven that the CLL method for steel girder bridges is an economical advance improving several facets of steel bridge construction.

The load testing of two steel CLL bridges showed that the concrete diaphragm maintained continuity across interior supports. Examining influence lines proved that the girders were behaving continuously. STAAD computer analysis models also showed that the bridge behaved more like a continuous configuration than a simply supported configuration. Thus, the CLL method for steel girder bridges is a success based on the original intent of providing continuity.

REFERENCES

Azizinamini, A., Lampe, N., Yakel, A. (2003). *Toward development of a steel bridge system – Simple for dead load and continuous for live load* (Thesis, University of Nebraska – Lincoln, 2003).

Azizinamini, A., Veen, L. V. (2004). Bridges made easy. *Roads and Bridges, 42*(11), 42-43.

Chung, W., Sotelino, E.D. (2005). Nonlinear finite-element analysis of composite steel girder bridges. *Journal of Structural Engineering, 131*(2), 304-313.

Dang, C. (2006). (Master's Report, Oklahoma State University, 2006).

Engel, R., Miller, R., Swanson, J. (2004). A summary of the PIC-22 fast-track bridge reconstruction project.

Engel, R., Weeks, M. (2001). PIC-22-16.96. (Drawings, Apr. 2001).

Henkle, D. (2001). Competitive edge. *Civil Engineering, July 2001,* 64-67.

Liang, Q. Q., Uy, B., Bradford, M. A., Ronagh, H. R. (2005). Strength analysis of steel-concrete composite beams in combined bending and shear. *Journal of Structural Engineering, 131*(10), 1593-1600.

Lin, M., Swanson, J. (2004). *Verification of AASHTO-LRFD specifications live load distribution factor formulas for HPS bridges* (Thesis, University of Cincinnati, 2004).

Mabsout, M. E., Tarhini, K. M., Frederick, G. R., Tayar, C. (1997). Finite-element analysis of steel girder highway bridges. *Journal of Bridge Engineering, 2*(3), 83-87.

Mistry, V. (1994). Economical steel bridge design. *Modern Steel Construction, 34*(3), 42-47.

Rubiez, C. (1996). Design aids for efficient short span steel bridges. *Modern Steel Construction, 36*(12), 20-21.

Stouffer, J. (2004). *Simplified economical bridge design feasibility report* (Master's Report, University of New Mexico, 2004).

Talbot, J. (2005). Simple made continuous. *NSBA Steel Bridge News, 6*(4), 1, 4-5.

Tedesco, J. W., Stallings, J. M., Tow, D.R. (1995). Finite element method analysis of bridge girder-diaphragm interaction. *Computers & Structures, 56*(2), 461-473.

Wade, D. (2000). Sonoma Ranch Blvd. Bridge. (Drawings, Dec. 2000).

Wasserman, E. (2004). Simplified continuity details for short and medium span composite steel girder bridges.

Weaver, D. L. (1996). Steel girder bridges. *The Construction Specifier, 49*(5), 109-117.

APPENDIX A

The following appendix contains stress versus truck position plots of the Las Cruces Bridge Test conducted on December 18, 2005. The stress is measured in units of ksi and the position of the truck is measured in units of ft. Please note that the strain gage locations close to the abutments and interior supports are measured 2 ft from the concrete diaphragm face. This appendix also contains plots of STAAD analysis results of the bottom flange stresses versus the field results taken from Chi Dang's report. Please note that FEA Model 1 is the continuous model while FEA Model 2 is the simply supported model.

TABLE OF FIGURES

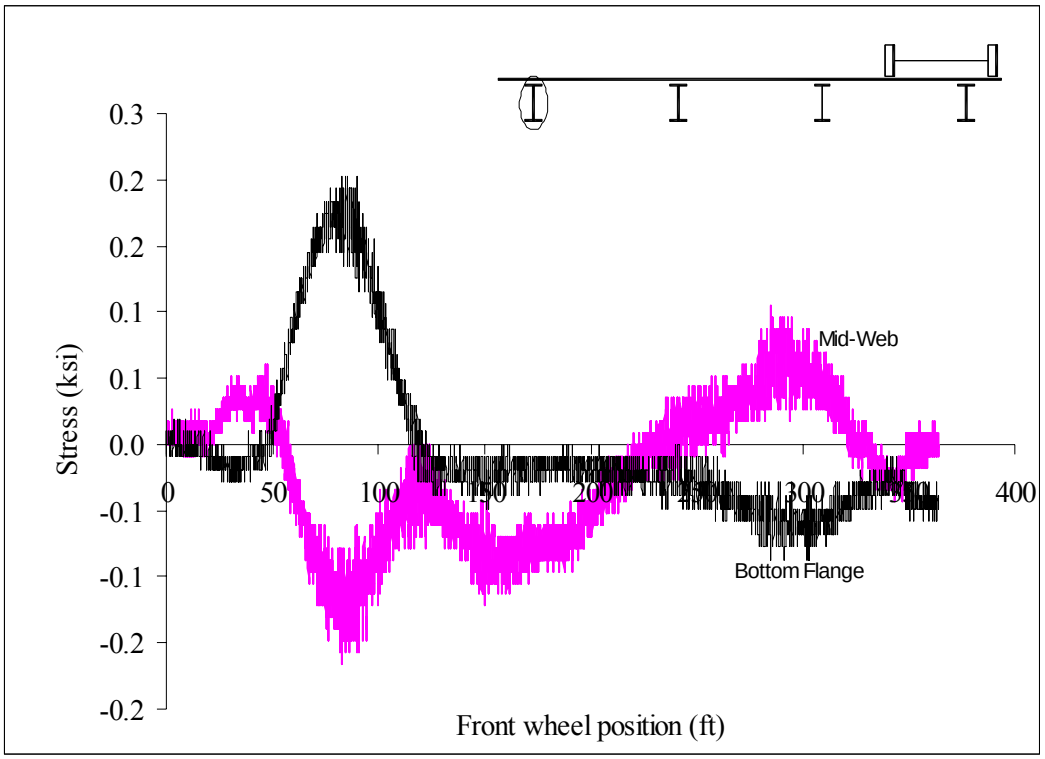

Figure A1: Las Cruces Bridge Test Run 1 S1 @ 2 ft from abutment

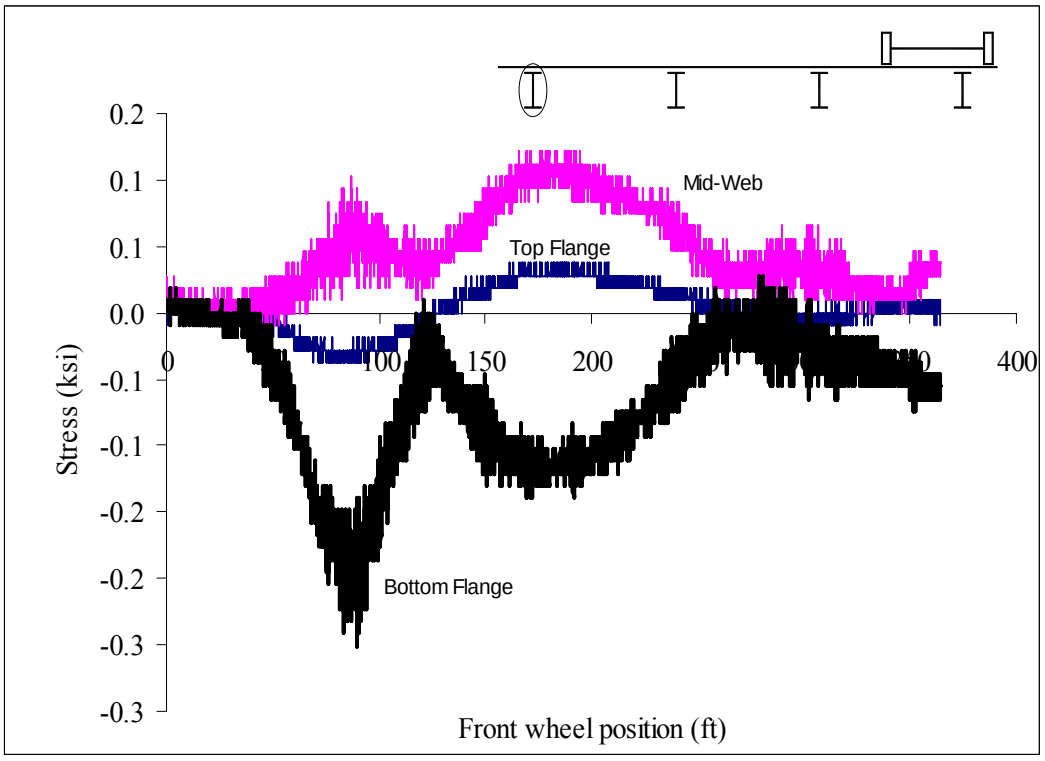

Figure A2: Las Cruces Bridge Test Run 1 S1 @ Midspan

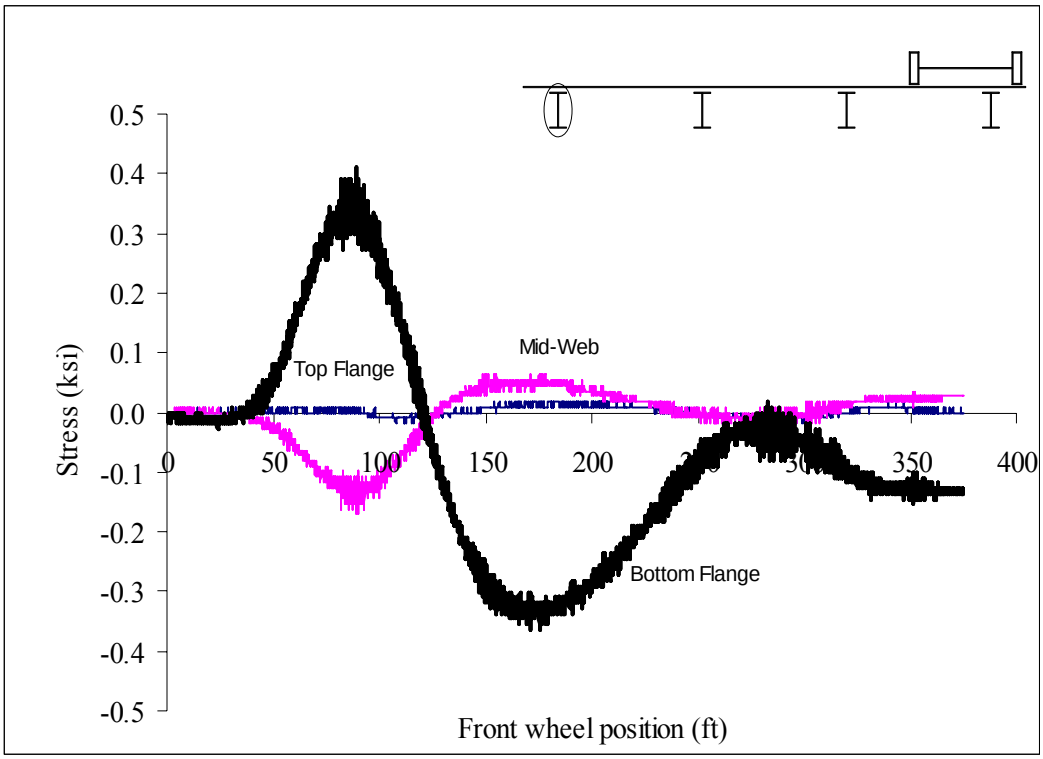

Figure A3: Las Cruces Bridge Test Run 1 S1 @ 2 ft from interior support

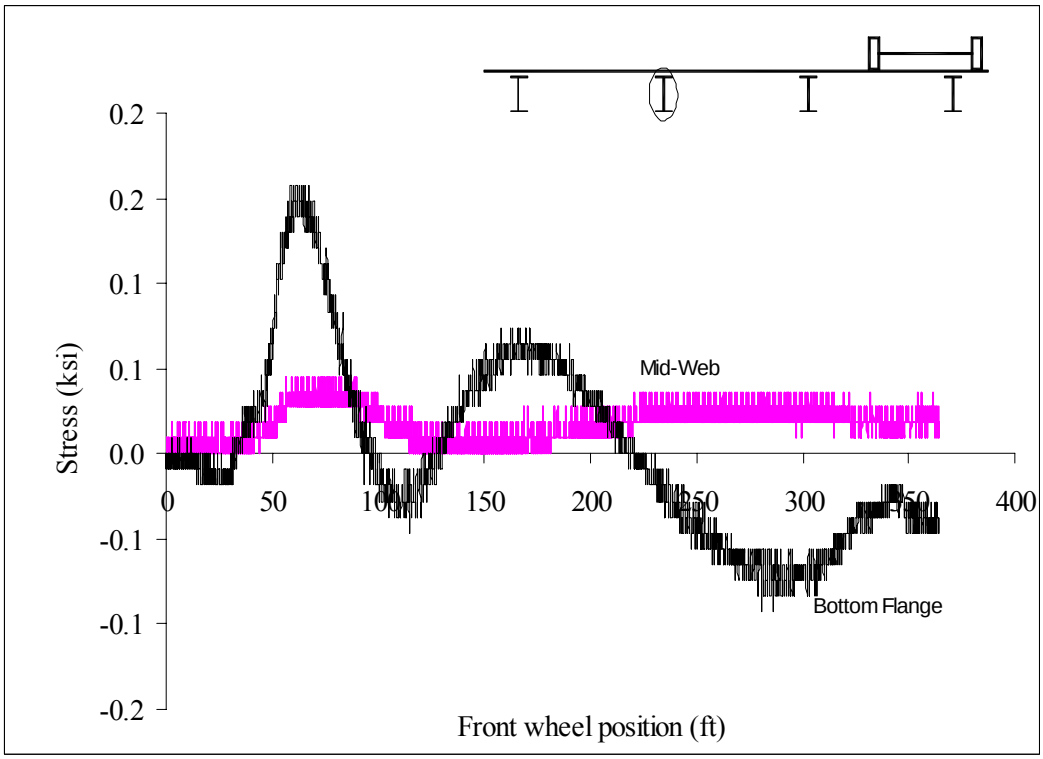

Figure A4: Las Cruces Bridge Test Run 1 S2 @ 2 ft from abutment

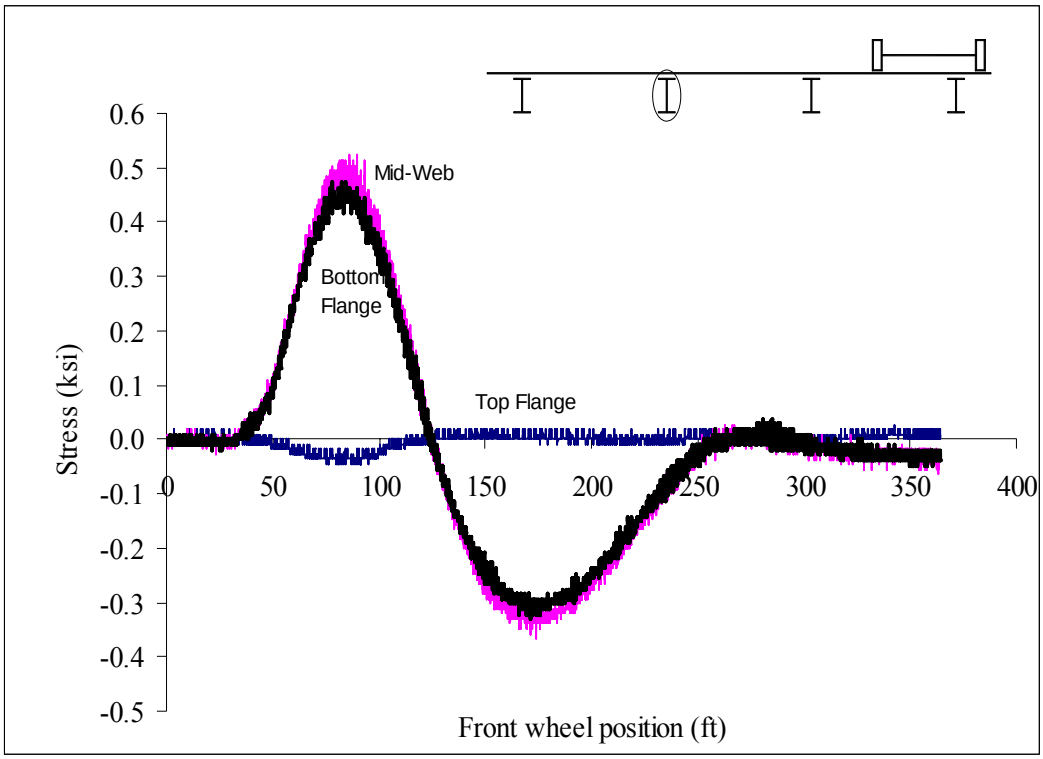

Figure A5: Las Cruces Bridge Test Run 1 S2 @ Midspan

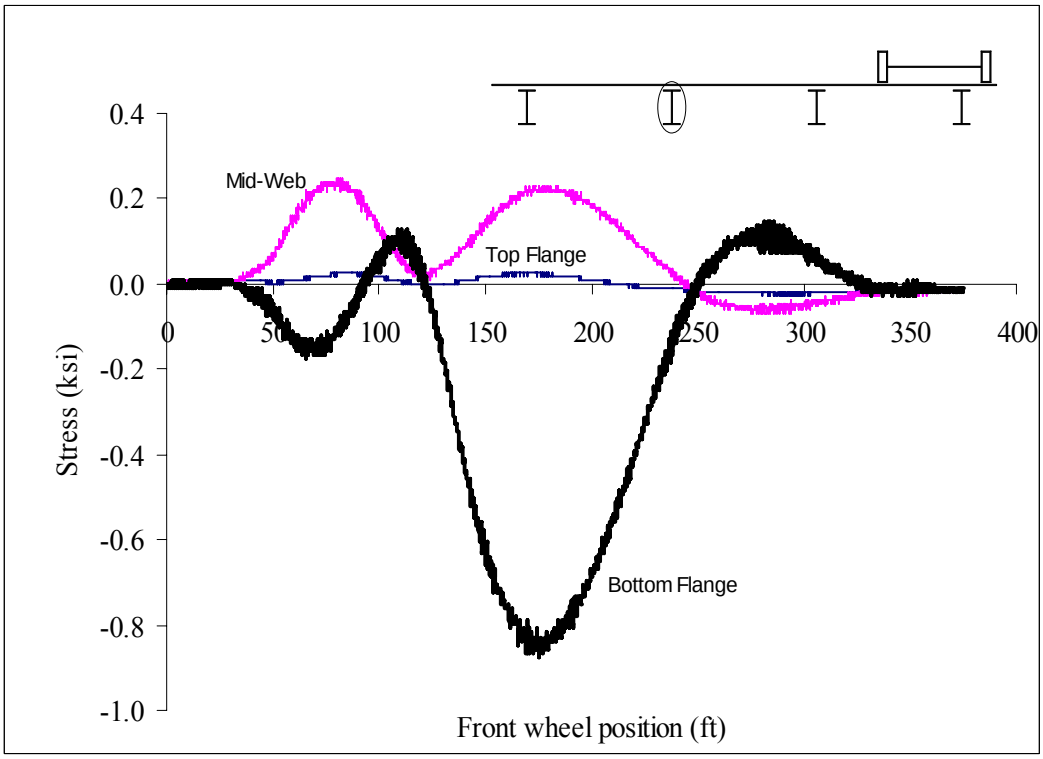

Figure A6: Las Cruces Bridge Test Run 1 S2 @ 2 ft from interior support

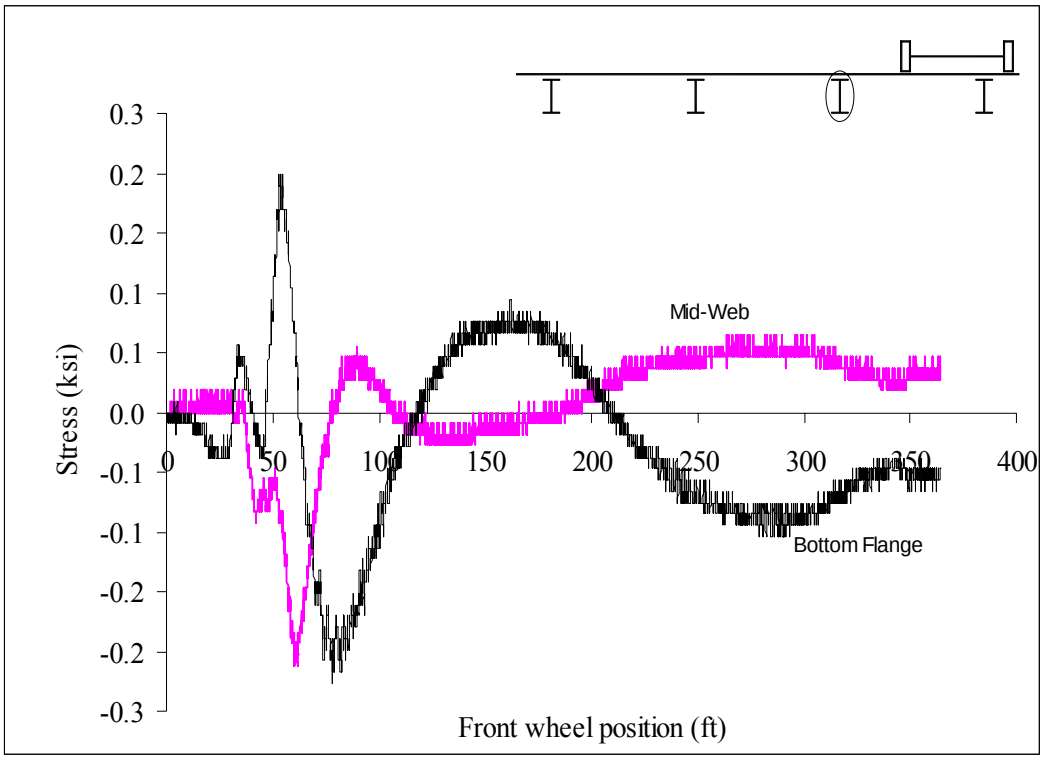

Figure A7: Las Cruces Bridge Test Run 1 S3 @ 2 ft from abutment

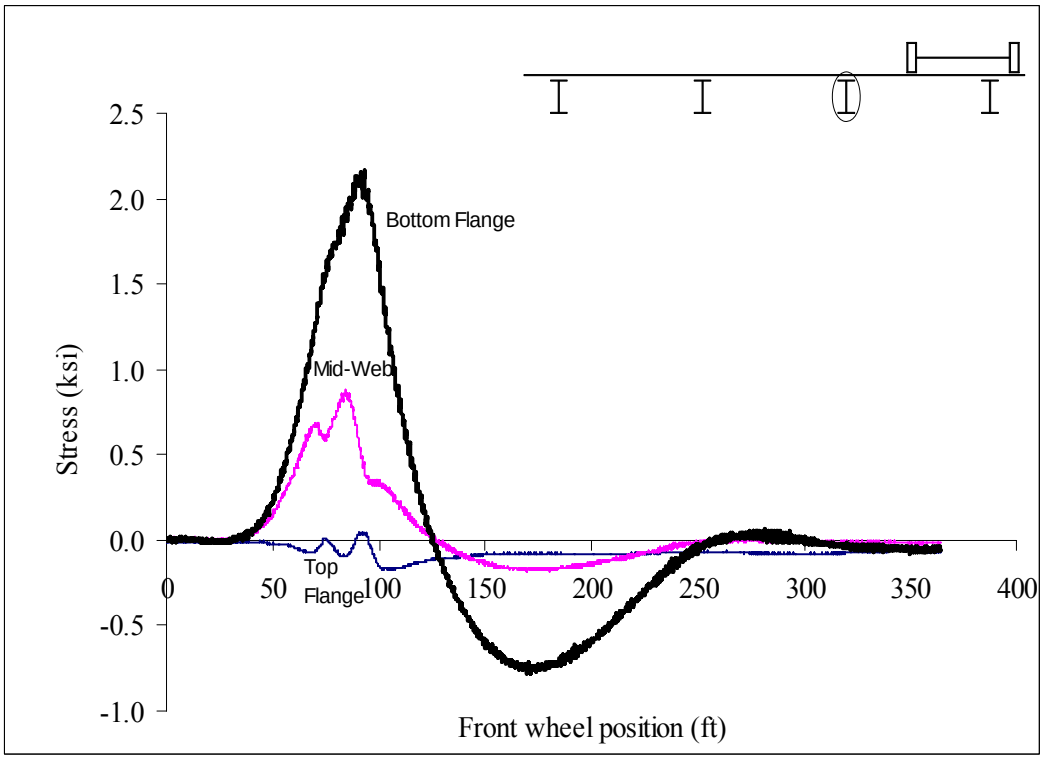

Figure A8: Las Cruces Bridge Test Run 1 S3 @ Midspan

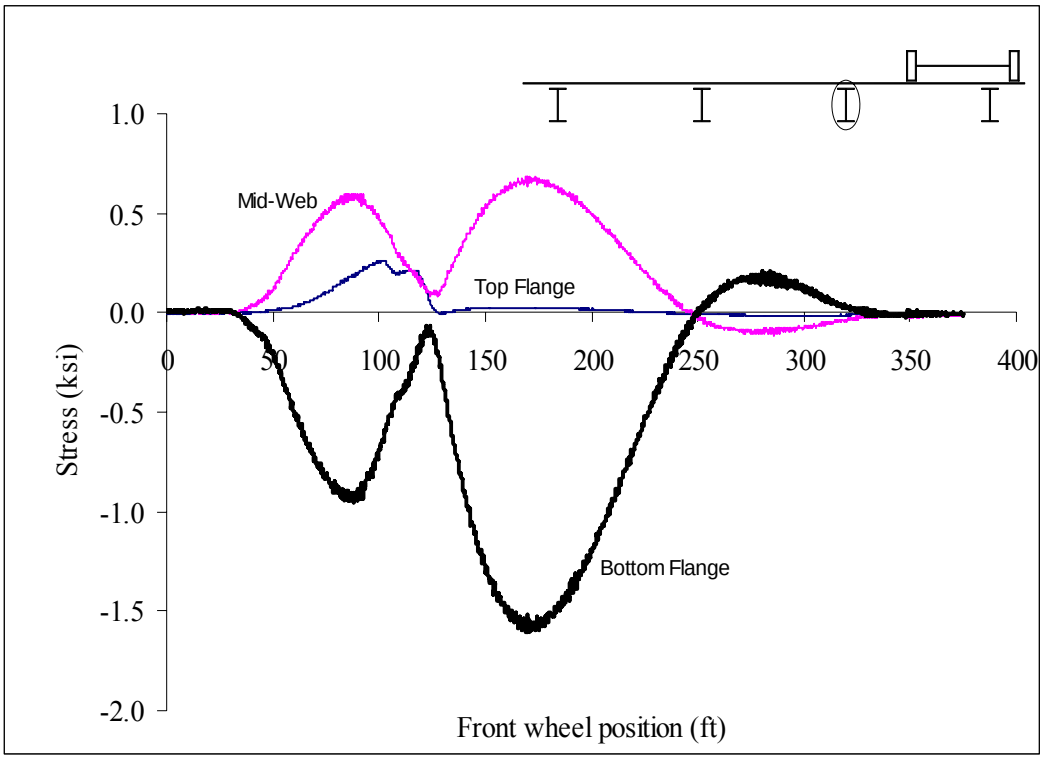

Figure A9: Las Cruces Bridge Test Run 1 S3 @ 2 ft from interior support

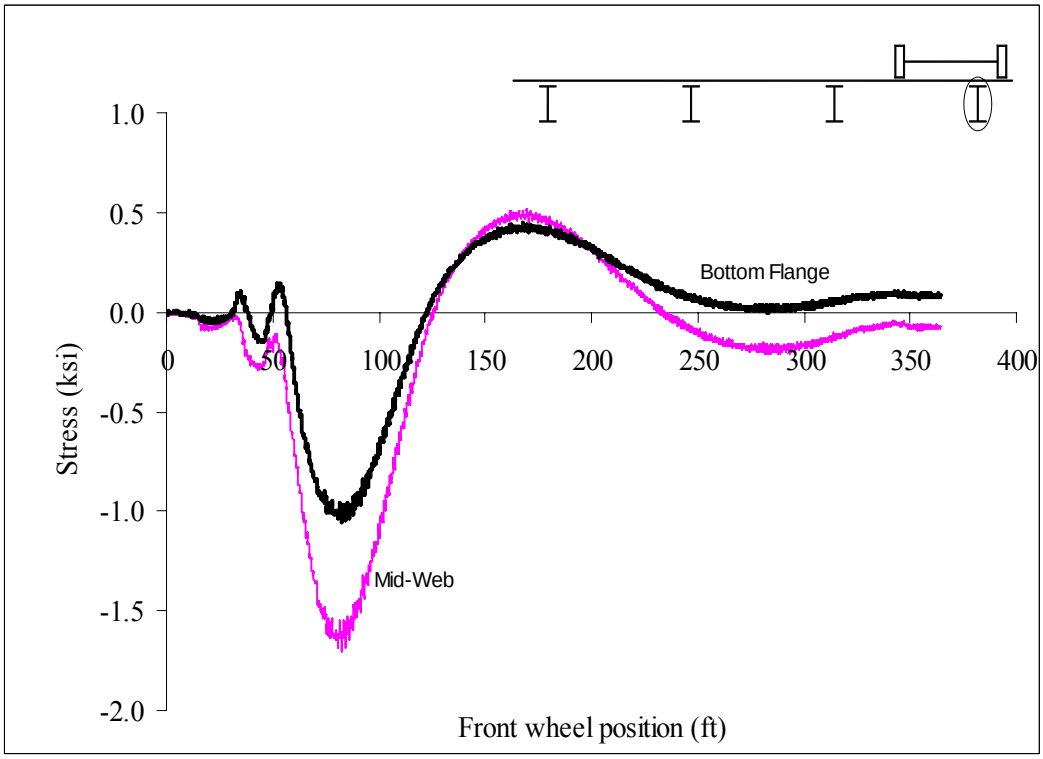

Figure A10: Las Cruces Bridge Test Run 1 S4 @ 2 ft from abutment

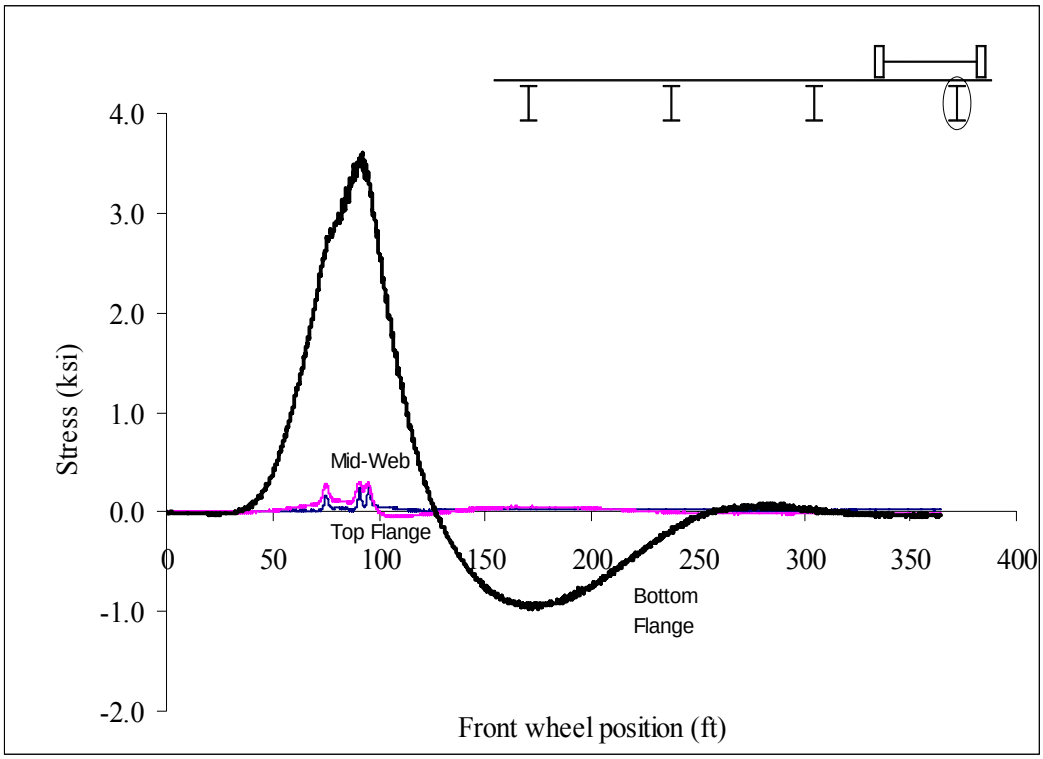

Figure A11: Las Cruces Bridge Test Run 1 S4 @ Midspan

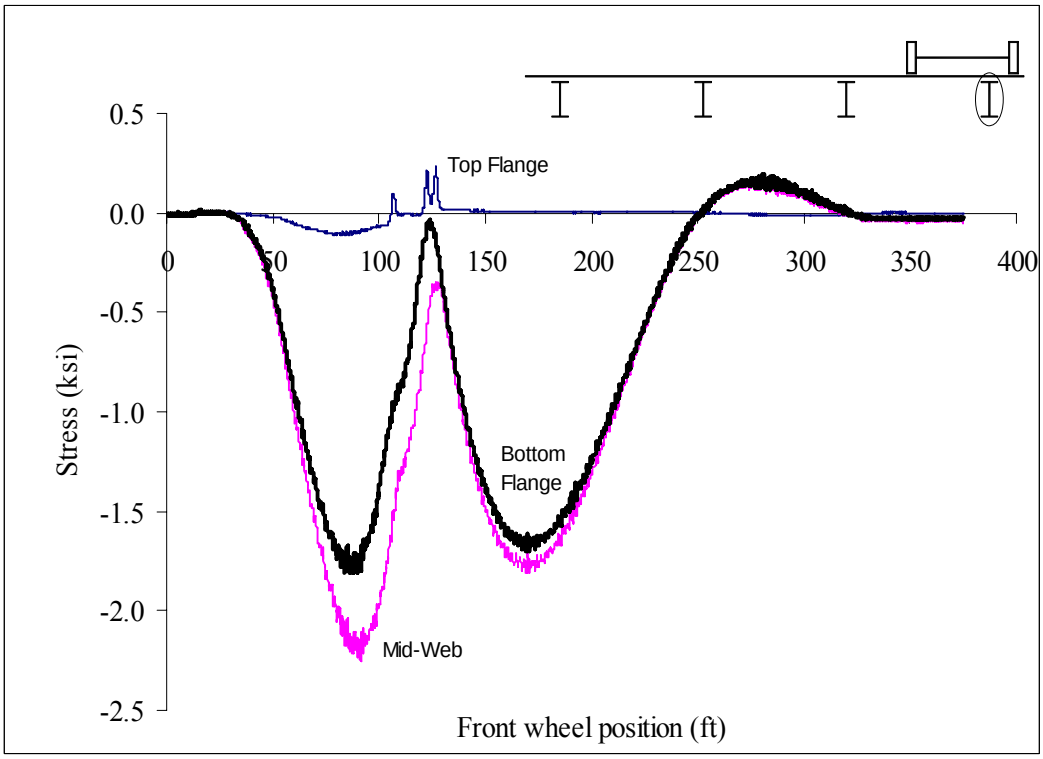

Figure A12: Las Cruces Bridge Test Run 1 S4 @ 2 ft from interior support

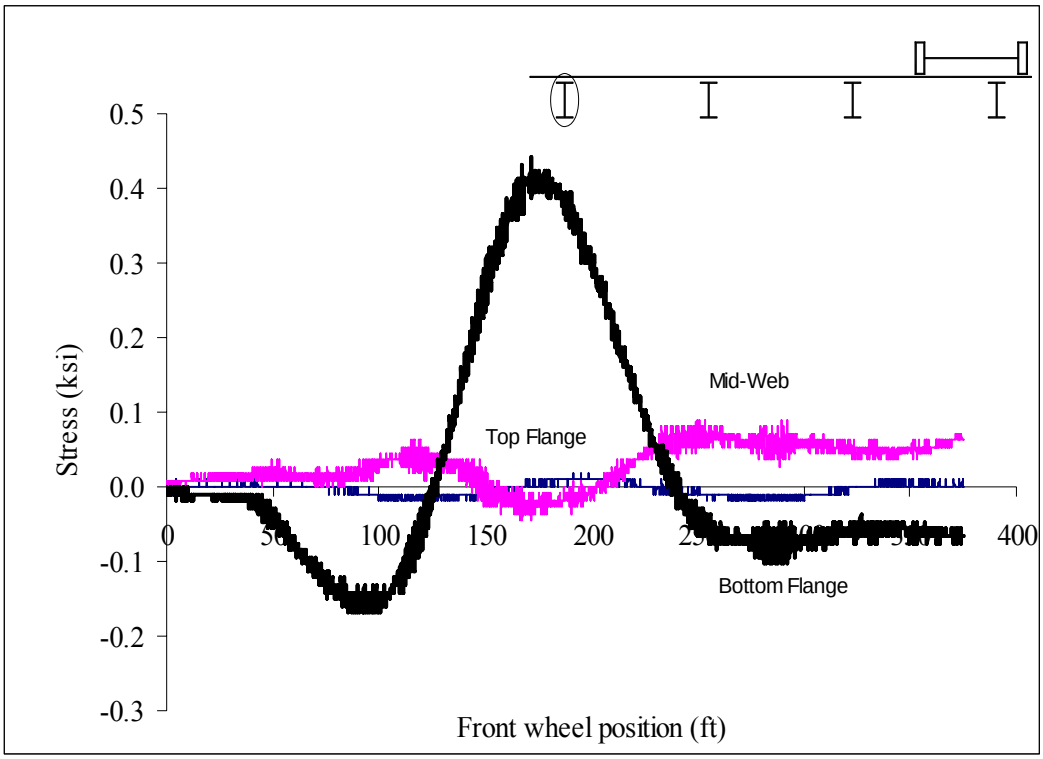

Figure A13: Las Cruces Bridge Test Run 1 S5 @ 2 ft from interior support

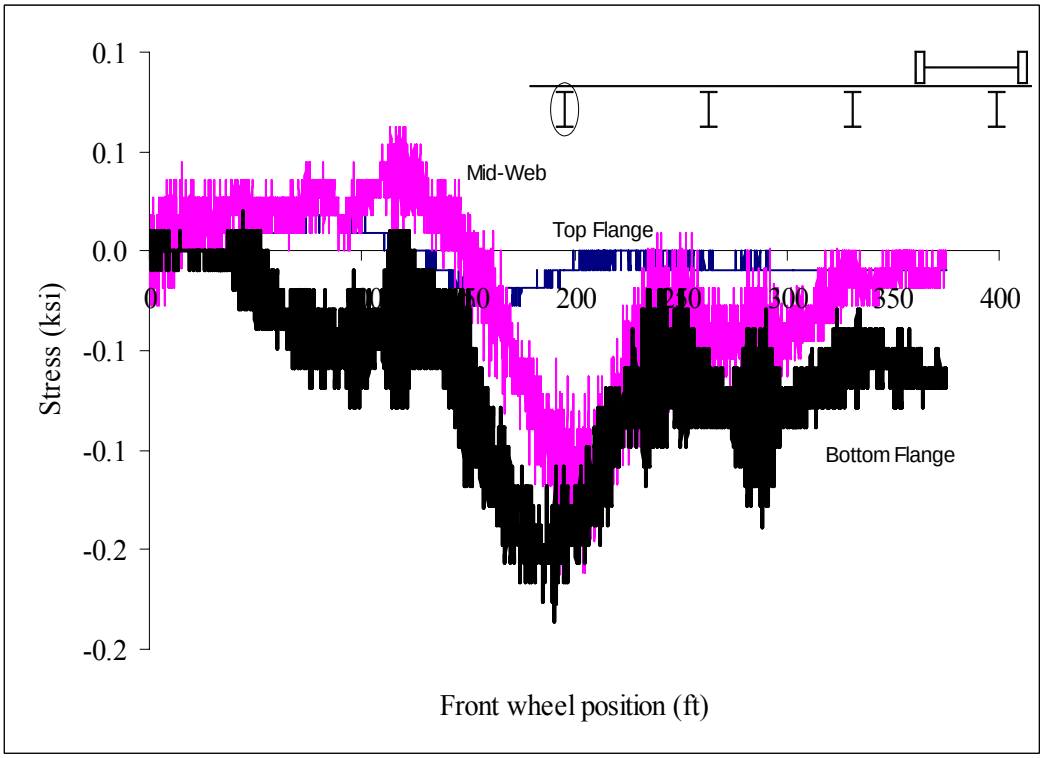

Figure A14: Las Cruces Bridge Test Run 1 S5 @ Midspan

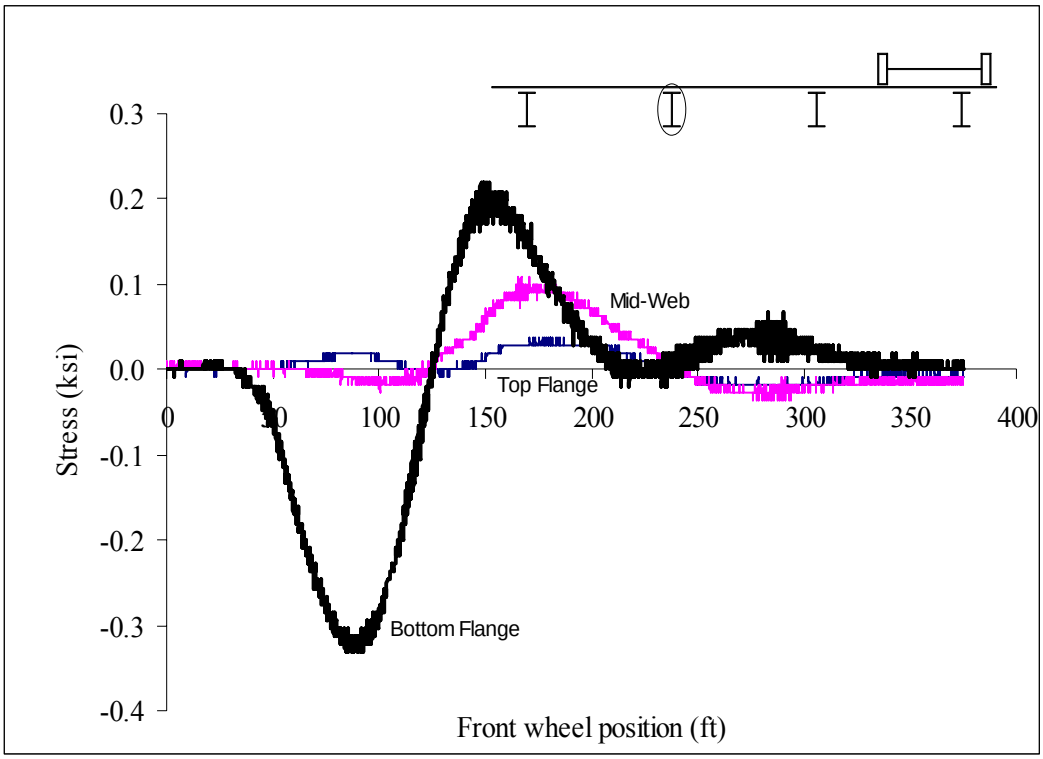

Figure A15: Las Cruces Bridge Test Run 1 S6 @ 2 ft from interior support

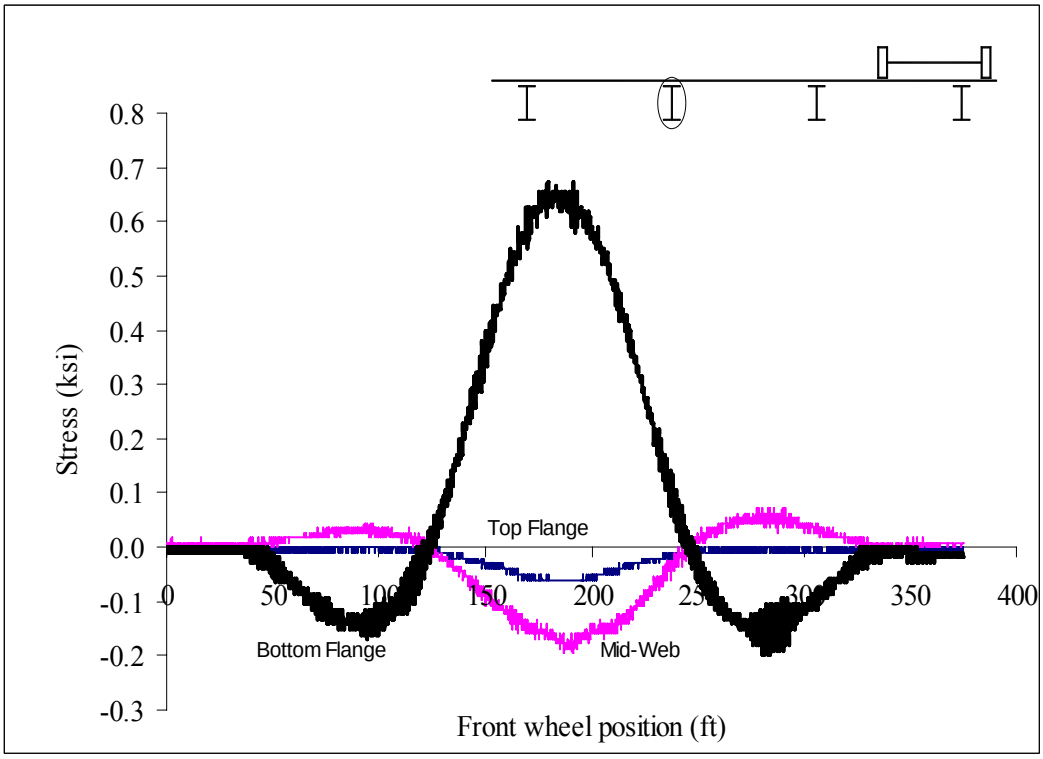

Figure A16: Las Cruces Bridge Test Run 1 S6 @ Midspan

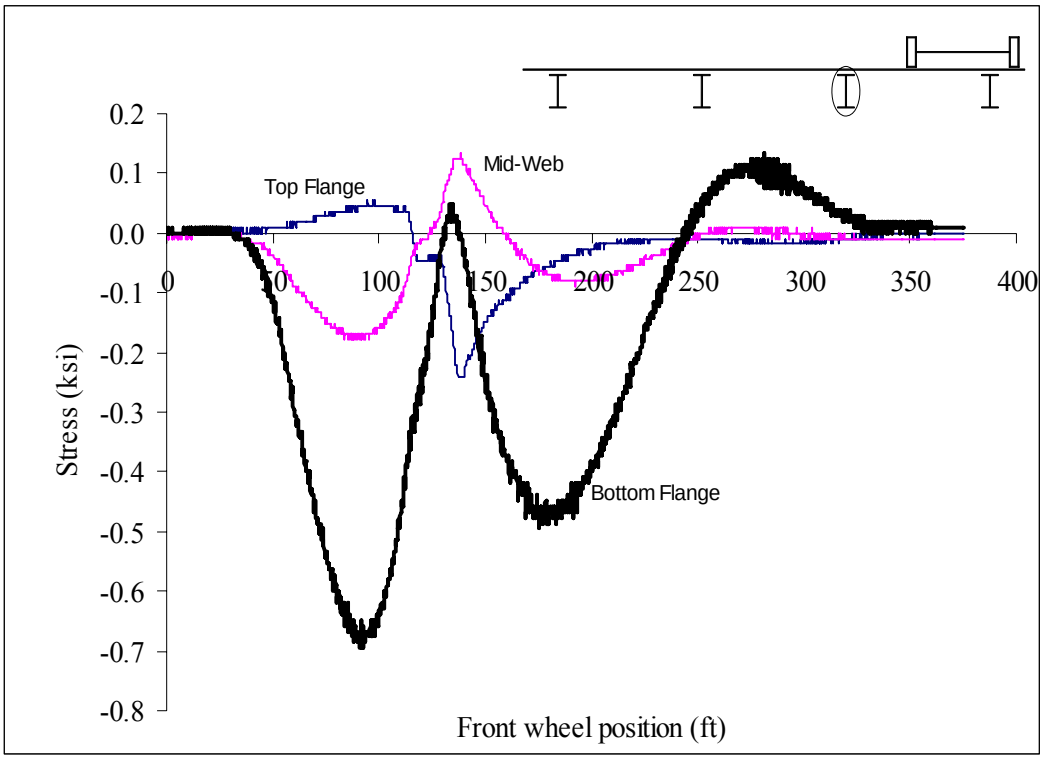

Figure A17: Las Cruces Bridge Test Run 1 S7 @ 2 ft from interior support

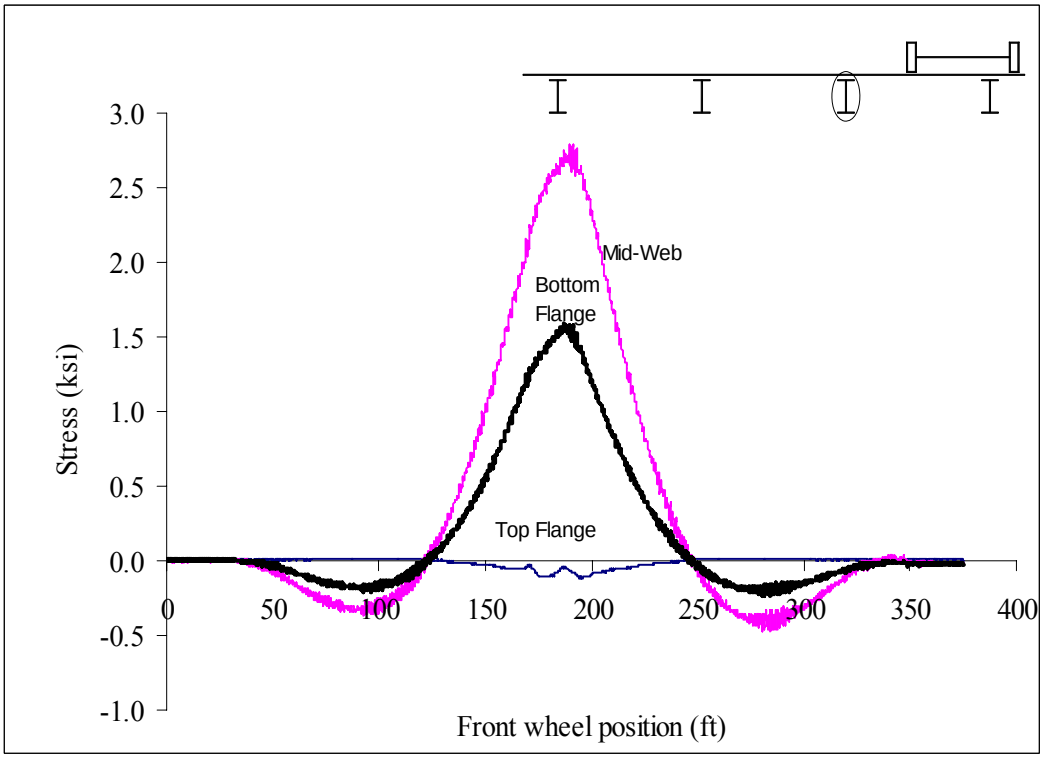

Figure A18: Las Cruces Bridge Test Run 1 S7 @ Midspan

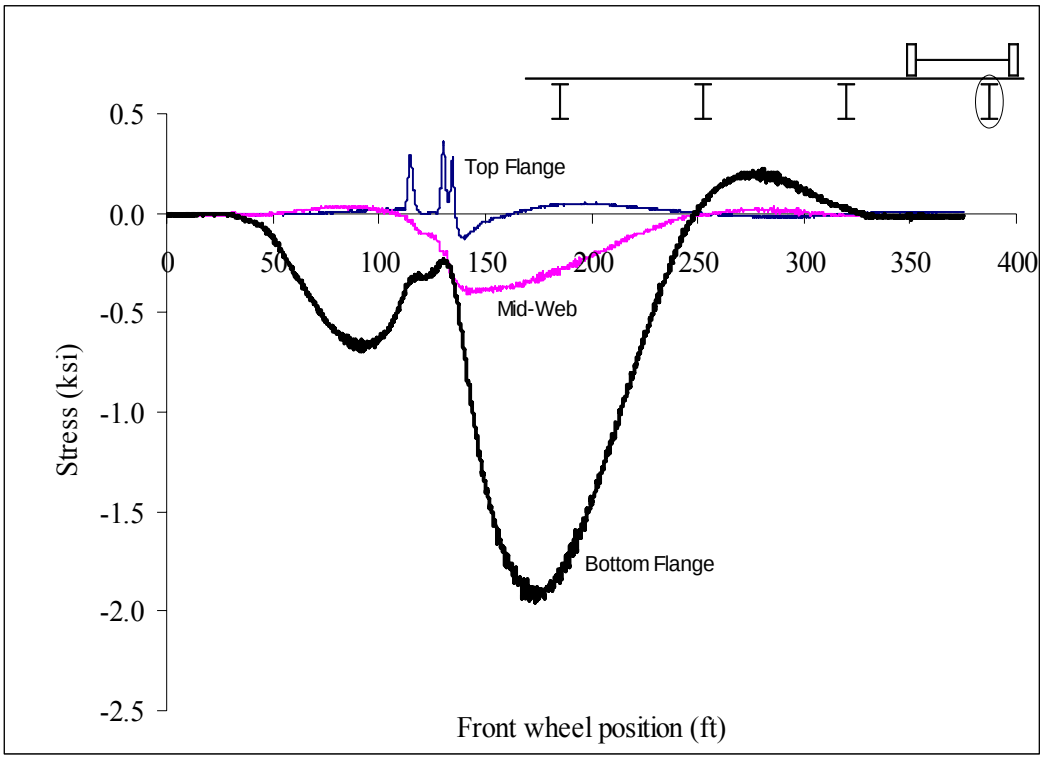

Figure A19: Las Cruces Bridge Test Run 1 S8 @ 2 ft from interior support

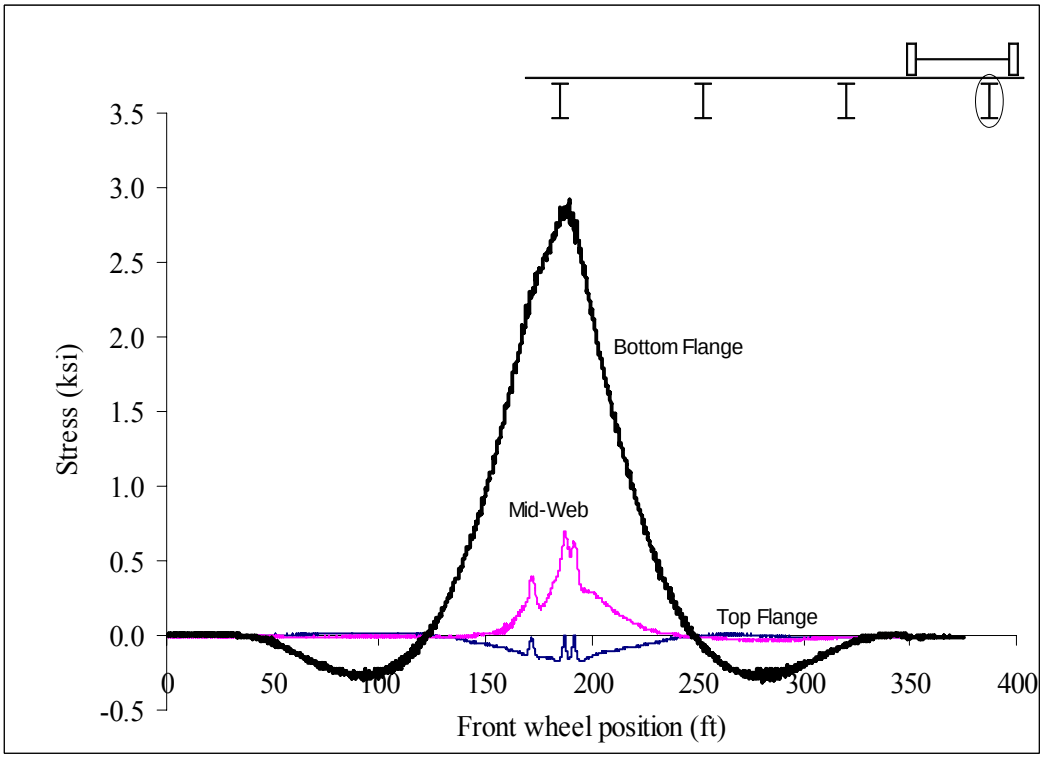

Figure A20: Las Cruces Bridge Test Run 1 S8 @ Midspan

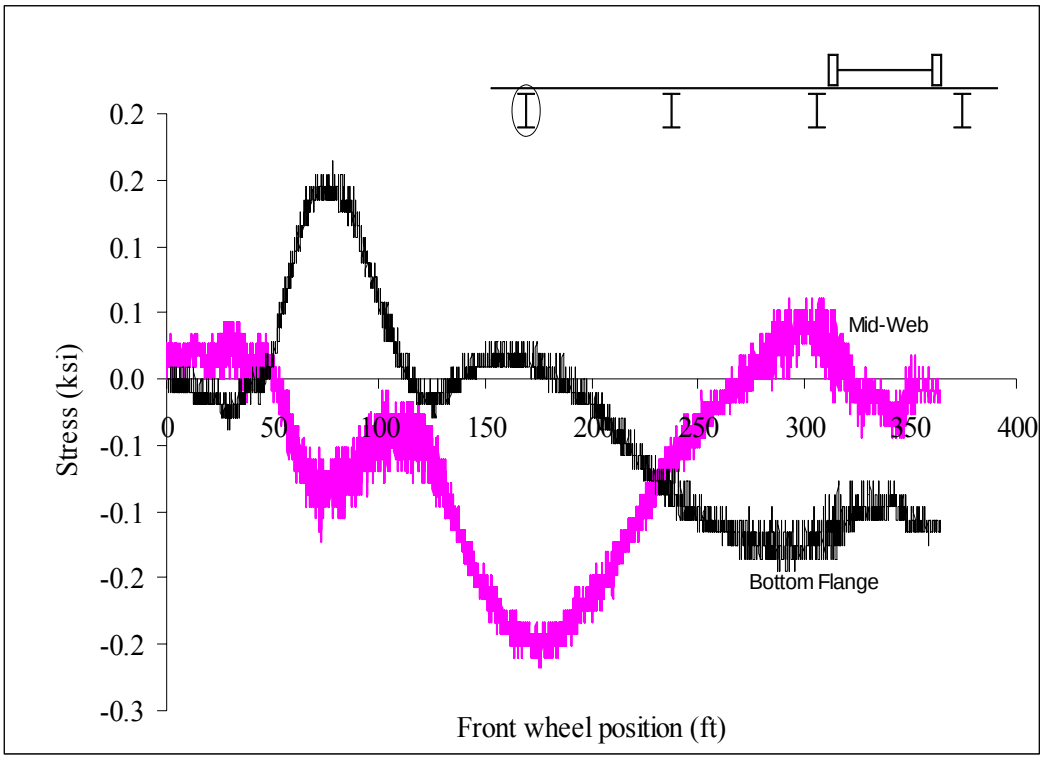

Figure A21: Las Cruces Bridge Test Run 2 S1 @ 2 ft from abutment

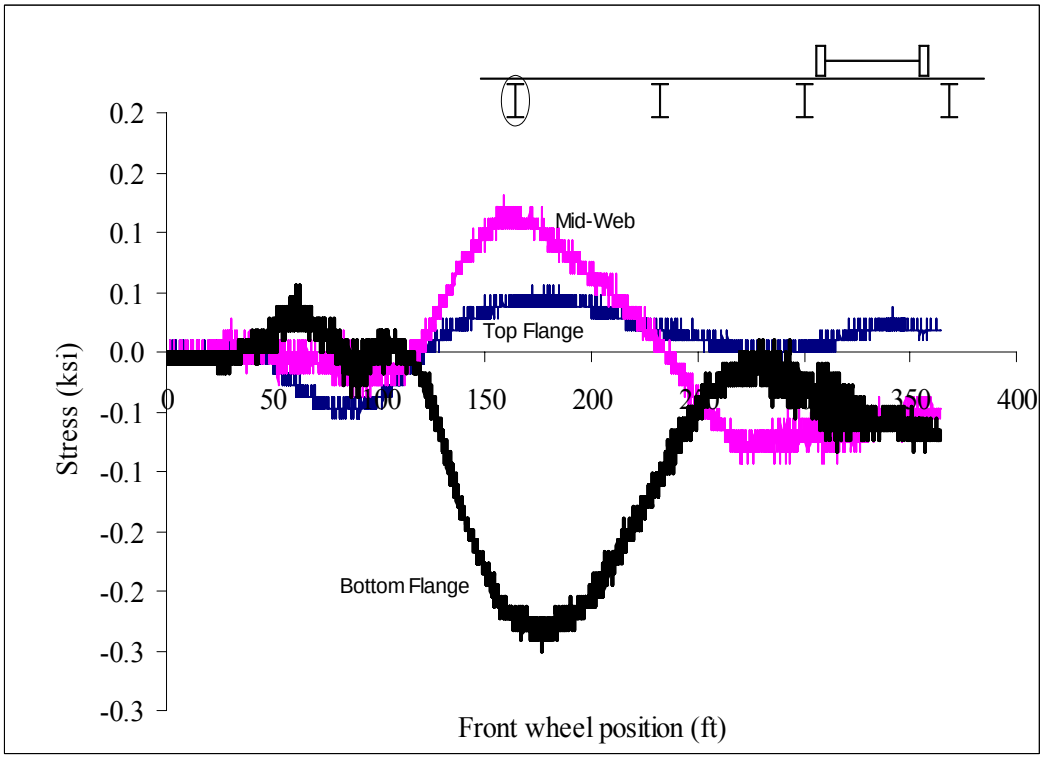

Figure A22: Las Cruces Bridge Test Run 2 S1 @ Midspan

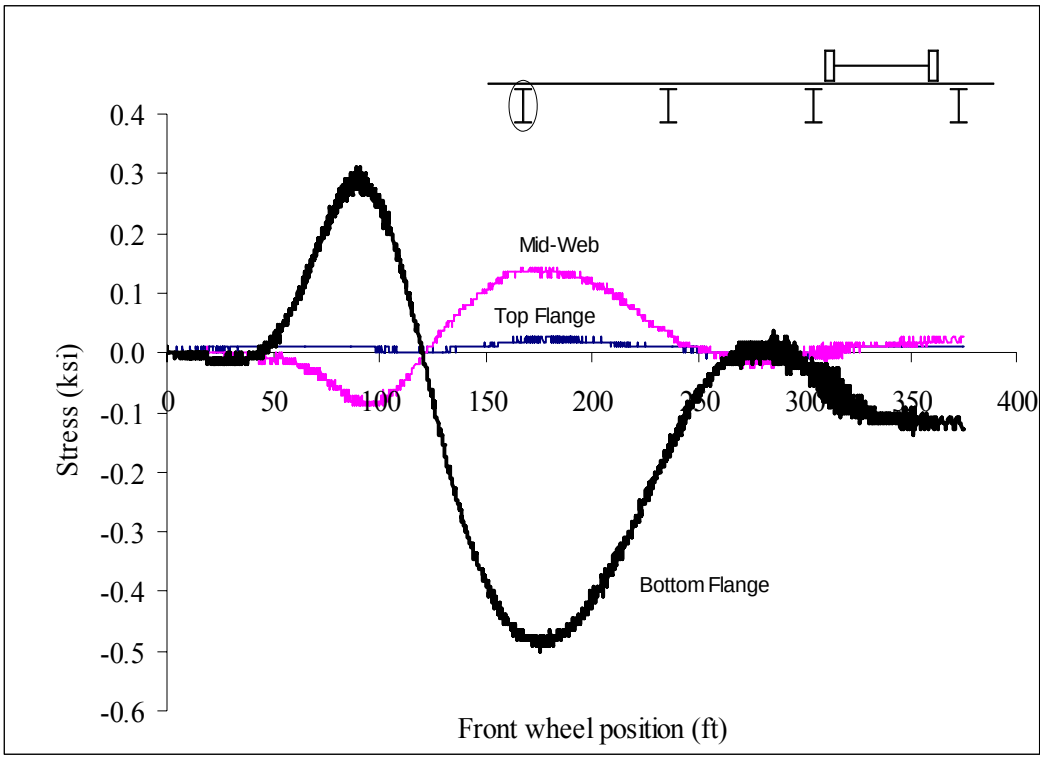

Figure A23: Las Cruces Bridge Test Run 2 S1 @ 2 ft from interior support

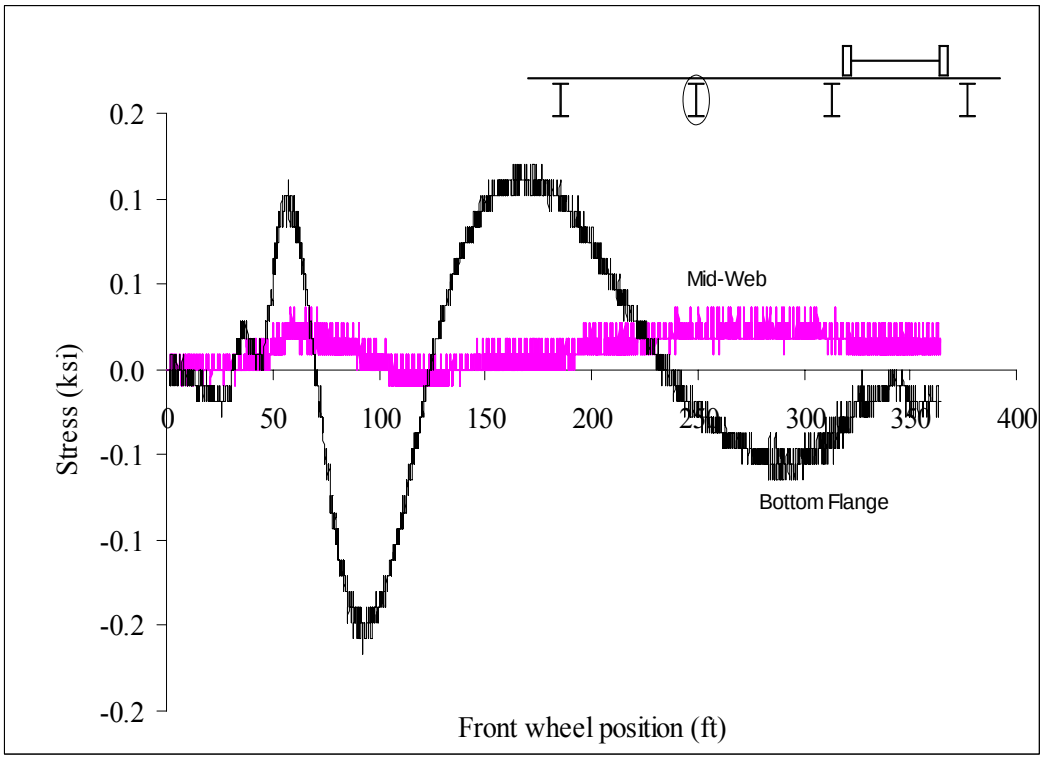

Figure A24: Las Cruces Bridge Test Run 2 S2 @ 2 ft from abutment

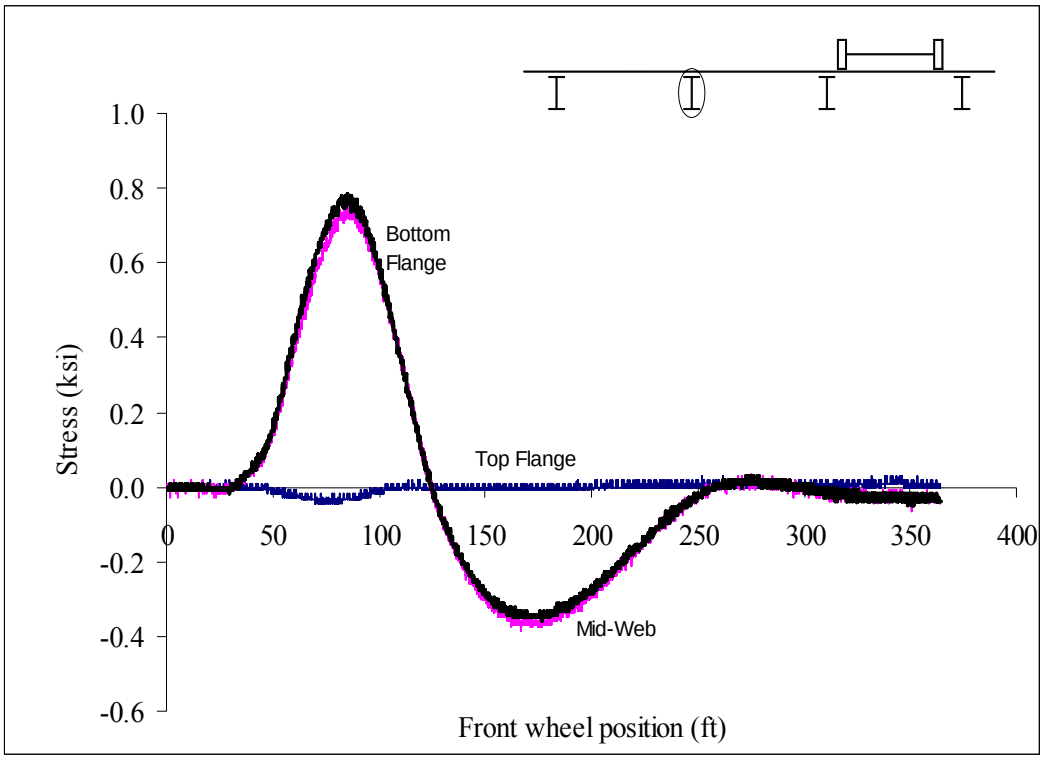

Figure A25: Las Cruces Bridge Test Run 2 S2 @ Midspan

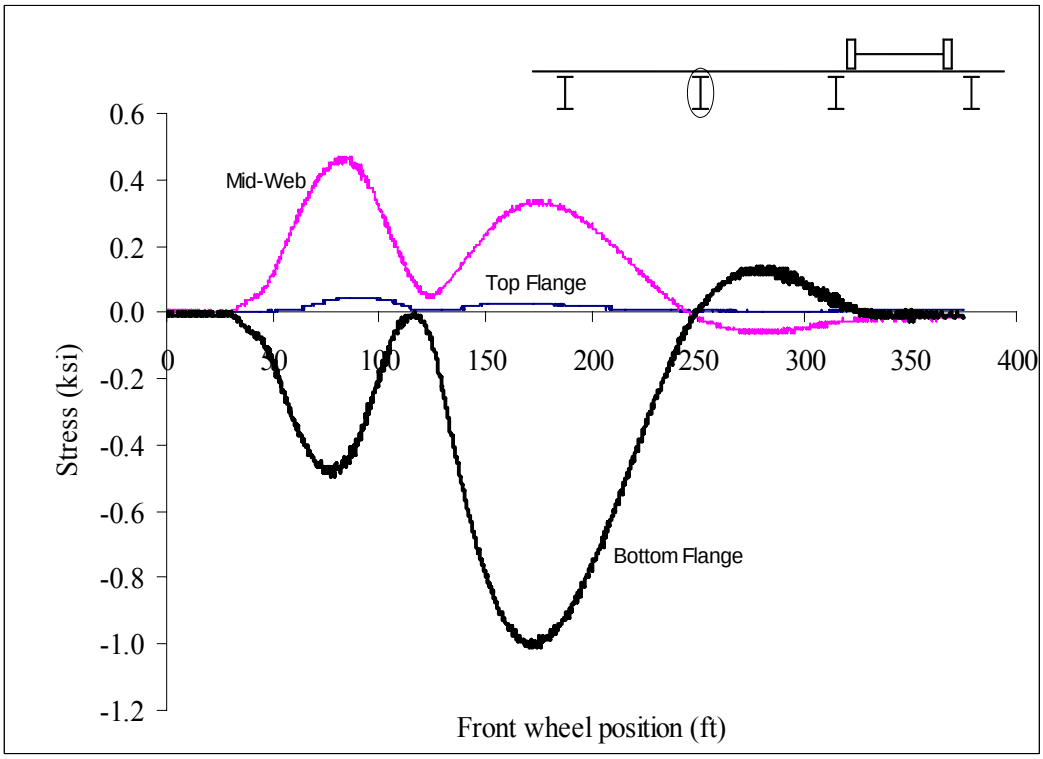

Figure A26: Las Cruces Bridge Test Run 2 S2 @ 2 ft from interior support

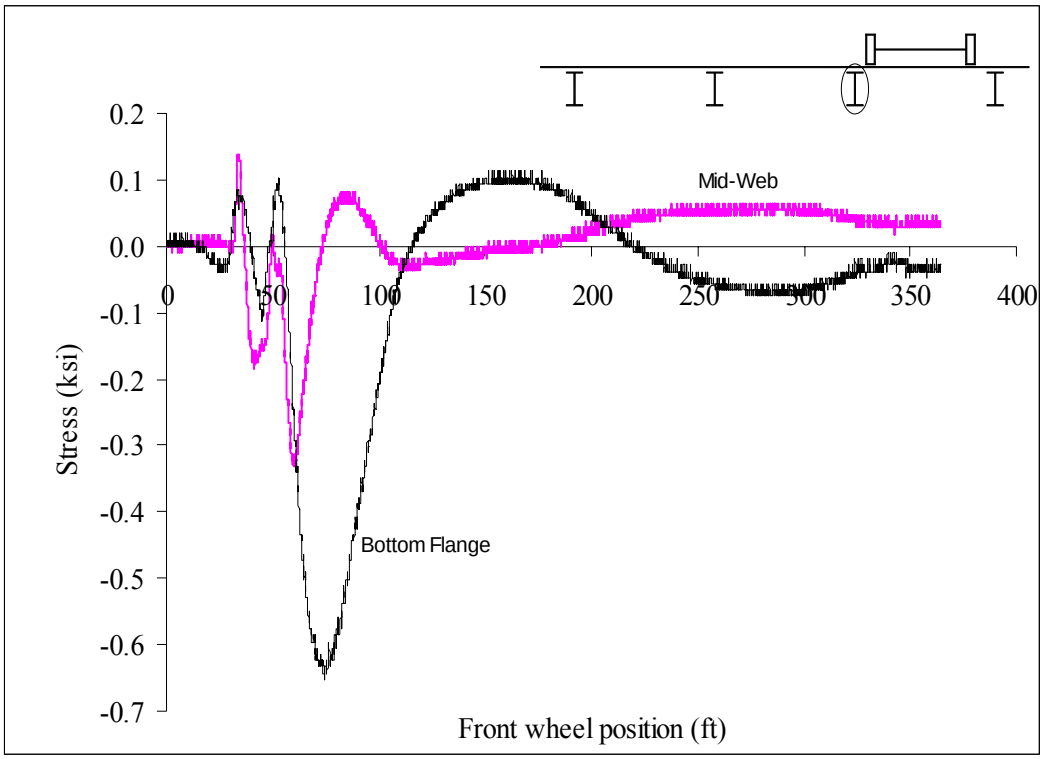

Figure A27: Las Cruces Bridge Test Run 2 S3 @ 2 ft from abutment

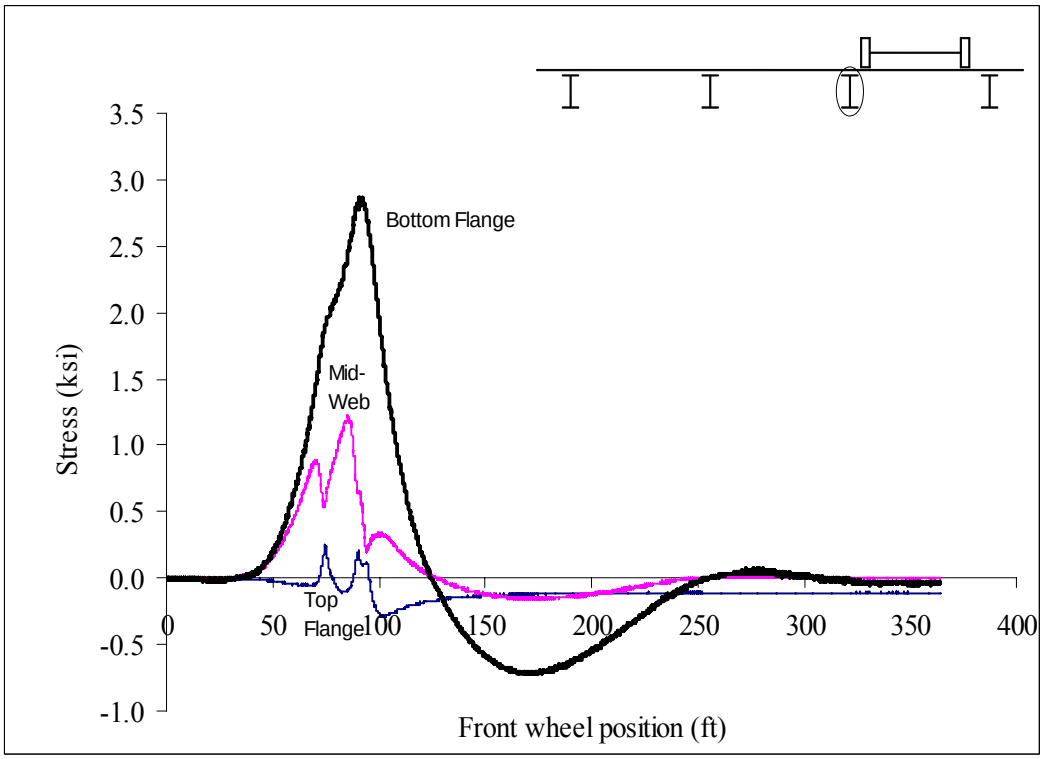

Figure A28: Las Cruces Bridge Test Run 2 S3 @ Midspan

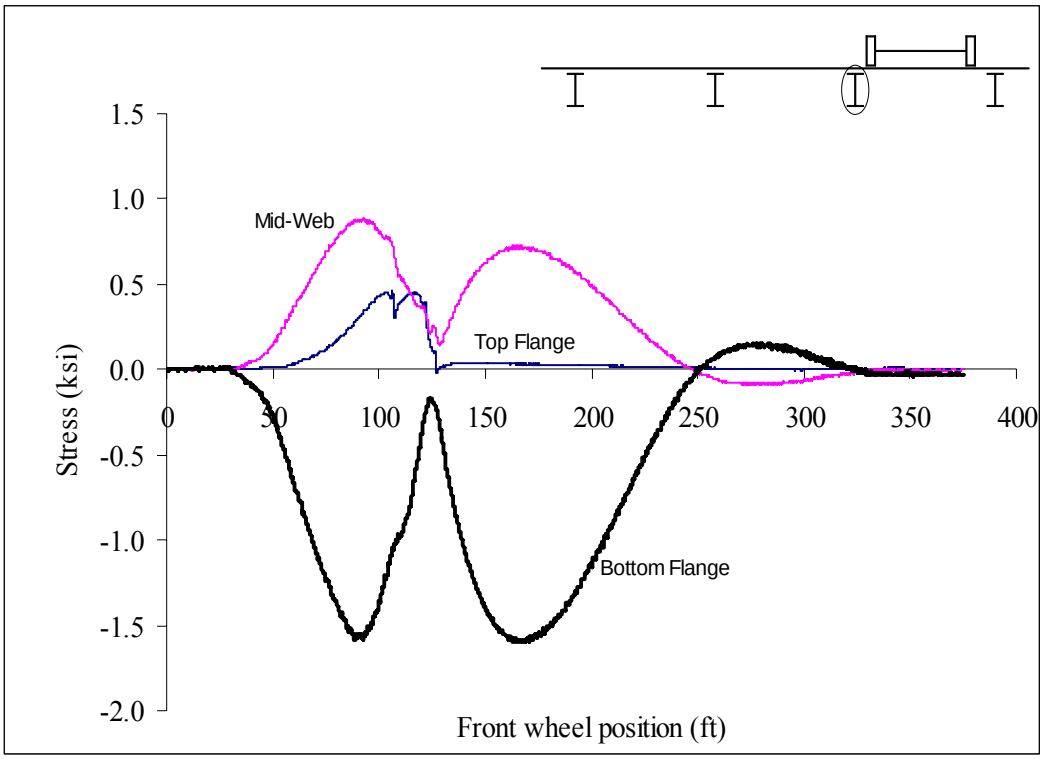

Figure A29: Las Cruces Bridge Test Run 2 S3 @ 2 ft from interior support

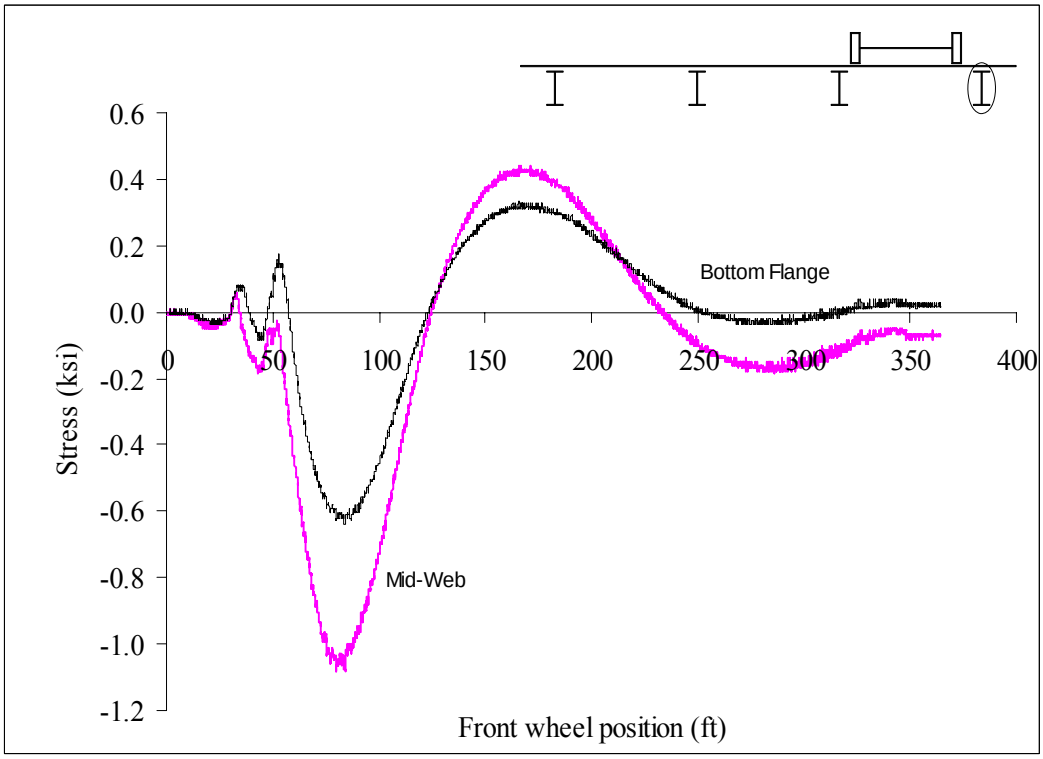

Figure A30: Las Cruces Bridge Test Run 2 S4 @ 2 ft from abutment

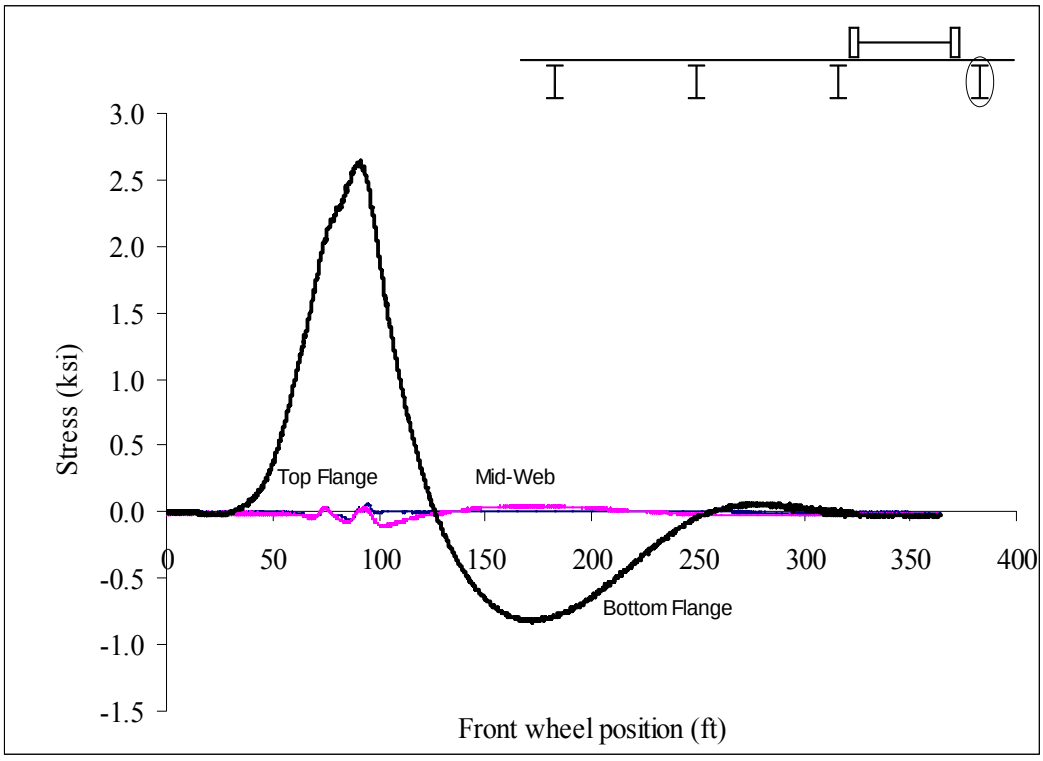

Figure A31: Las Cruces Bridge Test Run 2 S4 @ Midspan

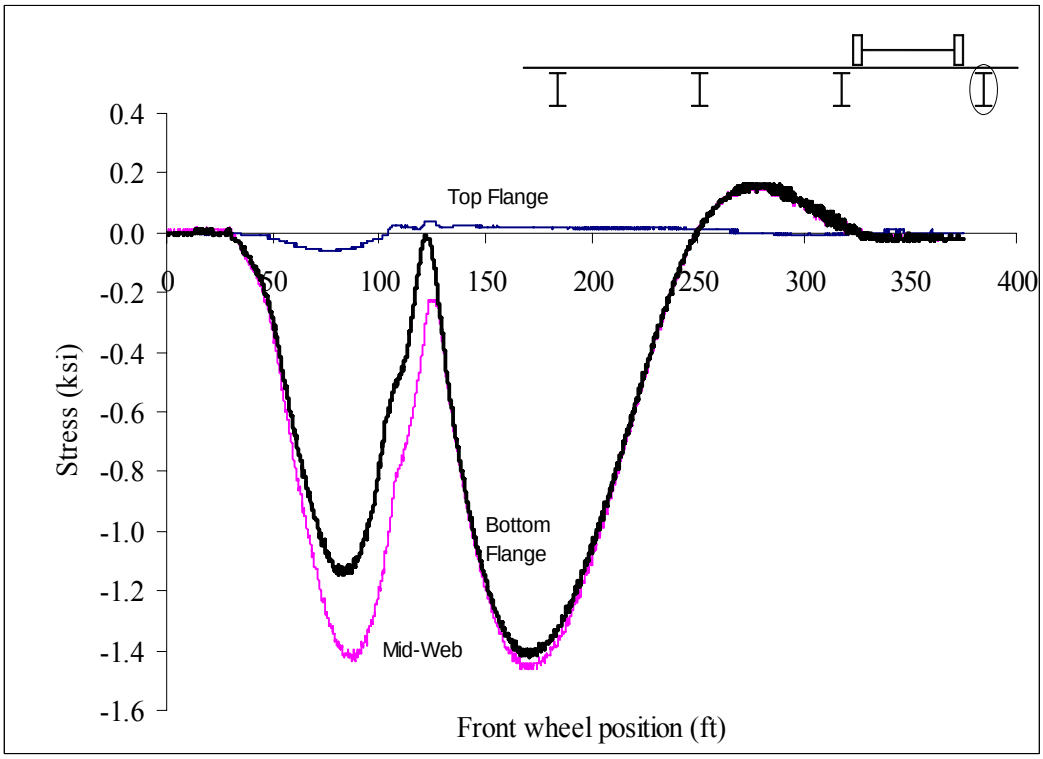

Figure A32: Las Cruces Bridge Test Run 2 S4 @ 2 ft from interior support

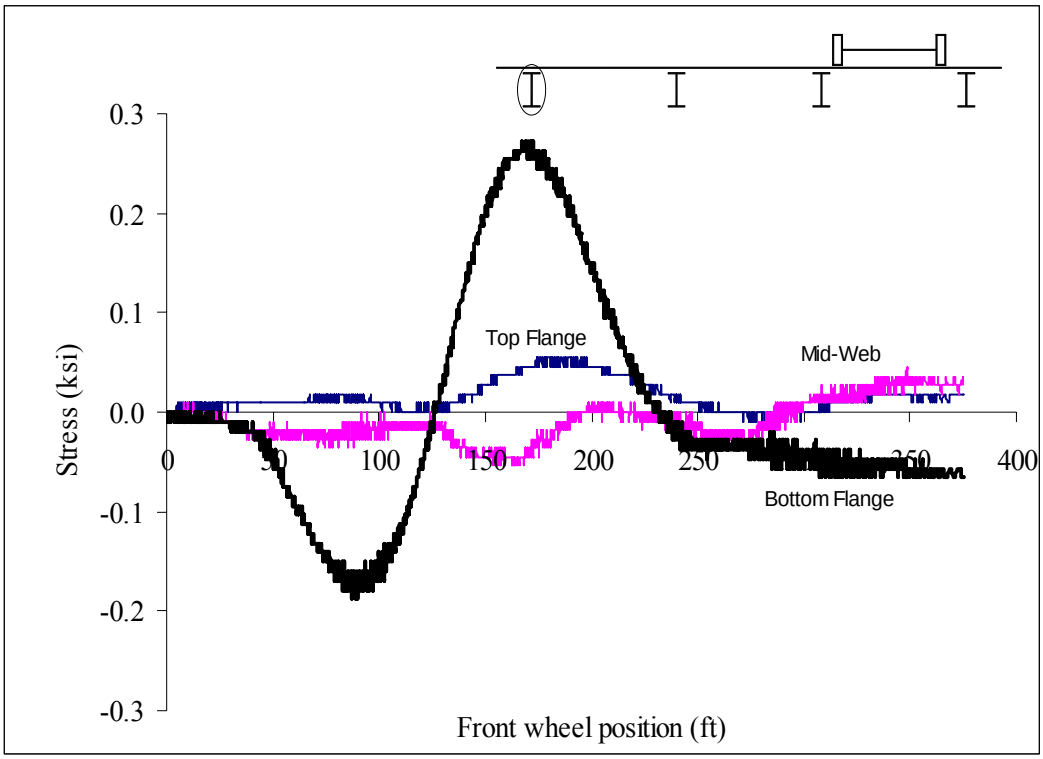

Figure A33: Las Cruces Bridge Test Run 2 S5 @ 2 ft from interior support

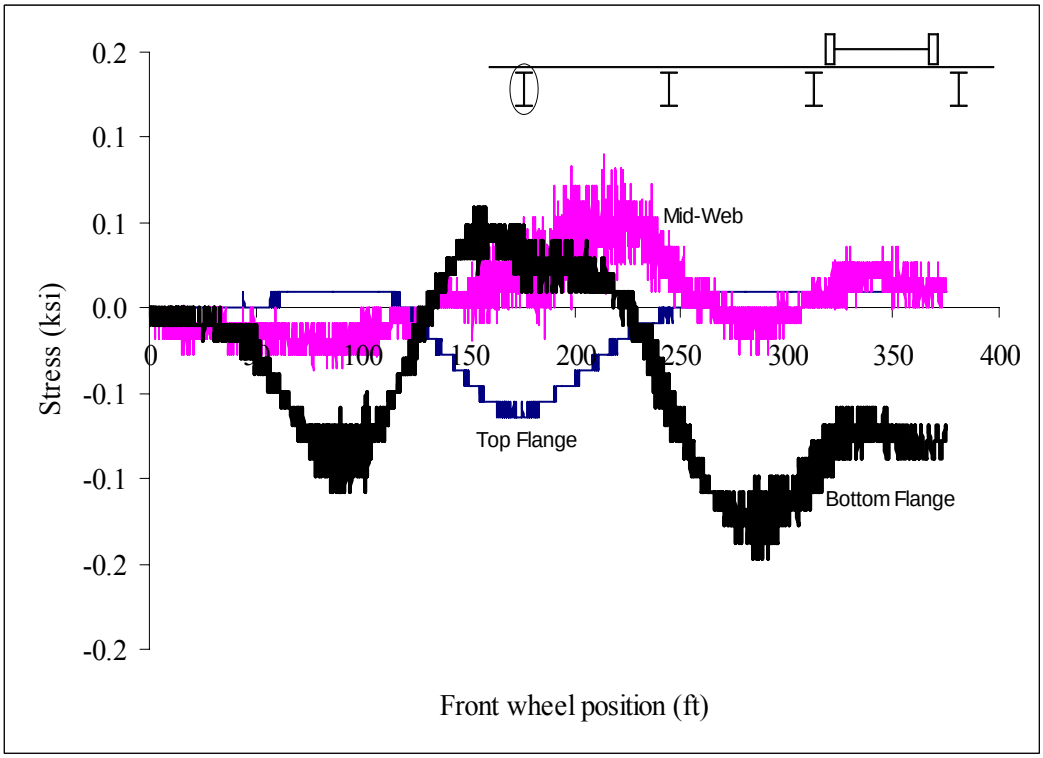

Figure A34: Las Cruces Bridge Test Run 2 S5 @ Midspan

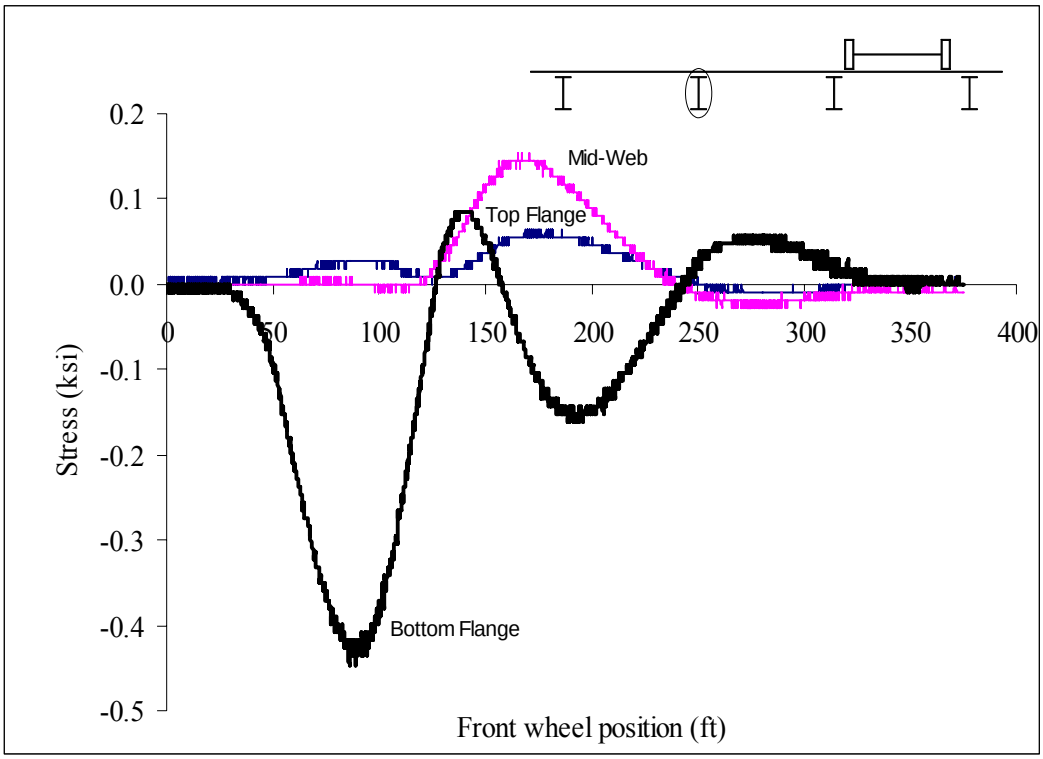

Figure A35: Las Cruces Bridge Test Run 2 S6 @ 2 ft from interior support

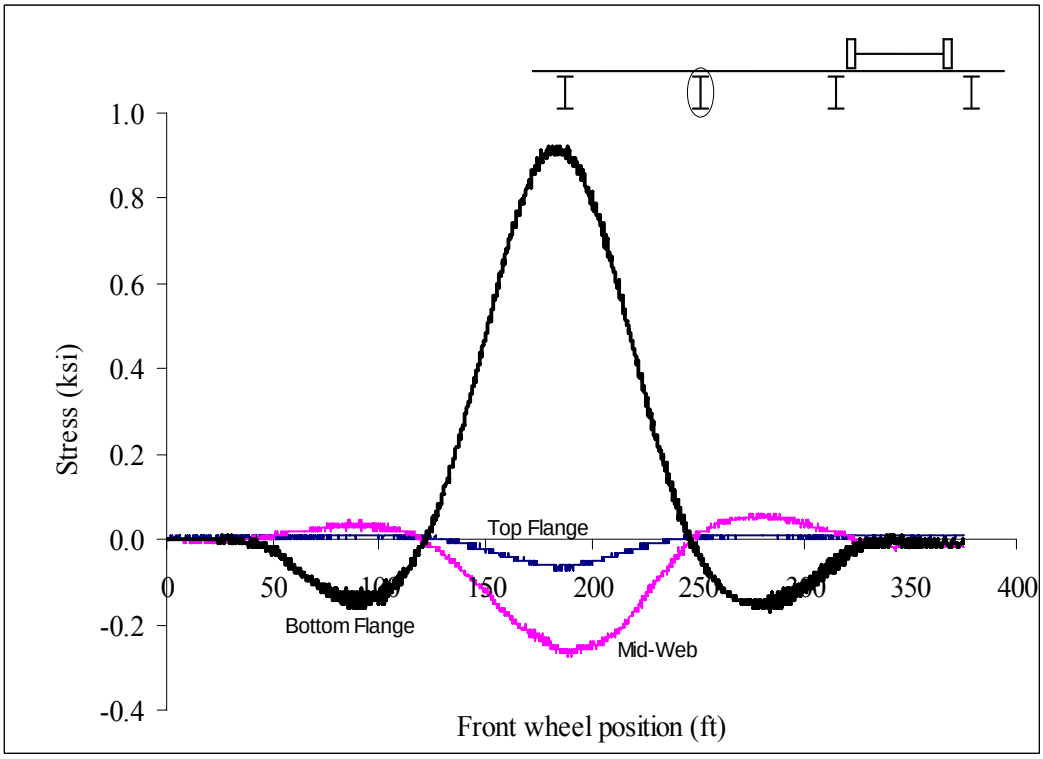

Figure A36: Las Cruces Bridge Test Run 2 S6 @ Midspan

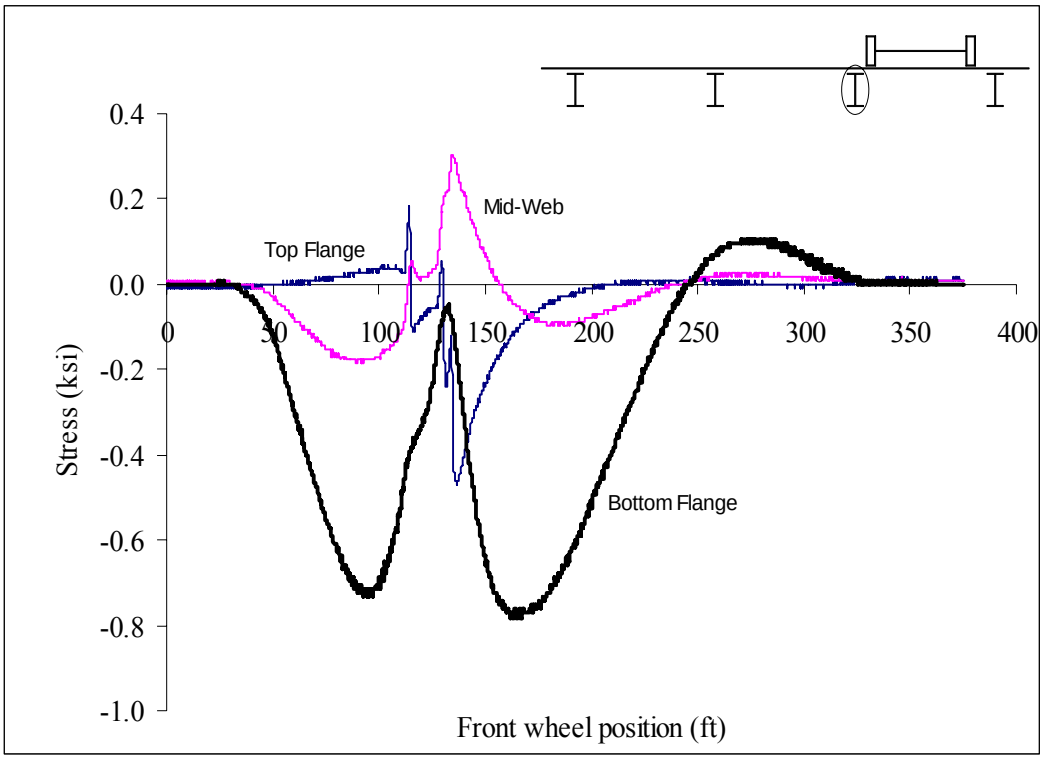

Figure A37: Las Cruces Bridge Test Run 2 S7 @ 2 ft from interior support

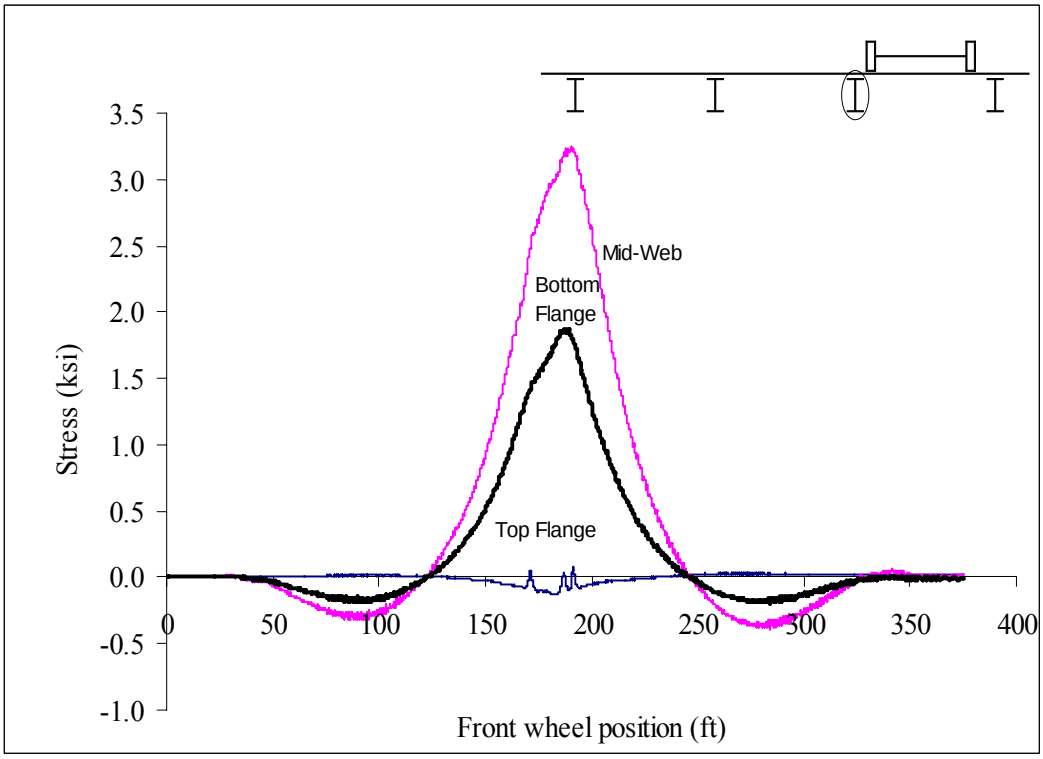

Figure A38: Las Cruces Bridge Test Run 2 S7 @ Midspan

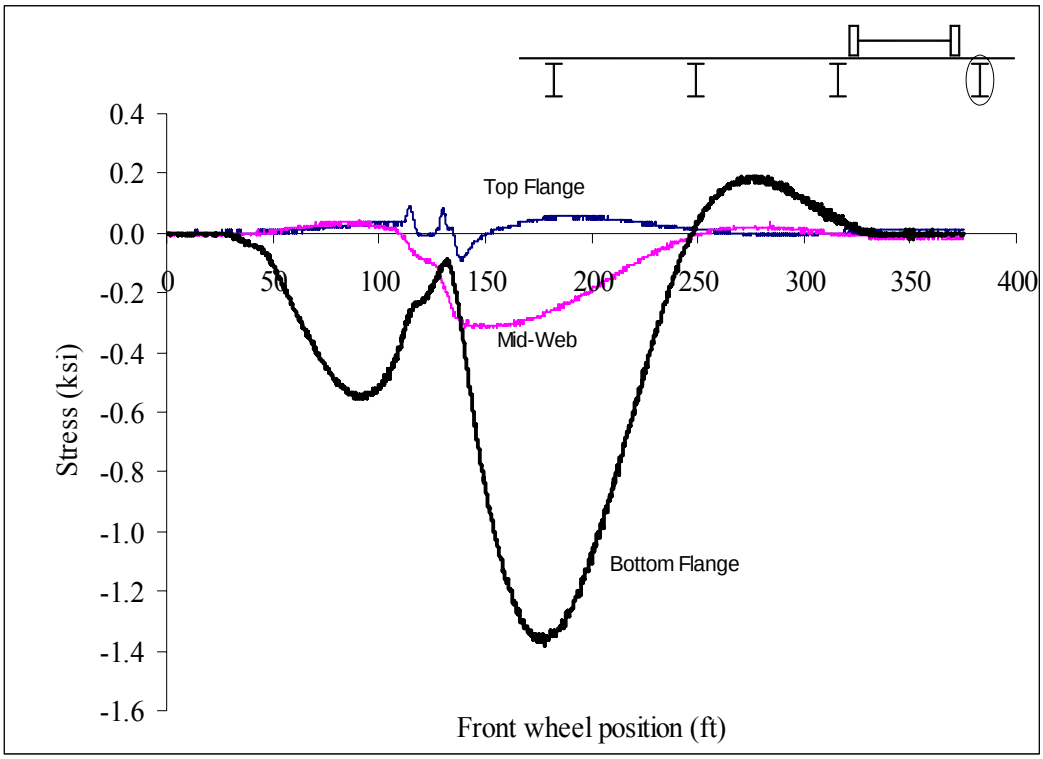

Figure A39: Las Cruces Bridge Test Run 2 S8 @ 2 ft from interior support

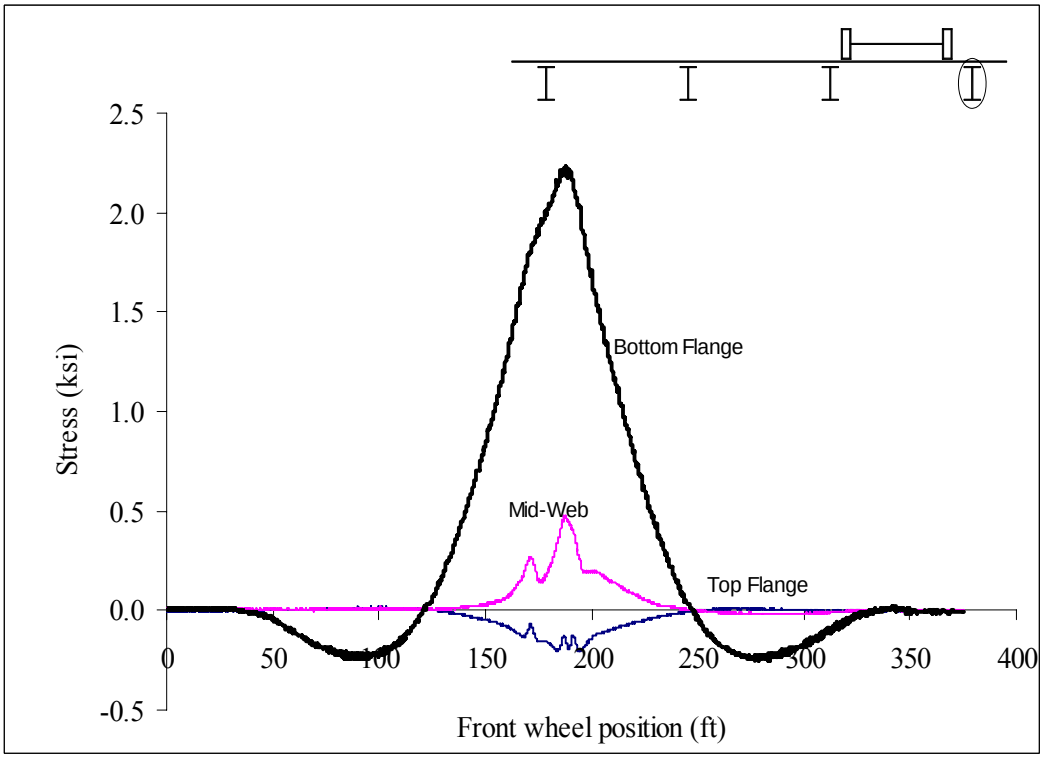

Figure A40: Las Cruces Bridge Test Run 2 S8 @ Midspan

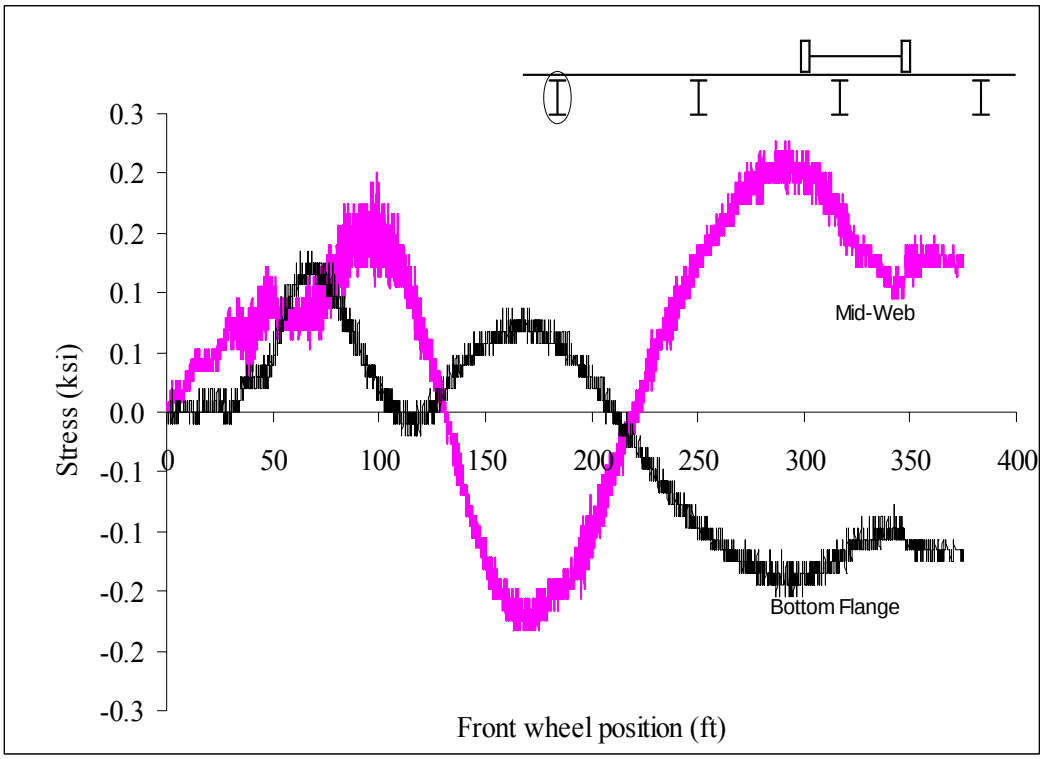

Figure A41: Las Cruces Bridge Test Run 3 S1 @ 2 ft from abutment

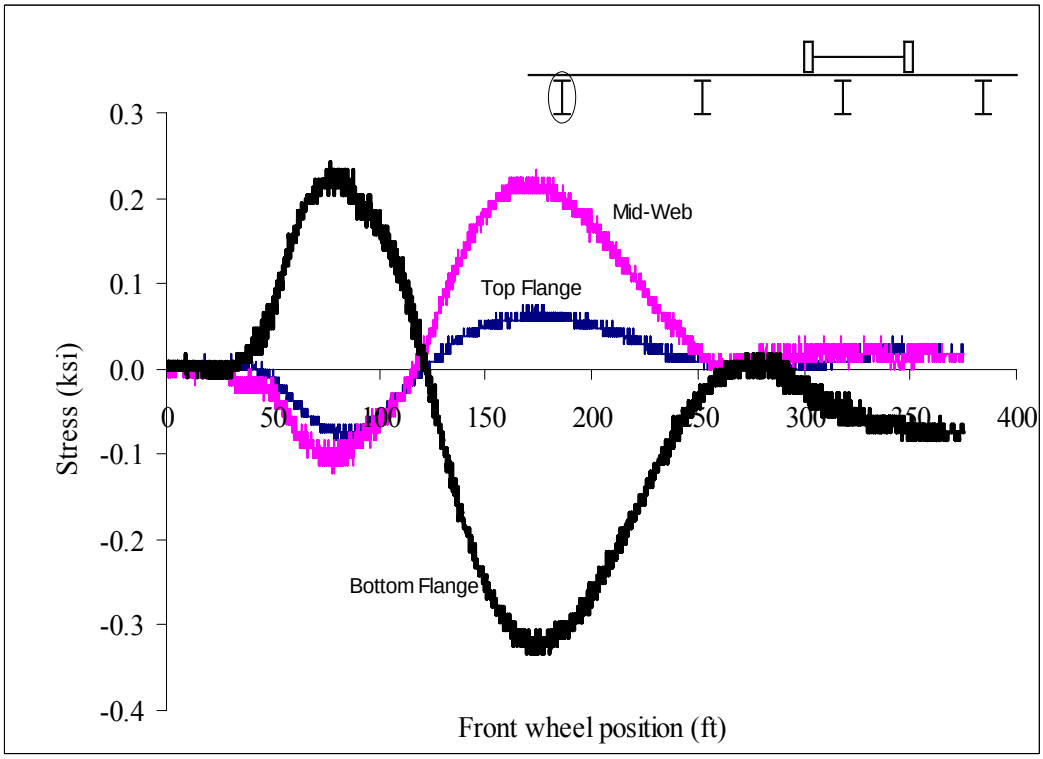

Figure A42: Las Cruces Bridge Test Run 3 S1 @ Midspan

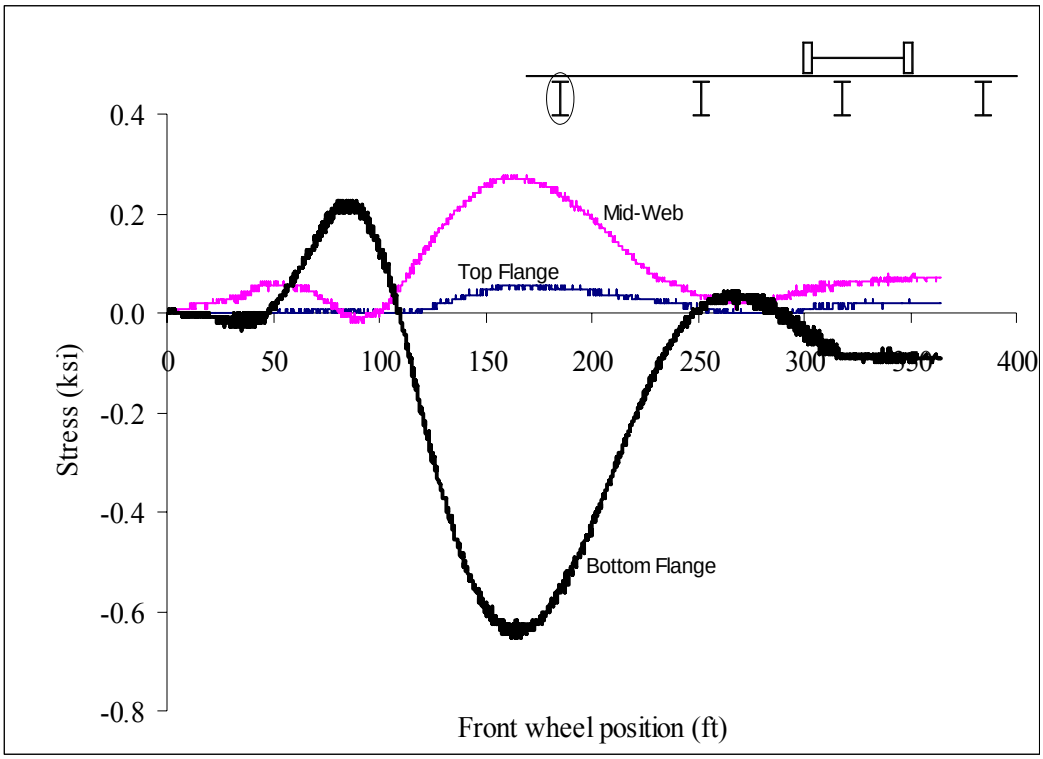

Figure A43: Las Cruces Bridge Test Run 3 S1 @ 2 ft from interior support

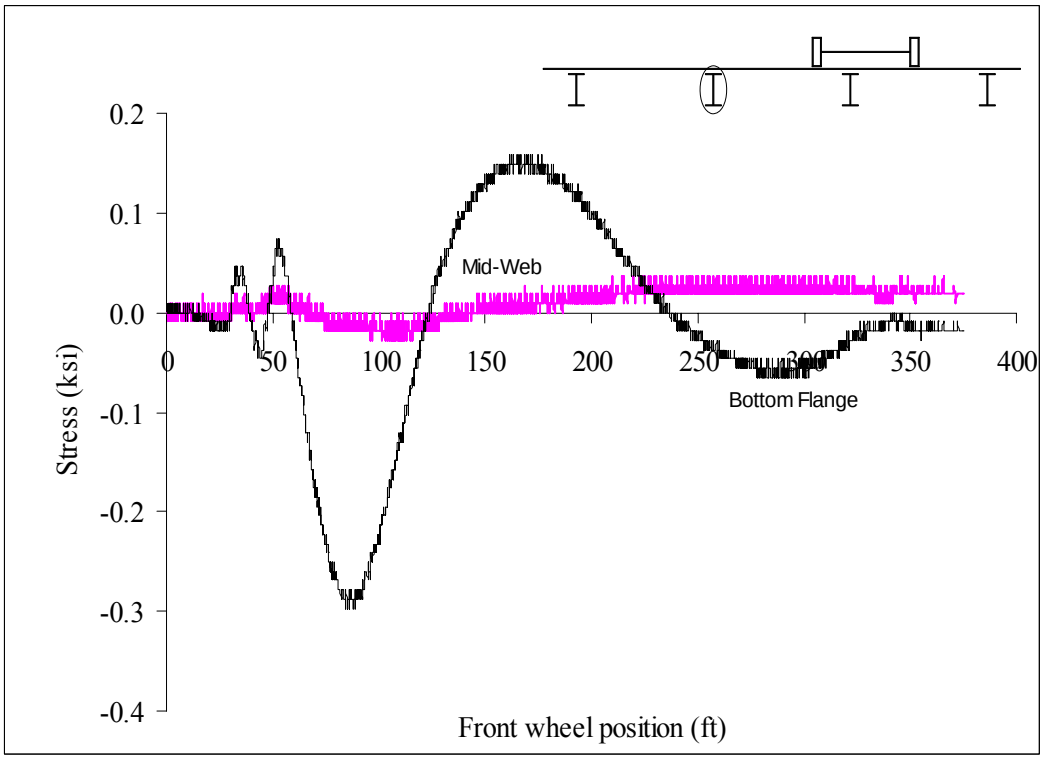

Figure A44: Las Cruces Bridge Test Run 3 S2 @ 2 ft from abutment

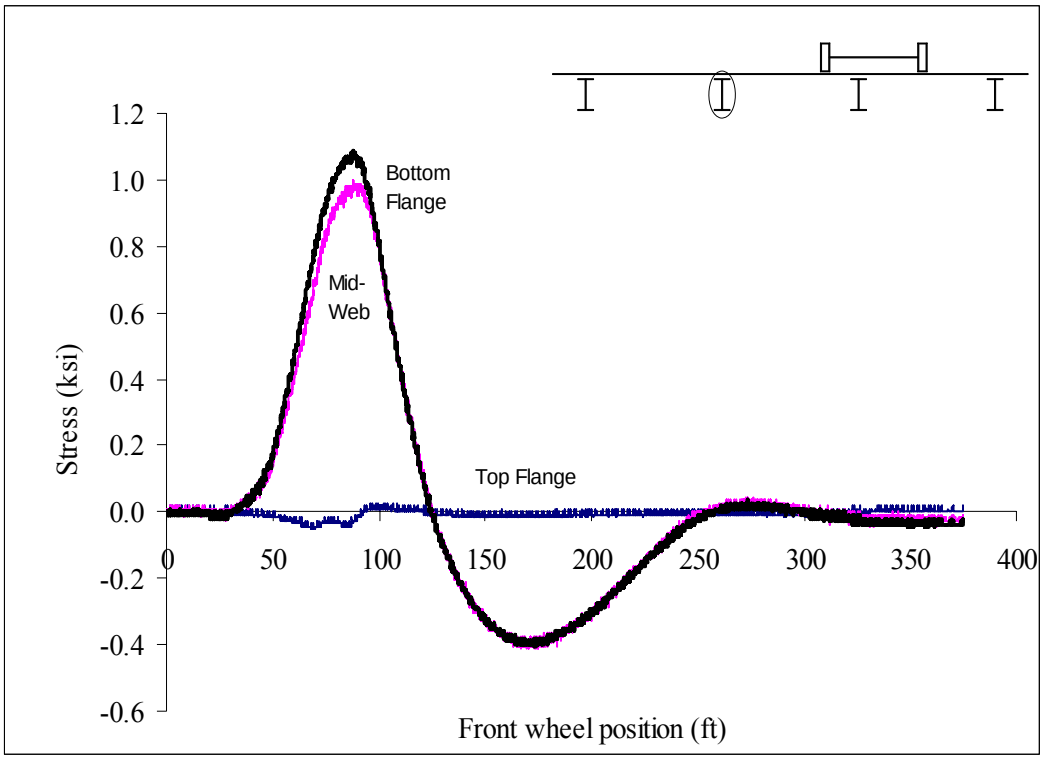

Figure A45: Las Cruces Bridge Test Run 3 S2 @ Midspan

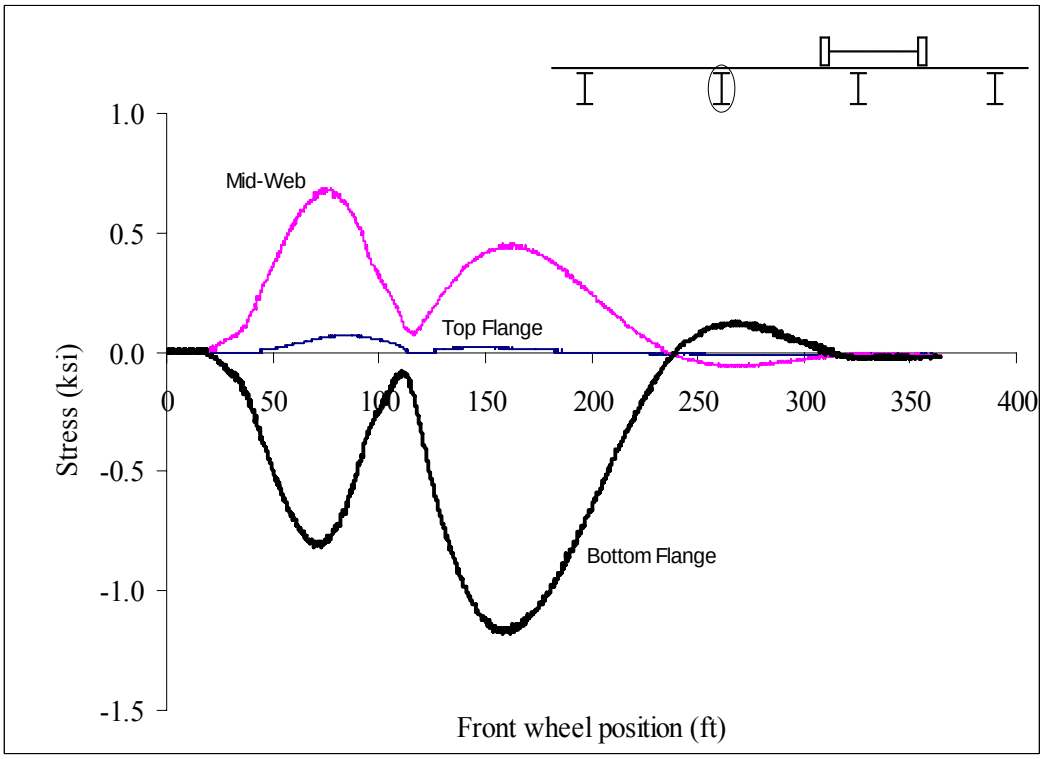

Figure A46: Las Cruces Bridge Test Run 3 S2 @ 2 ft from interior support

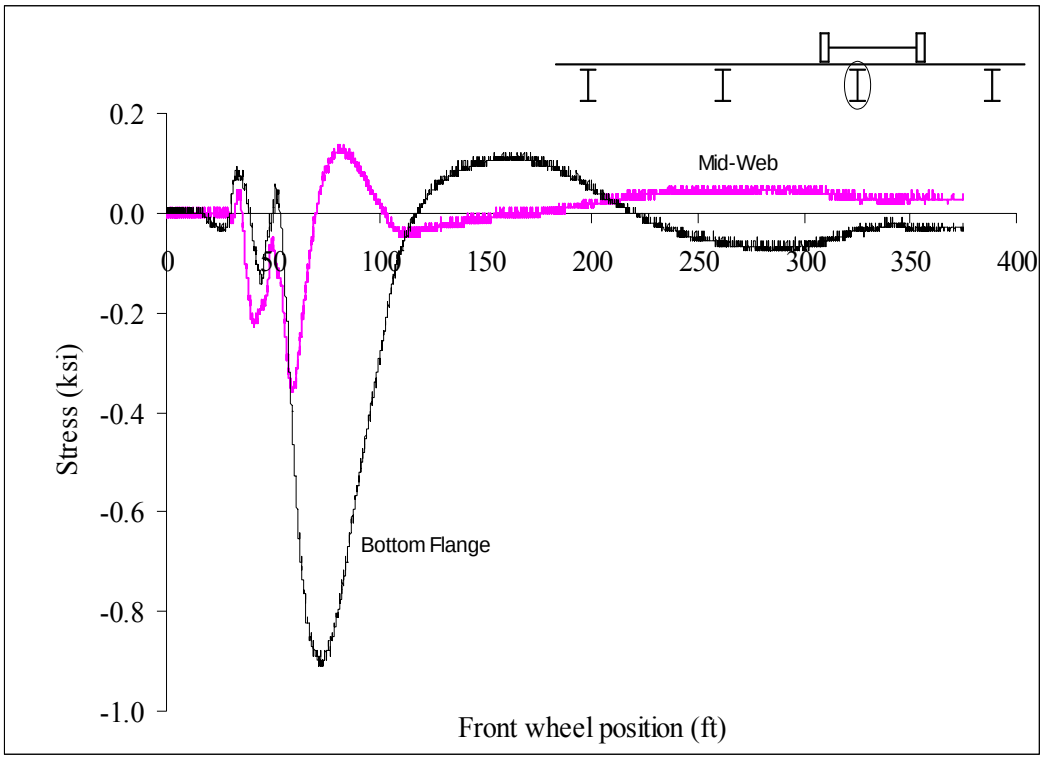

Figure A47: Las Cruces Bridge Test Run 3 S3 @ 2 ft from abutment

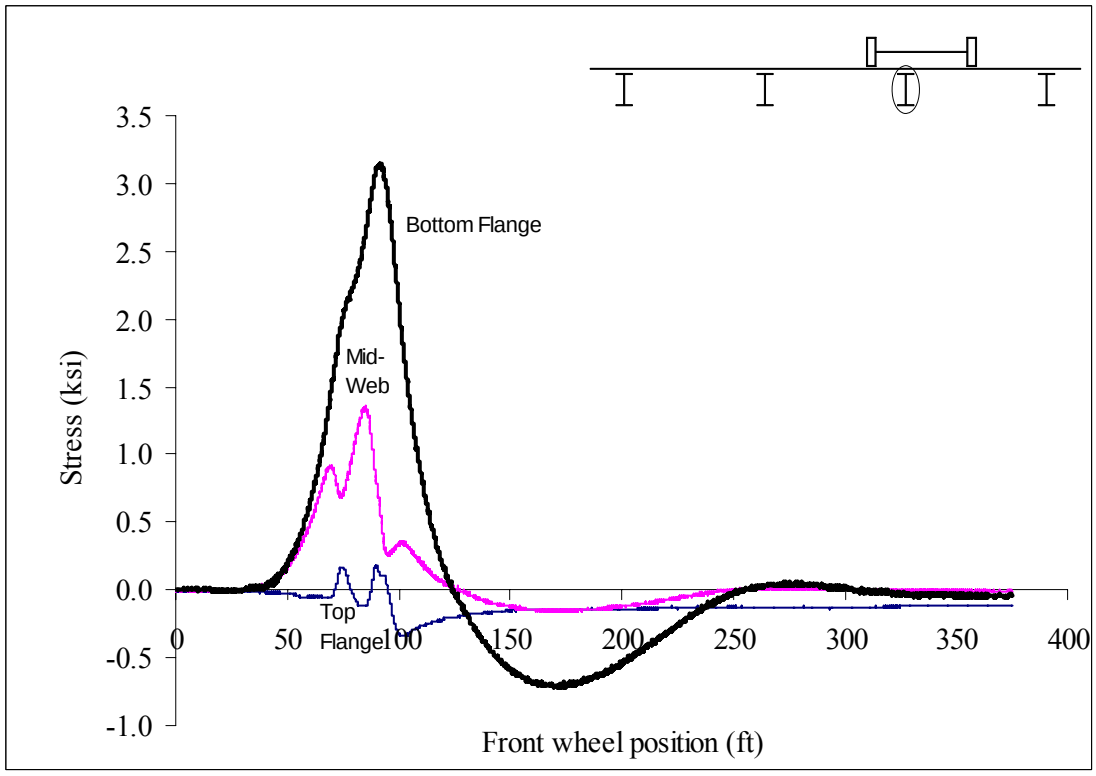

Figure A48: Las Cruces Bridge Test Run 3 S3 @ Midspan

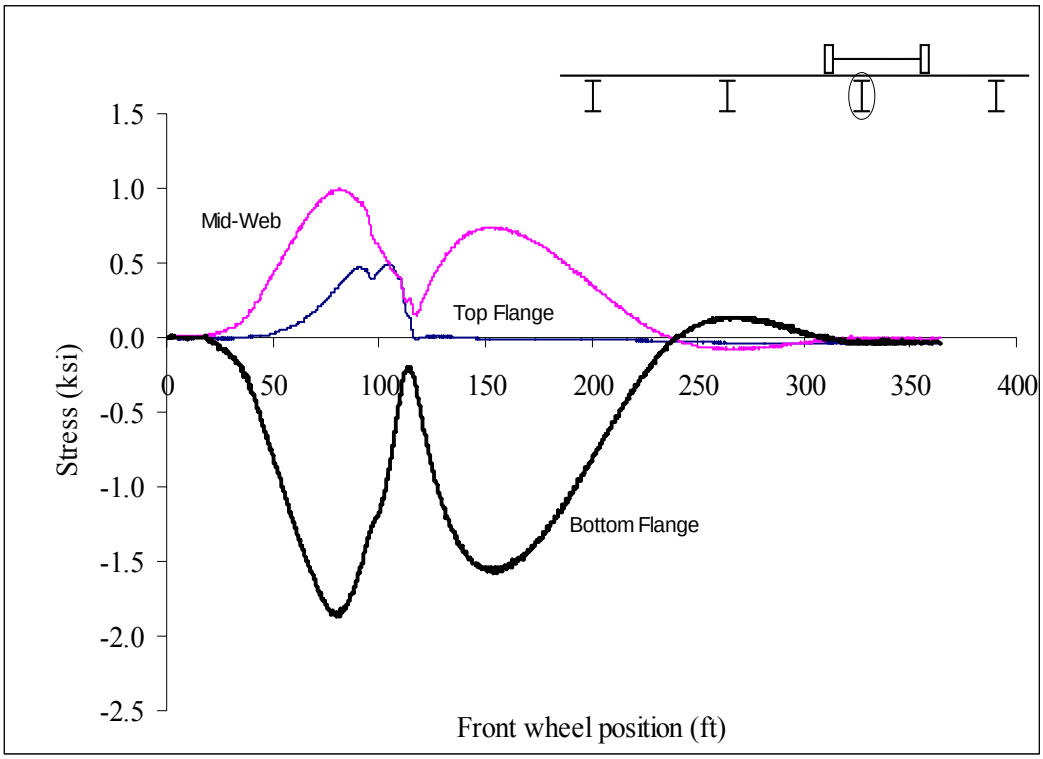

Figure A49: Las Cruces Bridge Test Run 3 S3 @ 2 ft from interior support

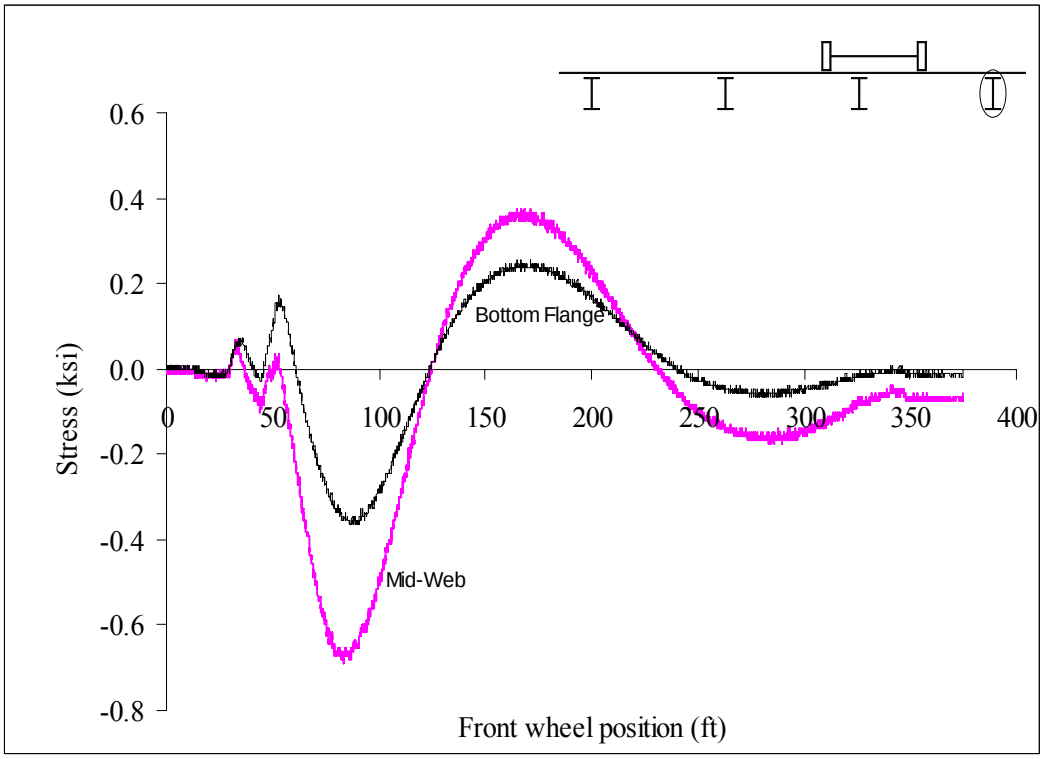

Figure A50: Las Cruces Bridge Test Run 3 S4 @ 2 ft from abutment

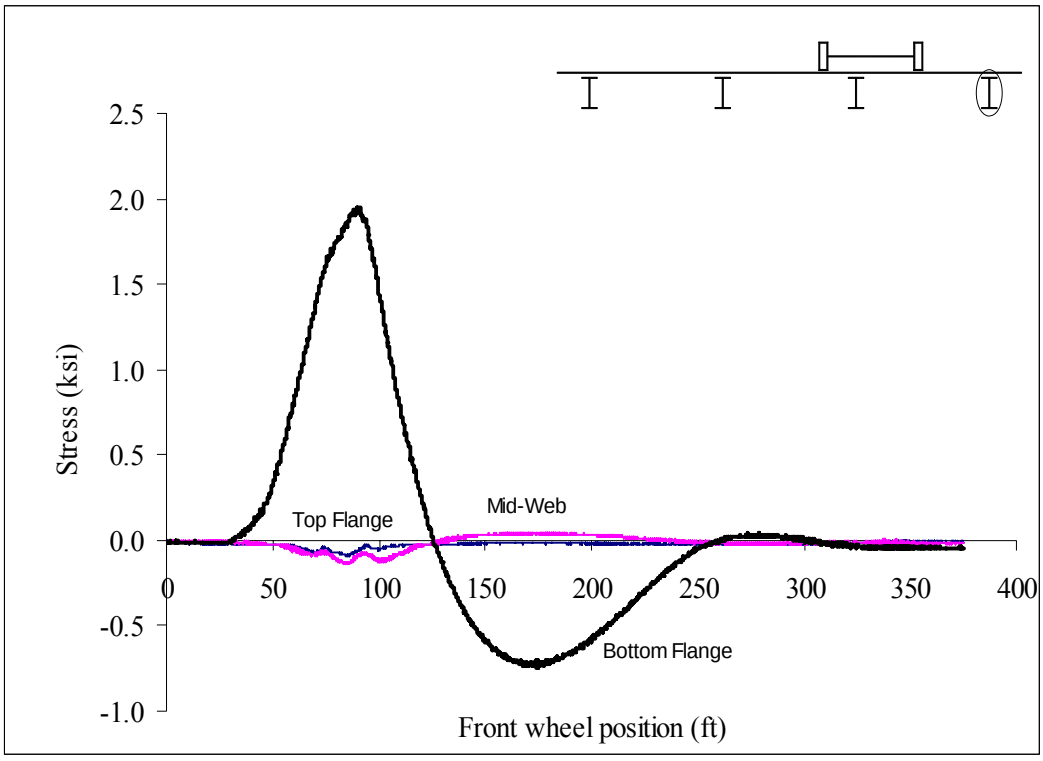

Figure A51: Las Cruces Bridge Test Run 3 S4 @ Midspan

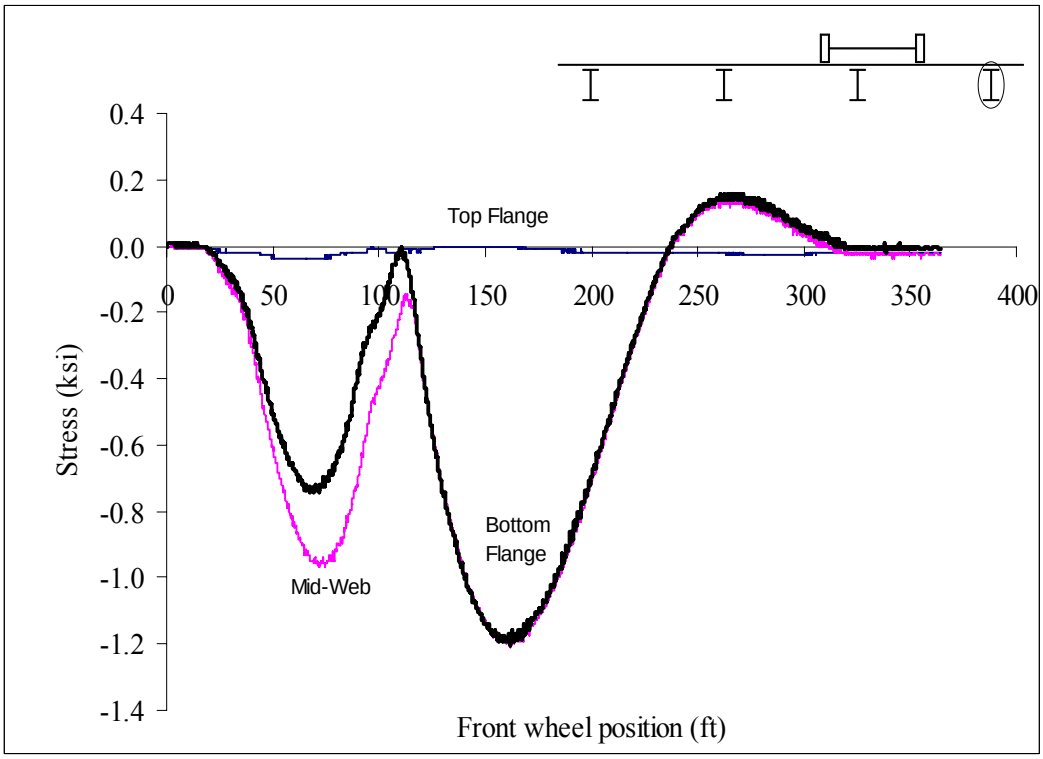

Figure A52: Las Cruces Bridge Test Run 3 S4 @ 2 ft from interior support

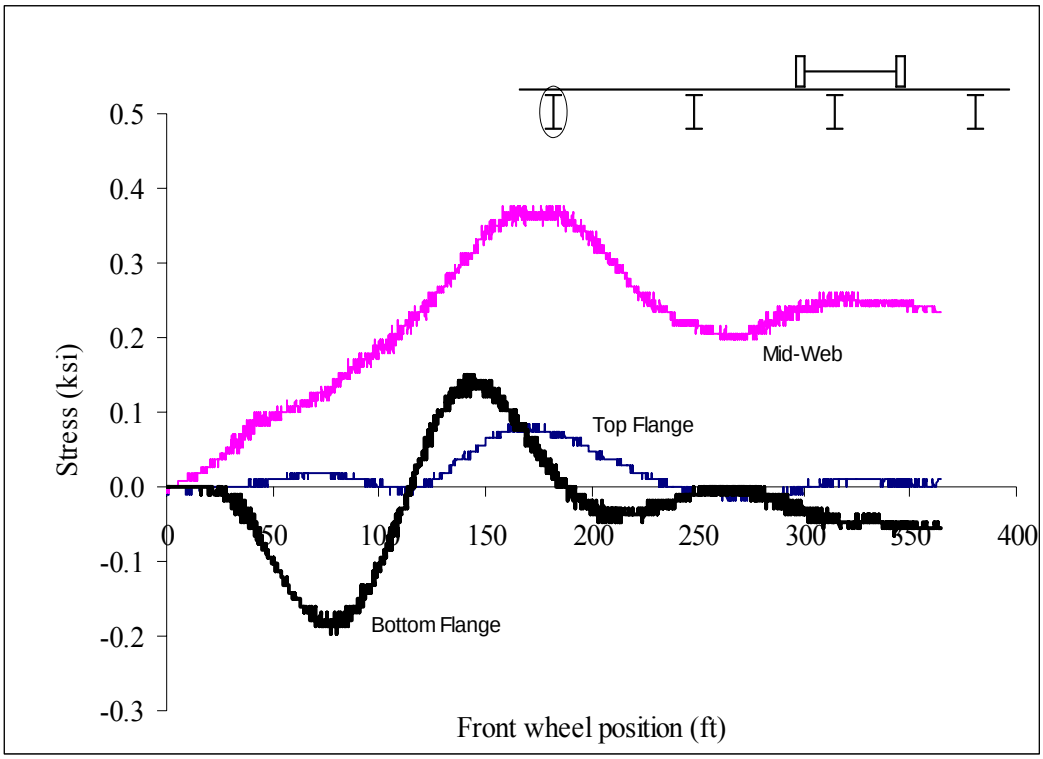

Figure A52: Las Cruces Bridge Test Run 3 S5 @ 2 ft from interior support

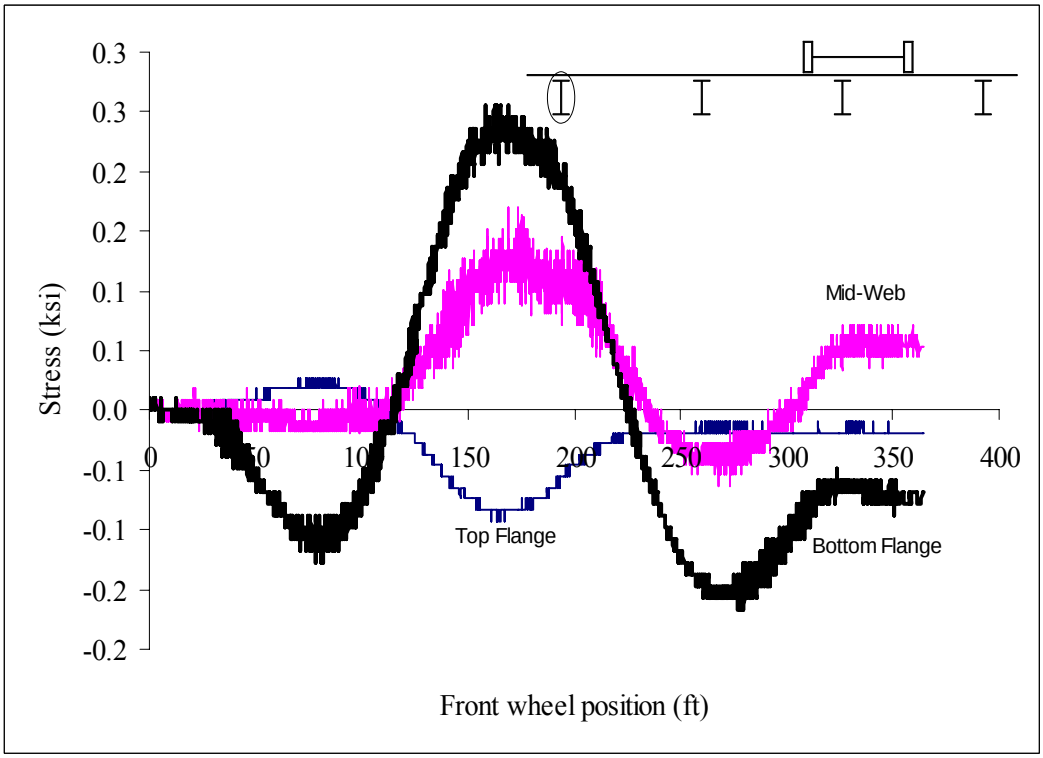

Figure A53: Las Cruces Bridge Test Run 3 S5 @ Midspan

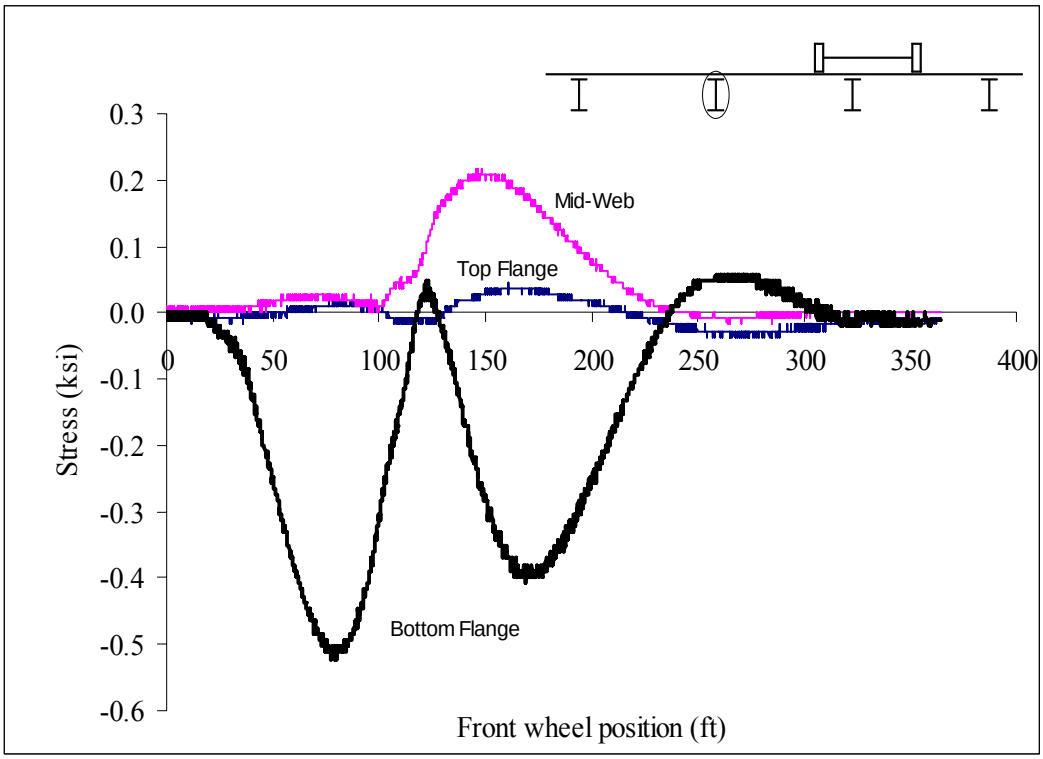

Figure A54: Las Cruces Bridge Test Run 3 S6 @ 2 ft from interior support

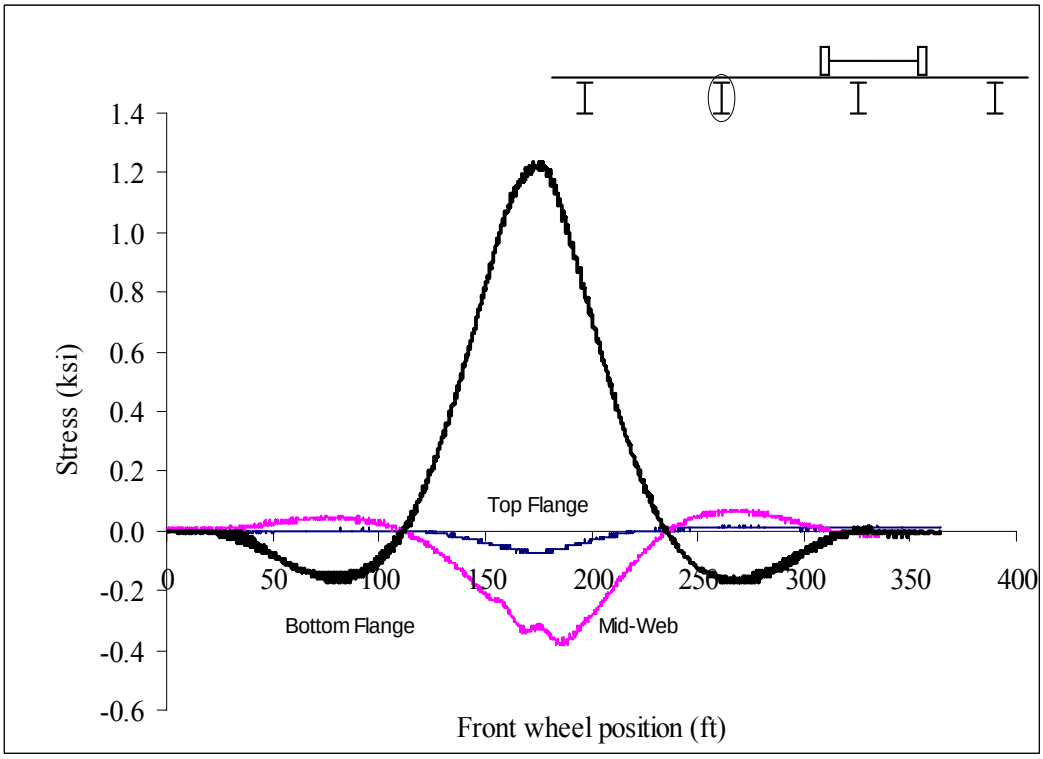

Figure A55: Las Cruces Bridge Test Run 3 S6 @ Midspan

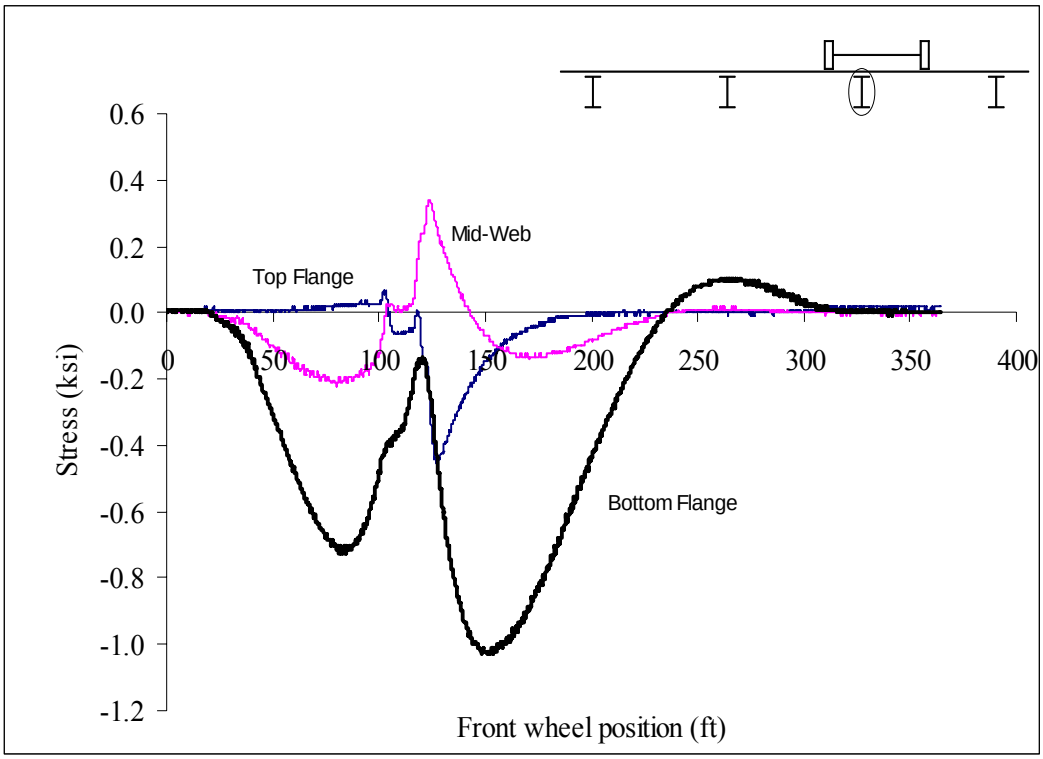

Figure A56: Las Cruces Bridge Test Run 3 S7 @ 2 ft from interior support

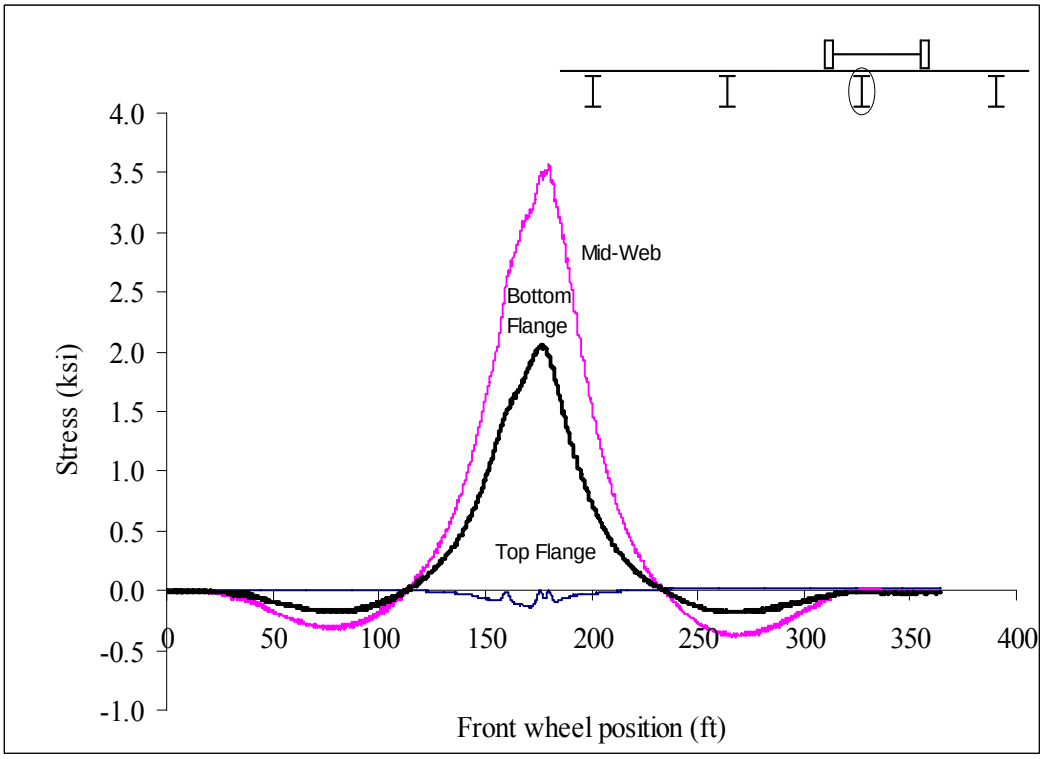

Figure A57: Las Cruces Bridge Test Run 3 S7 @ Midspan

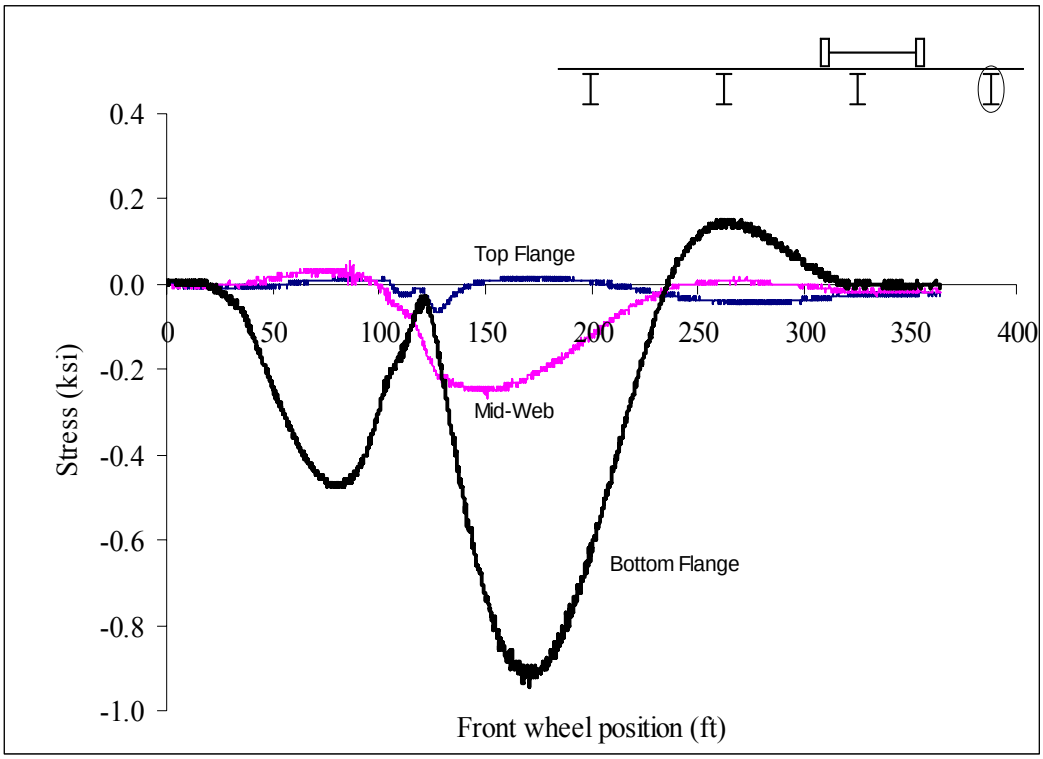

Figure A58: Las Cruces Bridge Test Run 3 S8 @ 2 ft from interior support

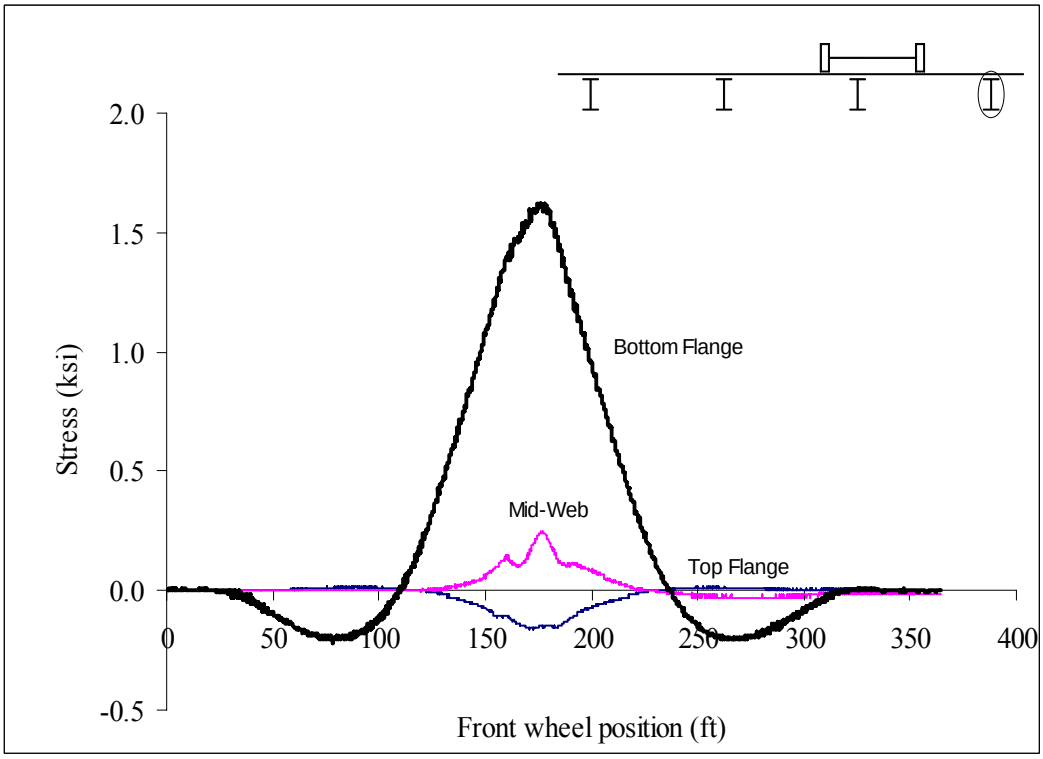

Figure A59: Las Cruces Bridge Test Run 3 S8 @ Midspan

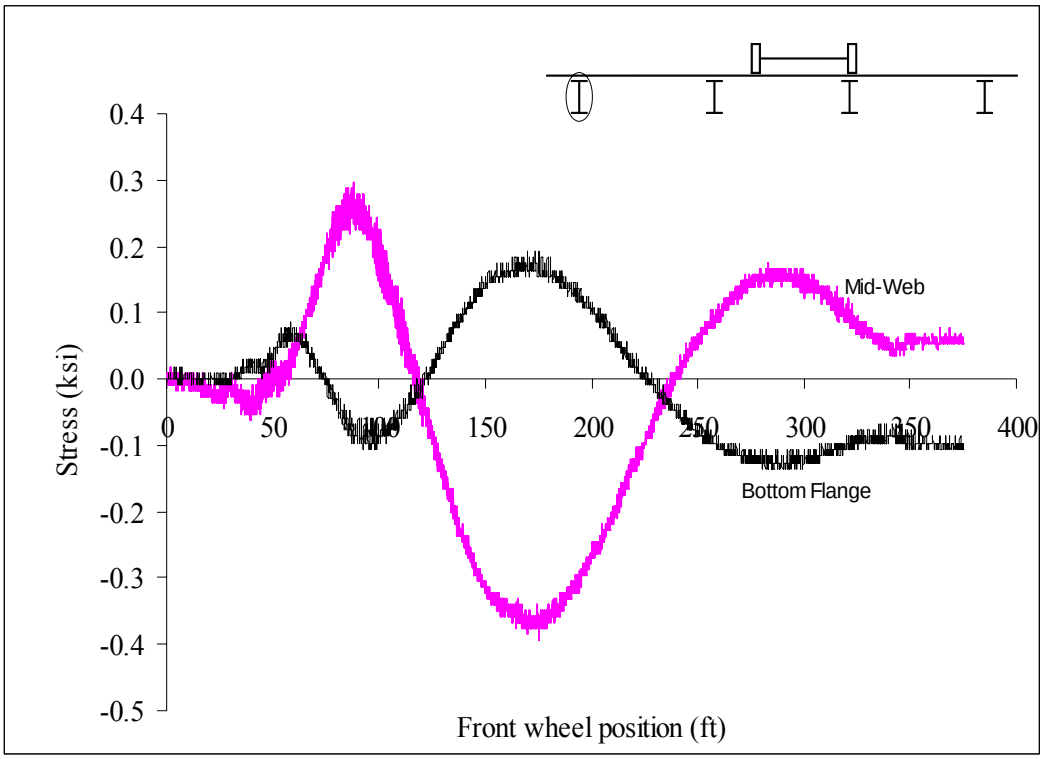

Figure A60: Las Cruces Bridge Test Run 4 S1 @ 2 ft from abutment

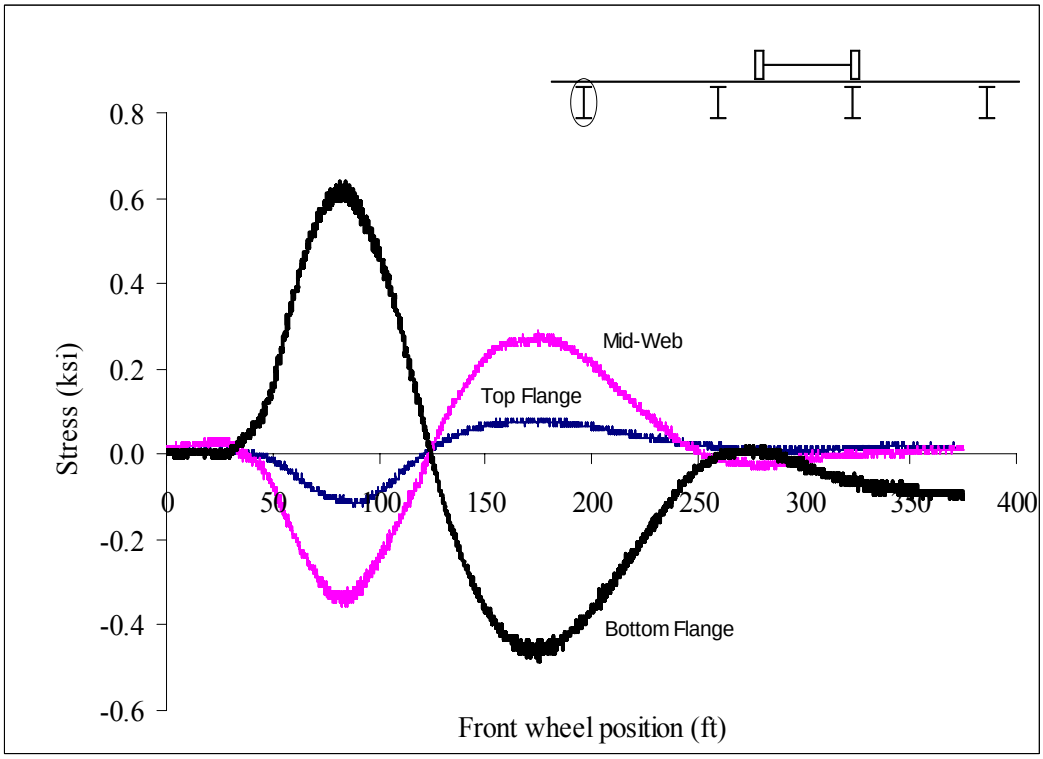

Figure A61: Las Cruces Bridge Test Run 4 S1 @ Midspan

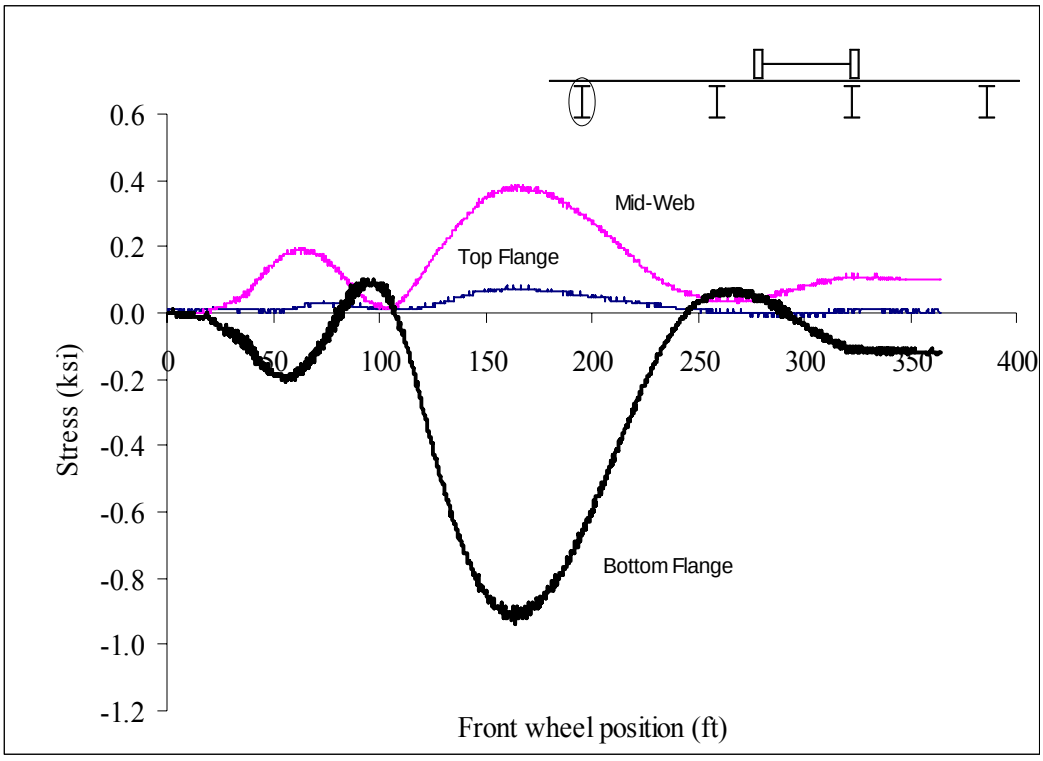

Figure A62: Las Cruces Bridge Test Run 4 S1 @ 2 ft from interior support

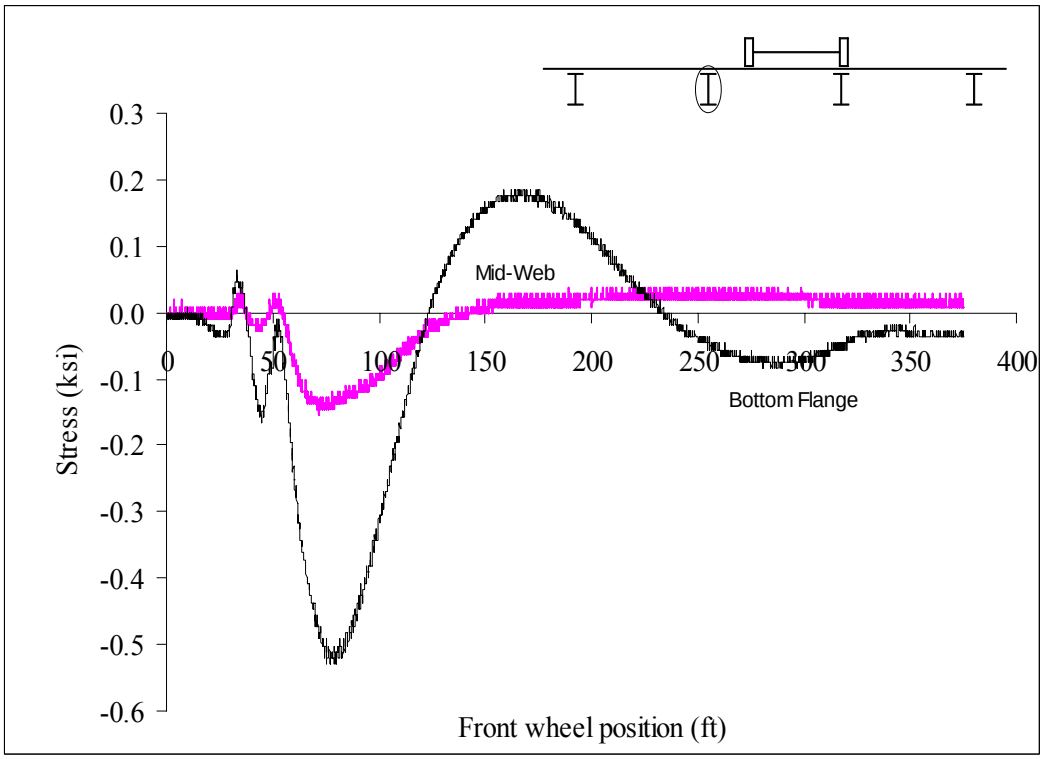

Figure A63: Las Cruces Bridge Test Run 4 S2 @ 2 ft from abutment

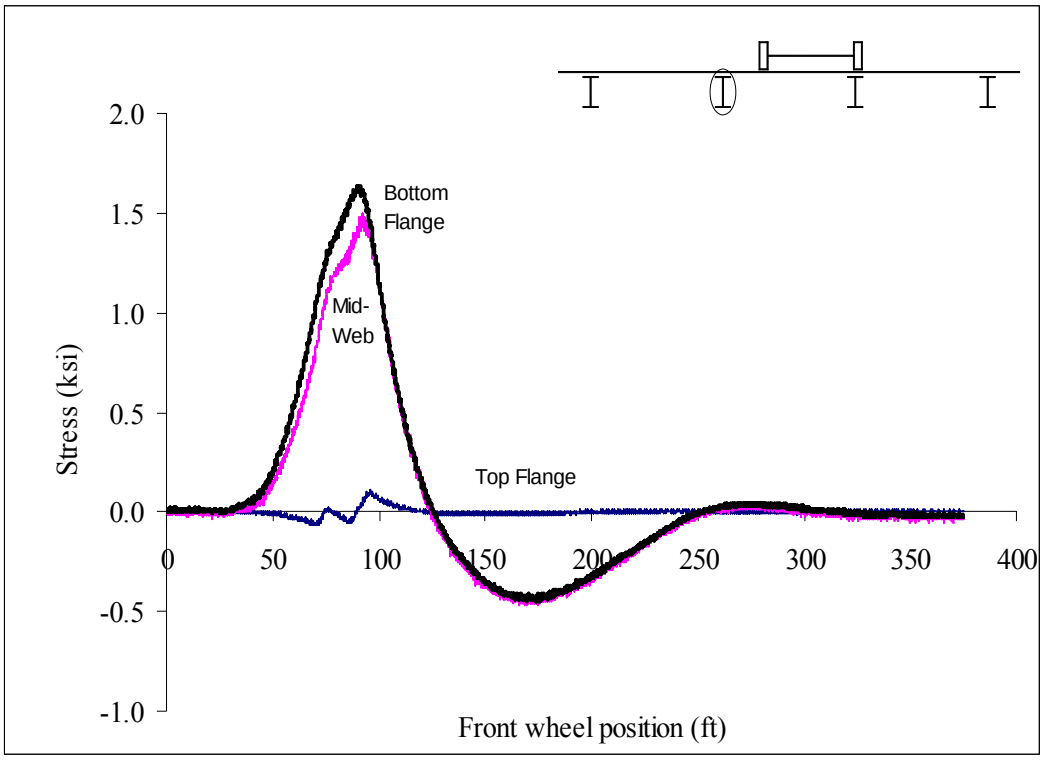

Figure A64: Las Cruces Bridge Test Run 4 S2 @ Midspan

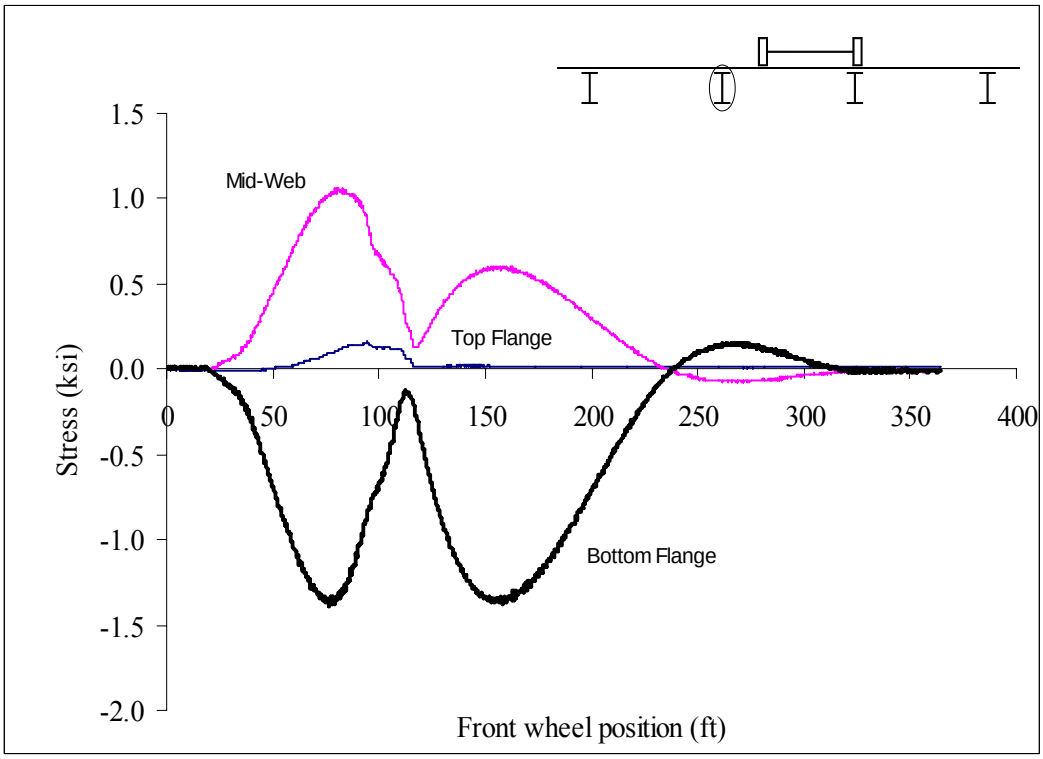

Figure A65: Las Cruces Bridge Test Run 4 S2 @ 2 ft from interior support

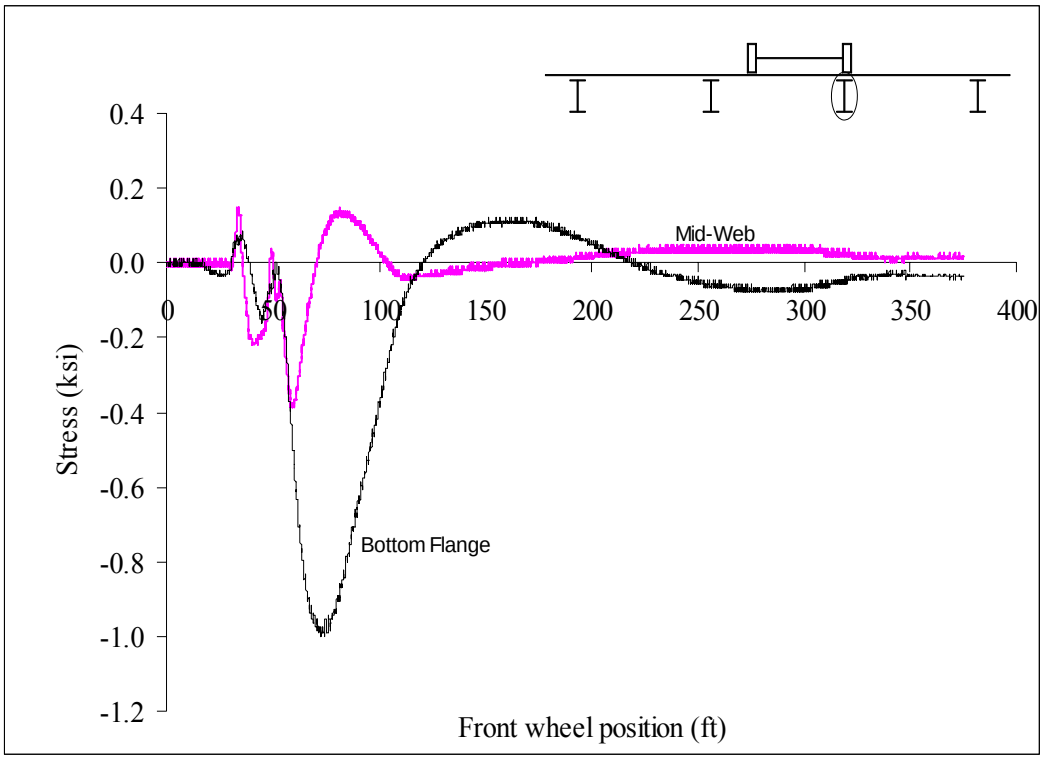

Figure A66: Las Cruces Bridge Test Run 4 S3 @ 2 ft from abutment

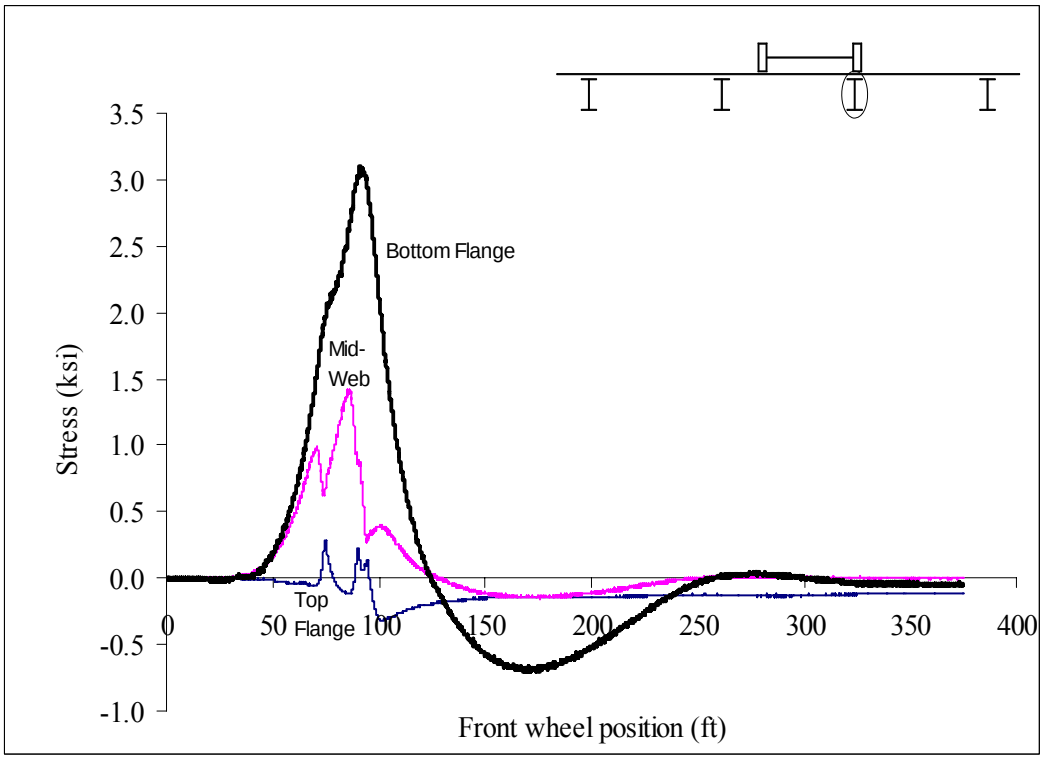

Figure A67: Las Cruces Bridge Test Run 4 S3 @ Midspan

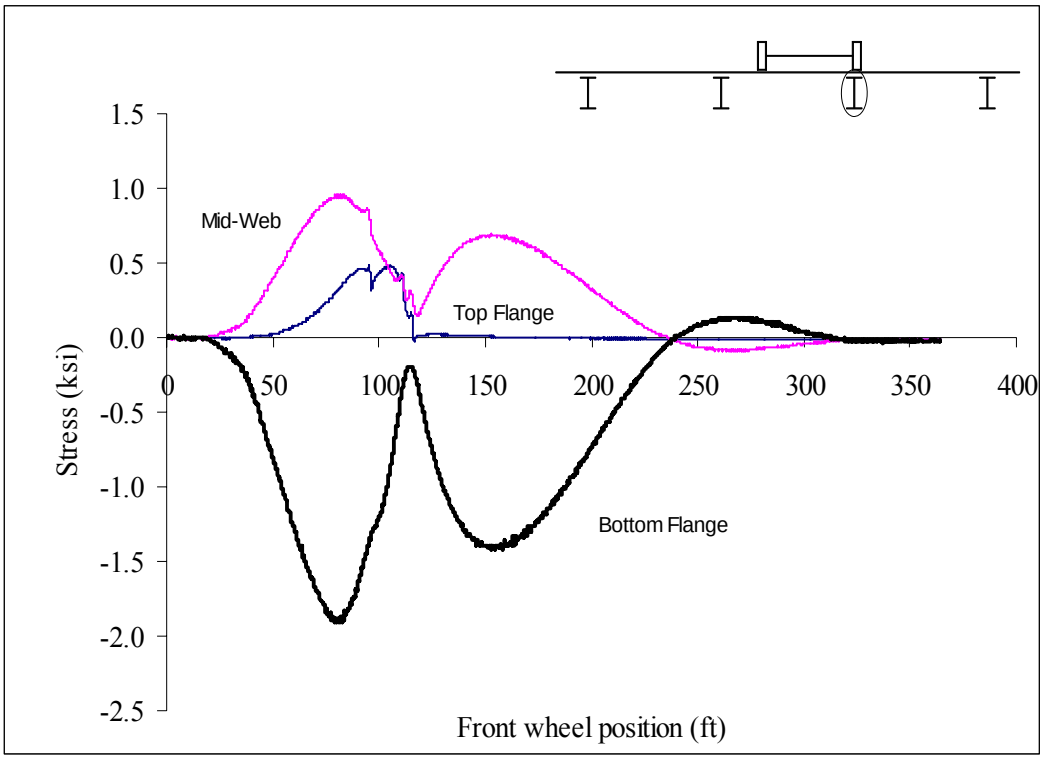

Figure A68: Las Cruces Bridge Test Run 4 S3 @ 2 ft from interior support

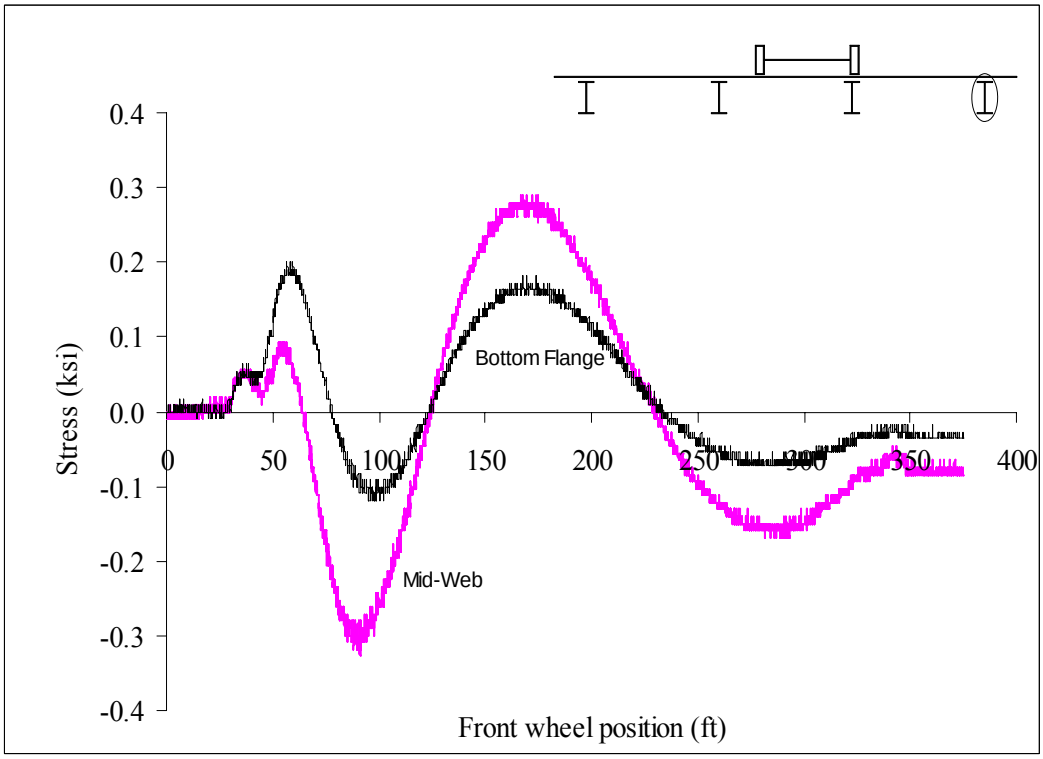

Figure A69: Las Cruces Bridge Test Run 4 S4 @ 2 ft from abutment

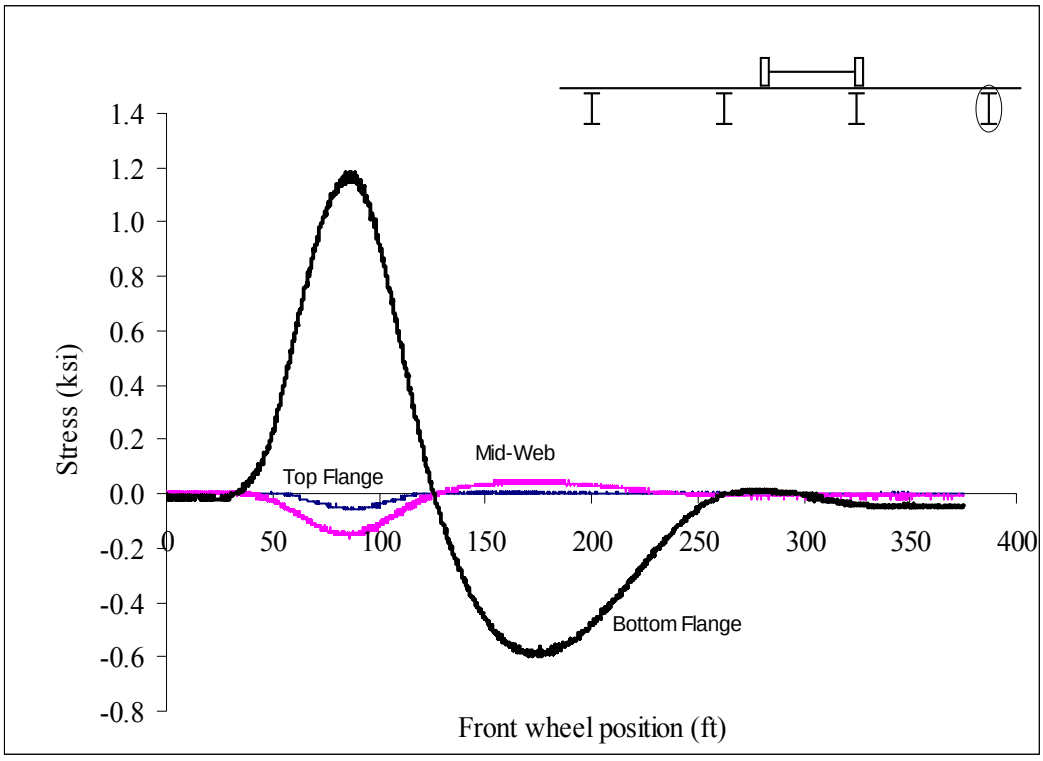

Figure A70: Las Cruces Bridge Test Run 4 S4 @ Midspan

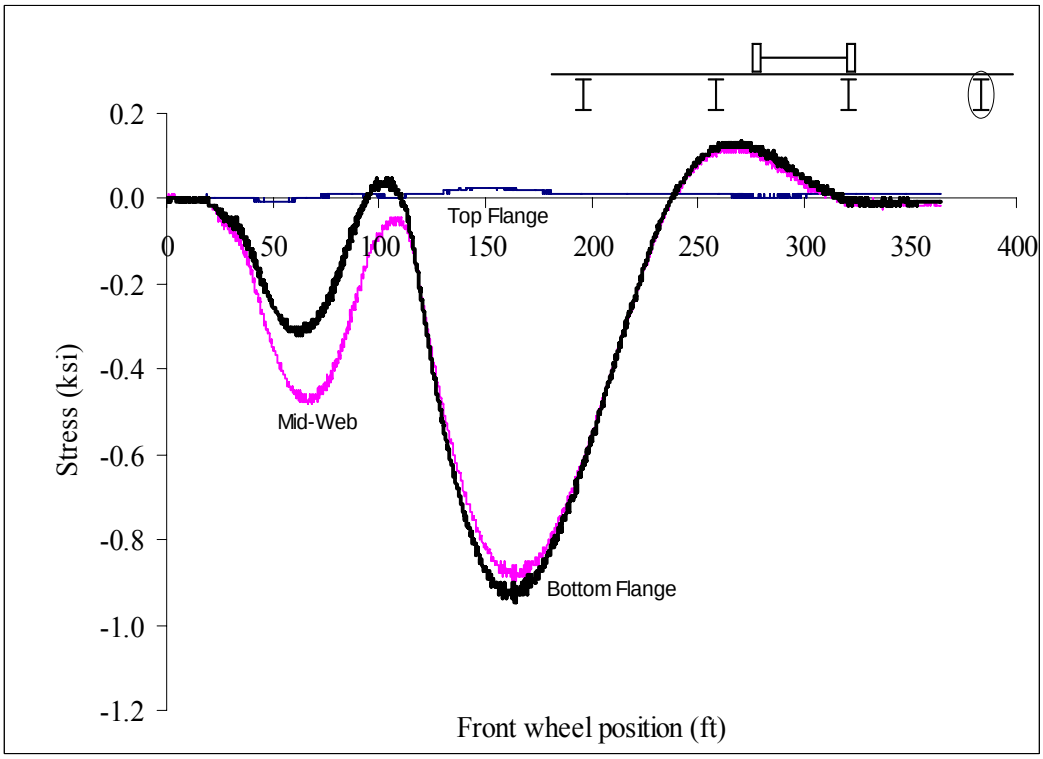

Figure A71: Las Cruces Bridge Test Run 4 S4 @ 2 ft from interior support

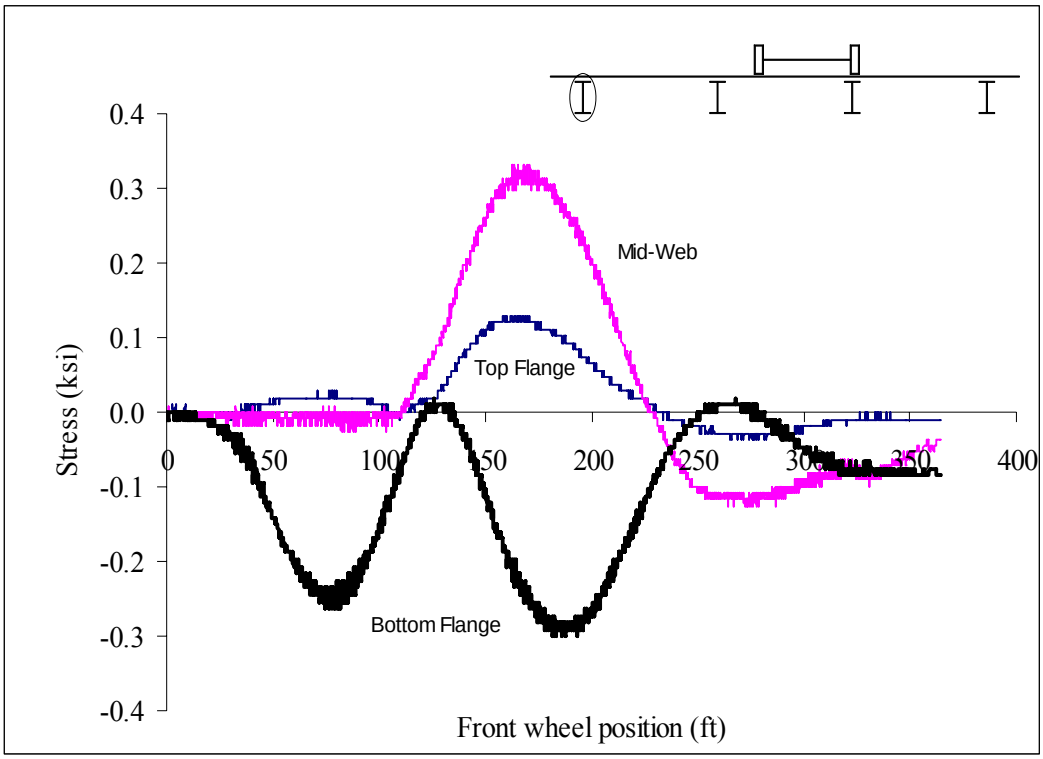

Figure A72: Las Cruces Bridge Test Run 4 S5 @ 2 ft from interior support

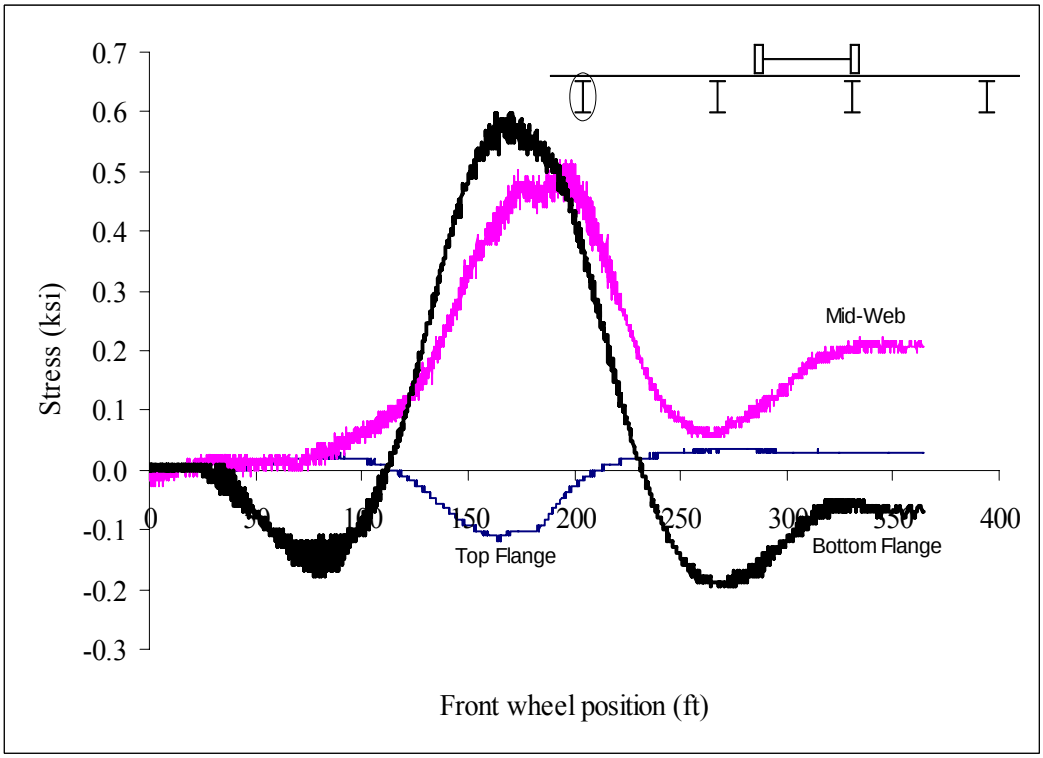

Figure A73: Las Cruces Bridge Test Run 4 S5 @ Midspan

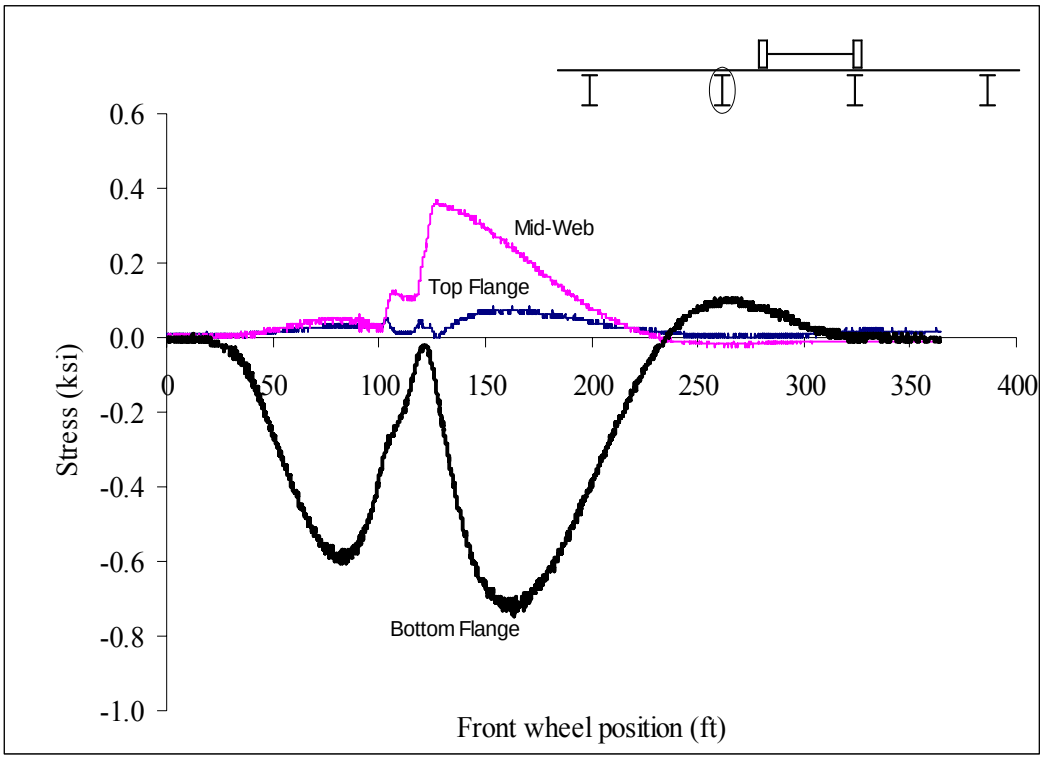

Figure A74: Las Cruces Bridge Test Run 4 S6 @ 2 ft from interior support

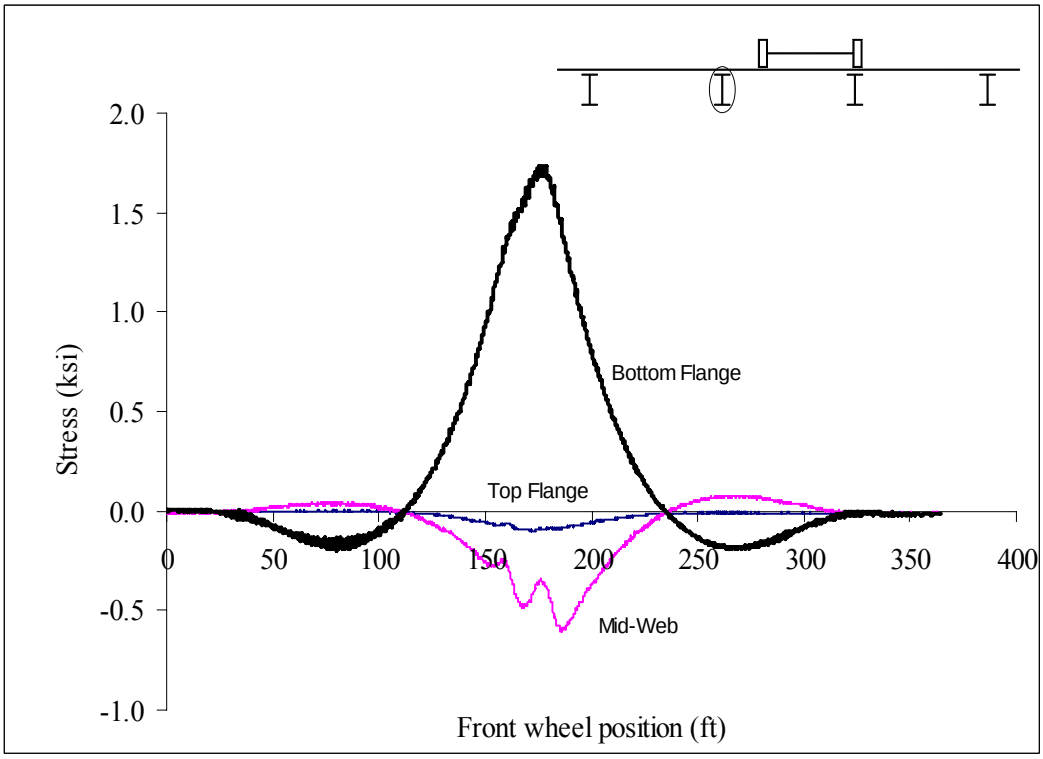

Figure A75: Las Cruces Bridge Test Run 4 S6 @ Midspan

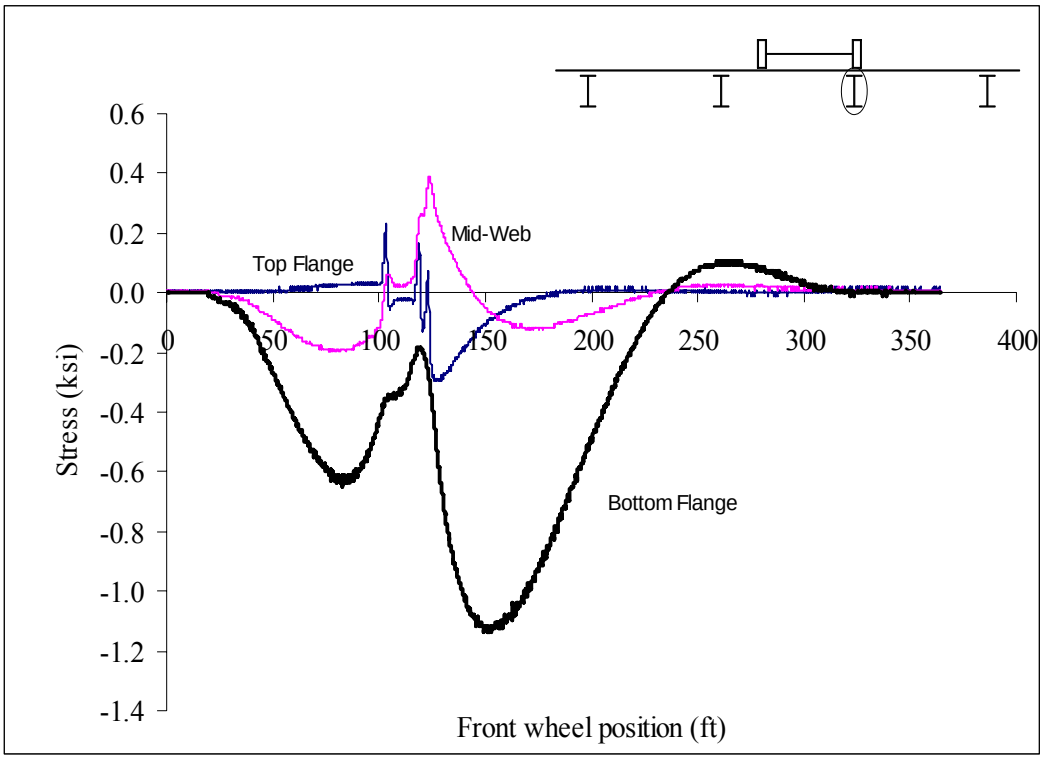

Figure A76: Las Cruces Bridge Test Run 4 S7 @ 2 ft from interior support

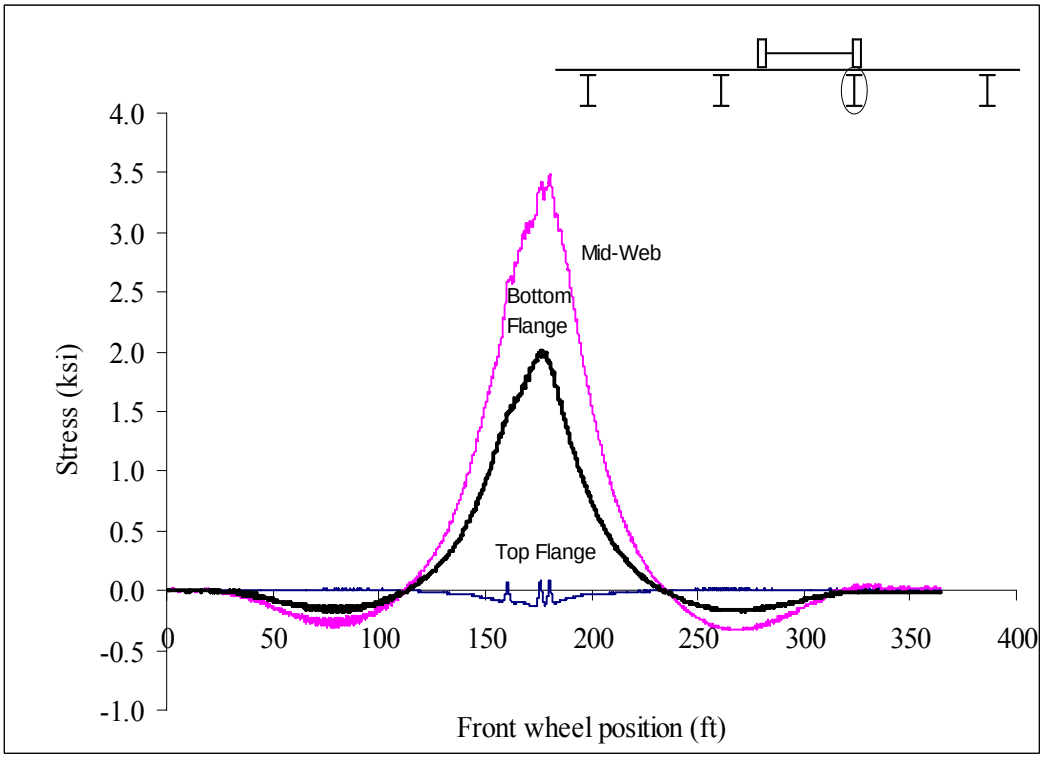

Figure A77: Las Cruces Bridge Test Run 4 S7 @ Midspan

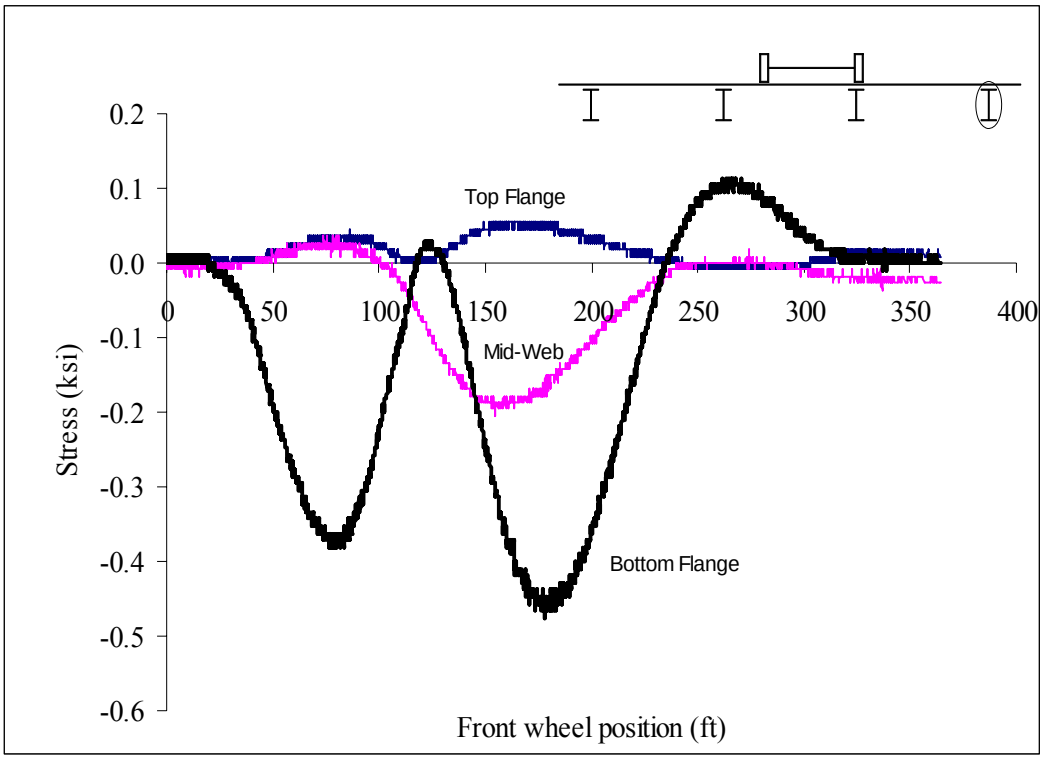

Figure A78: Las Cruces Bridge Test Run 4 S8 @ 2 ft from interior support

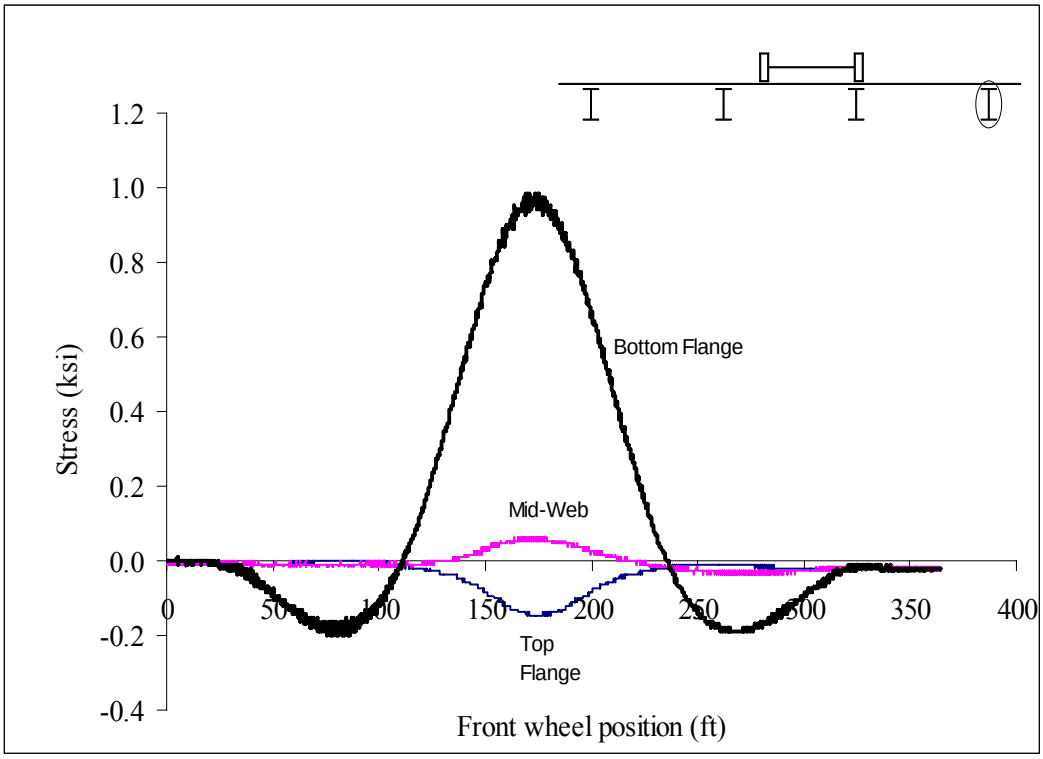

Figure A79: Las Cruces Bridge Test Run 4 S8 @ Midspan

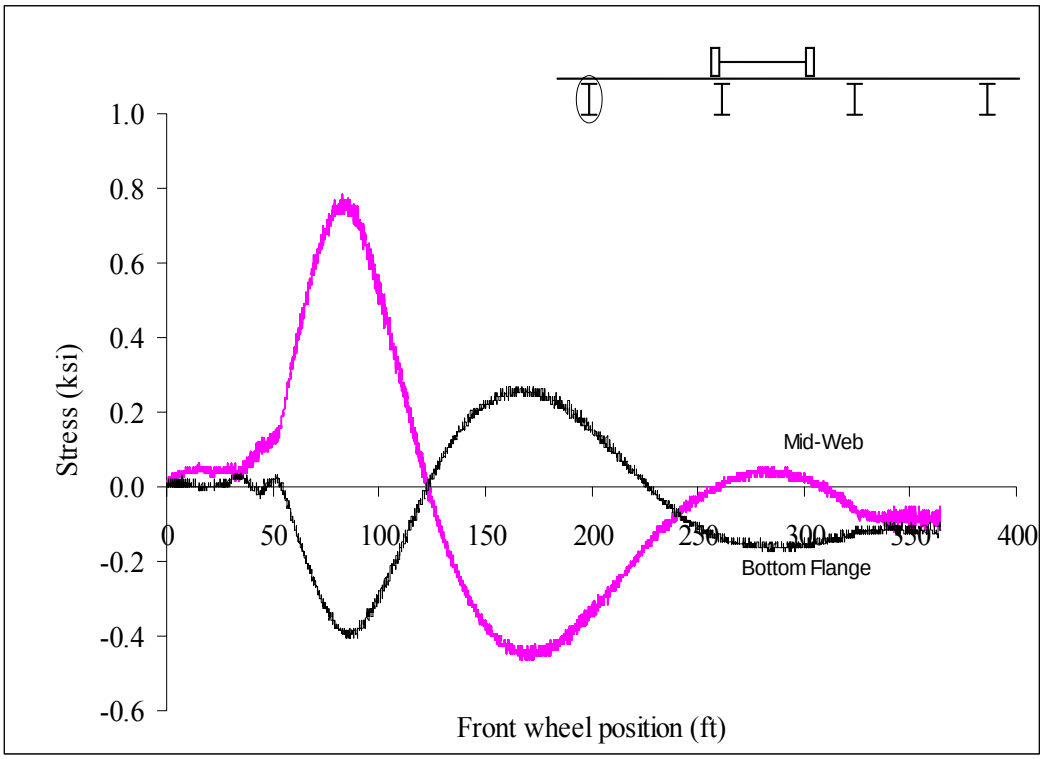

Figure A80: Las Cruces Bridge Test Run 5 S1 @ 2 ft from abutment

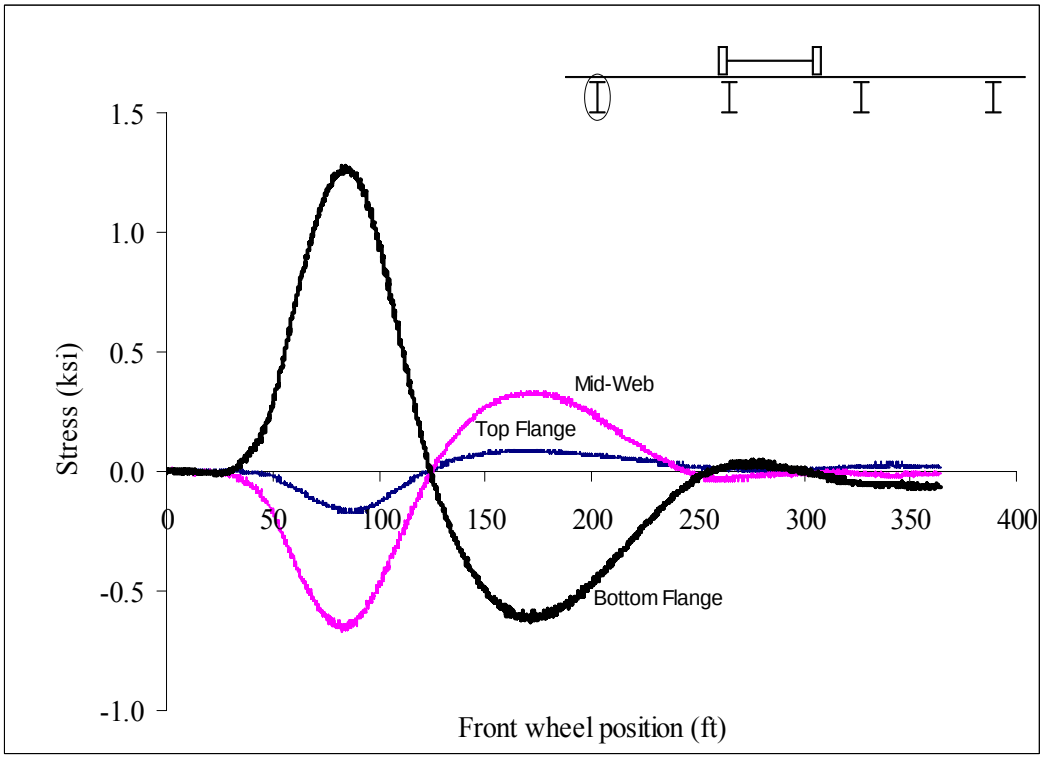

Figure A81: Las Cruces Bridge Test Run 5 S1 @ Midspan

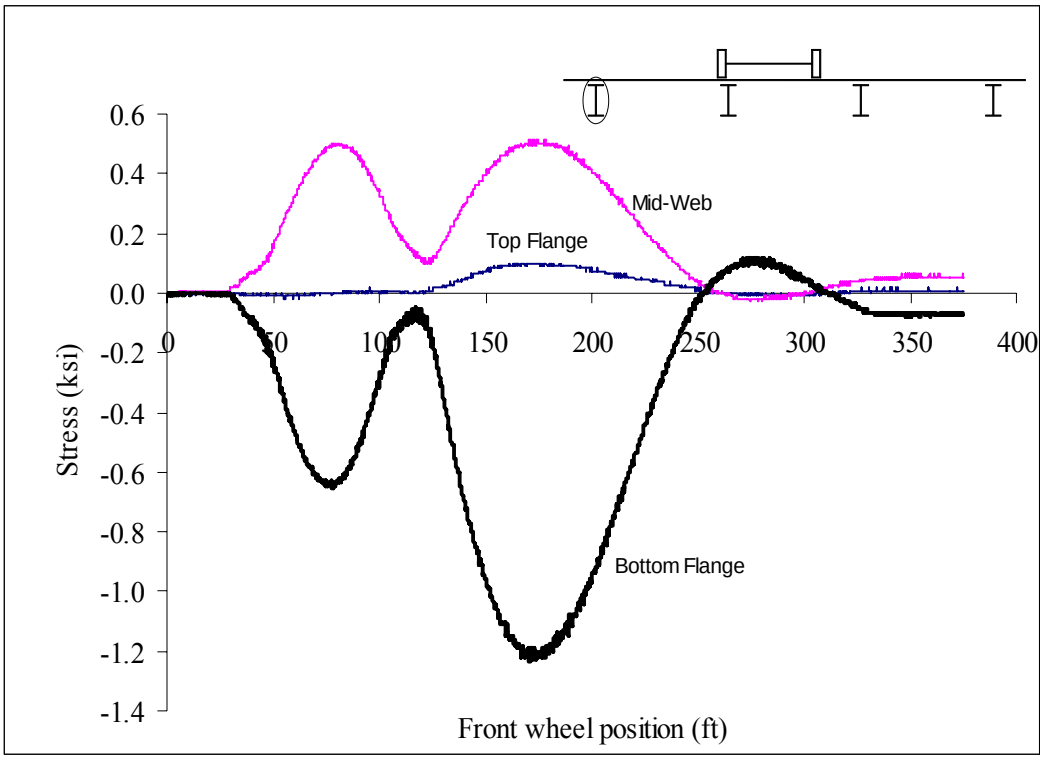

Figure A82: Las Cruces Bridge Test Run 5 S1 @ 2 ft from interior support

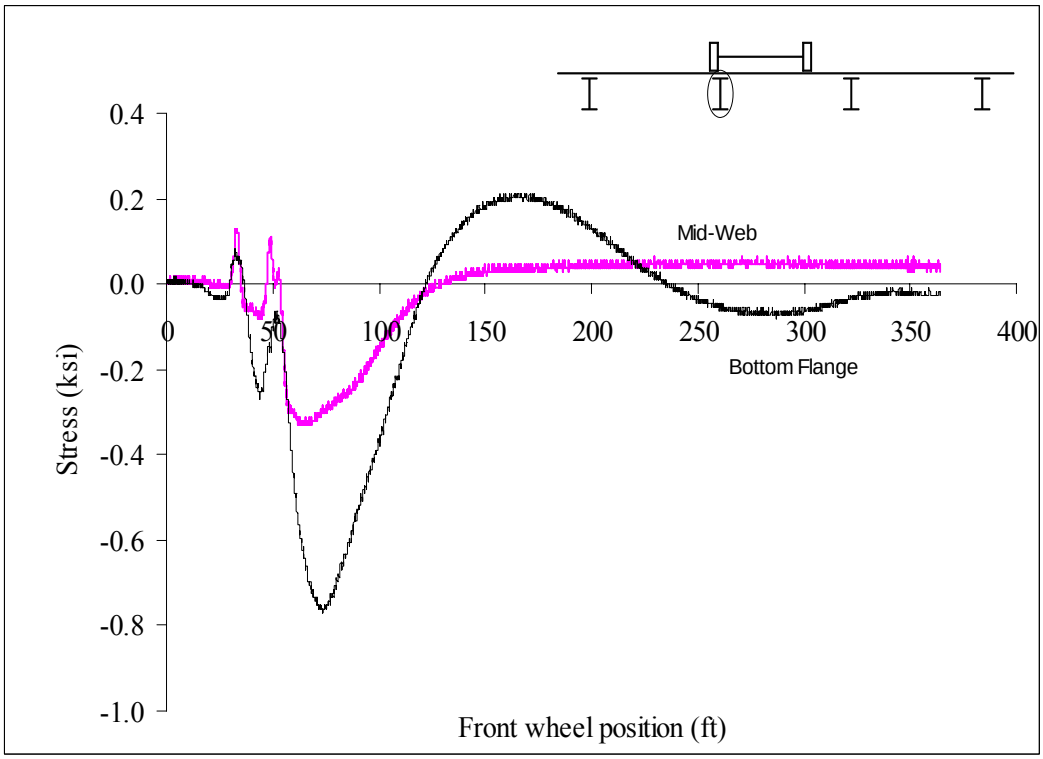

Figure A83: Las Cruces Bridge Test Run 5 S2 @ 2 ft from abutment

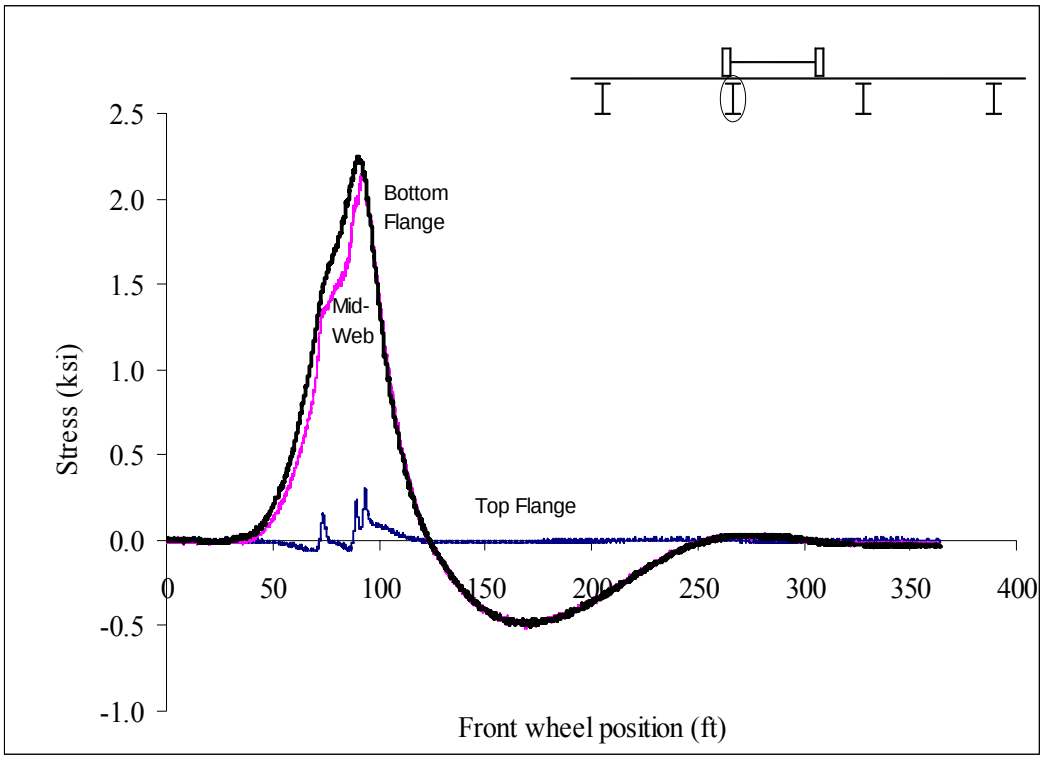

Figure A84: Las Cruces Bridge Test Run 5 S2 @ Midspan

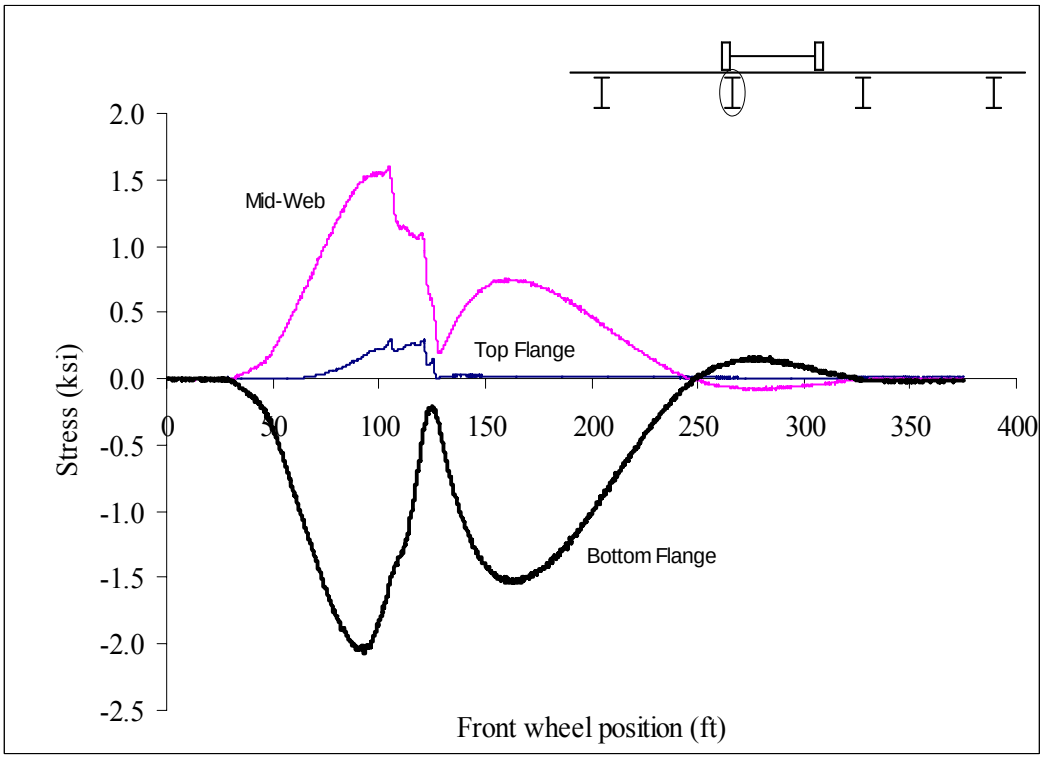

Figure A85: Las Cruces Bridge Test Run 5 S2 @ 2 ft from interior support

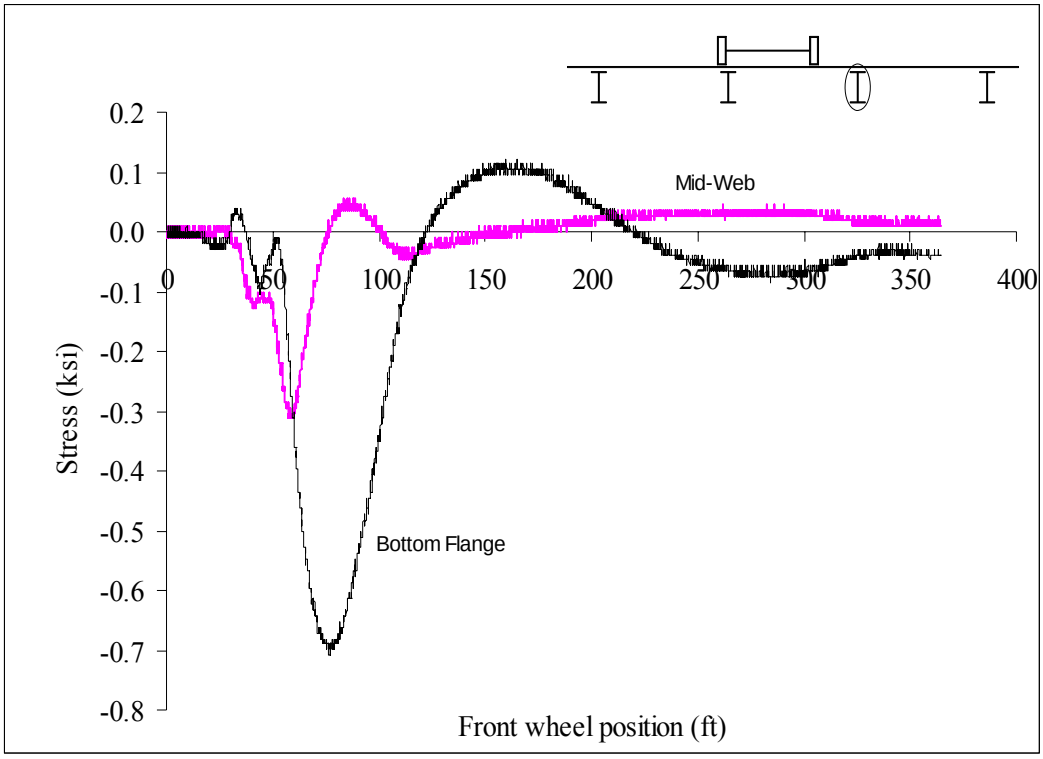

Figure A86: Las Cruces Bridge Test Run 5 S3 @ 2 ft from abutment

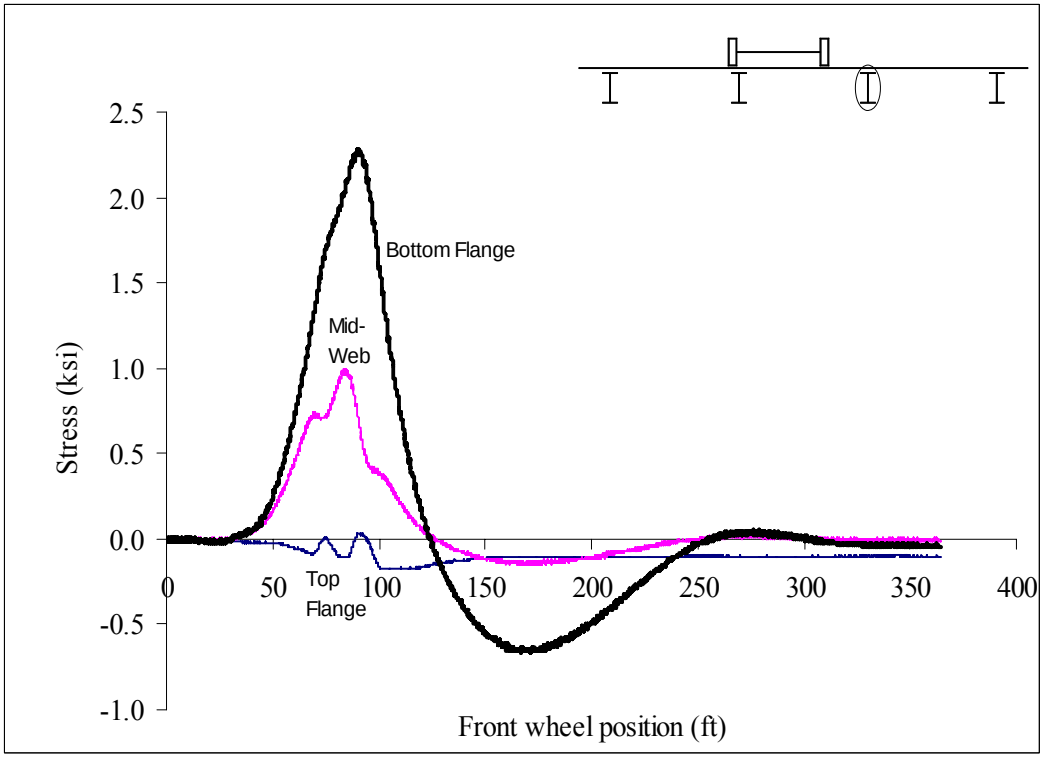

Figure A87: Las Cruces Bridge Test Run 5 S3 @ Midspan

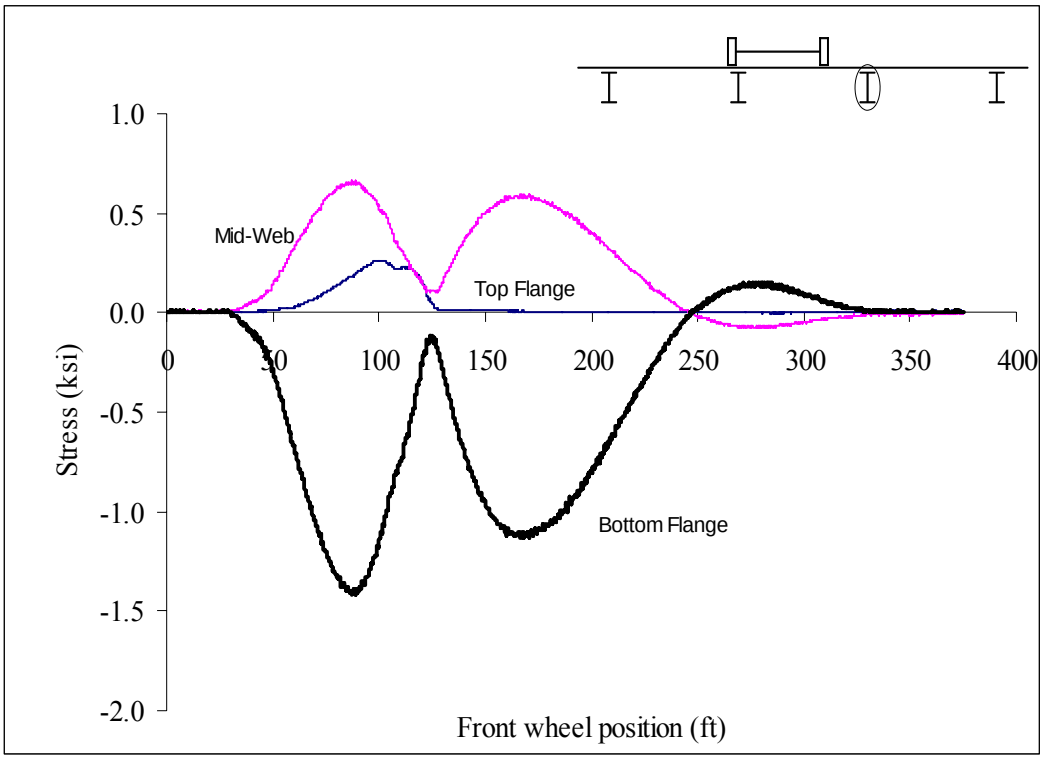

Figure A88: Las Cruces Bridge Test Run 5 S3 @ 2 ft from interior support

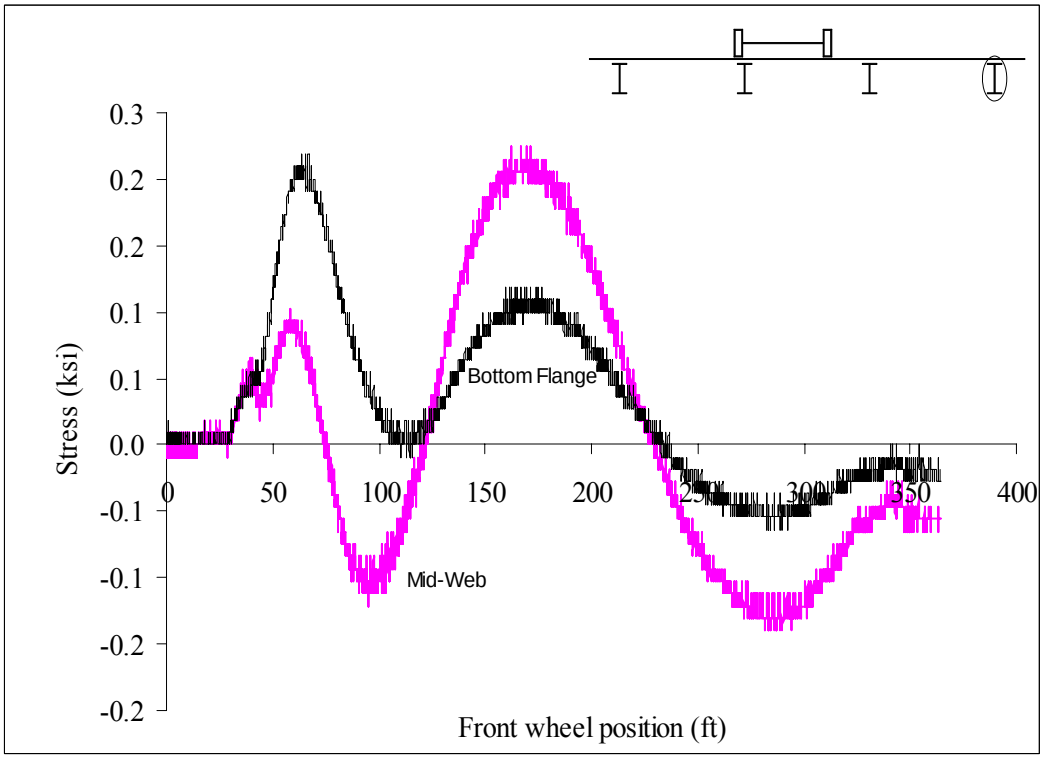

Figure A89: Las Cruces Bridge Test Run 5 S4 @ 2 ft from abutment

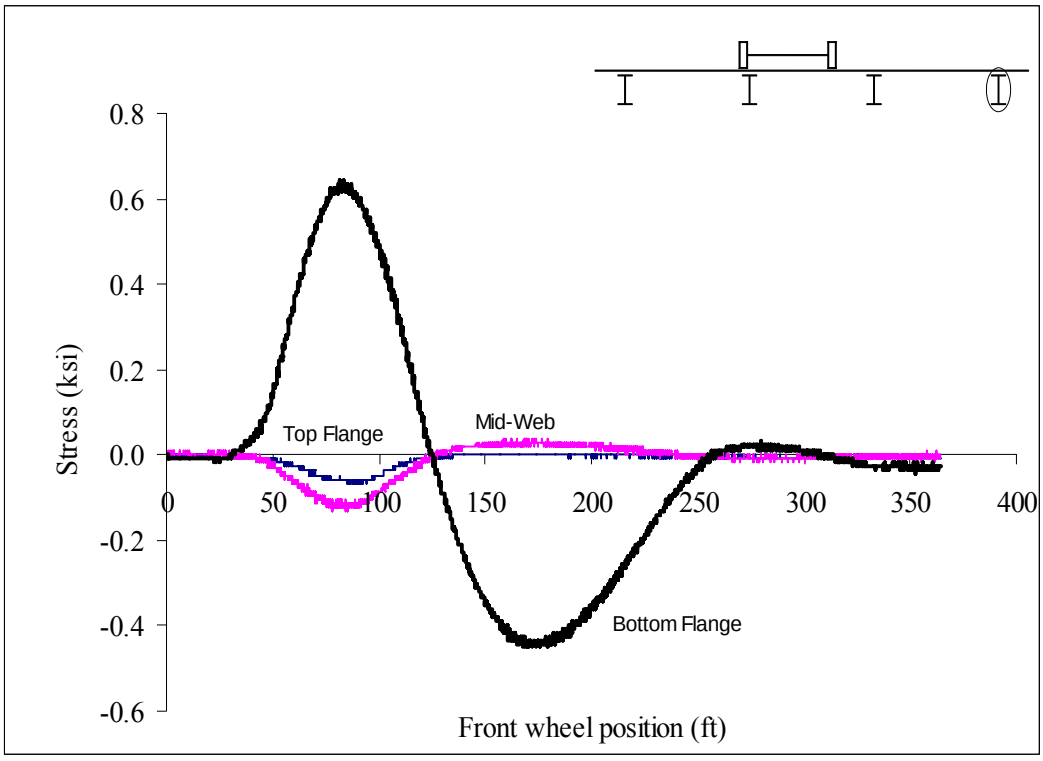

Figure A90: Las Cruces Bridge Test Run 5 S4 @ Midspan

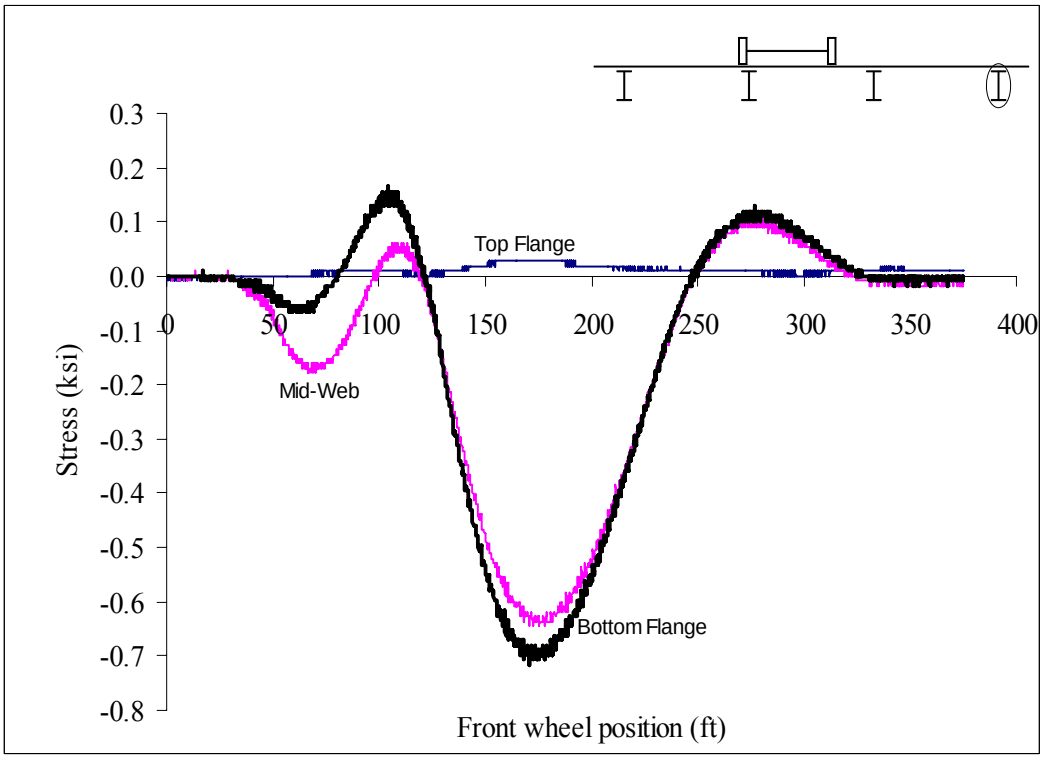

Figure A91: Las Cruces Bridge Test Run 5 S4 @ 2 ft from interior support

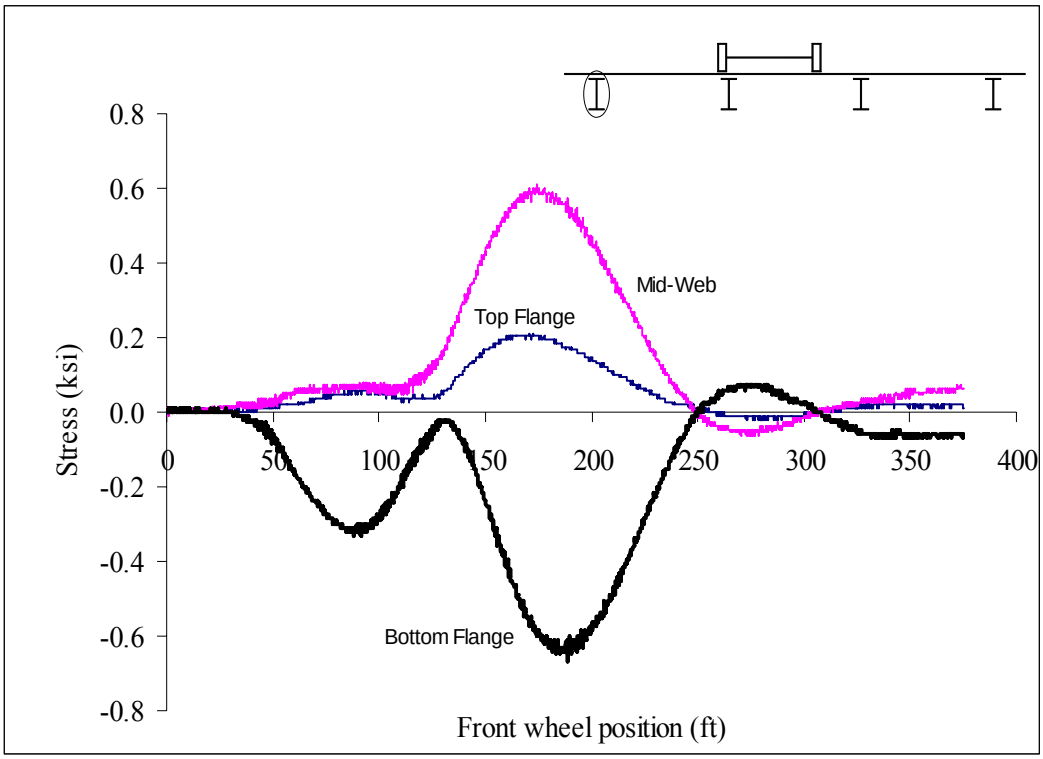

Figure A92: Las Cruces Bridge Test Run 5 S5 @ 2 ft from interior support

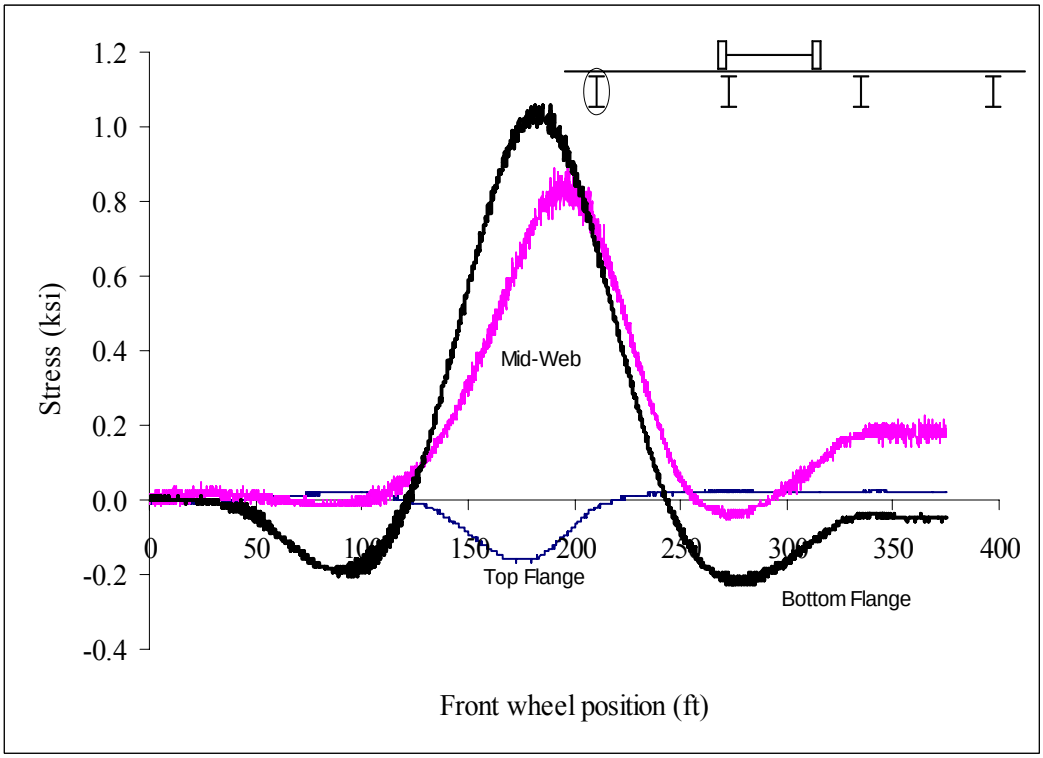

Figure A93: Las Cruces Bridge Test Run 5 S5 @ Midspan

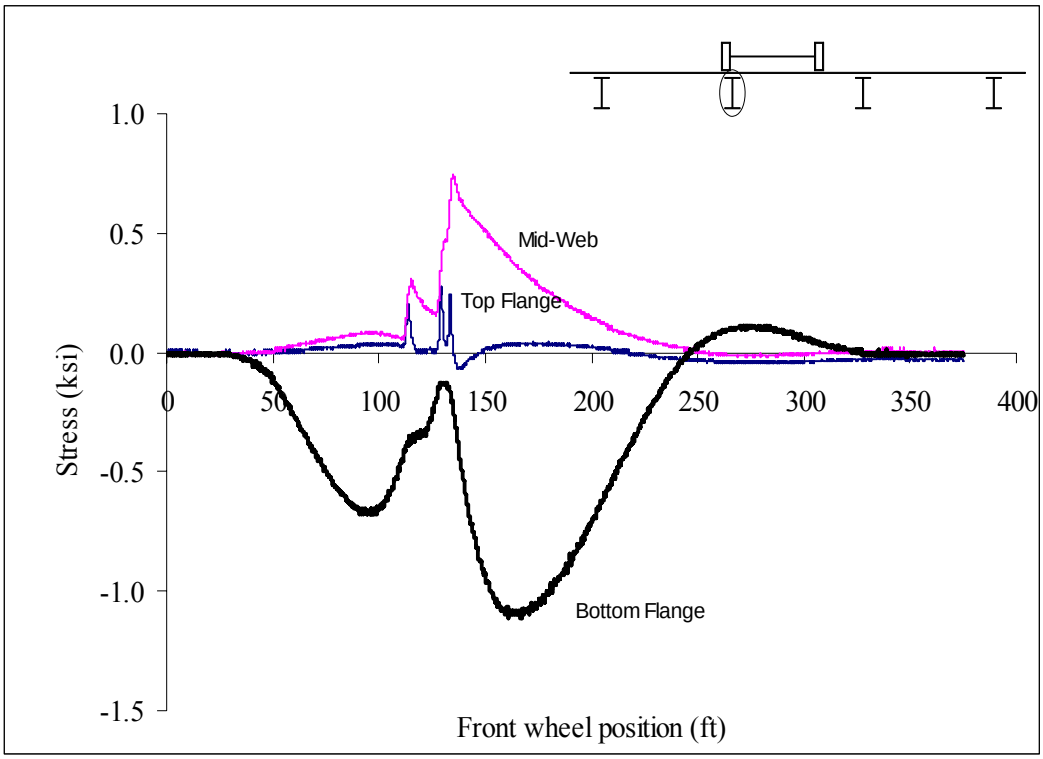

Figure A94: Las Cruces Bridge Test Run 5 S6 @ 2 ft from interior support

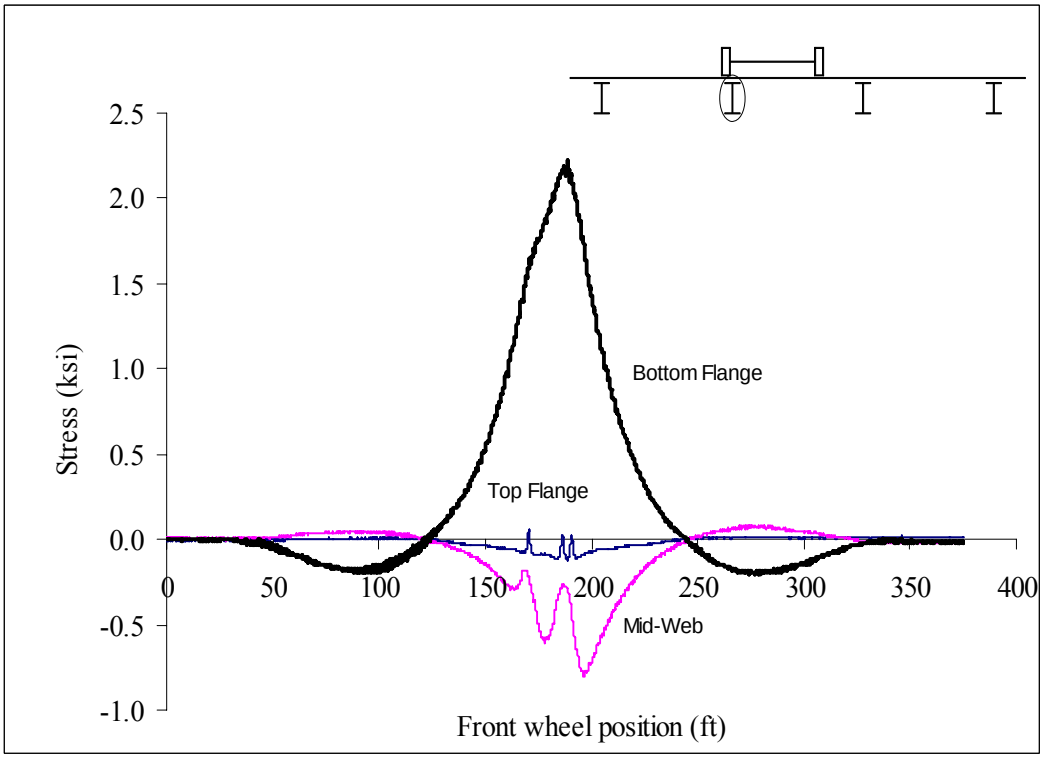

Figure A95: Las Cruces Bridge Test Run 5 S6 @ Midspan

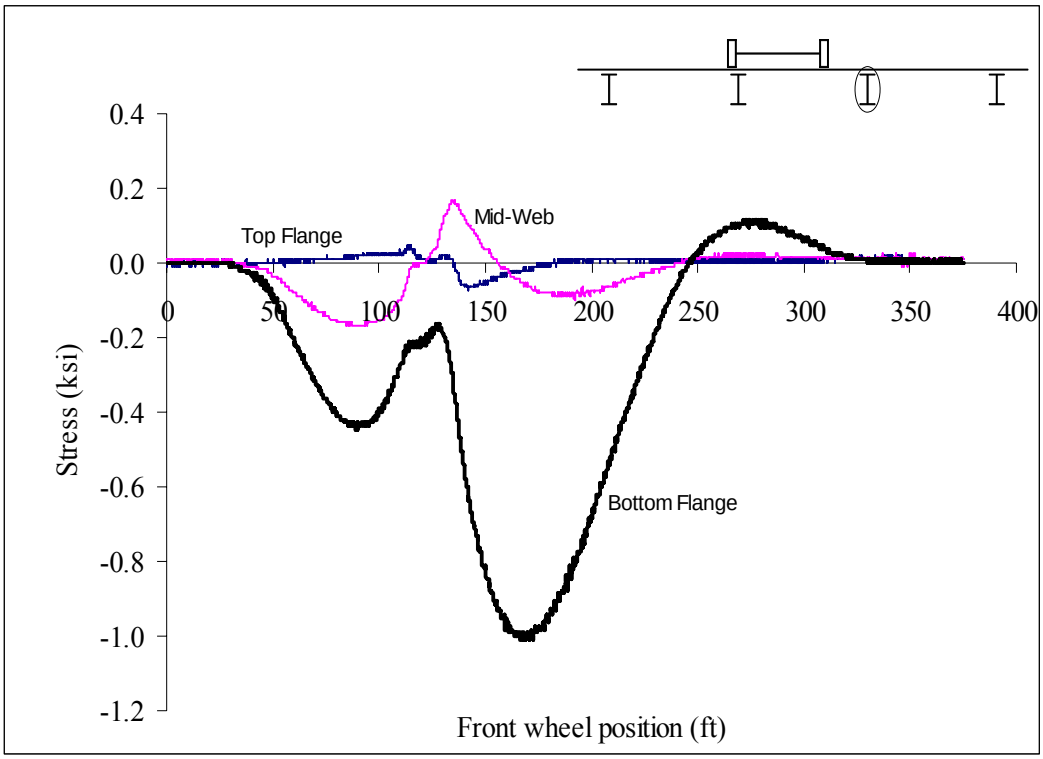

Figure A96: Las Cruces Bridge Test Run 5 S7 @ 2 ft from interior support

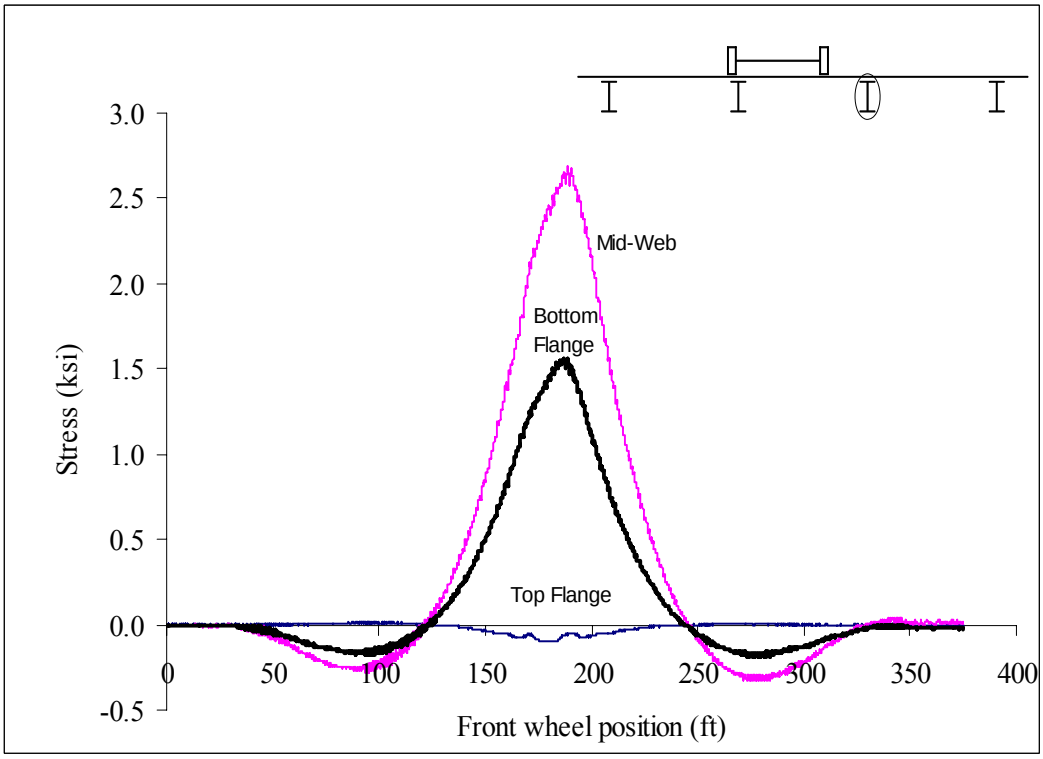

Figure A97: Las Cruces Bridge Test Run 5 S7 @ Midspan

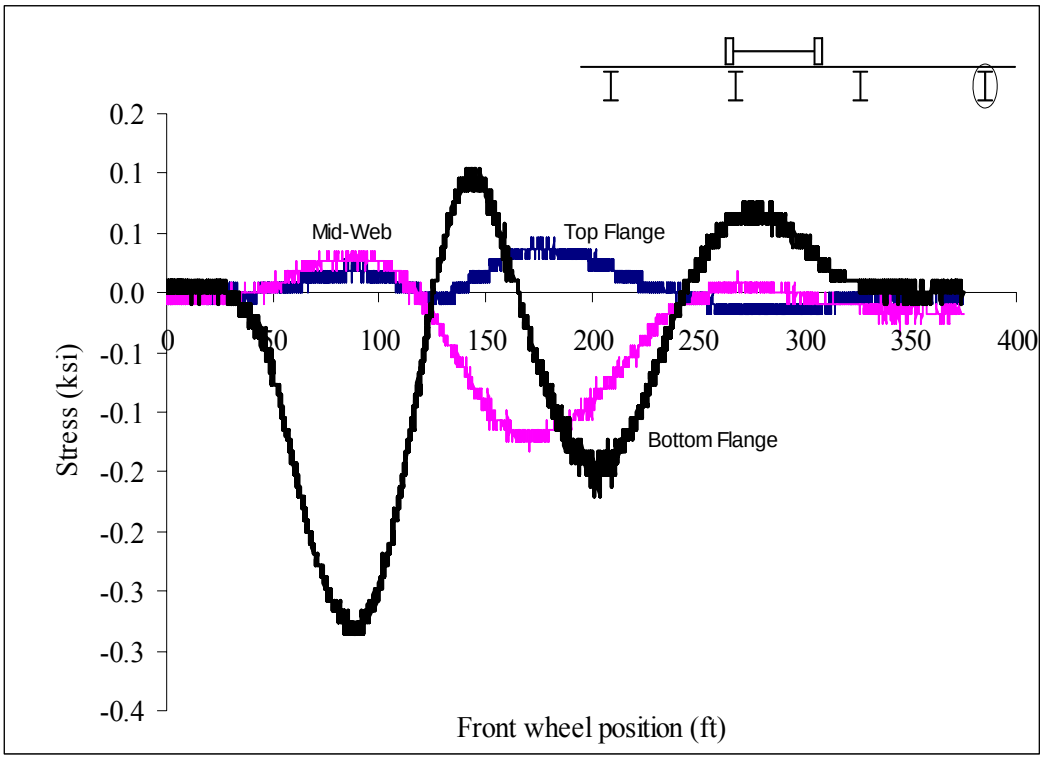

Figure A98: Las Cruces Bridge Test Run 5 S8 @ 2 ft from interior support

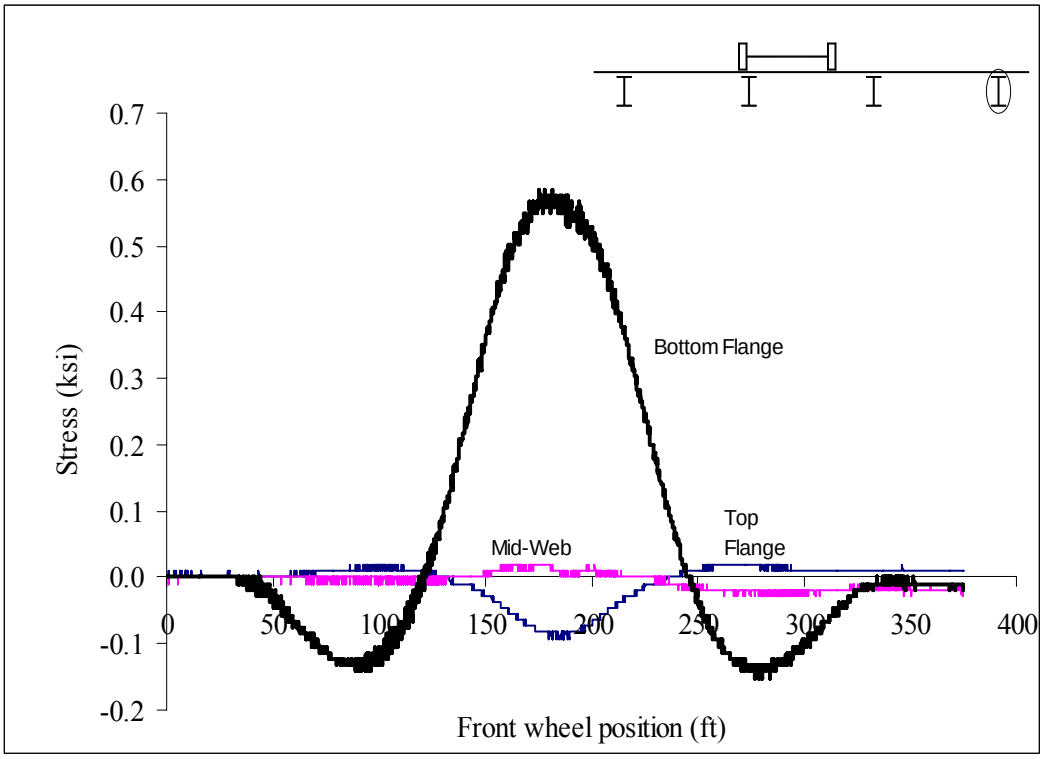

Figure A99: Las Cruces Bridge Test Run 5 S8 @ Midspan

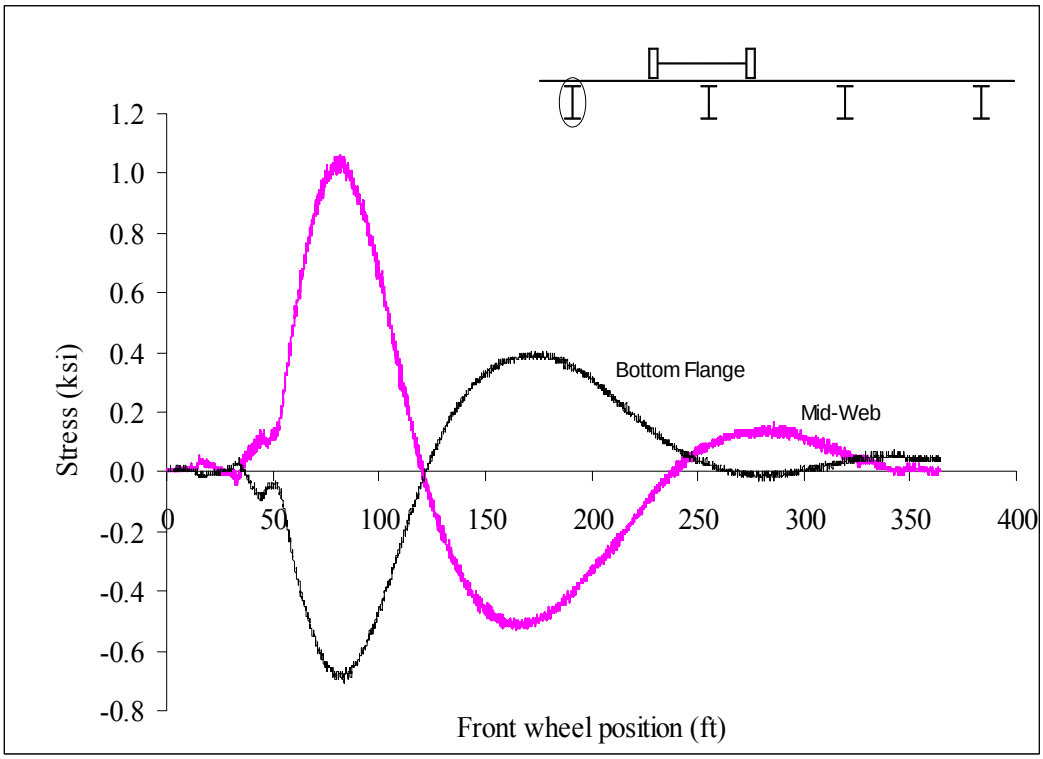

Figure A100: Las Cruces Bridge Test Run 6 S1 @ 2 ft from abutment

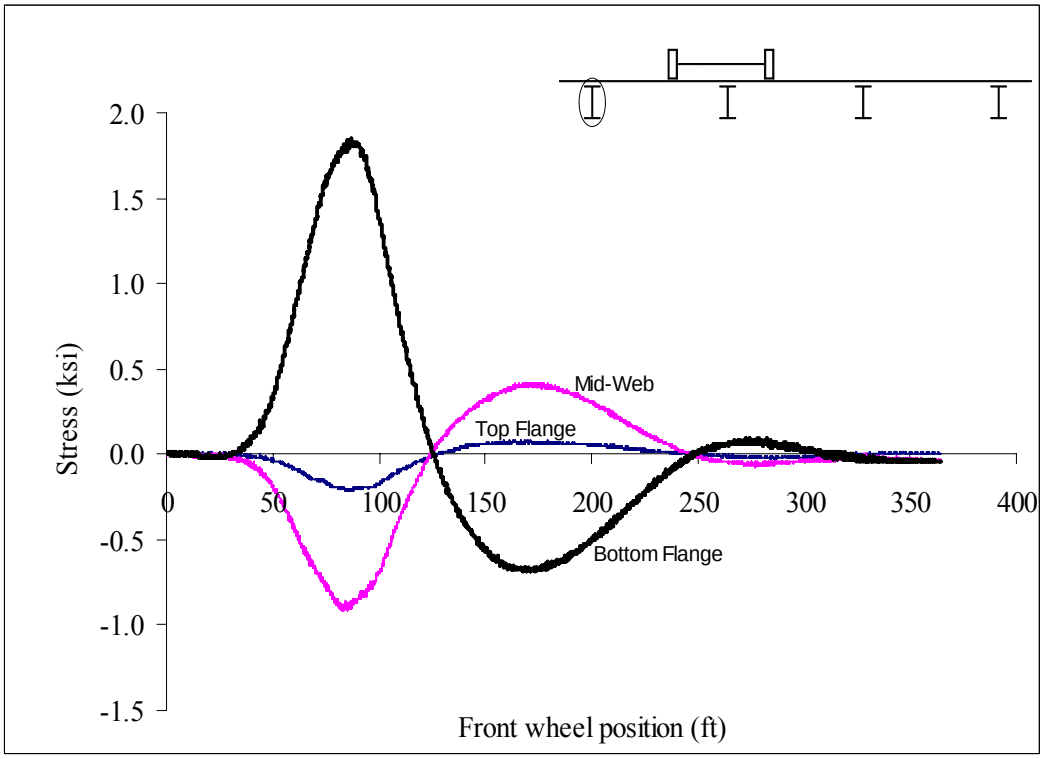

Figure A101: Las Cruces Bridge Test Run 6 S1 @ Midspan

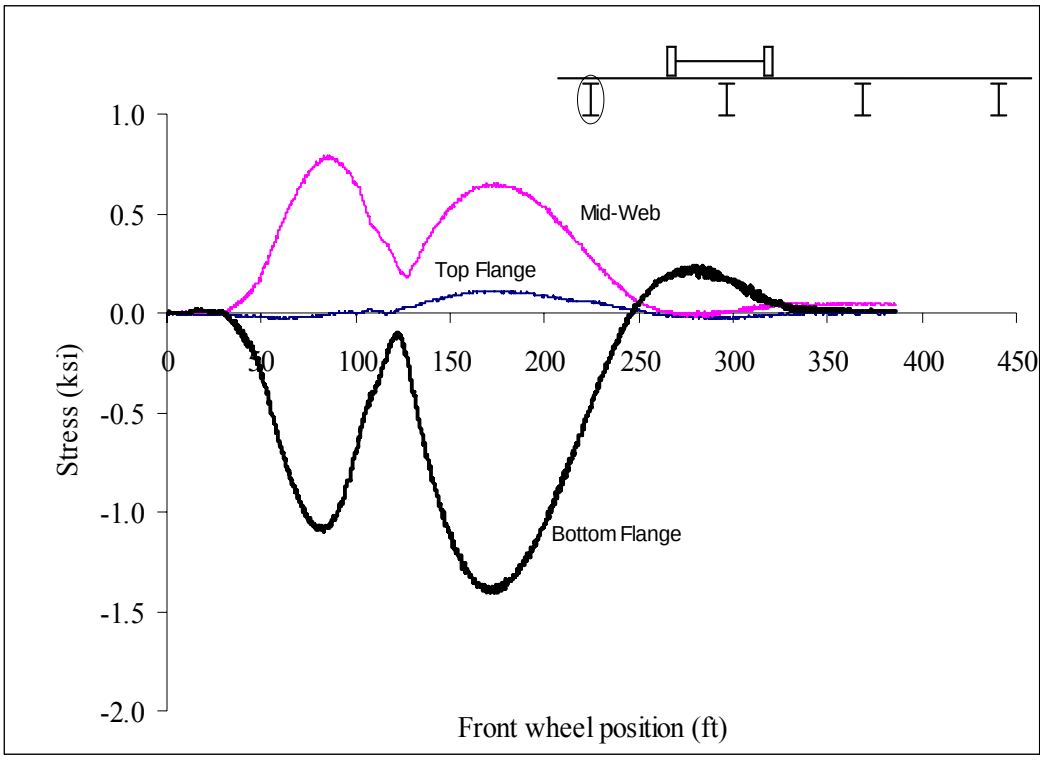

Figure A102: Las Cruces Bridge Test Run 6 S1 @ 2 ft from interior support

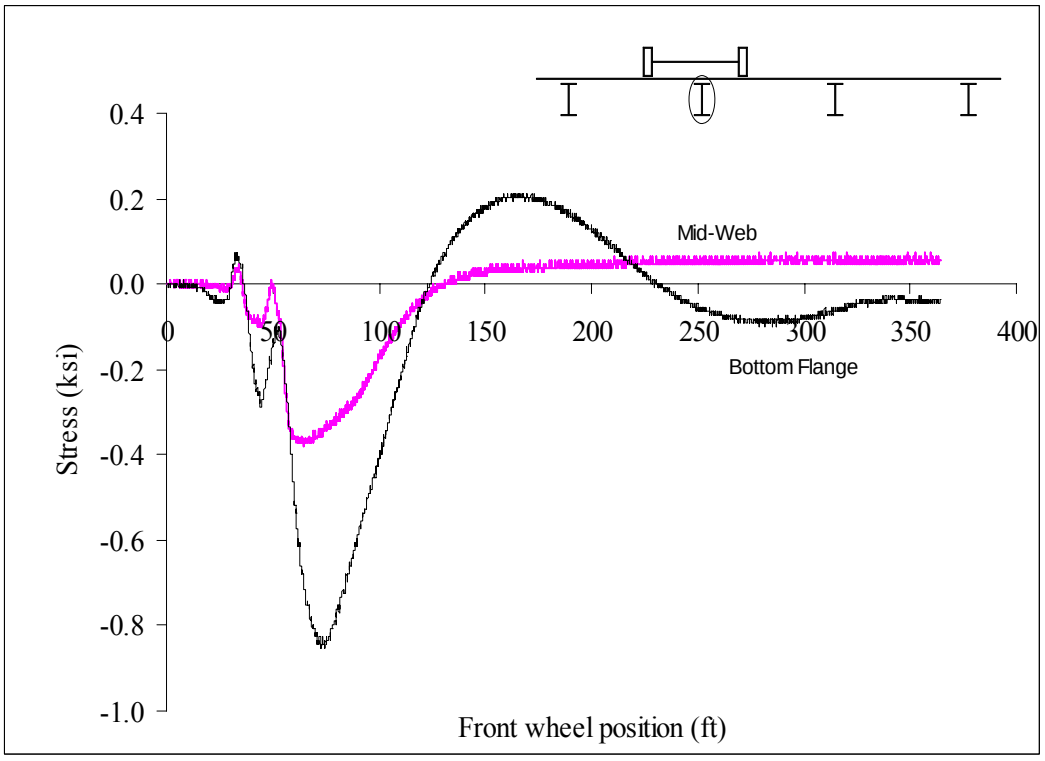

Figure A103: Las Cruces Bridge Test Run 6 S2 @ 2 ft from abutment

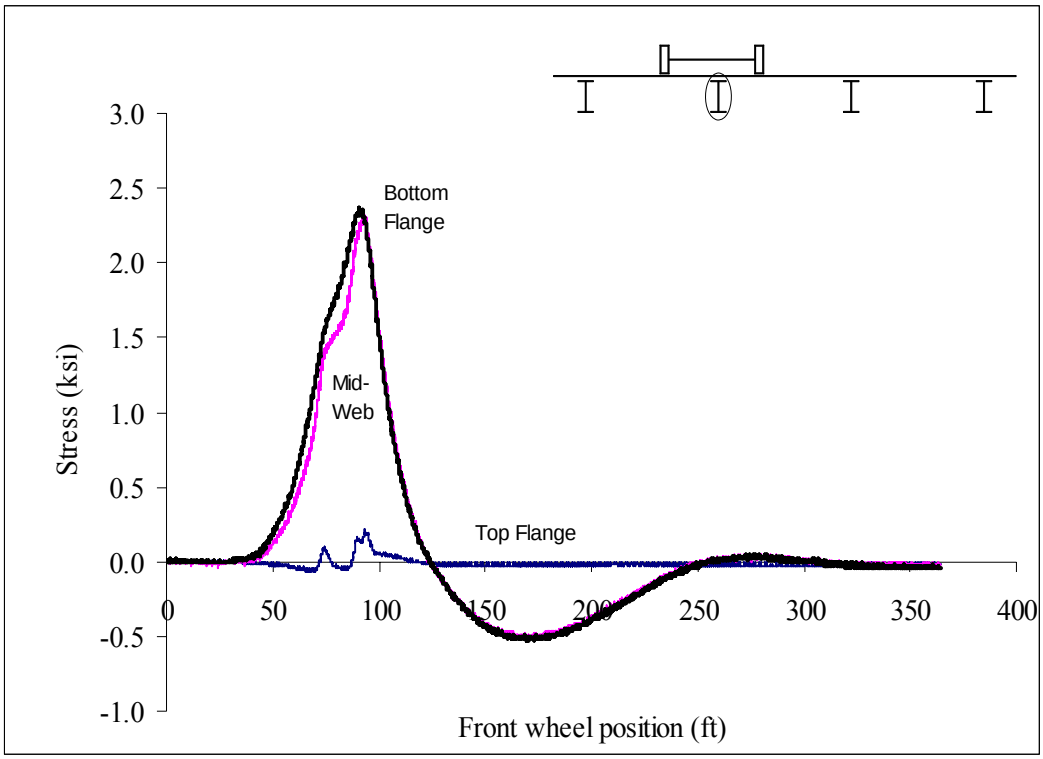

Figure A104: Las Cruces Bridge Test Run 6 S2 @ Midspan

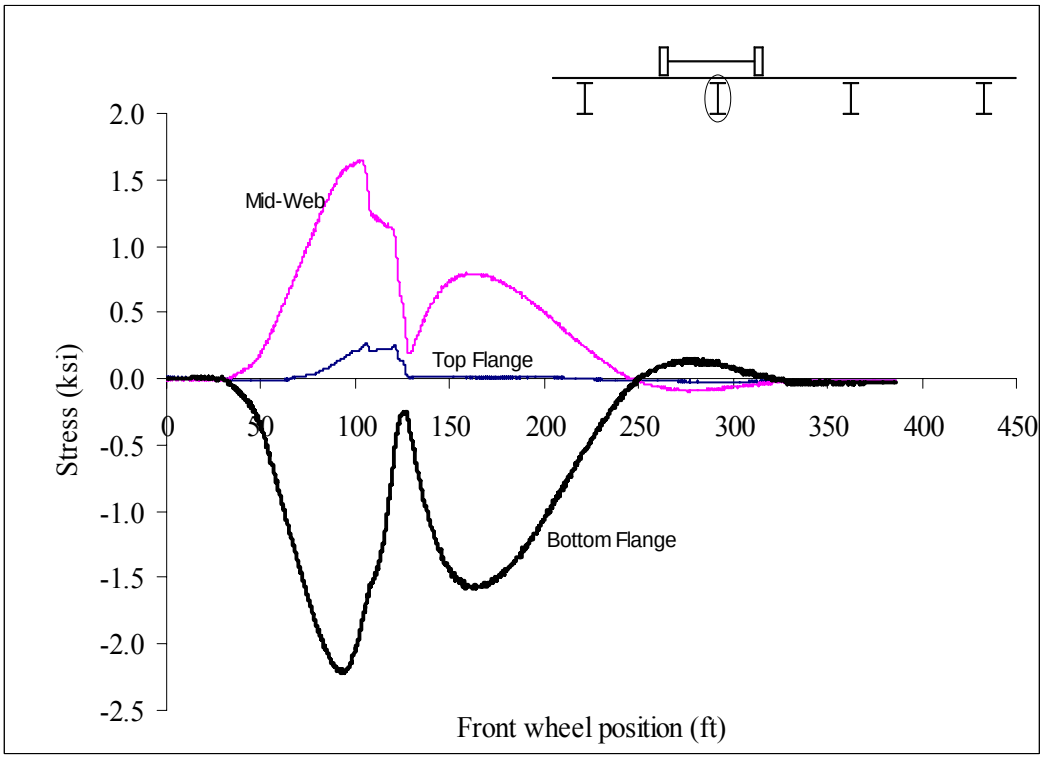

Figure A105: Las Cruces Bridge Test Run 6 S2 @ 2 ft from interior support

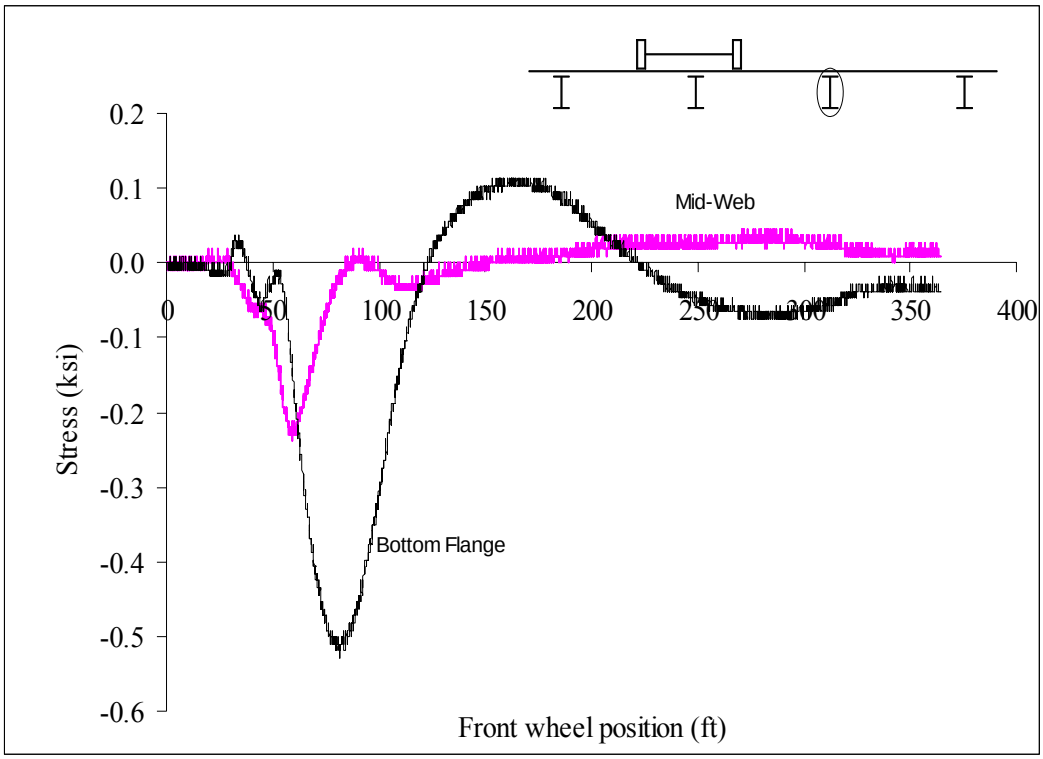

Figure A106: Las Cruces Bridge Test Run 6 S3 @ 2 ft from abutment

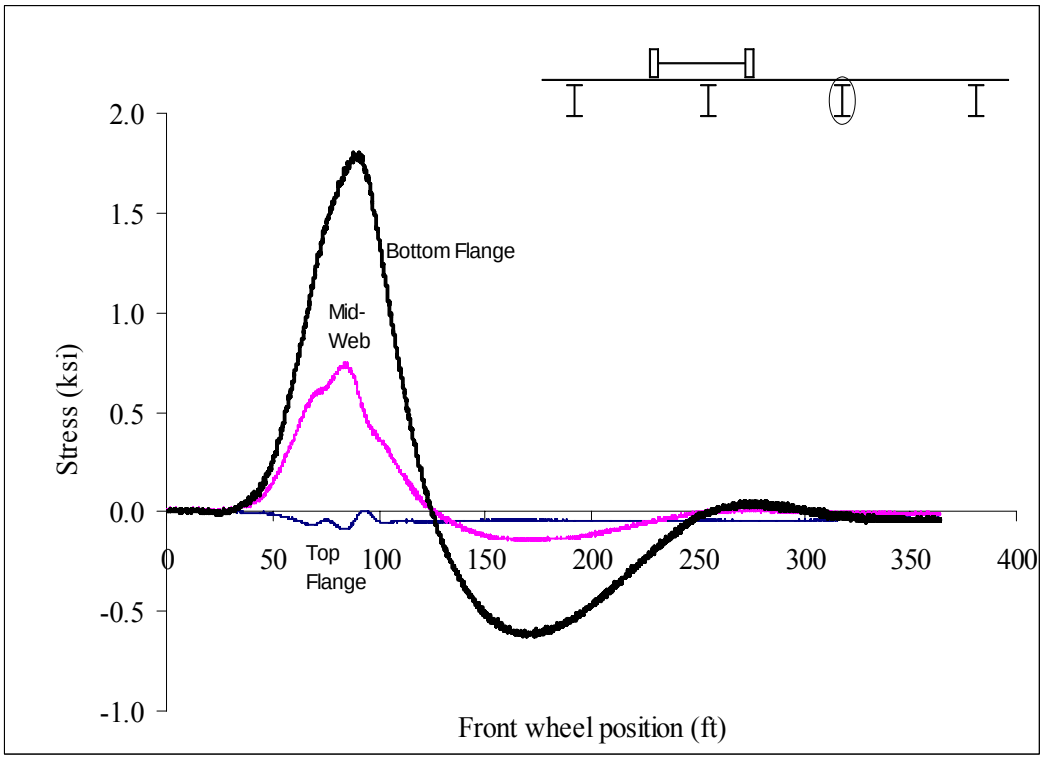

Figure A107: Las Cruces Bridge Test Run 6 S3 @ Midspan

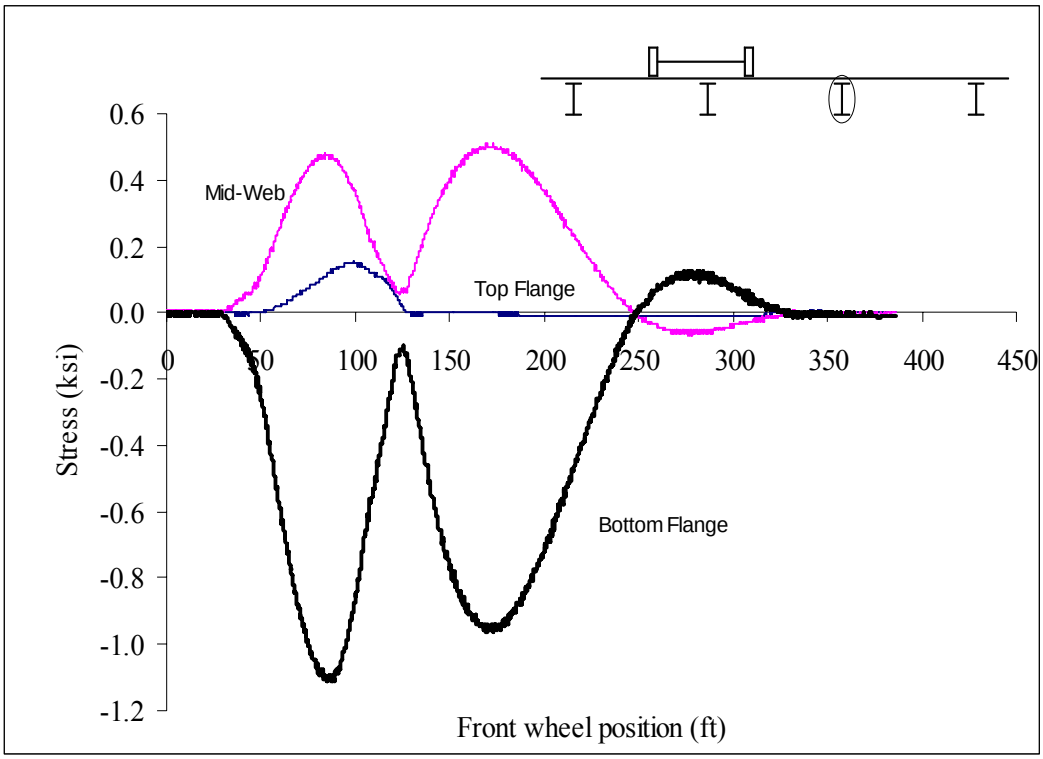

Figure A108: Las Cruces Bridge Test Run 6 S3 @ 2 ft from interior support

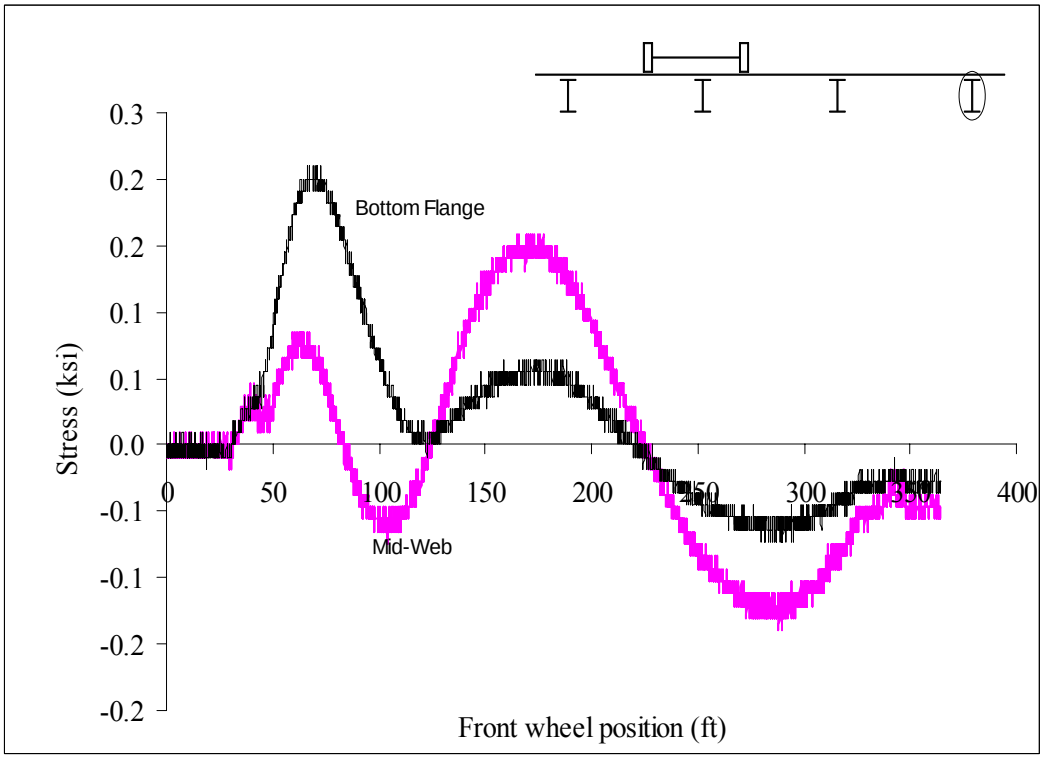

Figure A109: Las Cruces Bridge Test Run 6 S4 @ 2 ft from abutment

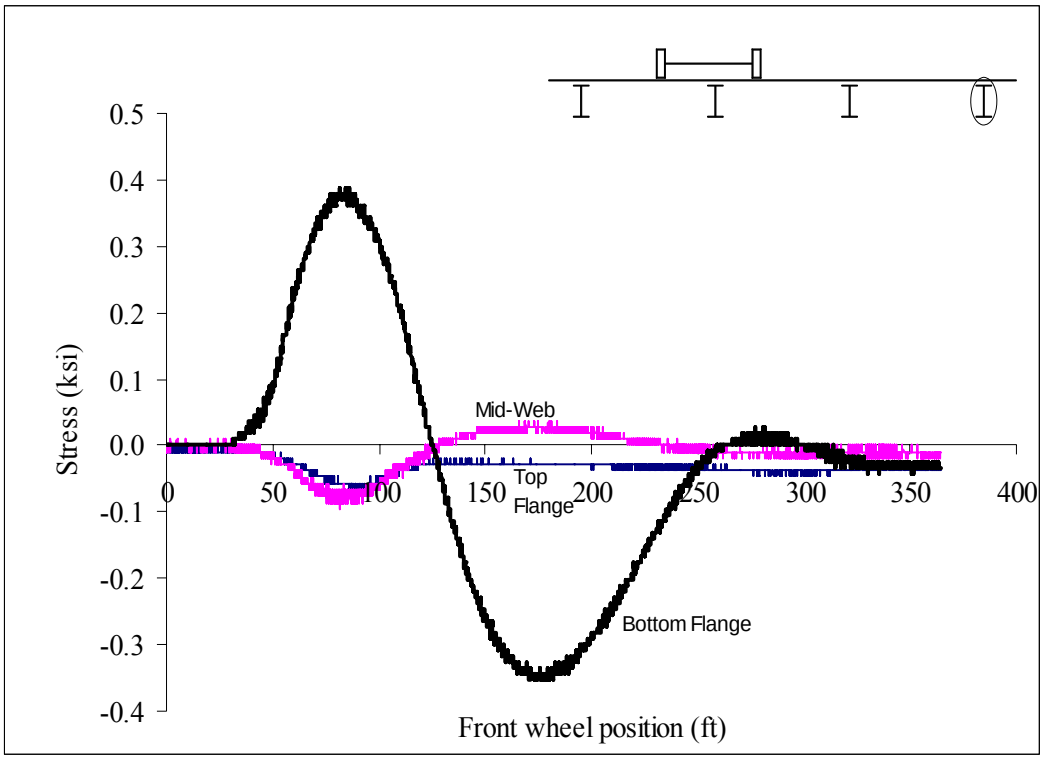

Figure A110: Las Cruces Bridge Test Run 6 S4 @ Midspan

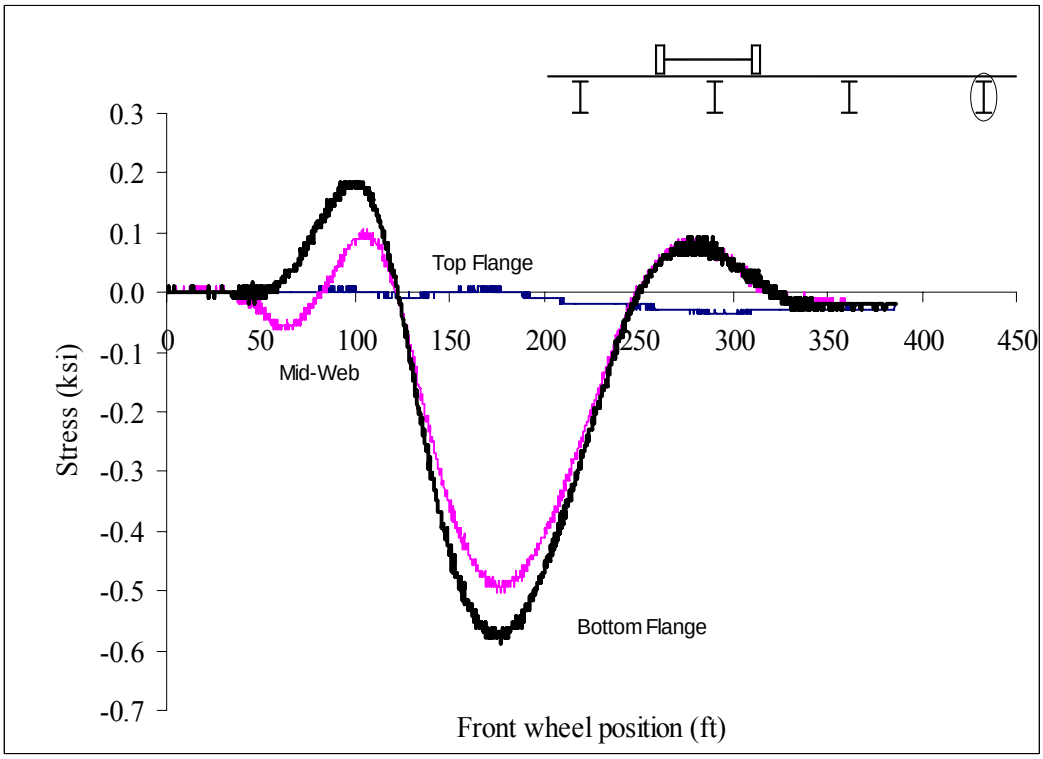

Figure A111: Las Cruces Bridge Test Run 6 S4 @ 2 ft from interior support

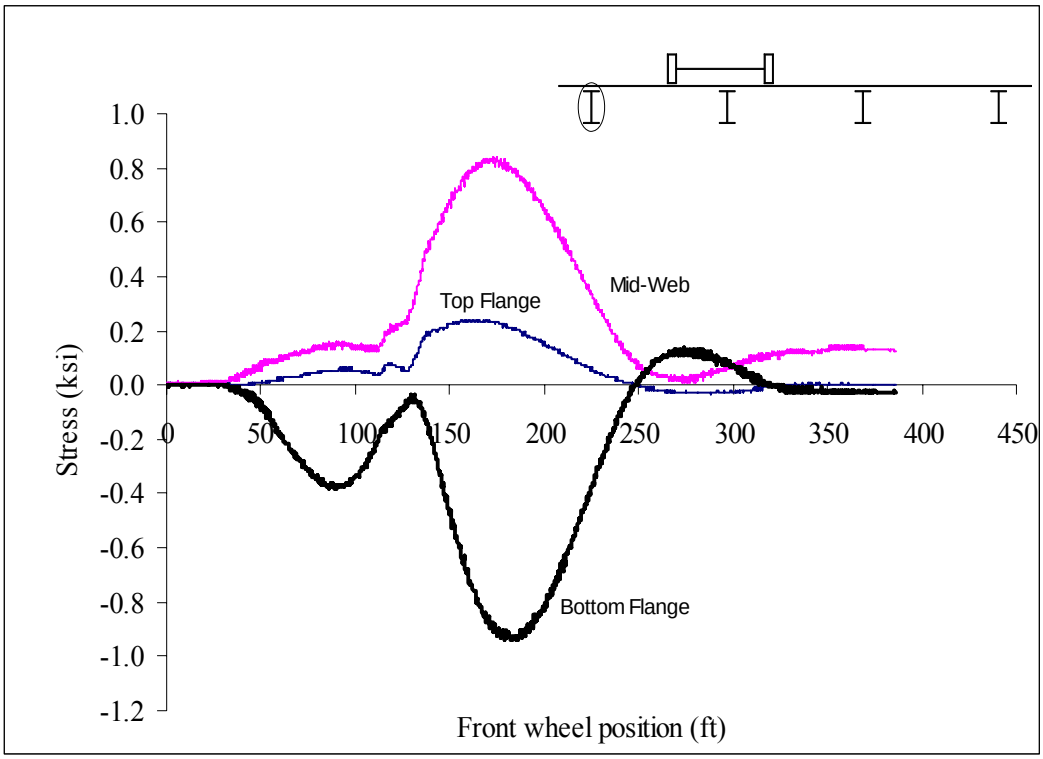

Figure A112: Las Cruces Bridge Test Run 6 S5 @ 2 ft from interior support

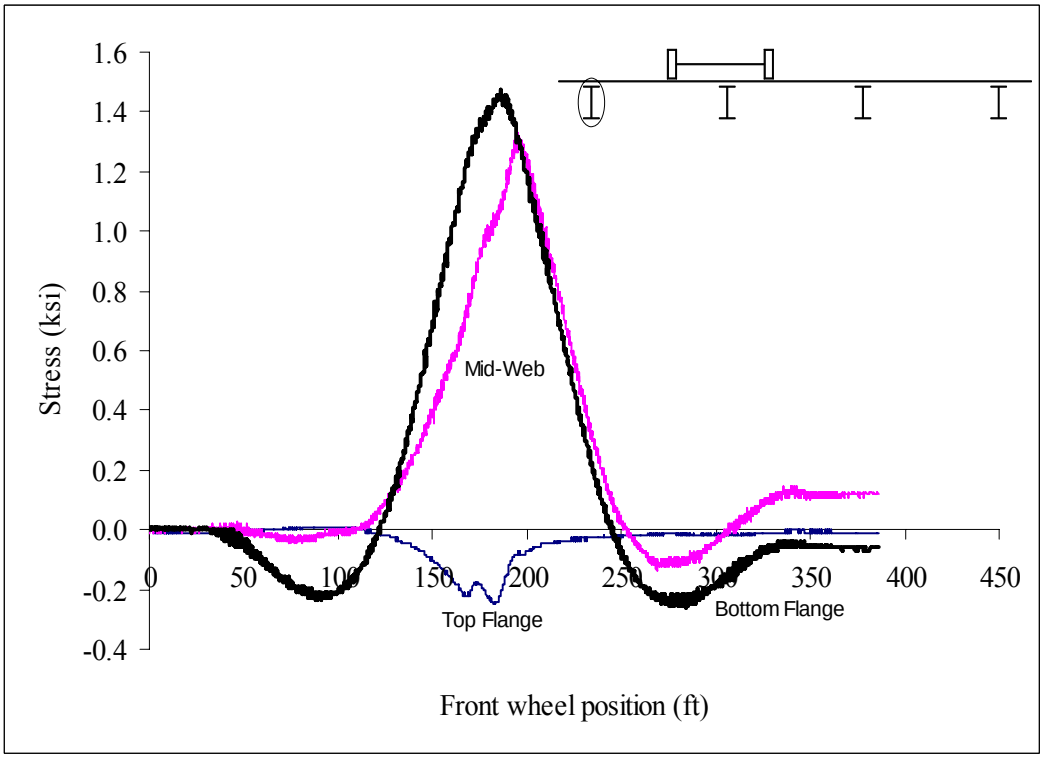

Figure A113: Las Cruces Bridge Test Run 6 S5 @ Midspan

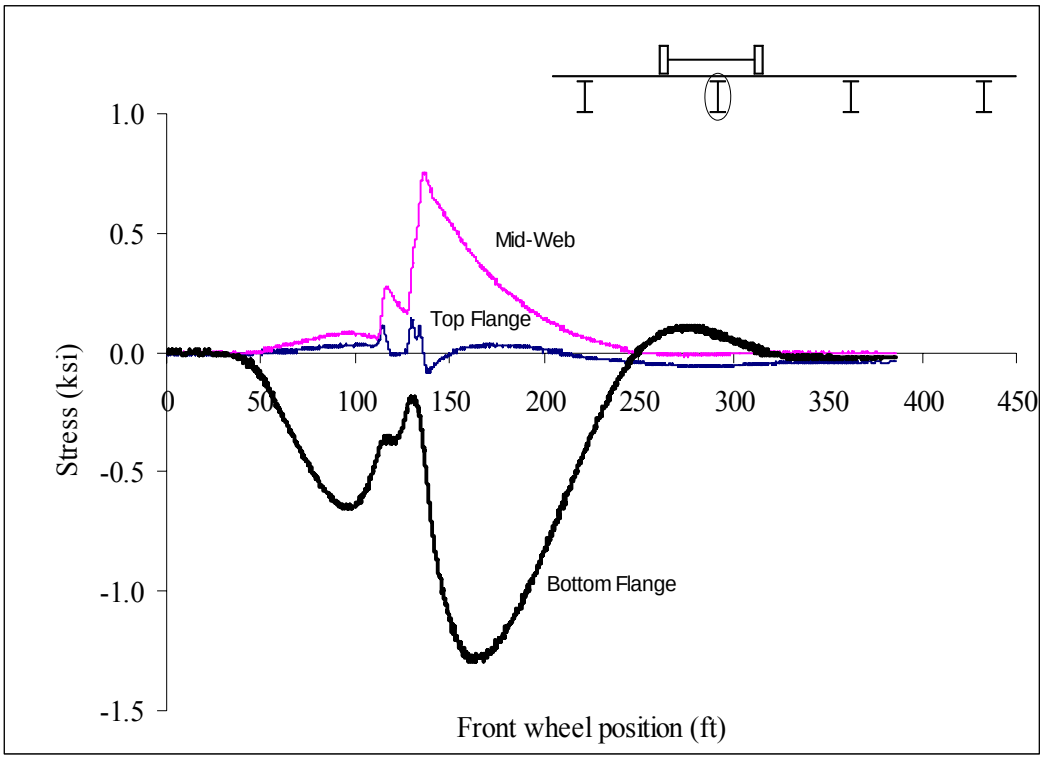

Figure A114: Las Cruces Bridge Test Run 6 S6 @ 2 ft from interior support

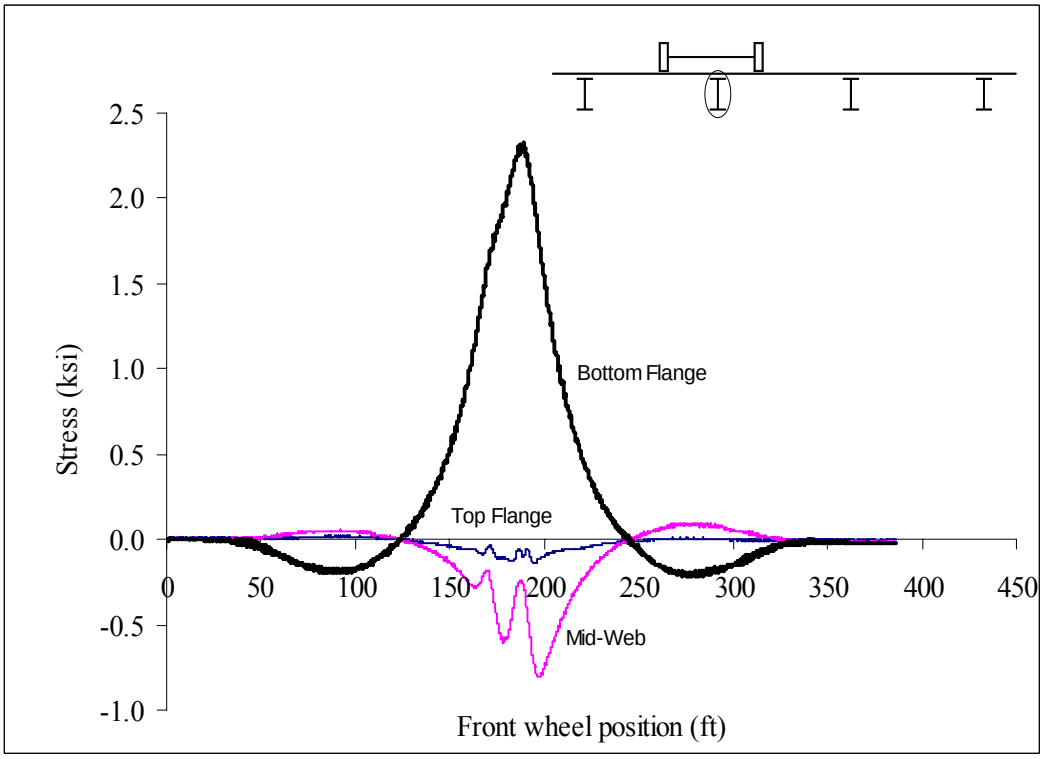

Figure A115: Las Cruces Bridge Test Run 6 S6 @ Midspan

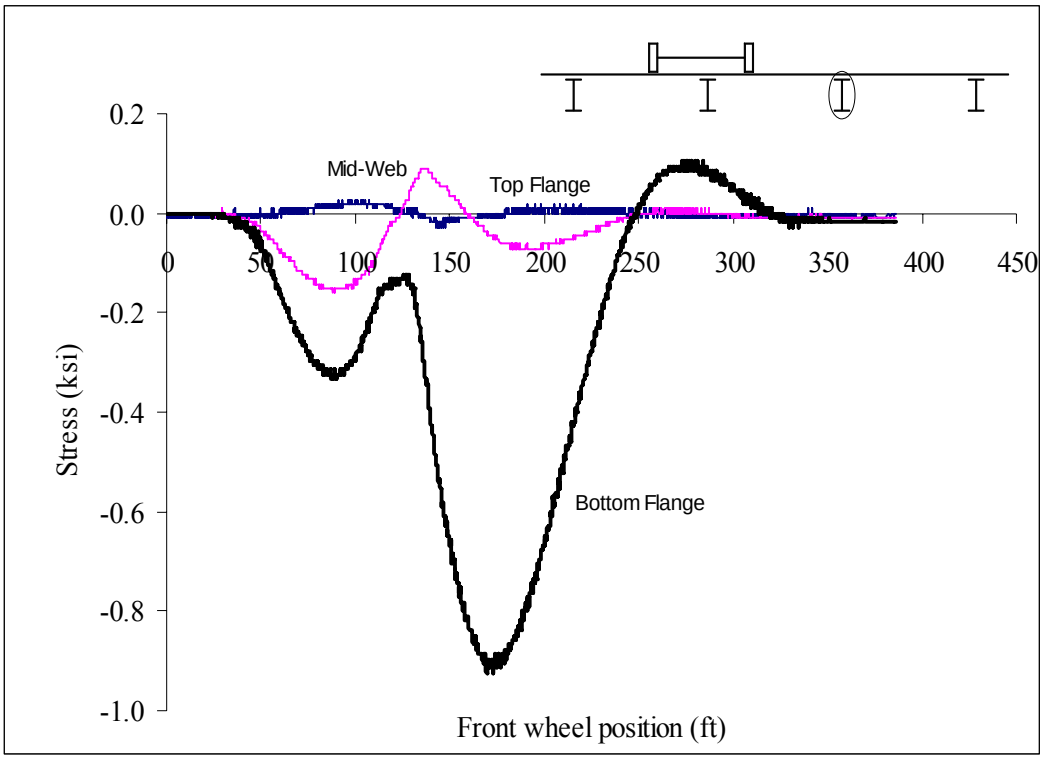

Figure A116: Las Cruces Bridge Test Run 6 S7 @ 2 ft from interior support

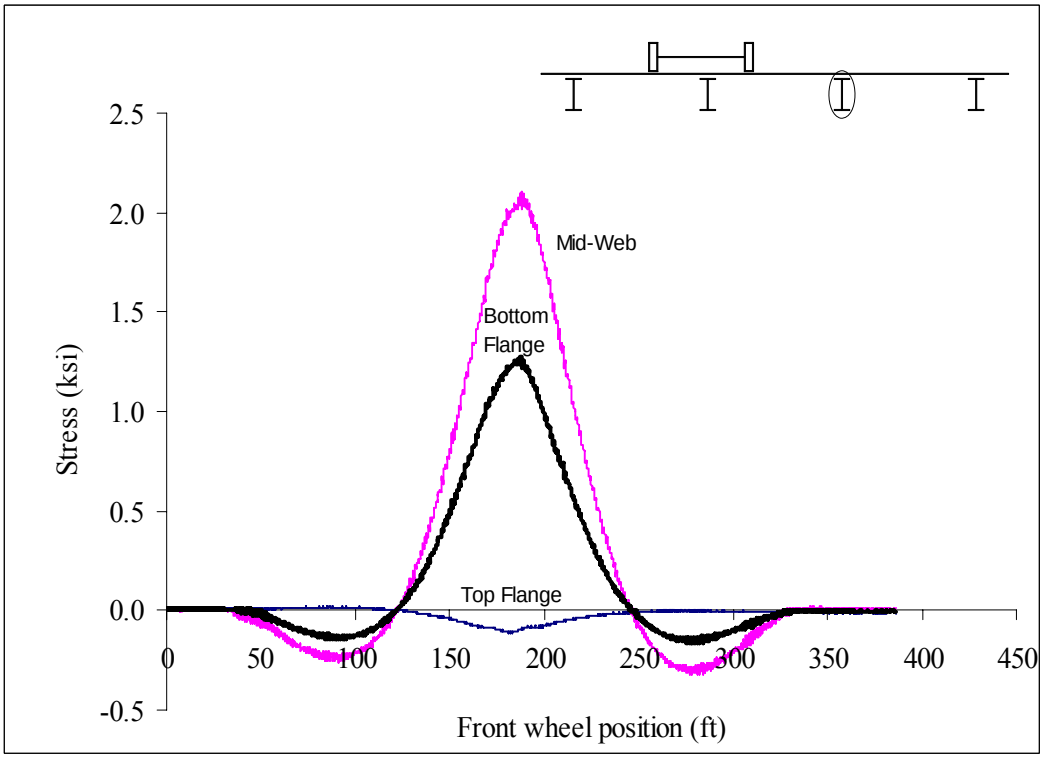

Figure A117: Las Cruces Bridge Test Run 6 S7 @ Midspan

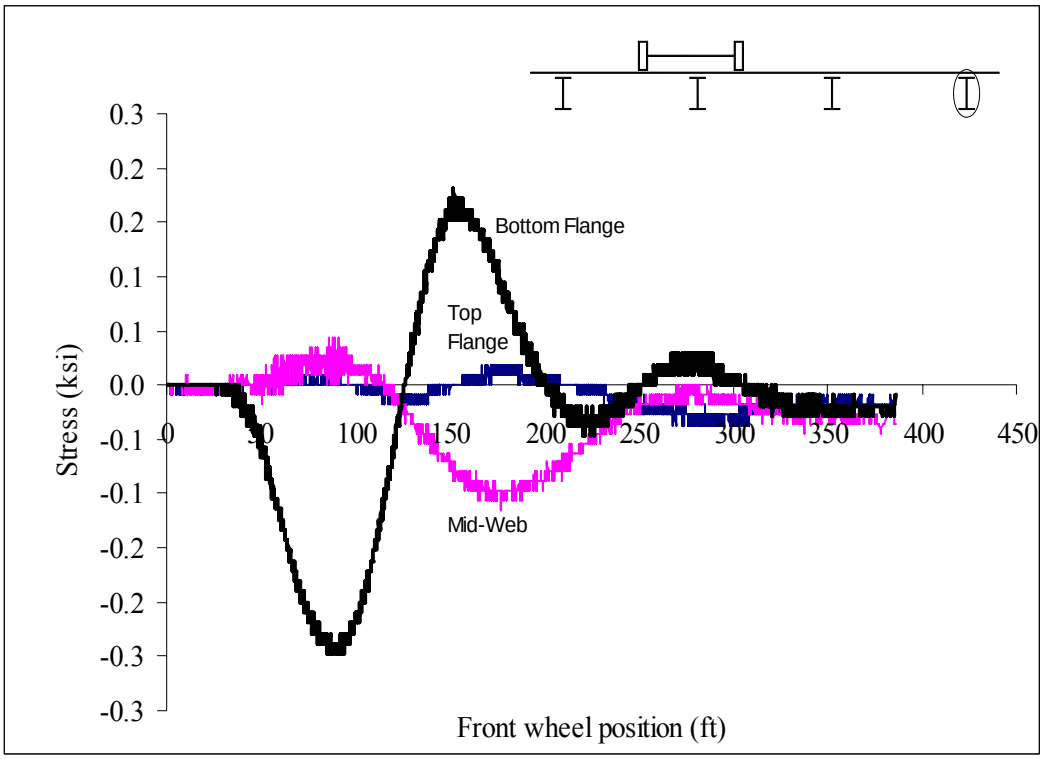

Figure A118: Las Cruces Bridge Test Run 6 S8 @ 2 ft from interior support

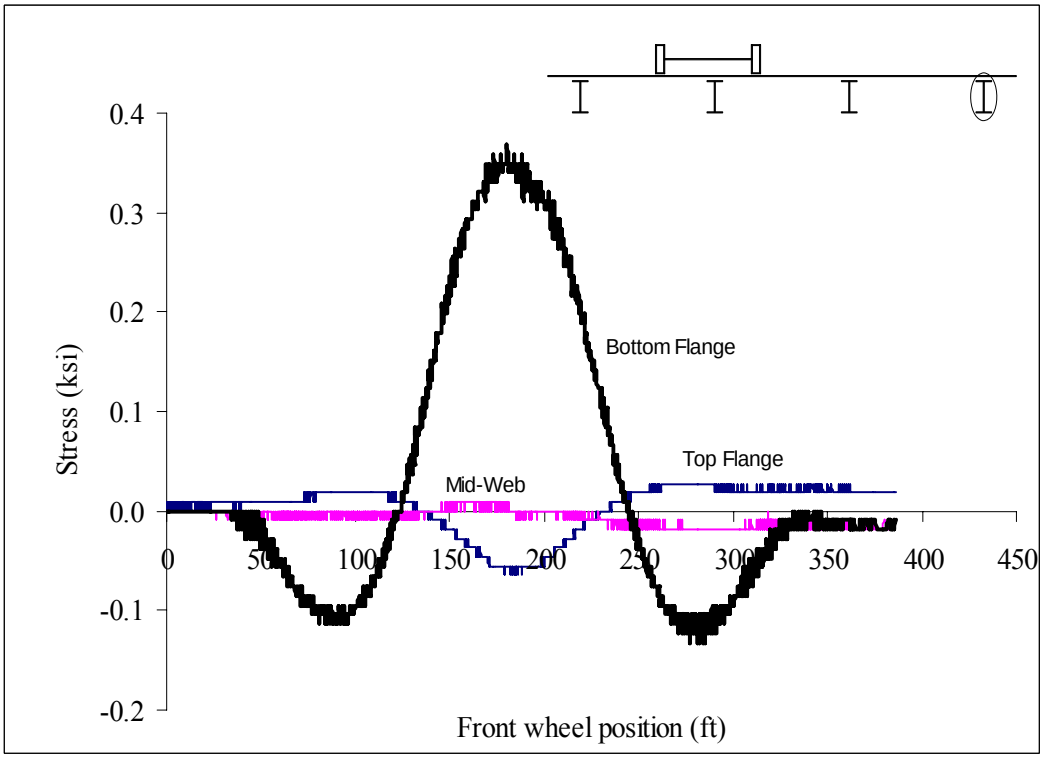

Figure A119: Las Cruces Bridge Test Run 6 S8 @ Midspan

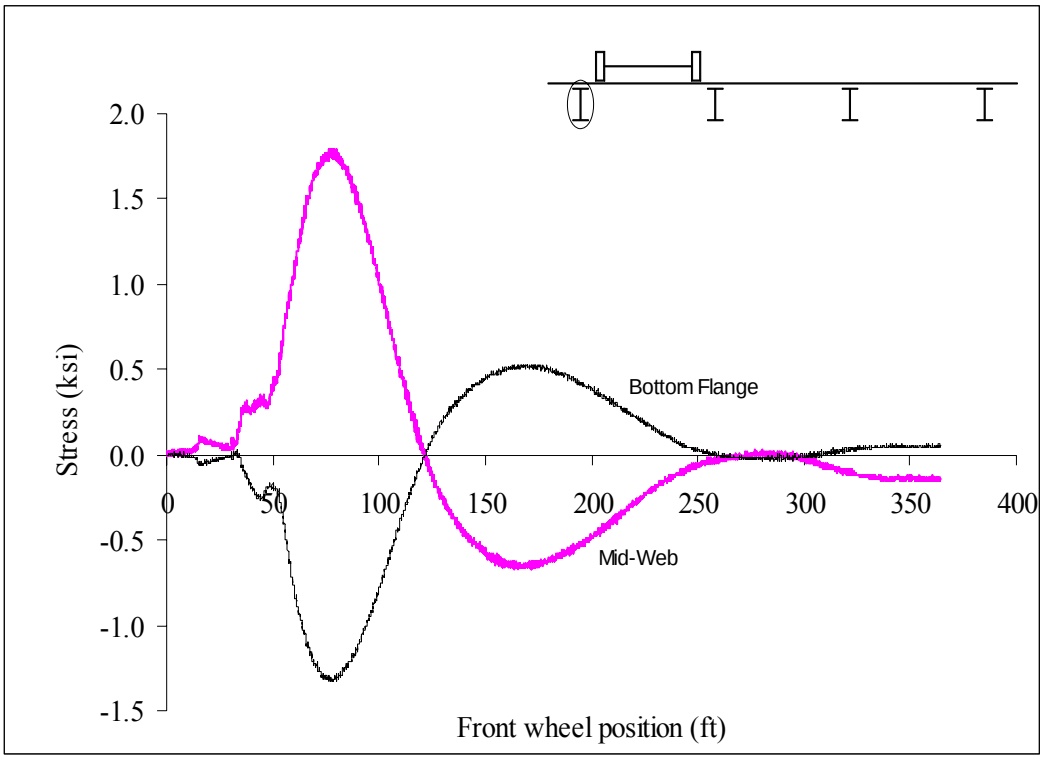

Figure A120: Las Cruces Bridge Test Run 7 S1 @ 2 ft from abutment

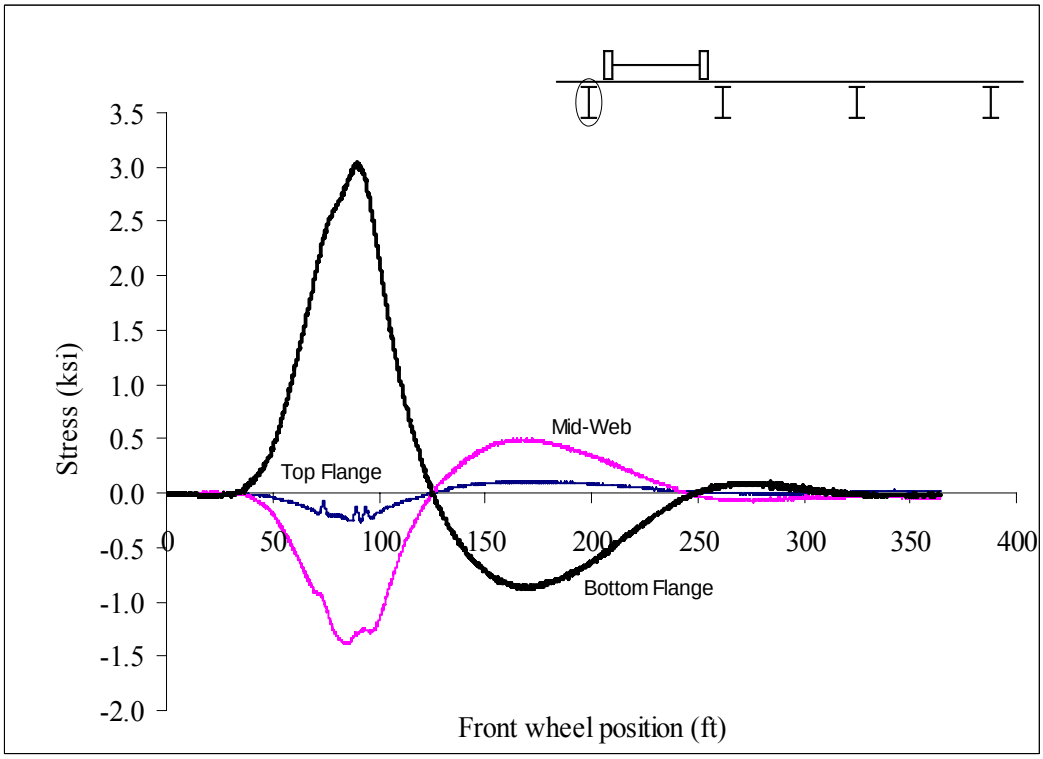

Figure A121: Las Cruces Bridge Test Run 7 S1 @ Midspan

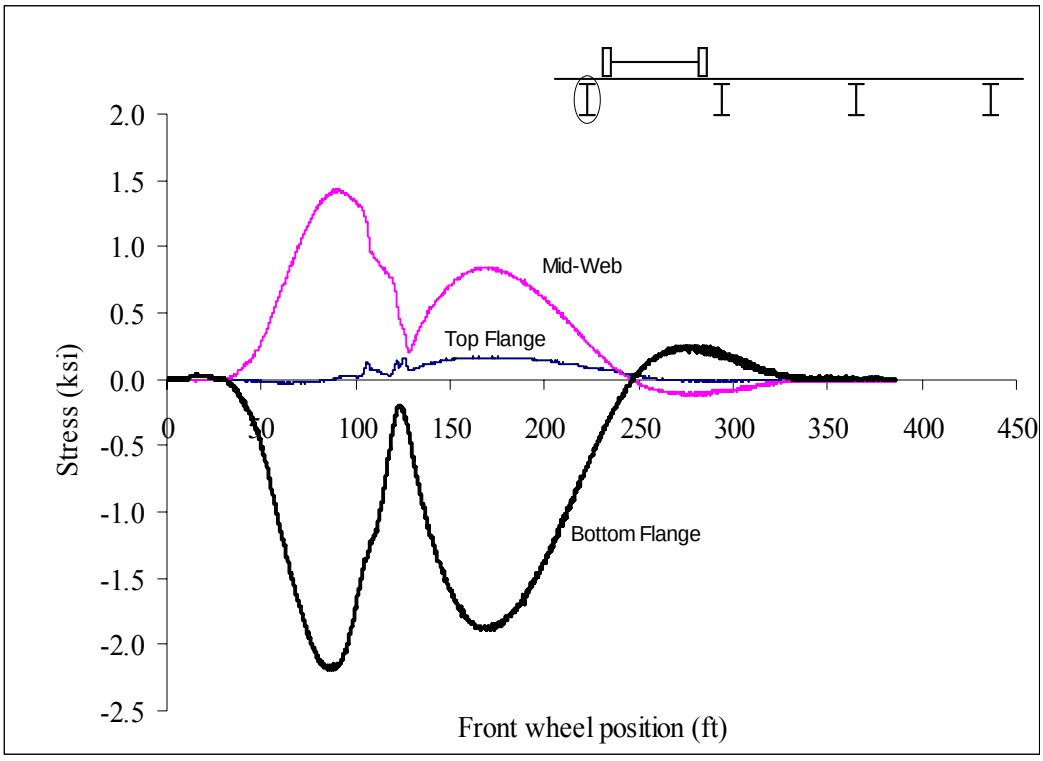

Figure A122: Las Cruces Bridge Test Run 7 S1 @ 2 ft from interior support

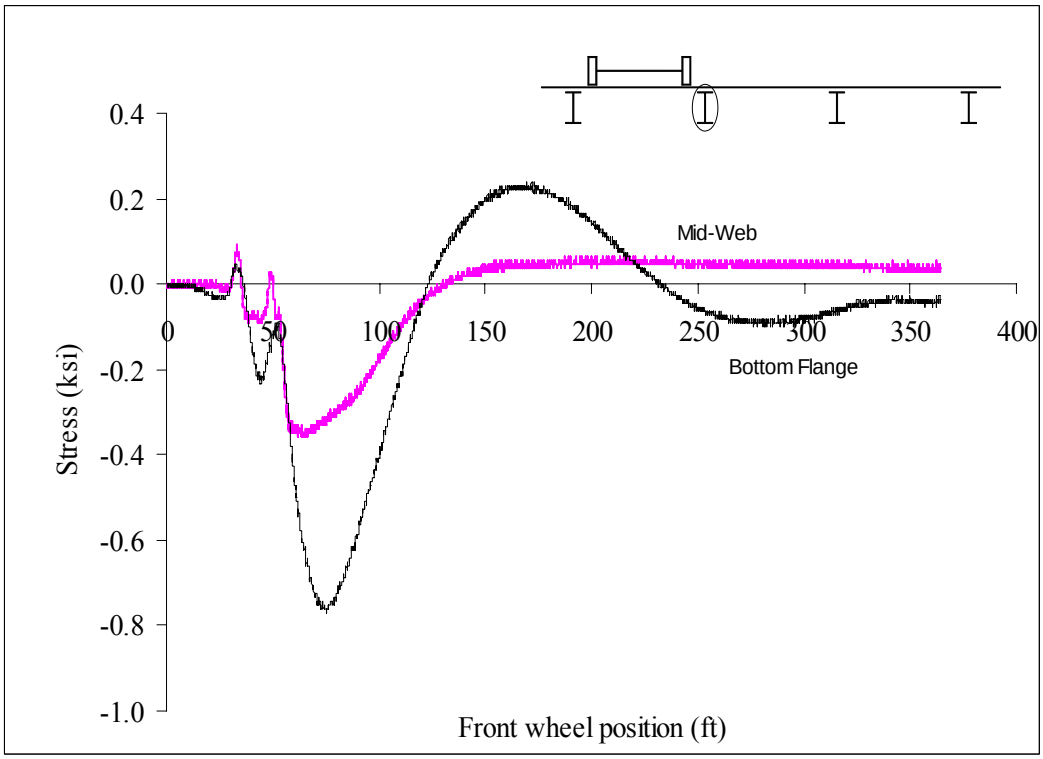

Figure A123: Las Cruces Bridge Test Run 7 S2 @ 2 ft from abutment

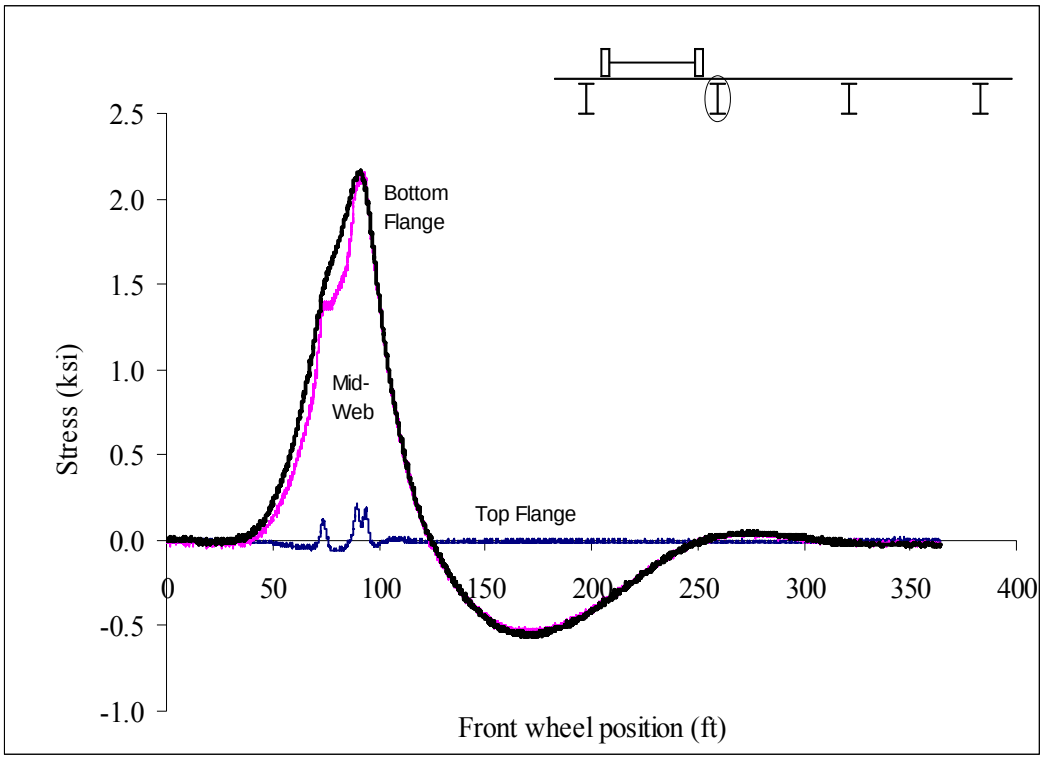

Figure A124: Las Cruces Bridge Test Run 7 S2 @ Midspan

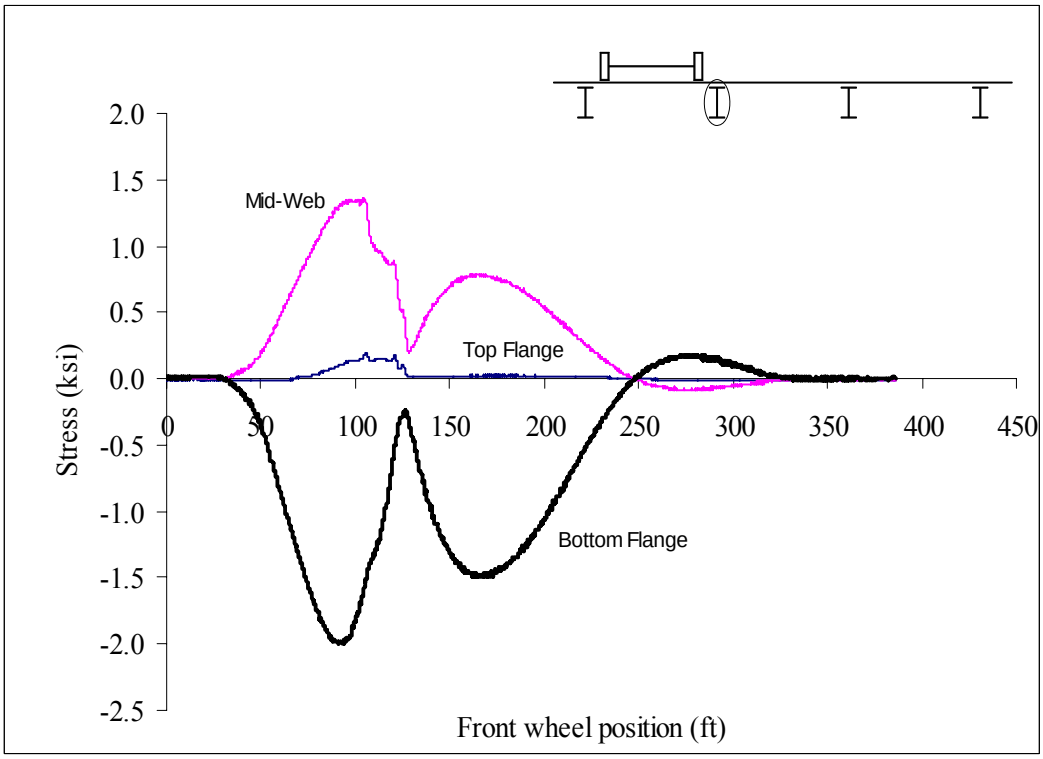

Figure A125: Las Cruces Bridge Test Run 7 S2 @ 2 ft from interior support

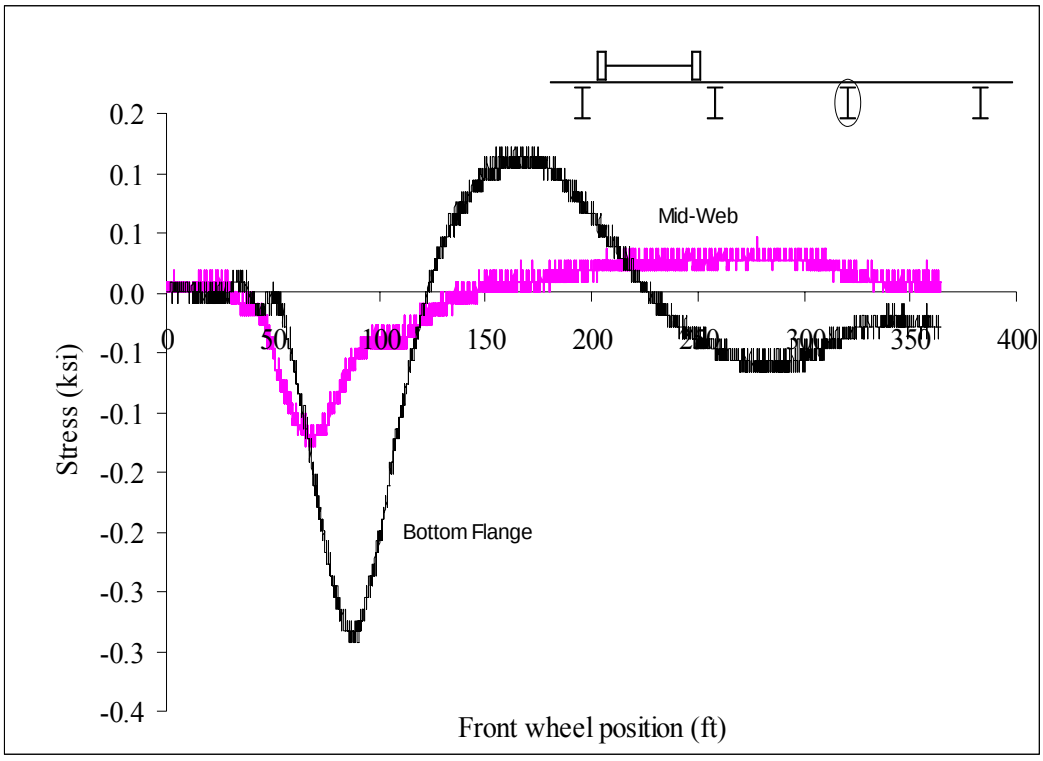

Figure A126: Las Cruces Bridge Test Run 7 S3 @ 2 ft from abutment

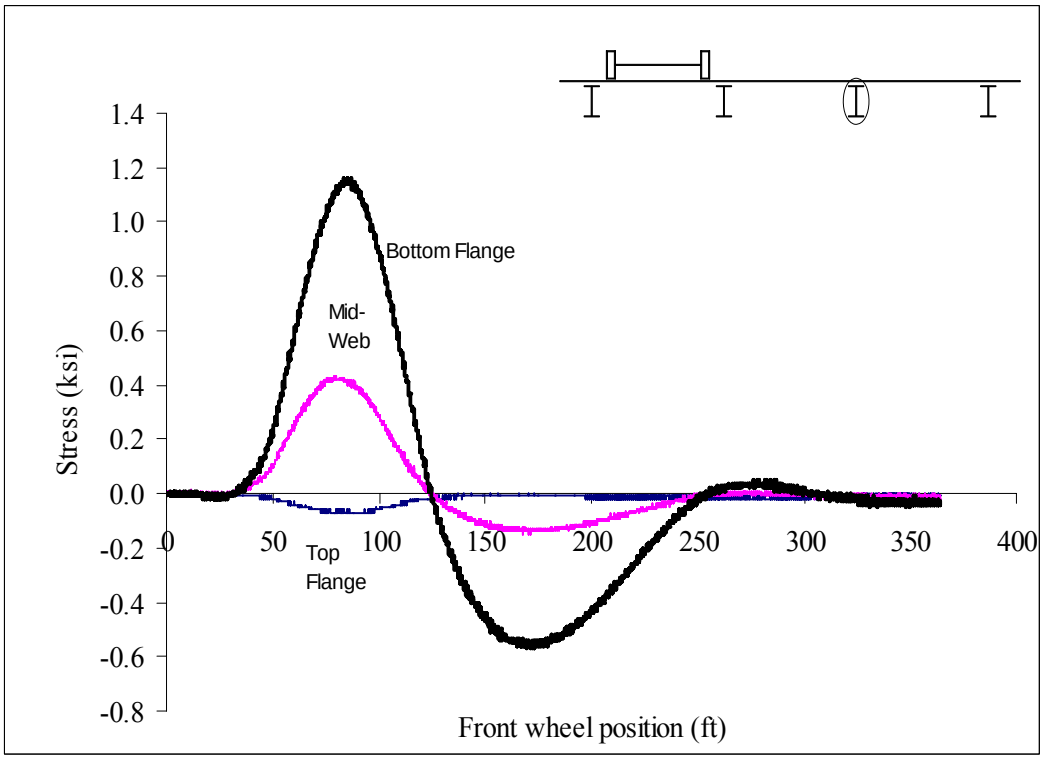

Figure A127: Las Cruces Bridge Test Run 7 S3 @ Midspan

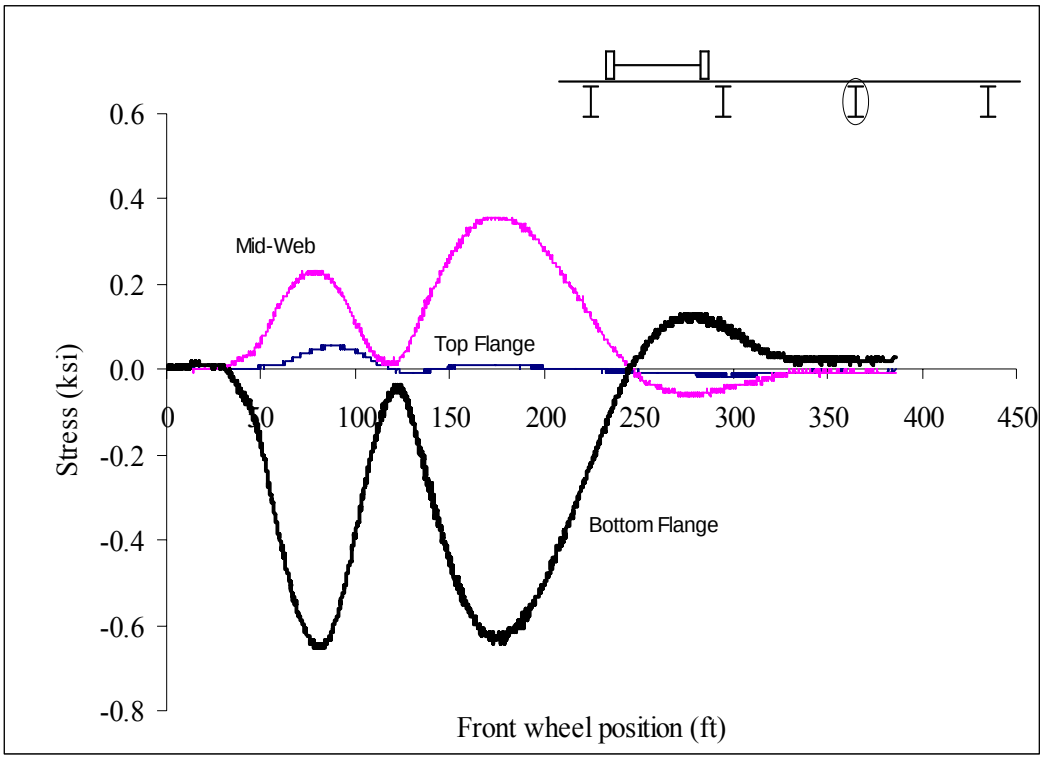

Figure A128: Las Cruces Bridge Test Run 7 S3 @ 2 ft from interior support

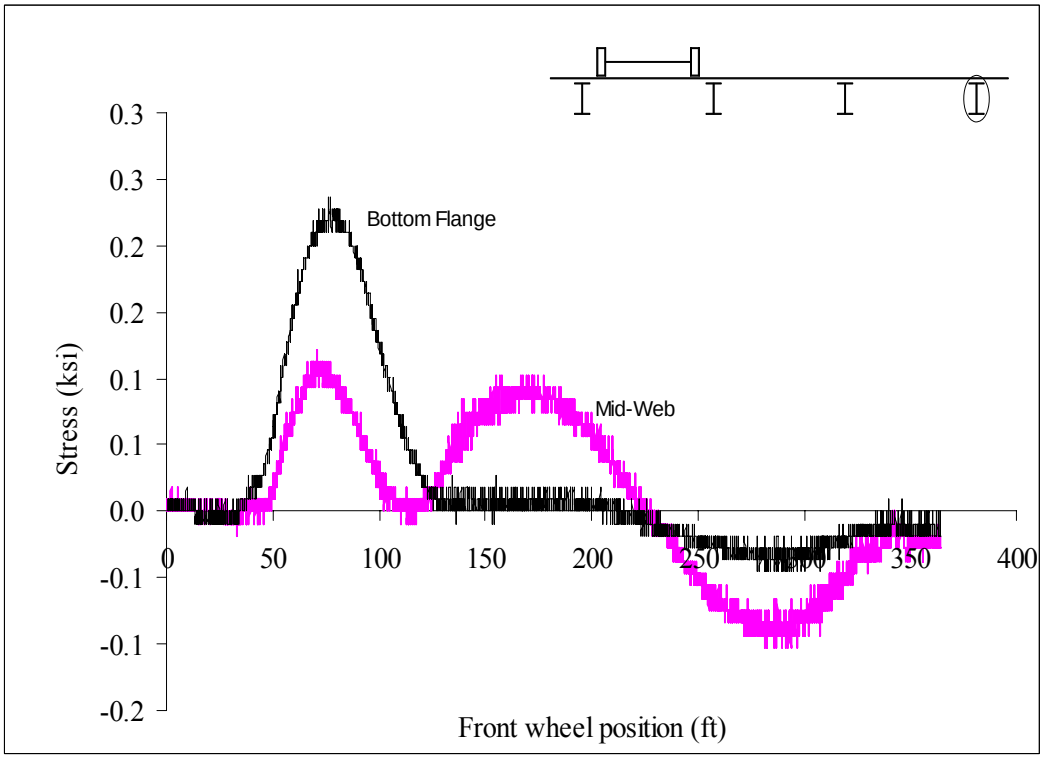

Figure A129: Las Cruces Bridge Test Run 7 S4 @ 2 ft from abutment

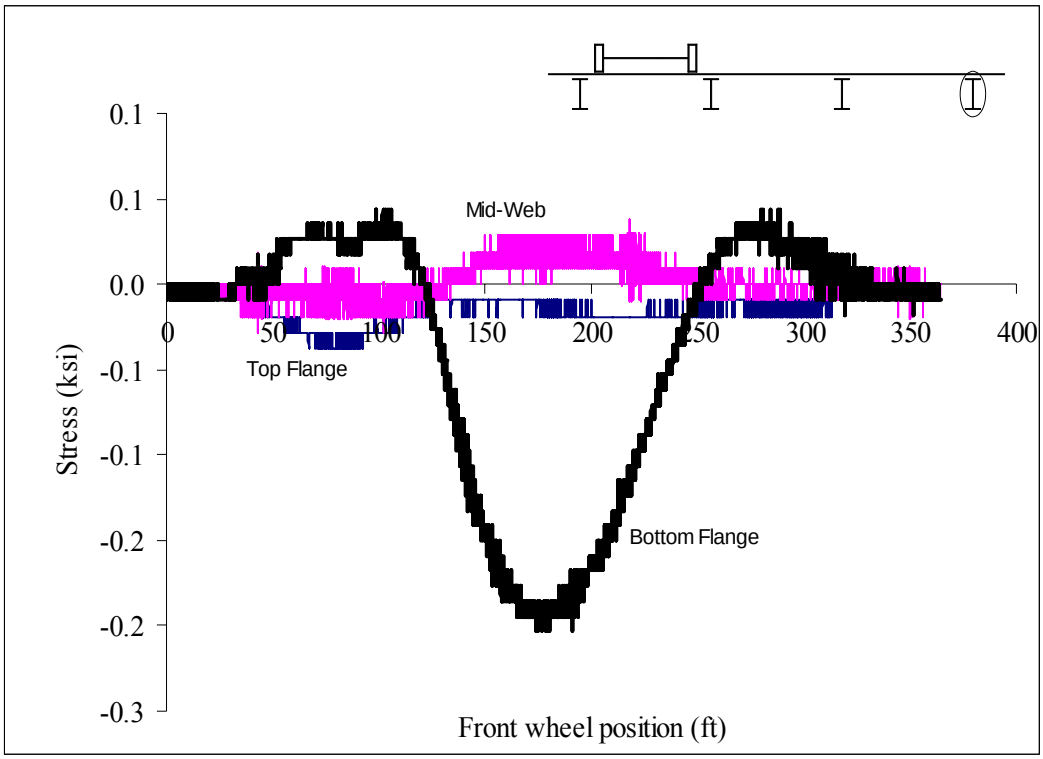

Figure A130: Las Cruces Bridge Test Run 7 S4 @ Midspan

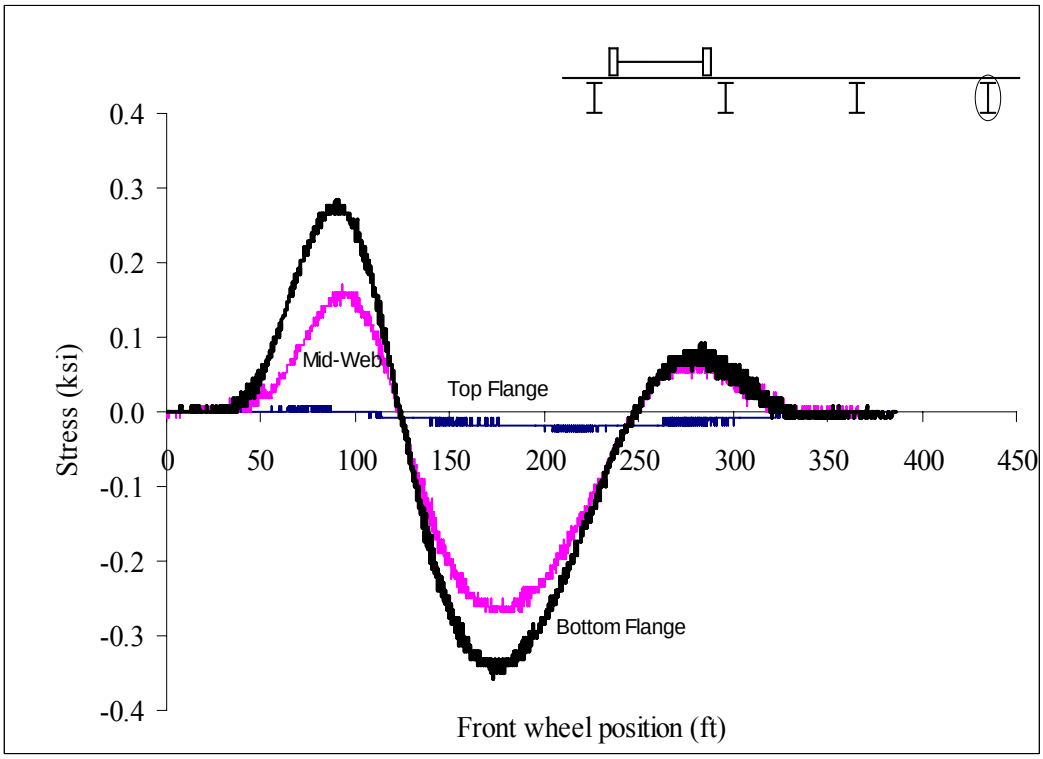

Figure A131: Las Cruces Bridge Test Run 7 S4 @ 2 ft from interior support

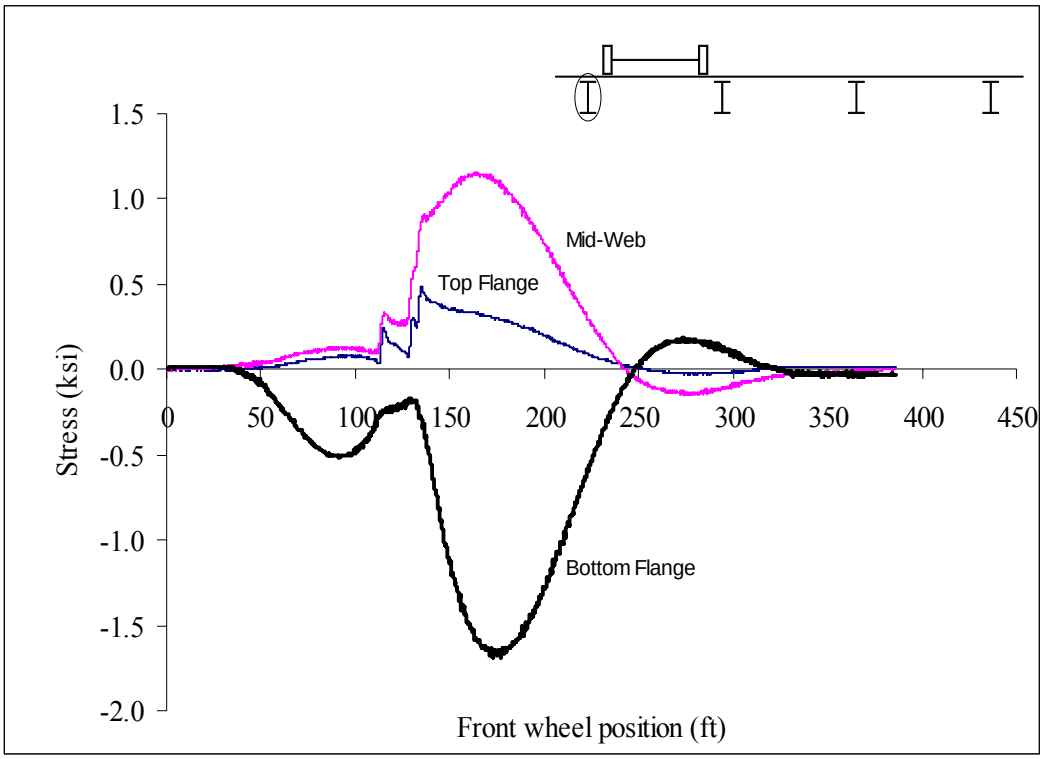

Figure A132: Las Cruces Bridge Test Run 7 S5 @ 2 ft from interior support

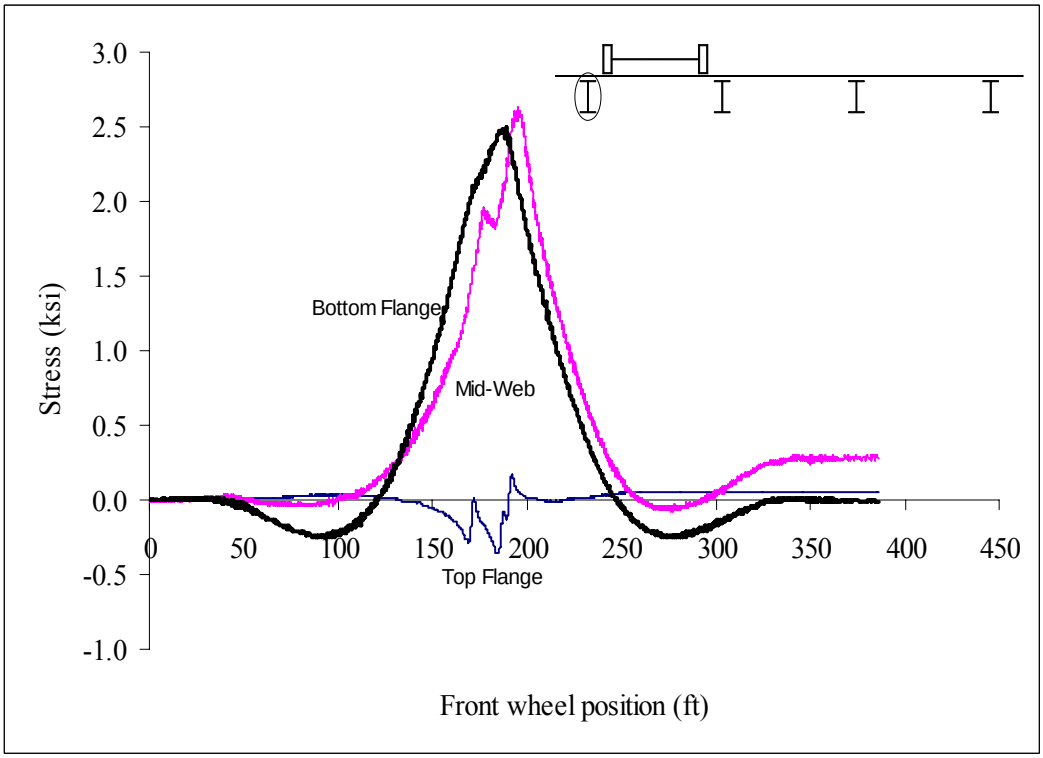

Figure A133: Las Cruces Bridge Test Run 7 S5 @ Midspan

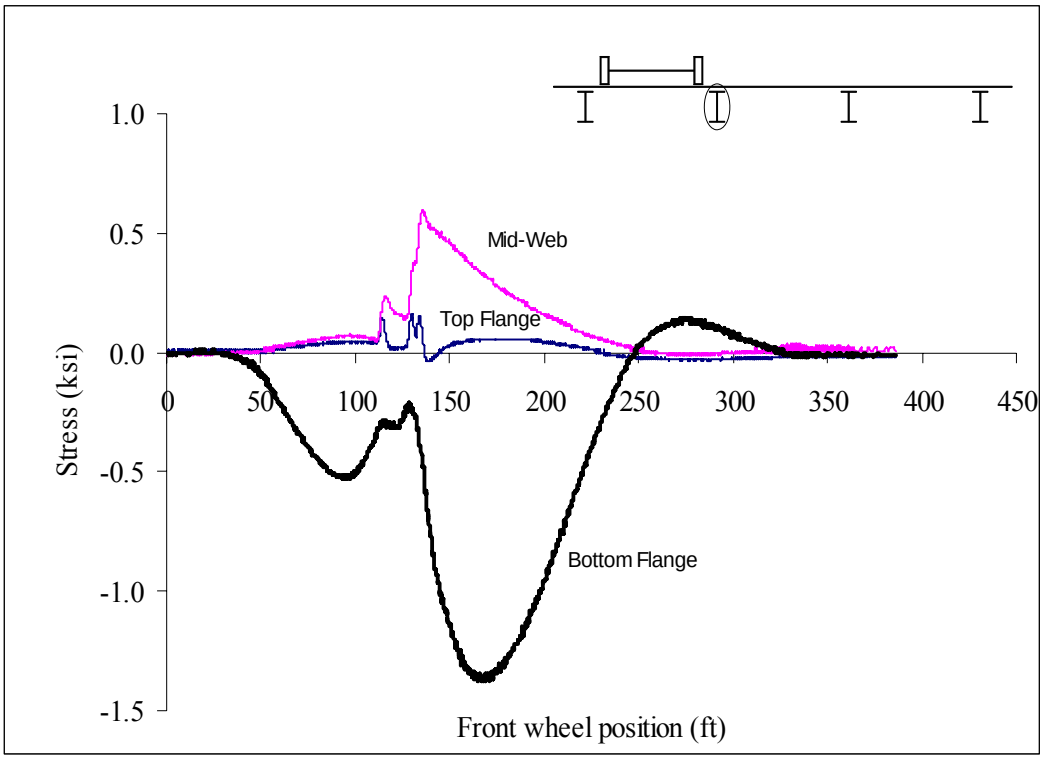

Figure A134: Las Cruces Bridge Test Run 7 S6 @ 2 ft from interior support

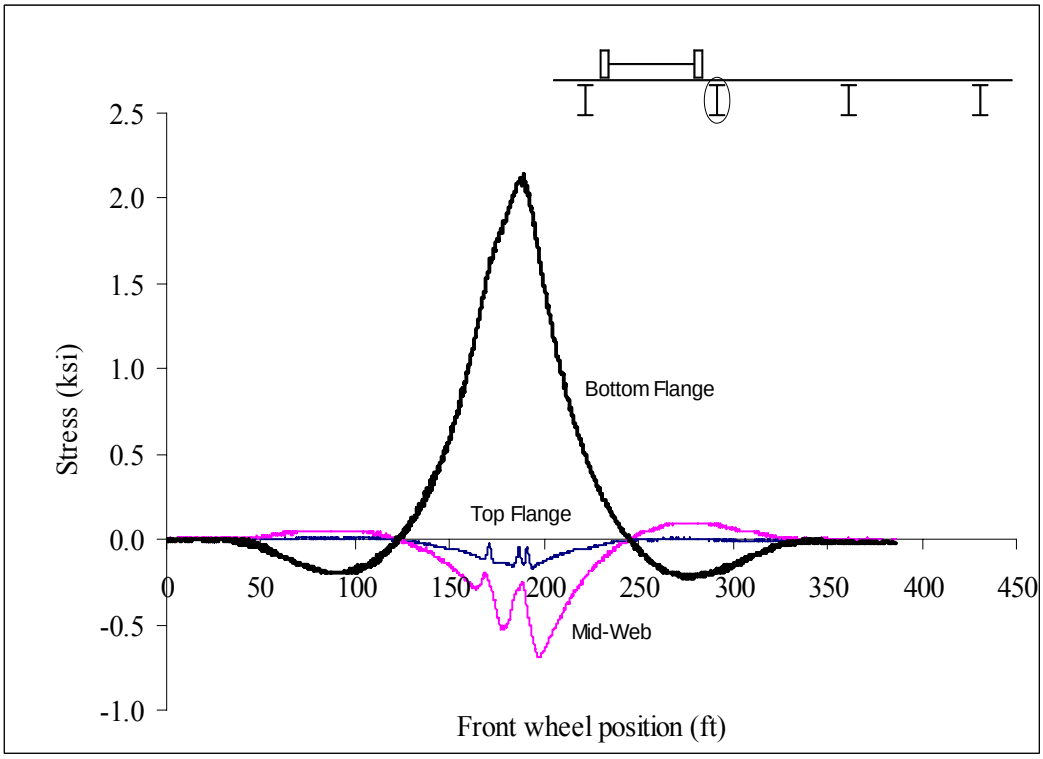

Figure A135: Las Cruces Bridge Test Run 7 S6 @ Midspan

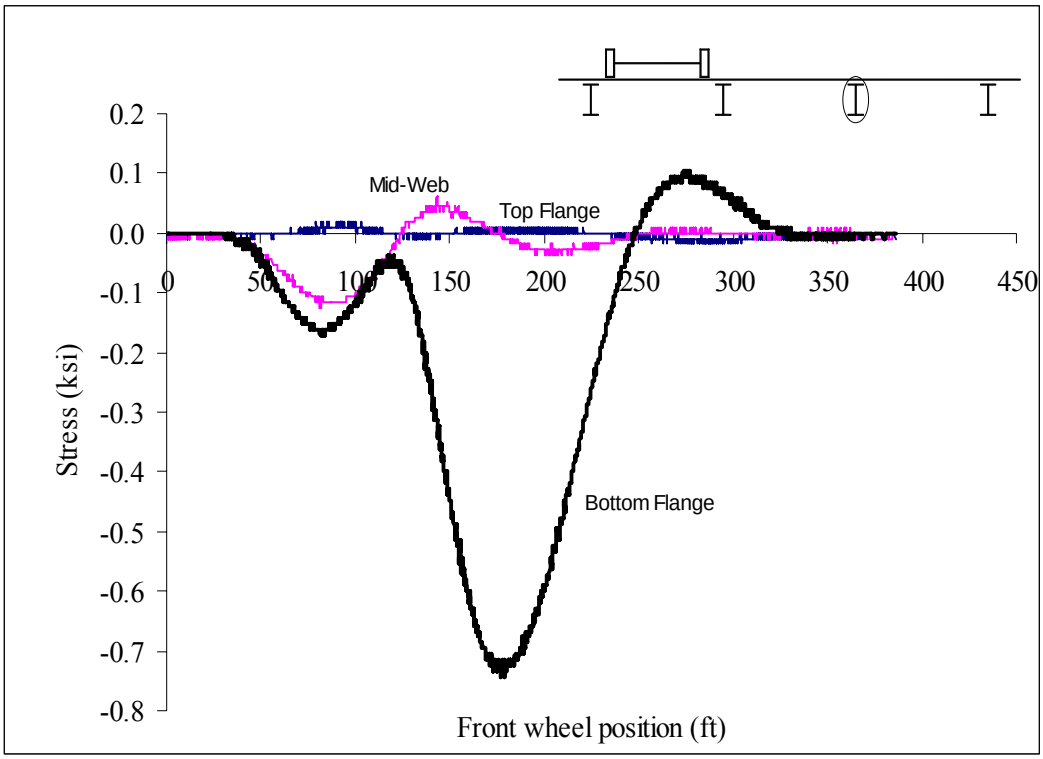

Figure A136: Las Cruces Bridge Test Run 7 S7 @ 2 ft from interior support

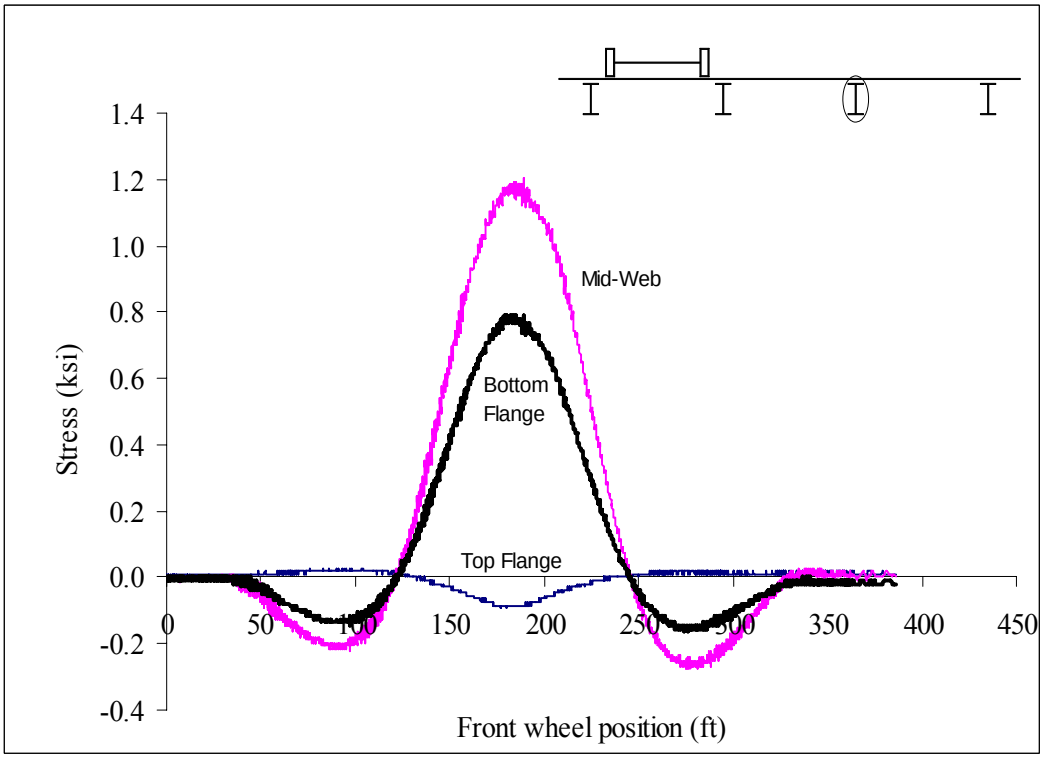

Figure A137: Las Cruces Bridge Test Run 7 S7 @ Midspan

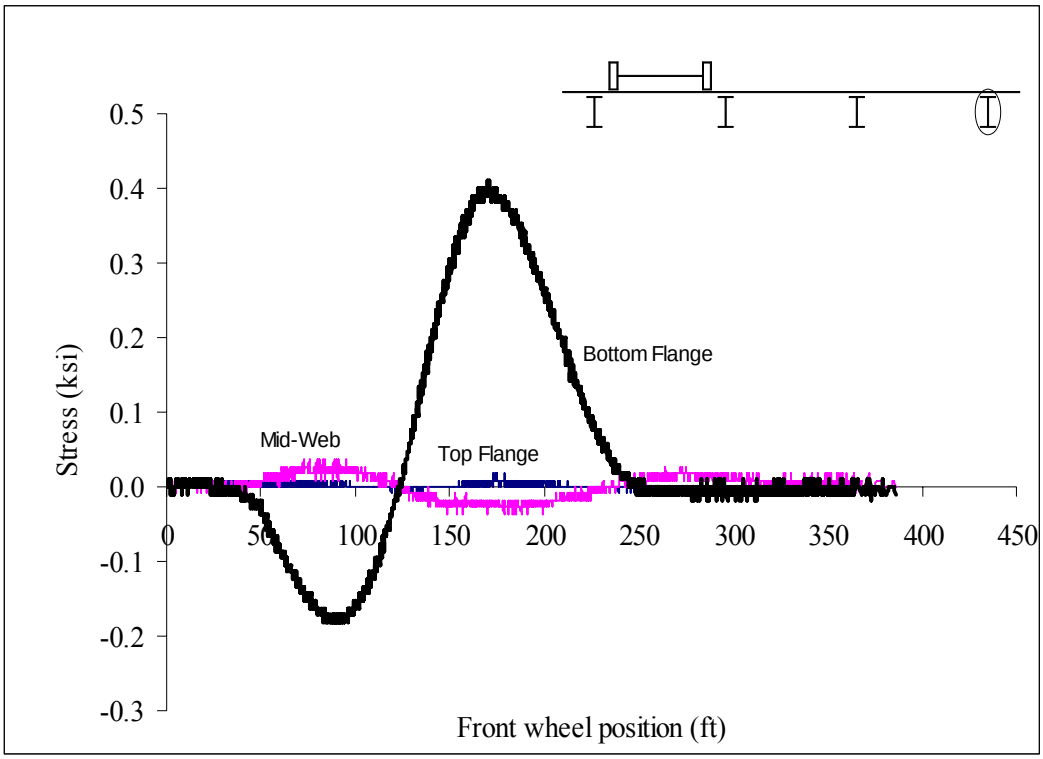

Figure A138: Las Cruces Bridge Test Run 7 S8 @ 2 ft from interior support

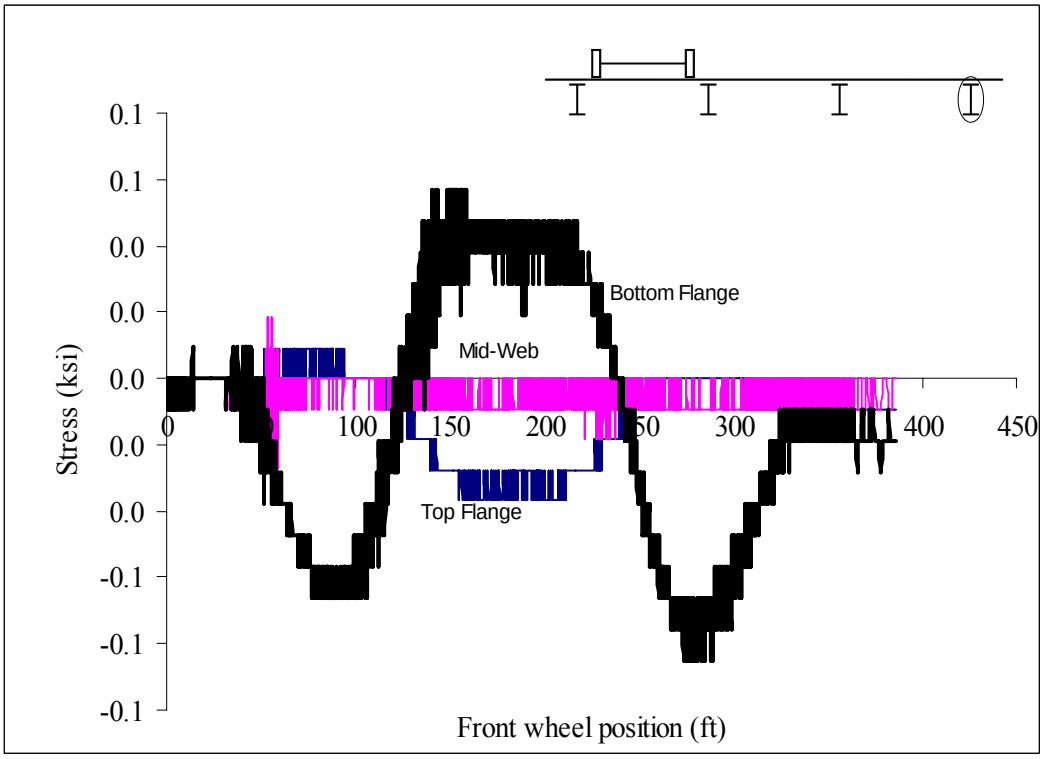

Figure A139: Las Cruces Bridge Test Run 7 S8 @ Midspan

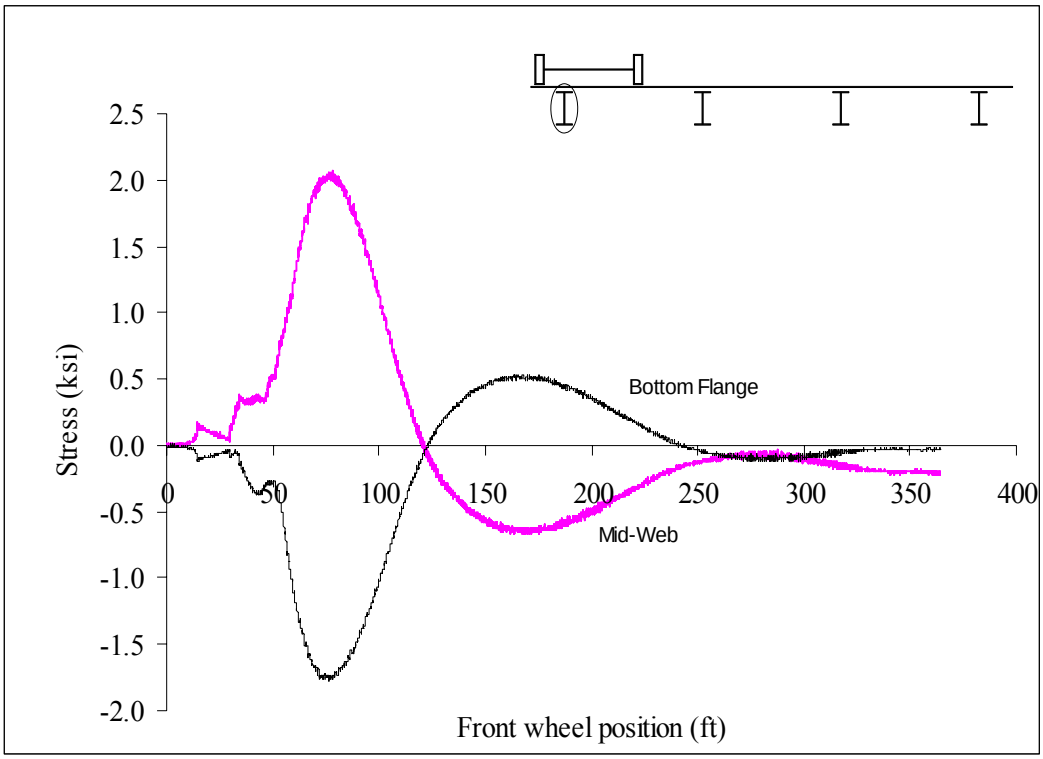

Figure A140: Las Cruces Bridge Test Run 8 S1 @ 2 ft from abutment

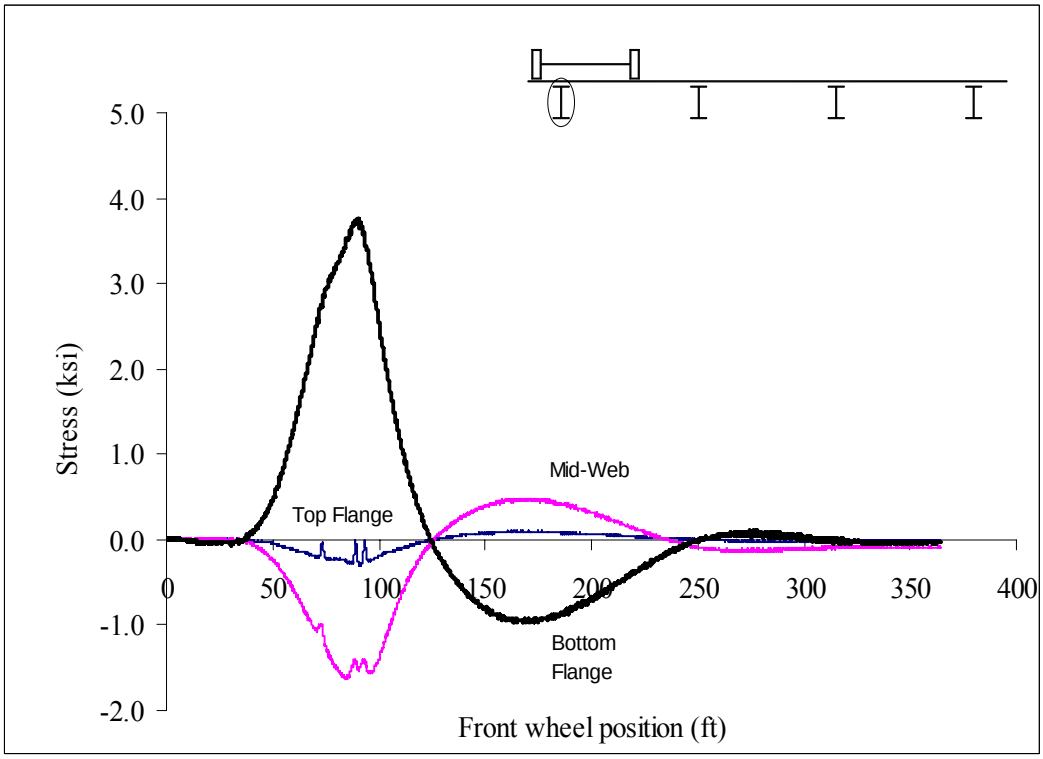

Figure A141: Las Cruces Bridge Test Run 8 S1 @ Midspan

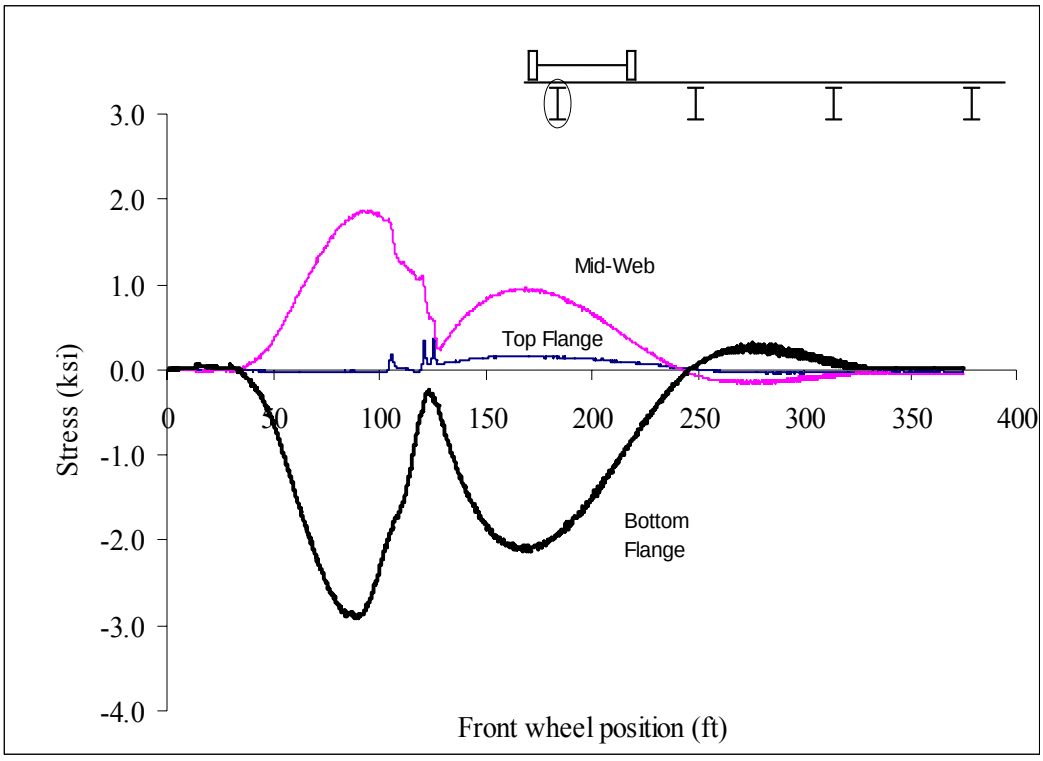

Figure A142: Las Cruces Bridge Test Run 8 S1 @ 2 ft from interior support

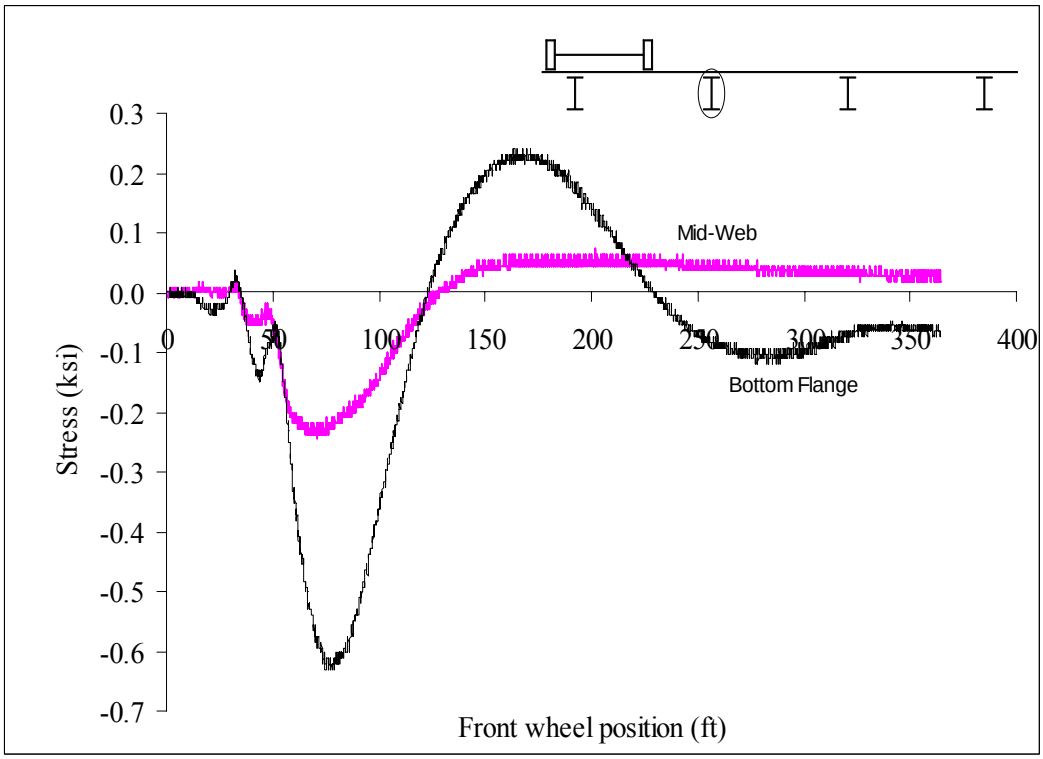

Figure A143: Las Cruces Bridge Test Run 8 S2 @ 2 ft from abutment

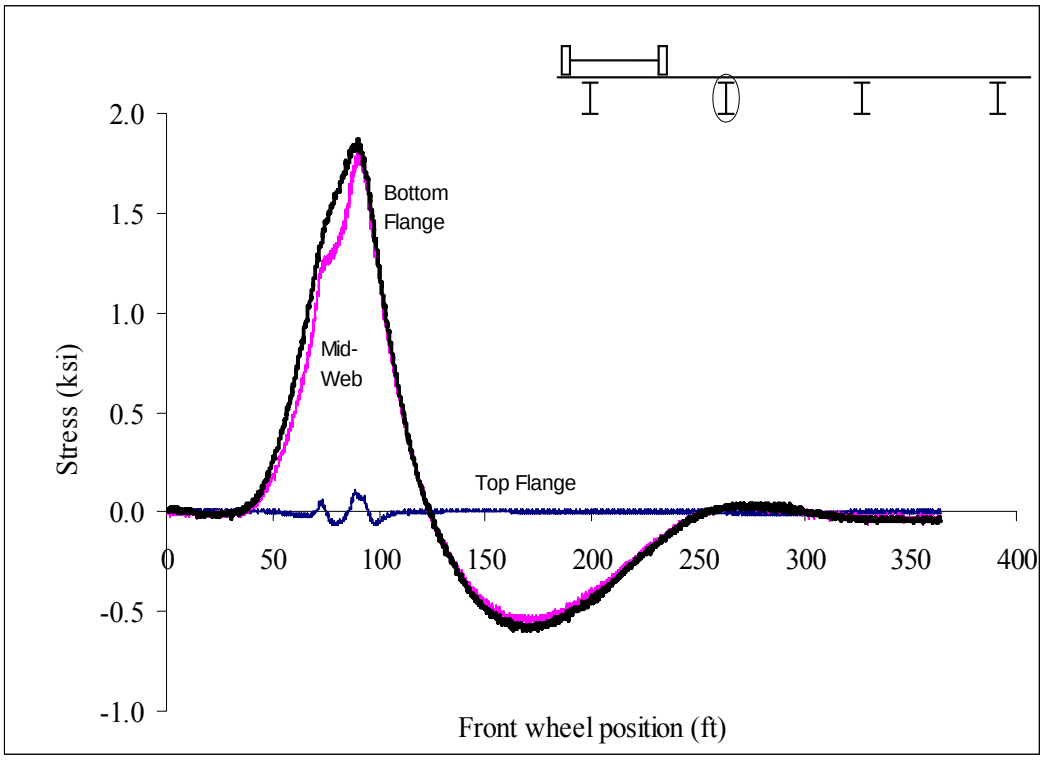

Figure A144: Las Cruces Bridge Test Run 8 S2 @ Midspan

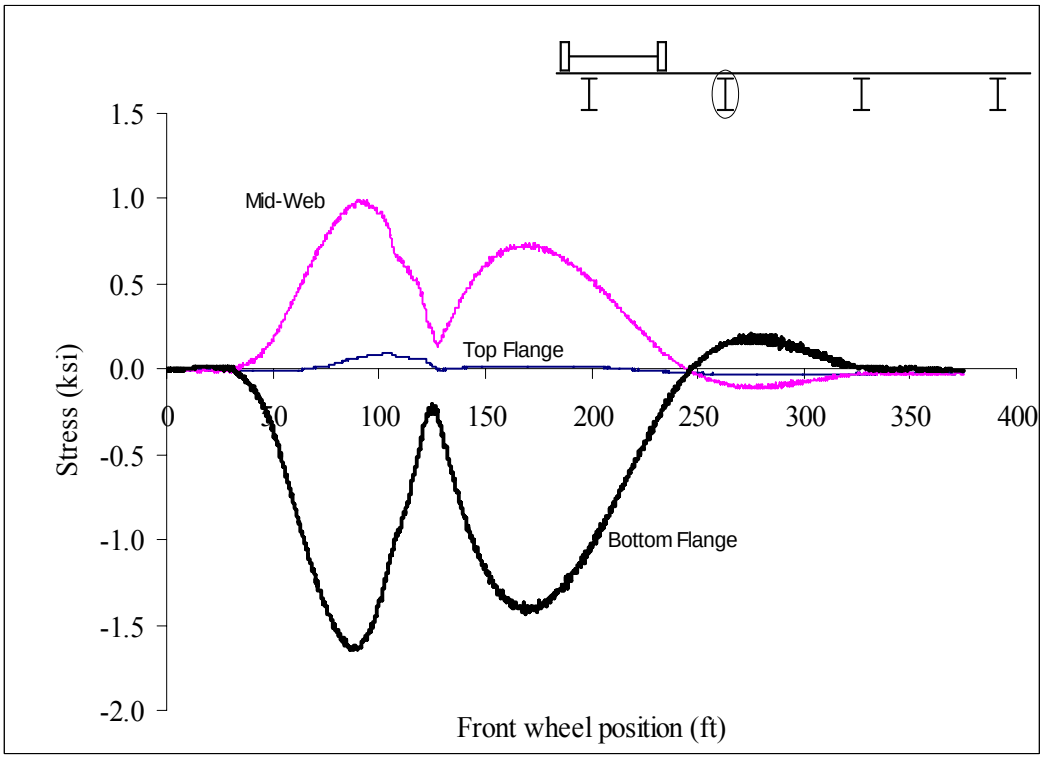

Figure A145: Las Cruces Bridge Test Run 8 S2 @ 2 ft from interior support

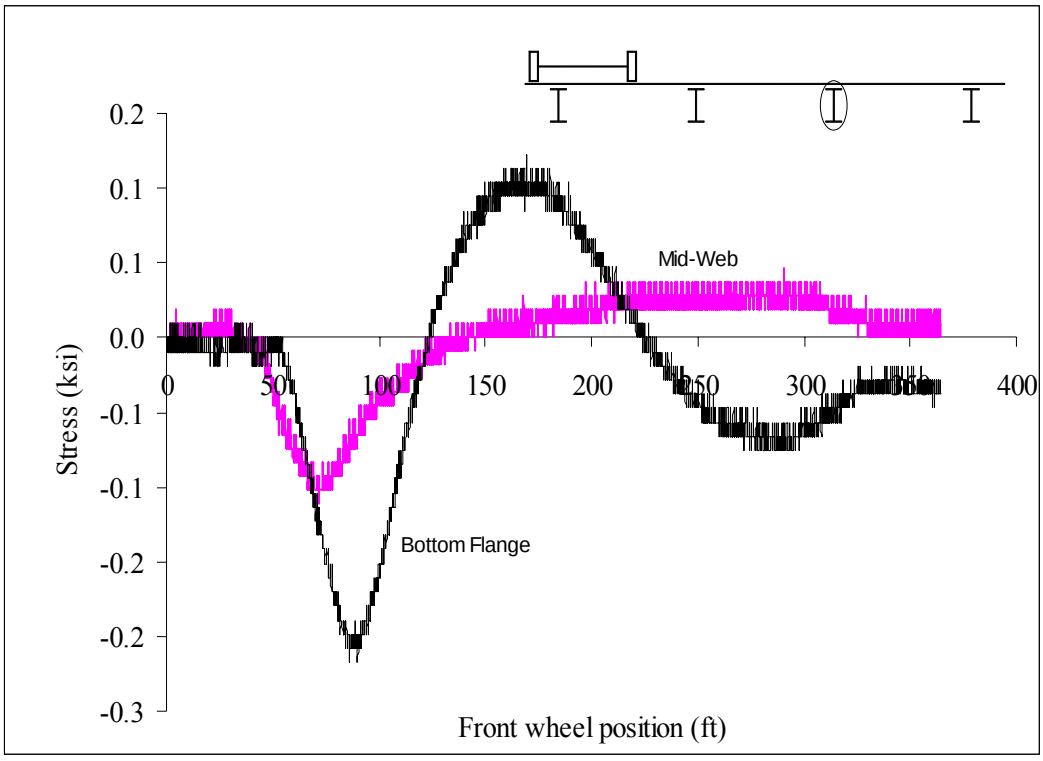

Figure A146: Las Cruces Bridge Test Run 8 S3 @ 2 ft from abutment

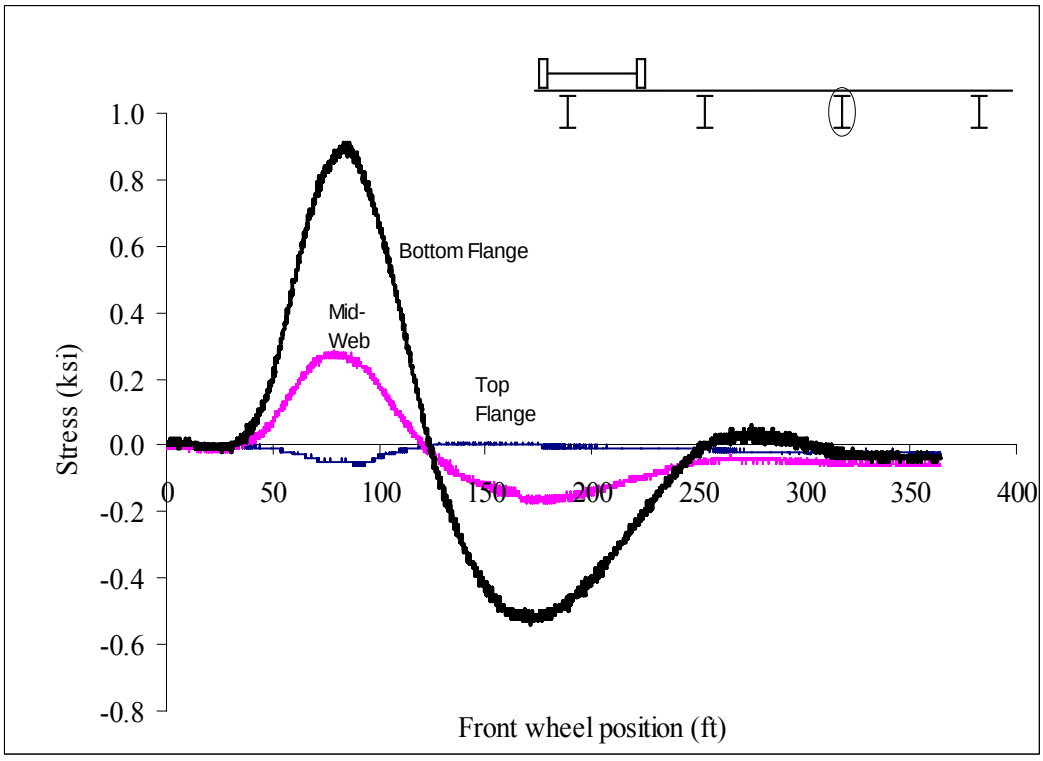

Figure A147: Las Cruces Bridge Test Run 8 S3 @ Midspan

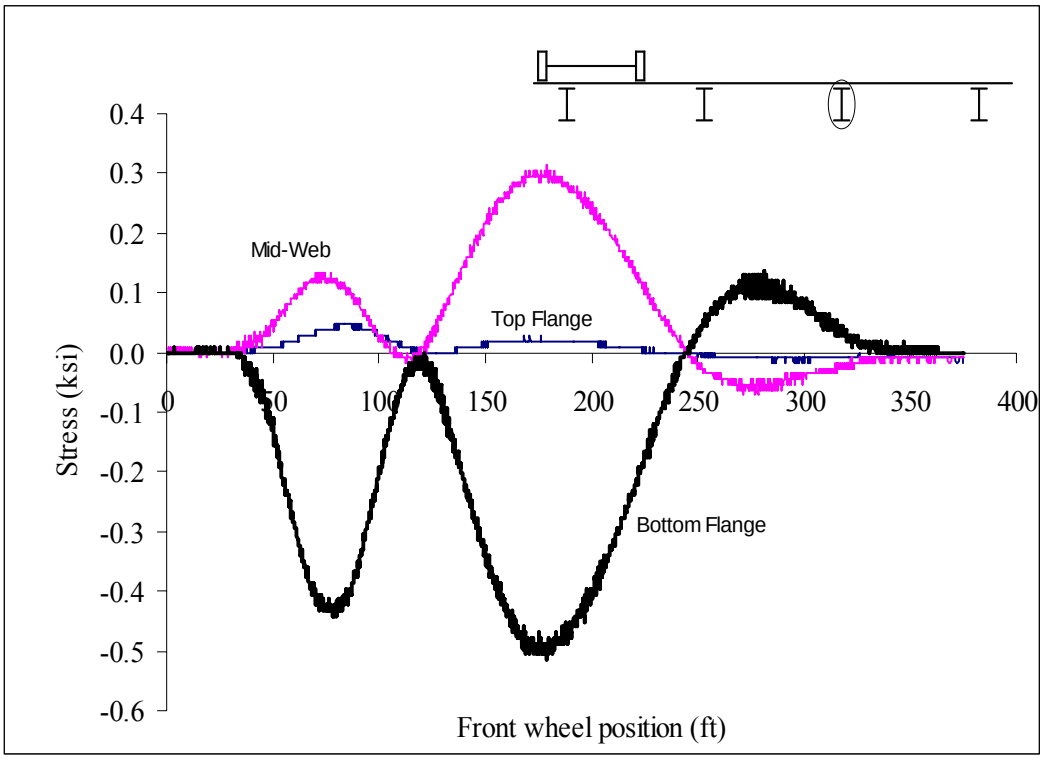

Figure A148: Las Cruces Bridge Test Run 8 S3 @ 2 ft from interior support

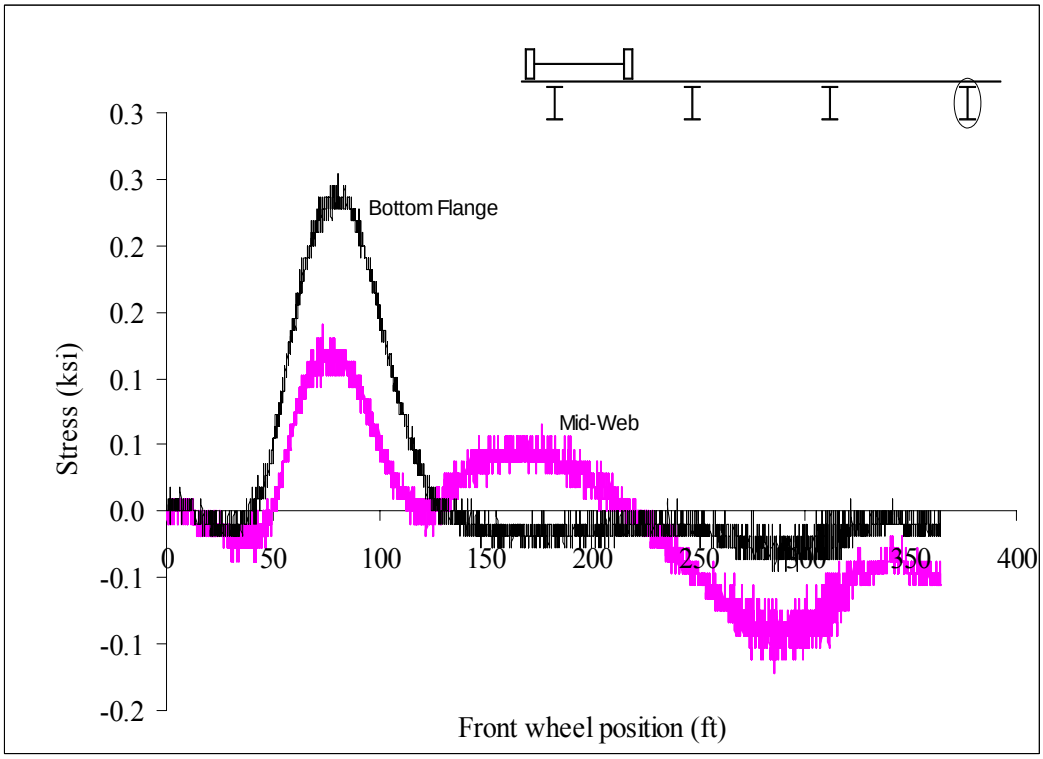

Figure A149: Las Cruces Bridge Test Run 8 S4 @ 2 ft from abutment

Figure A150: Las Cruces Bridge Test Run 8 S4 @ Midspan

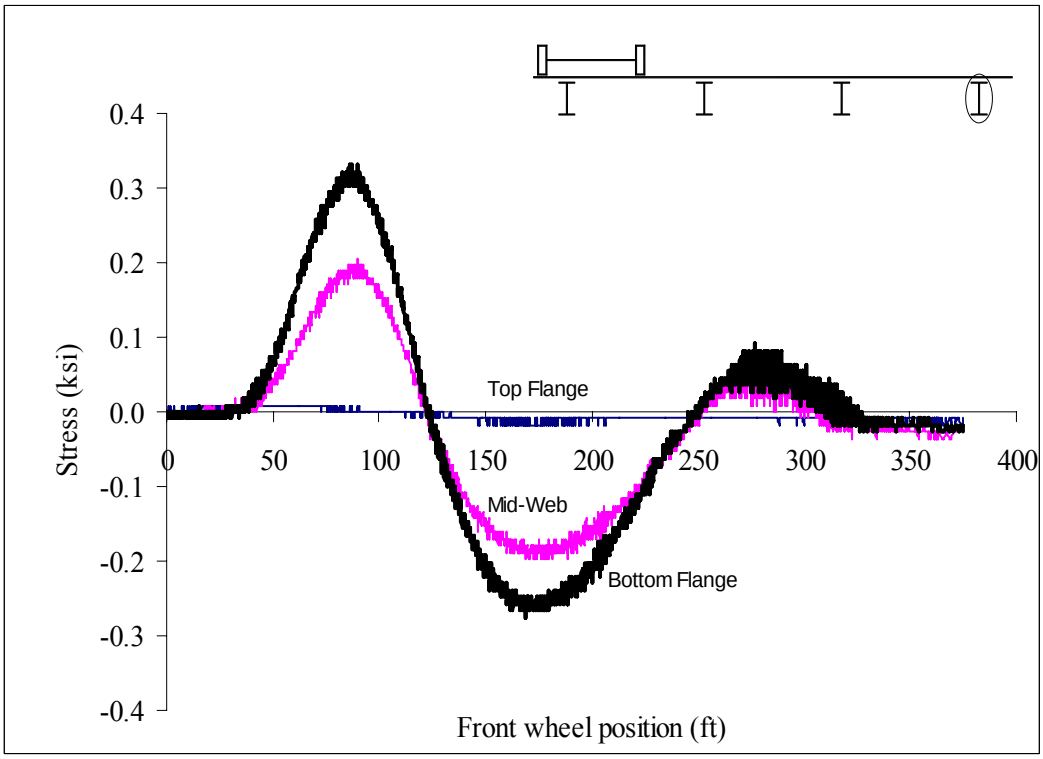

Figure A151: Las Cruces Bridge Test Run 8 S4 @ 2 ft from interior support

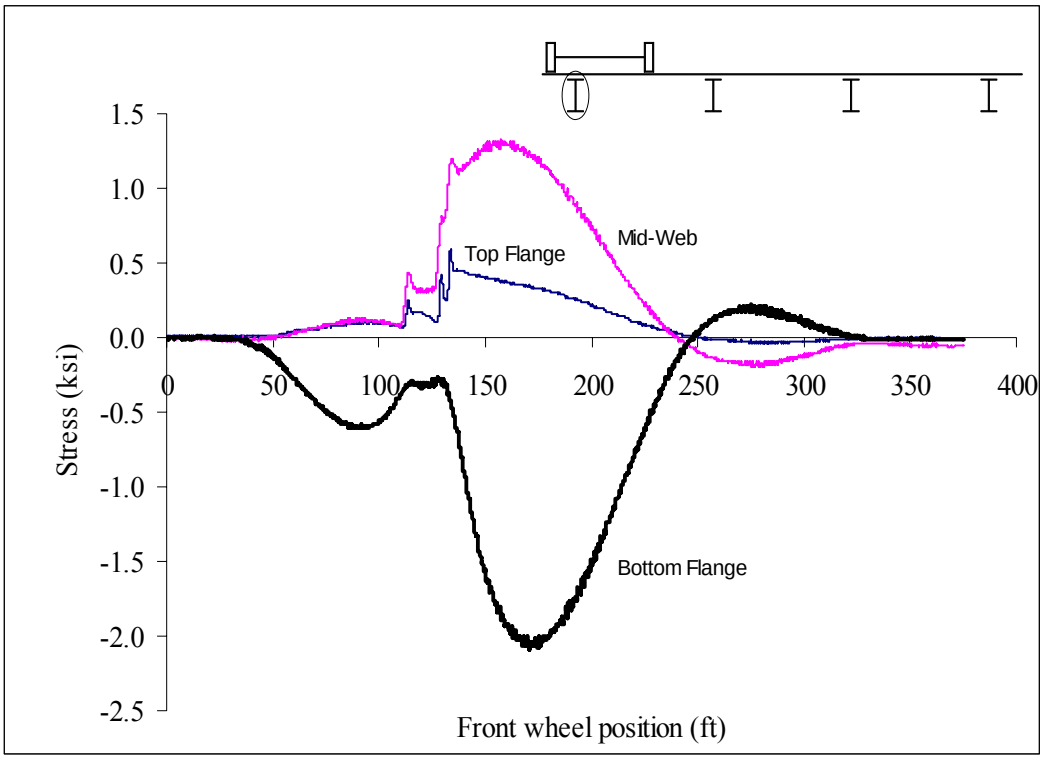

Figure A152: Las Cruces Bridge Test Run 8 S5 @ 2 ft from interior support

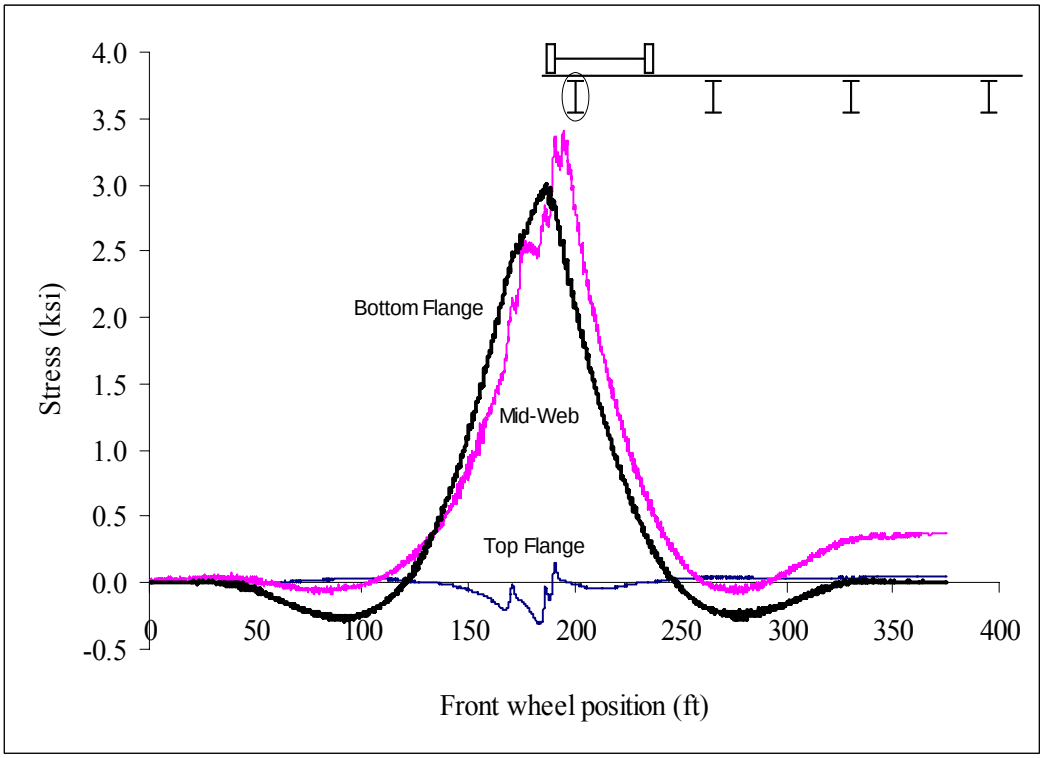

Figure A153: Las Cruces Bridge Test Run 8 S5 @ Midspan

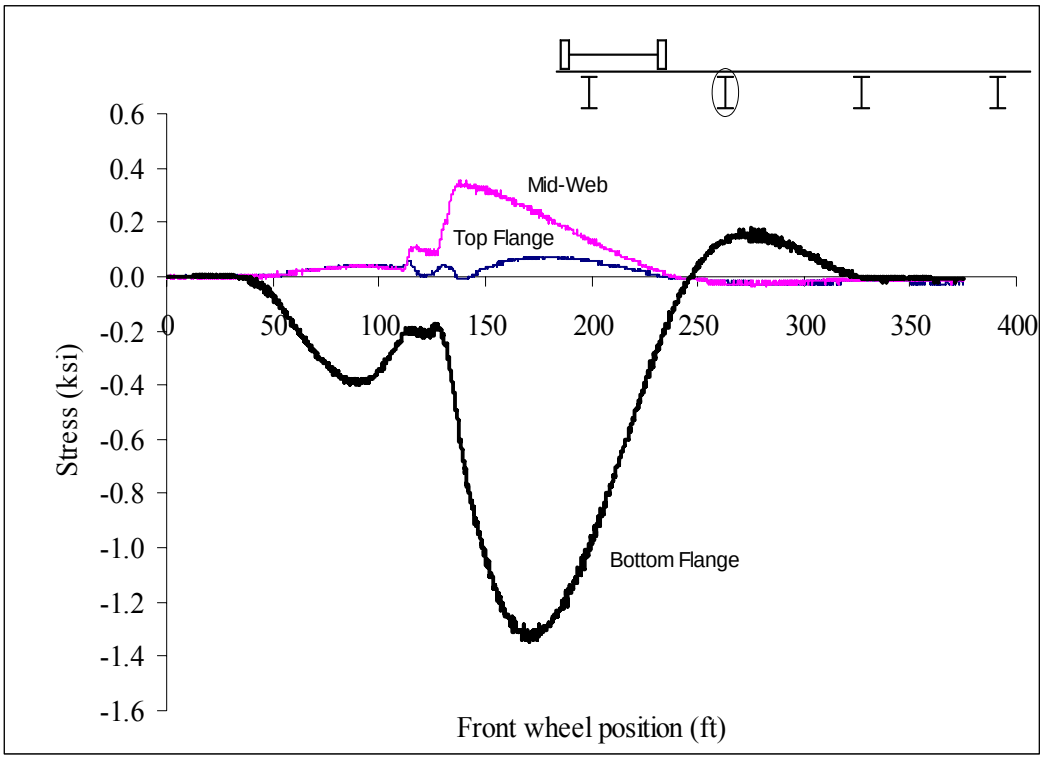

Figure A154: Las Cruces Bridge Test Run 8 S6 @ 2 ft from interior support

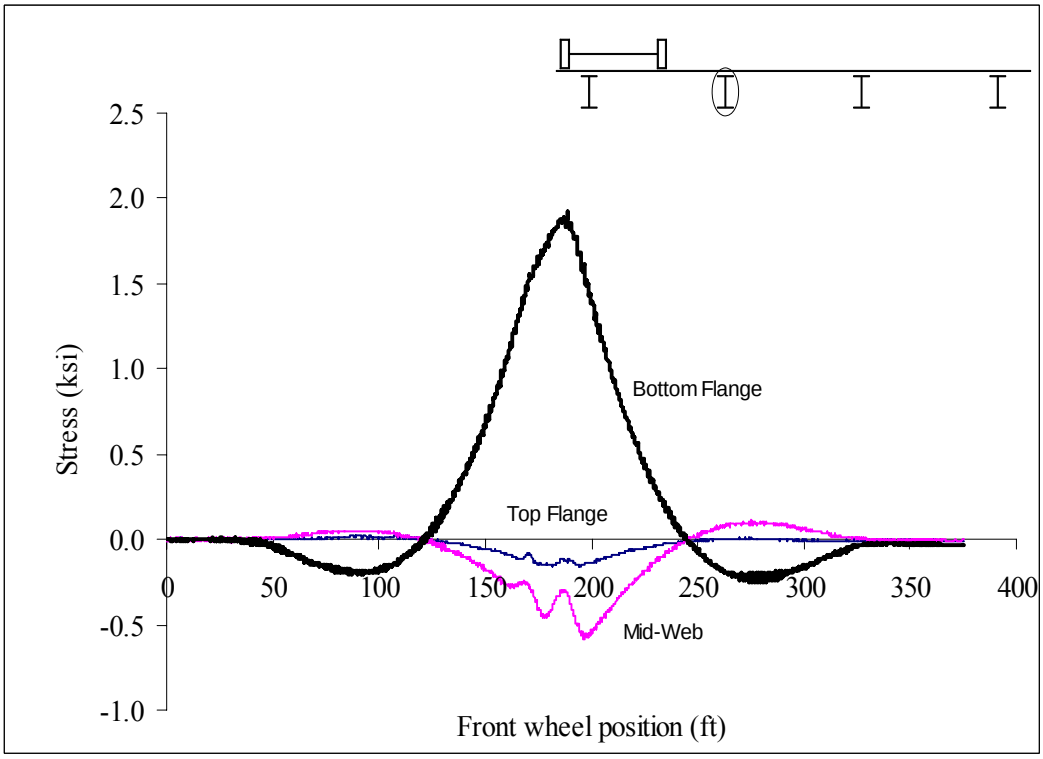

Figure A155: Las Cruces Bridge Test Run 8 S6 @ Midspan

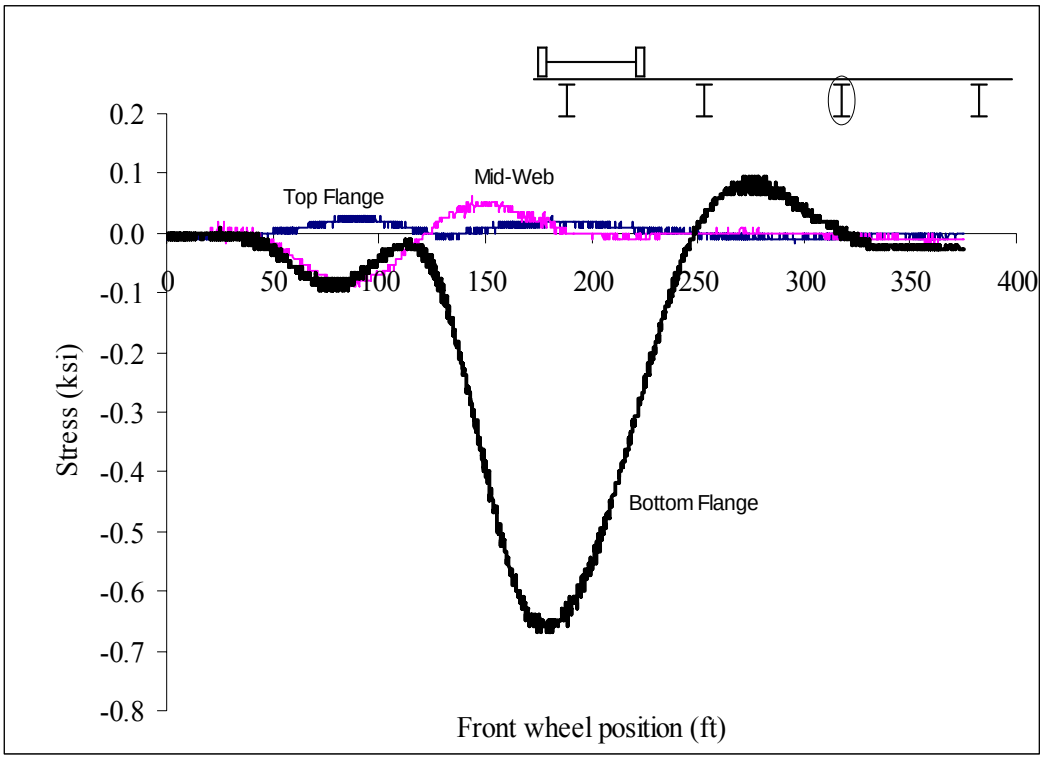

Figure A156: Las Cruces Bridge Test Run 8 S7 @ 2 ft from interior support

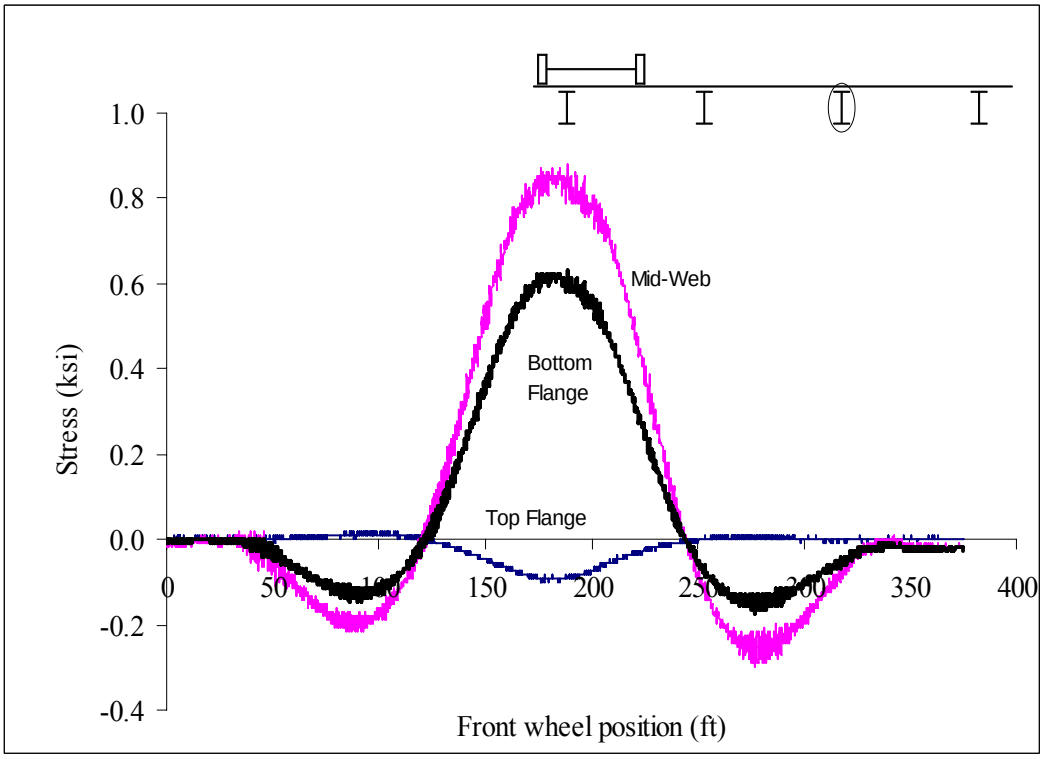

Figure A157: Las Cruces Bridge Test Run 8 S7 @ Midspan

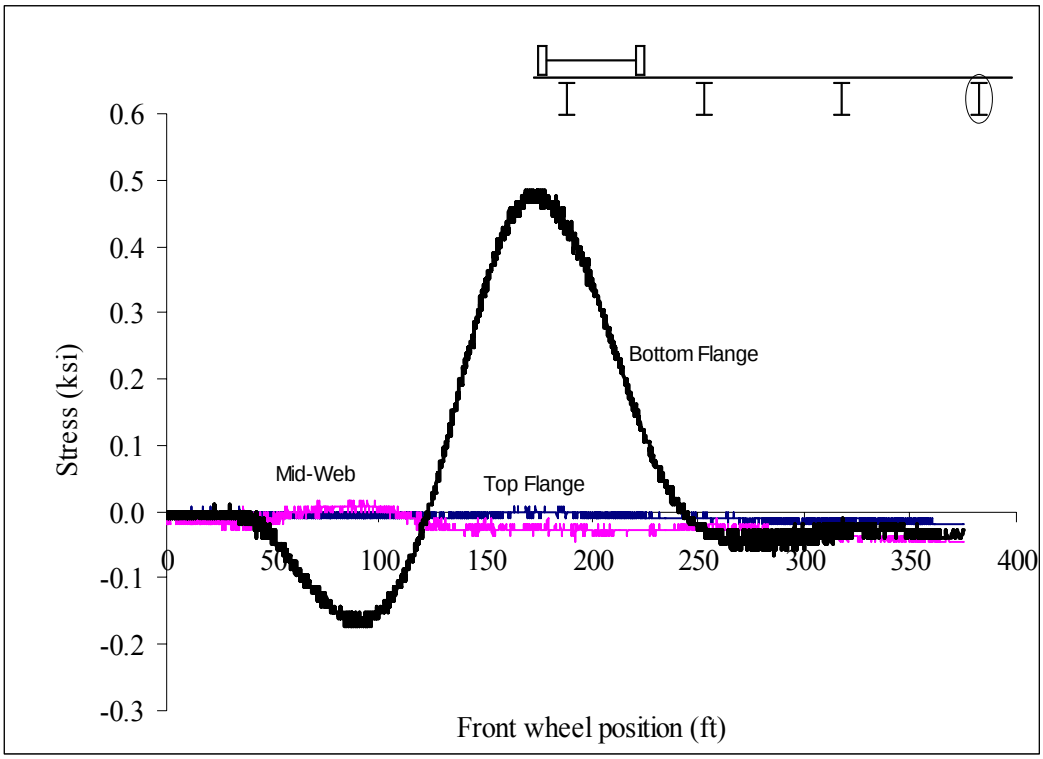

Figure A158: Las Cruces Bridge Test Run 8 S8 @ 2 ft from interior support

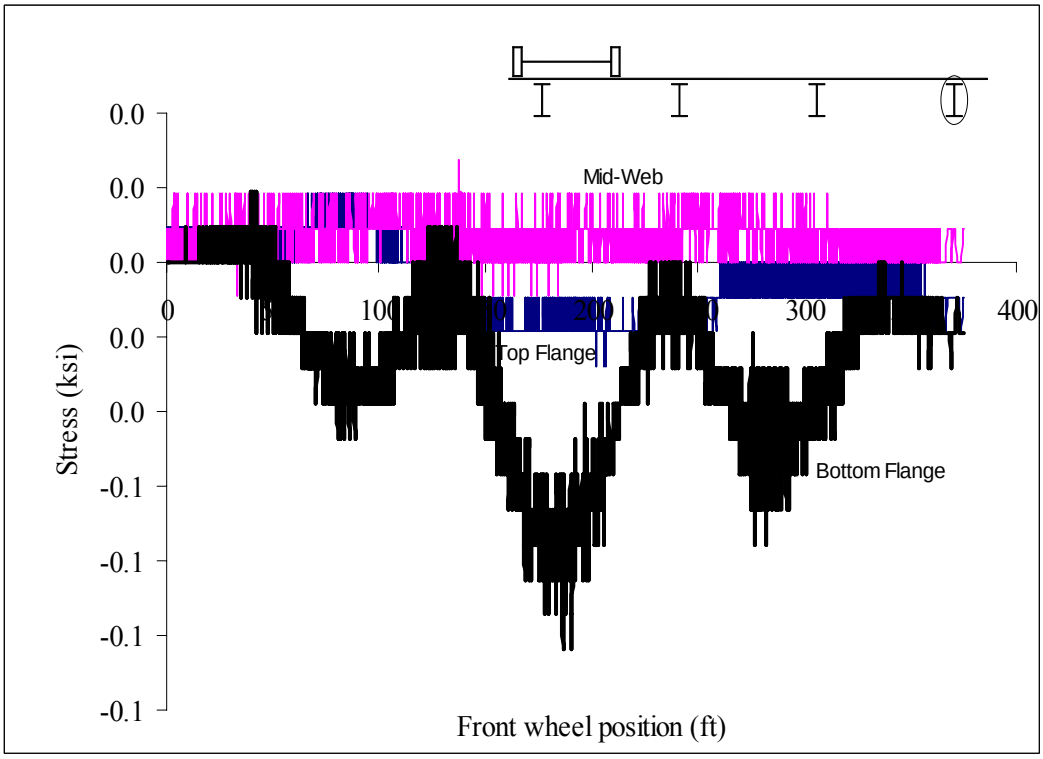

Figure A159: Las Cruces Bridge Test Run 8 S8 @ Midspan

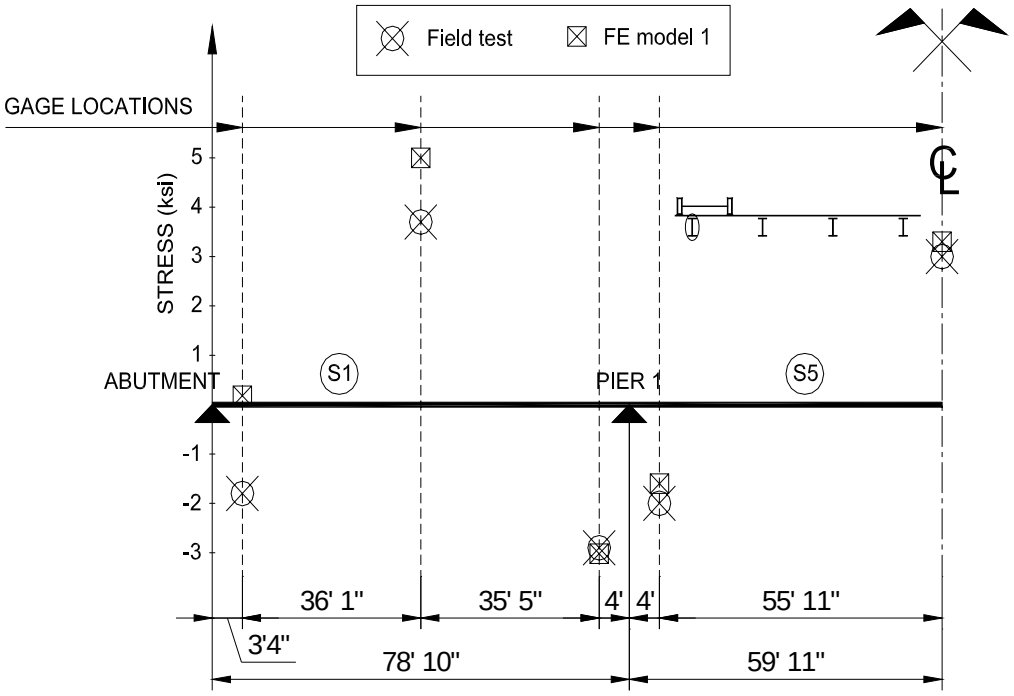

Figure A160: Las Cruces Load Test Results vs. FEA Results of Bottom Flange Stresses of S1 & S5 (Dang 2006)

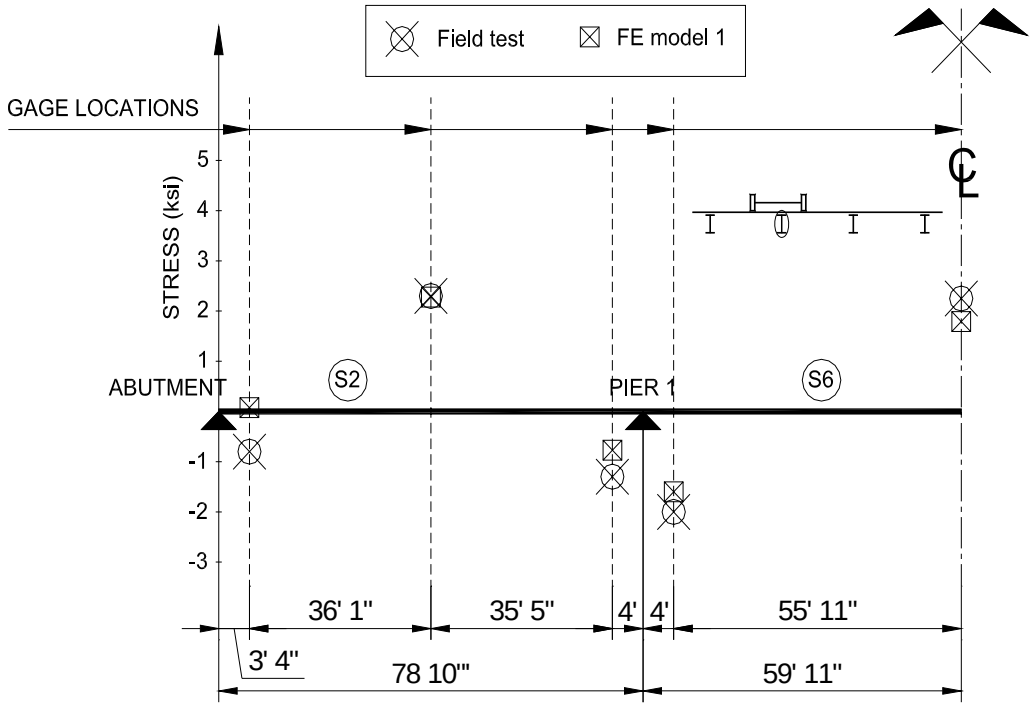

Figure A161: Las Cruces Load Test Results vs. FEA Results of Bottom Flange Stresses of S2 & S6 (Dang 2006)

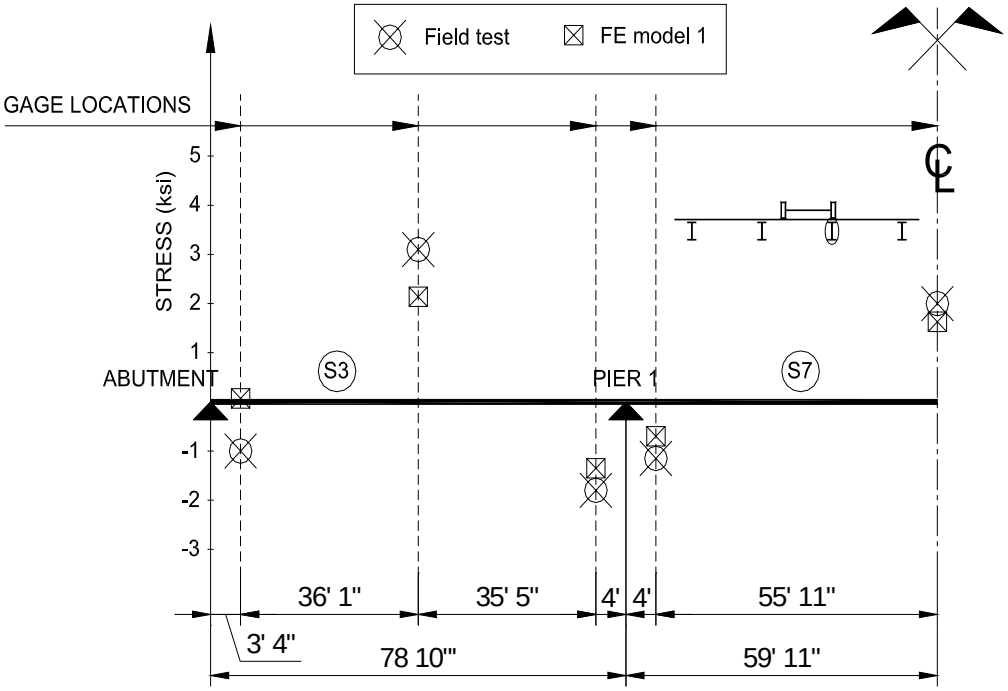

Figure A162: Las Cruces Load Test Results vs. FEA Results of Bottom Flange Stresses of S3 & S7 (Dang 2006)

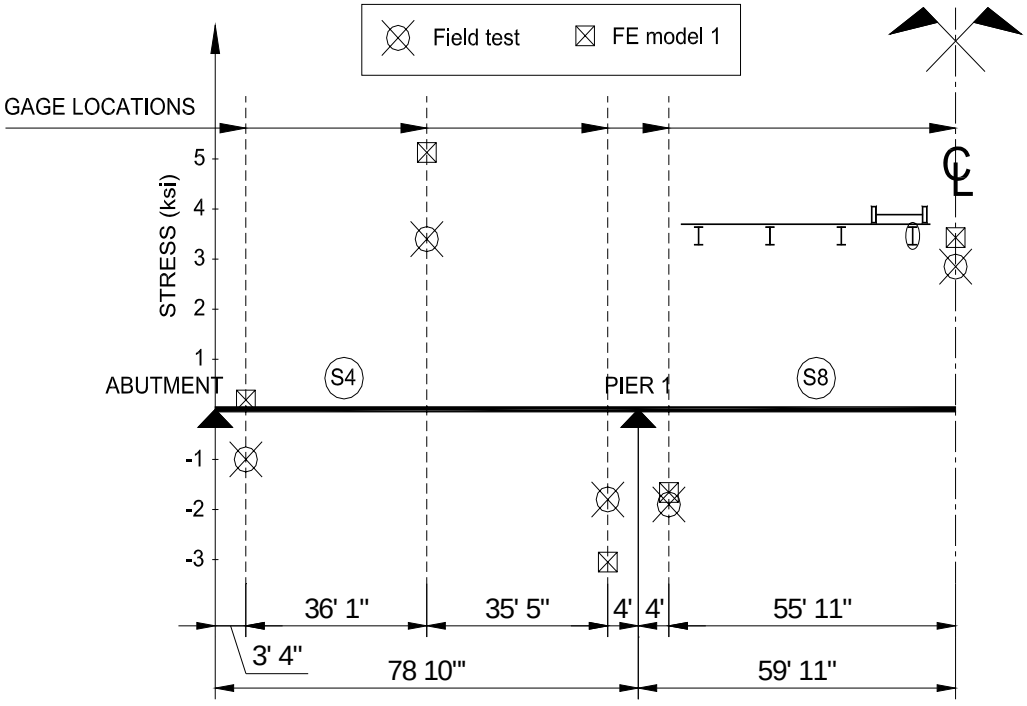

Figure A163: Las Cruces Load Test Results vs. FEA Results of Bottom Flange Stresses of S4 & S8 (Dang 2006)

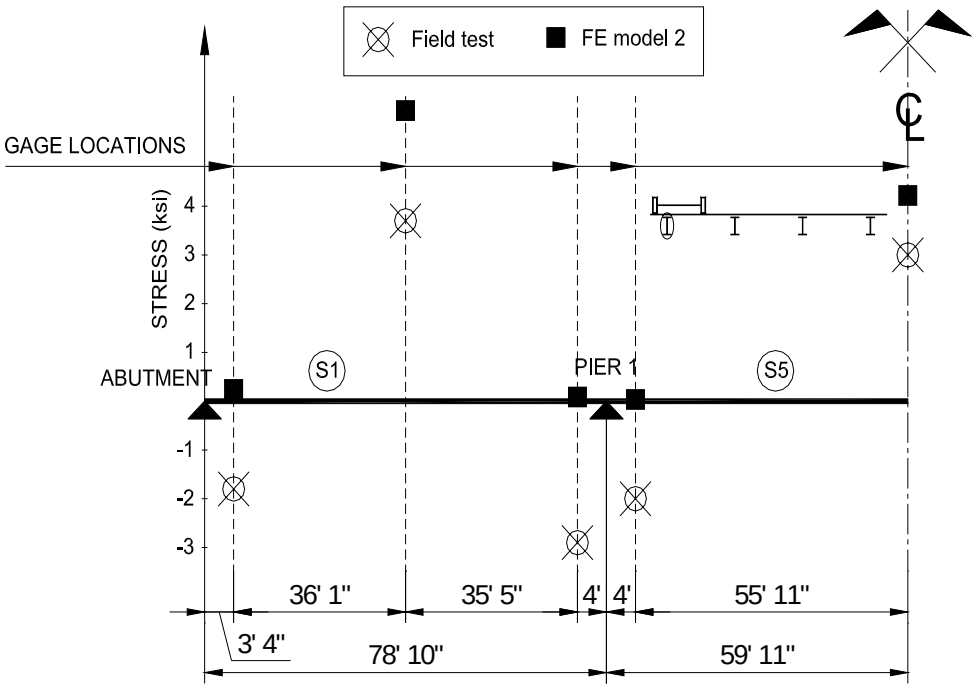

Figure A164: Las Cruces Load Test Results vs. FEA Results of Bottom Flange Stresses of S1 & S5 (Dang 2006)

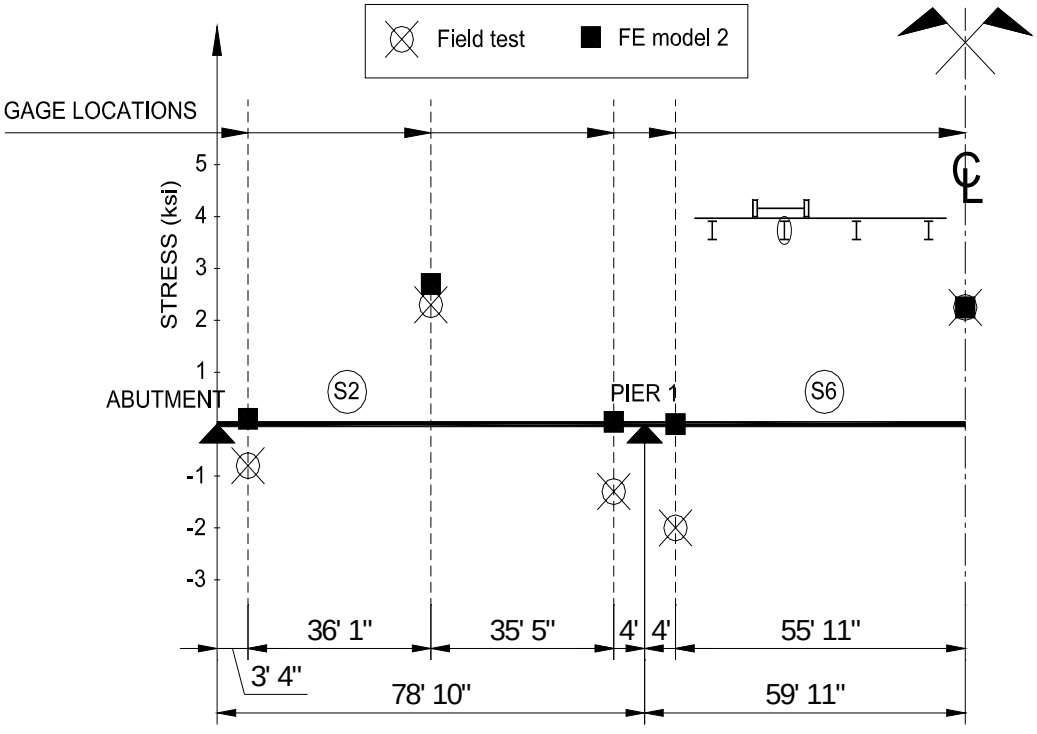

Figure A165: Las Cruces Load Test Results vs. FEA Results of Bottom Flange Stresses of S2 & S6 (Dang 2006)

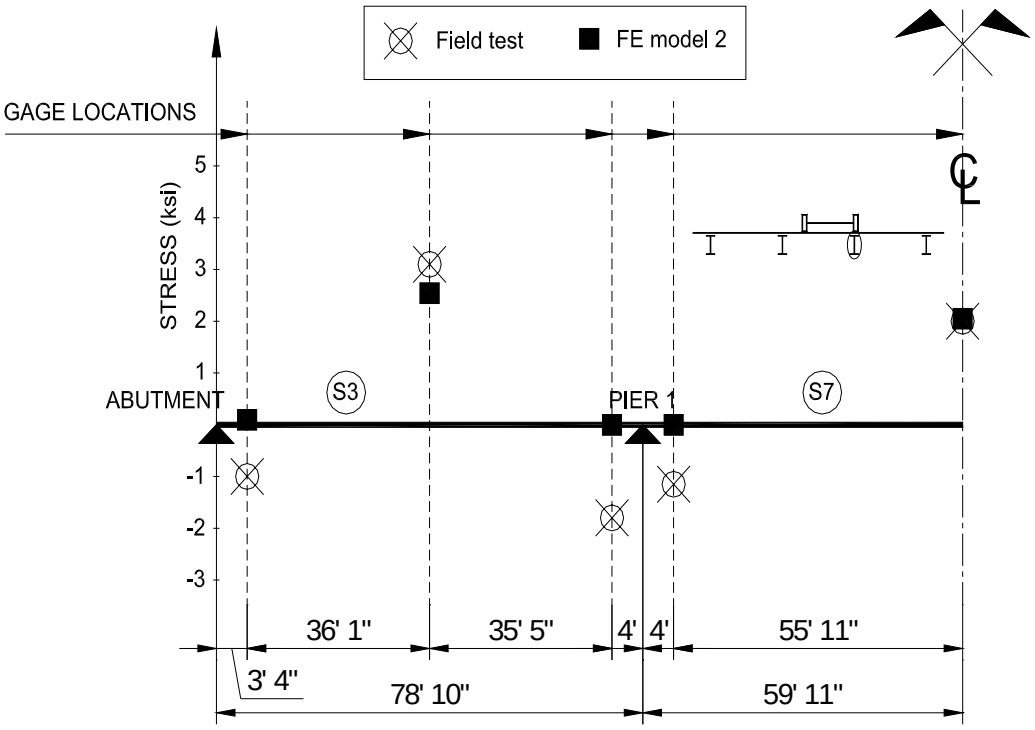

Figure A166: Las Cruces Load Test Results vs. FEA Results of Bottom Flange Stresses of S3 & S7 (Dang 2006)

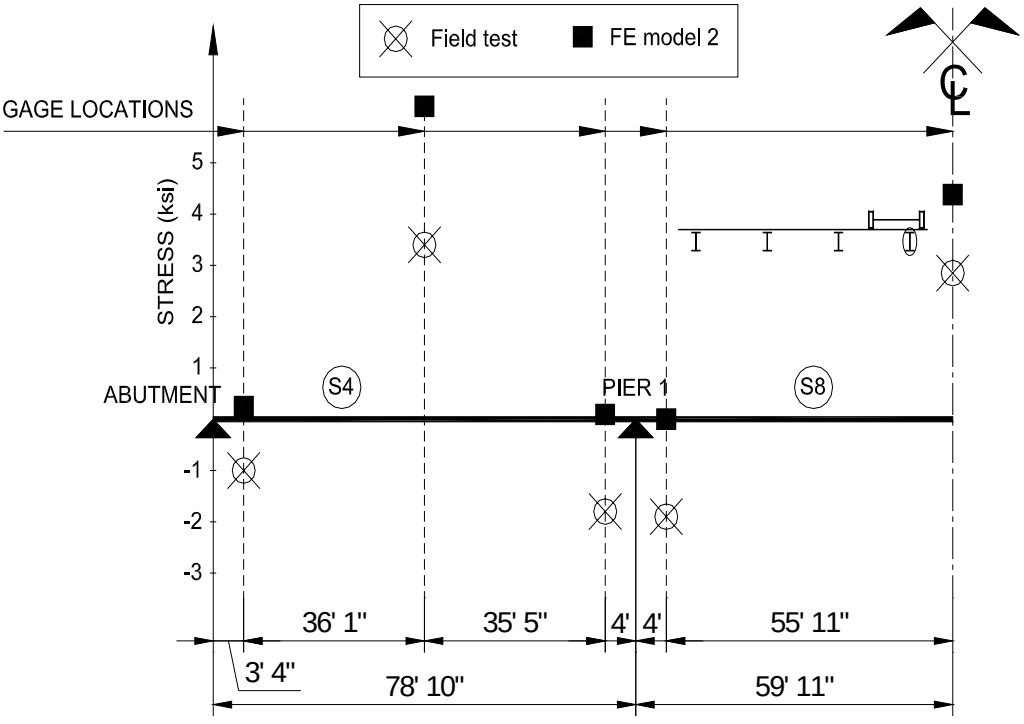

Figure A167: Las Cruces Load Test Results vs. FEA Results of Bottom Flange Stresses of S4 & S8 (Dang 2006)

APPENDIX B

The following appendix contains stress versus truck position plots of the Hatch Bridge Test conducted on December 19, 2005. The stress is measured in units of ksi and the position of the truck is measured in units of ft. Please note that the strain gage locations close to the interior supports are measured 3 ft from the concrete diaphragm face. This appendix also contains plots of STAAD analysis results of the bottom flange stresses versus the field results taken from Chi Dang's report. Please note that FEA Model 1 is the continuous model while FEA Model 2 is the simply supported model.

TABLE OF FIGURES

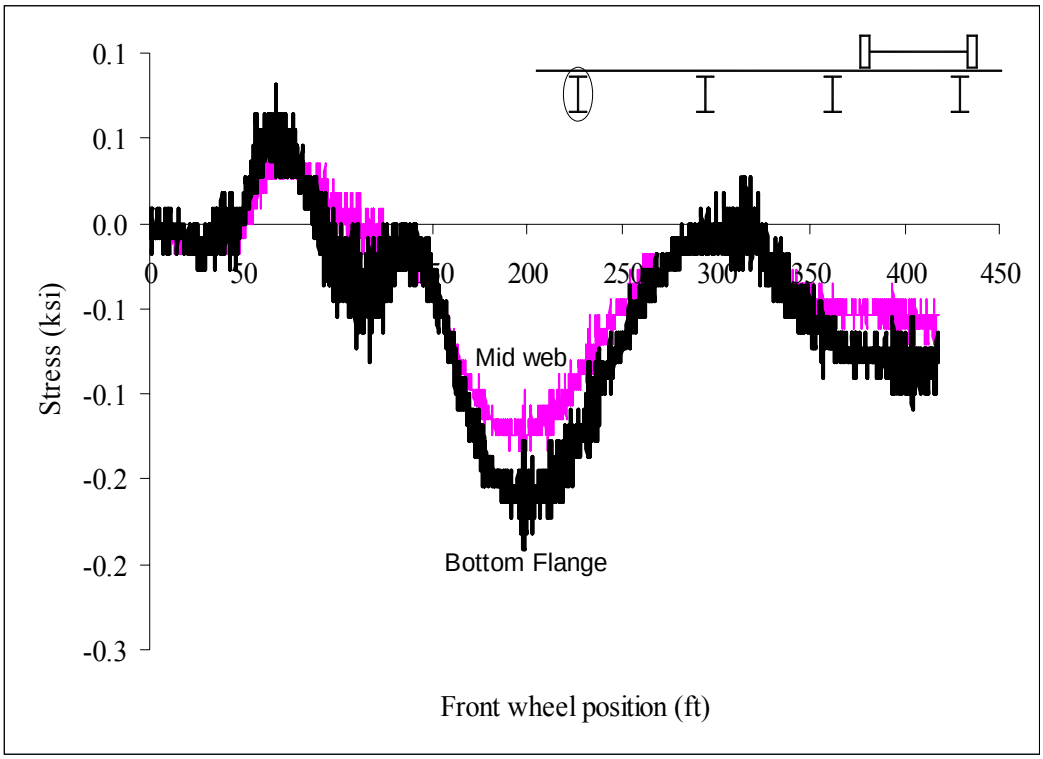

Figure B1: Hatch Bridge Test Run 1 S1 @ Midspan

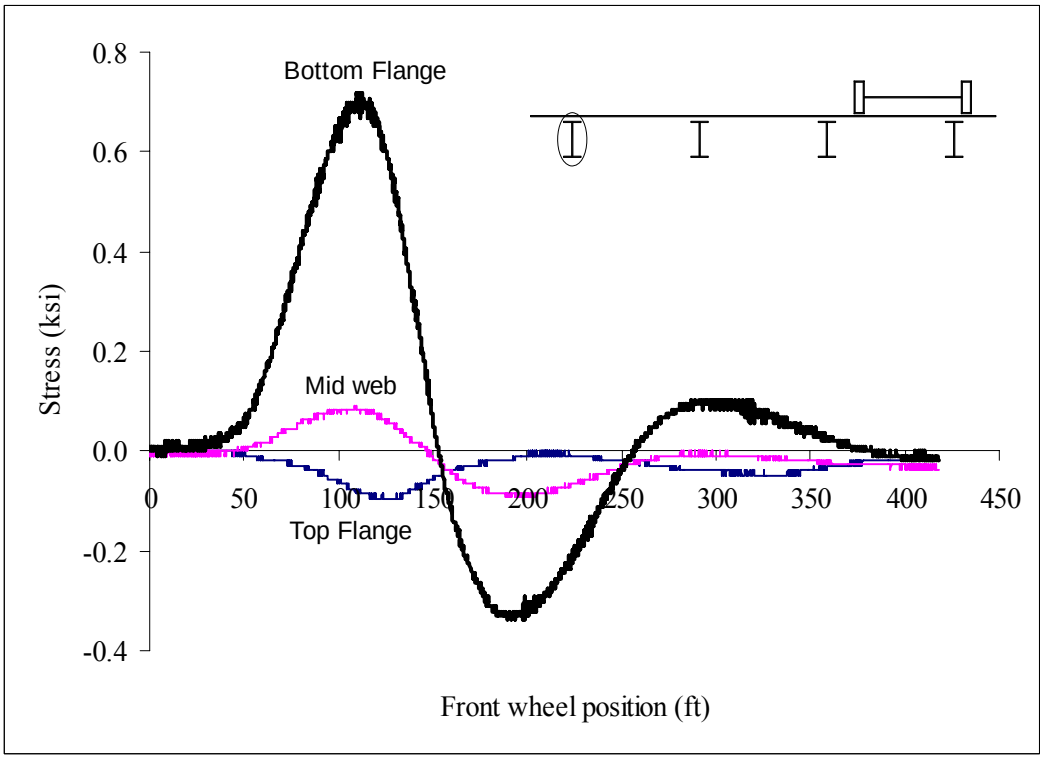

Figure B2: Hatch Bridge Test Run 1 S1 @ 3 ft west of interior support

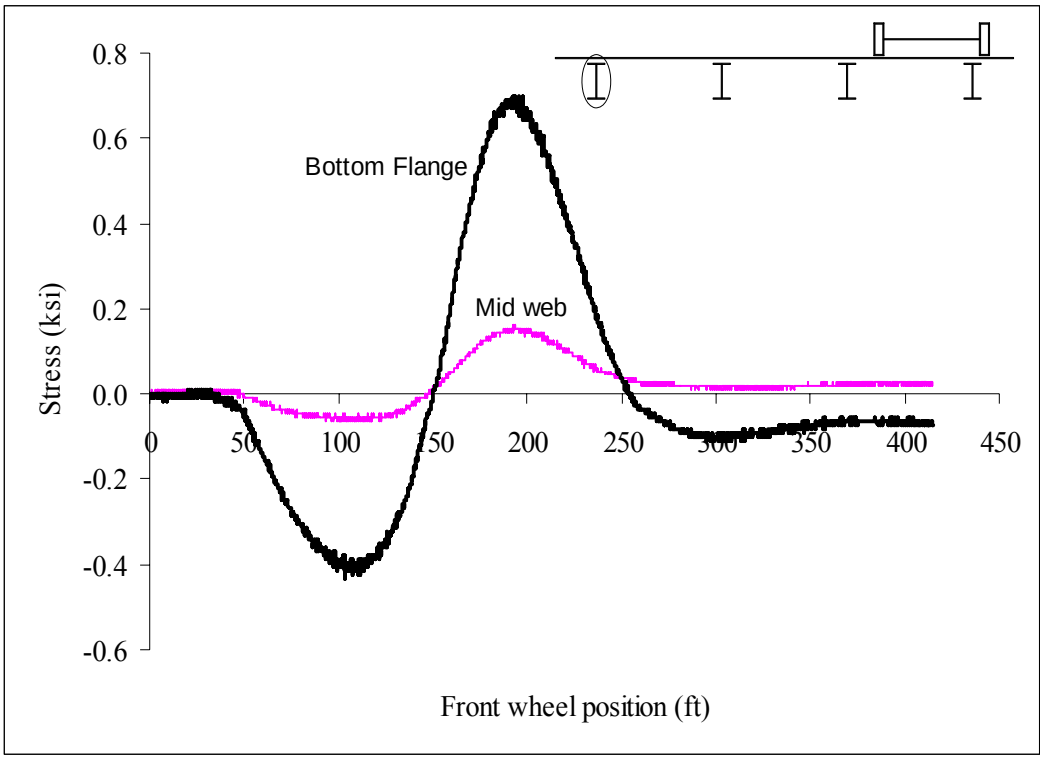

Figure B3: Hatch Bridge Test Run 1 S5 @ 3 ft east of interior support

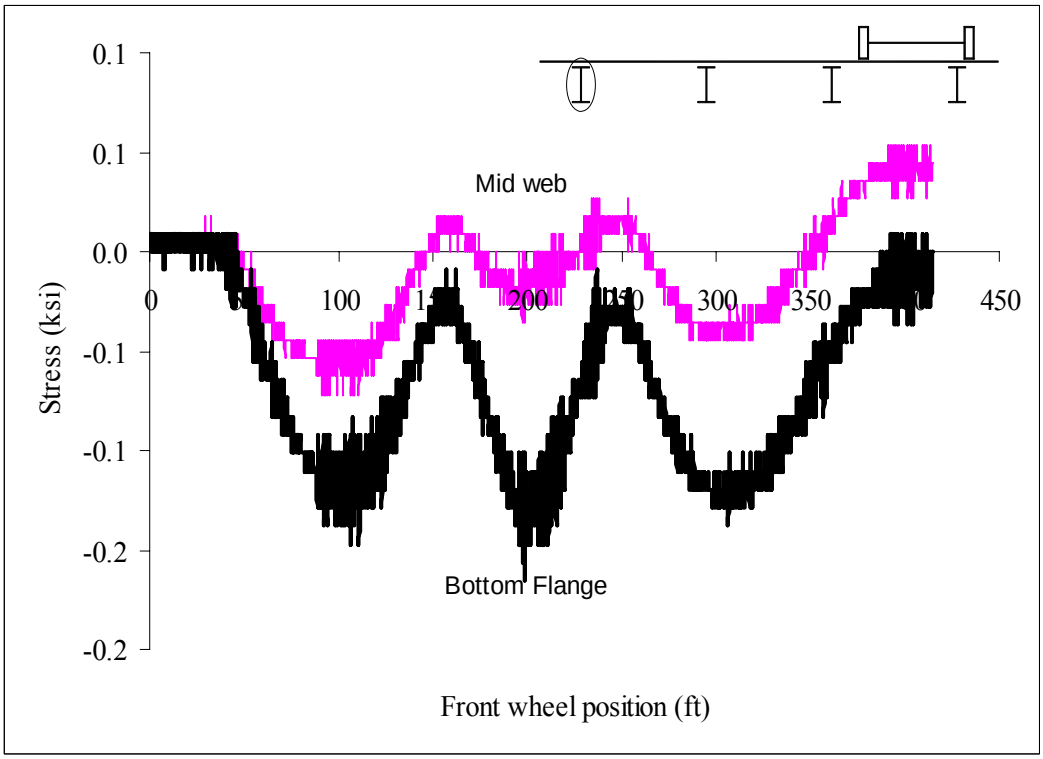

Figure B4: Hatch Bridge Test Run 1 S5 @ Midspan

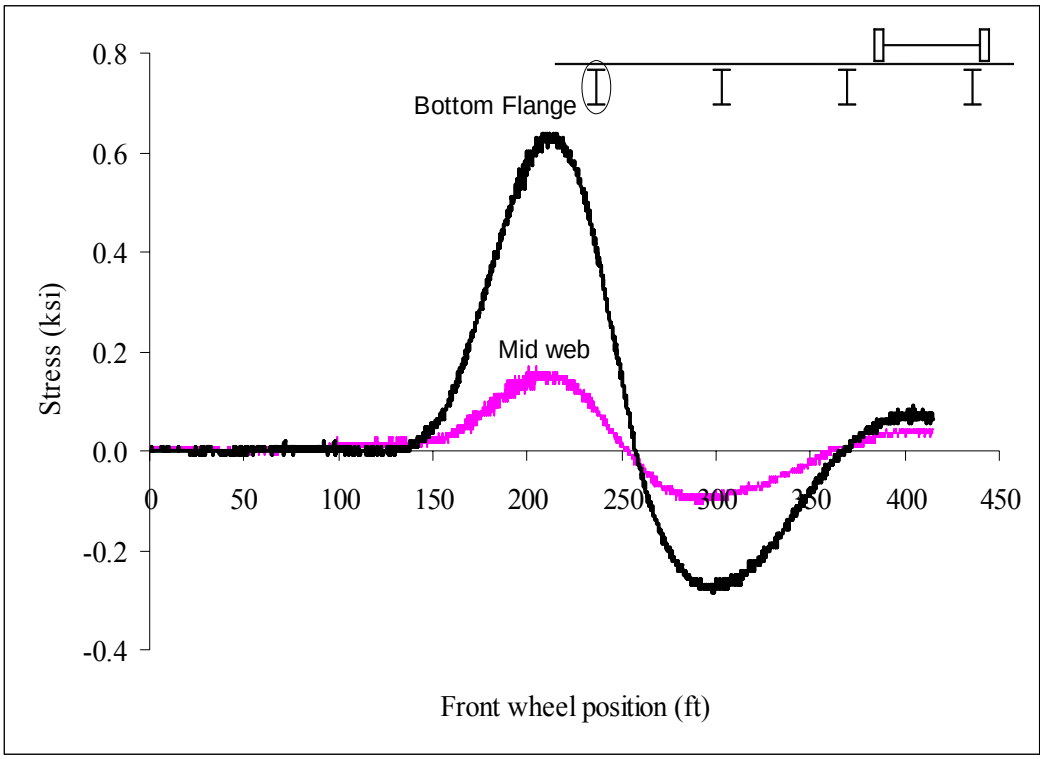

Figure B5: Hatch Bridge Test Run 1 S5 @ 3 ft west of interior support

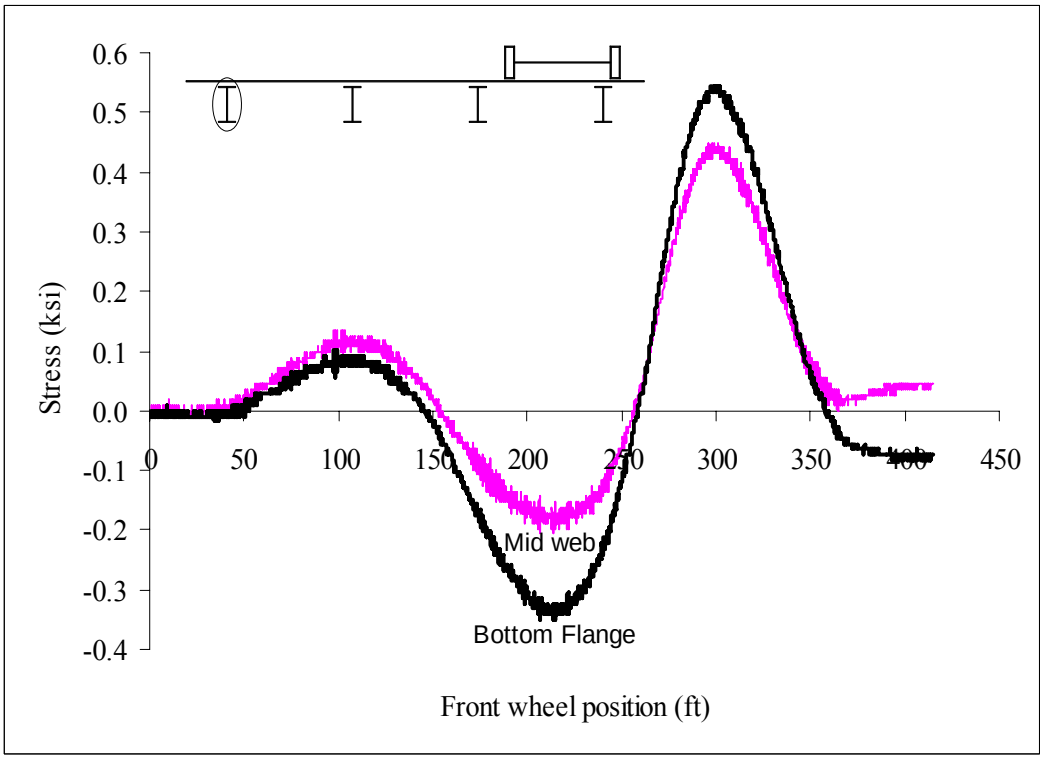

Figure B6: Hatch Bridge Test Run 1 S9 @ 3 ft east of interior support

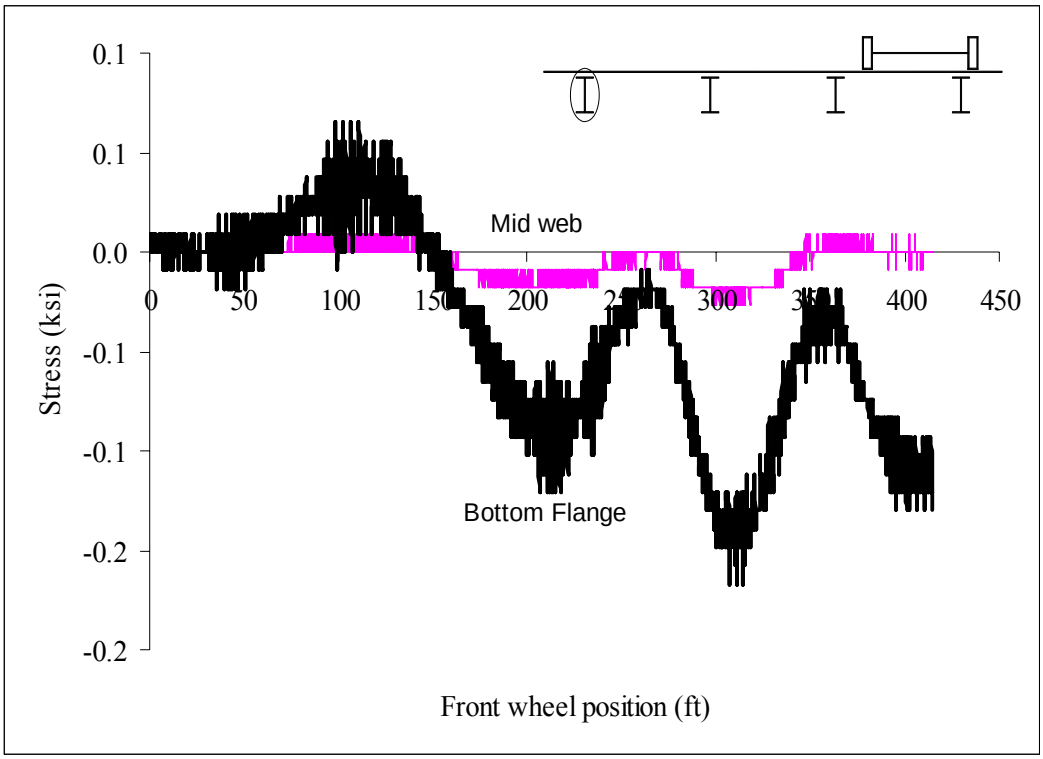

Figure B7: Hatch Bridge Test Run 1 S9 @ Midspan

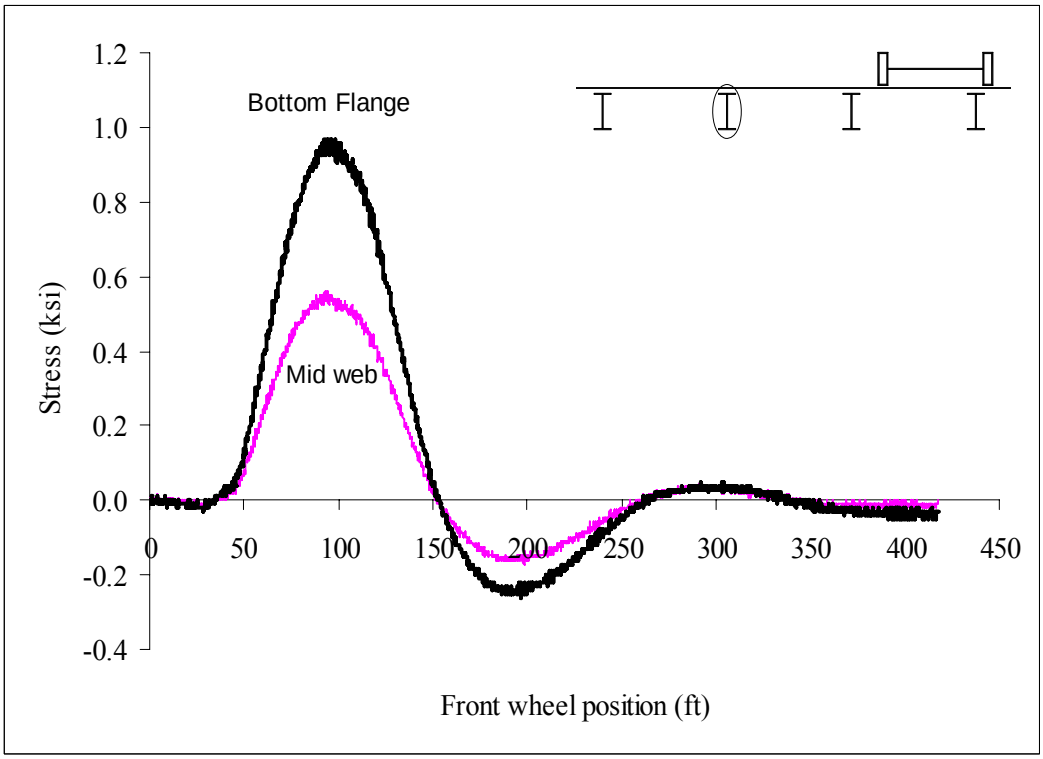

Figure B8: Hatch Bridge Test Run 1 S2 @ Midspan

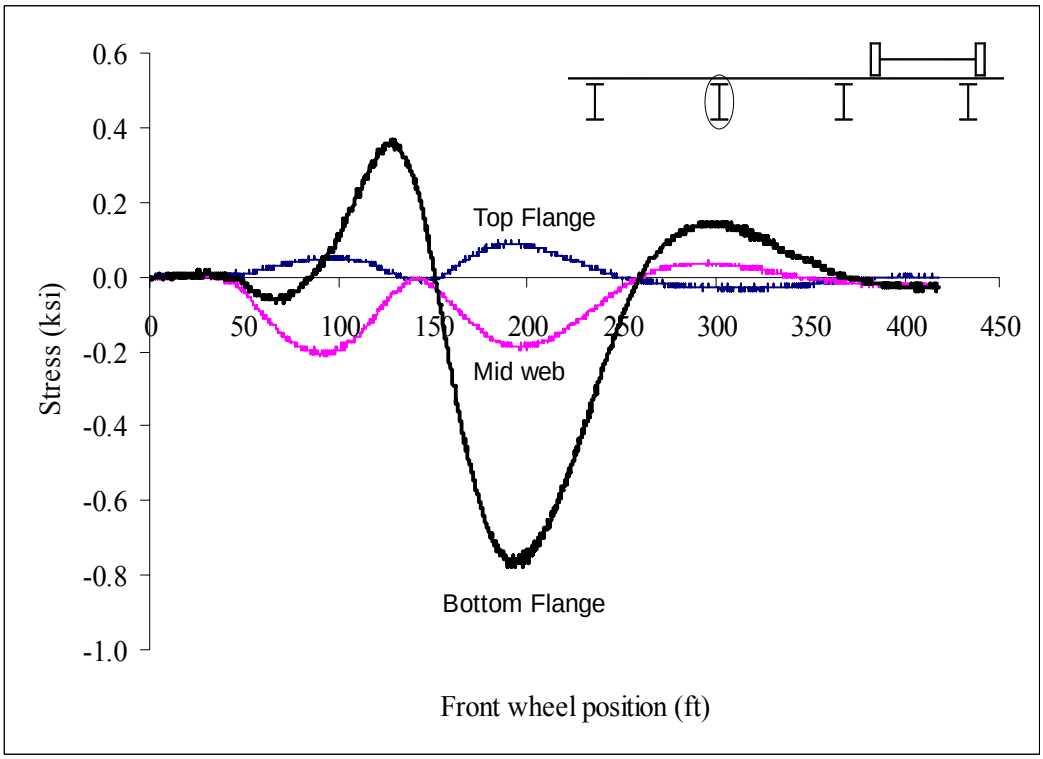

Figure B9: Hatch Bridge Test Run 1 S2 @ 3 ft west of interior support

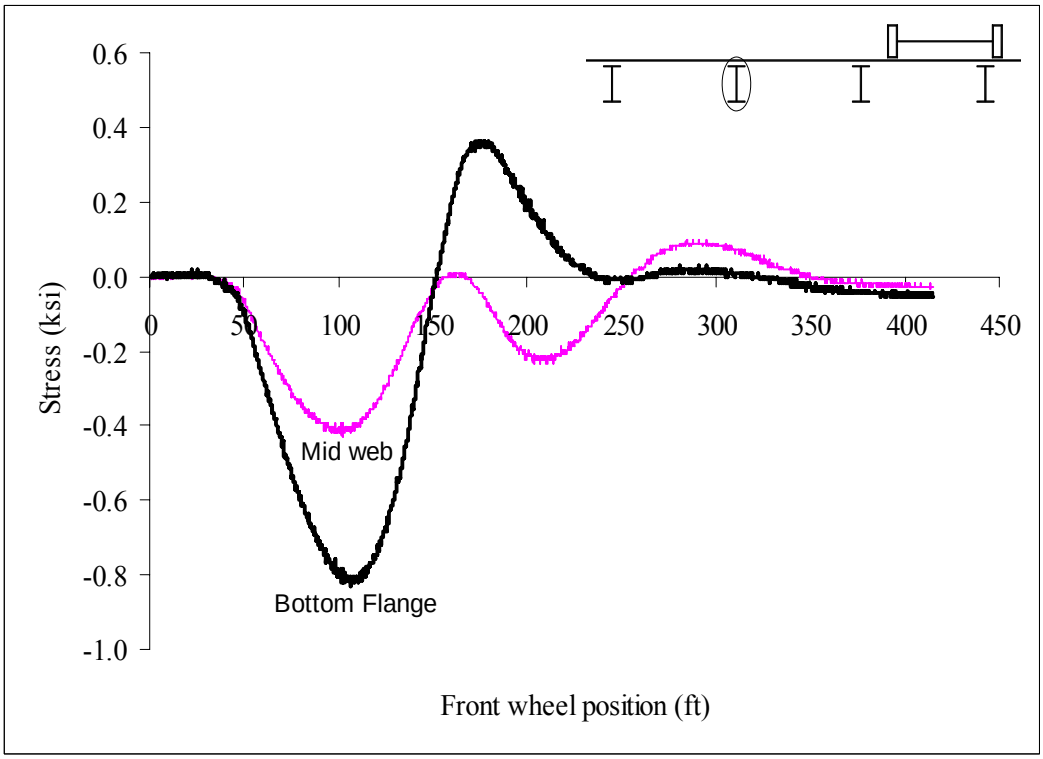

Figure B10: Hatch Bridge Test Run 1 S6 @ 3 ft east of interior support

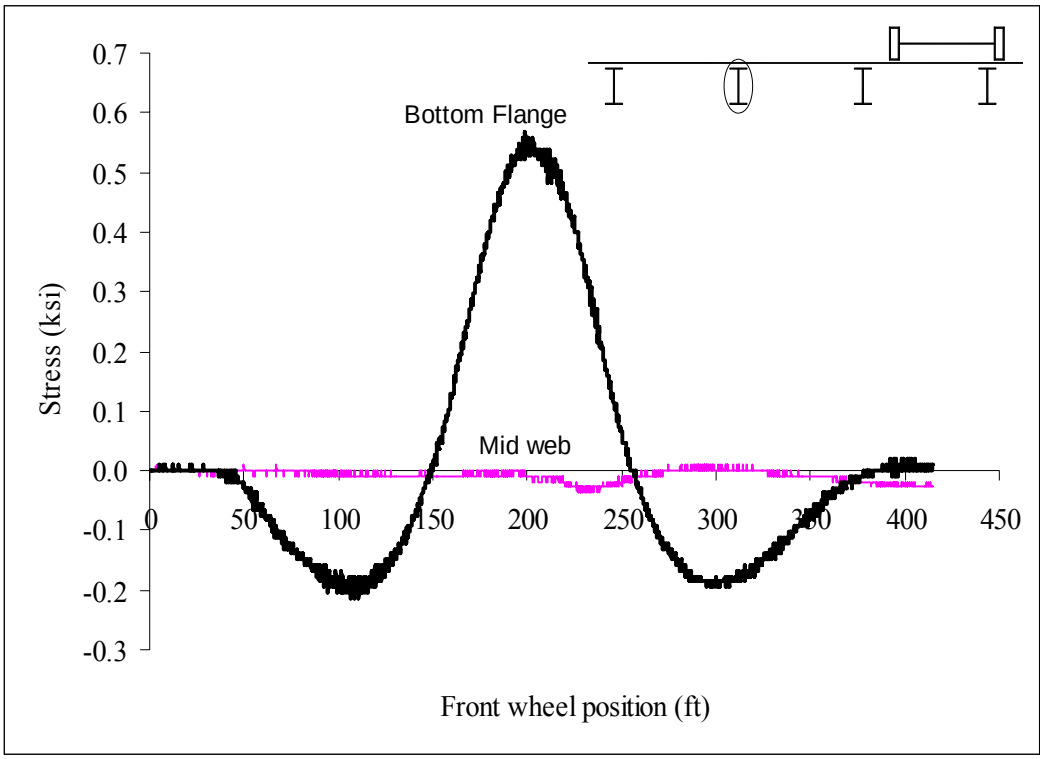

Figure B11: Hatch Bridge Test Run 1 S6 @ Midspan

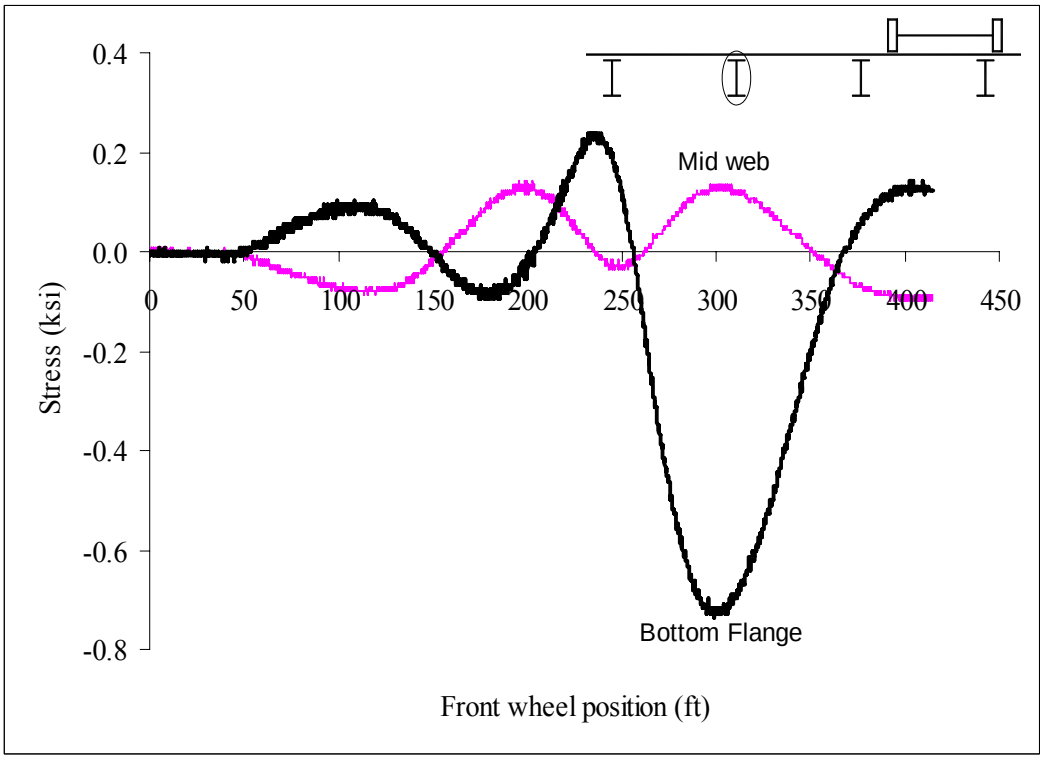

Figure B12: Hatch Bridge Test Run 1 S6 @ 3 ft west of interior support

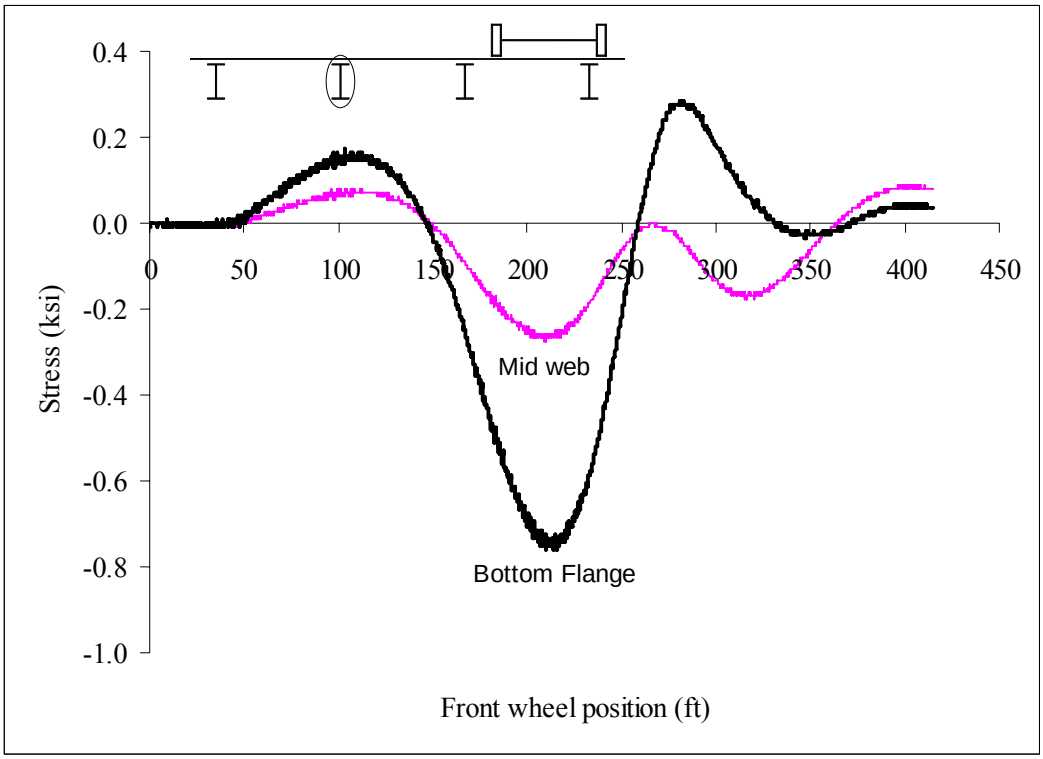

Figure B13: Hatch Bridge Test Run 1 S10 @ 3 ft east of interior support

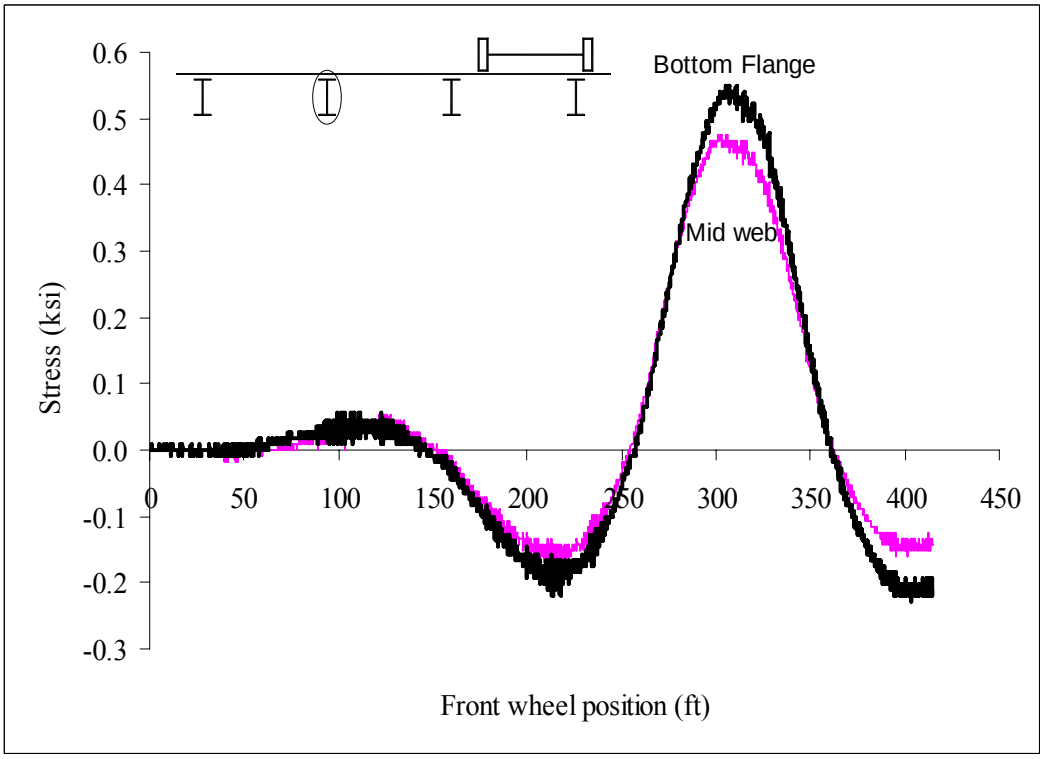

Figure B14: Hatch Bridge Test Run 1 S10 @ Midspan

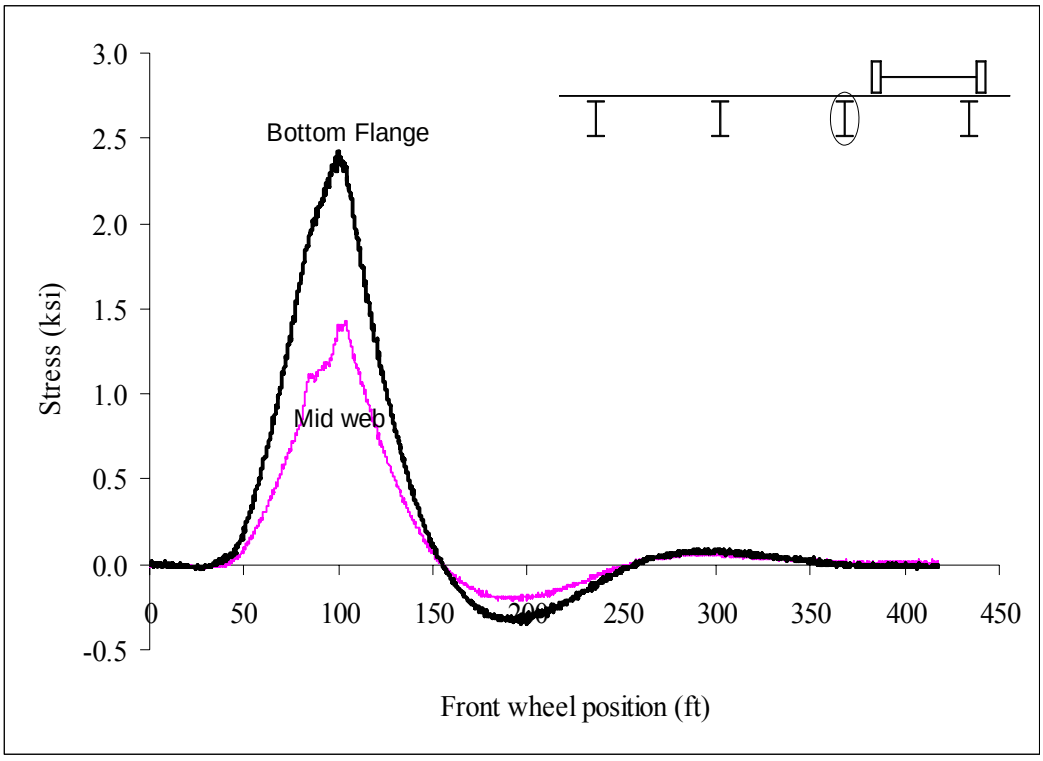

Figure B15: Hatch Bridge Test Run 1 S3 @ Midspan

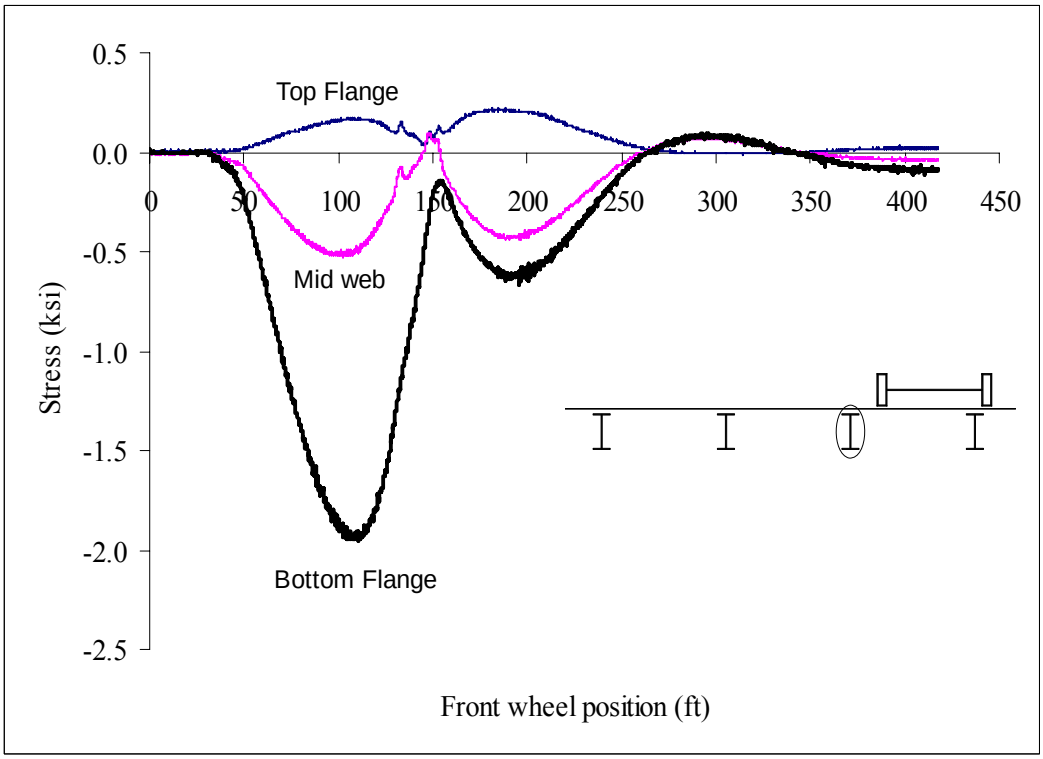

Figure B16: Hatch Bridge Test Run 1 S3 @ 3 ft west of interior support

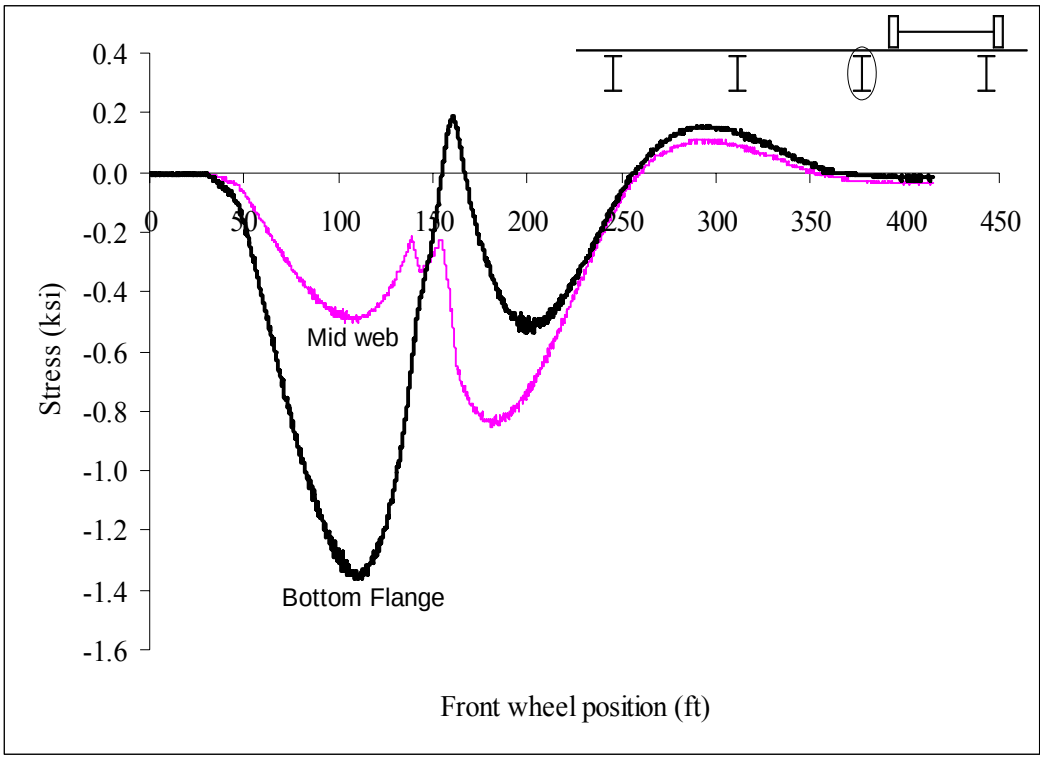

Figure B17: Hatch Bridge Test Run 1 S7 @ 3 ft east of interior support

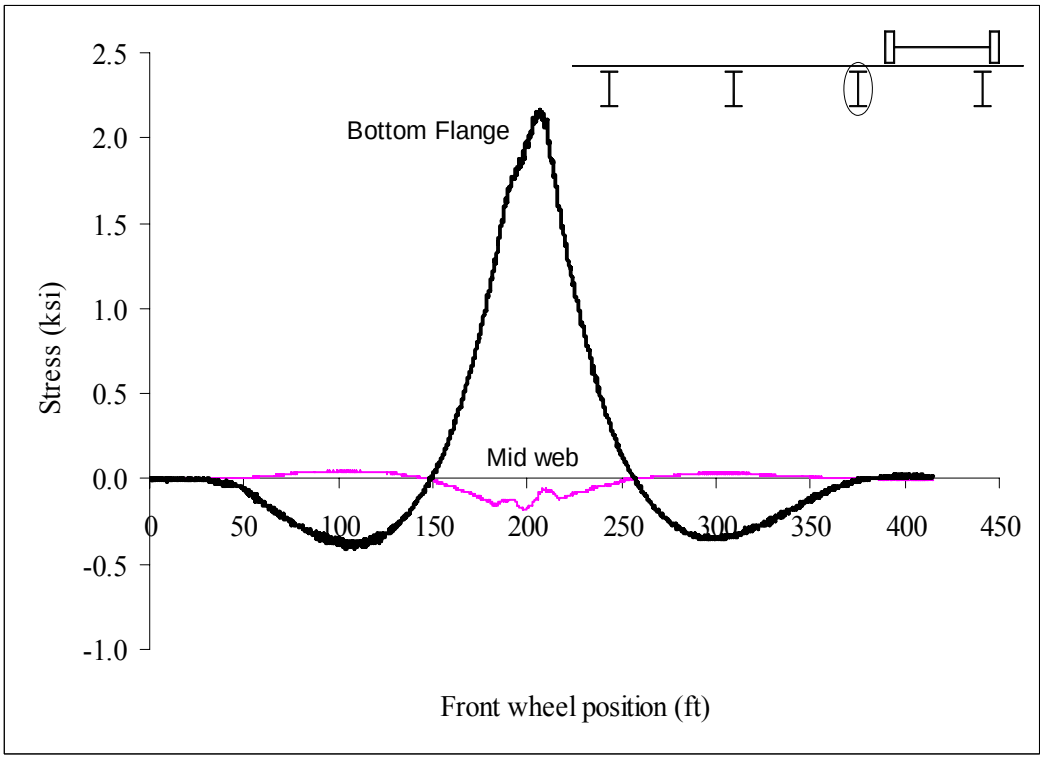

Figure B18: Hatch Bridge Test Run 1 S7 @ Midspan

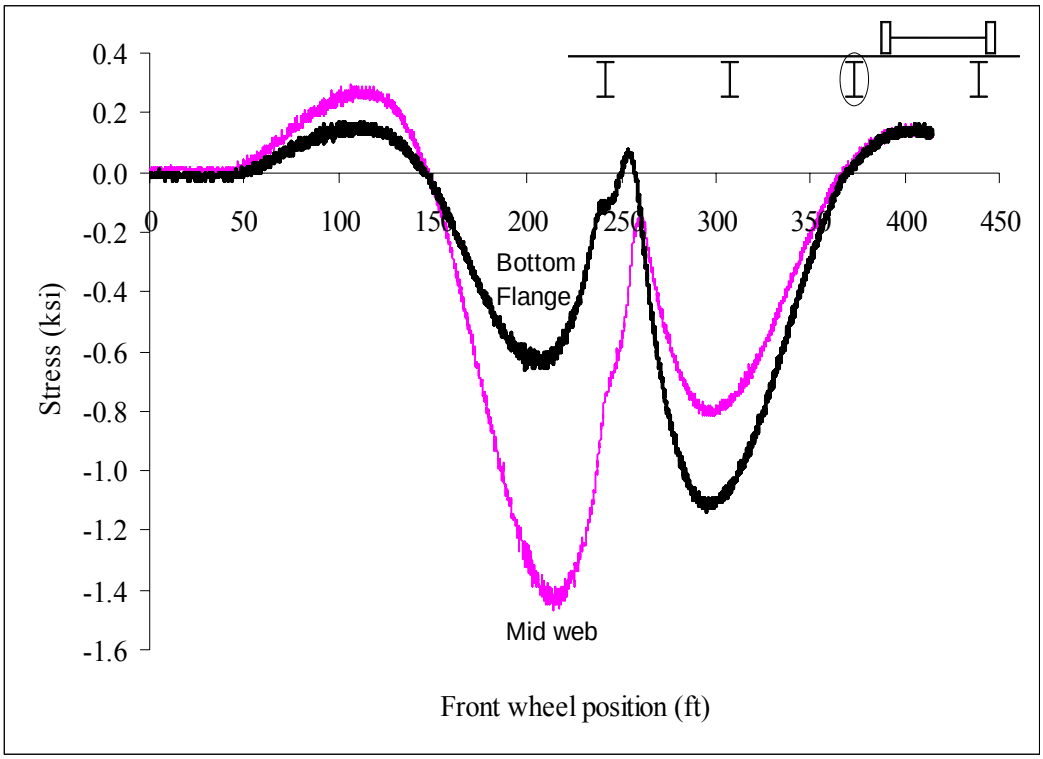

Figure B19: Hatch Bridge Test Run 1 S7 @ 3 ft west of interior support

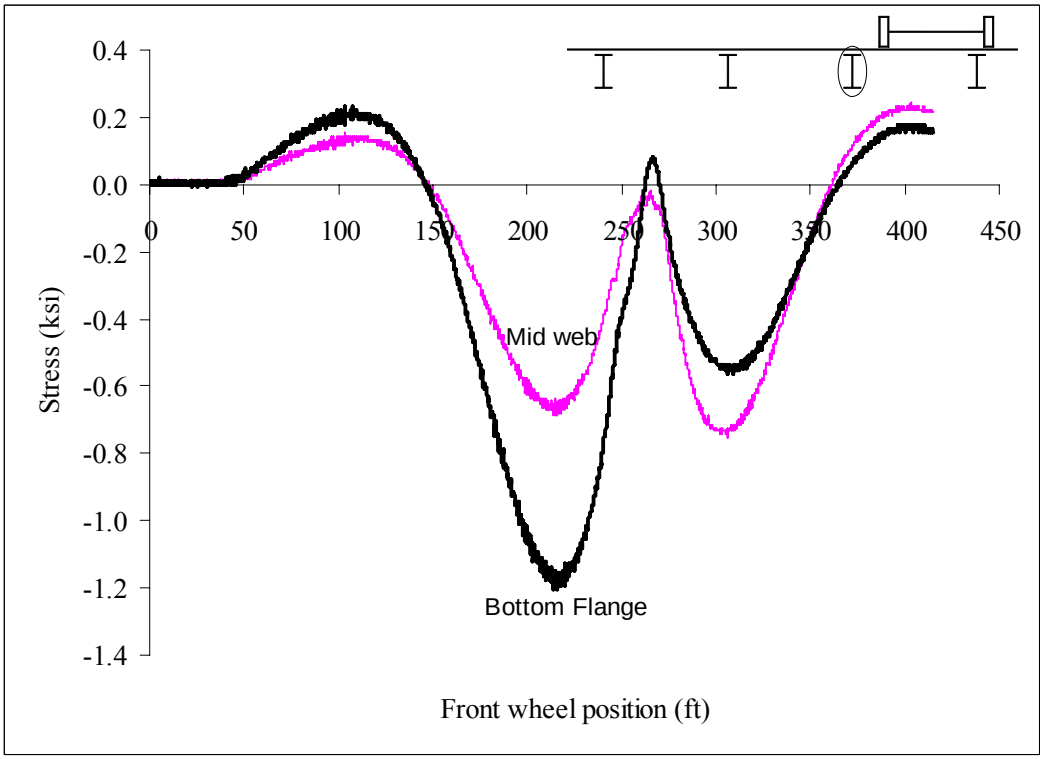

Figure B20: Hatch Bridge Test Run 1 S11 @ 3 ft east of interior support

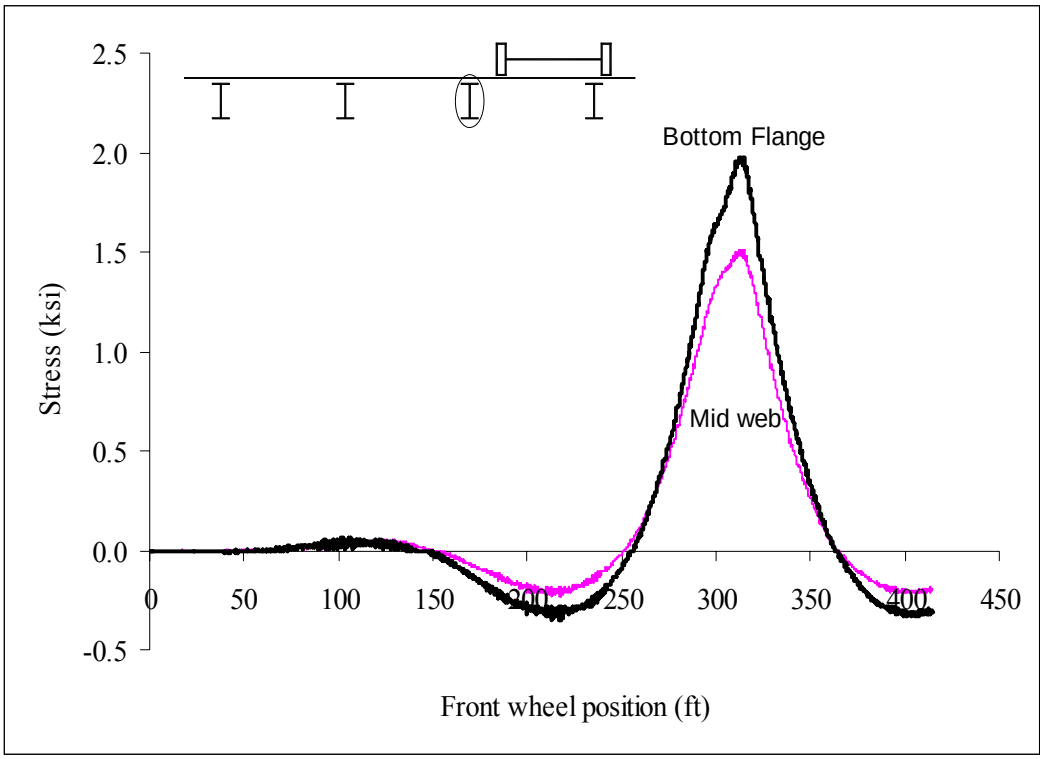

Figure B21: Hatch Bridge Test Run 1 S11 @ Midspan

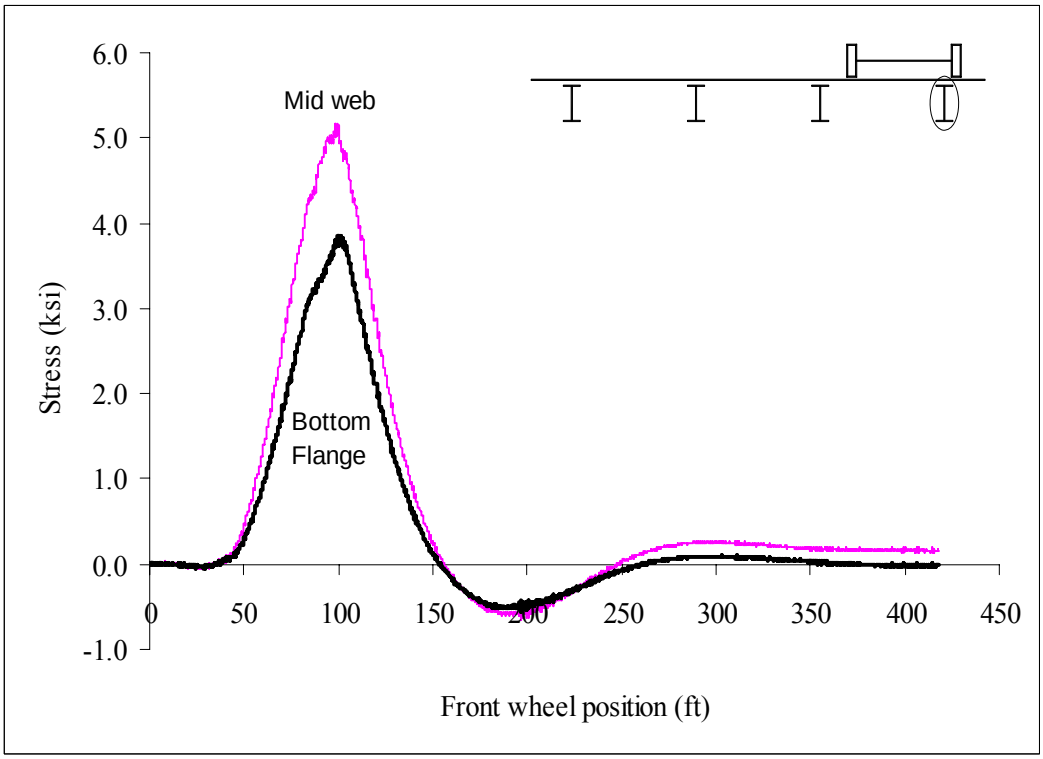

Figure B22: Hatch Bridge Test Run 1 S4 @ Midspan

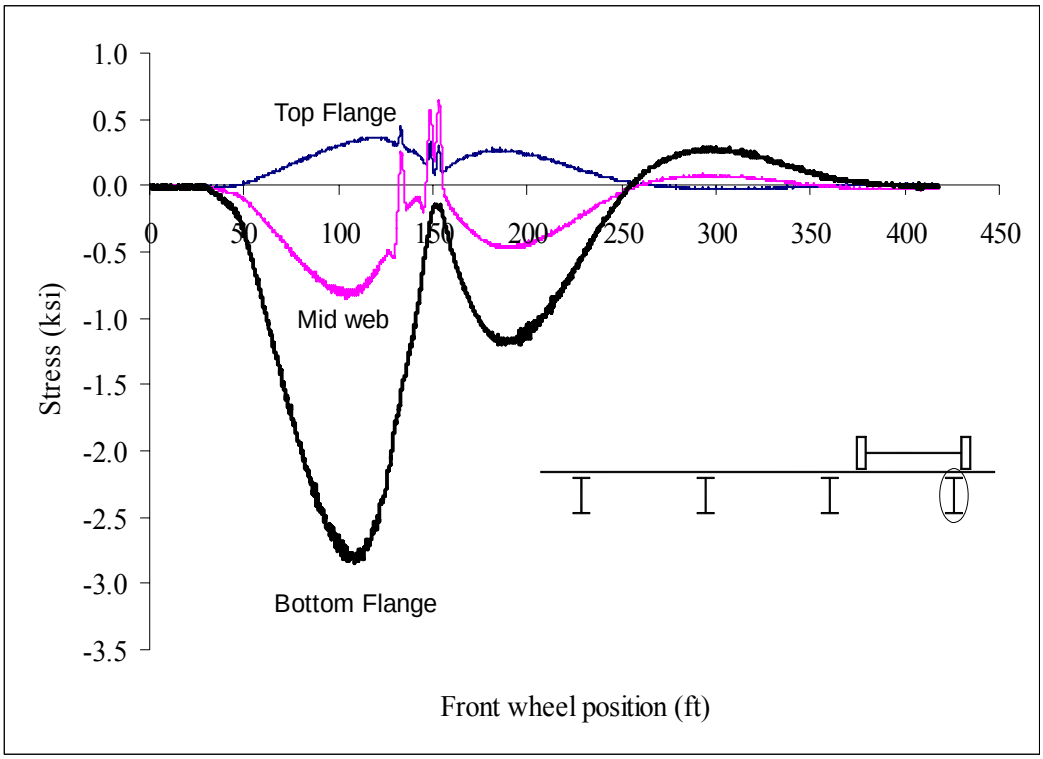

Figure B23: Hatch Bridge Test Run 1 S4 @ 3 ft west of interior support

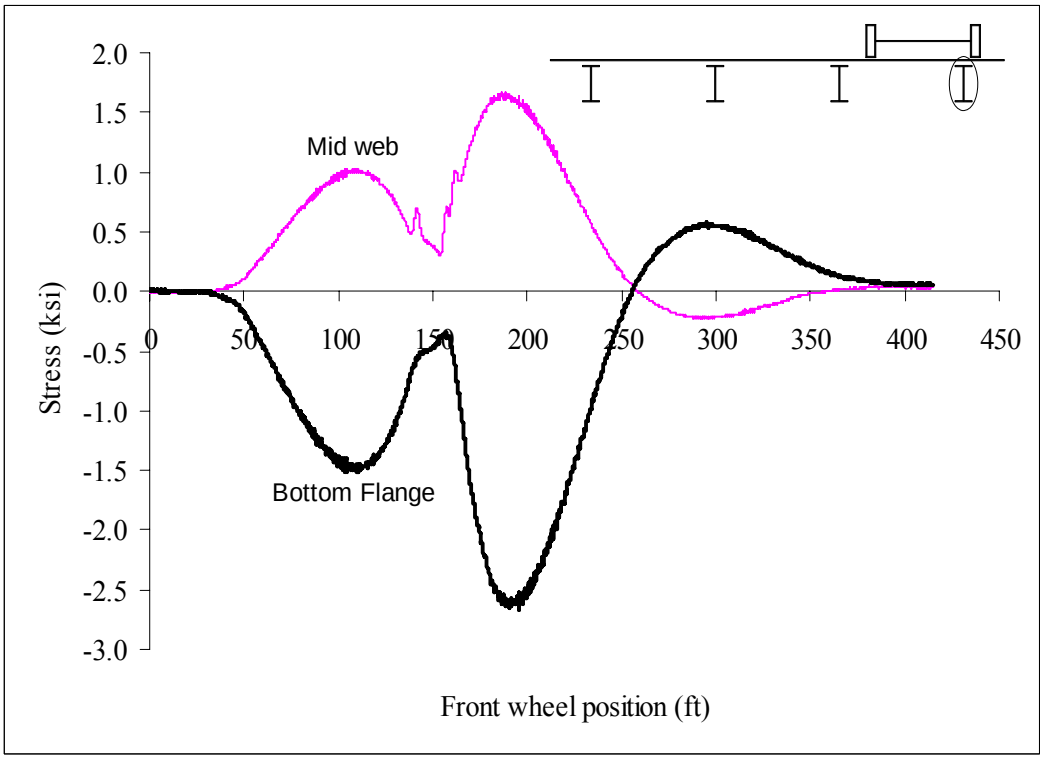

Figure B24: Hatch Bridge Test Run 1 S8 @ 3 ft east of interior support

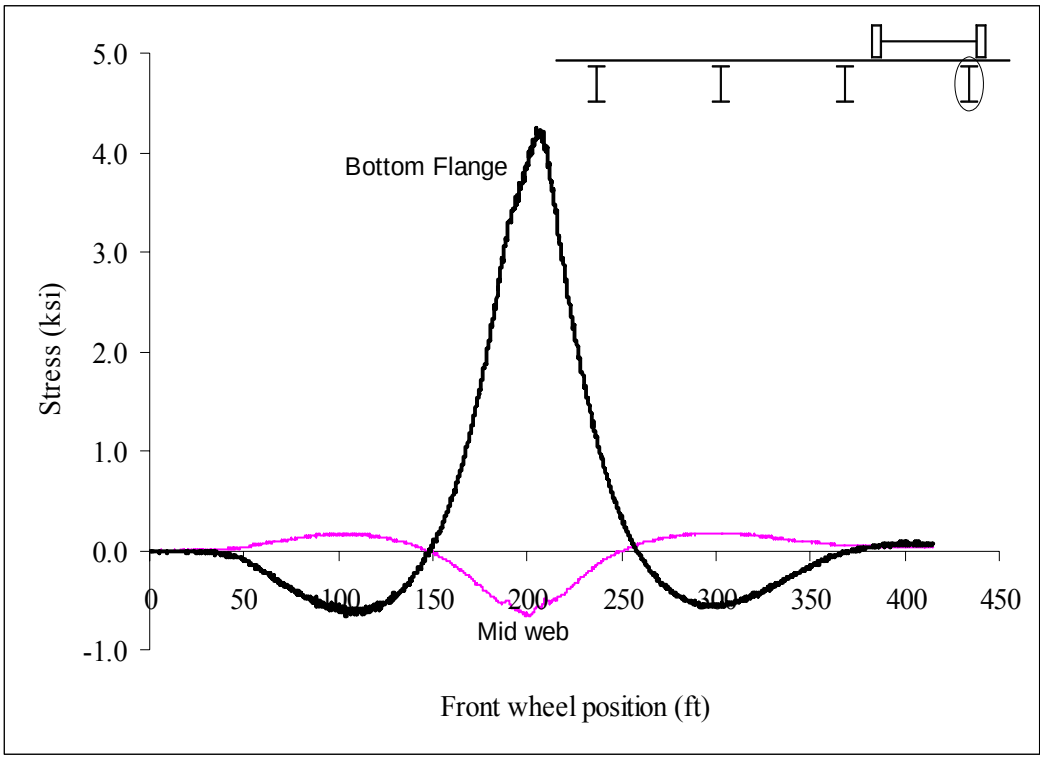

Figure B25: Hatch Bridge Test Run 1 S8 @ Midspan

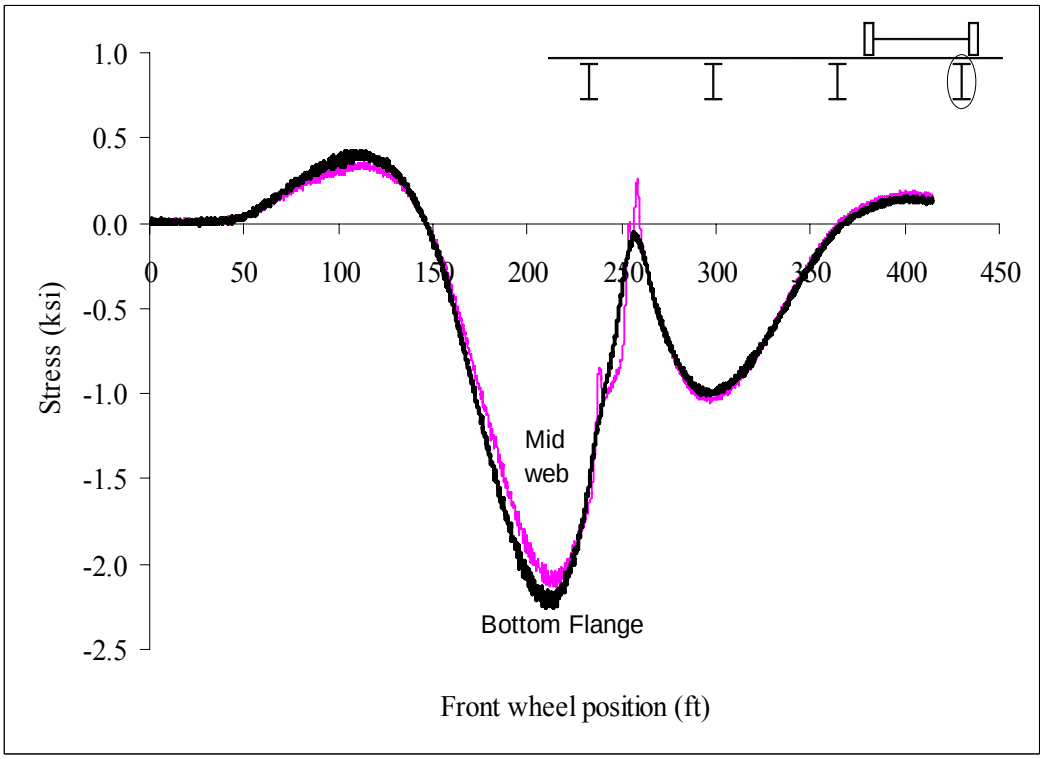

Figure B26: Hatch Bridge Test Run 1 S8 @ 3 ft west of interior support

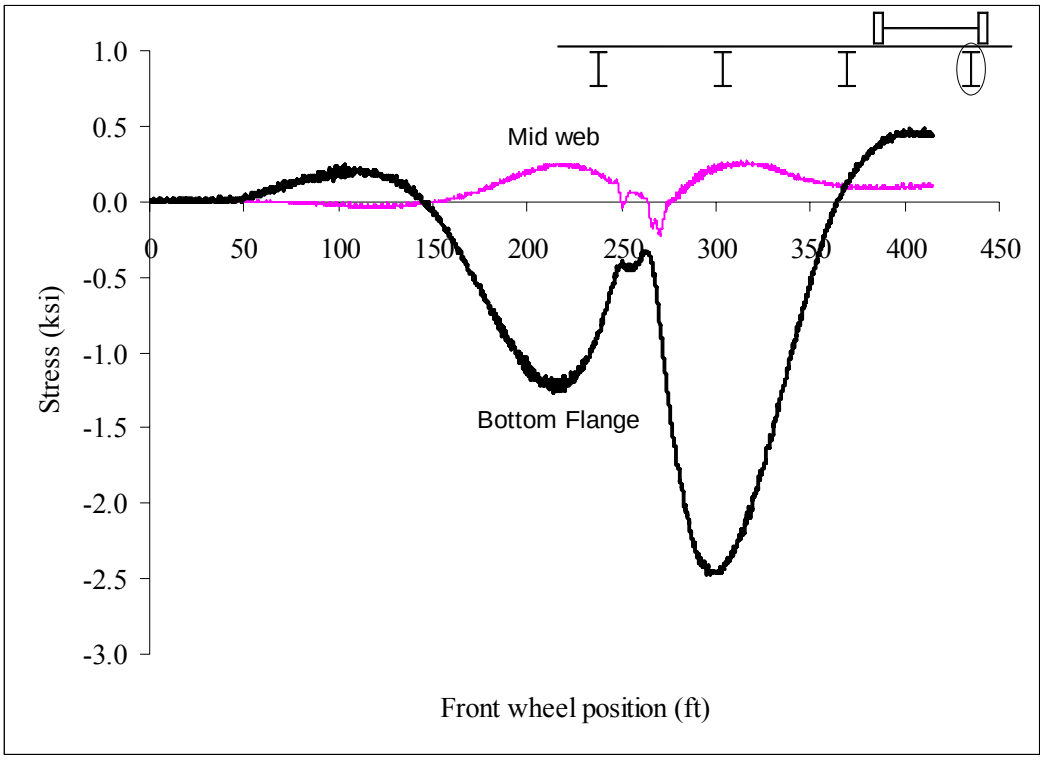

Figure B27: Hatch Bridge Test Run 1 S12 @ 3 ft east of interior support

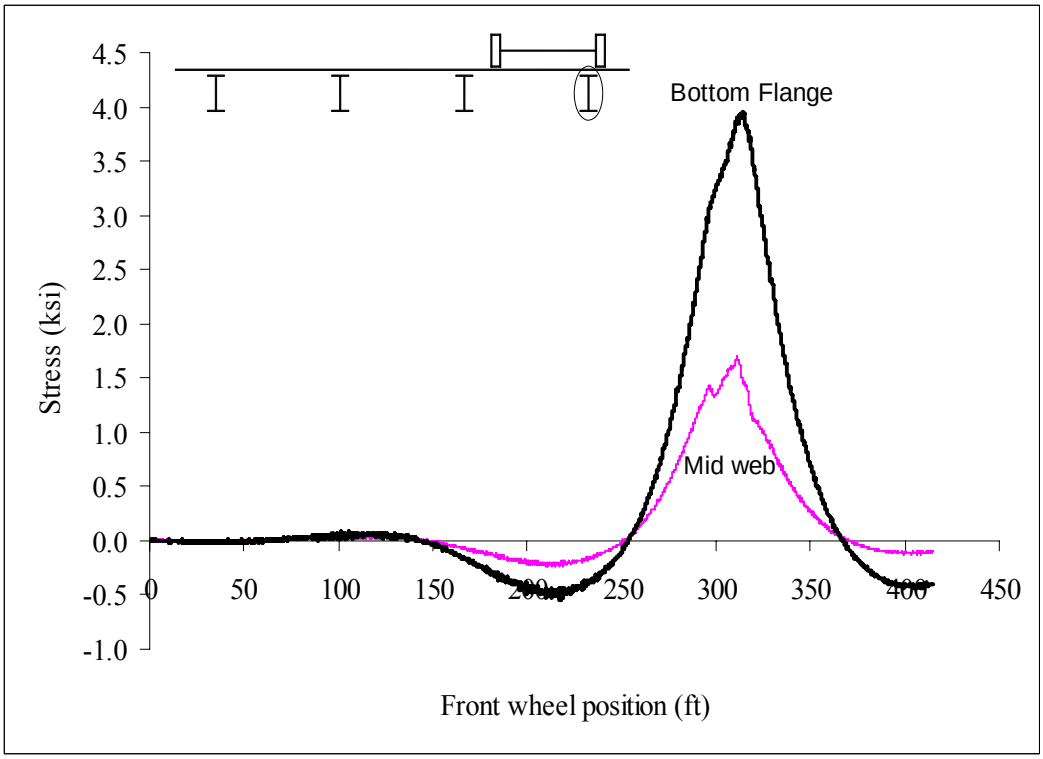

Figure B28: Hatch Bridge Test Run 1 S12 @ Midspan

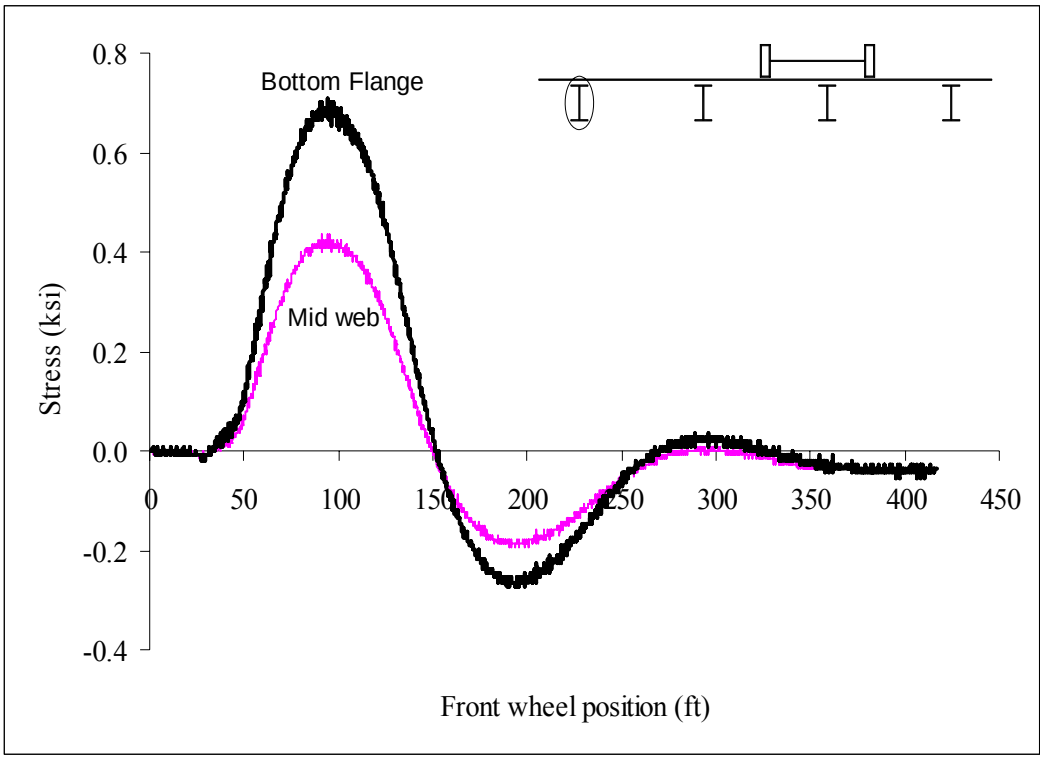

Figure B29: Hatch Bridge Test Run 2 S1 @ Midspan

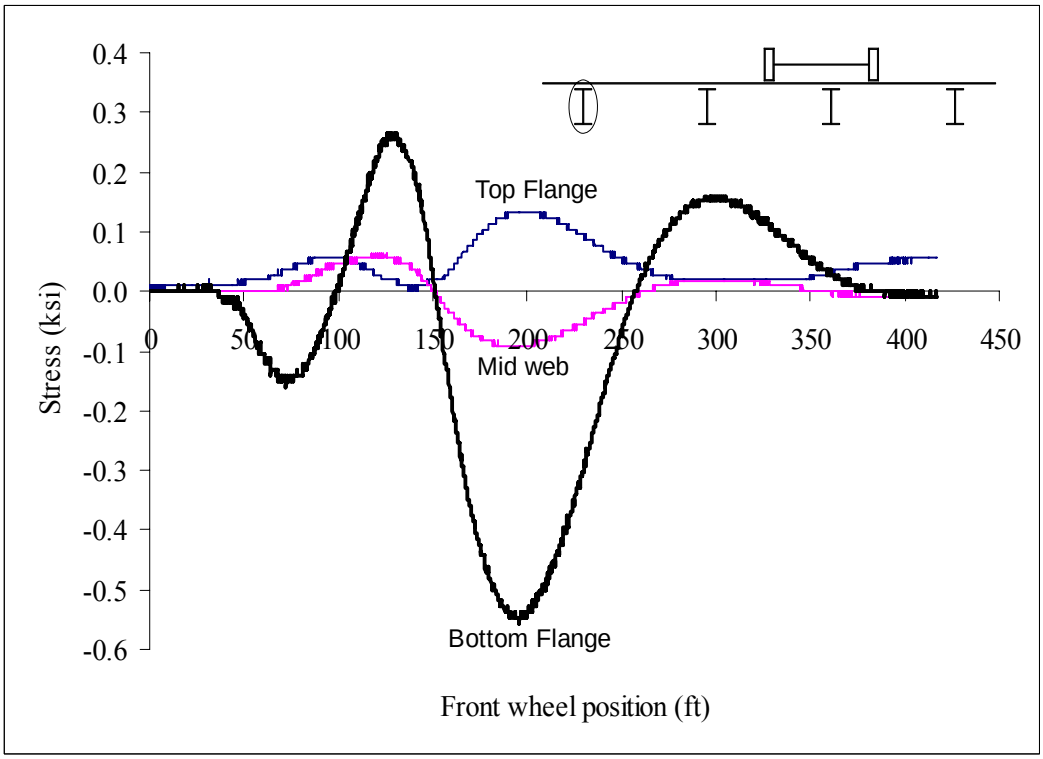

Figure B30: Hatch Bridge Test Run 2 S1 @ 3 ft west of interior support

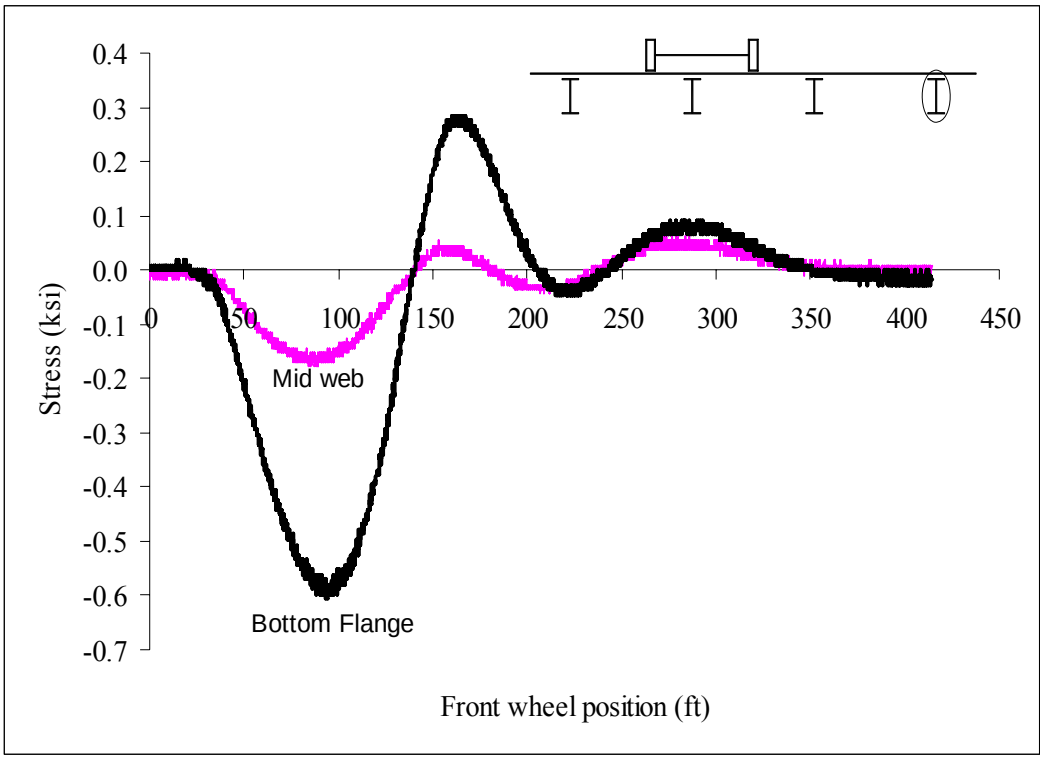

Figure B31: Hatch Bridge Test Run 2 S5 @ 3 ft east of interior support

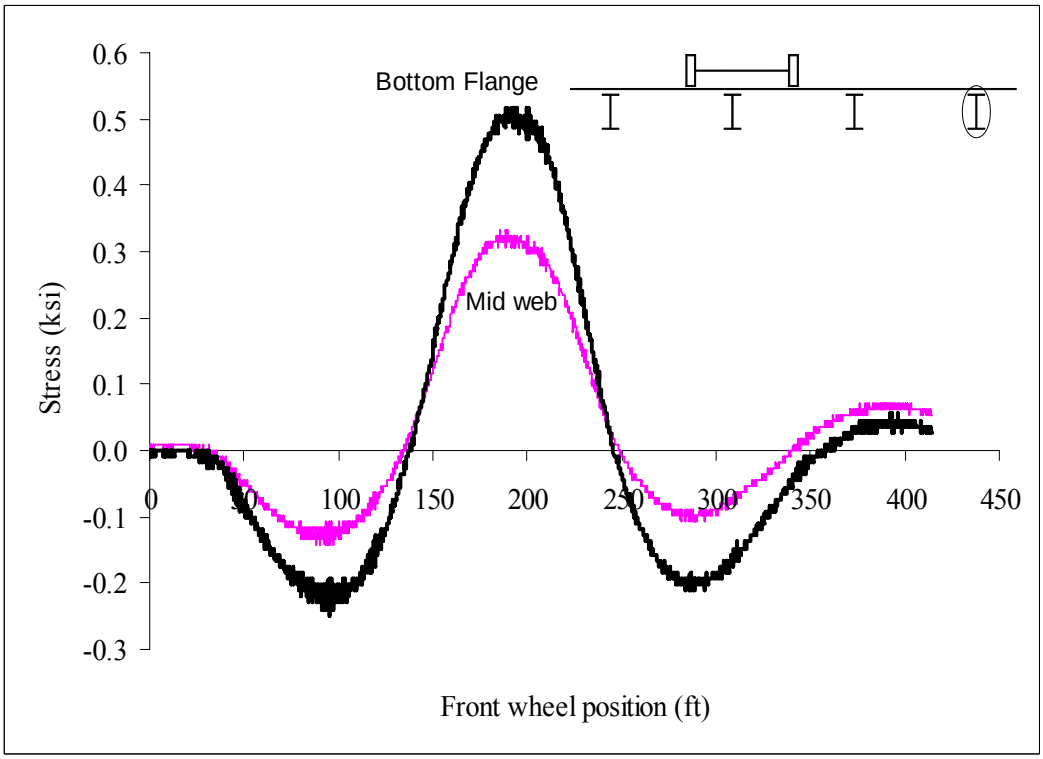

Figure B32: Hatch Bridge Test Run 2 S5 @ Midspan

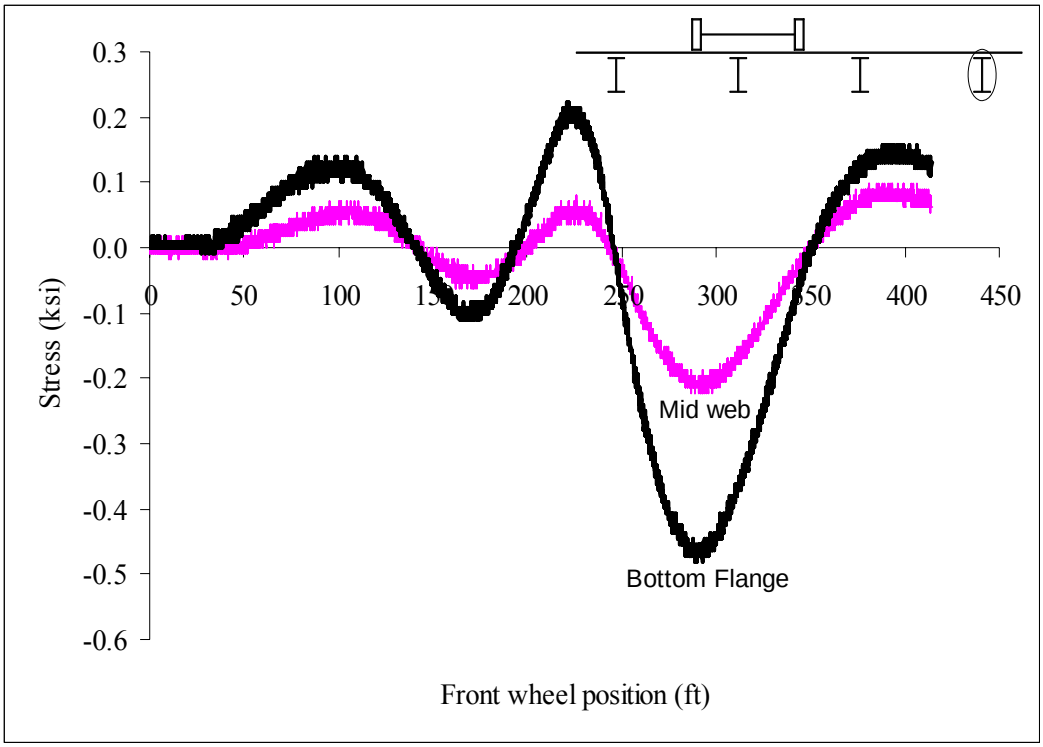

Figure B33: Hatch Bridge Test Run 2 S5 @ 3 ft west of interior support

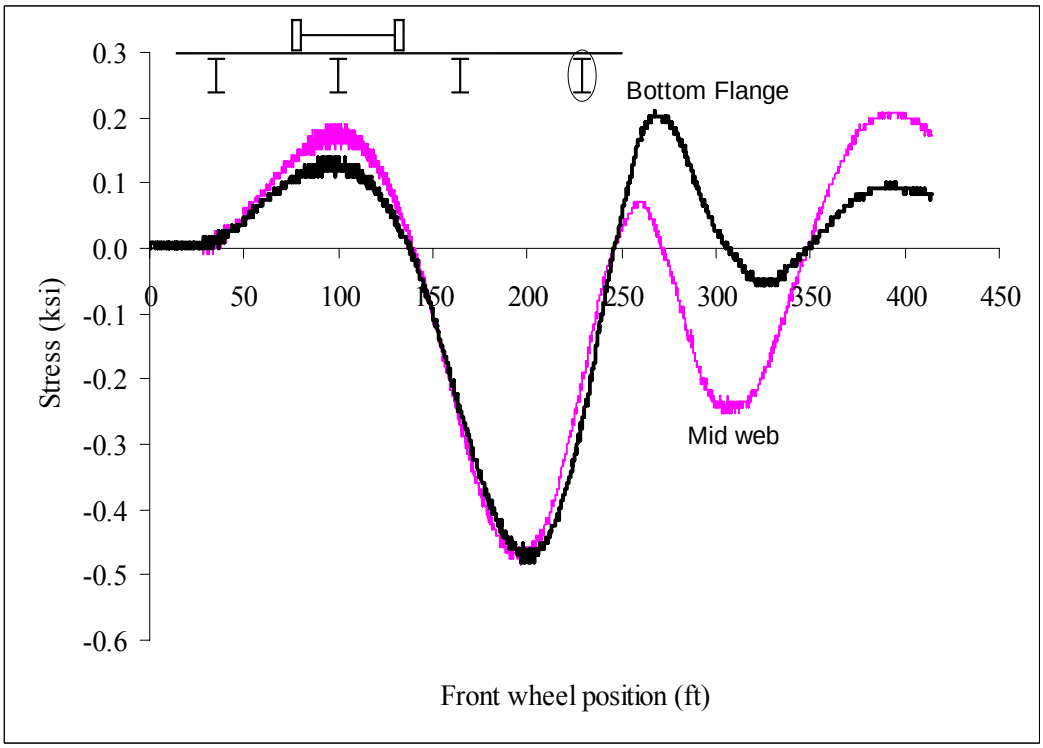

Figure B34: Hatch Bridge Test Run 2 S9 @ 3 ft east of interior support

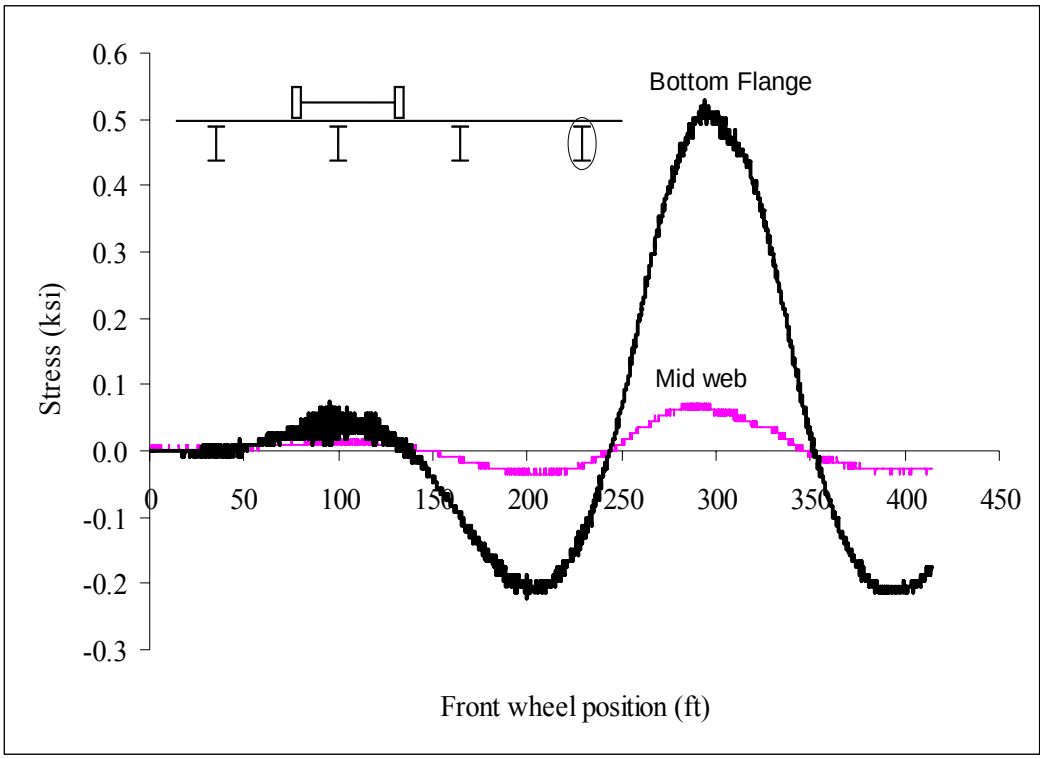

Figure B35: Hatch Bridge Test Run 2 S9 @ Midspan

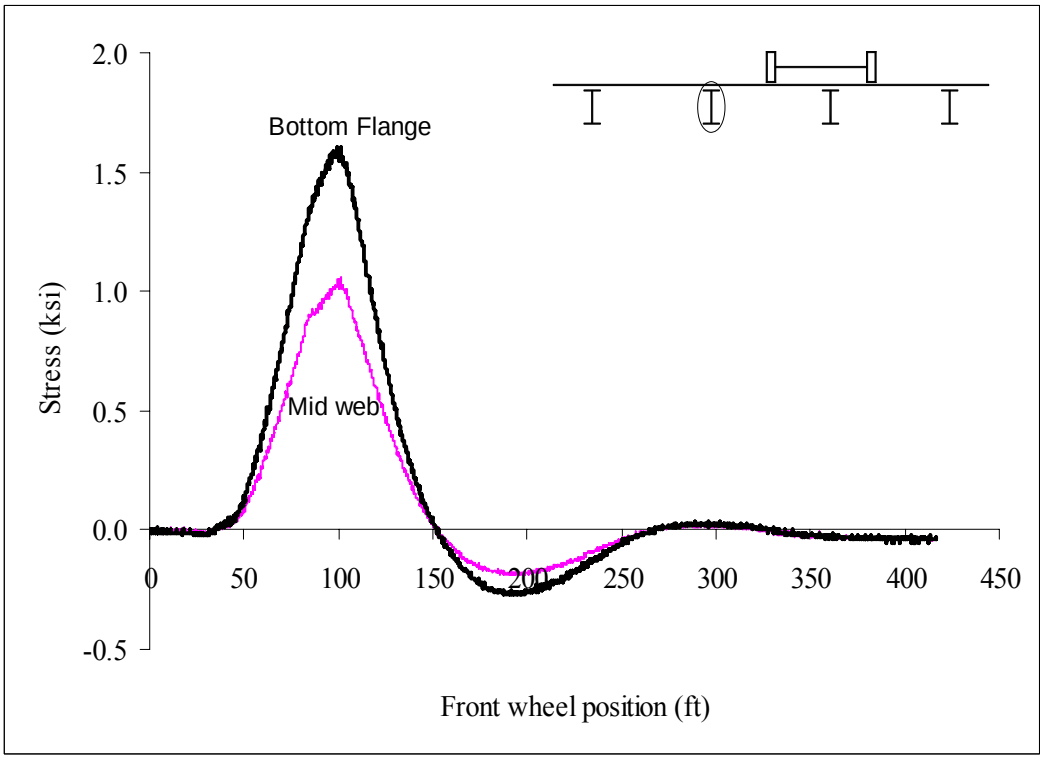

Figure B36: Hatch Bridge Test Run 2 S2 @ Midspan

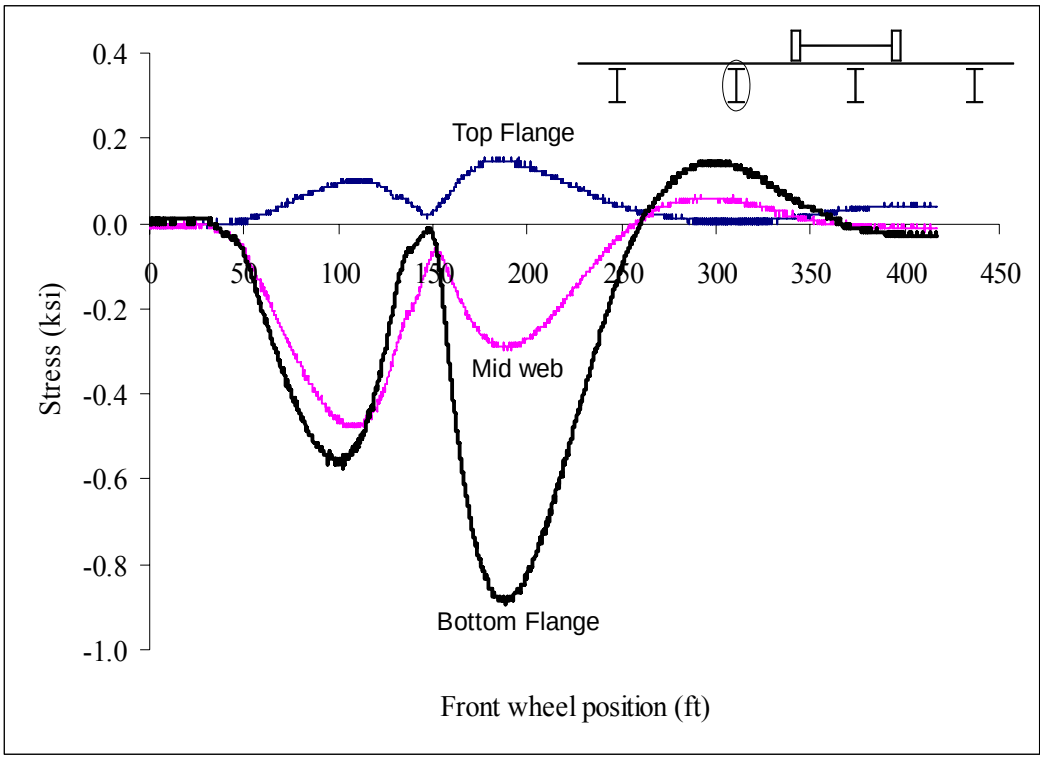

Figure B37: Hatch Bridge Test Run 2 S2 @ 3 ft west of interior support

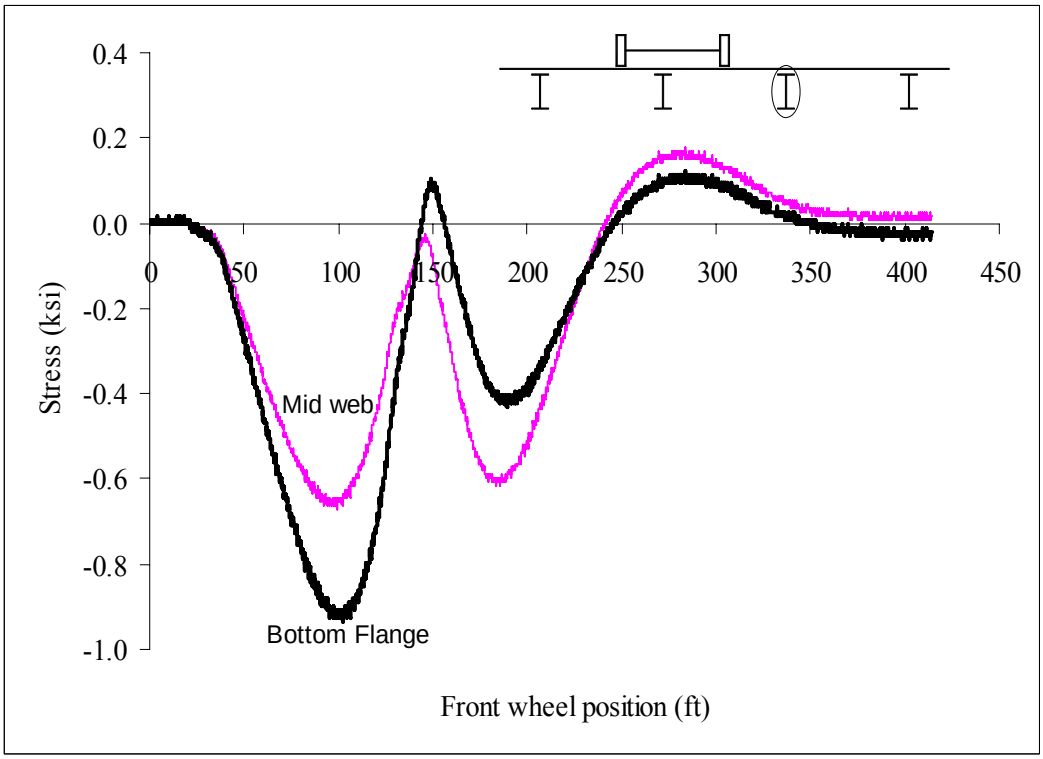

Figure B38: Hatch Bridge Test Run 2 S6 @ 3 ft east of interior support

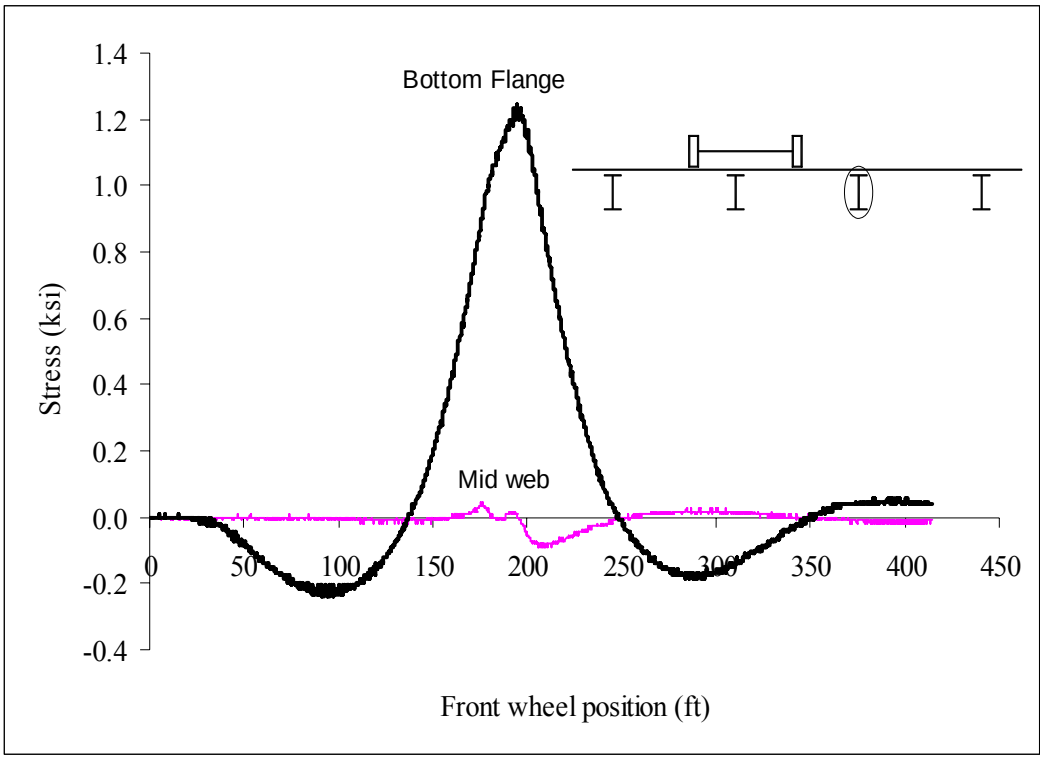

Figure B39: Hatch Bridge Test Run 2 S6 @ Midspan

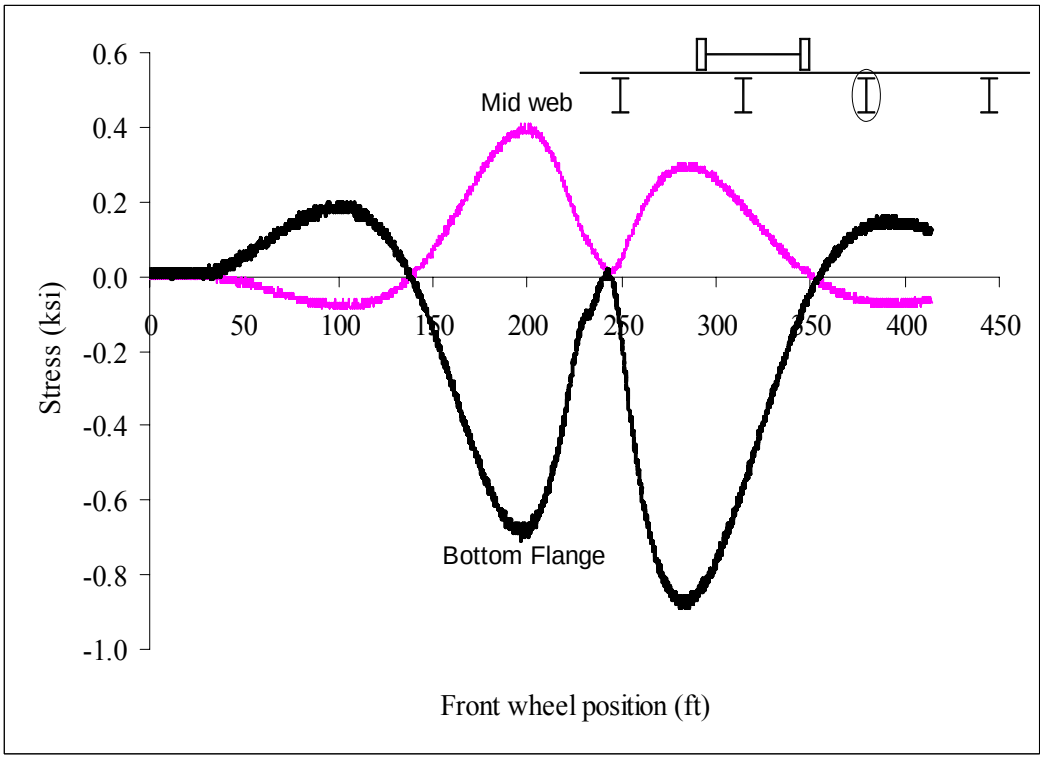

Figure B40: Hatch Bridge Test Run 2 S6 @ 3 ft west of interior support

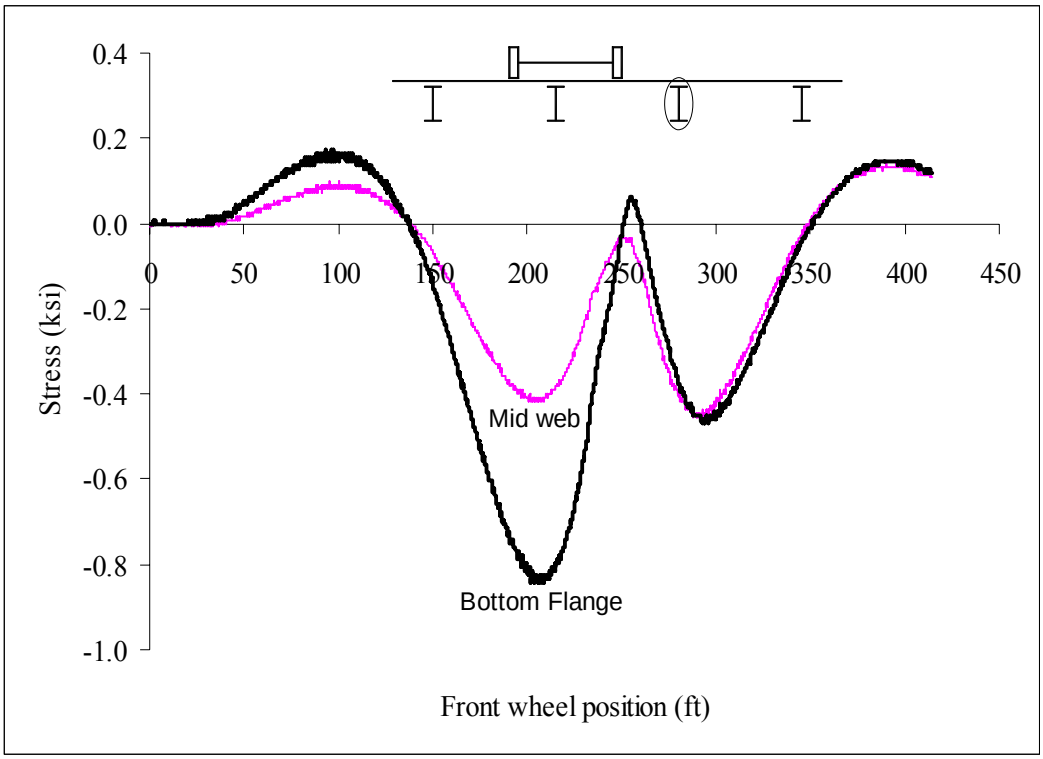

Figure B41: Hatch Bridge Test Run 2 S10 @ 3 ft east of interior support

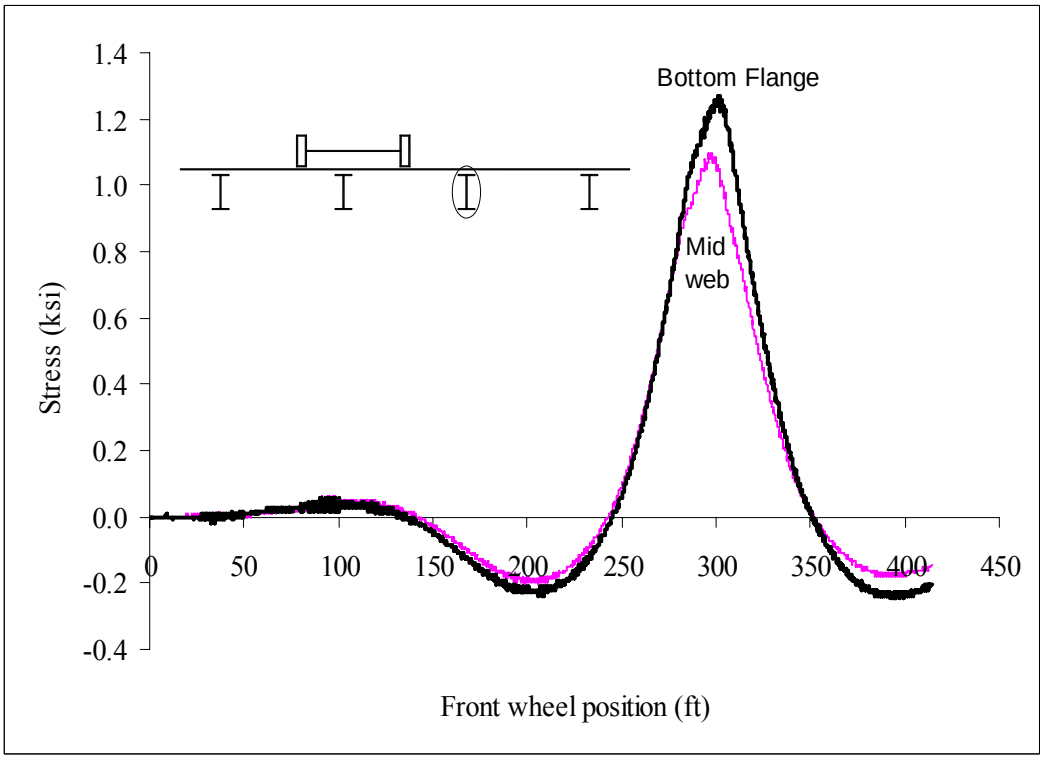

Figure B42: Hatch Bridge Test Run 2 S10 @ Midspan

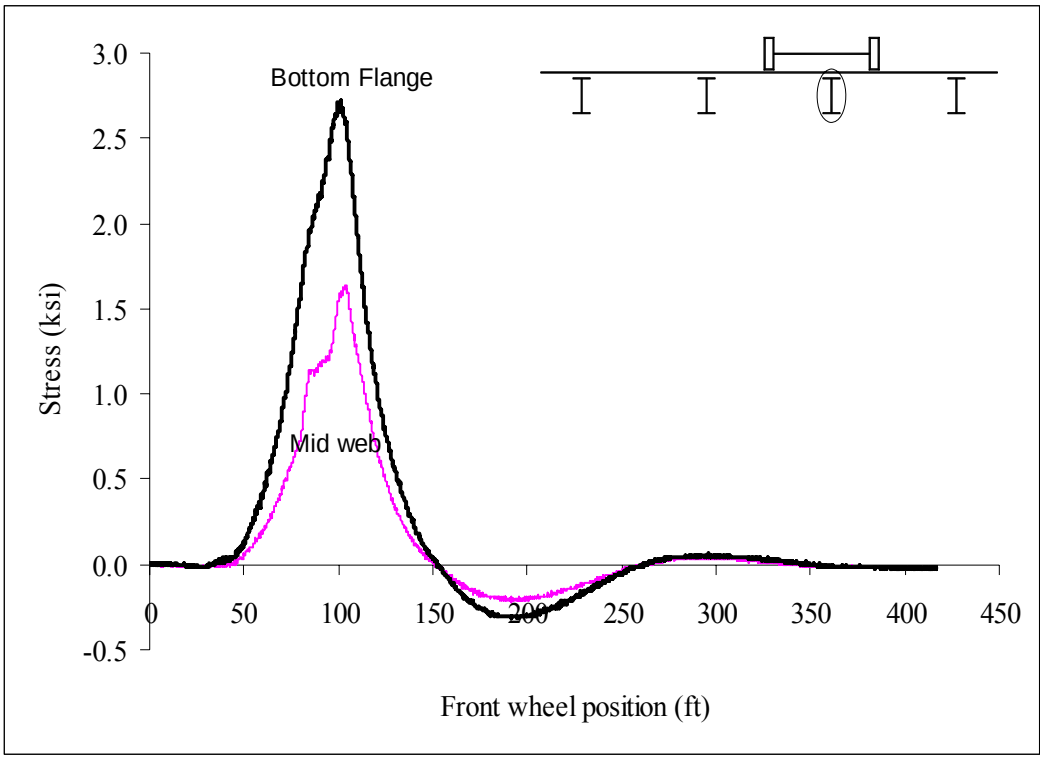

Figure B43: Hatch Bridge Test Run 2 S3 @ Midspan

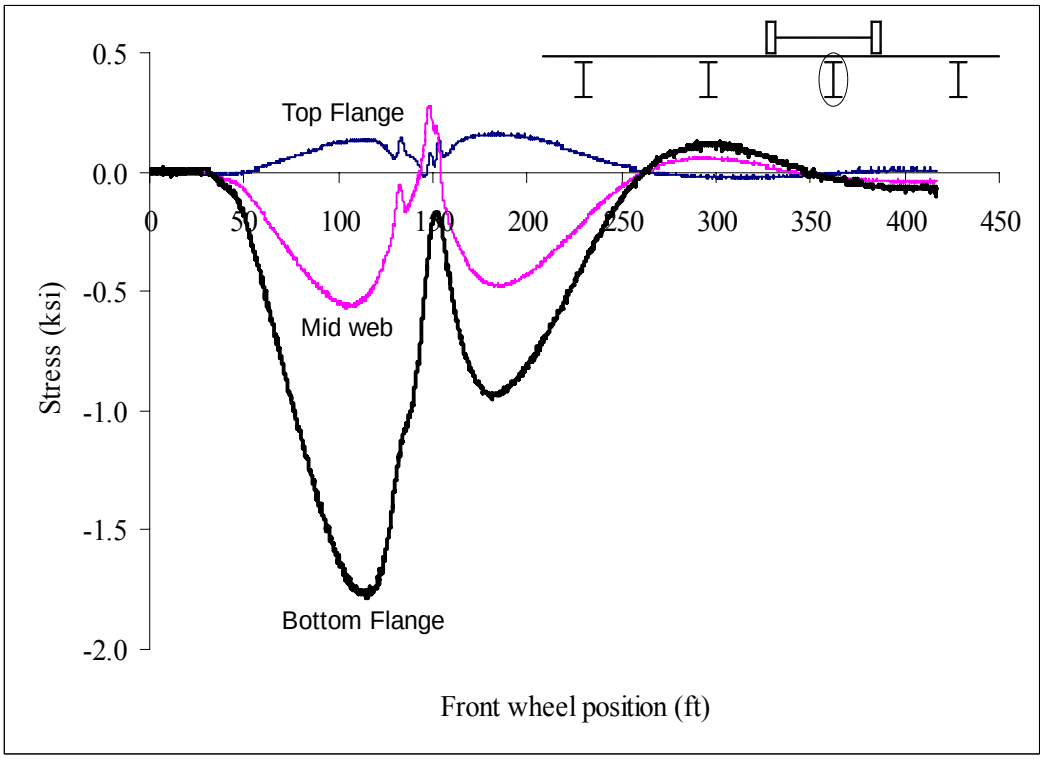

Figure B44: Hatch Bridge Test Run 2 S3 @ 3 ft west of interior support

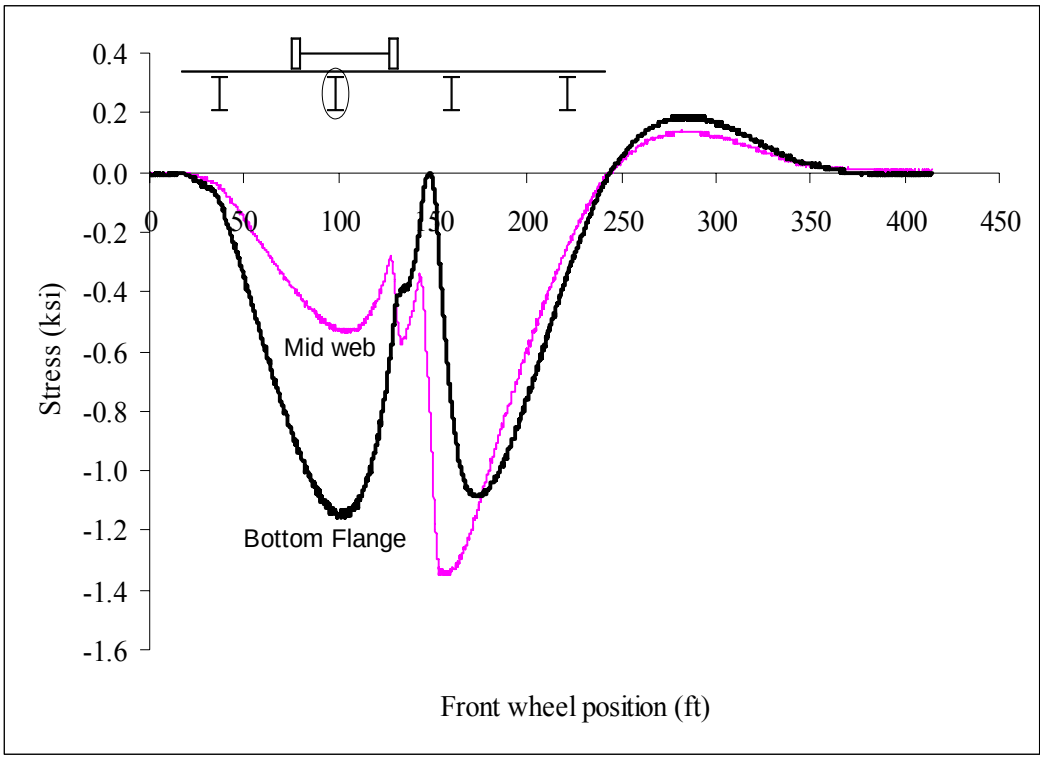

Figure B45: Hatch Bridge Test Run 2 S7 @ 3 ft west of interior support

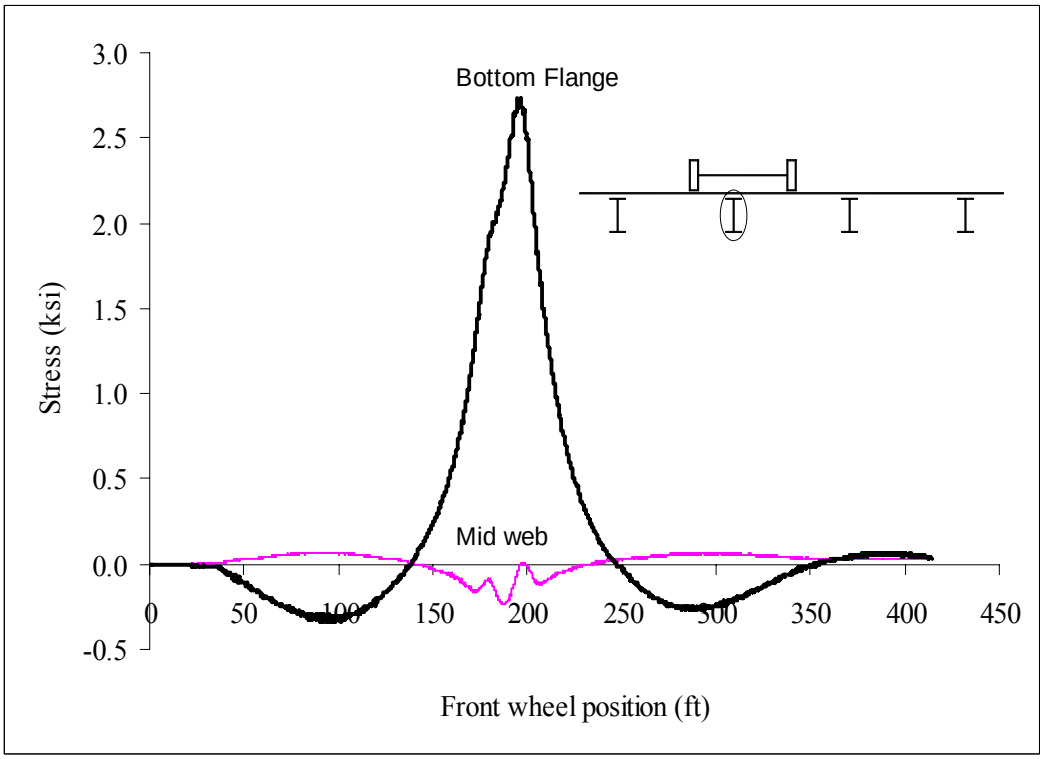

Figure B46: Hatch Bridge Test Run 2 S7 @ Midspan

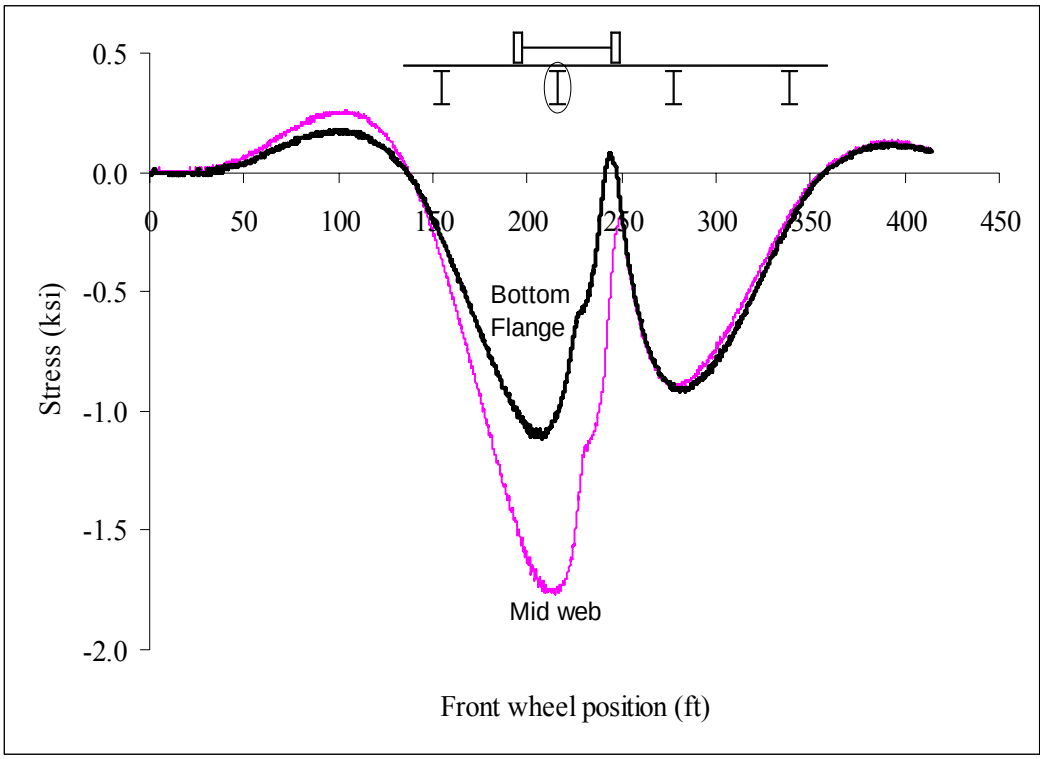

Figure B47: Hatch Bridge Test Run 2 S7 @ 3 ft west of interior support

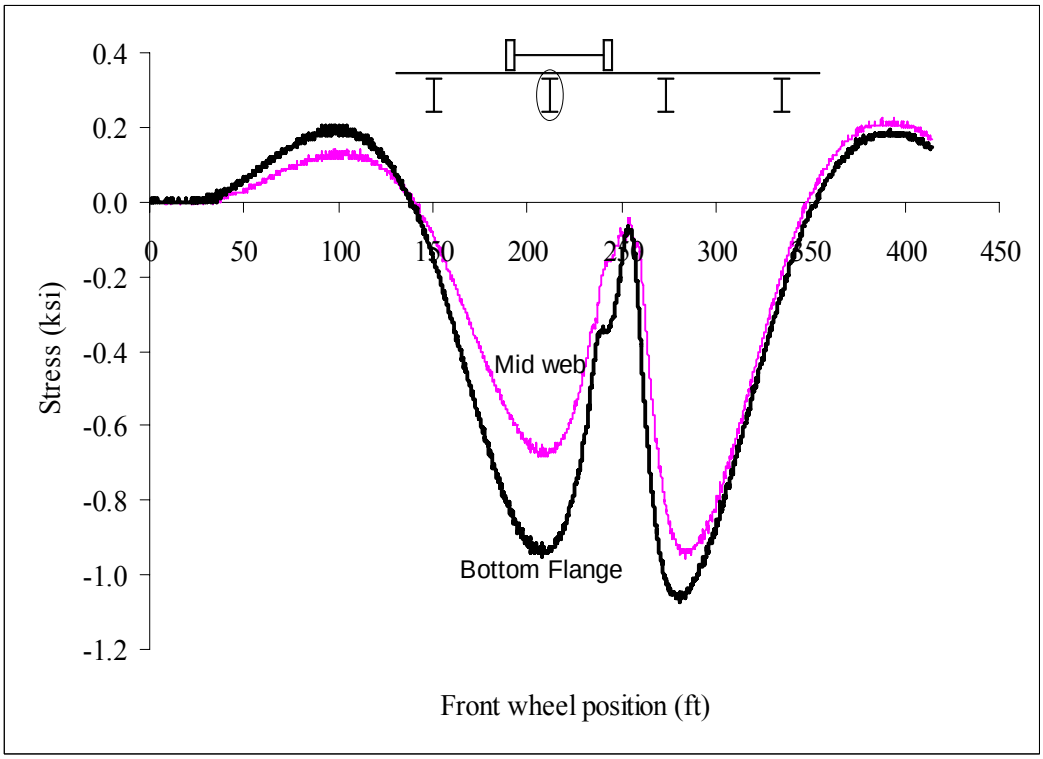

Figure B48: Hatch Bridge Test Run 2 S11 @ 3 ft east of interior support

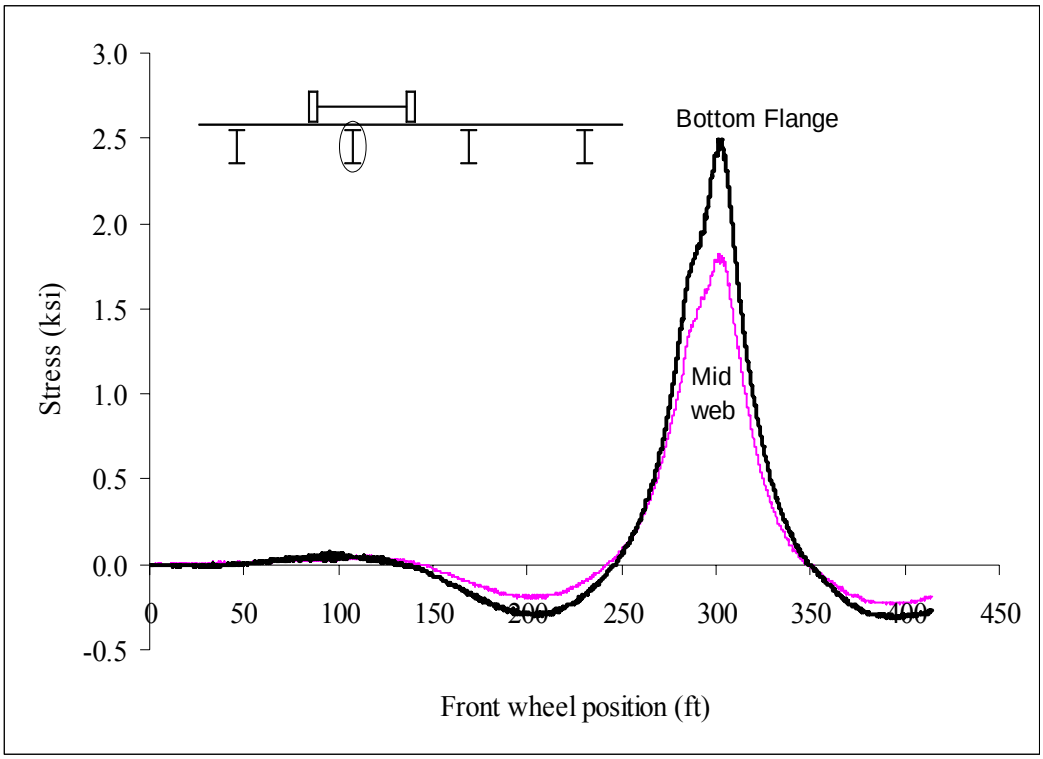

Figure B49: Hatch Bridge Test Run 2 S11 @ Midspan

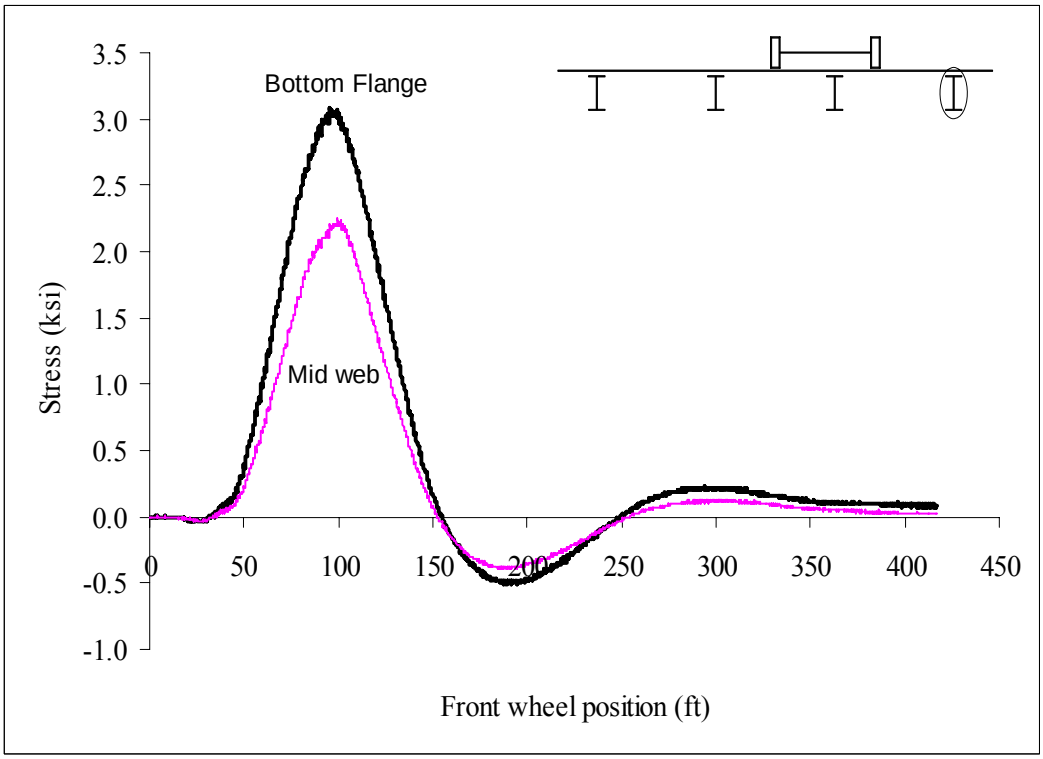

Figure B50: Hatch Bridge Test Run 2 S4 @ Midspan

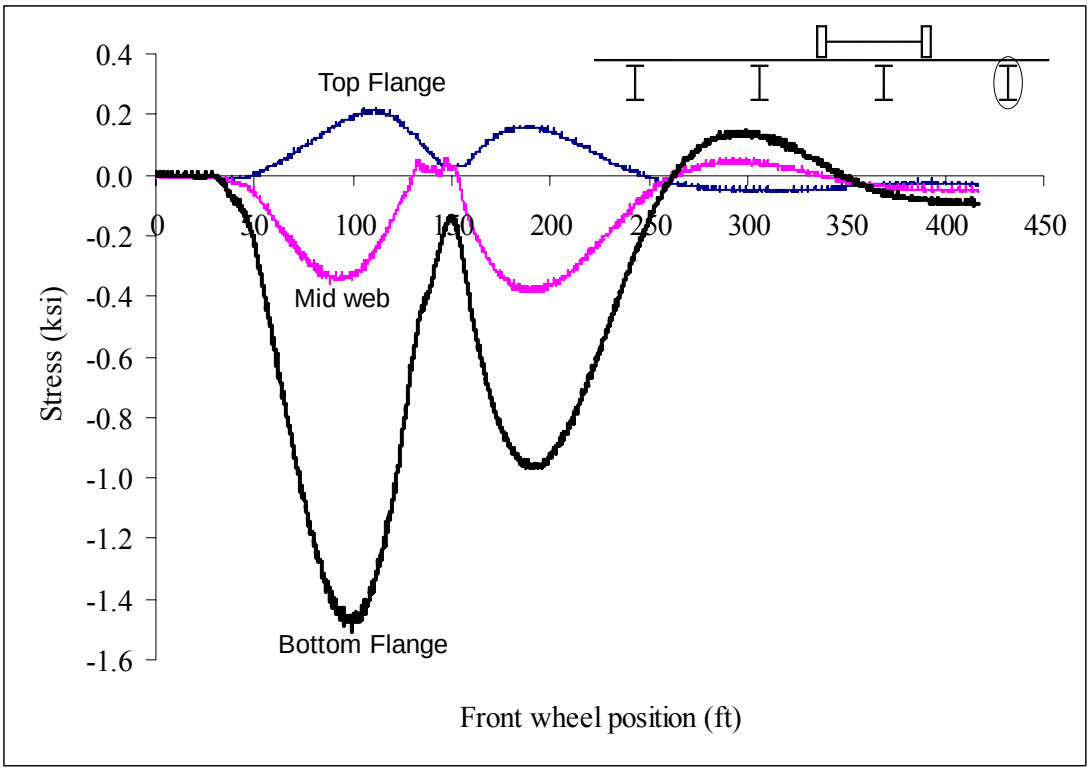

Figure B51: Hatch Bridge Test Run 2 S4 @ 3 ft west of interior support

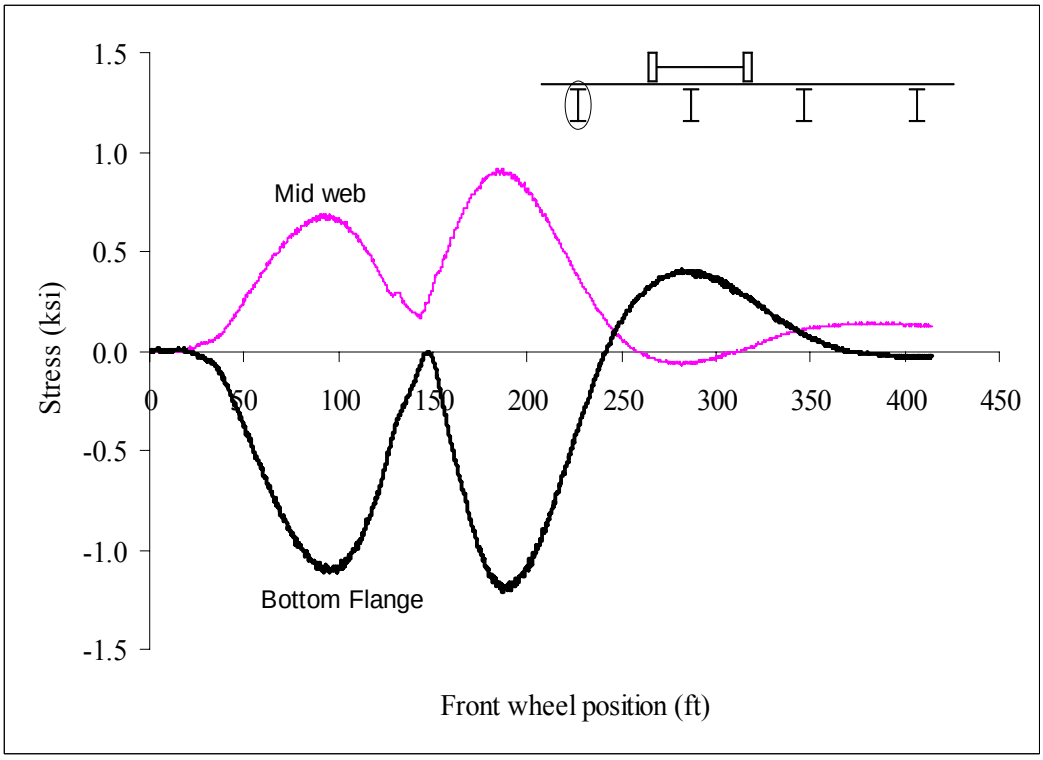

Figure B52: Hatch Bridge Test Run 2 S8 @ 3 ft east of interior support

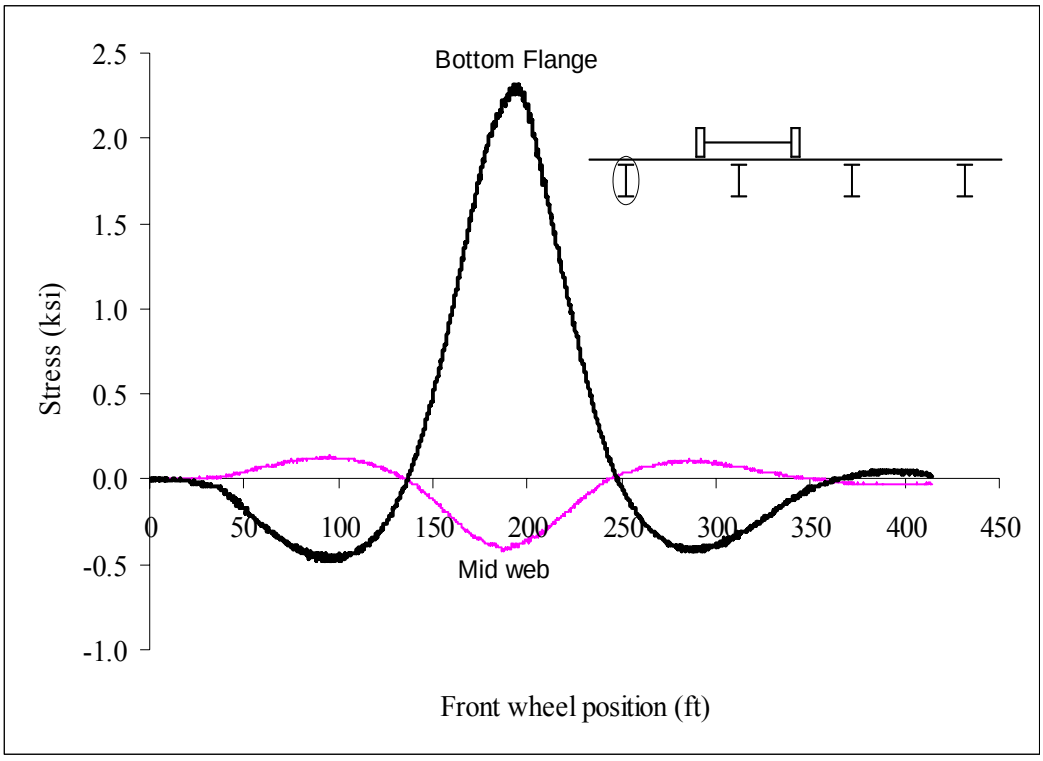

Figure B53: Hatch Bridge Test Run 2 S8 @ Midspan

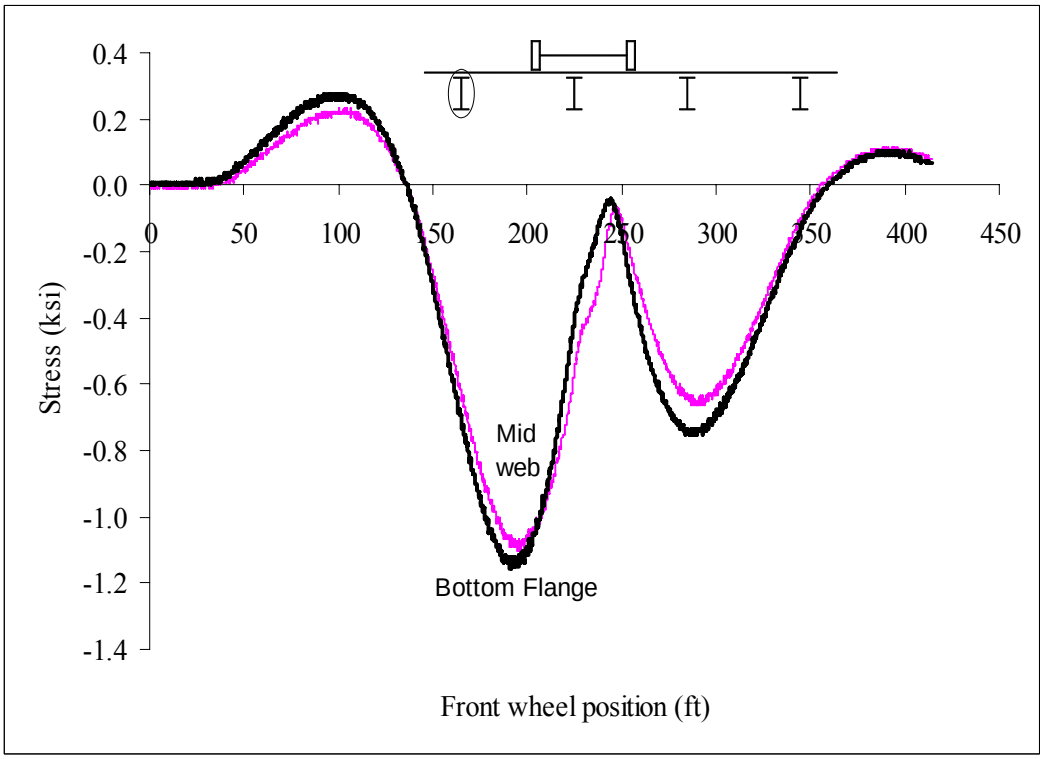

Figure B54: Hatch Bridge Test Run 2 S8 @ 3 ft west of interior support

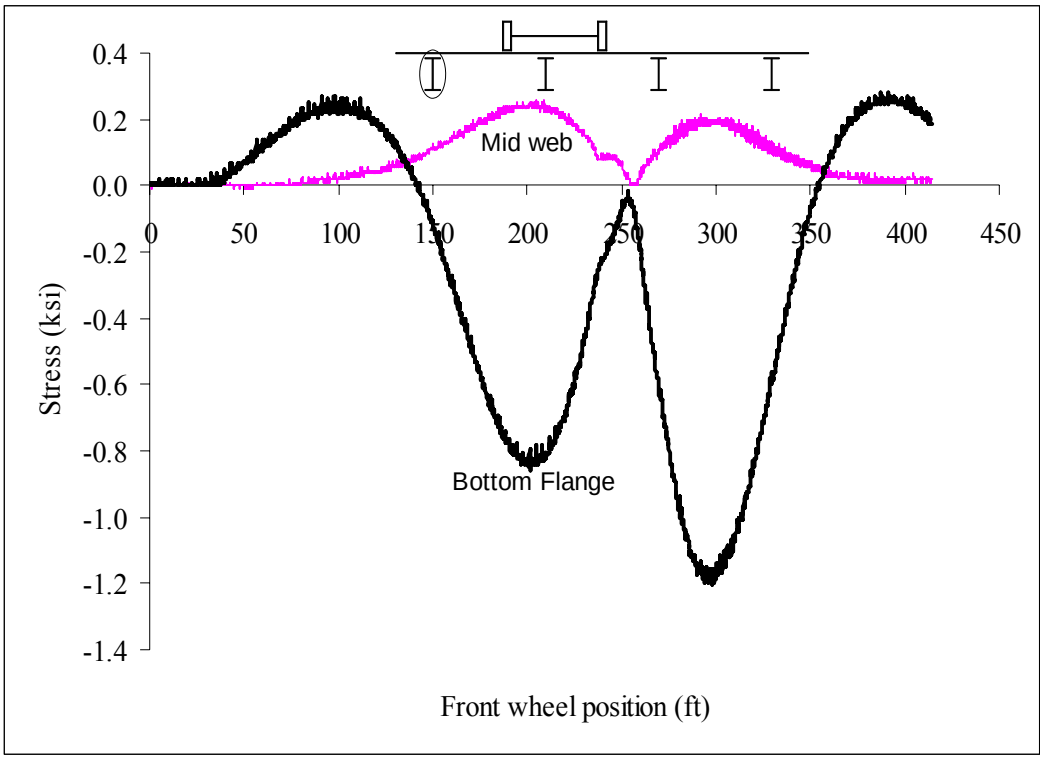

Figure B55: Hatch Bridge Test Run 2 S12 @ 3 ft east of interior support

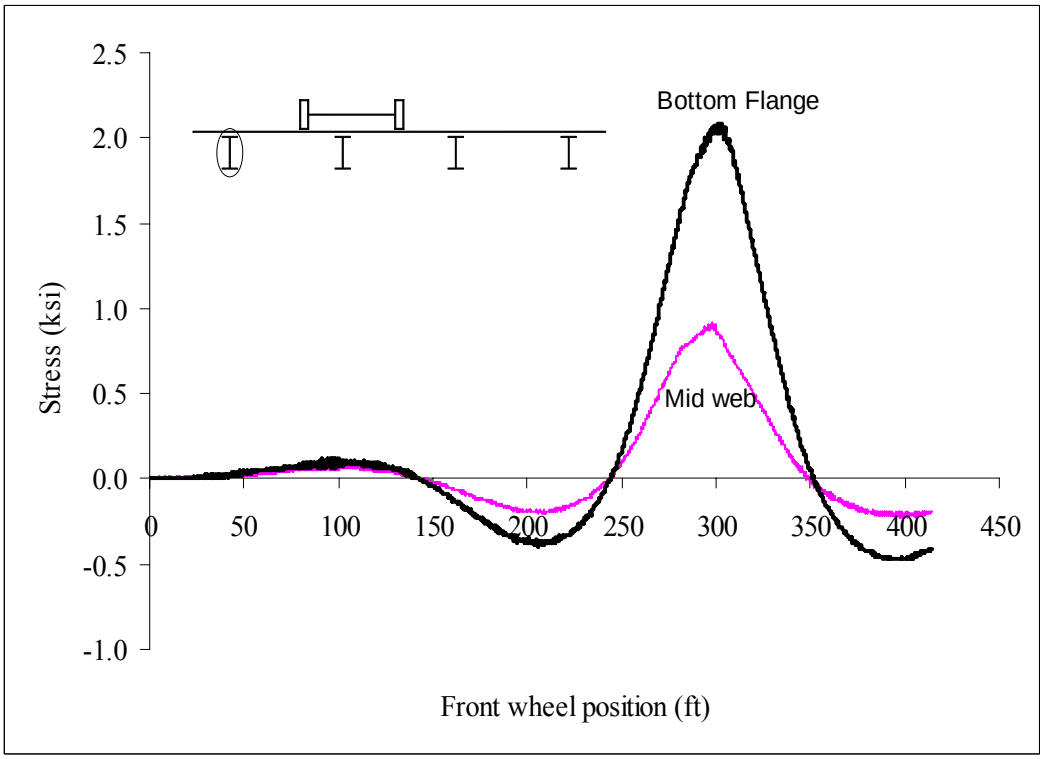

Figure B56: Hatch Bridge Test Run 2 S12 @ Midspan

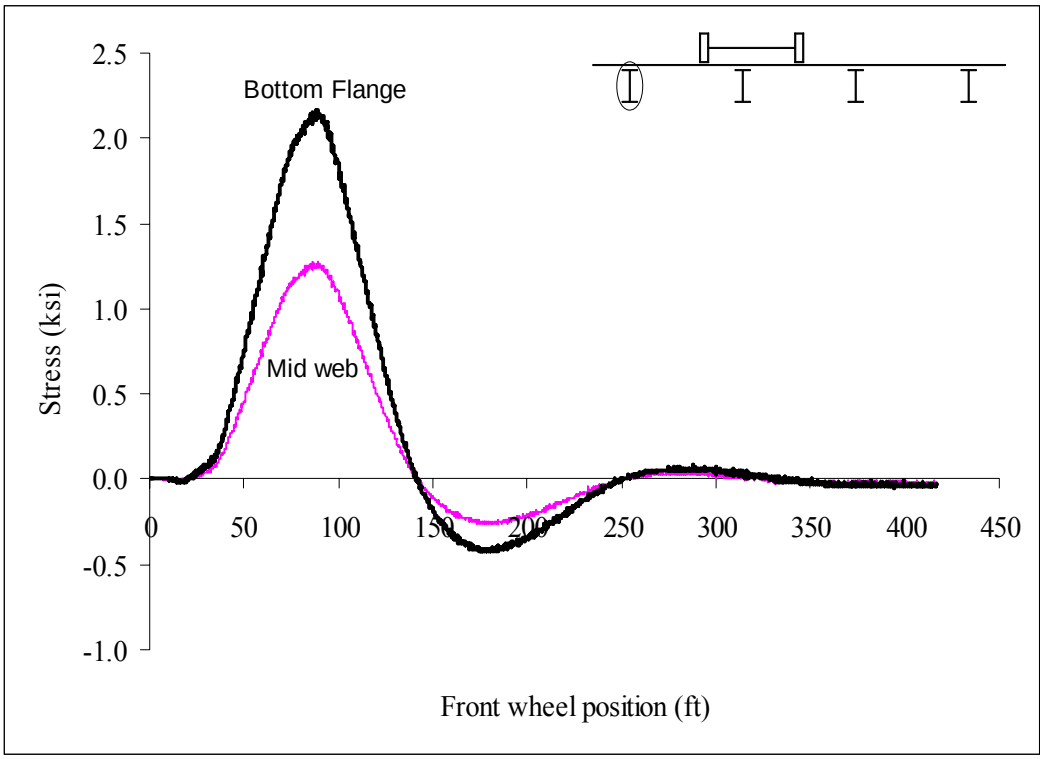

Figure B57: Hatch Bridge Test Run 3 S1 @ Midspan

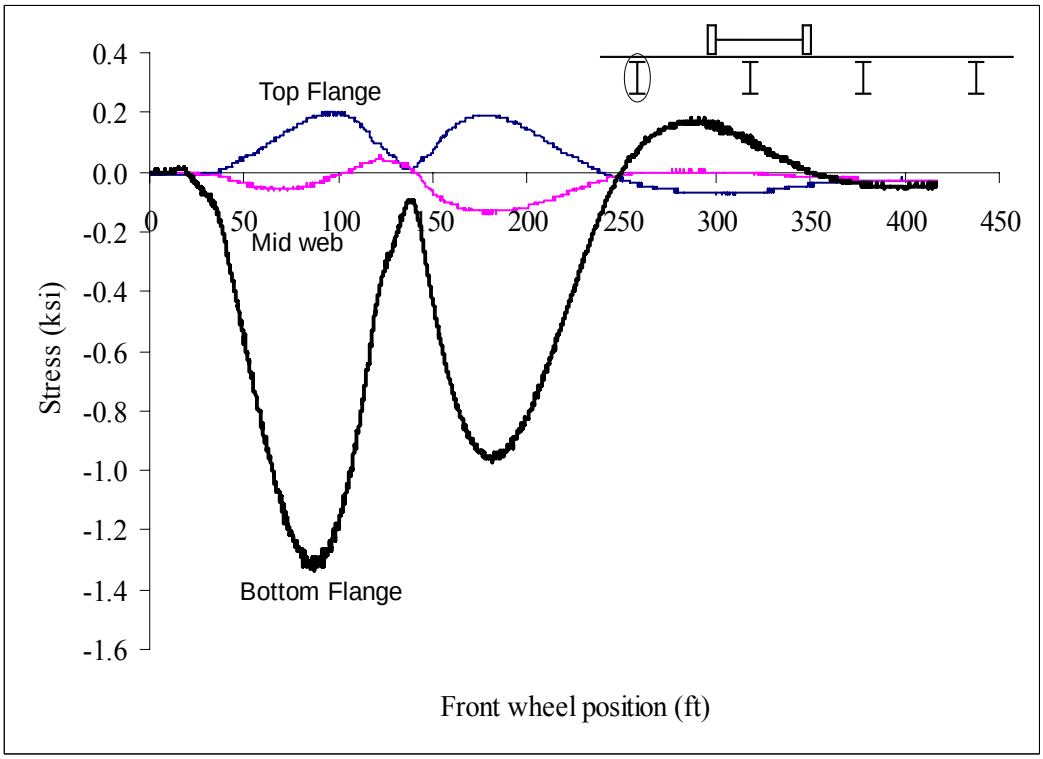

Figure B58: Hatch Bridge Test Run 3 S1 @ 3 ft west of interior support

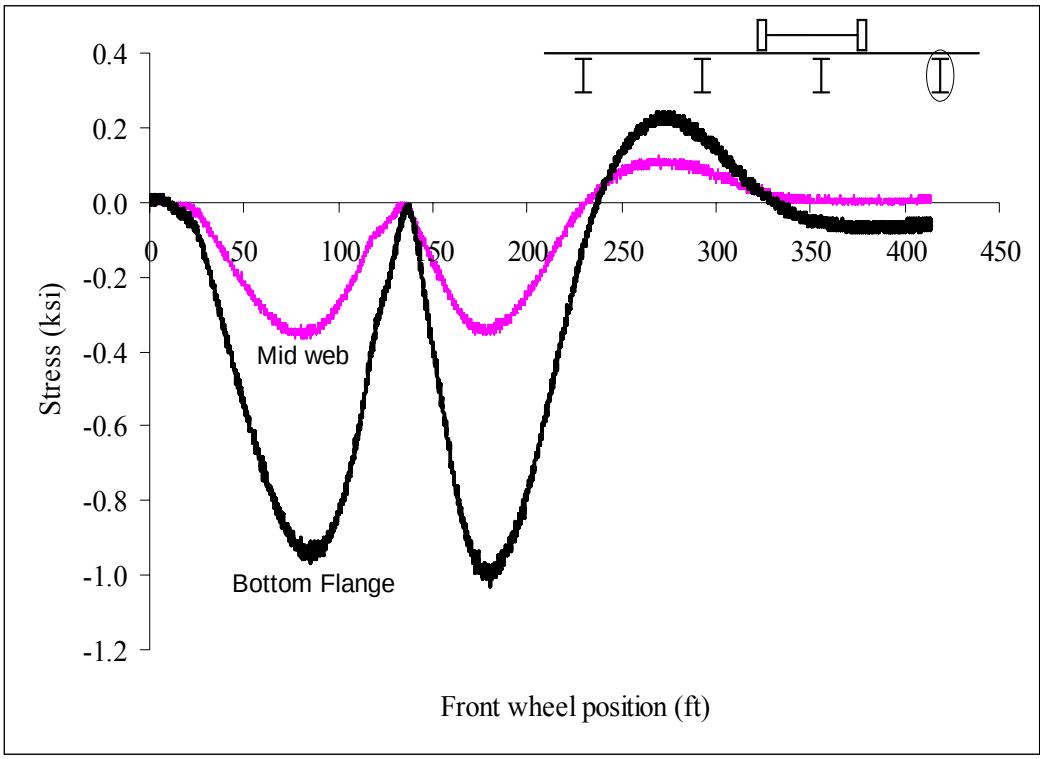

Figure B59: Hatch Bridge Test Run 3 S5 @ 3 ft east of interior support

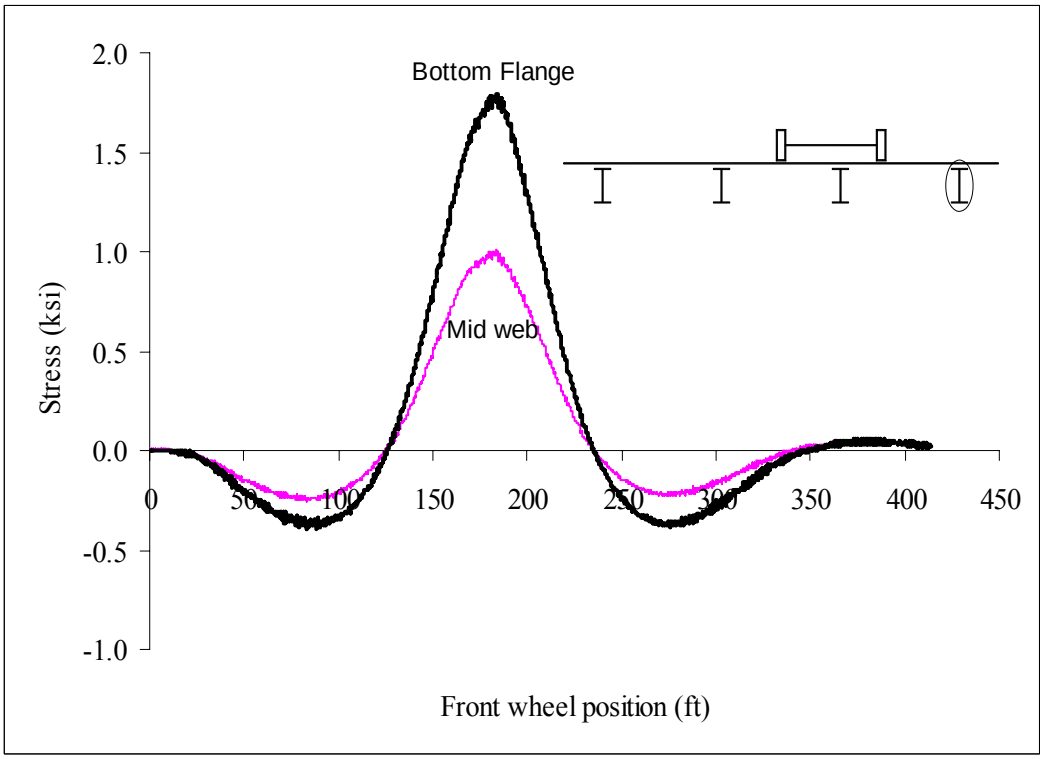

Figure B60: Hatch Bridge Test Run 3 S5 @ Midspan

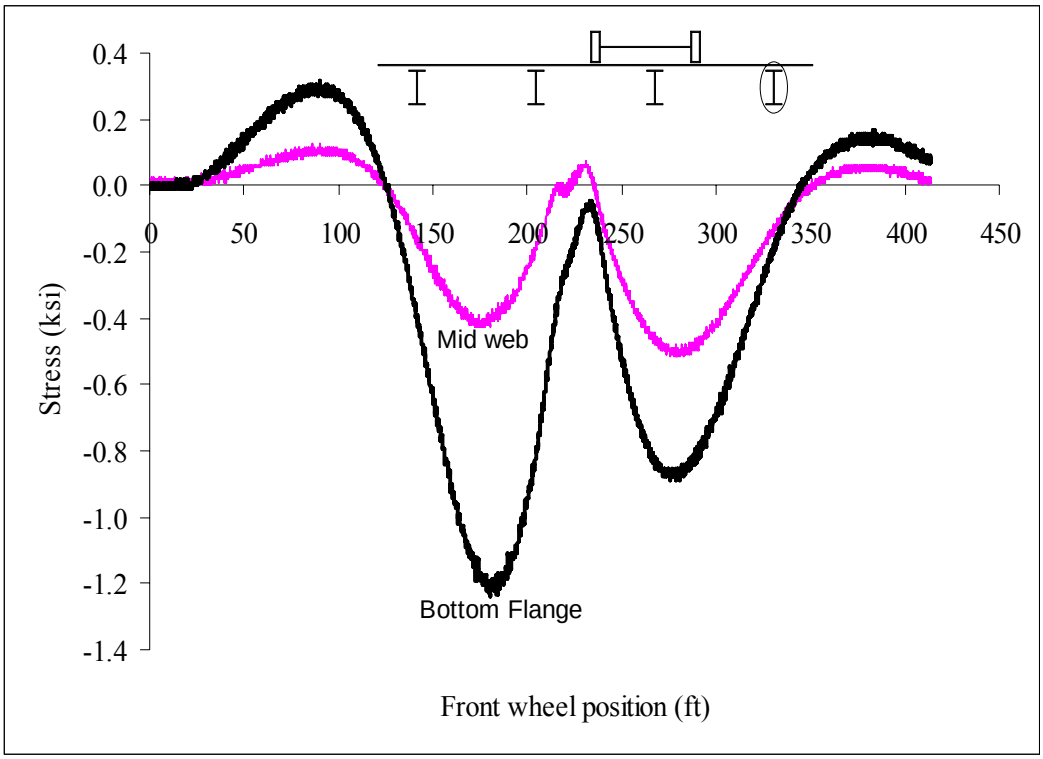

Figure B61: Hatch Bridge Test Run 3 S5 @ 3 ft west of interior support

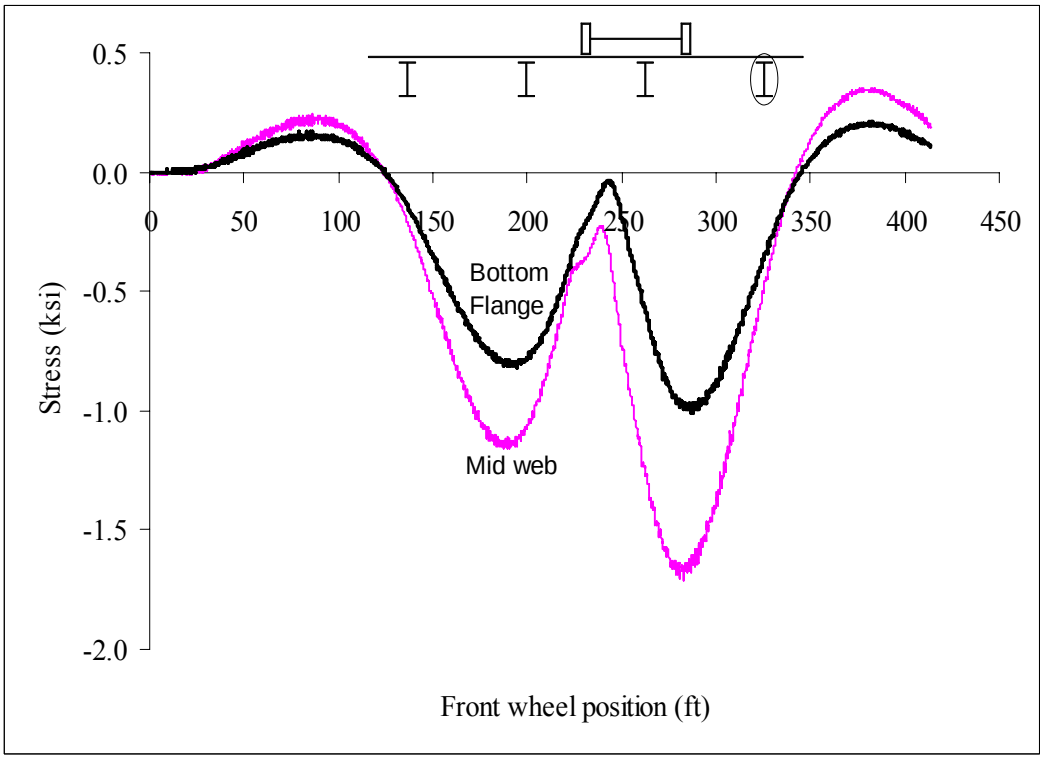

Figure B62: Hatch Bridge Test Run 3 S9 @ 3 ft east of interior support

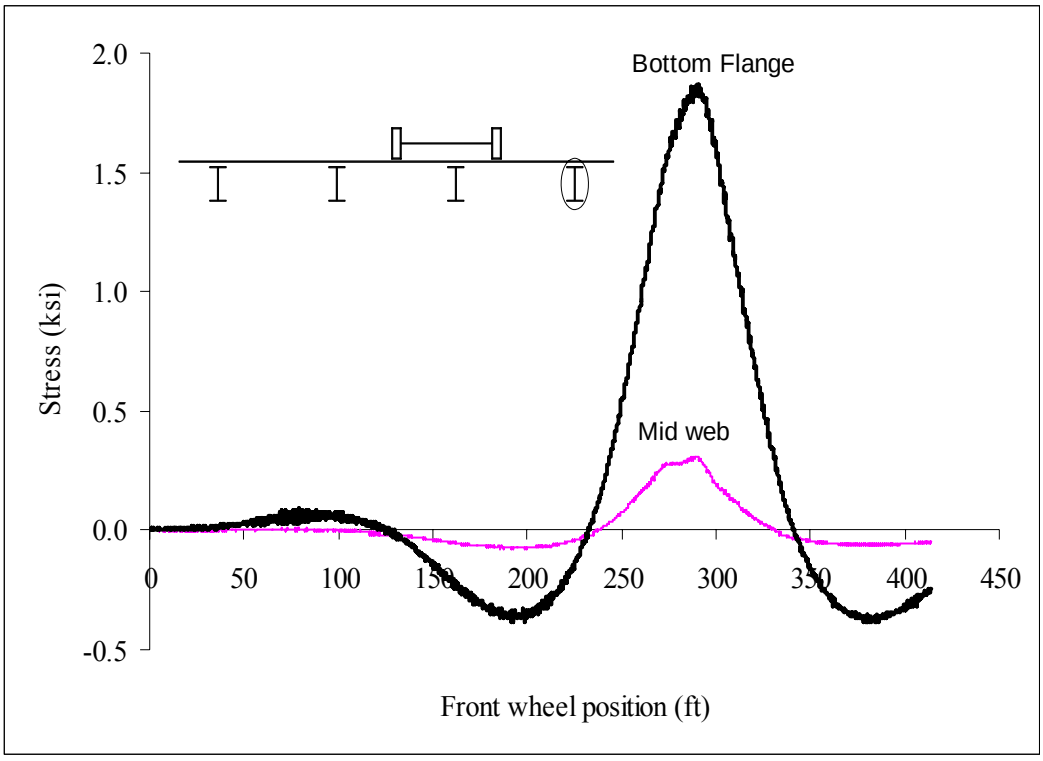

Figure B63: Hatch Bridge Test Run 3 S9 @ Midspan

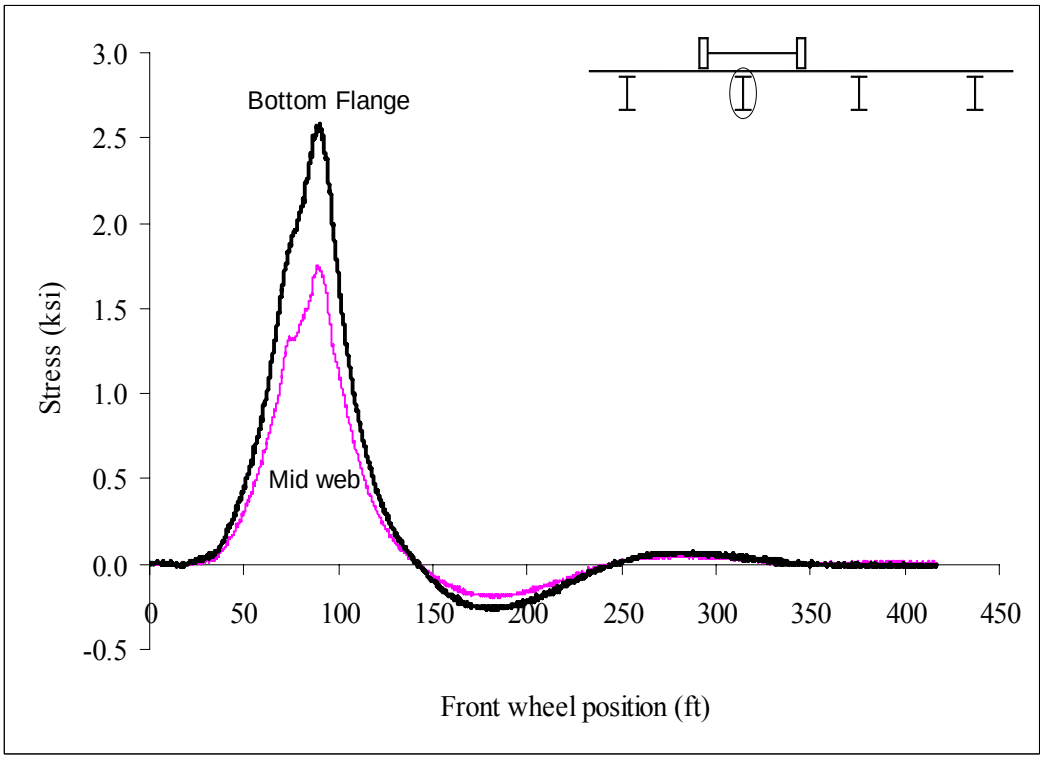

Figure B64: Hatch Bridge Test Run 3 S2 @ Midspan

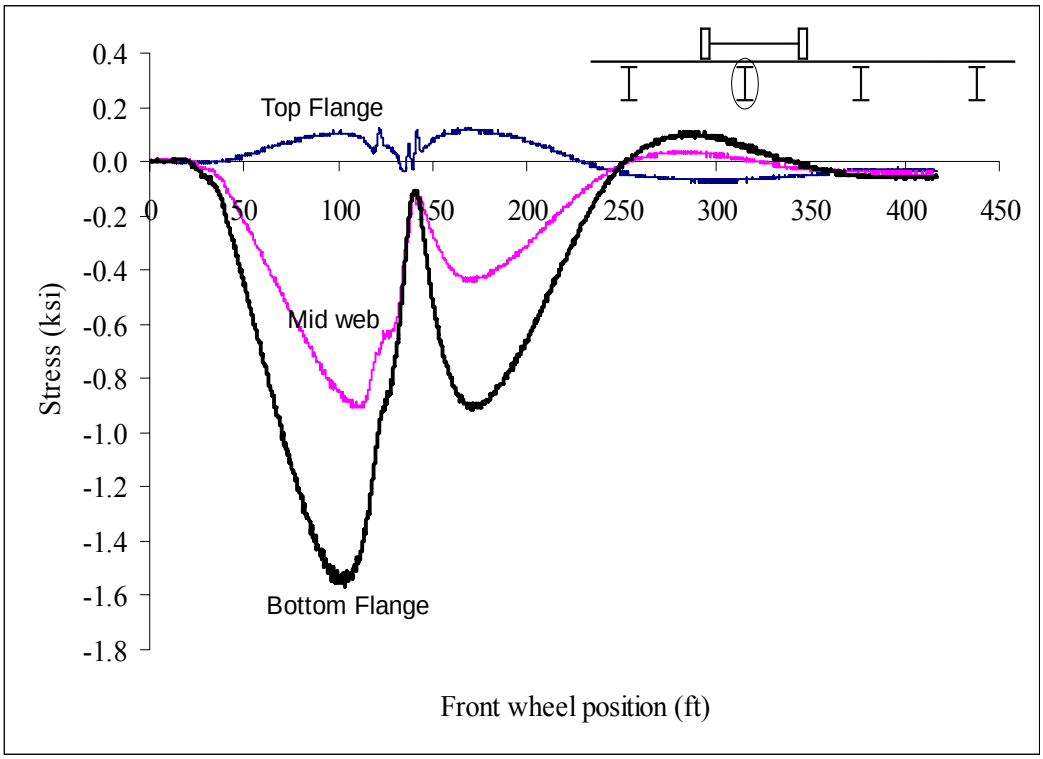

Figure B65: Hatch Bridge Test Run 3 S2 @ 3 ft west of interior support

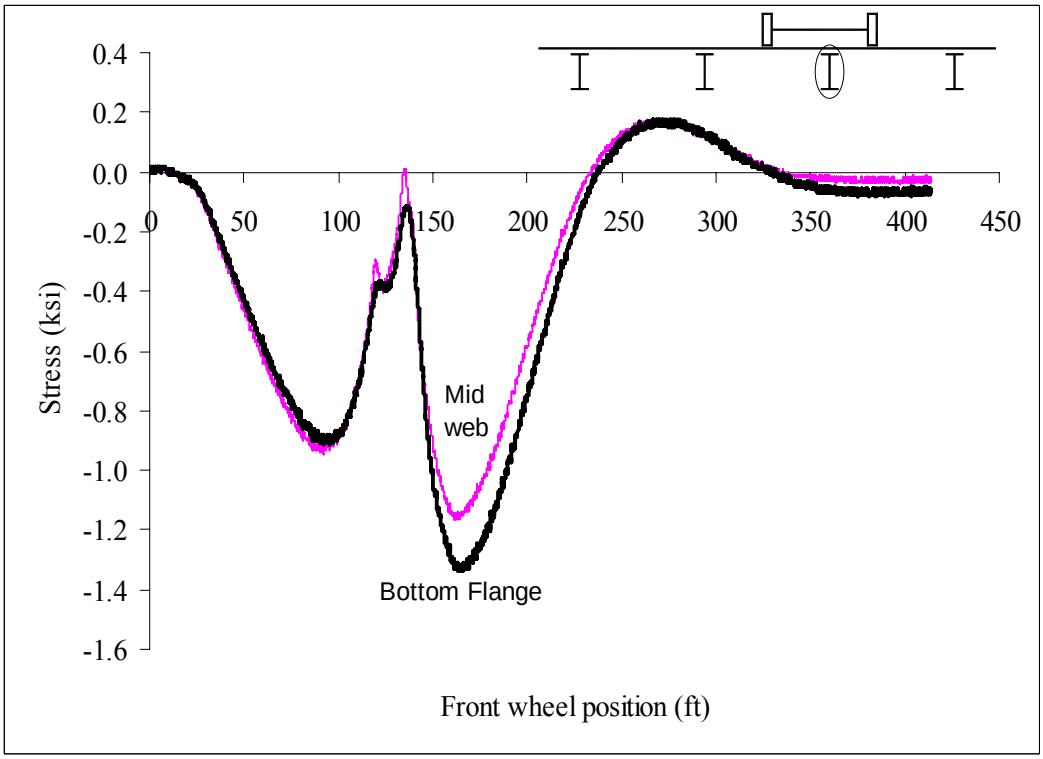

Figure B66: Hatch Bridge Test Run 3 S6 @ 3 ft east of interior support

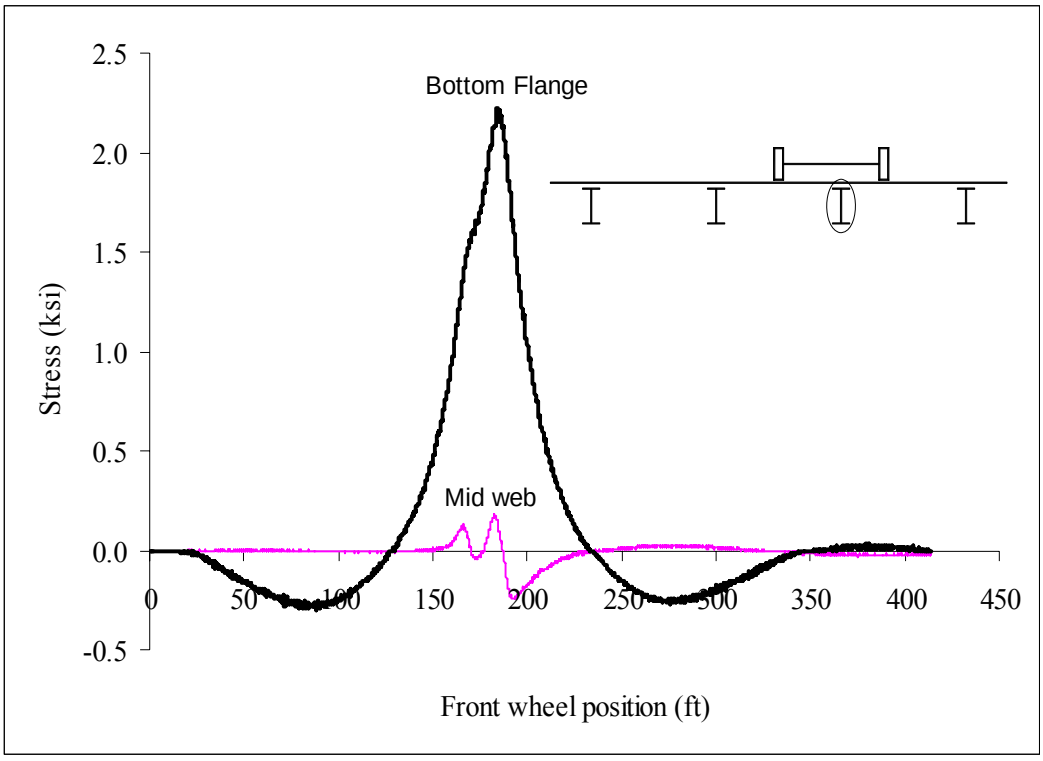

Figure B67: Hatch Bridge Test Run 3 S6 @ Midspan

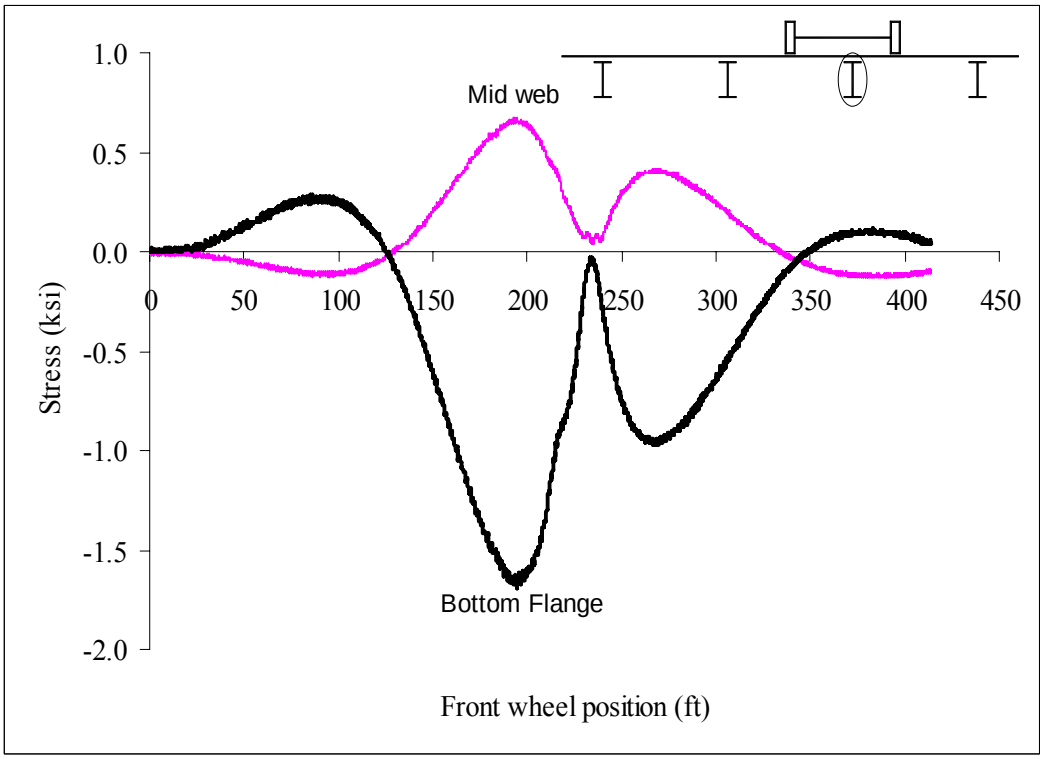

Figure B68: Hatch Bridge Test Run 3 S6 @ 3 ft west of interior support

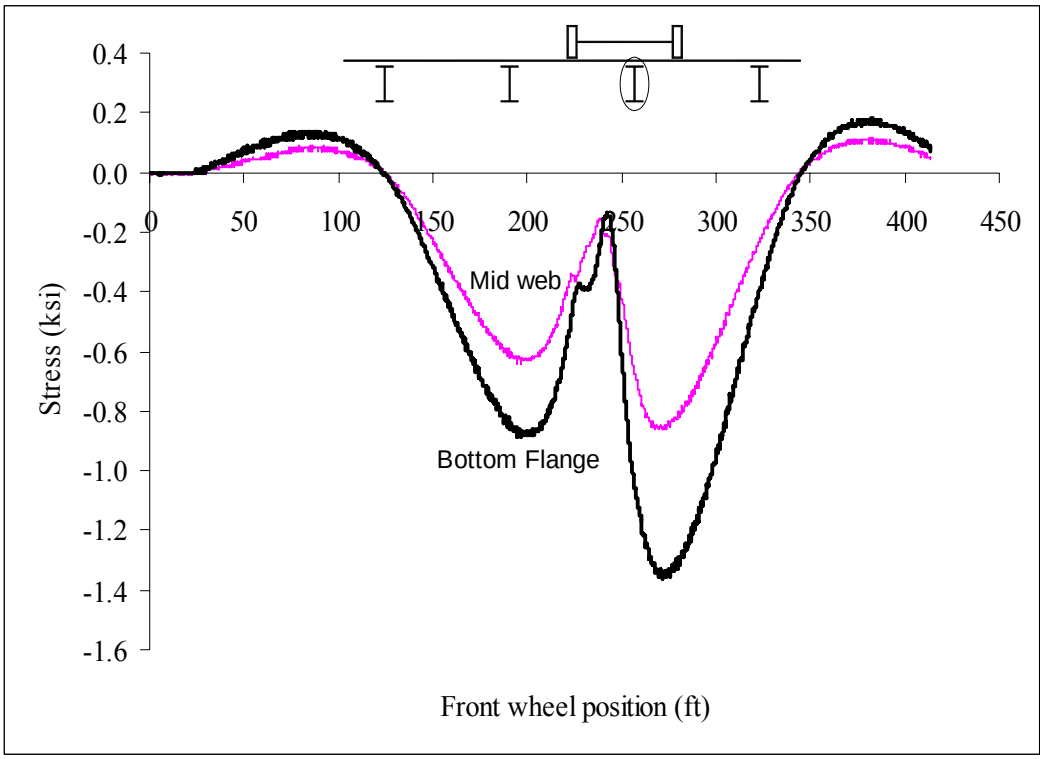

Figure B69: Hatch Bridge Test Run 3 S10 @ 3 ft east of interior support

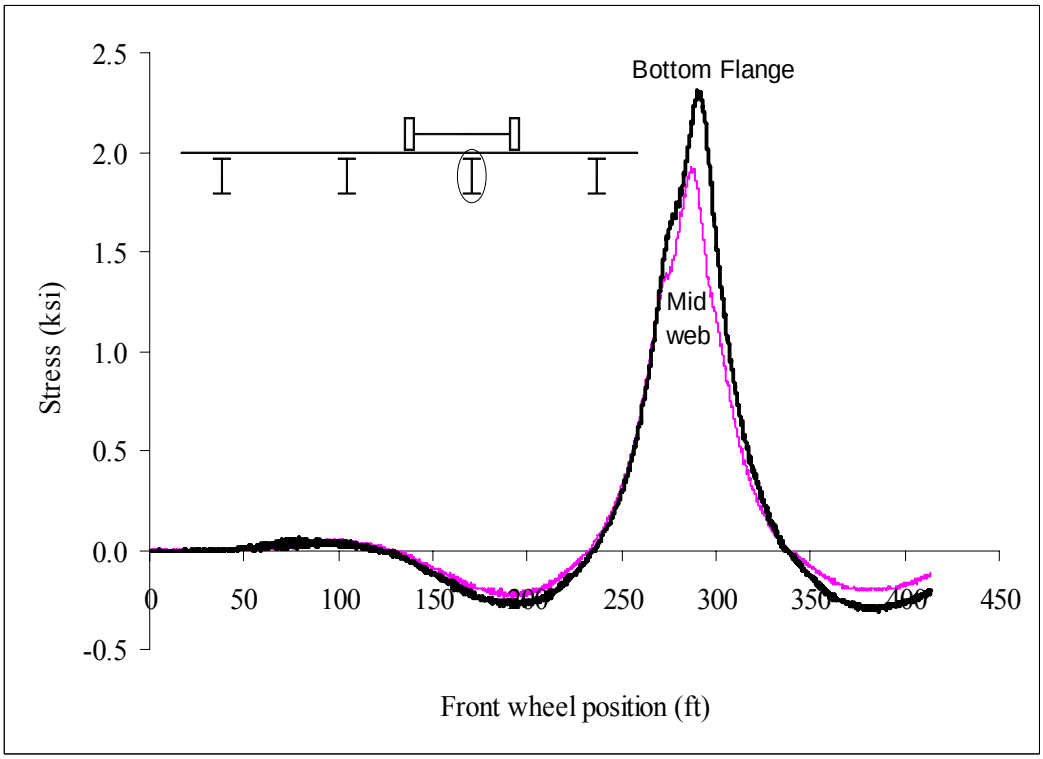

Figure B70: Hatch Bridge Test Run 3 S10 @ Midspan

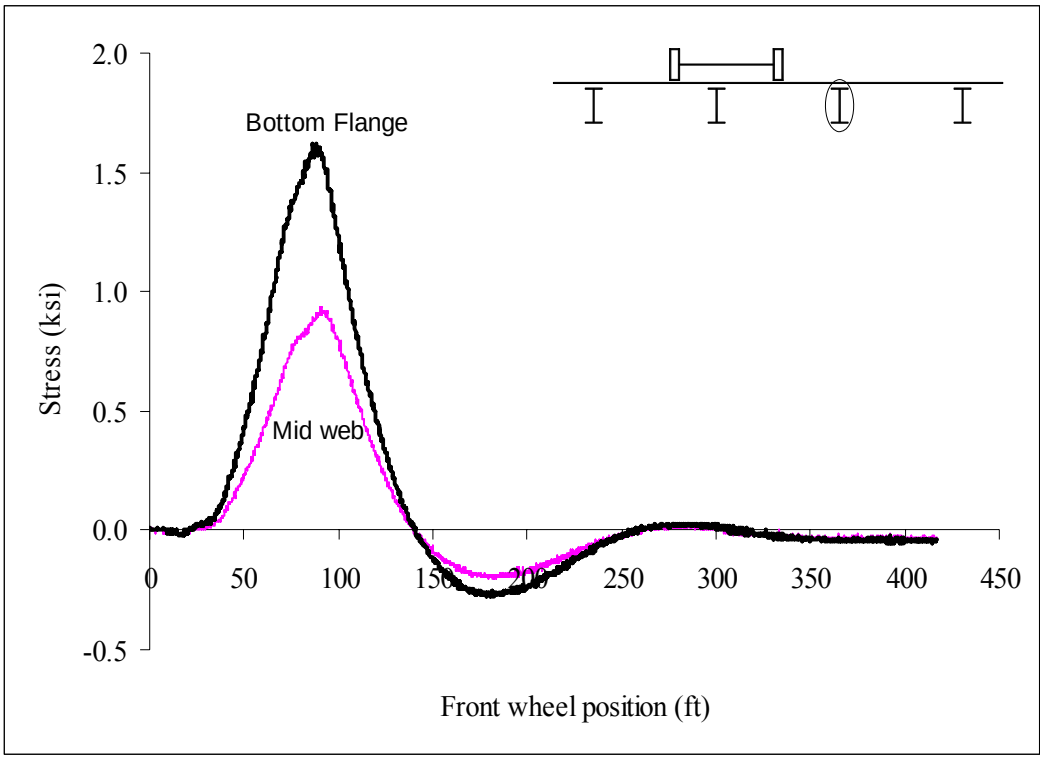

Figure B71: Hatch Bridge Test Run 3 S3 @ Midspan

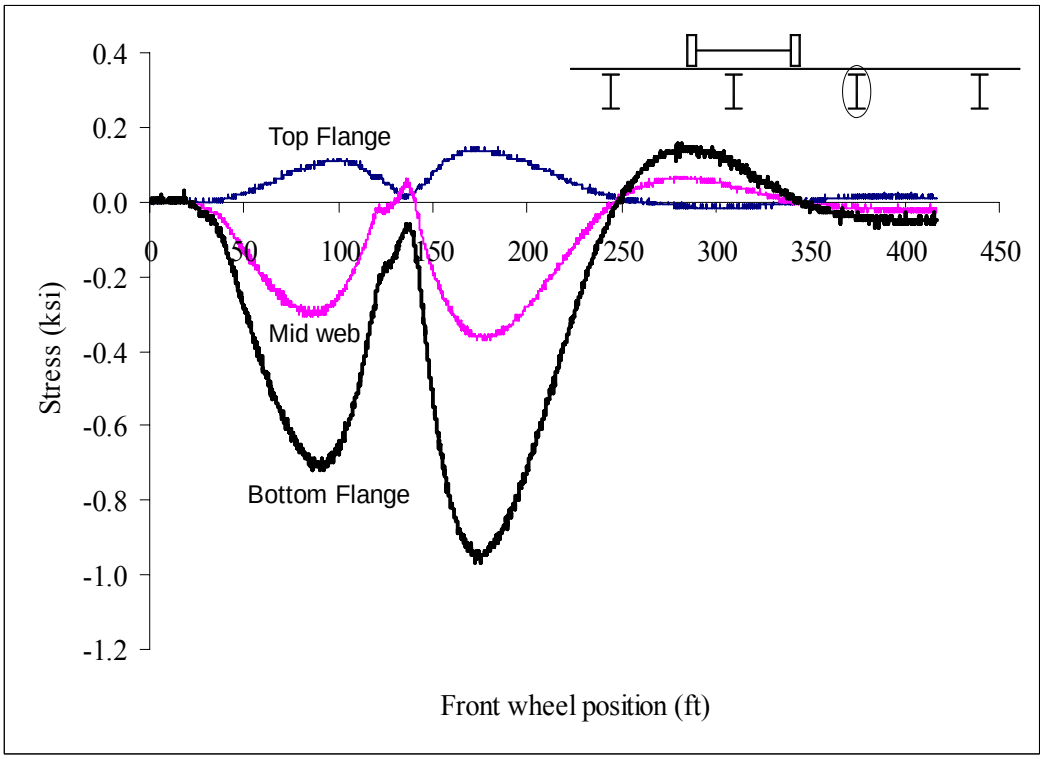

Figure B72: Hatch Bridge Test Run 3 S3 @ 3 ft west of interior support

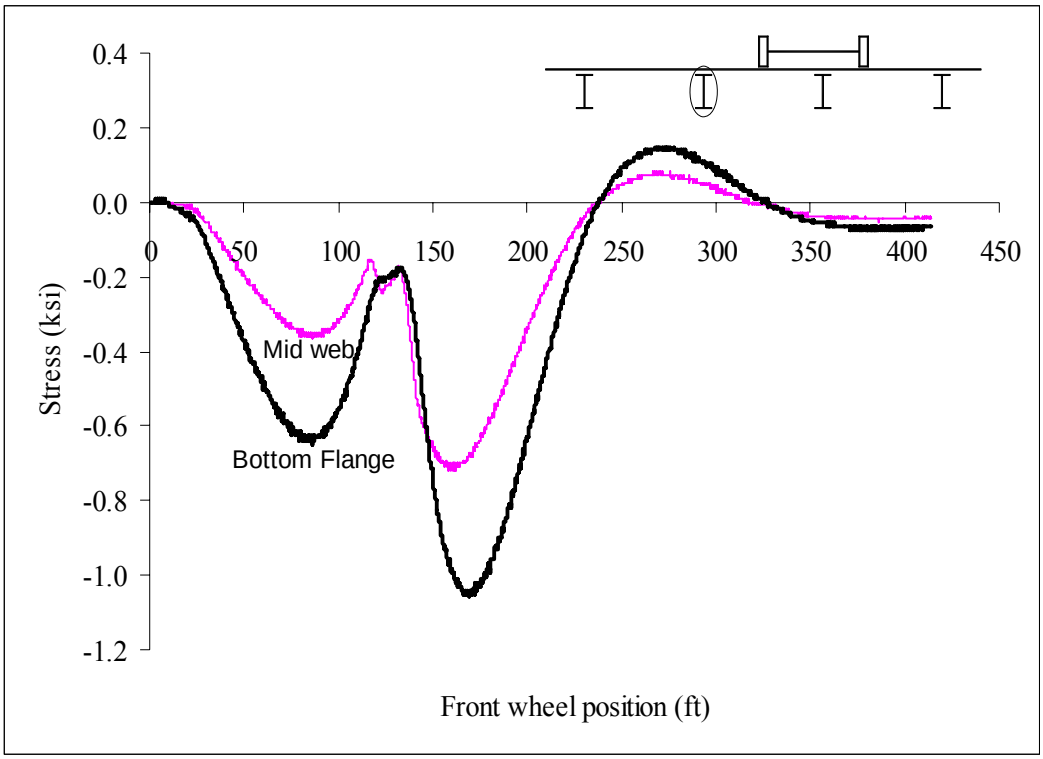

Figure B73: Hatch Bridge Test Run 3 S7 @ 3 ft east of interior support

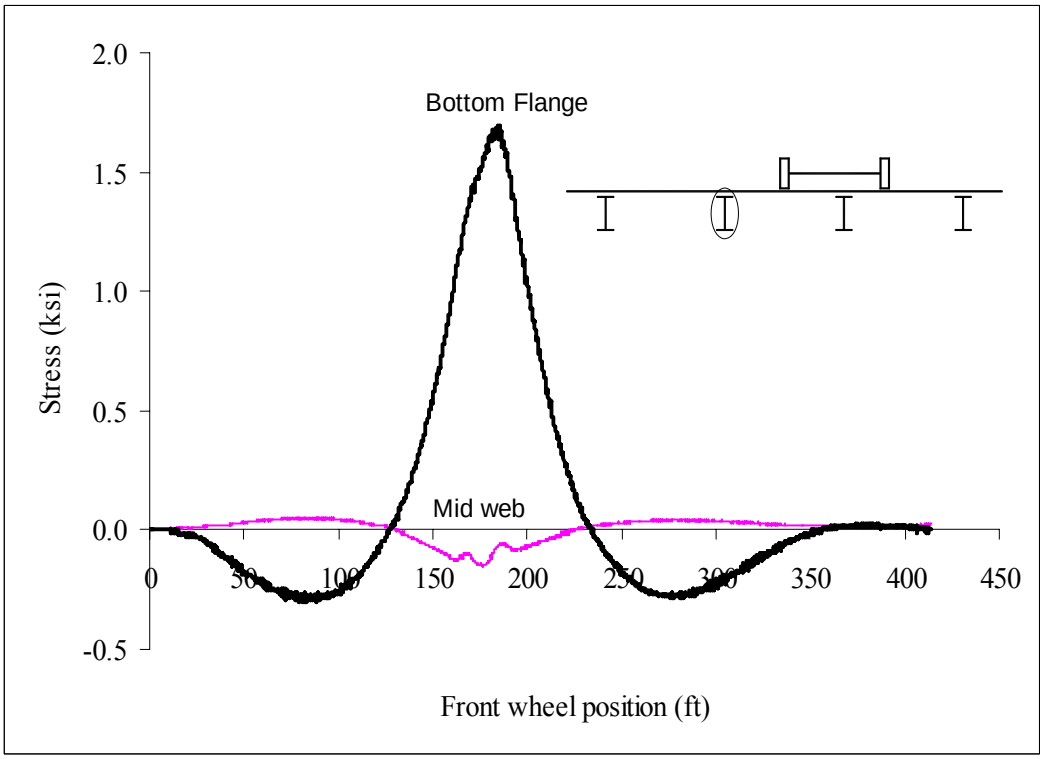

Figure B74: Hatch Bridge Test Run 3 S7 @ Midspan

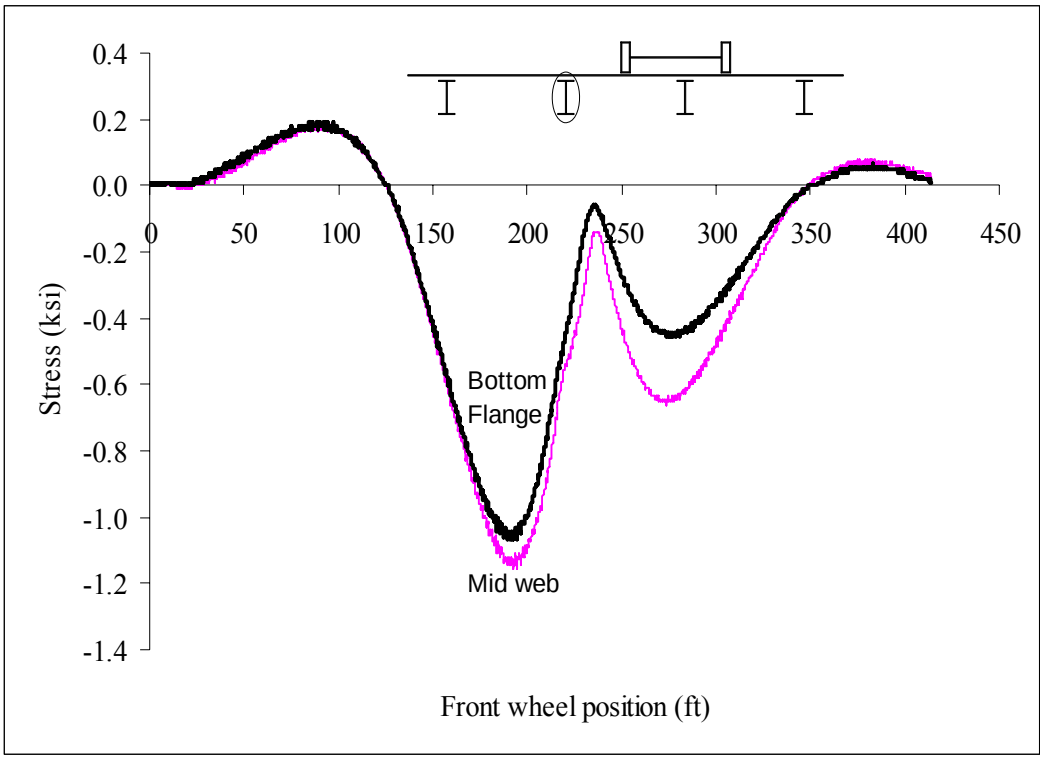

Figure B75: Hatch Bridge Test Run 3 S7 @ 3 ft west of interior support

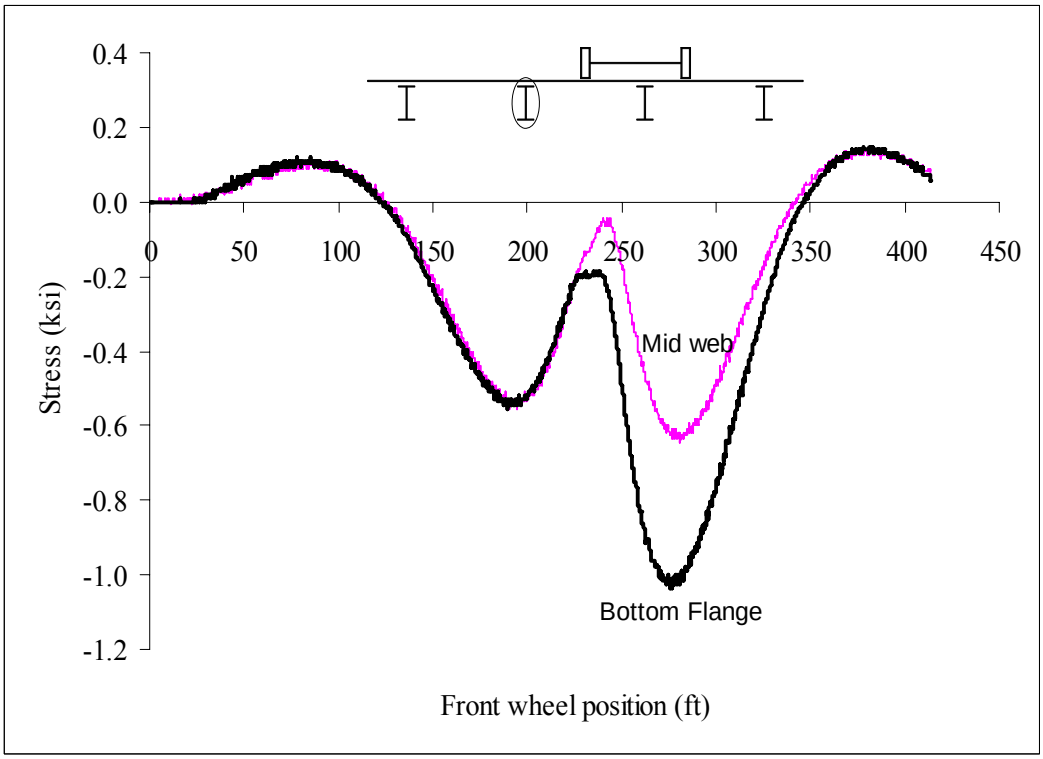

Figure B76: Hatch Bridge Test Run 3 S11 @ 3 ft east of interior support

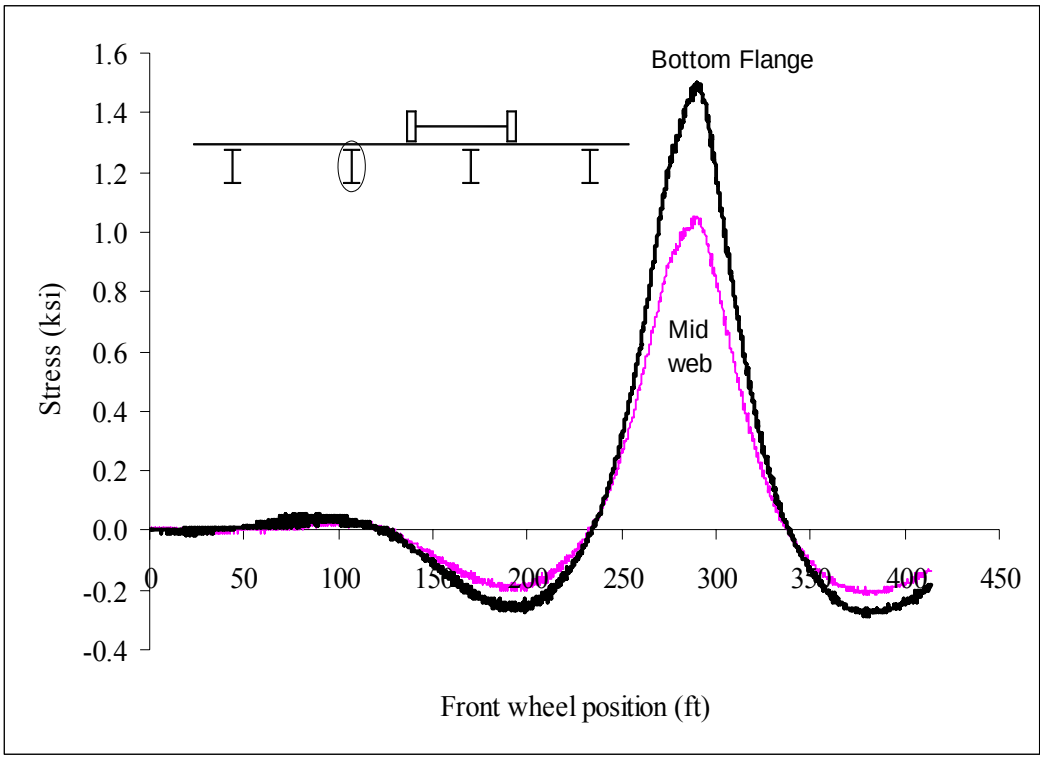

Figure B77: Hatch Bridge Test Run 3 S11 @ Midspan

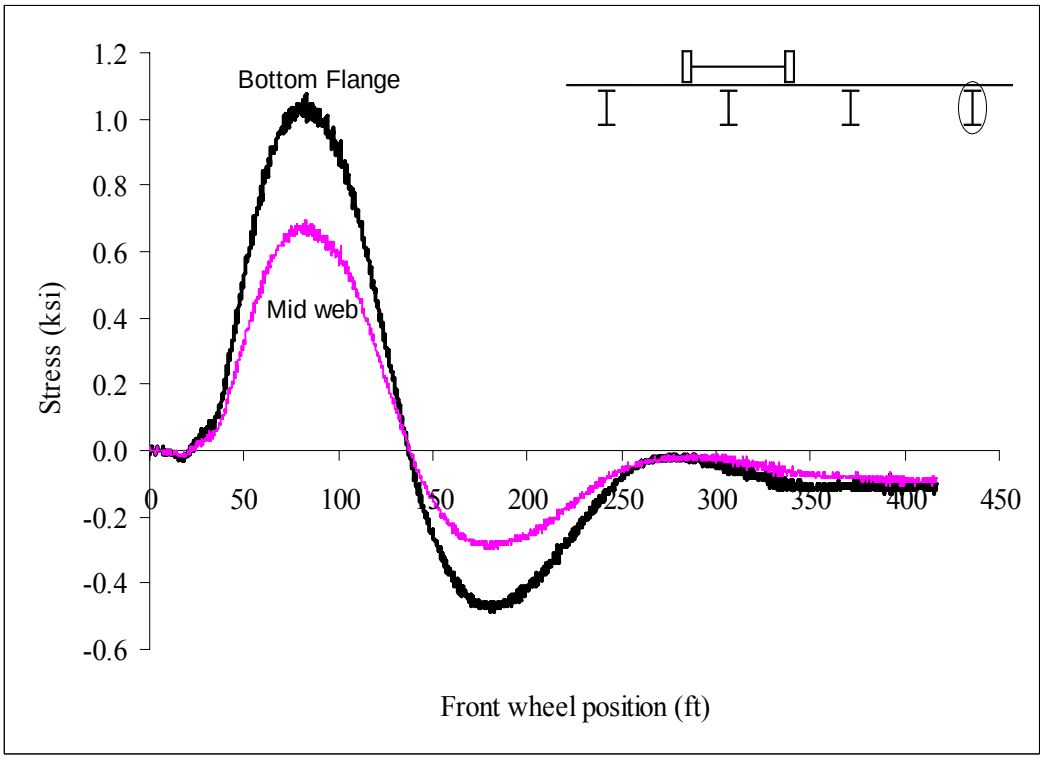

Figure B78: Hatch Bridge Test Run 3 S4 @ Midspan

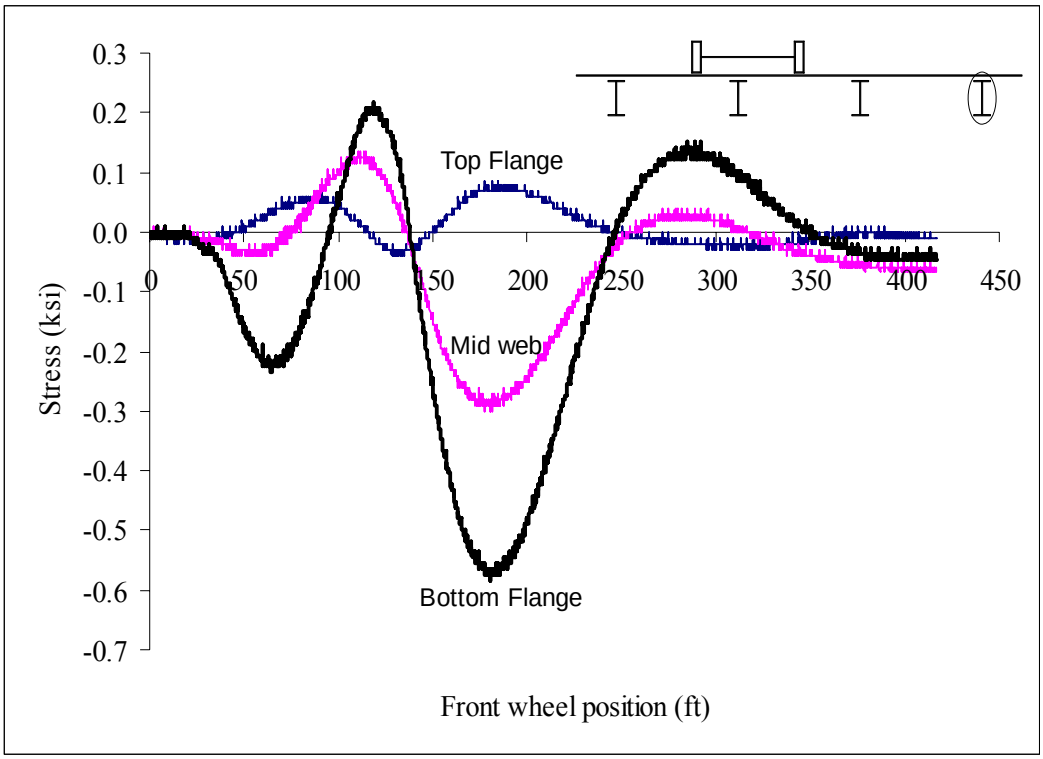

Figure B79: Hatch Bridge Test Run 3 S4 @ 3 ft west of interior support

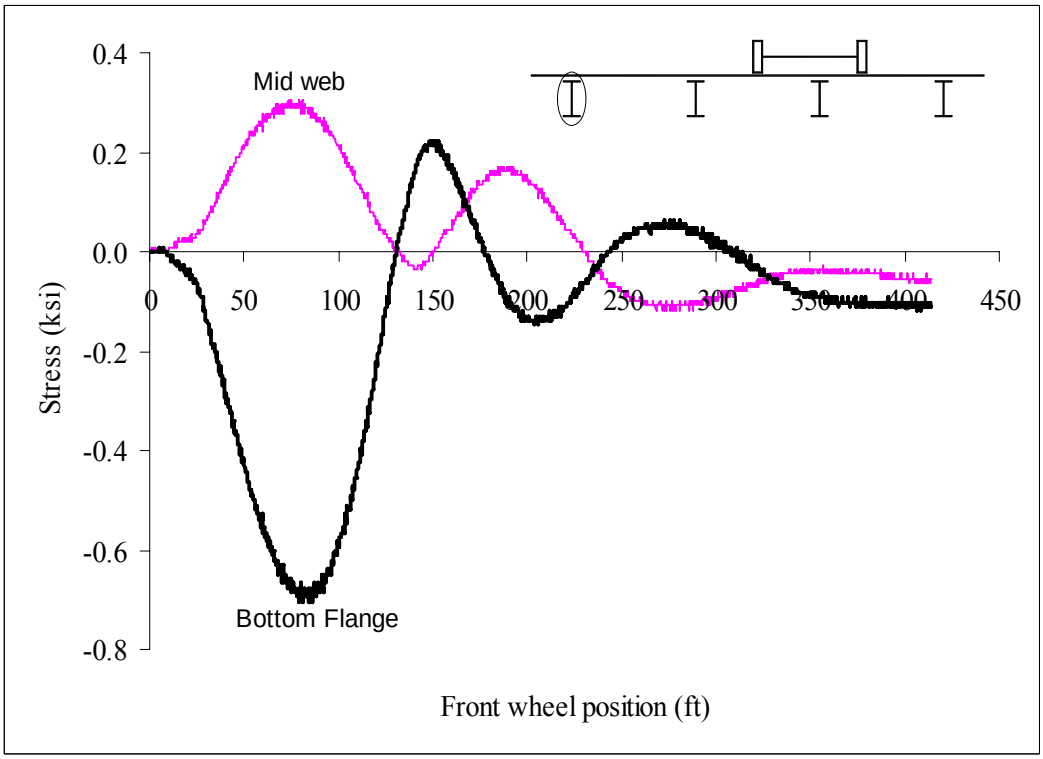

Figure B80: Hatch Bridge Test Run 3 S8 @ 3 ft east of interior support

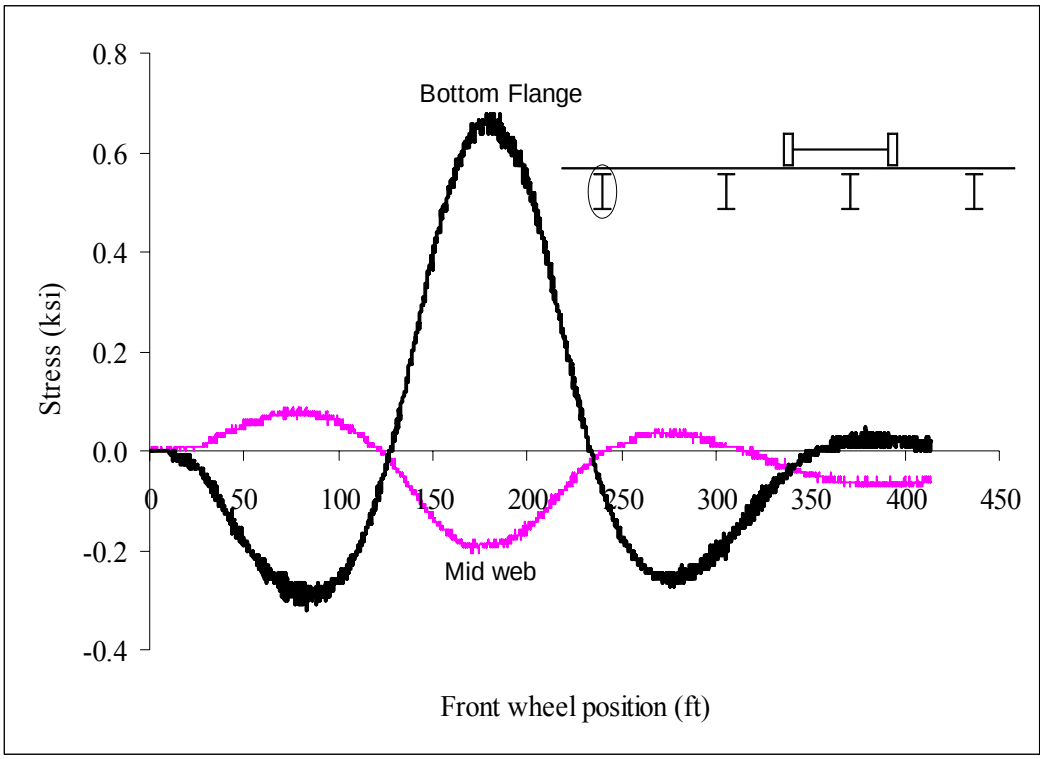

Figure B81: Hatch Bridge Test Run 3 S8 @ Midspan

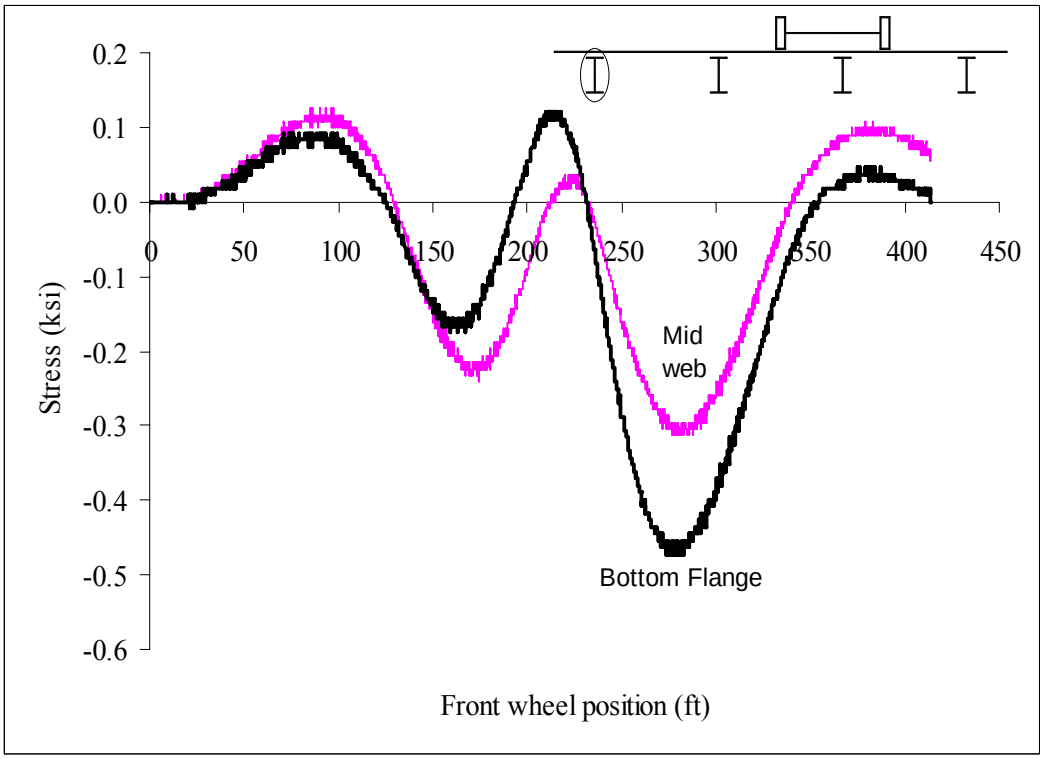

Figure B82: Hatch Bridge Test Run 3 S8 @ 3 ft west of interior support

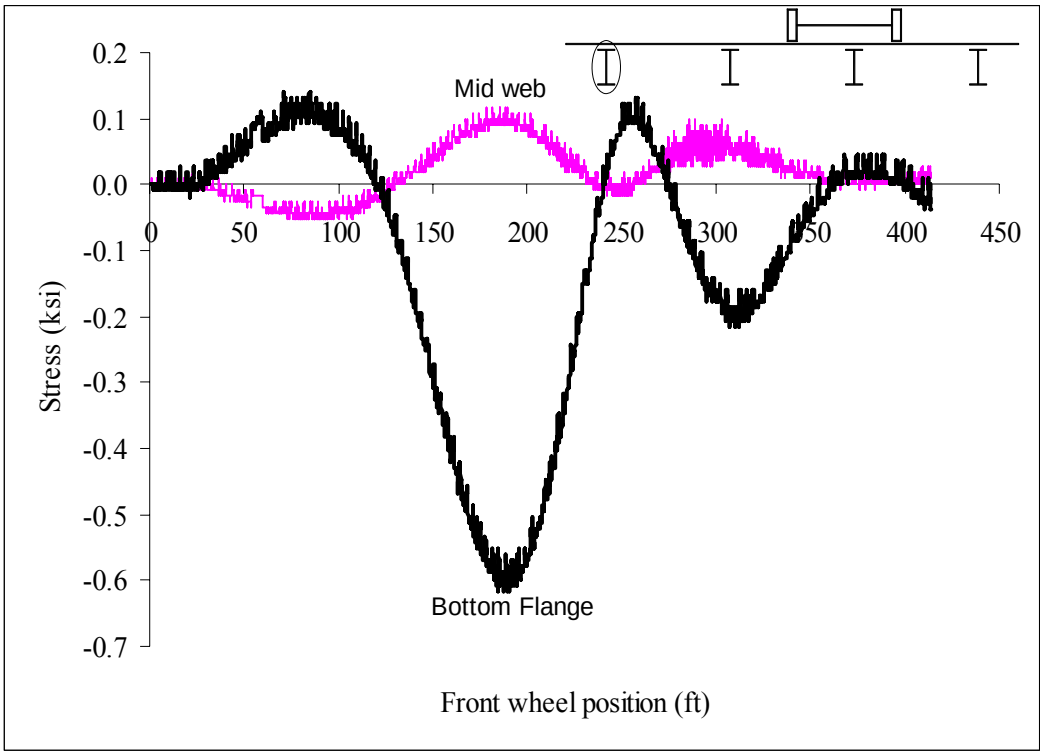

Figure B83: Hatch Bridge Test Run 3 S12 @ 3 ft east of interior support

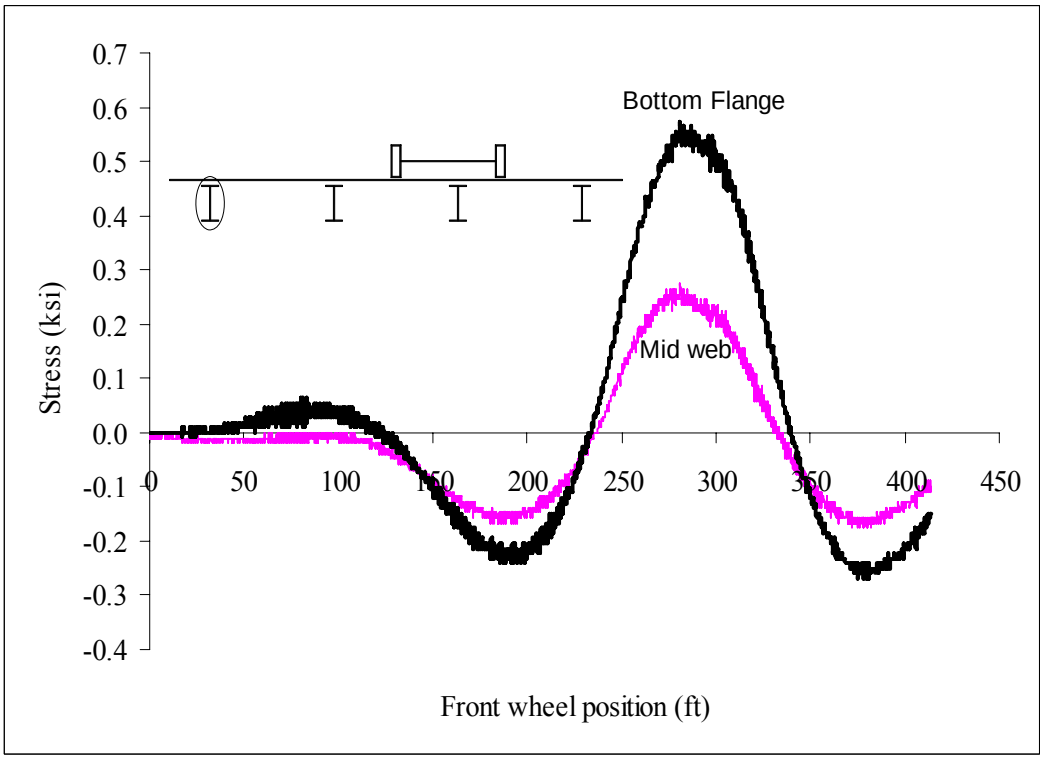

Figure B84: Hatch Bridge Test Run 3 S12 @ Midspan

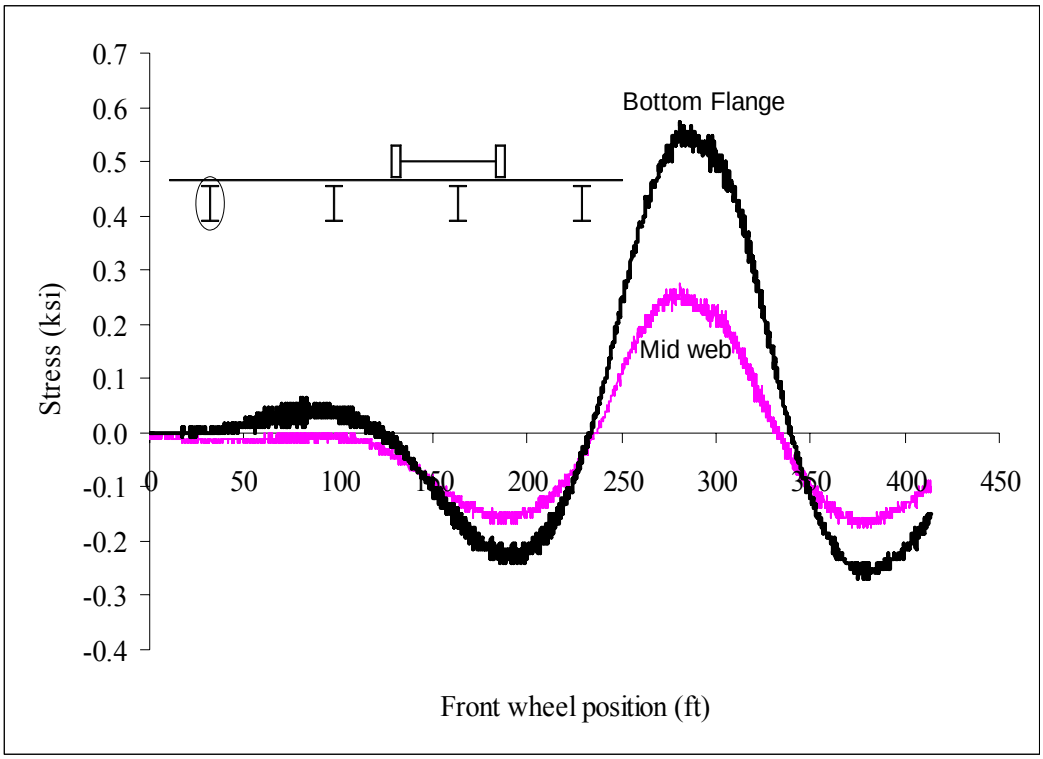

Figure B85: Hatch Bridge Test Run 4 S1 @ Midspan

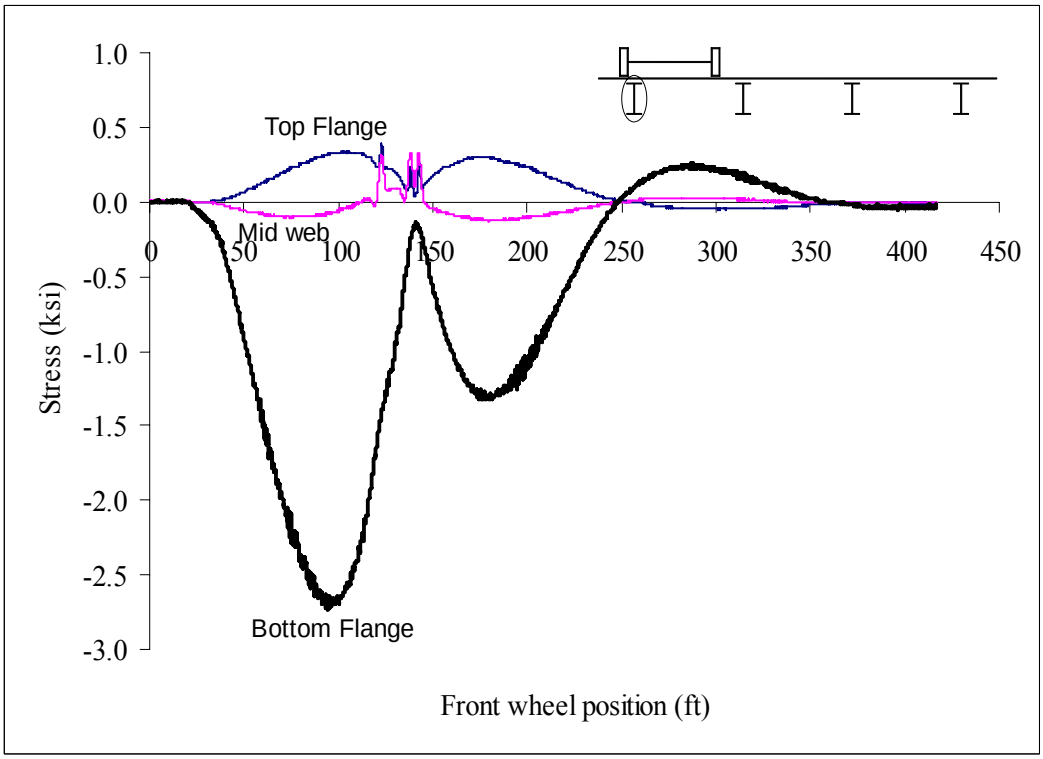

Figure B86: Hatch Bridge Test Run 4 S1 @ 3 ft west of interior support

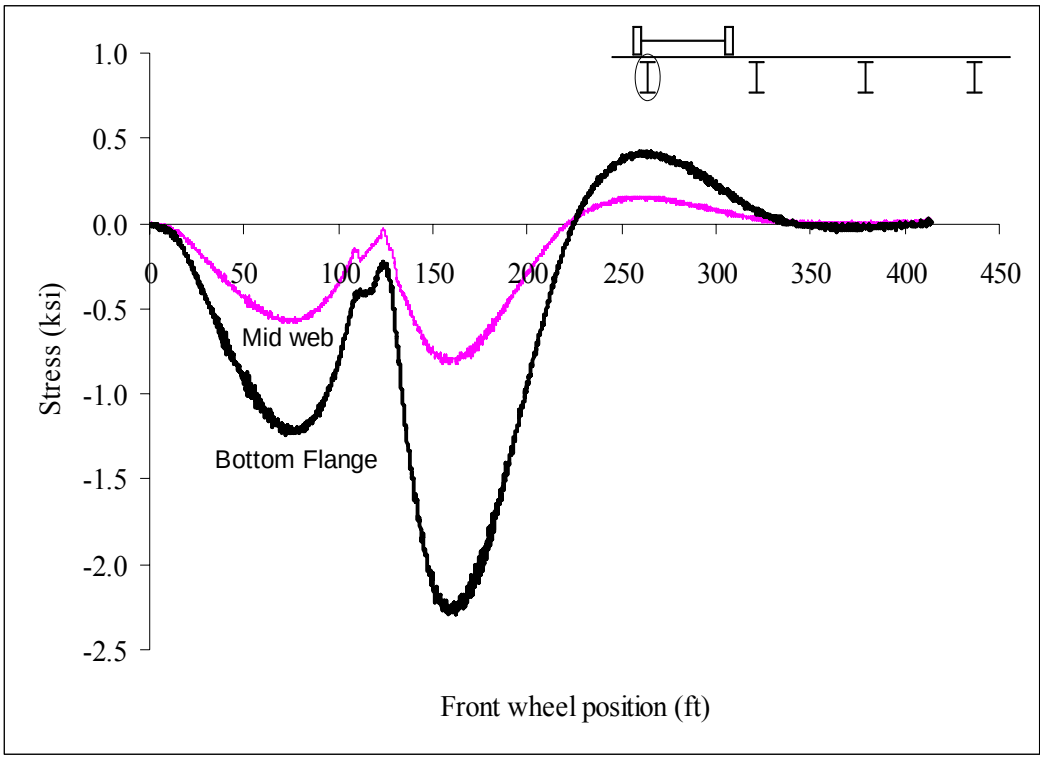

Figure B87: Hatch Bridge Test Run 4 S5 @ 3 ft east of interior support

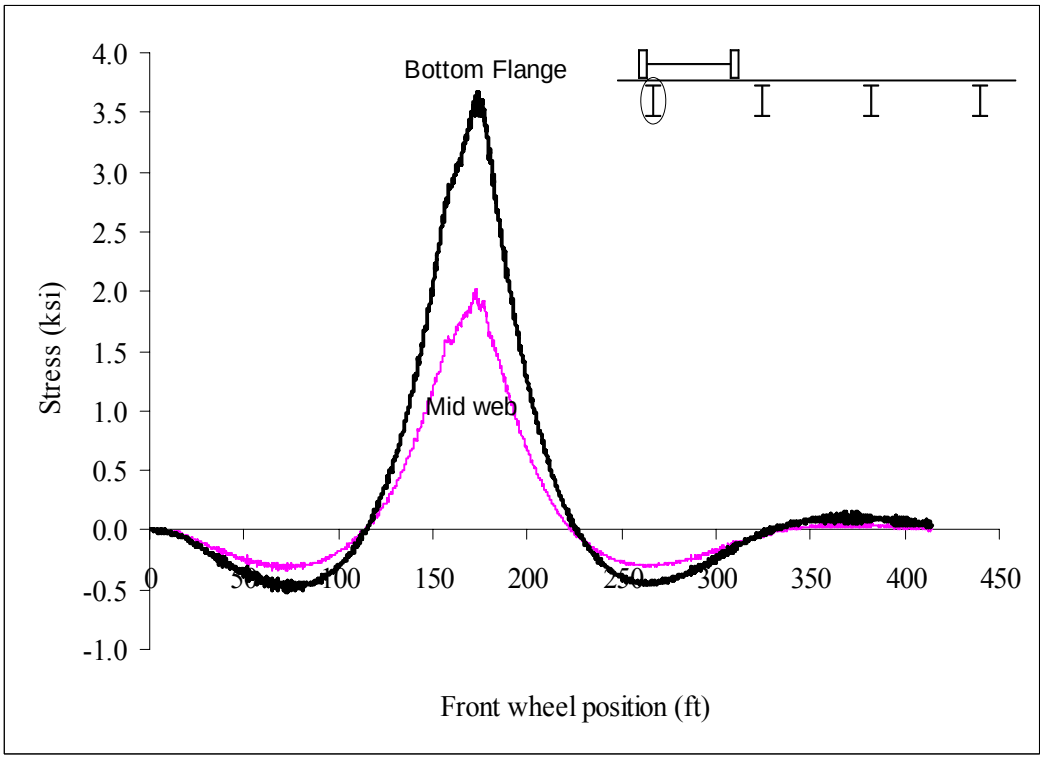

Figure B88: Hatch Bridge Test Run 4 S5 @ Midspan

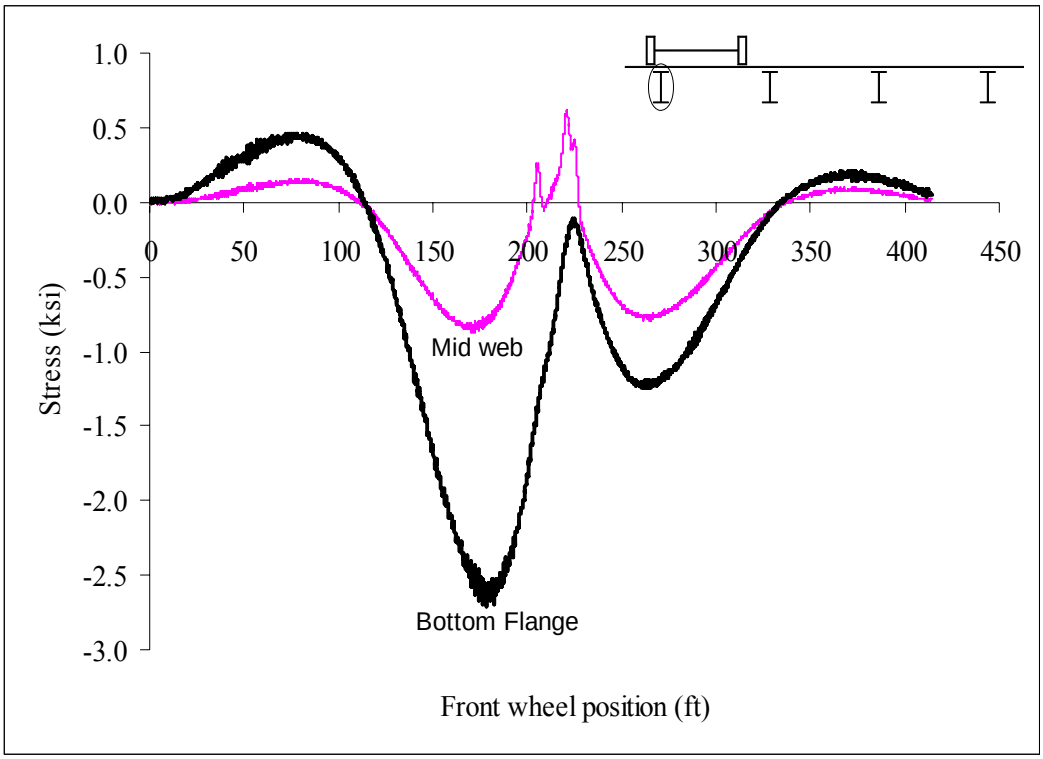

Figure B89: Hatch Bridge Test Run 4 S5 @ 3 ft west of interior support

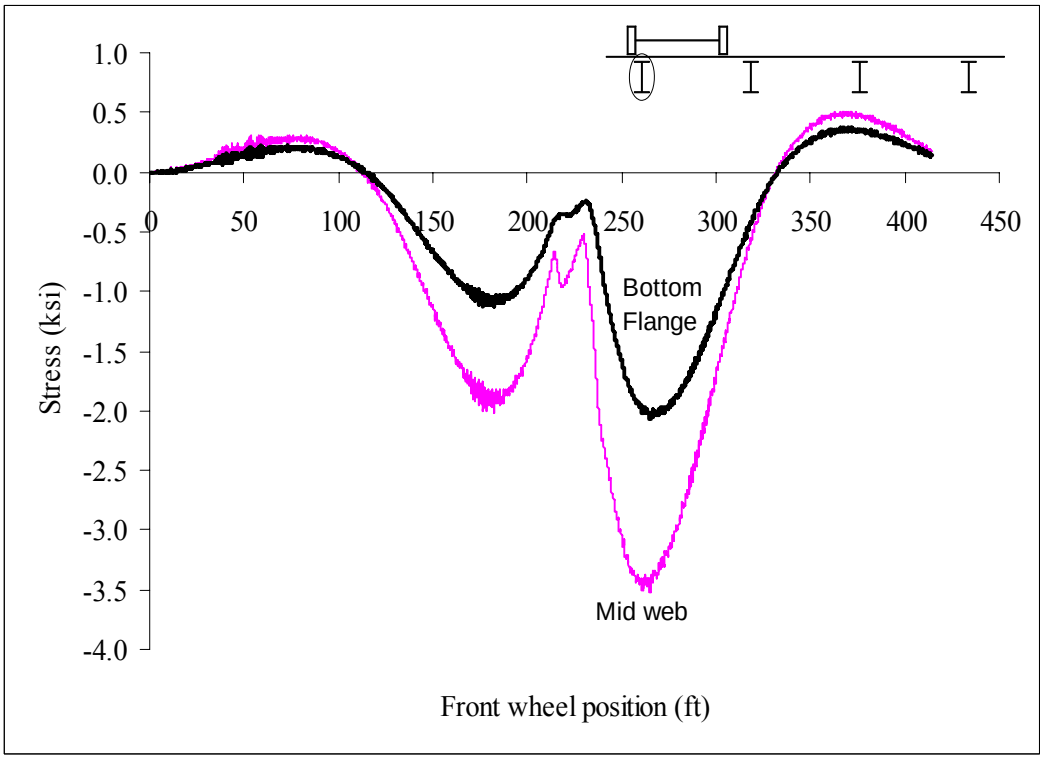

Figure B90: Hatch Bridge Test Run 4 S9 @ 3 ft east of interior support

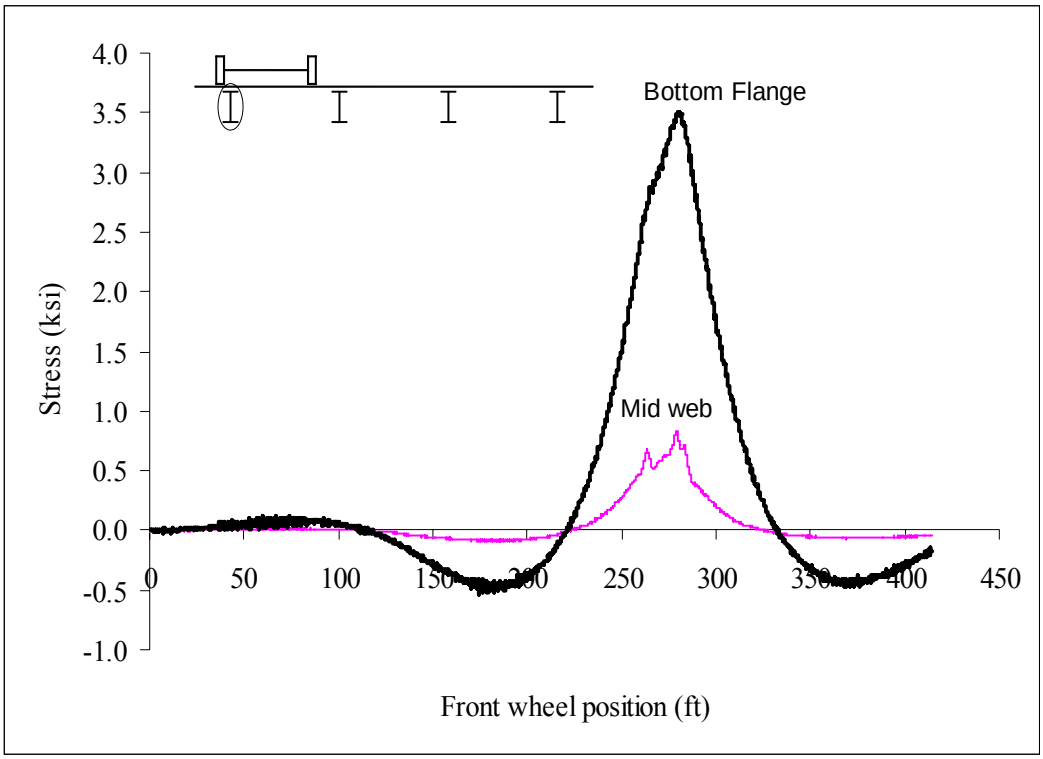

Figure B91: Hatch Bridge Test Run 4 S9 @ Midspan

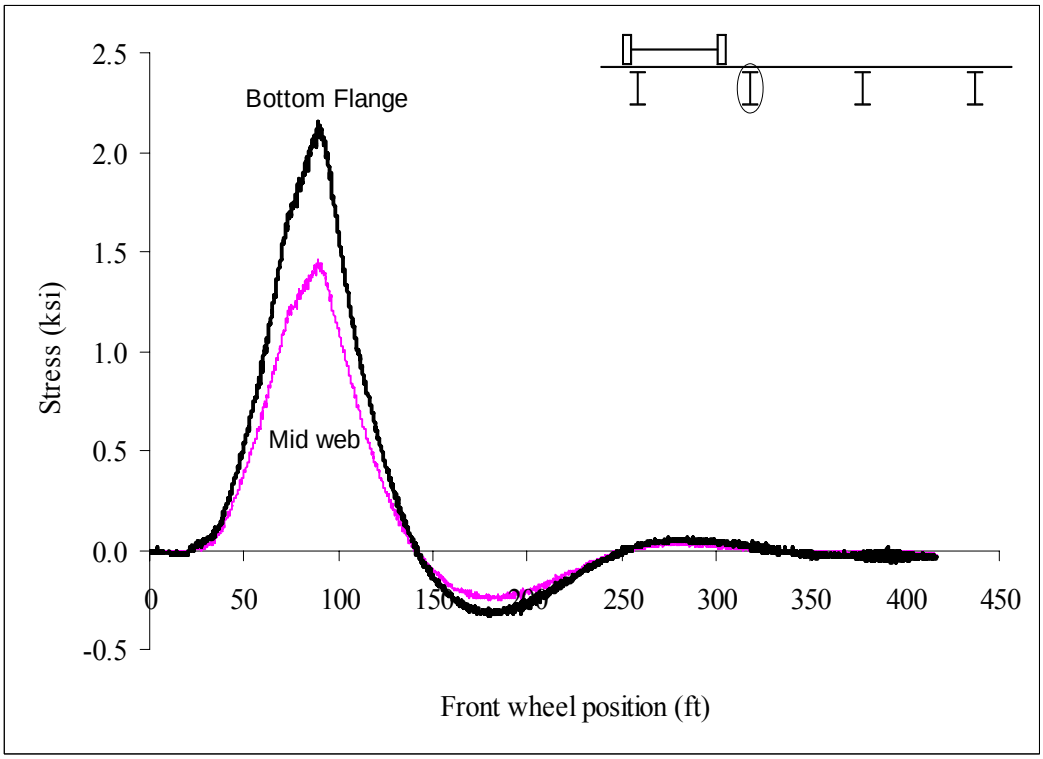

Figure B92: Hatch Bridge Test Run 4 S2 @ Midspan

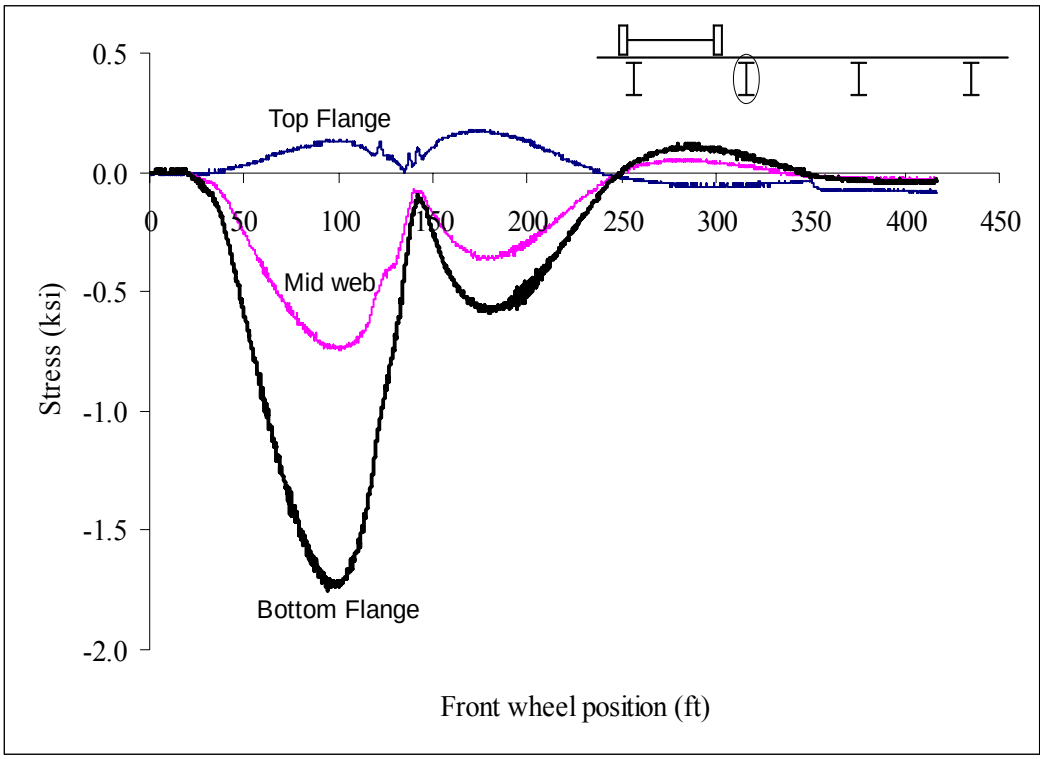

Figure B93: Hatch Bridge Test Run 4 S2 @ 3 ft west of interior support

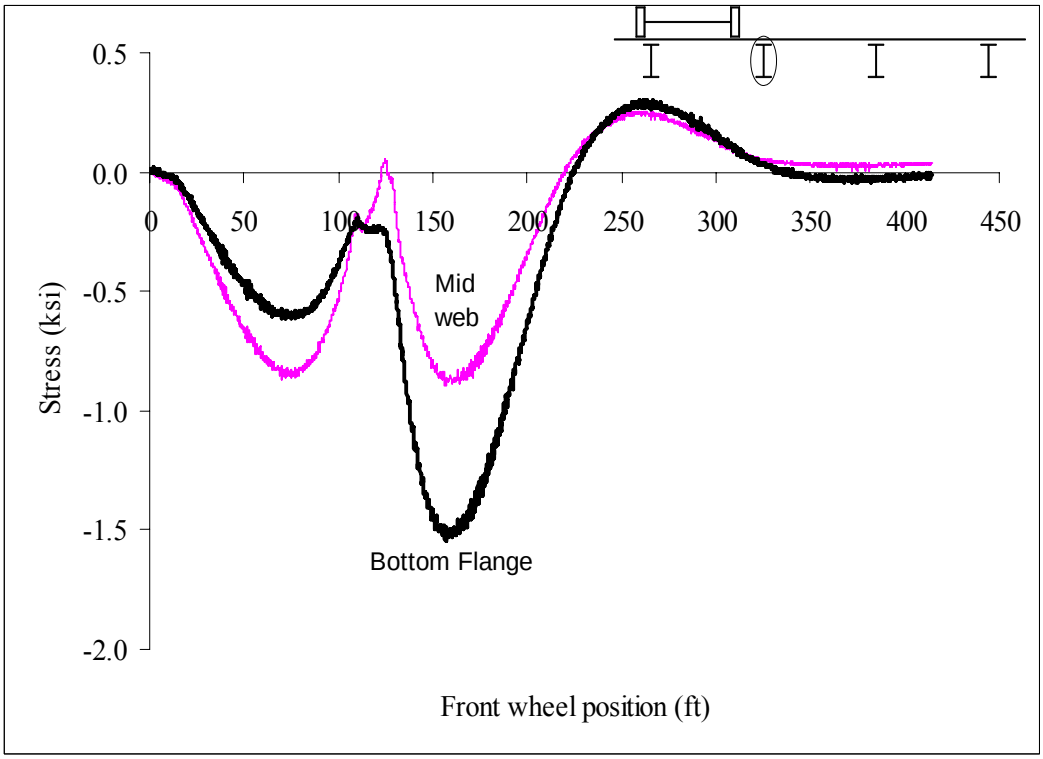

Figure B94: Hatch Bridge Test Run 4 S6 @ 3 ft east of interior support

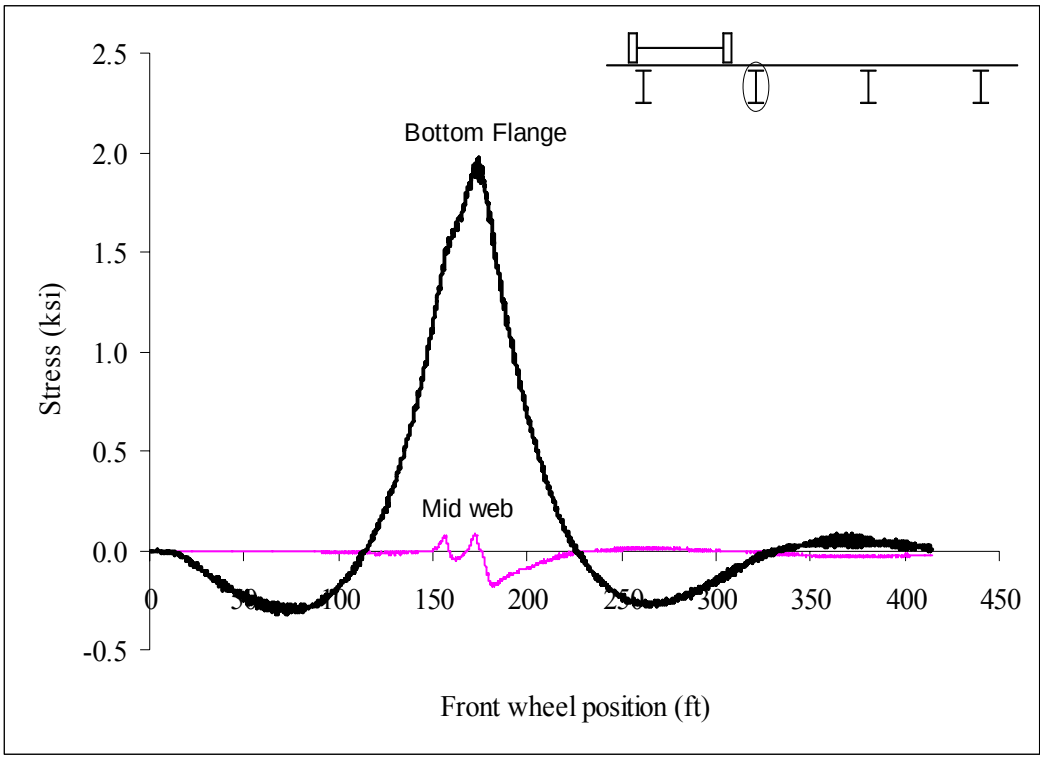

Figure B95: Hatch Bridge Test Run 4 S6 @ Midspan

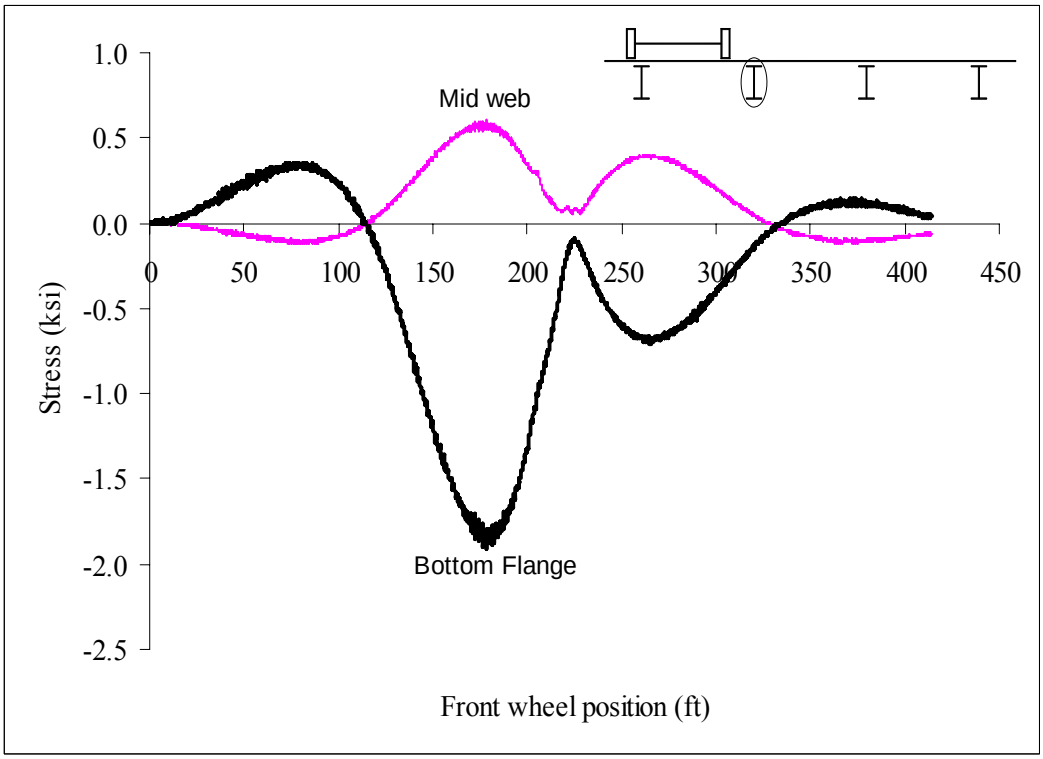

Figure B96: Hatch Bridge Test Run 4 S6 @ 3 ft west of interior support

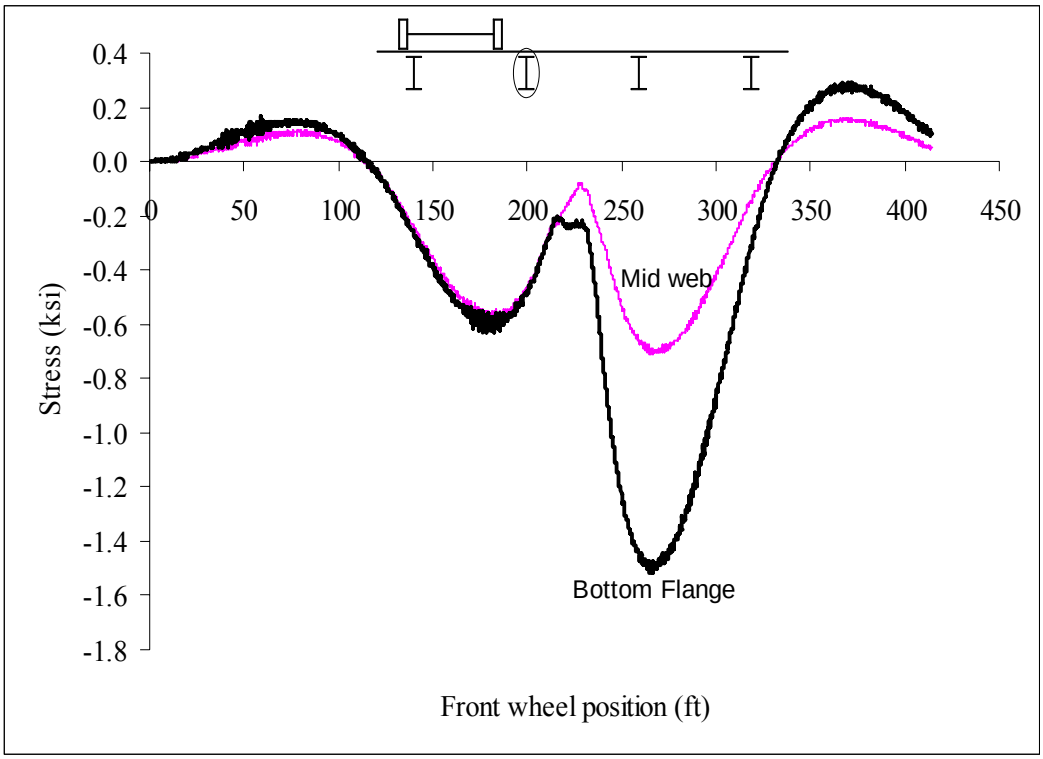

Figure B97: Hatch Bridge Test Run 4 S10 @ 3 ft east of interior support

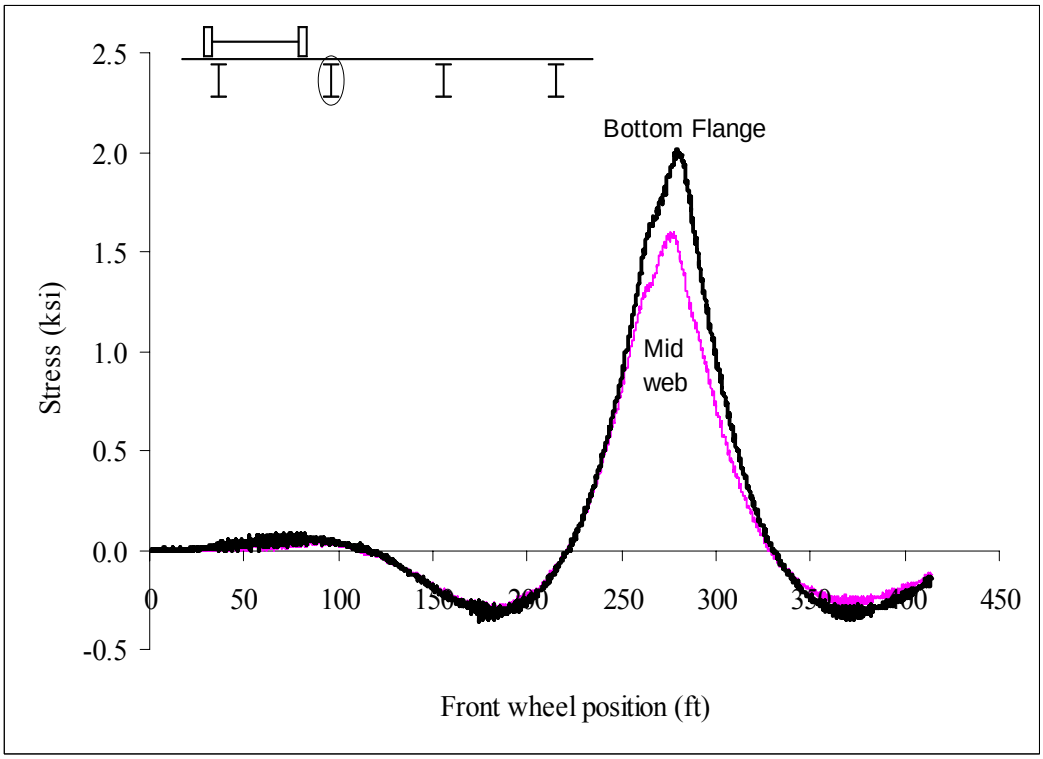

Figure B98: Hatch Bridge Test Run 4 S10 @ Midspan

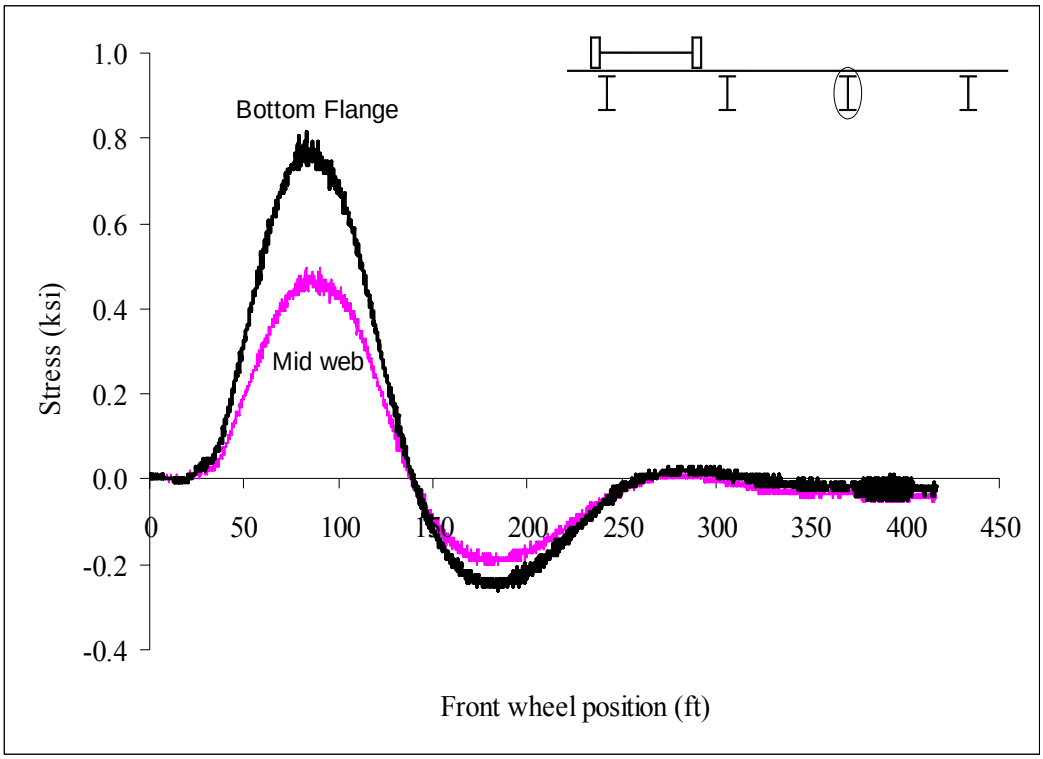

Figure B99: Hatch Bridge Test Run 4 S3 @ Midspan

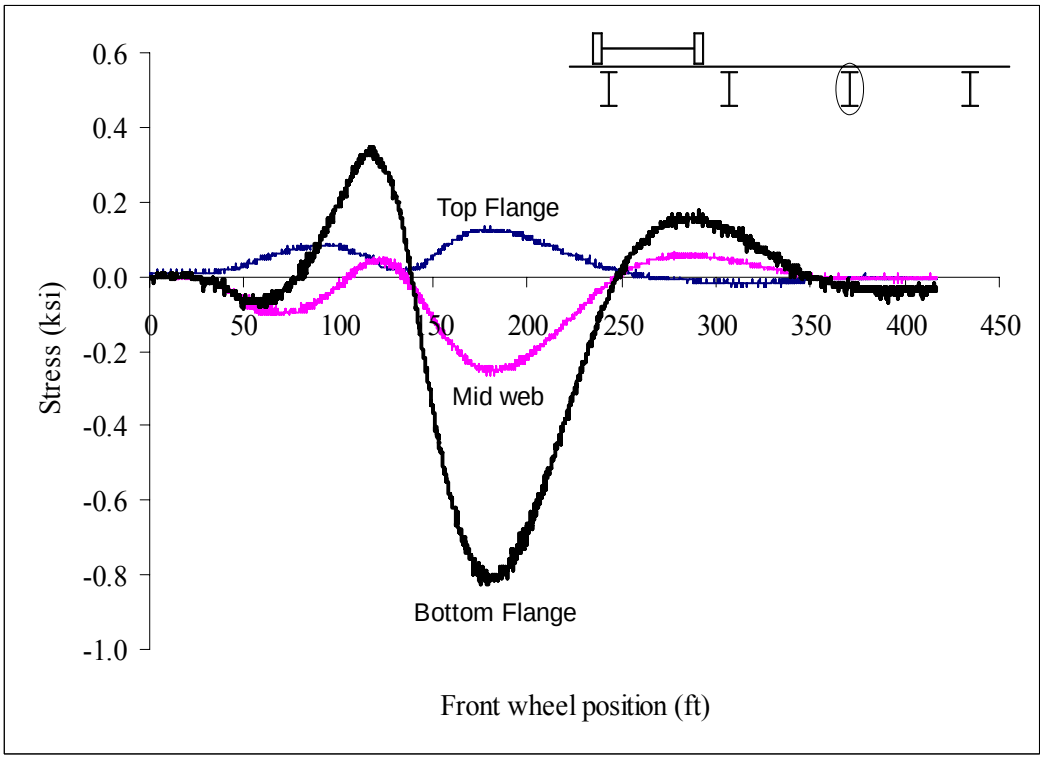

Figure B100: Hatch Bridge Test Run 4 S3 @ 3 ft west of interior support

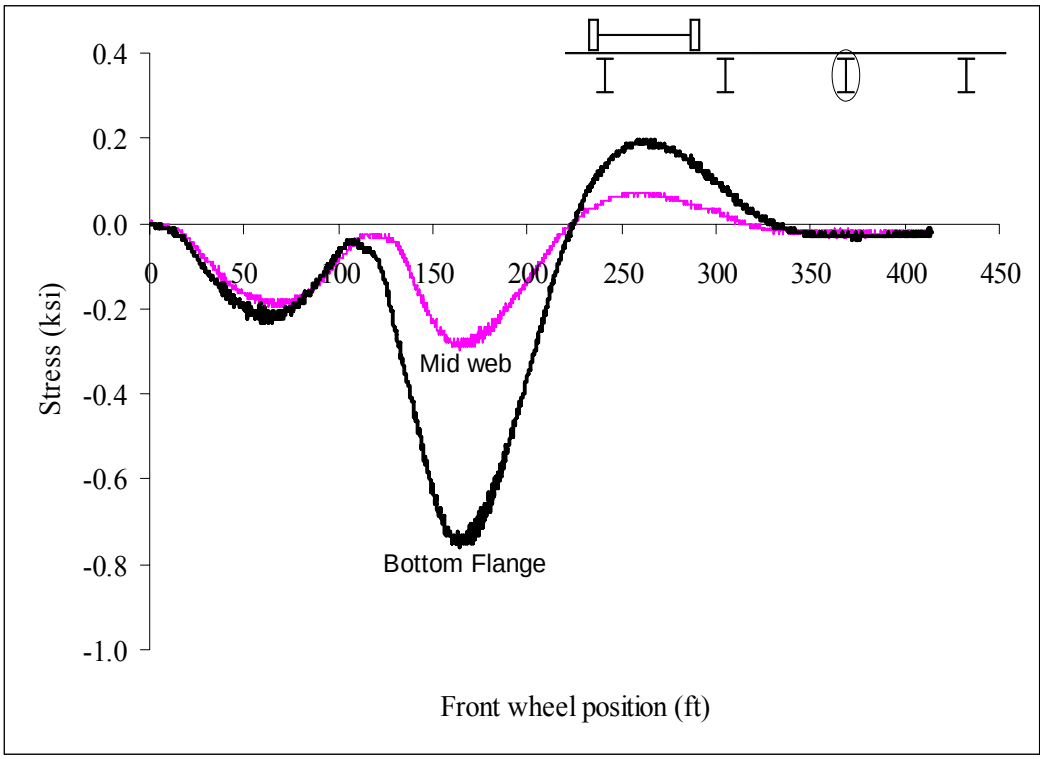

Figure B101: Hatch Bridge Test Run 4 S7 @ 3 ft east of interior support

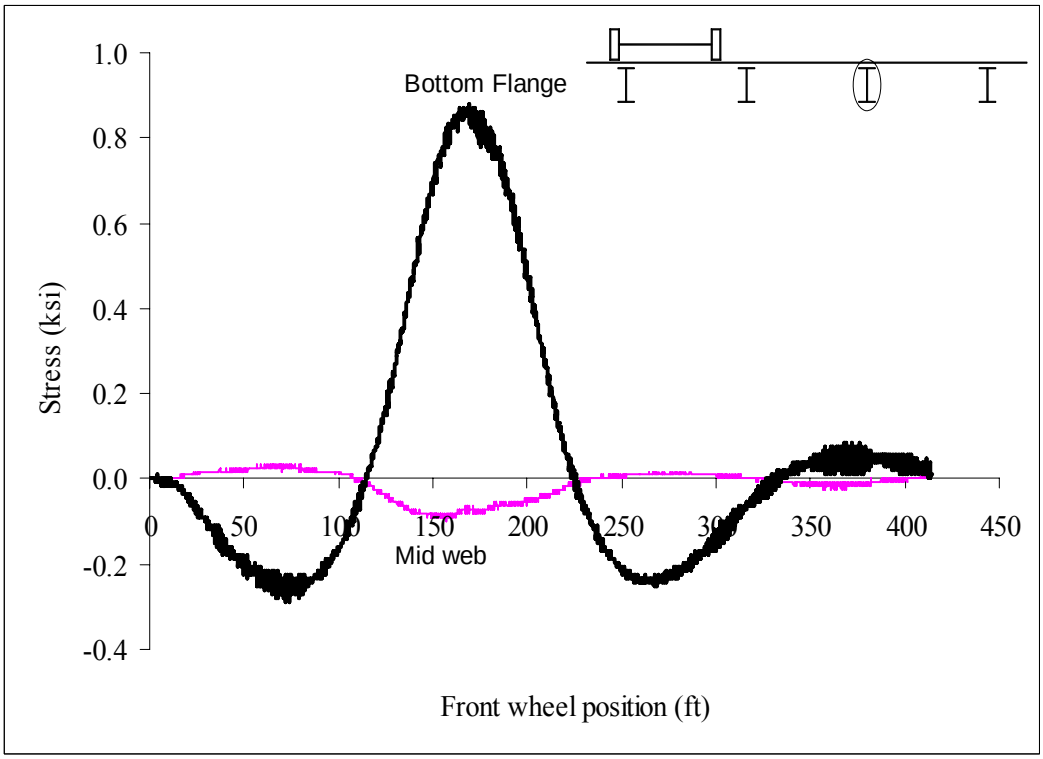

Figure B102: Hatch Bridge Test Run 4 S7 @ Midspan

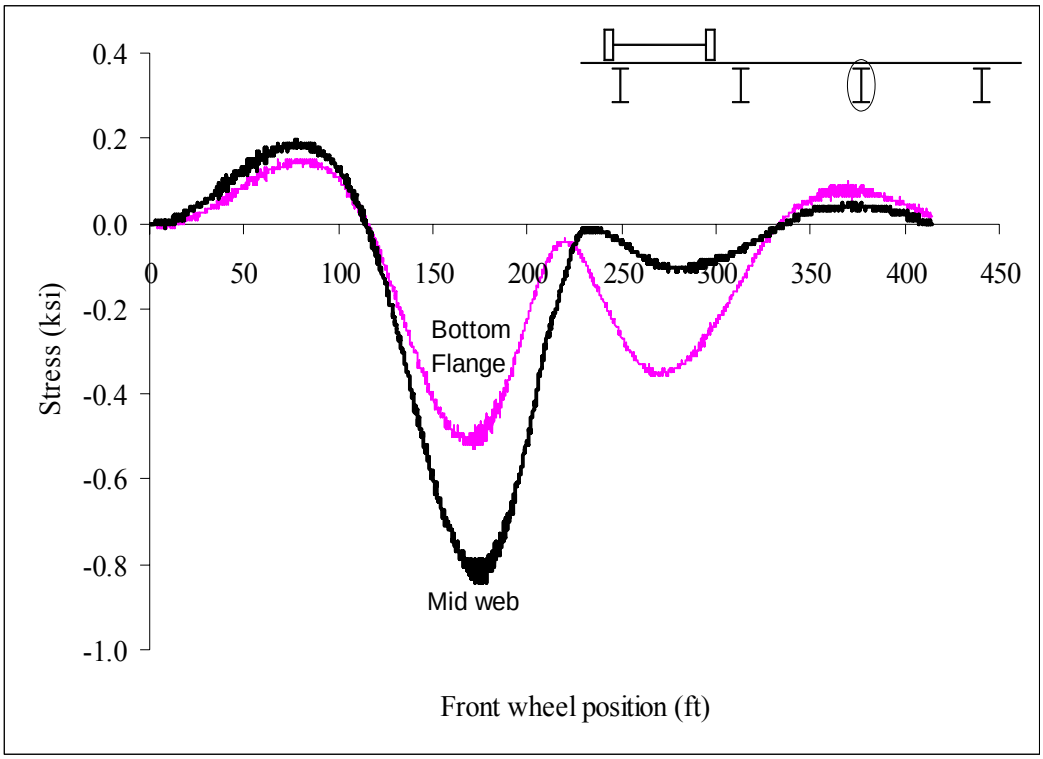

Figure B103: Hatch Bridge Test Run 4 S7 @ 3 ft west of interior support

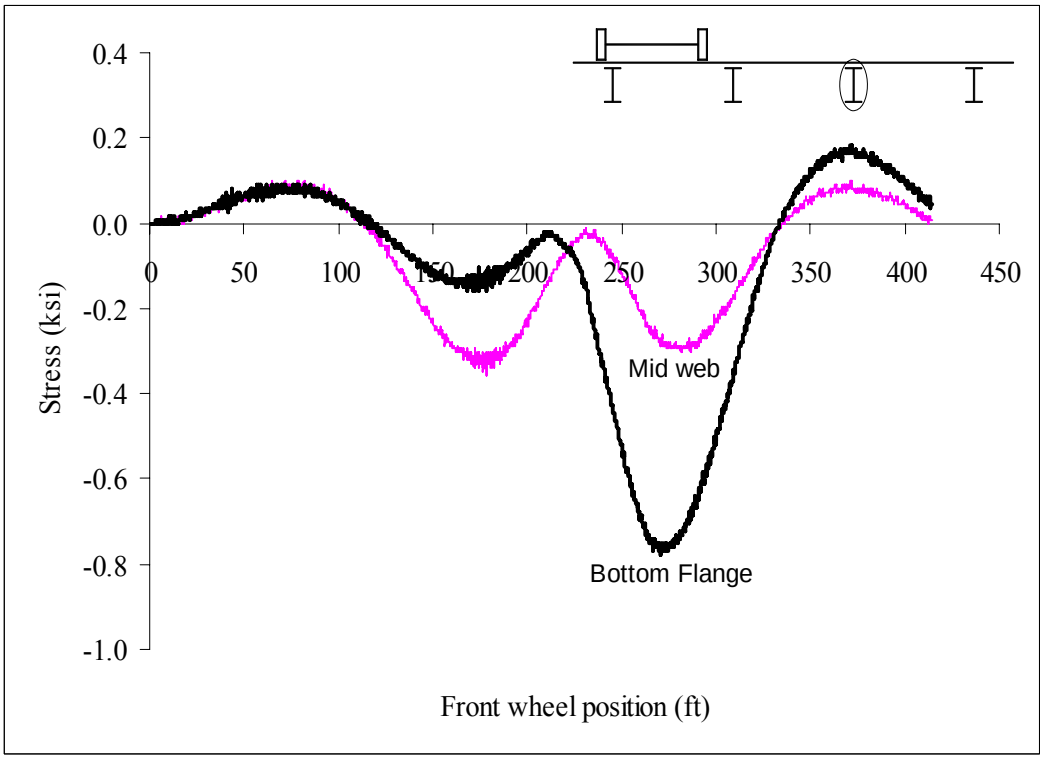

Figure B104: Hatch Bridge Test Run 4 S11 @ 3 ft east of interior support

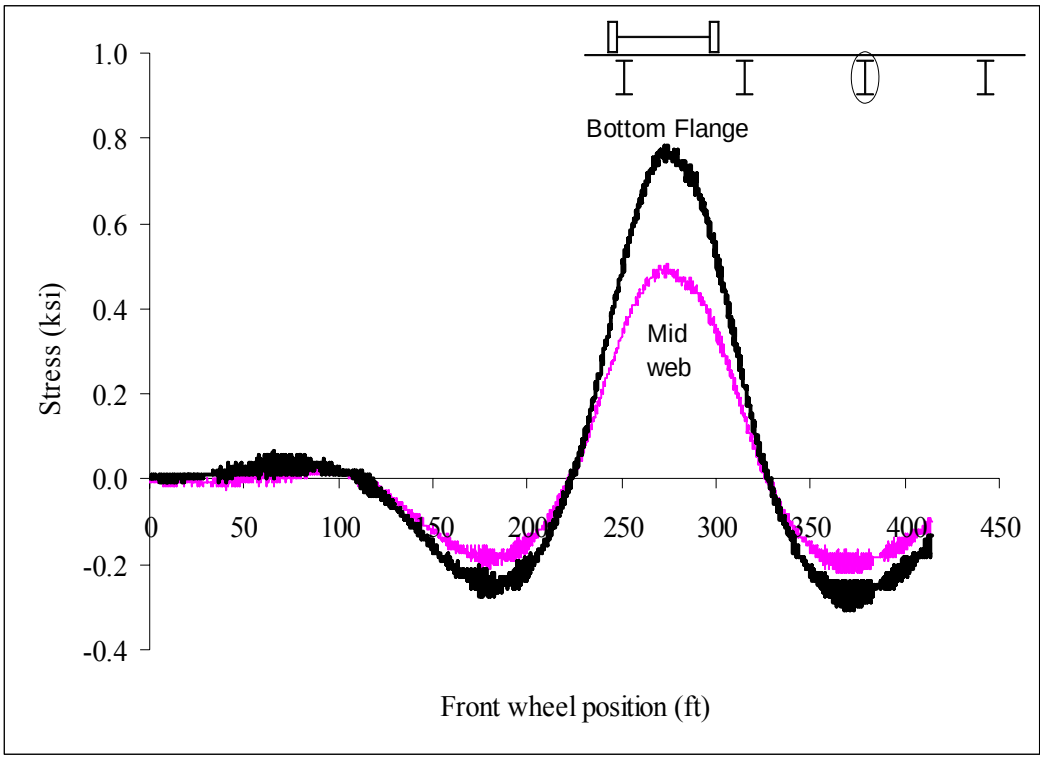

Figure B105: Hatch Bridge Test Run 4 S11 @ Midspan

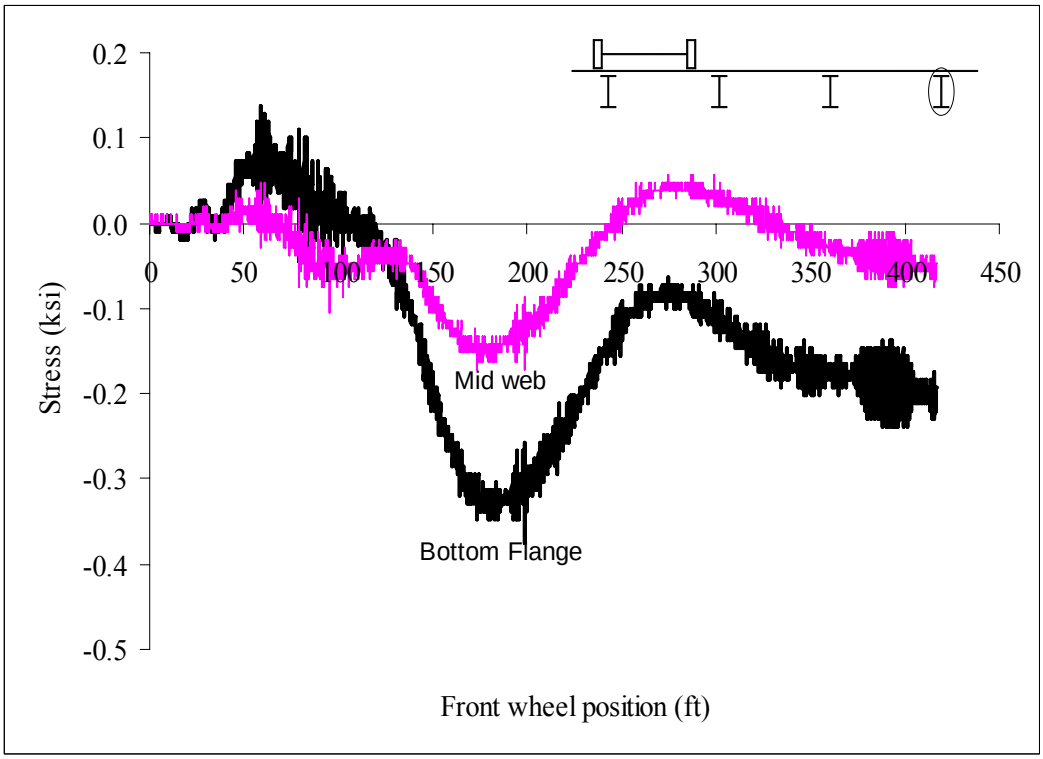

Figure B106: Hatch Bridge Test Run 4 S4 @ Midspan

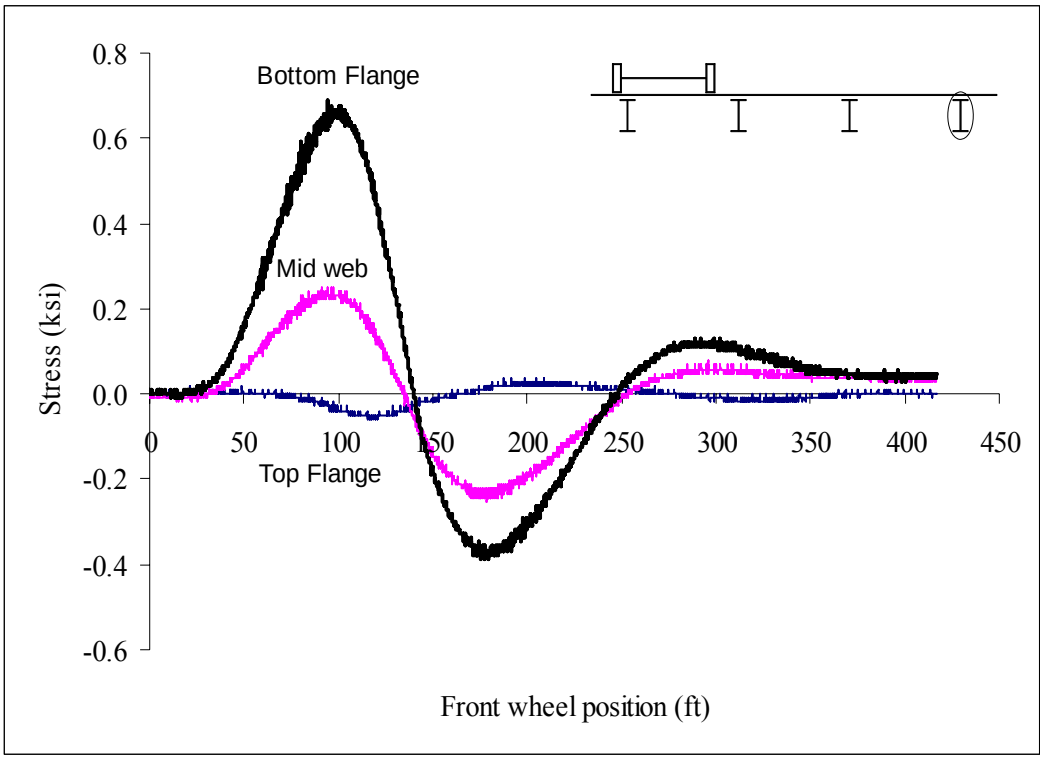

Figure B107: Hatch Bridge Test Run 4 S4 @ 3 ft west of interior support

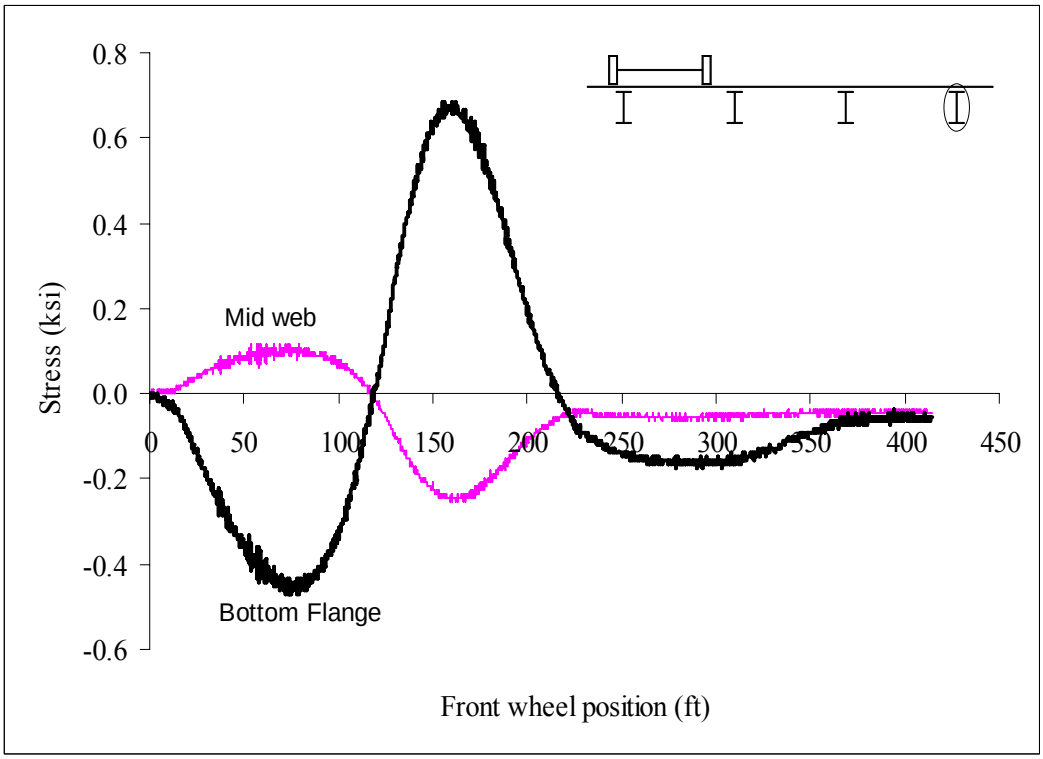

Figure B108: Hatch Bridge Test Run 4 S8 @ 3 ft east of interior support

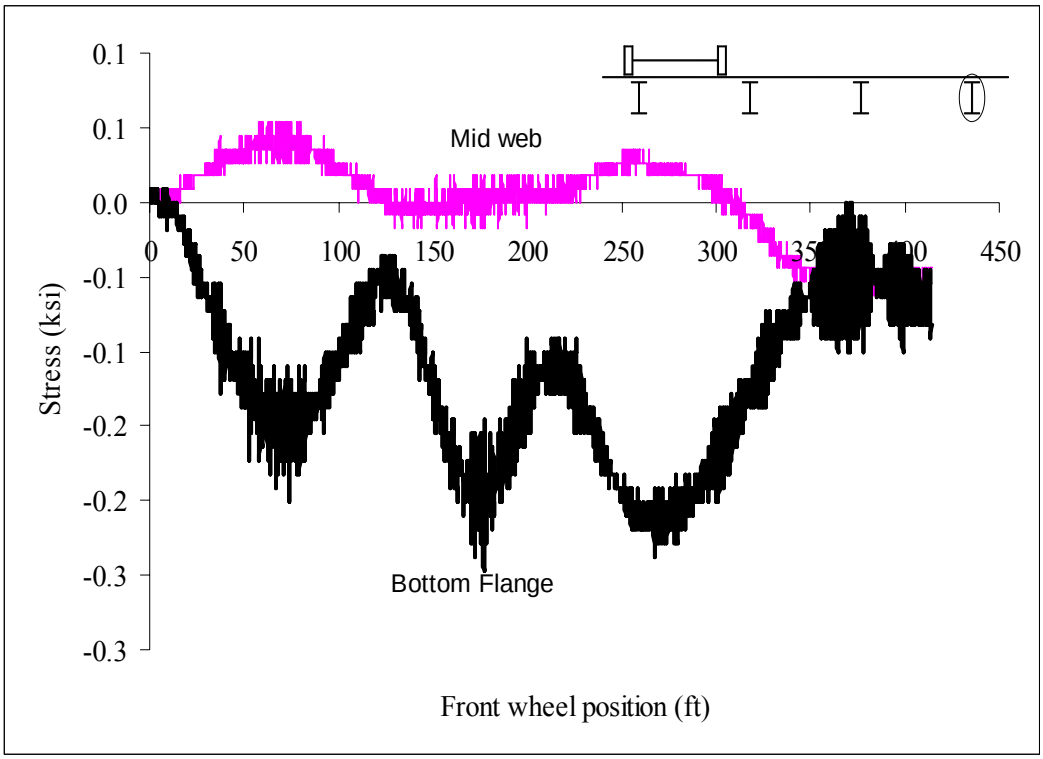

Figure B109: Hatch Bridge Test Run 4 S8 @ Midspan

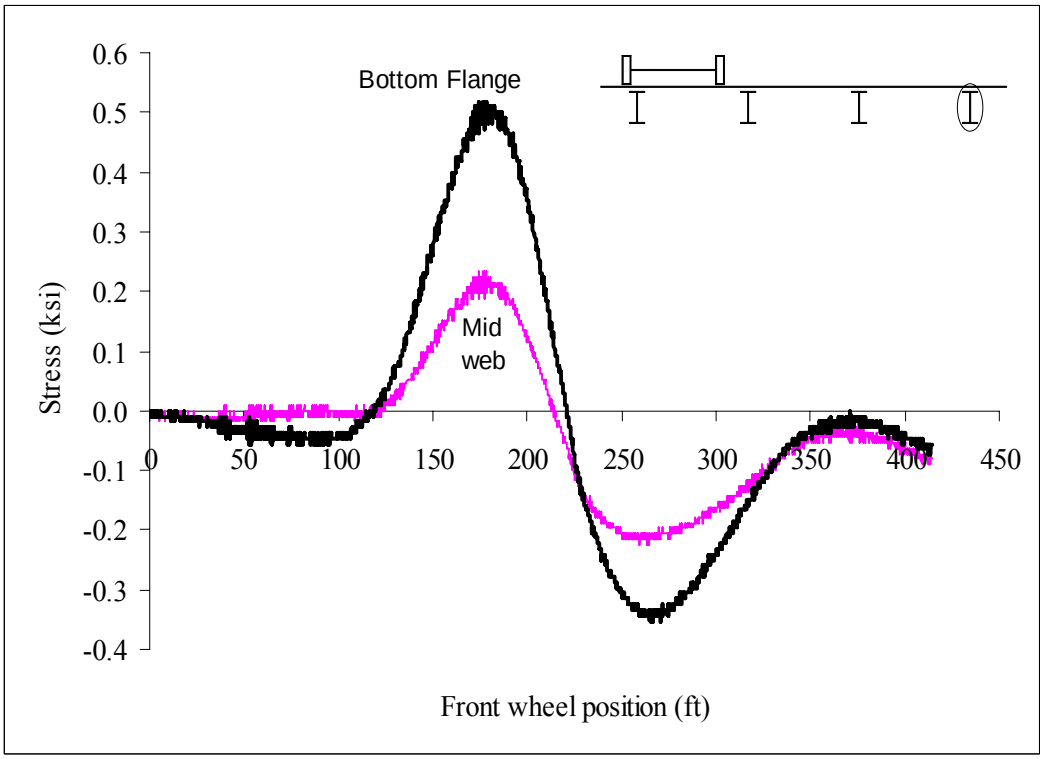

Figure B110: Hatch Bridge Test Run 4 S8 @ 3 ft west of interior support

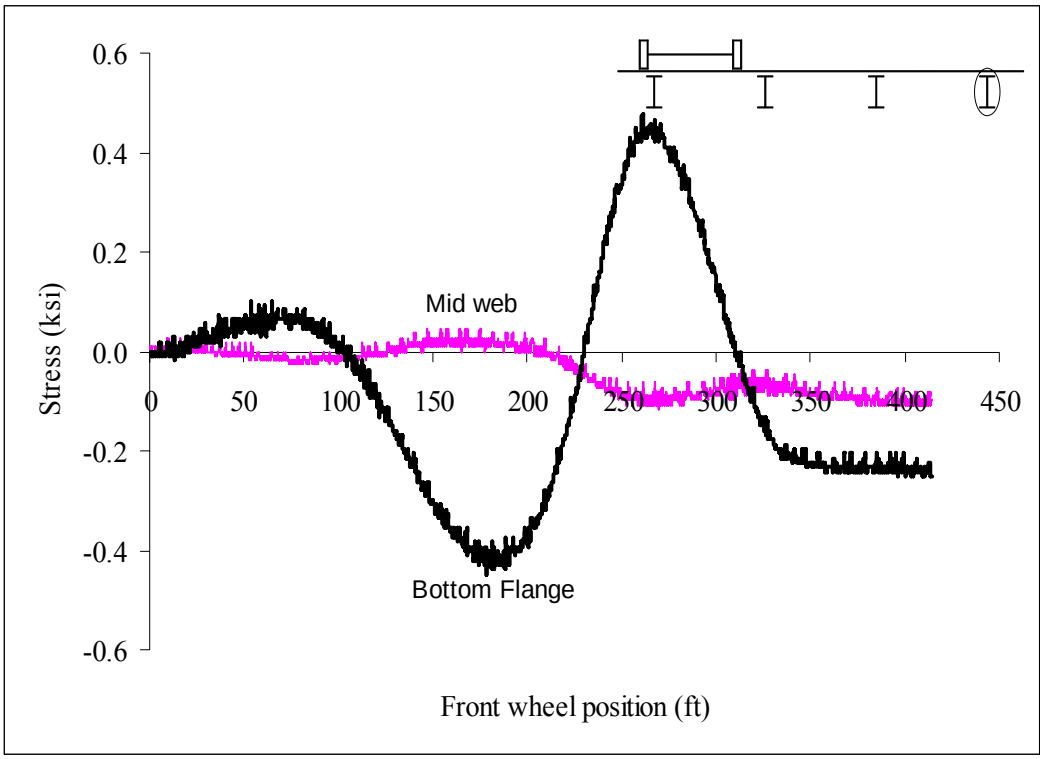

Figure B111: Hatch Bridge Test Run 4 S12 @ 3 ft east of interior support

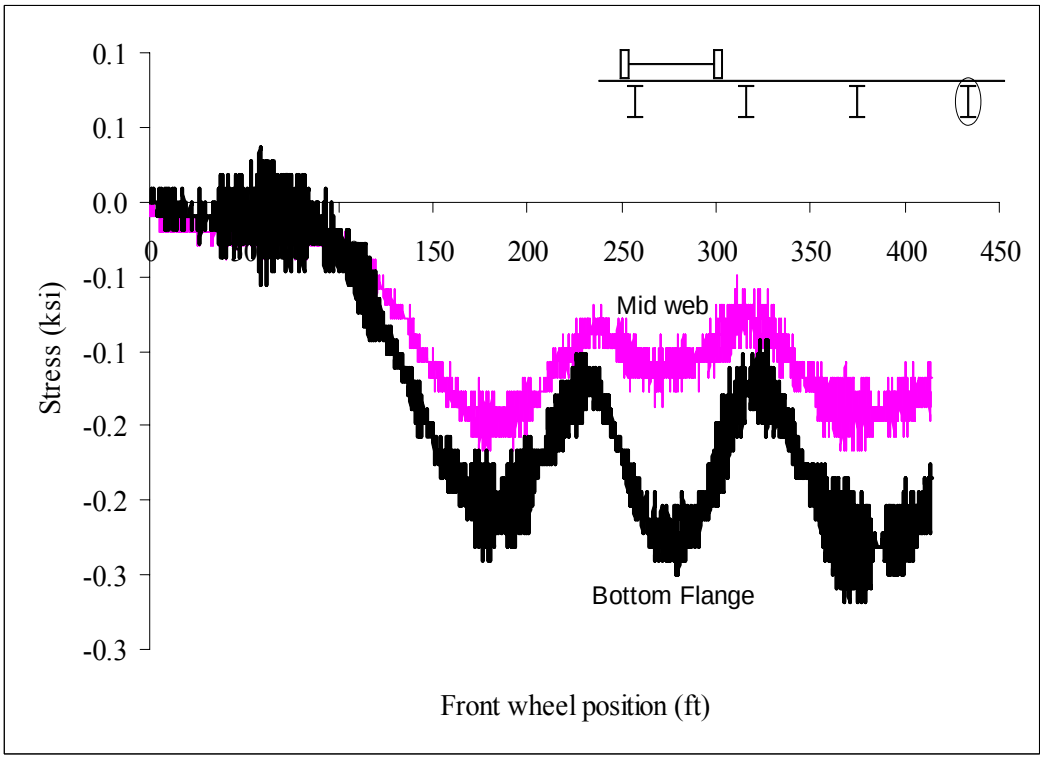

Figure B112: Hatch Bridge Test Run 4 S12 @ Midspan

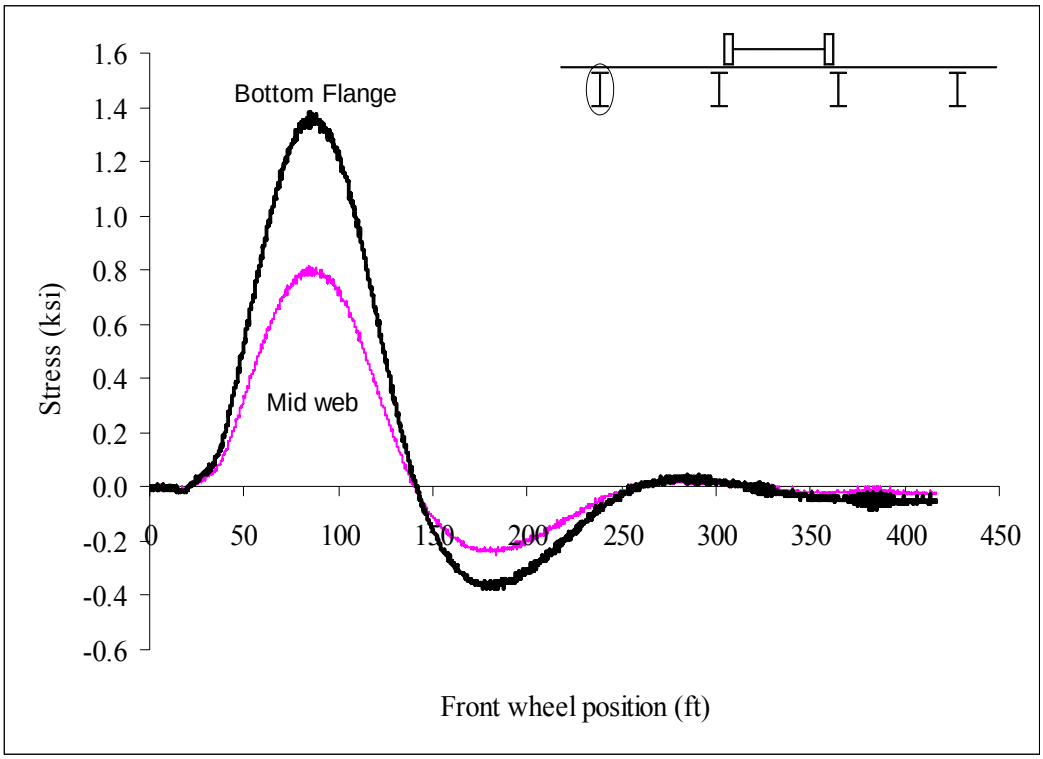

Figure B113: Hatch Bridge Test Run 5 S1 @ Midspan

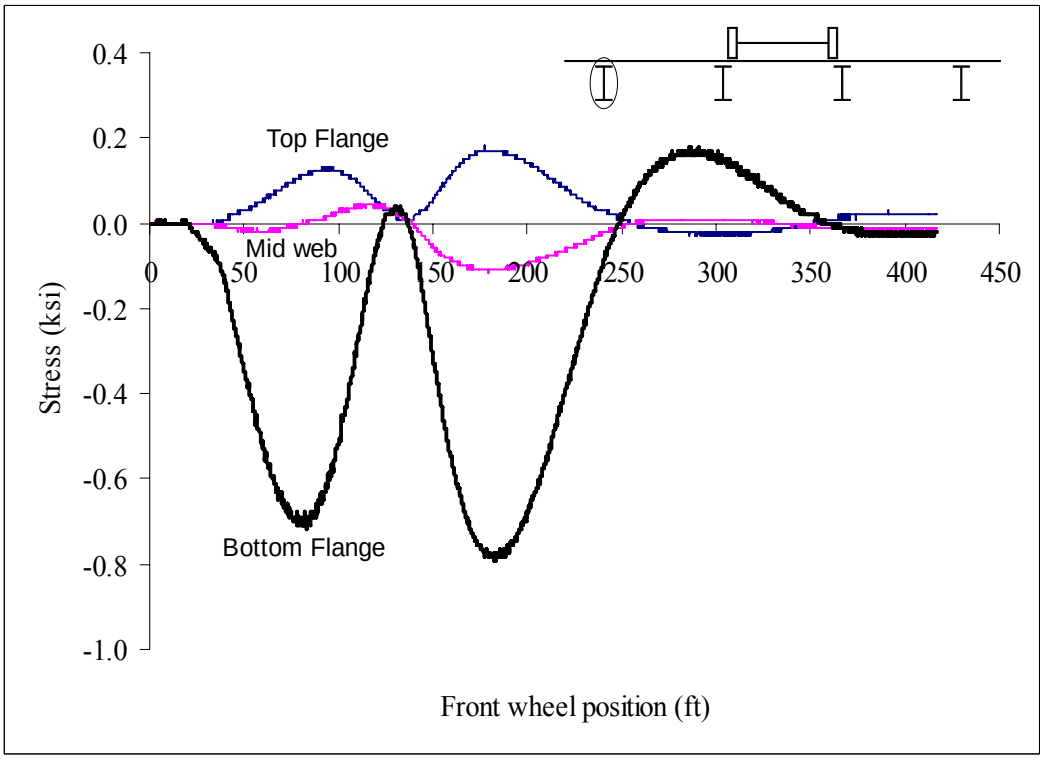

Figure B114: Hatch Bridge Test Run 5 S1 @ 3 ft west of interior support

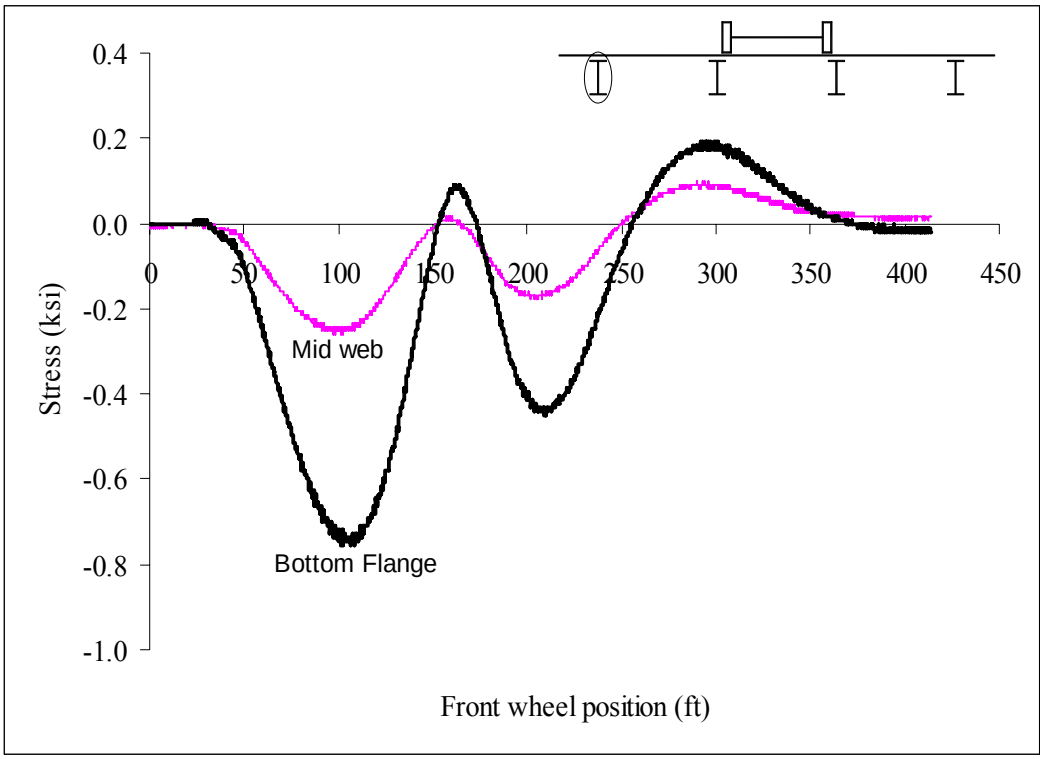

Figure B115: Hatch Bridge Test Run 5 S5 @ 3 ft east of interior support

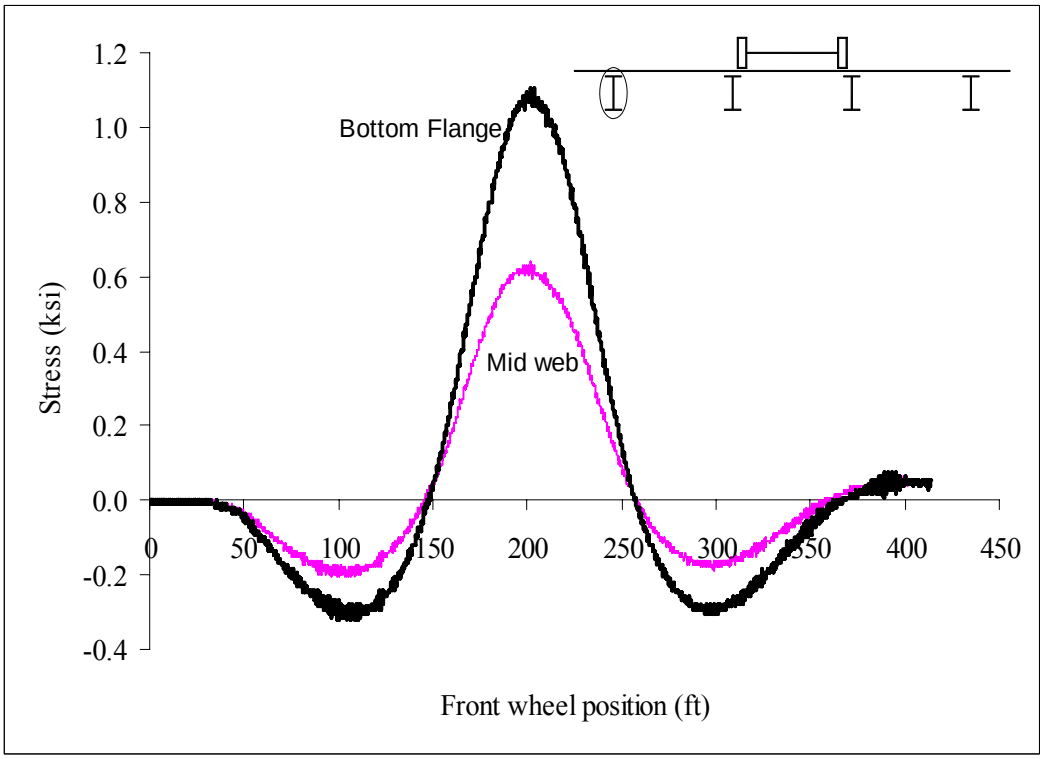

Figure B116: Hatch Bridge Test Run 5 S5 @ Midspan

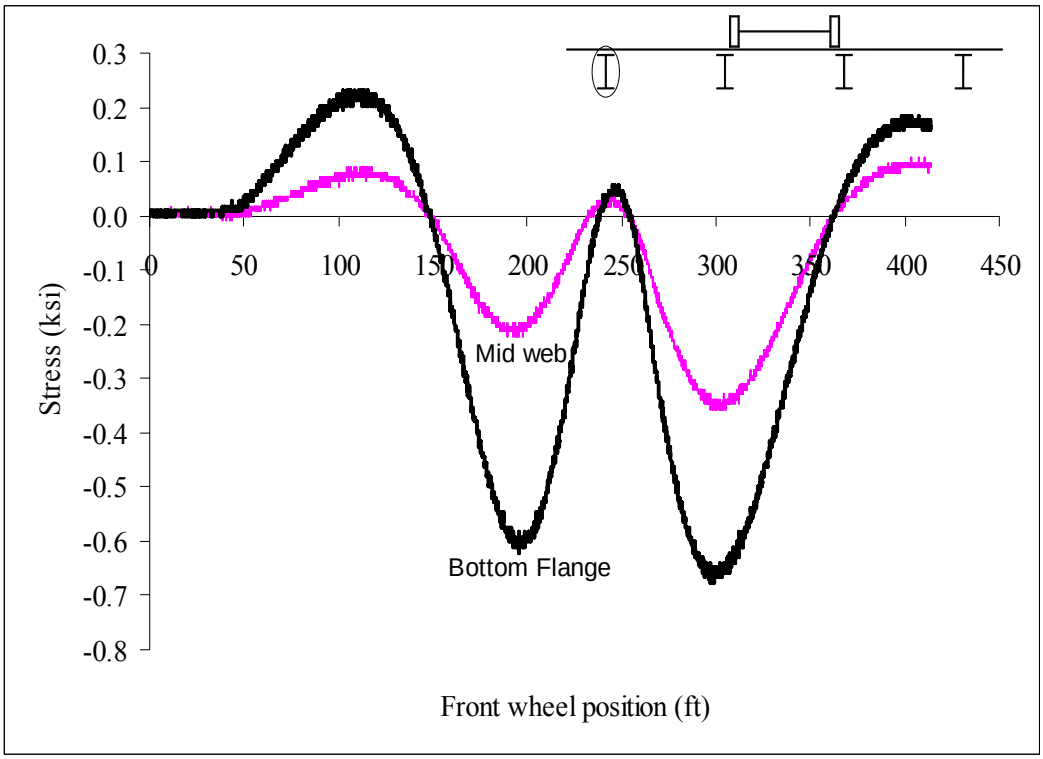

Figure B117: Hatch Bridge Test Run 5 S5 @ 3 ft west of interior support

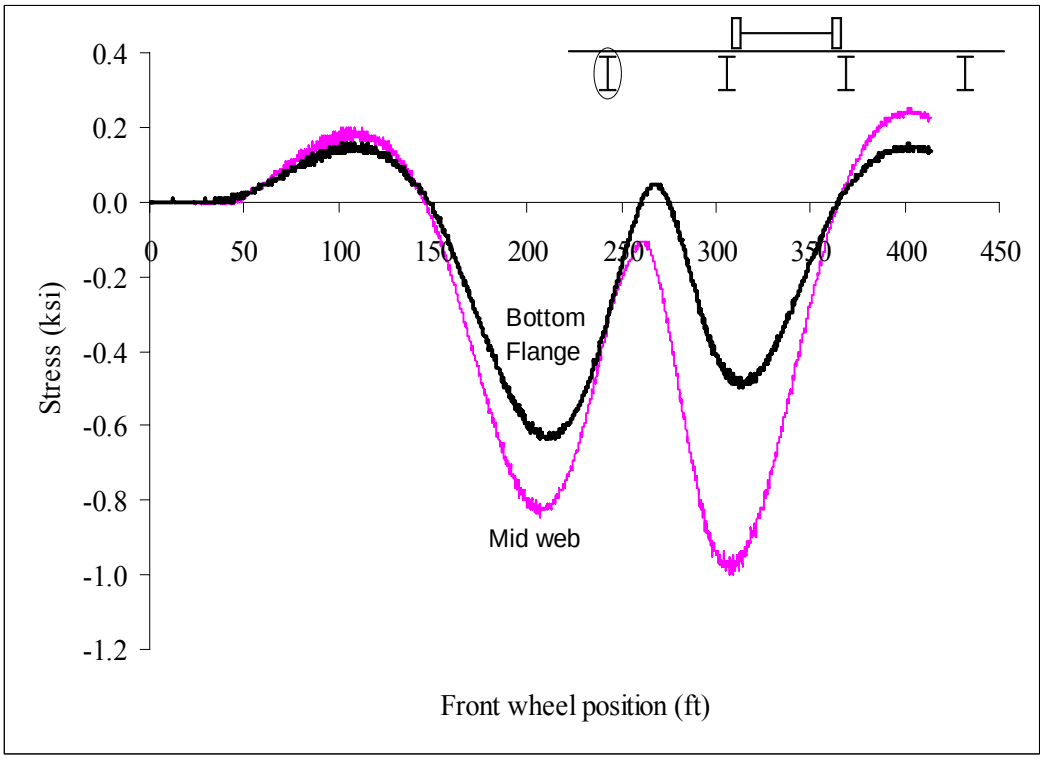

Figure B118: Hatch Bridge Test Run 5 S9 @ 3 ft east of interior support

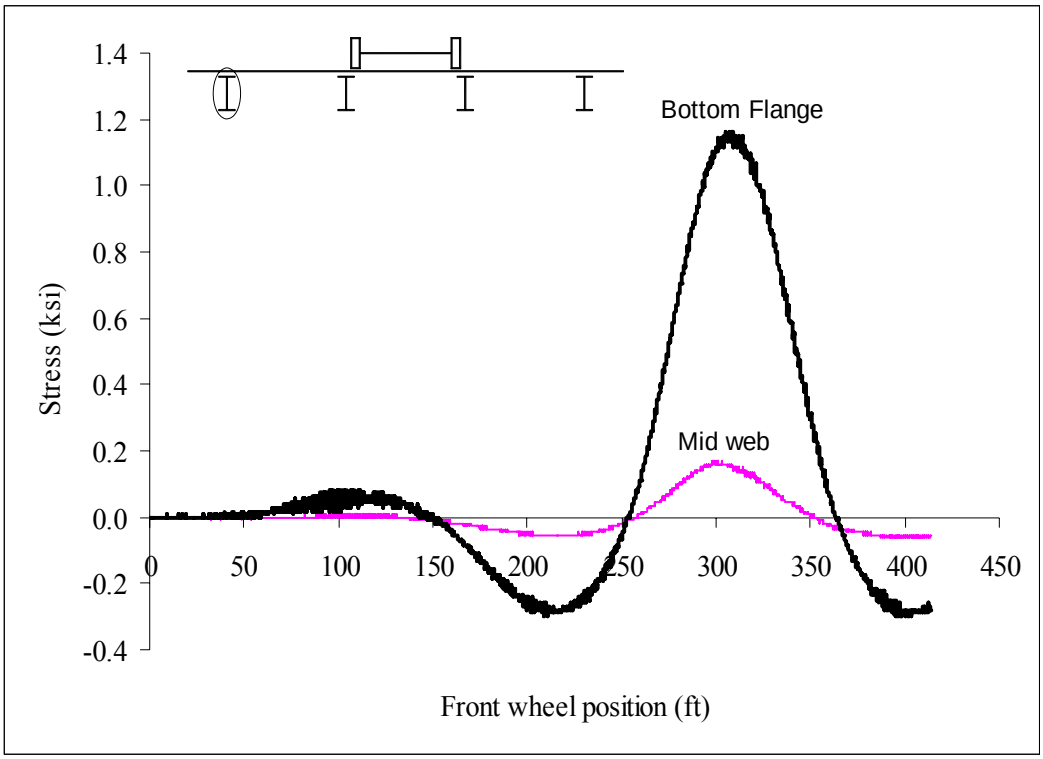

Figure B119: Hatch Bridge Test Run 5 S9 @ Midspan

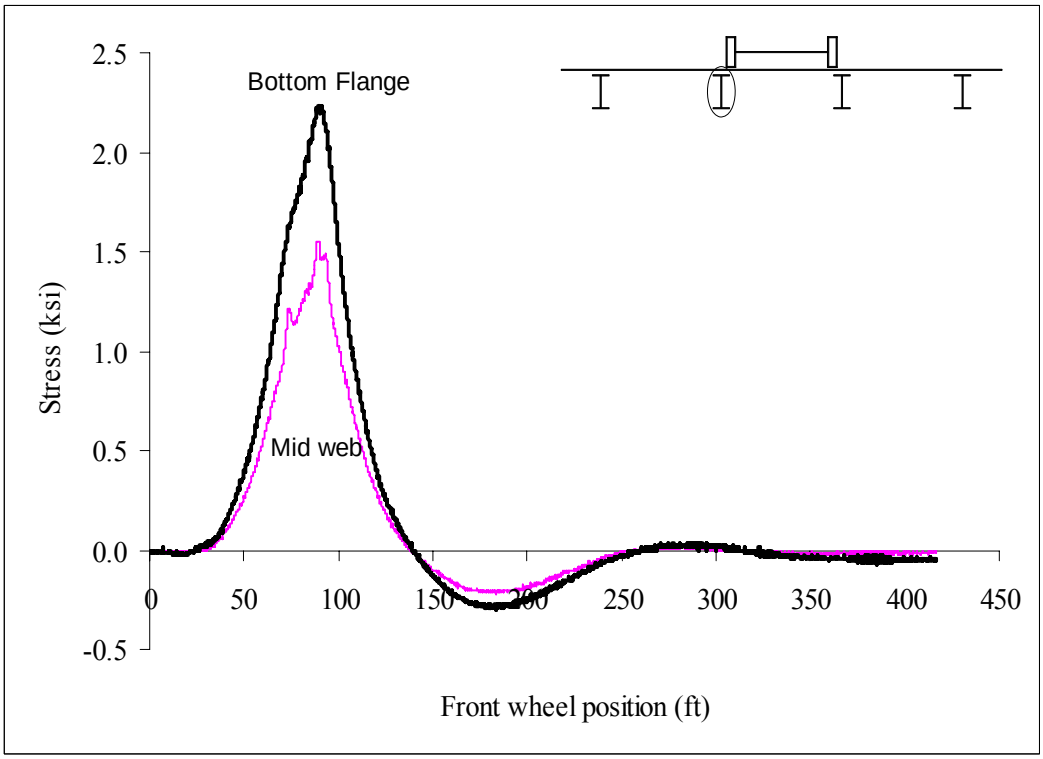

Figure B120: Hatch Bridge Test Run 5 S2 @ Midspan

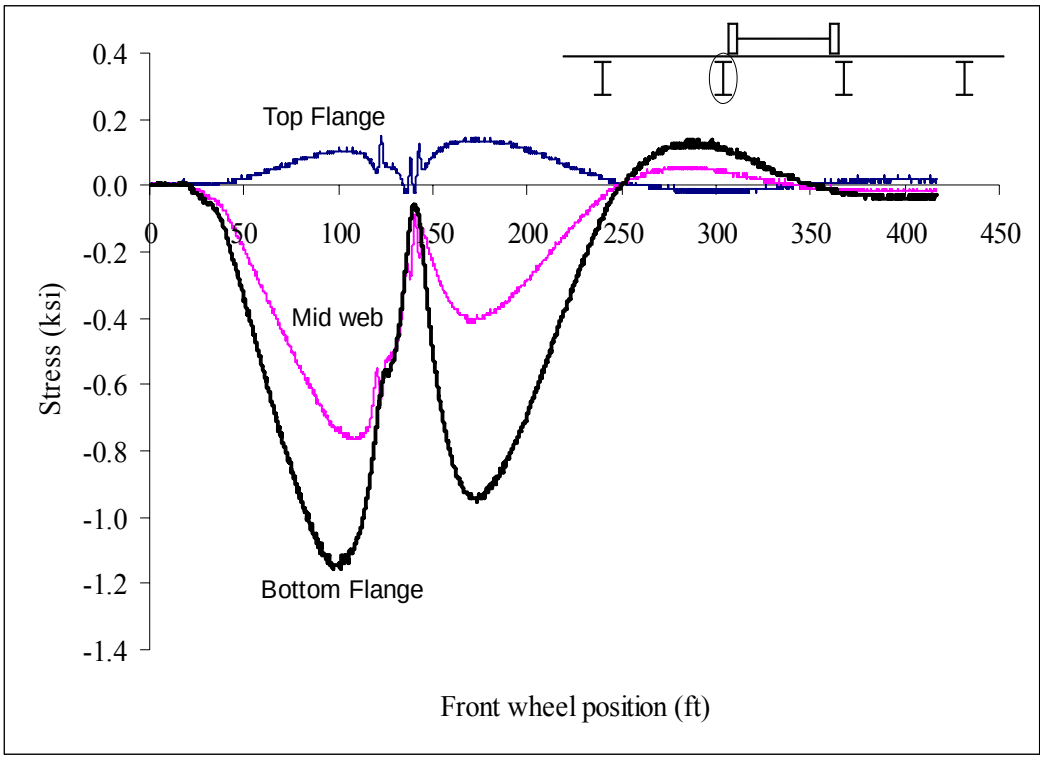

Figure B121: Hatch Bridge Test Run 5 S2 @ 3 ft west of interior support

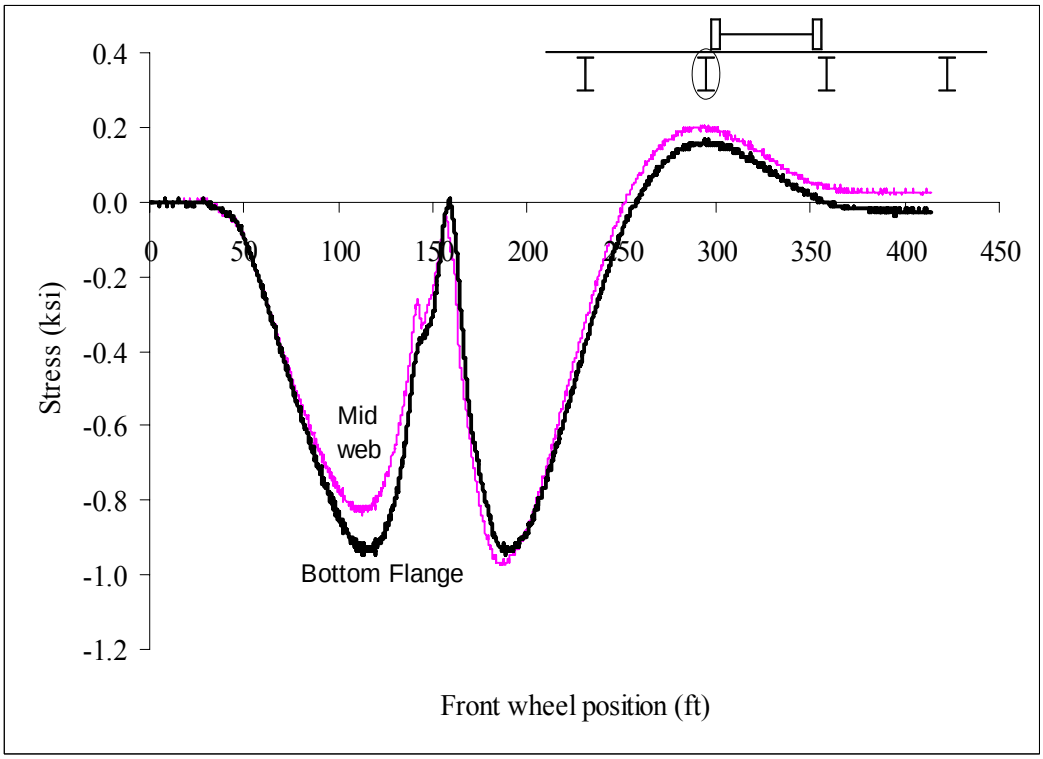

Figure B122: Hatch Bridge Test Run 5 S6 @ 3 ft east of interior support

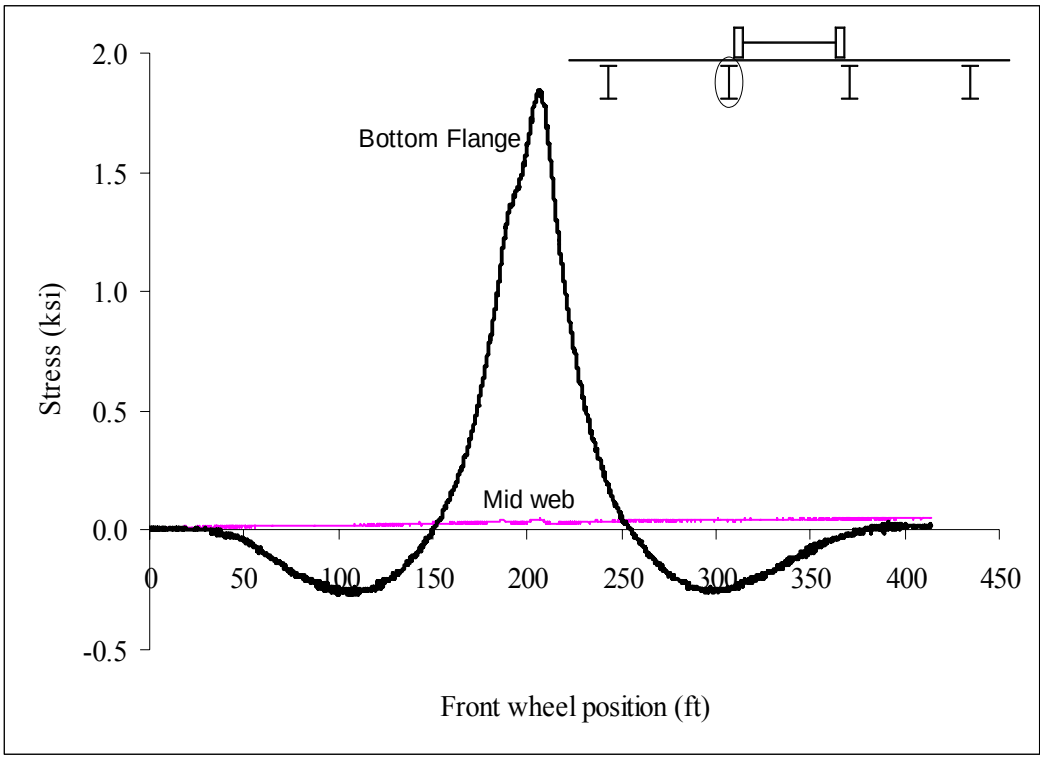

Figure B123: Hatch Bridge Test Run 5 S6 @ Midspan

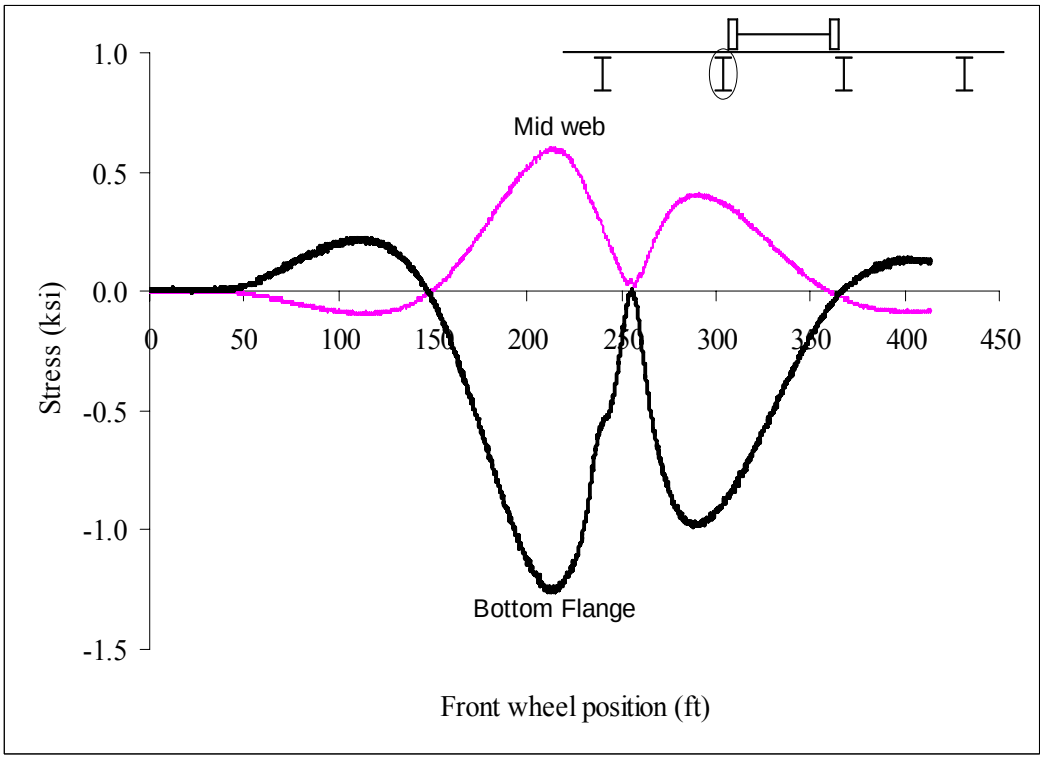

Figure B124: Hatch Bridge Test Run 5 S6 @ 3 ft west of interior support

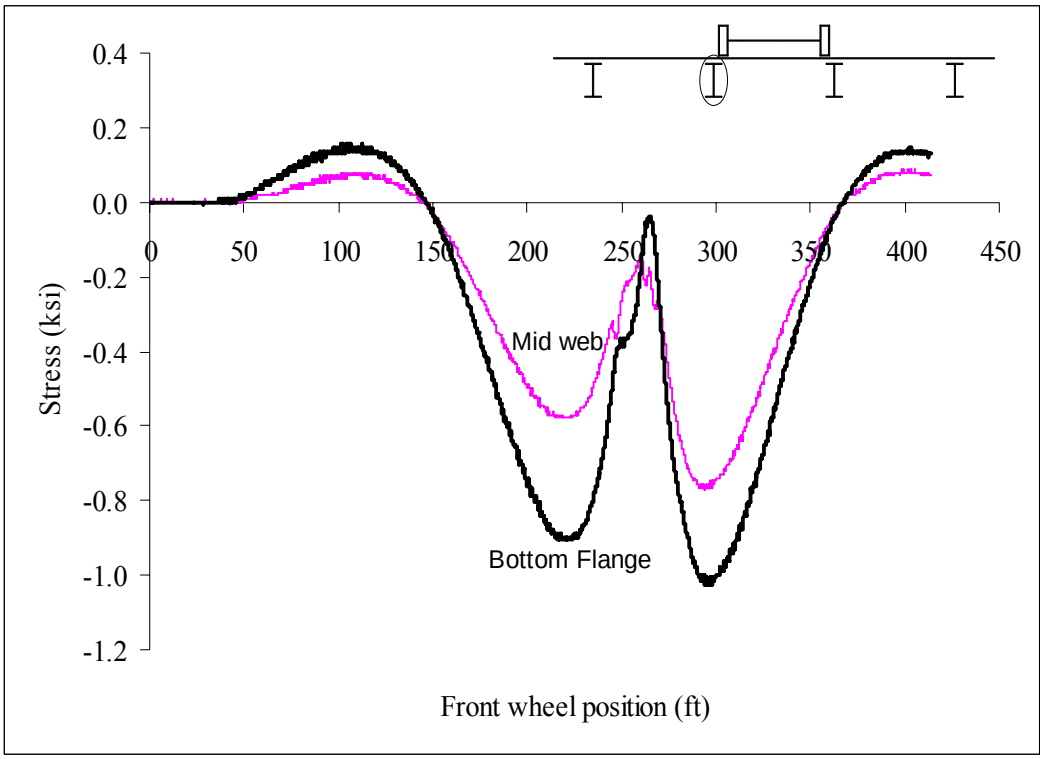

Figure B125: Hatch Bridge Test Run 5 S10 @ 3 ft east of interior support

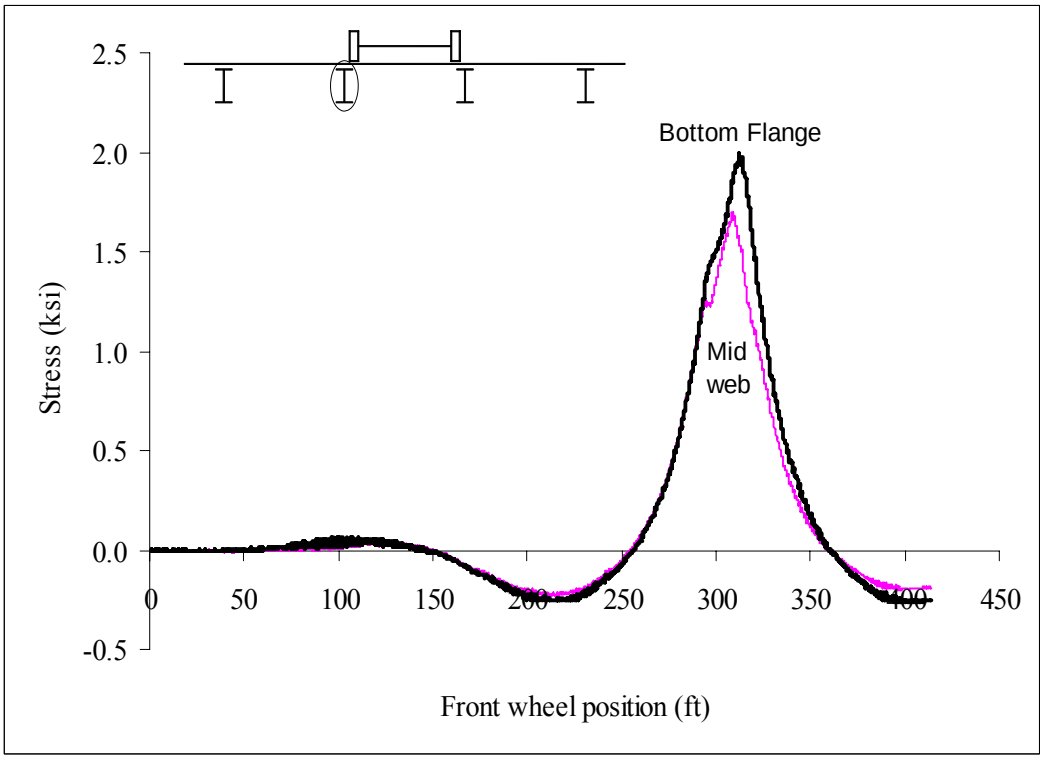

Figure B126: Hatch Bridge Test Run 5 S10 @ Midspan

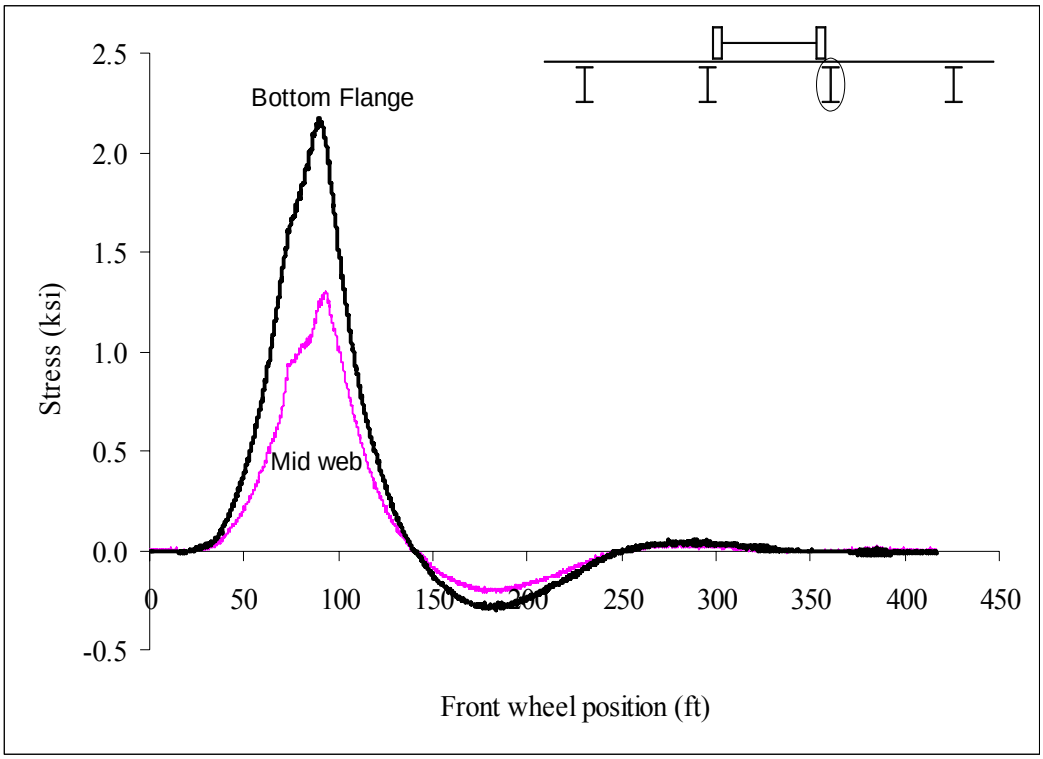

Figure B127: Hatch Bridge Test Run 5 S3 @ Midspan

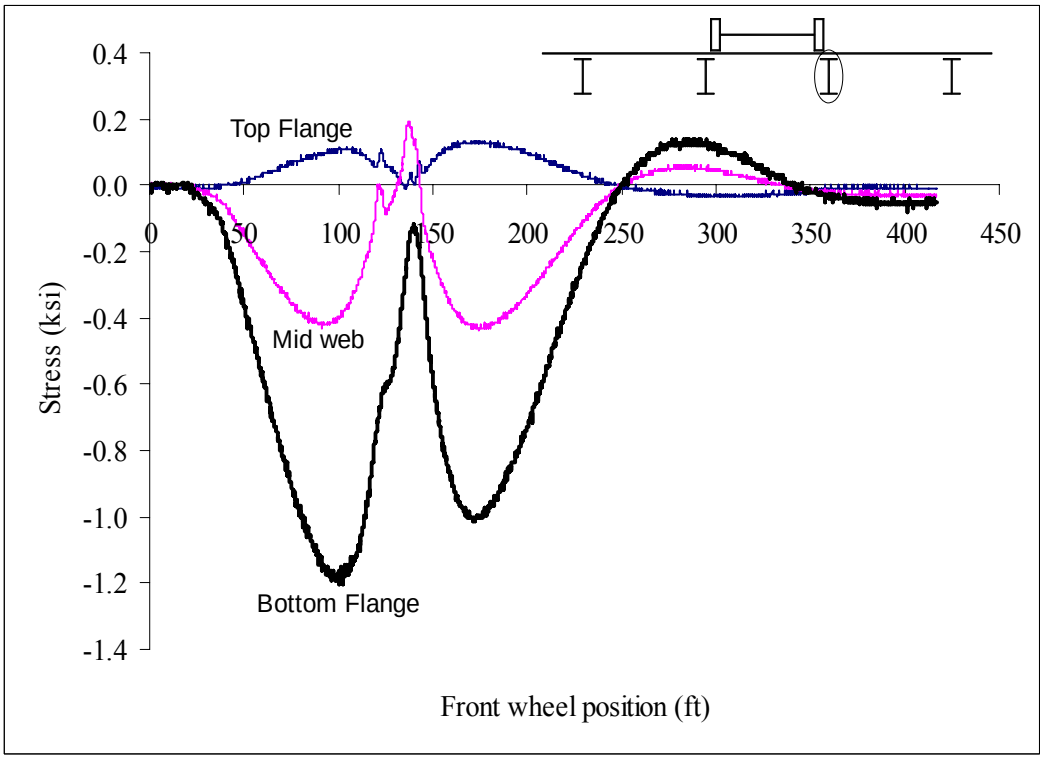

Figure B128: Hatch Bridge Test Run 5 S3 @ 3 ft west of interior support

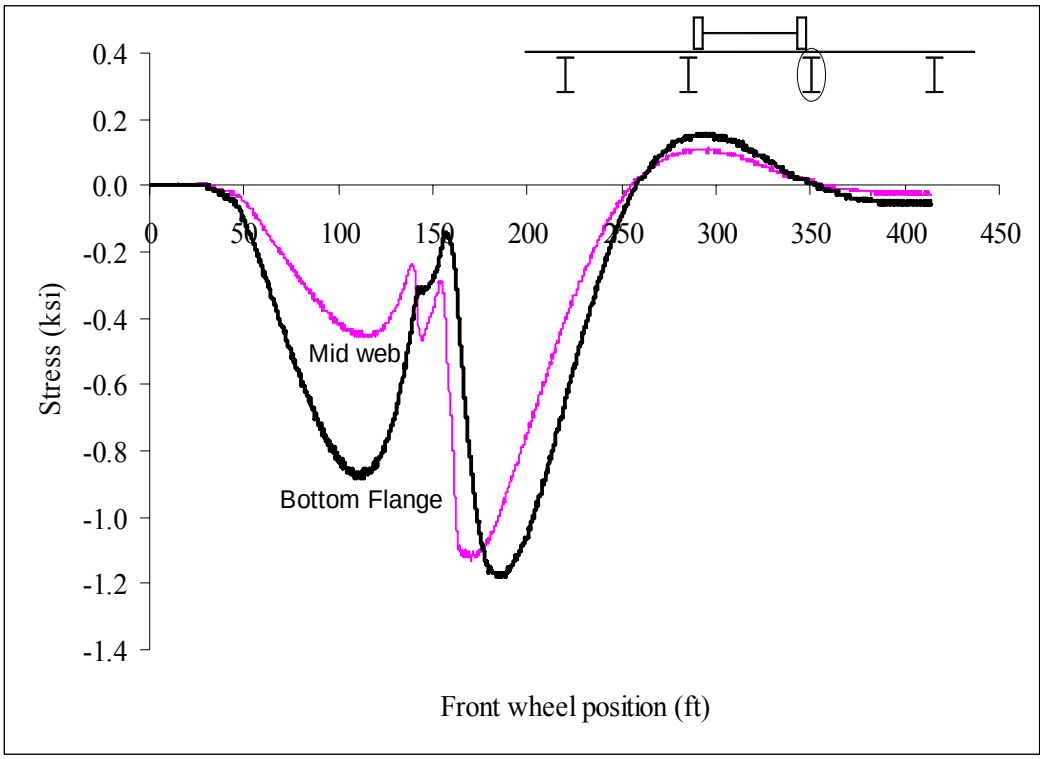

Figure B129: Hatch Bridge Test Run 5 S7 @ 3 ft east of interior support

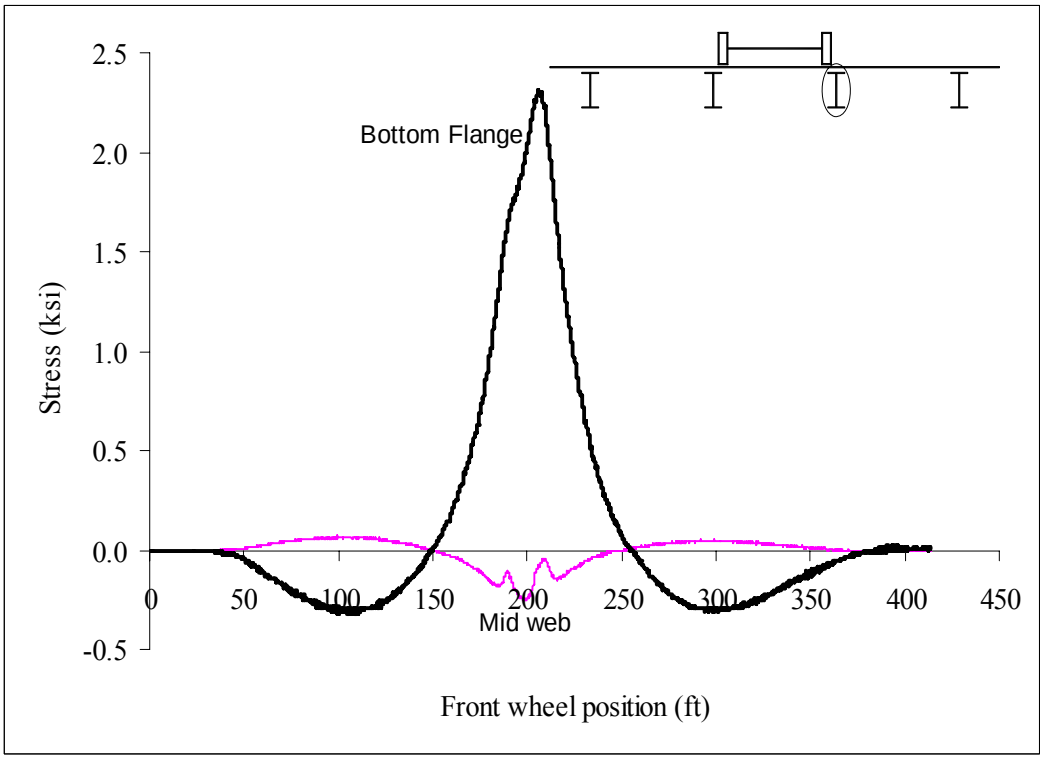

Figure B130: Hatch Bridge Test Run 5 S7 @ Midspan

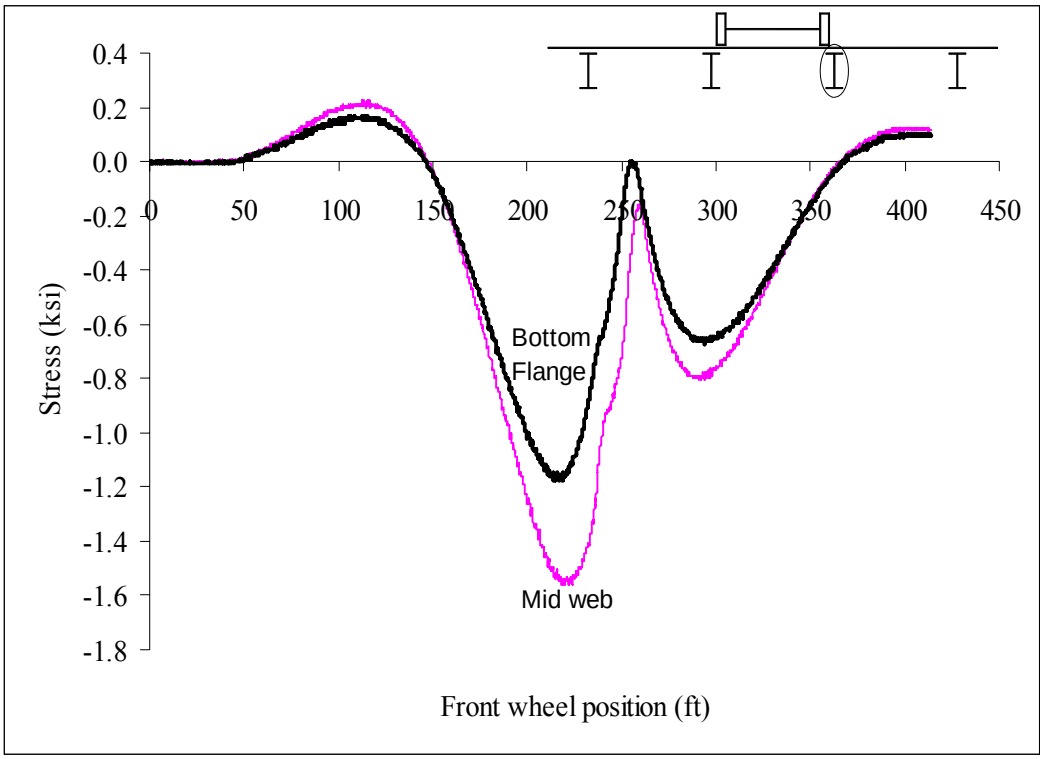

Figure B131: Hatch Bridge Test Run 5 S7 @ 3 ft west of interior support

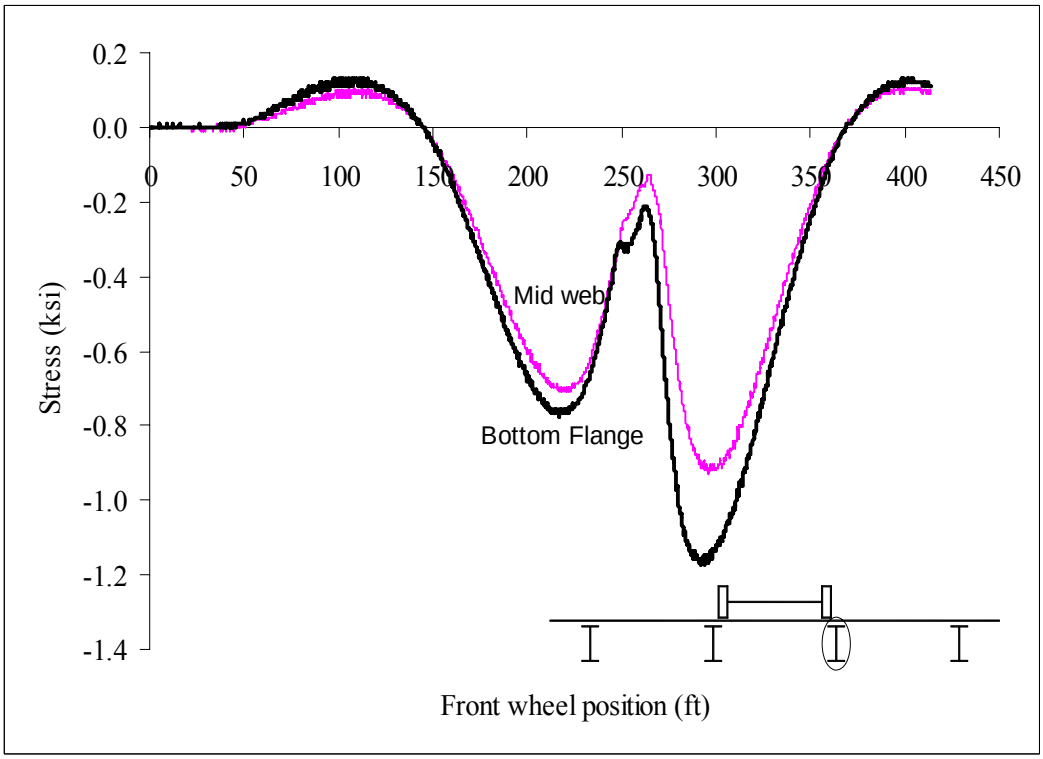

Figure B132: Hatch Bridge Test Run 5 S11 @ 3 ft east of interior support

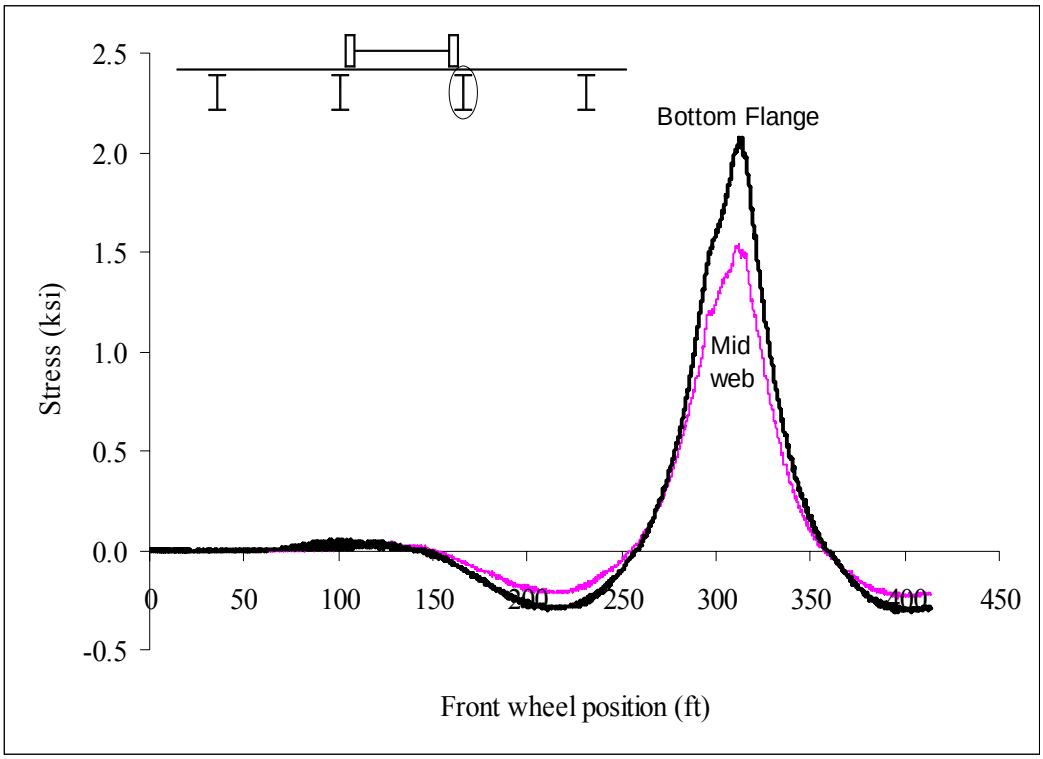

Figure B133: Hatch Bridge Test Run 5 S11 @ Midspan

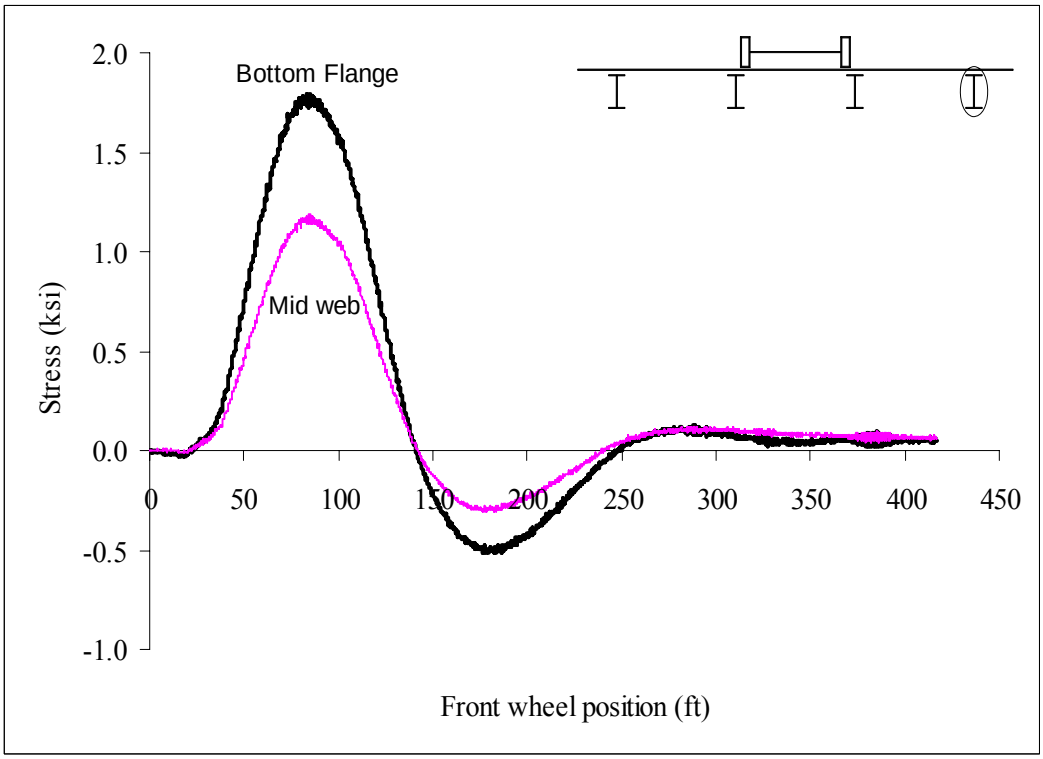

Figure B134: Hatch Bridge Test Run 5 S4 @ Midspan

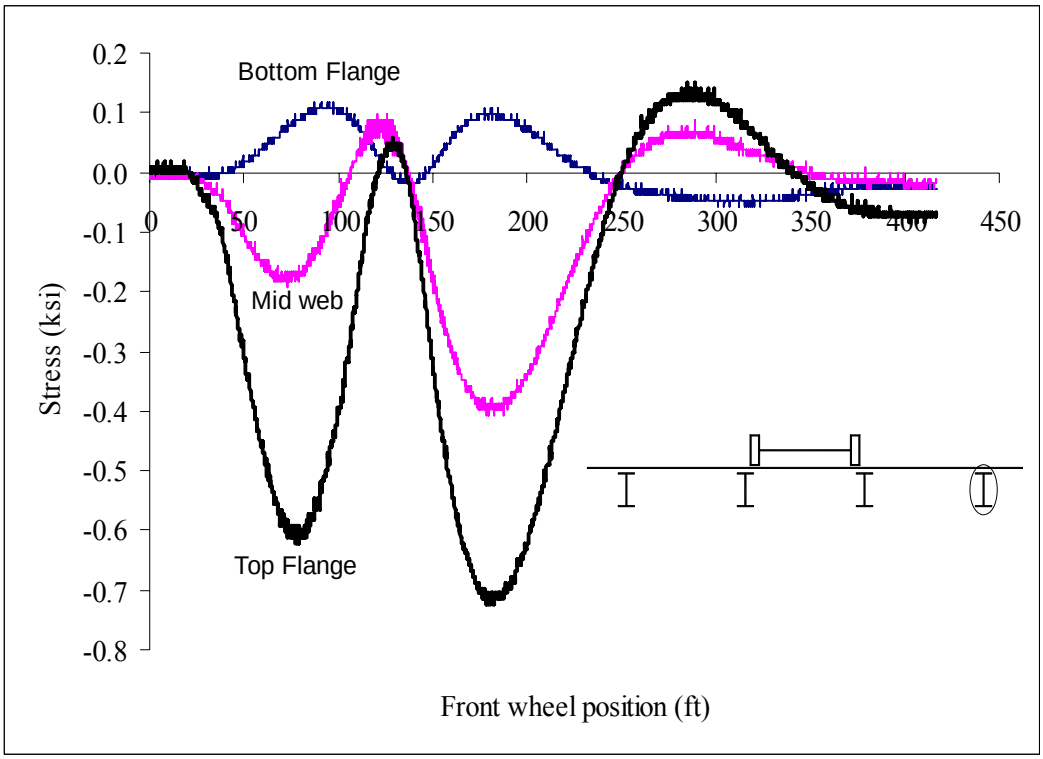

Figure B135: Hatch Bridge Test Run 5 S4 @ 3 ft west of interior support

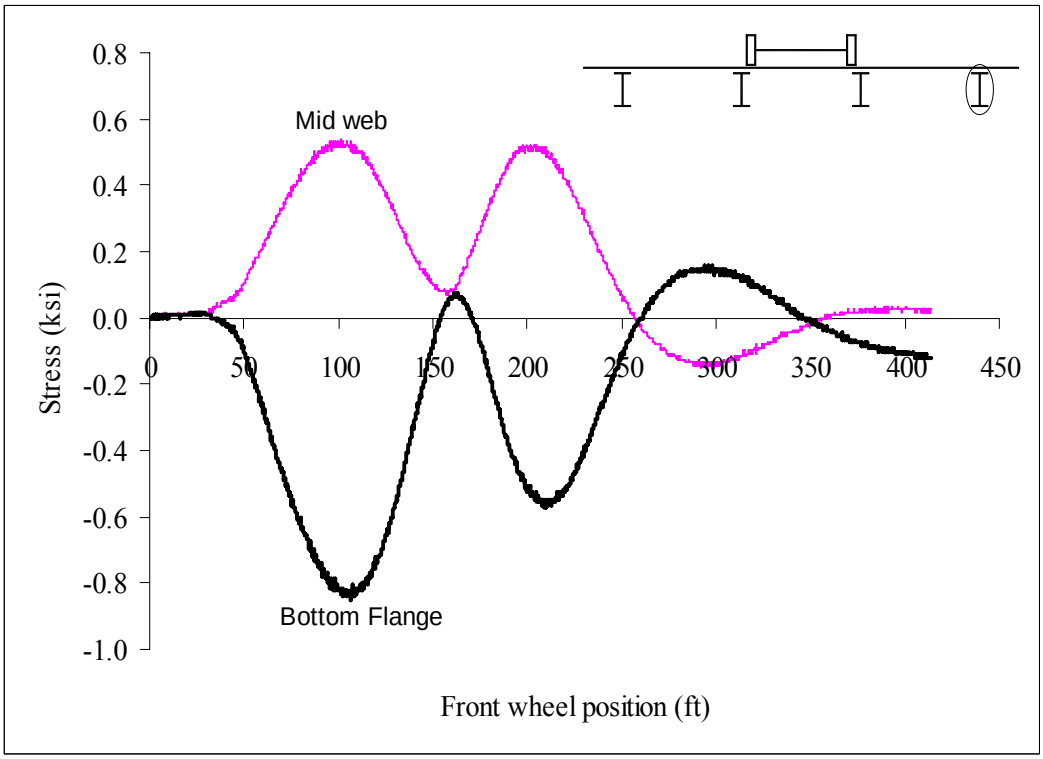

Figure B136: Hatch Bridge Test Run 5 S8 @ 3 ft east of interior support

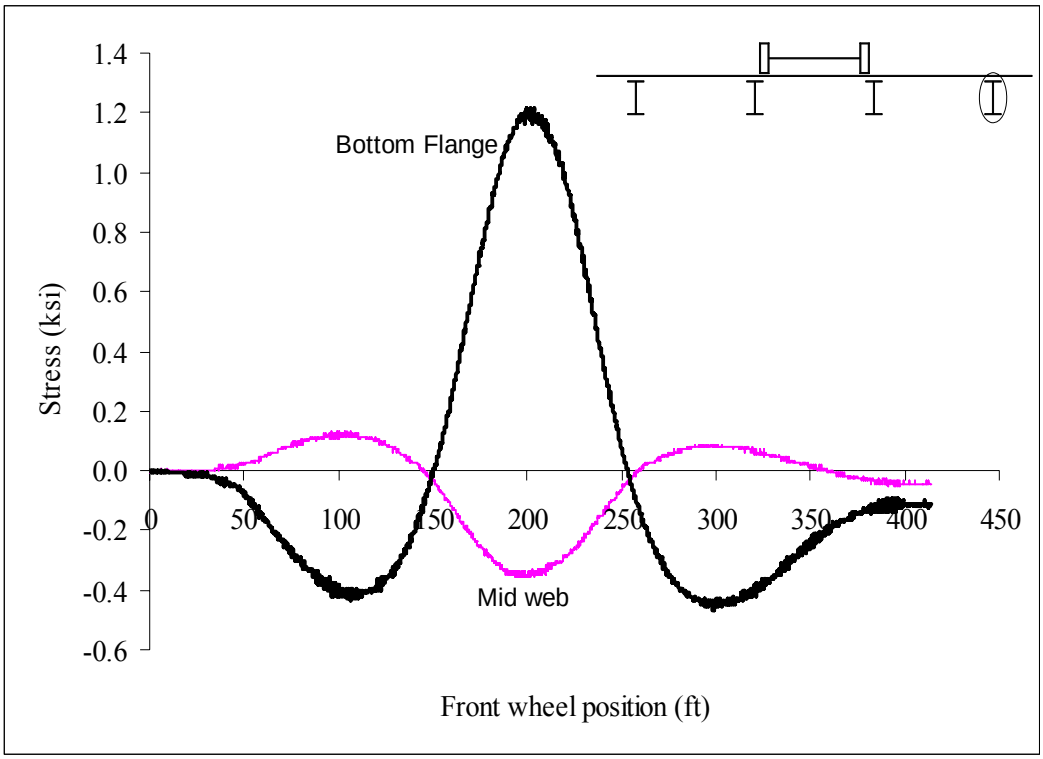

Figure B137: Hatch Bridge Test Run 5 S8 @ Midspan

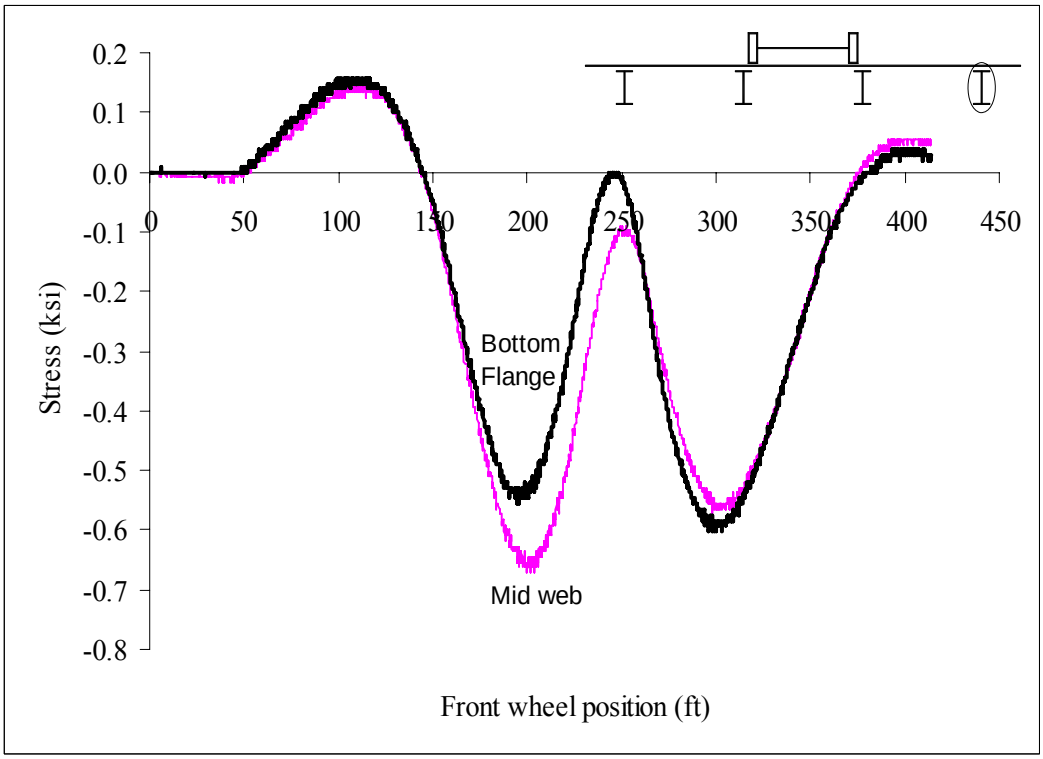

Figure B138: Hatch Bridge Test Run 5 S8 @ 3 ft west of interior support

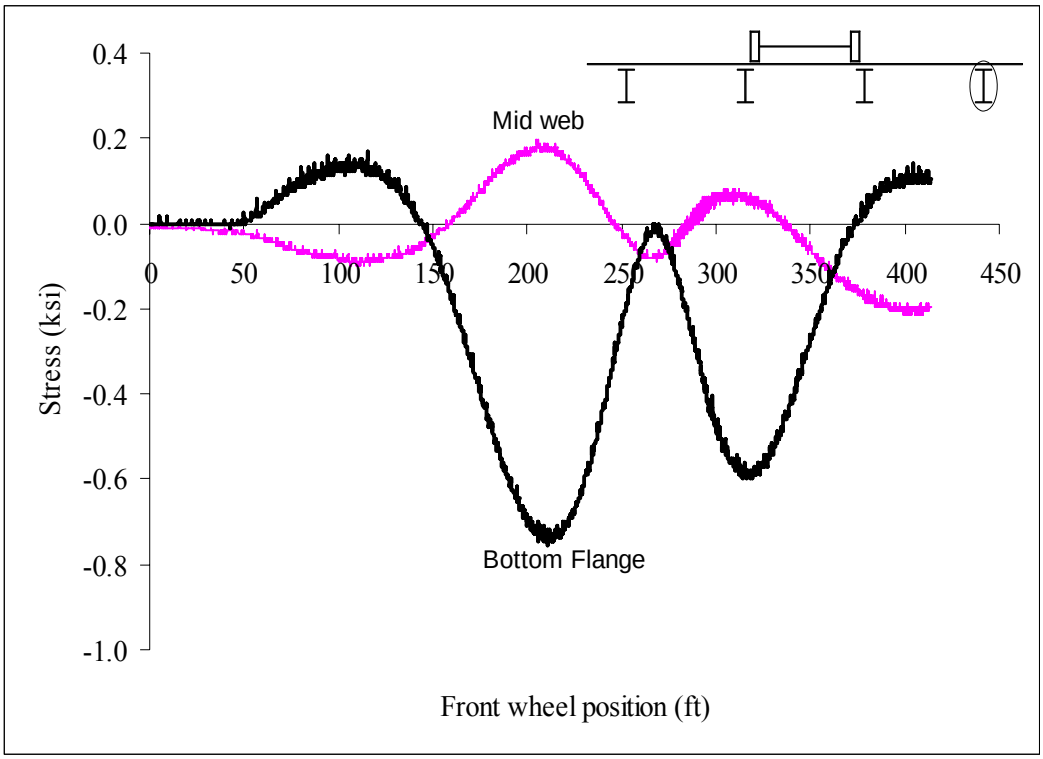

Figure B139: Hatch Bridge Test Run 5 S12 @ 3 ft east of interior support

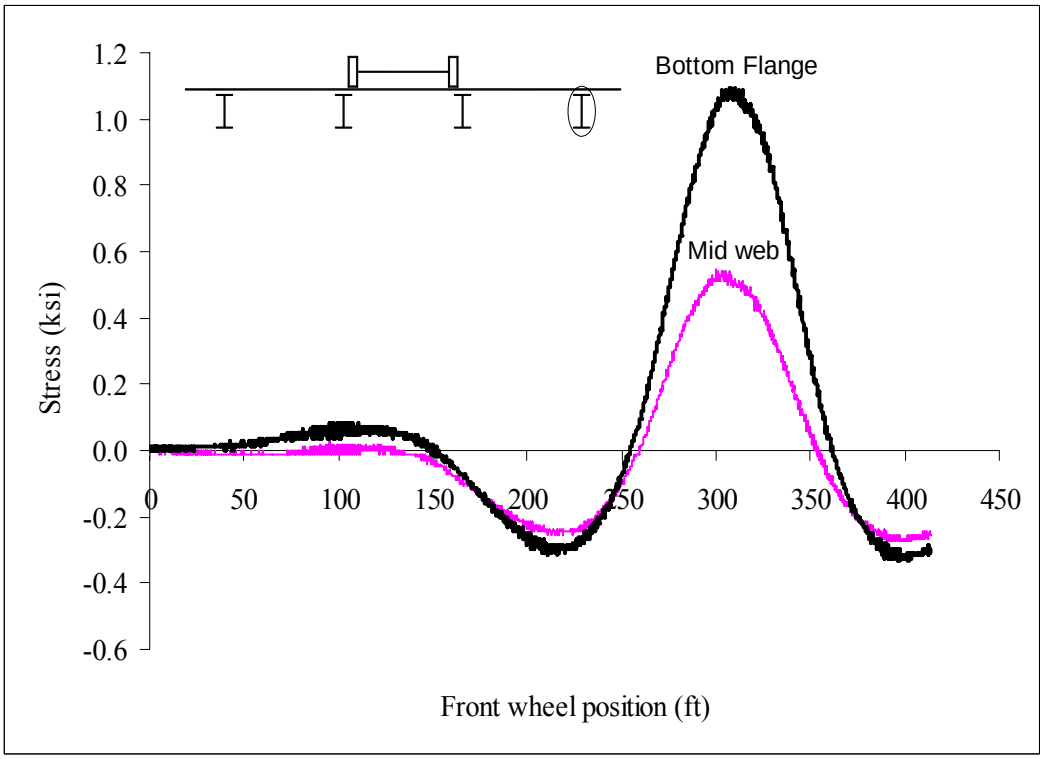

Figure B140: Hatch Bridge Test Run 5 S12 @ Midspan

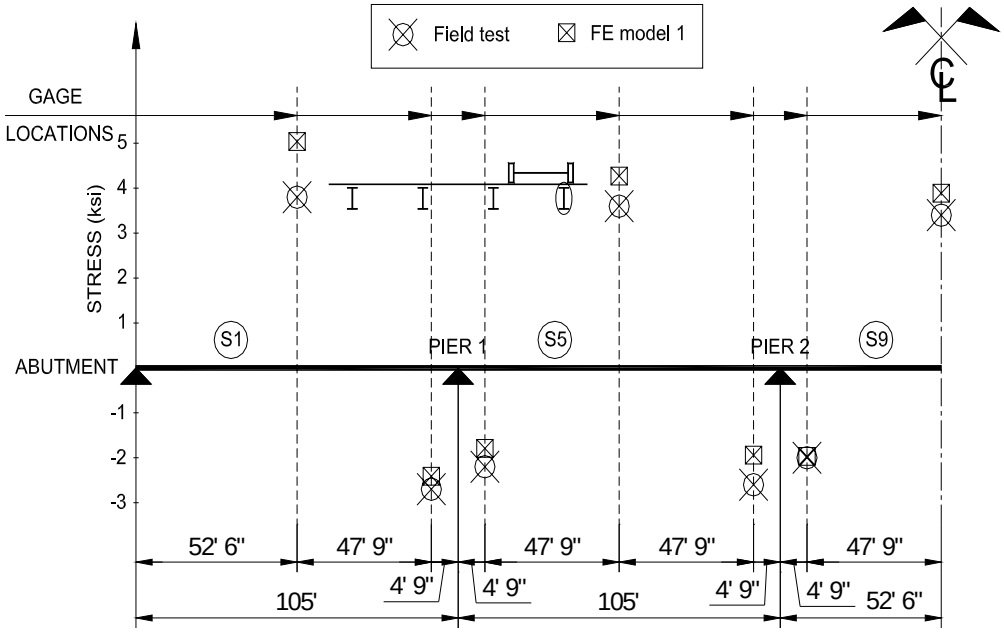

Figure B141: Hatch Load Test Results vs. FEA Results of Bottom Flange Stresses of S1, S5, & S9 (Dang 2006)

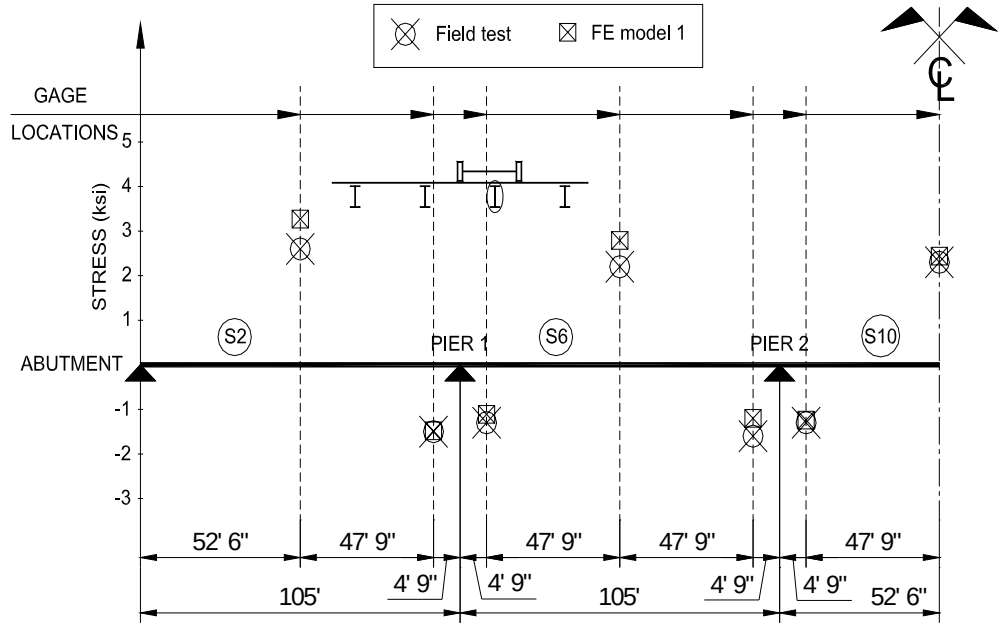

Figure B142: Hatch Load Test Results vs. FEA Results of Bottom Flange Stresses of S2, S6, & S10 (Dang 2006)

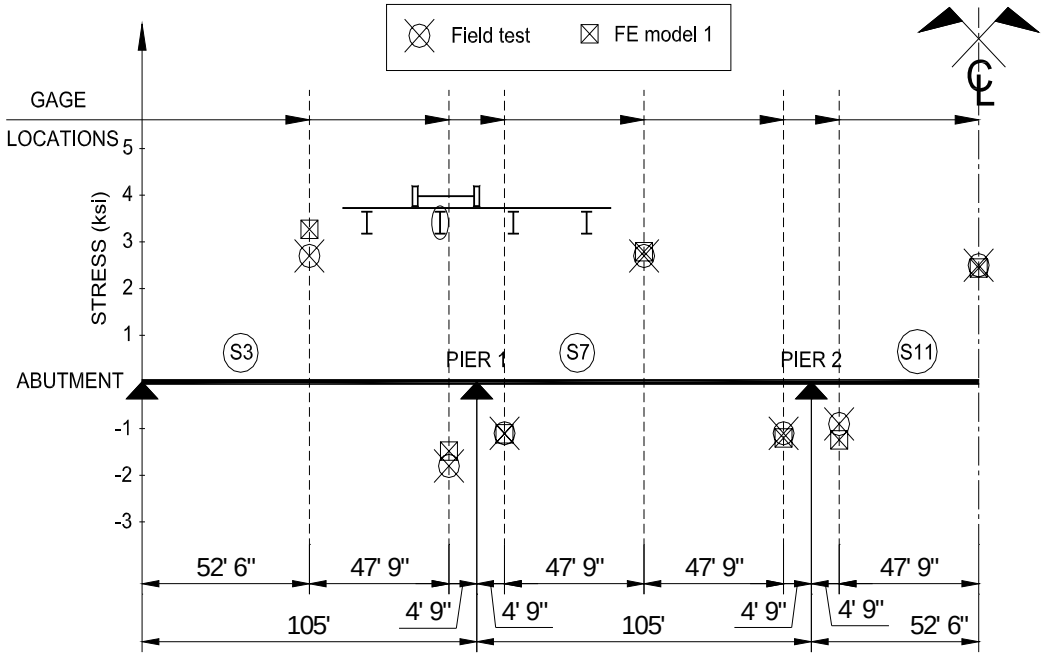

Figure B143: Hatch Load Test Results vs. FEA Results of Bottom Flange Stresses of S3, S7, & S11 (Dang 2006)

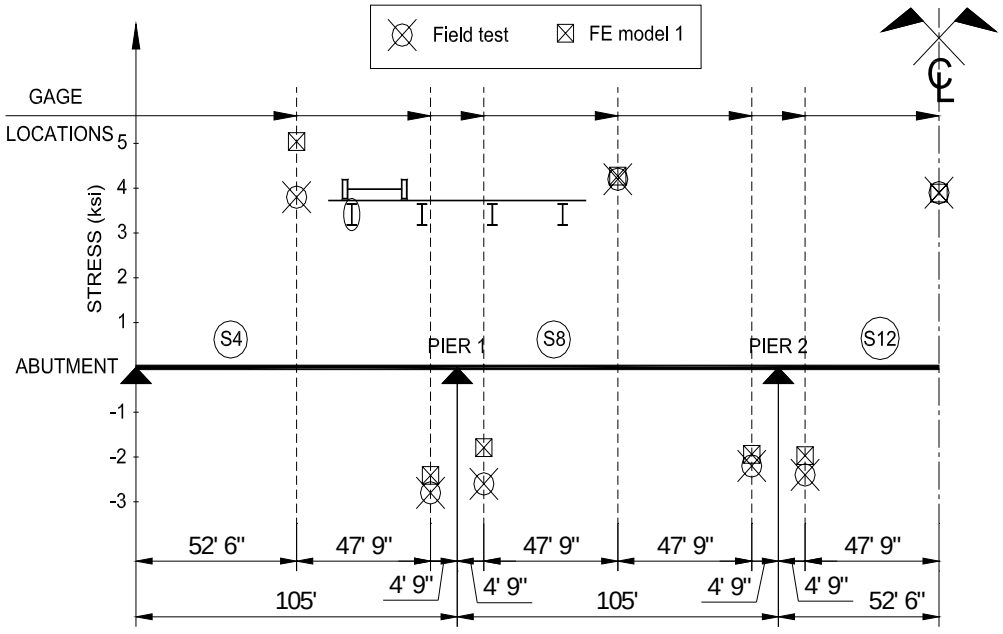

Figure B144: Hatch Load Test Results vs. FEA Results of Bottom Flange Stresses of S4, S8, & S12 (Dang 2006)

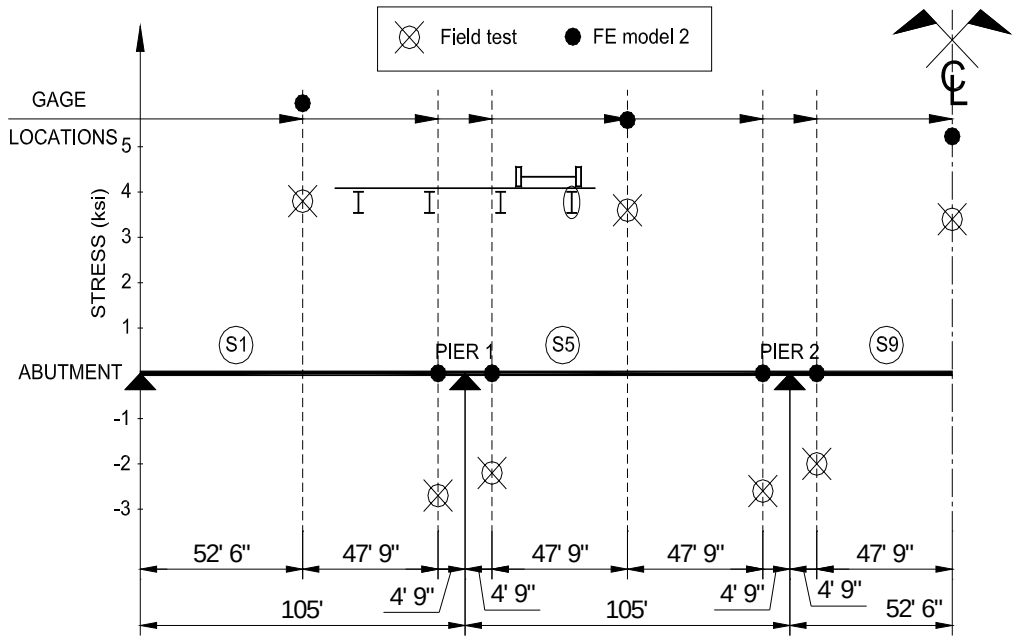

Figure B145: Hatch Load Test Results vs. FEA Results of Bottom Flange Stresses of S1, S5, & S9 (Dang 2006)

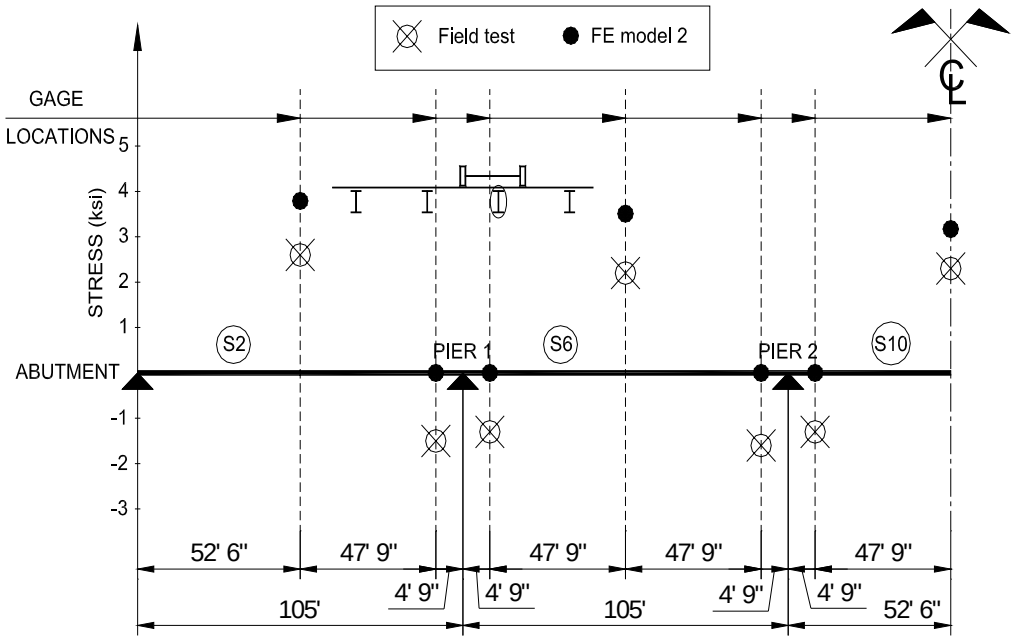

Figure B146: Hatch Load Test Results vs. FEA Results of Bottom Flange Stresses of S2, S6, & S10 (Dang 2006)

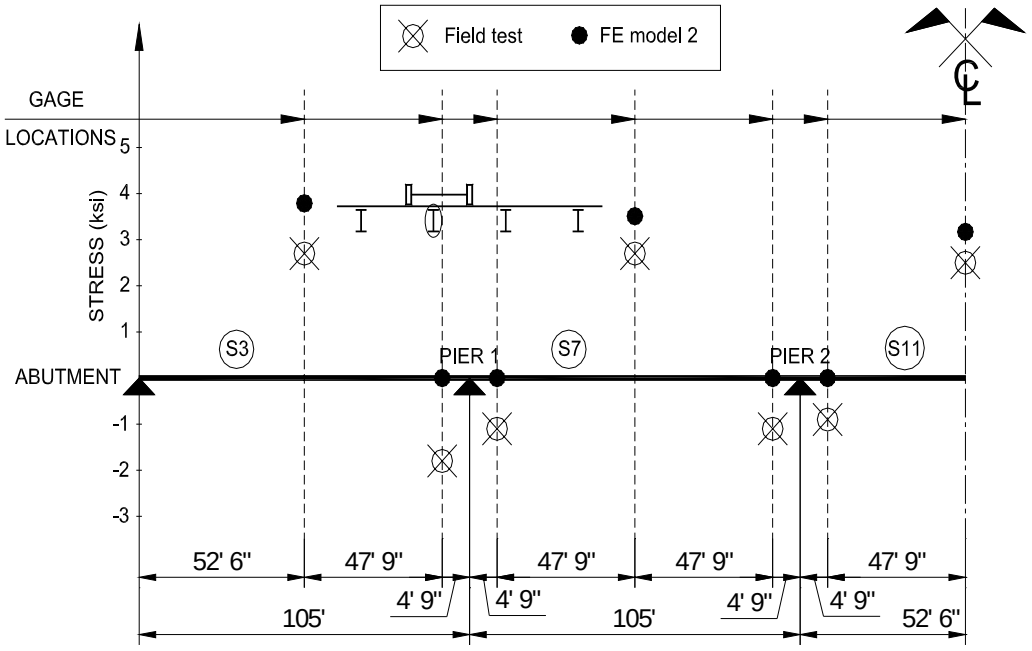

Figure B147: Hatch Load Test Results vs. FEA Results of Bottom Flange Stresses of S3, S7, & S11 (Dang 2006)

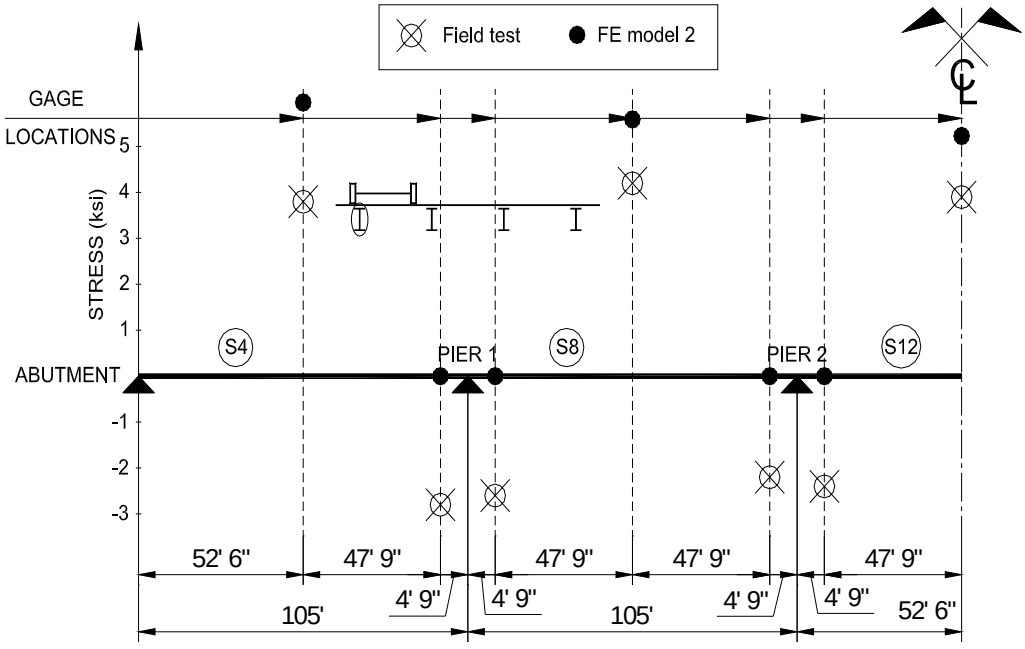

Figure B148: Hatch Load Test Results vs. FEA Results of Bottom Flange Stresses of S4, S8, & S12 (Dang 2006)

APPENDIX C

Steel Bridge Design and Construction Questionnaire

Charles M. Bowen, PhD
Assistant Professor of Civil Engineering
(405) 744-5257

Daniel E. Morales
Graduate Research Assistant
(405) 744-5222

1. Do you have any experience with the design or construction of steel bridges? If so, list any projects you have been involved with.

2. Have you worked on any bridge projects using a different structural material besides steel? If so, please answer the following set of questions.

   Compare/contrast the two types of bridges based on:

   Cost:

   Erection:

   Fabrication:

   Maintenance:

   Design Simplicity:

3. Do you feel as though the design method of minimizing the weight of steel in bridges is a sufficient method to compete with other bridges (E.I. Prestressed Concrete Bridges) in terms of cost effectiveness?

4. Do you have any knowledge or experience concerning field splicing? List any projects you have worked on with field splices.

5. If knowledge is known about field splicing please answer the following questions.

   How does field splicing affect the design/construction of steel bridges in terms of:

   Cost:

   Erection:

   Fabrication:

   Design Simplicity:

6. In your professional opinion, would research into the possible elimination of field splices be beneficial to the steel bridge industry?

7. Have you heard of the simplified economical bridge design developed by Atorod Azizinamini in coordination with the National Bridge Research Organization (NaBRO) and the Nebraska Department of Roads (NDOR)?

8. Do you have any concerns about this new method of construction?

VITA

Daniel Enrique Morales

Candidate for the Degree of

Master of Science

Thesis: FEASIBILITY STUDY OF CONTINUOUS FOR LIVE LOAD STEEL BRIDGES

Major Field: Civil Engineering

Biographical:

Education: Graduated from Booker T. Washington High School, Tulsa, Oklahoma in May 2000; received Bachelor of Science degree in Civil Engineering from Oklahoma State University, Stillwater, Oklahoma in December 2004. Completed the requirements for the Master of Science degree with a major in Civil Engineering at Oklahoma State University in December 2006.

Experience: Employed as a non-arterial street surveyor by Poe & Assoc. Inc., summer of 2000; employed as a civil engineering intern by City of Tulsa Public Works, summer of 2001 and 2002; employed as a civil engineering intern by U.S. Army Corps. Of Engineers – Tulsa District, summer of 2003 and 2004; employed as a graduate research assistant by the Oklahoma State University Department of Civil and Environmental Engineering, 2005; currently employed as a civil engineer by U.S. Army Corps. Of Engineers – Tulsa District, summer of 2006 to present.

Professional Memberships: American Society of Civil Engineers, Chi Epsilon Honor Society

Name: Daniel Morales Date of Degree: December, 2006

Institution: Oklahoma State University Location: Stillwater, Oklahoma

Title of Study: FEASIBILITY STUDY OF CONTINUOUS FOR LIVE LOAD STEEL BRIDGES

Pages in Study: 261 Candidate for the Degree of Master of Science

Major Field: Civil Engineering

Currently in the United States, the precast, pre-stressed concrete design method dominates the new construction market in the short to medium span range bridges.

One approach to help make steel bridges more competitive with pre-stressed concrete bridges is the continuous for live load method (CLL). The method employs a simply supported interior end restraint configuration for dead loads and a subsequent modification to a continuous span configuration for live loads by way of a concrete diaphragm at interior supports.

To determine the feasibility and effectiveness of this method, a cost analysis, an in-situ field load test, and finite element analysis were performed on two CLL bridges in service in New Mexico, USA. The continuous for live load method was found to be more cost and time effective as compared with traditional continuous steel bridge construction. Additionally, it was determined that both case study bridges maintained continuity across the interior supports.

Adviser's Approval: Charles M. Bowen